Impact des chromosomes sexuels sur la différenciation sexuelle du cerveau : aperçu d'une espèce de souris sauvage avec une inversion du sexe naturelle

Louise Heitzmann

▶ **To cite this version:**

Louise Heitzmann. Impact des chromosomes sexuels sur la différenciation sexuelle du cerveau : aperçu d'une espèce de souris sauvage avec une inversion du sexe naturelle. Sciences agricoles. Université de Montpellier, 2022. Français. NNT : 2022UMONG064 . tel-04087607

HAL Id: tel-04087607

https://theses.hal.science/tel-04087607v1

Submitted on 3 May 2023

HAL is a multi-disciplinary open access archive for the deposit and dissemination of scientific research documents, whether they are published or not. The documents may come from teaching and research institutions in France or abroad, or from public or private research centers.

L'archive ouverte pluridisciplinaire **HAL**, est destinée au dépôt et à la diffusion de documents scientifiques de niveau recherche, publiés ou non, émanant des établissements d'enseignement et de recherche français ou étrangers, des laboratoires publics ou privés.

THÈSE POUR OBTENIR LE GRADE DE DOCTEUR DE L'UNIVERSITÉ DE MONTPELLIER

En Ecologie, Evolution, Ressources Génétiques, Paléobiologie

École doctorale Gaia

Unité de recherche ISEM

Impact des chromosomes sexuels sur la différenciation sexuelle du cerveau : aperçu d'une espèce de souris sauvage avec une inversion du sexe naturelle

Présentée par Louise Heitzmann
Le 30 novembre 2022

Sous la direction de Pierre Boursot et Frédéric Veyrunes

Devant le jury composé de

Anna LINDHOLM, Professeure, Université de Zurich	Rapporteure
Catherine PEICHEL, Professeure, Université de Bern	Rapporteure
Patrice DAVID, DR, CNRS, CEFE	Président
Aline MUYLE, CR, CNRS, CEFE	Examinatrice
Sylvie RETAUX, DR, CNRS, DECA	Examinatrice
Agnès MARTIN, CR, CNRS, IGF	Invitée
Pierre BOURSOT, DR, CNRS, ISEM	Invité
Frédéric VEYRUNES, CR, CNRS, ISEM	Co-directeur

UNIVERSITÉ DE MONTPELLIER

Acknowledgements

I think I could not start without thanking Fred. Fred, I do not think there will be enough thank you to explain my gratitude. You trusted me from even before the project started, and you never doubted since. I could not have done this without you : you brought me so much, as a brilliant scientist, but also as the optimistic, kind, and warm person that you are. This past three years and a half have been a blast, and I could not have done this without you. So again, thank you.

I would like to thank Pierre. B, you have always been present when I needed it, you were always considerate, with relevant and brilliant comments. Always with (terrible) jokes also, but I have the same sense of humour and I reckon it is the best.

Paulo, you have been a friend, a supervisor, you have been a rock in the past three years on so many levels. And because we break our heads so many times working on the evolution of sex chromosome in the APM, thank you !!

I want to thank the “Sexe and Speciation” team, it was so much fun to be with you guys, you were always there for me: Guila, Carole, Pierre, Hamilcar (I count on you to maintain the nice vibes in the team). Special thanks to Julie who taught me everything in the lab life (with Faby), the nice discussions, and for being a friend. But I would like to thank you all for that too. Thank you the extended lab team: Faby, Sandra and Fadela, Théo Pierre Richard DelaRemarque, for all these lunches together, for always welcoming me in your office, for your mental and scientific support.

I would like to thank many people from the lab: Marie-ka, for your motivational support when I was extracting RNA, holding the count-down. Special thanks to PierrO, you bring so much to the student in the lab, you are always here when we need it, you always have a smile, a joke. Thank you to all my friends in the lab but a special thanks to my best people, my “babitch team”: Arthur and Alex’, always here for a football on table, for talking, visiting me to see if I am still alive, I could not have done this without you; Alice, sisterhood, babe toussa toussa, thank you for being an amazing friend. Thanks to my other partners in crime: Martinez, we are the best team ever! Laura for your kindness and constant support: you are an amazing person. Thanks to Maurine, PierreBarry, Arthur, Tainou, Nathan, Sophie, Felix, Tanguy, Iago and all the person in the lab for making these three years (and more) fantastic.

I also want to thank Manu V., which, even though he is not in paper, supervised me as well. You always have the right and critical thought which makes us think and improve the work. Beyond that, you’ve always been considerate and welcoming.

I would like to thank Agnès, for many reasons but especially for supervising on the neuro part of this work, for trusting me, for being fun, and for all the nice conversations. I could not have done this without you either, you made me feel like I was part of your team, which I would also like to thank: Evelyne, Anne, which have been so helpful, and always a pleasure to talk to you and listen to ‘It’s just an illusion” from Imagination, while puzzling with the countless number of brain slices to put them back into order. Special thanks to Stas’, for always being there when I needed it: scientifically and humanly speeking, I am glad to have you as a friend !

I thank the team at IGH: Xavier, Brigitte, Francis for your help, the nice discussions, and making me feel like I was part of the team.

I would like to thank the people from IGF/IGH, especially the people guarding the lab: always nice talking to you, and letting me steal wooden pallets.

I would like to thank my PhD committee: especially Thomas for making me do my committee twice in a row, PierrO, Richard, Michel, Manu. You all helped me with constructive interactions and by believing in me.

Thanks to my students as well, I guess I taught you as much as you taught me: for all the relevant discussions and some even far beyond your program. It has been a pleasure !

I have to thank Nico, my physiotherapist, who saw me almost as often as if I was doing a PhD there, between my knees, the double twisted ankle, the elbow etc… You were also a huge mental support, thank you for that. Thanks to your partners in crime as well for being supportive and being interested in my work: Antoine and Vincent.

A huge thanks to my friend, notably Charlène, Jérémy, JY, for always being there and supportive and just being you (which is mostly making fun of me, but I love you guys anyway).

To Léa and Tazzio, you have been there for me for so many years, thanks for your help, your love, your words and your friendship.

Pierro, my friend, my brother, thank you so much for who you are and for being there for me, for crossing the country on a whim to come see me and your strong support all these years !!! I love you man ! Thanks to your family : your brother for telling me when there is an observation at sea, your parents, for always welcoming me, especially when we invade Contis (thanks everyone in Contis: Dan, La Cabane and mostly the Bordeu family).

I would like to thank my roommates at the Chatal : Laura, Guigui, Manu, Manon, Agnès, Nathan 1, Nathan 2, Mathieu, Morgui, “le F.”, Arhur, Milo. You have always been there for me, feeding me when I would come back very (very) late from the lab, for your support, for this wonderful time spent together: parties, transhumance, etc. Thank you !!

And finally, I would like to thank my family: my parents, my sister, Mathieu, Alice the crab and my sunshine, Zoe the shrimp, Pops’, Nono, Rico, and all the others for being part of my life everyday (present and in my head).

This work is dedicated to Raph’, my cousin with Klinefelter syndrome, it all started with him who initiated my interest for sex chromosomes. Thank you Raph’ !

Résumé de la thèse

Mâles et femelles diffèrent sur de nombreux traits, que cela soit au niveau des traits morphologiques, physiologiques ou comportementaux. Ce dimorphisme sexuel est généralement associé à la sélection sexuelle (par exemple, le choix du partenaire, ou la compétition intra-sexuelle), et c'est d'ailleurs Darwin, en 1871, avec ses observations sur la grande diversité de traits extravagants retrouvés majoritairement chez les mâles, qui a définit ce principe fondamental. Mais le dimorphisme sexuel peut aussi être lié à la résolution -ou à la résolution partielle-, des conflits sexuels générés par la présence de traits bénéfiques pour un sexe, mais délétères pour l'autre. Par exemple, chez les Ongulés, les mâles présentent des cornes ou des bois, beaucoup plus développés que chez les femelles (voire absents chez ces dernières), dont ils se servent pour combattre d'autres mâles, ce qui augmente leur chance d'accéder à des femelles et de se reproduire. Or la production de ces bois/cornes peut être coûteuse pour les femelles, dans le sens où ça ne leur confère aucun avantage sélectif, tandis que l' énergie investie aurait pu être allouée dans d'autres traits. Les conflits entre les sexes peuvent ainsi générer une dynamique co-évolutive d'adaptation et de contre-adaptation entre ces derniers, alimentant la grande diversité de phénotypes sexuels observés chez les animaux comme chez les plantes. Depuis Darwin, de nombreuses études ont été réalisées tentant de comprendre les mécanismes proximaux et ultimes conduisant au dimorphisme sexuel.

Chez les vertébrés, on a longtemps pensé que le facteur biologique immédiat à la base du dimorphisme sexuel était les hormones stéroïdes gonadiques, qui influencent l'expression des gènes et des phénotypes qui en découlent. Ce paradigme est encore plus ancré pour les différences comportementales ainsi que les circuits-neuronaux sous-jacents, où les études se sont concentrées uniquement sur les hormones pour rechercher et expliquer la différentiation sexuelle du cerveau (par exemple Breedlove et al., 1999 ; Phoenix et al., 1959). Pourtant, chez les espèces ayant un déterminisme du sexe génétique, les chromosomes sexuels, notamment s'ils sont différenciés (e.g. le Y chez les mammifères possède une poignée de gènes contrairement au chromosome X qui, lui, en est riche, et ces gènes sont spécifiques à la fonction mâle) peuvent être propices aux conflits sexuels ainsi qu' à leur résolution. En outre, il a été démontré des différences entre mâles et femelles qui apparaissent avant la différenciation des gonades, sous-tendant un rôle des chromosomes sexuels, et mettant en lumière la limite d'une vision hormone-centrée de la différenciation sexuelle du cerveau.

Au cours des deux dernières décennies, plusieurs études, utilisant pour la plupart des souris génétiquement modifiées, ont montré que les chromosomes sexuels peuvent avoir une influence directe

sur la différenciation sexuelle du cerveau. Cependant, le rôle de ces derniers est loin d'être compris et la plupart des études concernées ont une vision médicale, afin de mieux comprendre et de prédire certaines maladies pour lesquelles le sexe peut être un facteur de risque. De surcroît, l'utilisation de souris génétiquement modifiées peut représenter certaines limites d'interprétations, notamment lorsque l'on s'intéresse à des phénotypes façonnés par la sélection naturelle et sexuelle.

La souris naine africaine, *Mus minutoides*, appartenant au sous-genre *Nannomys*, est une souris sauvage qui s'est révélée être une espèce de souris particulièrement fascinante et permettant, qui plus est, d'aborder les questions du lien genotype-phenotype sexuel au niveau du cerveau. On retrouve chez cette souris trois chromosomes sexuels : les classiques X et Y, ainsi qu'un troisième chromosome féminisant, nommé X*. Ce chromosome a pour origine une mutation sur le chromosome X (datant d'il y a environ un million d'années) et présente, depuis, des divergences notables avec ce dernier: arrêt de la recombinaison, remaniements chromosomiques et duplications/délétions de gènes. En outre, la mutation à l'origine de ce chromosome est dite féminisante, puisqu'elle induit une inversion du sexe chez les individus qui portent le chromosome X* et le Y. On retrouve donc trois génotypes femelles dans les populations naturelles : XX, XX*, X*Y et un seul génotype mâle, XY. Les femelles X*Y sont des femelles à part entière, avec la présence d'ovaires fonctionnels et comparables entre les femelles (au stade adulte du moins). Les femelles X*Y ont même un plus grand succès reproducteur que les femelles XX et XX*. En revanche, elles sont plus agressives que les autres femelles, elles ont une force de morsure comparable à celle des mâles, et il en va de même pour les comportements liés à l'anxiété (qui semble être réduite chez ces femelles). Ces traits, que l'on retrouve généralement plus souvent chez les mâles, sous-tendent une masculinisation partielle du cerveau des femelles X*Y, mettant ainsi en évidence une dichotomie entre le sexe gonadique et le sexe phénotypique chez cette espèce. Ces différents phénotypes observés questionnent donc la différenciation du cerveau des femelles (et des mâles), ainsi que l'impact direct des chromosomes sexuels sur la différenciation sexuelle du cerveau et des phénotypes subséquents .

J'ai consacré les travaux de ma thèse à déterminer et caractériser la différenciation sexuelle du cerveau chez la souris naine africaine. J'ai entrepris une approche intégrative, combinant des expériences comportementales, de neurobiologie et de transcriptomique pour évaluer différents aspects du cerveau. Ces approches ont été déterminantes pour moi, puisqu'elles m'ont permis d'établir un lien direct entre génotype et phénotype, et donc d'avoir une vision plus globale sur le système. En effet, ce travail a permis de nombreuses collaborations et d'intégrer diverses disciplines de la biologie ce qui, je suppose, en fait sa force.

Les travaux présentés ici se concentrent sur deux axes :

Partie 1 . Les comportements sociaux et parentaux.

1. Est-ce que l'inversion de sexe chez les femelles X*Y influence les comportements de soins maternels ?

2. Est-ce que la lactation est aussi impactée par l'inversion de sexe, et est-ce qu'elle pourrait indiquer une différence de valeur sélective entre les femelles ?

3. Est-ce que l'agressivité accrue des femelles est liée à l'action directe des chromosomes sexuels ou des hormones stéroïdiennes ?

Partie 2 : La différenciation sexuelle du transcriptome du cerveau

4. Le transcriptome du cerveau reflète -t-il le sexe gonadique où le sexe génotypique ?, Peut-on identifier des candidats à la base des différences phénotypiques observées entre les femelles ?

5. Projet annexe basé sur le transcriptome du rein : Est-ce que les chromosomes sexuels non recombinants dégénèrent ? Auquel cas, ils pourraient aussi prendre part aux différences phénotypiques observées.

Partie 1 . Les comportements sociaux et parentaux

1. Est-ce que l'inversion de sexe chez les femelles X*Y influence les comportements de soins maternels ?

1. Heitzmann, L., Challe, M., Perez, J., Castell, L., Galibert, E., Martin, A., Valjent, E., and Veyrunes, F. (2022). Genotypic sex shapes maternal care in the African Pygmy mouse, Mus minutoides. BioRxiv. https://doi.org/10.1101/2022.04.05.487174. Revu et accepté par PCI pour recommandation.

On a longtemps considéré que les comportements sexuellement dimorphiques, tels que les soins parentaux, étaient principalement, voire exclusivement, déterminés par les hormones gonadiques. Au cours de ces deux dernières décennies, quelques études ont remis en question ce point de vue, mettant en évidence l'influence directe du complément chromosomique sexuel (XX vs XY ou ZZ vs ZW). La souris naine africaine, *Mus minutoides*, est une souris sauvage dont l'inversion sexuelle XY naturelle est induite par un troisième chromosome féminisant, appelé X*, conduisant à trois génotypes femelles : XX, XX* et X*Y. Ici, nous montrons que l'inversion sexuelle chez les femelles X*Y façonne une stratégie de soins maternels divergente de celle des femelles XX et XX*, plutôt que d'en impacter leur qualité. En outre, nous montrons que l'inversion sexuelle peut également avoir un impact sur le système dopaminergique dans le noyau périventriculaire antéroventral de l'hypothalamus, ce qui est cohérent avec une composante des soins maternels : ramener les petits dans le nid. En combinant l'écologie comportementale et la neurobiologie chez un rongeur soumis à la sélection naturelle, nous évaluons les candidats potentiels pour la base neuronale des comportements maternels et renforçons le rôle sous-estimé des chromosomes sexuels dans la mise en place des différences comportementales et au niveau du système nerveux, entre les sexes. Tout bien considéré, nous mettons en évidence l'émergence d'un troisième phénotype sexuel, remettant en question la vision binaire des sexes phénotypiques.

2. Est-ce que la lactation est aussi impactée par l'inversion de sexe et est-ce qu'elle pourrait indiquer une différence de valeur sélective entre les femelles ?

Louise D. Heitzmann, Anne Guillou, Evelyne Galibert, Marie Challe, Agnes O. Martin[1] & Frederic[1] Veyrunes

La lactation est un trait complexe spécifique aux femelles et crucial pour la survie des descendants. La lactation, c'est-à-dire la production et l'éjection du lait de la glande mammaire, est induite par la prolactine (PRL), une hormone sécrétée par l'hypophyse (production), et par l'ocytocine (éjection), un neuropeptide qui régule un large éventail de comportements sociaux (ex : les soins maternels, les liens de couple). Nous nous sommes spécifiquement concentrés sur la prolactine, car l'ocytocine a été développée dans la section précédente et aucune différence n'a été trouvée entre les femelles. Le but de ce projet est de combiner trois aspects de la lactation : le contrôle neuronal de la prolactine par l'axe hypothalamo-hypophysaire, la quantification des niveaux de prolactine circulante, et le suivi du poids des portées comme indicateur de la qualité de la lactation. Les données présentées ici sont principalement des méthodes qui sont encore en cours d'optimisation (notamment pour la quantification de la prolactine), avec quelques résultats préliminaires d'une étude en cours. Ce projet est particulièrement intéressant car la prolactine est régulée par la dopamine qui est susceptible d'être influencée par les chromosomes sexuels, avec, par exemple, plusieurs études montrant des différences dans les niveaux de dopamine dues à l'expression de *Sry* (exprimé dans le cerveau des femelles X*Y). En conséquence, des niveaux de lactation plus élevés chez les femelles X*Y apporteraient de nouvelles perspectives passionnantes sur les conséquences de l'inversion du sexe chez la souris naine africaine ; cela pourrait apporter un soutien supplémentaire à la valeur sélective accrue des femelles X*Y, et au maintien du système grâce à des phénotypes adaptatifs.

3. Est-ce que l’agressivité accrue des femelles est liée à l’action directe des chromosomes sexuels ou des hormones stéroïdiennes ?

Louise Heitzmann, Marc Fichter, Julie Perez, Xavier Hautecoeur, Theo Deremarque & Frederic Veyrunes

Les différences entre les sexes en matière d'agressivité sociale sont courantes dans le règne animal, les mâles étant généralement plus agressifs que les femelles. Les causes proximales de ce dimorphisme sexuel impliquent les hormones stéroïdes avec notamment la testostérone, mais aussi les chromosomes sexuels avec un déséquilibre de gènes liés au sexe. Cependant, l'influence directe des chromosomes sexuels est loin d'être comprise car les études sont peu nombreuses et parce que nous ne pouvons généralement pas distinguer la contribution relative des gènes liés au sexe, de celle des hormones (c'est-à-dire que les sexes génotypiques et gonadiques sont indissociables). La souris naine africaine est une espèce de souris sauvage présentant une dissociation entre le sexe gonadique et le sexe génotypique. En raison d'une mutation sur le chromosome X à l'origine d'un troisième chromosome sexuel, nommé X*, et induisant une inversion de sexe, il existe trois génotypes femelles dans les populations naturelles : XX, XX* et X*Y, tandis que tous les mâles sont XY. Il est intéressant de noter qu'une étude précédente a montré que les femelles X*Y sont plus agressives que les femelles XX et XX*. Afin de démêler les contributions relatives des gènes liés au sexe et des hormones dans la régulation de l’ agressivité, nous avons reconduit le même test de comportement agonistique chez les femelles de la même population de souris naine africaine. Après les essais, nous avons mesuré les concentrations en testostérone chez les femelles et quantifié l'expression des gènes liés au sexe connus pour réguler les comportements d’ agression, que nous avons corrélés avec les niveaux d'agressivité. Même si nos résultats doivent être approfondis, nous avons montré que les gènes liés au sexe, plutôt que les hormones stéroïdiennes, sont plus susceptibles de stimuler l'agressivité chez les femelles X*Y. Tout bien considéré, les espèces dotées d'un système de déterminisme du sexe atypique et façonné par l'évolution, comme chez la souris naine africaine, peuvent apporter une aide considérable pour comprendre le rôle direct des gènes liés au sexe quant à la mise en place de différences entre les sexes au niveau des comportements et du cerveau.

Partie 2: La différenciation sexuelle du transcriptome du cerveau

4. Le transcriptome du cerveau reflète -t-il le sexe gonadique où le sexe génotypique ?, Peut-on identifier des candidats à la base des différences phénotypiques observées entre les femelles ?

Louise D. Heitzmann, Paul A. Saunders, Julie Perez, Pierre Boursot & Frederic Veyrunes

Les hormones gonadiques et les chromosomes sexuels déterminent les différences entre sexes au niveau du cerveau et des phénotypes qui en découlent. Cependant, la contribution relative de ces deux facteurs reste difficile à déterminer car le sexe gonadique et le sexe génotypique sont généralement confondus. La souris naine africaine, *Mus minutoides*, possède un système de détermination du sexe polygénique, impliquant une dissociation entre les sexes gonadique et génotypique. Dans les populations naturelles, il existe un seul génotype mâle, XY, mais trois génotypes femelles : XX, XX* et X*Y, en raison d'un chromosome X* féminisant. En outre, tous les chromosomes sexuels sont fusionnés aux autosomes, ce qui génère des néo-X, néo-X* et néo-Y chromosomes sexuels. Les femelles X*Y présentent des divergences phénotypiques frappantes par rapport aux autres femelles : un taux d'ovulation plus élevé, des comportements maternels divergents et une agressivité accrue. Ces phénotypes suggèrent des divergences sous-jacentes au niveau du transcriptome du cerveau qui serait donc influencé par le complément de chromosomes sexuels (par l'expression directe de gènes liés au sexe et la régulation de l'expression autosomale, ou via les hormones). Ici, nous comparons le transcriptome du cerveau des quatre génotypes sexuels chez *M. minutoides*. Nous rapportons que, bien que le transcriptome reflète principalement le sexe gonadique (83% des gènes différentiellement exprimés), les chromosomes sexuels ont également une influence d'interaction omniprésente, qui est prédominante pour une proportion significative (17%) de gènes et dont les profils d'expression corroborent les différents phénotypes femelles. Ces gènes exprimés différemment sont enrichis sur les chromosomes sexuels et néo-chromosomes sexuels, ce qui suggère un rôle direct du complément des chromosomes sexuels, et une dynamique évolutive entraînée par le nouveau mode de transmission des chromosomes sexuels. De plus, notre analyse met en lumière plusieurs gènes candidats à corréler avec les variations phénotypiques observées entre femelles, impliqués dans les fonctions reproductives (e.g. *Amhr2*), ou les comportements sociaux via la voie dopaminergique (e.g. *MaoA*). Enfin, nous avons trouvé une expression préférentielle des allèles X par rapport aux allèles X*, suggérant une inactivation biaisée du X* dans le cerveau des femelles XX*. Au final, nous montrons que le système de détermination du sexe a profondément impacté le transcriptome du cerveau, ce qui apporte des perspectives excitantes sur les bases moléculaires du dimorphisme sexuel et de la résolution des conflits sexuels.

5. Projet annexe basé sur le transcriptome du rein : Est-ce que les chromosomes sexuels non recombinants dégénèrent ? Auquel cas, ils pourraient aussi prendre part aux différences phénotypiques observées.

Ce chapitre est basé sur un projet parallèle sur l'évolution des chromosomes et néo-chromosomes sexuels chez la souris pygmée africaine, en collaboration avec le Dr Paul Saunders. Dans ce projet, j'entreprends des analyses similaires à celles que j'ai développées sur le transcriptome du cerveau, afin d'évaluer l'évolution de l'expression des gènes dans les régions non recombinantes liées au sexe (ex : analyses d'expression différentielle, de « clustering » et d' expression allèle-spécifique). Les chromosomes X/X* et les néo-chromosomes sexuels ayant cessé de recombiner, ces méthodes pourraient aider à détecter des signes de dégénérescence au niveau de l'expression génique. Les données présentées ici sont basées sur des analyses qui sont encore en cours, et notre plan sera de publier ces résultats en même temps que les analyses de Paul, décrivant l'arrêt de la recombinaison et l'évolution des séquences dans les régions non recombinantes. Ces résultats, bien qu'ils fassent partie d'un projet différent, peuvent néanmoins apporter un éclairage sur la question de savoir si la dégénérescence des chromosomes sexuels peut également induire une divergence phénotypique entre les femelles, et ainsi décrire un autre axe de la relation génotype-phénotype.

Table of Contents

Introduction.....2
1 The evolution of sexual dimorphism.....6
1.1 Evolution of anisogamy and costs of males : the beginning of a female struggle.....6
1.2 The reinforcing role of separate sexes, intra-locus and inter-locus sexual conflicts.....8
2 Proximate causes at the basis of sexual dimorphism.....9
2.1 The standard and hormone-centered view of sexual differentiation in vertebrates.....11
2.2 The role of sex chromosomes.....14
2.2.1 Why sex chromosomes ?.....14
2.2.2 X and Z chromosomes implications.....14
2.2.3 Y and W implications.....16
3 Genetically modified mice to assess sexual differentiation of the brain: a powerful tool but to a certain extent.....16
4 The African pygmy mouse.....18
5 Research questions.....21
Part 1: Social and parental behaviours.....23
1 Genotypic sex shapes maternal care in the African pygmy mouse, *Mus minutoides*.....24
2 Impact of sex reversal on maternal care: focus on lactation.....52
3 Disentangling between hormonal and sex-linked genetic bases of territorial aggression in sex-reversed X*Y females.....64
Part 2: Sexual differentiation of the brain transcriptome.....84
4 Brain transcriptomic architecture of a wild mouse species with sex reversal: a three sex chromosome orchestra.....85
5 The evolution of gene expression on sex and neo-sex chromosomes: detecting signs of degeneration ?.....115
General discussion.....126
Cited references.....136
Supplemental Information.....151
S.1 Genotypic sex shapes maternal care in the African pygmy mouse, *Mus minutoides*.....152
S.2 Impact of sex reversal on maternal care: focus on lactation.....166
S.3 Brain transcriptomic architecture of a wild mouse species with sex reversal: a three sex chromosome orchestra.....168
S.4 The evolution of gene expression on sex and neo-sex chromosomes: detecting signs of degeneration ?.....235
Annexe.....243

Introduction

Why do females and males differ while they share most, if not all, of their genome has fascinated biologists for over a century, mostly inspired by the founder of sexual selection processes, Charles Darwin. In 'the Descent of Man and Selection in Relation to Sex', Darwin (1871) emphasized the role of sexual selection in shaping sex differences in behaviours and morphology, although differences in ecology between the sexes may also participate to the evolution of sexual dimorphism. He shed light on the great diversity of sophisticated ornaments, behaviours and weaponry characteristics found in males but not in females. Because these traits are not found in both sexes, he proposed that they must confer a reproductive advantage by increasing males' chance to find and gain access to a mate, and to be chosen by females. Hence, in contrast, females develop traits related to maternal care and/or choosiness.

Sophisticated male traits are found in a great diversity of taxa. In peacock spiders (*Maratus sp.)* for example, males have a fan-shaped abdomen ornamented with iridescent colour patterns that they display during courtship, while females usually have cryptic colours, with two or three shades and choose the male they mate with (Girard & Endler, 2014). Similarly, in the *Anolis proboscis* lizard, males have a rostral appendage, like a soft horn, they display during courtship and use it to stimulate females by rubbing the tip of the appendage on females' body (Fig. 1) (Quirola et al., 2017). In ungulate species, males have antlers or horns used in male-male fights in which the winner will mate with a female that usually lacks these characteristics (Clutton-Brock, 1982; McPherson & Chenoweth, 2012), or less developed (Fig. 1). These phenotypic divergences are assumed to arise from a stronger competition on males to find a mate. In comparison, females are usually the rare sex, that can either choose to mate among the strongest or the most attractive male, such as in the *Anolis proboscis*.

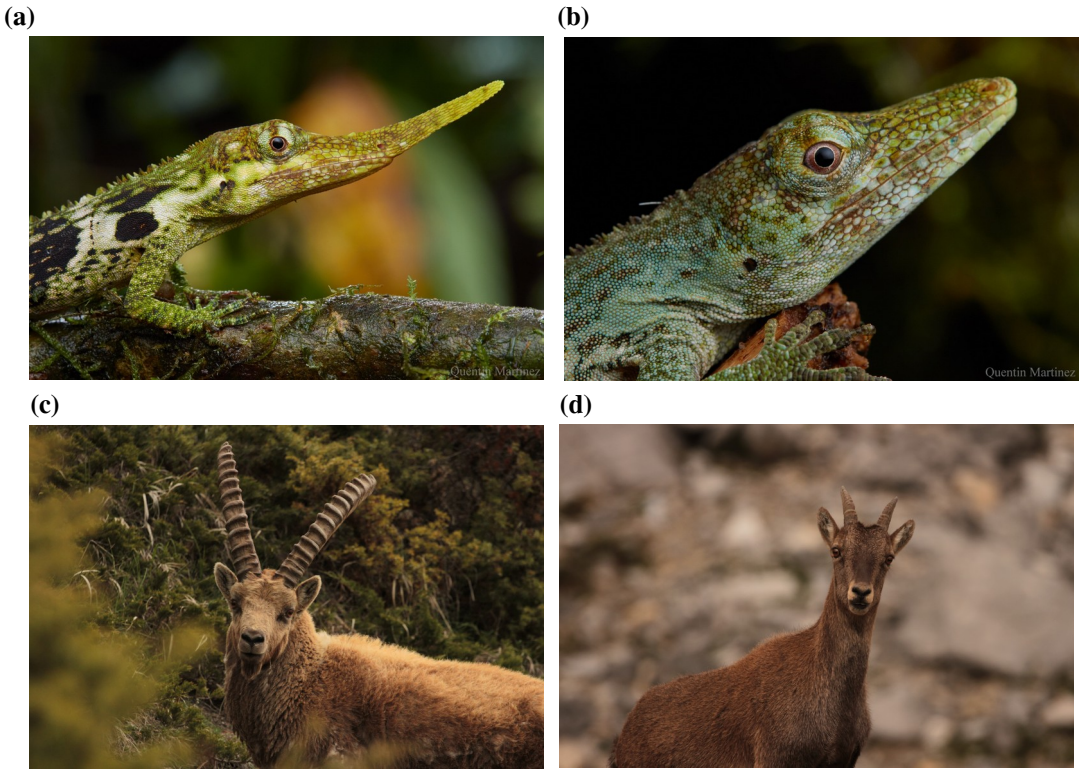

Figure 1. Sexual dimorphism in vertebrates. In the *Anolis proboscis* lizard, males (a) and females (b) differ in colouration, although they remain cryptic, and males have a horn-like rostral appendage which they use during courtship to stimulate and attract females. © Quentin Martinez. In the Alpine ibex (*Capra ibex*), males (c) have large horns with sophisticated shapes they use during male-male fights to gain access to females. Horns in females (d) are less developed. © Alexandre Assemat.

Ornaments, weaponery structures and other 'fancy' traits (e.g. courtship behaviours) displayed by males are considered as honest signals about males' condition : they are cues of healthiness and genetic quality (Hamilton & Zuk, 1982; Zahavi, 1975) that a female can pass on to her sons. However, these traits can also be passed on to females, which may come at a cost. First it requires energy that will not be allocated to other traits, which can be disadvantageous if there is no female-female competition to mate, nor male choice. Secondly, they increase predation risks because individuals are more visible not only to conspecific, but also to predators. Furthermore, females can directly suffer from male beneficial traits. For example in elephant seals, larger and stronger males tend to mate more but the larger the male is, the more likely the females are to be injured or killed during mating (Le Boeuf & Mesnick, 1990). Other traits including harassing behaviours and morpho-anatomical structures to assure mating can also be harmful to females, and can lead to the evolution of female resistance and counter-adaptation (e.g. spiny male genitalia in seed beetles; Rönn et al., 2007). On both instances (ornaments and armaments), sexual dimorphism might be the result of an underlying conflict between males and females over traits that are beneficial to one sex, but detrimental to the other. These examples illustrate and underpin the principle of sexually antagonistic selection.

Since Darwin's observations, studies have been focused on animals because sexual dimorphism in plants was thought to be rare or less spectacular. However, in dioecious (separate sexes) flowering plants, there are considerable differences in vegetative and reproductive morphology as well as in life history traits (reviewed in Barrett & Hough, 2013). For instance, male plants in some species, such as the Canada thistle (*Cirsium arvense*), have different and more complex odours (i.e., more molecules) than female plants (Ashman, 2009). Another study bias since Darwin stems from the focus on males, which led to a stereotypical view of sexual dimorphism. Males are the most attractive sex, highly aggressive, while females are choosy and display higher levels of maternal care. But sexual dimorphism also includes female-female competition, choosy or caring males (reviewed in Clutton-Brock & Huchard, 2013). In the spotted hyena (*Crocuta crocuta*) for instance, females are the dominant sex in the social hierarchy and are larger than males (Clutton-Brock & Huchard, 2013; Frank, 1986). All things considered, sexual dimorphism evolved independently in a great diversity of plant and animal taxa, in many forms, which raises questions on its evolutionary and proximate causes. To answer these questions, we must first go back to the prior basis of sex differences and probably the most ancient form of sexual conflict : anisogamy.

Box 1. Terminology and definitions

Mating types: loci enabling and controlling fertilization. Mating types prevent self-fertilization due to self-incompatibilities. The formation of a zygote requires the fusion of two distinct mating types (e.g. in fungi).

Isogamy : gametes of similar morphology. Fusion usually occurs between distinct mating types. Isogamy concerns most unicellular organism.

Anisogamy : production of dimorphic gametes. One is large, immobile, rich in food reserves, and is associated with female functions. The other gamete is small, motile, lack food reserves, and is associated with male functions. The formation of a zygote requires the fusion of these two types of gametes. Anisogamy concerns most multicellular organism.

Syngamy: fusion of gametes.

Simultaneous hermaphroditism: condition of individuals that carry both female and male organs at the same time. In contrast, **sequential hermaphrodites** start with one sex and switch to the other sex at some point in their lifetime.

Gonochorism (dioecy in plants): condition of separate sexes: one individual is female and one is male.

Heterogamety : production of gametes with two distinct sex chromosomes in species with genetic sex determination system : X and Y in males, or Z and W chromosomes in females (e.g mammals and birds, respectively). In contrast, XX (females) and ZZ (males) individuals are the homogametic sex. Sex chromosomes can be highly differentiated (heteromorphic) such as in mammals, or undifferentiated (homomorphic) such as in boas.

Intra-locus sexual conflict (IASC): conflict arising from different phenotypic optima between the sexes at a specific locus.

Inter-locus sexual conflict (IRSC): conflict arising when the phenotypic optimum for one sex at a given locus is detrimental for the phenotypic optimum of the other sex at another locus. IRSC is observed during interactions between the sexes and will usually involve phenotypes that maximize reproduction in males, and phenotypes that maximize resistance to males in females (e.g. coercive matings where males harass and harm females).

1 The evolution of sexual dimorphism

1.1 Evolution of anisogamy and costs of males : the beginning of a female struggle

Sexual dimorphism takes its first shape on the fundamental basis of sexual reproduction, with the evolution of two types of gametes: a large, immobile and nutrient rich gamete (egg) in females, and a small, motile and nutrient-deprived gamete (sperm) in males. Though these differences do not require separate sexes, by convention we refer to the large gamete as female, as it is produced by female gonads, and the small gamete as male, produced by male gonads (e.g. Bell, 1978; Parker et al., 1972). Differences in gamete morphology, termed anisogamy (see Box 1 for definitions of terms used), is common in multicellular plants and animals (Beukeboom & Perrin, 2014b; Lehtonen et al., 2016). In contrast, the production of gamete of the same size, i.e., isogamy, is the norm in unicellular organisms, though exceptions occur in both and notably in fungi (Bachtrog et al., 2014; Billiard et al., 2011; Lehtonen et al., 2016; Parker et al., 1972; Smith, 1982). Theoretically, isogamy is presumed to be the ancestral state, with independent transitions to anisogamy in multiple lineages. It is Parker et al (1972) that first proposed a model for the transition from isogamy to anisogamy based on selection for increased zygote size. He proposed a positive correlation between zygote size and food reserves as well as between food reserves and survival, under the assumption that the production of gametes is limited by the energy and mass allocable by individuals, i.e., you can either produce a lot of small gametes or a few large gametes. Accordingly, because large gametes increase the fitness of a zygote, selection will favour them. But why do large gametes always fuse with small gametes ?, and why don't large gametes invade ? If producing a large gamete increases a zygote's chances of survival, fusions between two large gametes would be even more advantageous.

One hypothesis is that large and small gametes were bipolars, with two distinct mating types that preceded the emergence of dimorphism. Mating types were self-incompatible thus preventing the fusion (i.e., syngamy) of gametes of the same size. In theoretical models, mating types can also evolve following the transition to anisogamy, however it does not explain why large gametes do not fuse in the first place, considering their selective advantage. The main theory, which is not incompatible with mating types, is that intermediate gametes are less fit because they have less resources necessary for the survival of a zygote in comparison to large gametes (Bell, 1978; Lehtonen & Parker, 2014; Parker et al., 1972; Smith, 1978). Similarly, they are less motile and produced in lower numbers due to limited energy allocable; there is a balance between mass and number production, as well as between mass and motility, i.e., larger gametes are slower and require more energy to move than small gametes. This creates a disruptive selection for large and small gametes to maximize chances of

encounters (selection on small gamete) -especially when fertilization is external-, and to maximize the fitness of zygotes (selection on large gamete). Because sperms are produced in large numbers while there are only a few eggs, not all sperms will find a mate, creating a competition between male gametes. If one male gamete of larger size is produced, the energy invested in its production will be disadvantageous as the chances of mating are very low due to the numerous competitors, especially since it should also affect its motility. On this basis, gamete competition should be enough to maintain anisogamy (Davies et al., 2012; Lehtonen & Parker, 2014; Parker, 1982; Parker et al., 1972).

Once anisogamy evolves, it automatically creates an asymmetric investment in gametes and zygote's development between the sexes, especially in species with internal fertilization, with caring females and opportunistic competitive males (Davies et al., 2012; Kokko & Jennions, 2008; Lehtonen & Parker, 2014; Trivers, 1972). Beyond gametes' production, parental investment is also often biased towards maternal care, such as in mammals, insects and reptiles, albeit paternal care is most common in fish, and biparental is more common in birds (Clutton-Brock, 1991; Gans, 1996; Wong et al., 2013). Nevertheless, the asymmetric investment and production of gametes implies that males can mate multiple times and sire many offspring, while females usually have less descendant than males. The differences in reproductive success are the foundation of Bateman's gradient principle (Bateman, 1948), in which there is a proportional relationship between copulatory occurrences and reproductive success in males. But because female is the limiting sex, it implies a greater intensity of sexual selection in males due to a strong competition to access a partner, which is thought to drive sexual dimorphism (Darwin, 1871).

On the other hand, the greater investment by females generates a sexual conflict, and shed light on the cost of sex. The latter is even greater in species with separate sexes with what John Maynard Smith (1978) called, the 'cost of males'. The cost of males refers to the cost of producing males that will not invest into their own progeny (at least at the zygote level), while in an asexual population, females invest their energy in producing a 100% of caring daughters. These conflicts, leading to sex differences in parental care for instance, are thought to play a crucial role in the evolution of sexual dimorphism as well (Bedhomme & Chippindale, 2007; R. M. Cox & Calsbeek, 2009).

In fact, it is the combination of both sexual selection and sexual conflicts that mainly drives the evolution of sexual dimorphism, though a few exceptions occur (Bedhomme et al., 2009; Pélissié et al., 2012). For example, in a simultaneous hermaphroditic snail species, *Physa acuta*, there is no sexual dimorphism (except for gametes) although there are signs of sexual selection : i) males have a greater reproductive success than females, ii) males show variance between mating and reproductive

success indicative of a post-copulatory selection, and iii) larger males have a greater reproductive success albeit they have a similar mating success. However, the lack of sexual dimorphism in hermaphroditic species is not surprising as both sexes are present in an individual, which constrains the resolution of sexual conflicts (Abbott, 2011; Bedhomme et al., 2009; Bedhomme & Chippindale, 2007). In fact, while the evolution of anisogamy might be the prelude to the evolution of sexual dimorphism, it is the separation of sexes, i.e., gonochorism or dioecy, that allowed for its exacerbation, fed by the long-standing tug of war between the sexes.

1.2 The reinforcing role of separate sexes, intra-locus and inter-locus sexual conflicts

Sexual dimorphism in species with separate sexes can reach its paroxysm because each sex will tend to reach its own phenotypic optimum. As exemplified by the evolution of anisogamy, many phenotypes have divergent optima between the sexes. For instance, in peacock spiders while "sexy" ornaments increase the chances of access to a mate in males, extravagant colours are disadvantageous in females because it will not increase their reproductive success and it will make them more visible to predators. It is noteworthy that in animals, the mating system (monogamy, polygyny, polyandry or promiscuity) and the sex ratio in a population can change the intensity of sexual selection, which will influence sexual conflicts over traits. For instance, sexual dimorphism tends to decrease with strict monogamy (Alexander et al., 1979; Clutton-Brock, 1985) due to a lower strength of selection i.e., there is no constant competition between males. Nevertheless, traits that maximize the fitness of one sex (usually male), while detrimental to the other (usually females) are under sexually antagonistic selection -the motor of sexual conflicts-, which drives sexual dimorphism (Abbott, 2011; Bedhomme & Chippindale, 2007; R. M. Cox & Calsbeek, 2009; Rowe & Day, 2006).

Sexual conflicts over traits encoded by a same locus, i.e., intra-locus sexual conflict (IASC) are observed when females' optimal expression for an allele differ from males' optimum. Sex-specific selective pressure can induce the evolution of sex-biased or sex-limited gene expression, where each sex moves towards its optimal expression level, which thus reduce, if not solve, IASC (Mank et al., 2008, 2013; Rayner et al., 2019). All things being equal, the evolution of gene differential expression will then drive sexual dimorphism. As a matter of fact, it has even been shown that variations in sex-biased gene expression intensity underpin phenotypic variance (Pointer et al., 2013; Rayner et al., 2019). On that instance, highly differentially expressed genes should correlate with strong sexual dimorphism. In contrast to IASC, inter-locus sexual conflict (IRSC) arises from different loci that interact during male-female encounters, i.e., where one's behaviour can be detrimental for the other's optimal fitness. In nurse sharks for instance, males grasp and harm females with their teeth while mating to ensure copulation, referred as coercive mating (Afonso et al., 2016). Interestingly, females

display behaviours such as staying at the surface with their flank side up, and/or hit the sea surface with their caudal fin, while moving to resist males and prevent mating. Though coercive mating can increase chances of copulation and paternity, it is harmful for females and selection will favour traits in females that resist males. Similarly in water striders, males have claspers they use to maintain females during copulation but which comes at a cost to females (e.g. superfluous mating, physical harassment) (Arnqvist & Rowe, 1995). However, females possess abdominal spines, structures that help counteract males' oppression and decrease mating costs. Hence, IRSC leads to the co-evolution of adaptive and counter-adaptive traits assuring mating in males, and resistance in females.

Taken together, these evolutionary processes modify the genetic architecture of sexual dimorphism, and shape the expression of genes under sexually antagonistic selection and sexual selection. The emergence of anisogamy have settled the basis for the evolution of sexual dimorphism, and the separation of sexes combined with sexual selection and sexual conflicts have opened ways to a great diversity of sexually dimorphic traits. Now, what is the proximate basis of sexual dimorphism ?, which biological and environmental factors are acting behind these evolutionary processes to settle sex differences ? Two factors mediating sexual differentiation will be discussed below: gonadal hormones, which were long thought to be the sole actor in vertebrates, and sex chromosomes, especially when they are highly genetically differentiated. To discuss the relative contribution of these two biological factors, we will thus focus on species with genetic sex determination systems from now on.

2 Proximate causes at the basis of sexual dimorphism

In the term sexual dimorphism underlies a process of sexual differentiation. In plants and 'invertebrates', it is perhaps in insects that sexual differentiation has been the most described. The doublesex (*Dsx*) gene at the basis of sex determination is also the core regulator of sexual differentiation, either directly or through the regulation of other genes (Hopkins & Kopp, 2021). Hormones such as ecdysone are also involved and seem to interact with *Dsx* to influence phenotypes, as illustrated by sex differences in the size of mandibles in beetles, or the lost of wings in female winter moths (Fig 2a,b) (Hopkins & Kopp, 2021; Derks et al., 2015; Niitsu et al., 2014). In plants, it seems that both sex chromosomes and hormones (e.g. auxin) drive sexual dimorphism (Chailakhyan, 1979; Liu et al., 2021; Zemp et al., 2016). In *Silene latifolia* for instance, flower buds are sexually dimorphic, which correlates with an enrichment of genes with a sex-biased expression on the sex chromosomes (Fig. 2c,d) (Zemp et al., 2016) and with an impact of the Y chromosome (Scotti & Delph, 2006). In contrast, in decapods, males are larger than females as a result of hormonal secretions from the male-specific androgenic gland (distinct from testes) (Sagi et al., 1997). Albeit

mechanisms are still not fully understood, both sex chromosomes and hormones can contribute to sex differences. Yet, in vertebrates, for which mechanisms of sexual differentiation have been widely described, the role of sex chromosomes has been considerably neglected at the benefit of an extensive work on gonadal hormones.

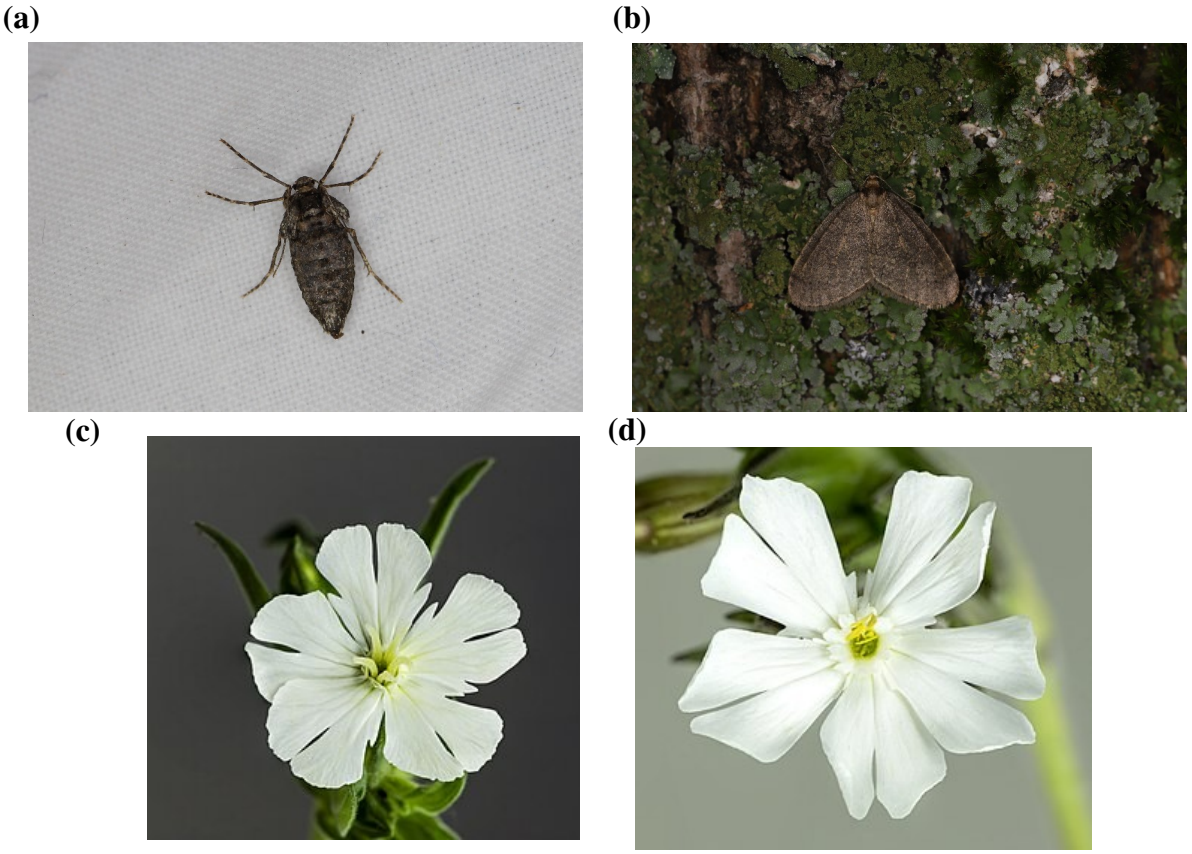

Figure 2. Sexual dimorphism in insects and plants is influenced by sex chromosomes and hormones. (a) In the winter moth *Operophtera brumata,* females (a) have vestigial wings in comparison to males (b).This dimorphism has been suggested to be driven by *Dsx*, although there are evidence for the role of ecdysone, a steroid hormone, in another moth species (Derks et al., 2015; Niitsu et al., 2014) . © Adrien Jailloux. In *Silene latifolia,* flower buds are sexually dimorphic, which is consistent with an enrichment of genes with a sex-biased expression on the sex chromosomes (Zemp et al., 2016). The female is on the left (c) and the male is on the right (d). ©Didier Descouens.

2.1 The standard and hormone-centered view of sexual differentiation in vertebrates

In the standard view of sexual differentiation, genotypic sex or environmental cues (e.g. temperature) determine gonadal sex, and gonads secrete steroid hormones (androgens and estrogens) that will drive the sexual differentiation of non-gonadal tissues (Fig. 3) (Arnold, 2009b, 2017, p. 201; Arnold & Breedlove, 1985; Breedlove et al., 1999). In fact, steroid hormones were long thought to be the sole biological factor at the basis of sexual dimorphism. This paradigm stems from studies on sex differences in brain and behaviours in eutherian mammals, with the decisive input of Phoenix et al's work (1959) on the necessary role of gonadal hormones to shape male or female-typical behaviours.

Following the differentiation of gonads, which starts around 6 weeks in humans, 11.5 days in mice or 6 days in birds (Chue & Smith, 2011; Rey et al., 2000), hormones induce the differentiation of tissues influencing gene expression, cells' development and functions. In fact, two surges of steroid hormones, occurring perinatally and at adutlhood, are critical and essential to drive the differentiation. The former is called the organizational period, where androgen and estrogen set in place the neural circuitry[1] essential for sex typical behaviours, with irreversible effects (Arnold, 2009b; Arnold & Breedlove, 1985; Breedlove et al., 1999; Phoenix et al., 1959). For example, female guinea pigs exposed to testosterone during their fetal development display male-typical mounting behaviours, even after gonadectomy (Phoenix et al., 1959). Since, it has been shown that it is not only testosterone but its aromatization to estradiol[2], that is crucial for the masculinization of brain neural circuits: injection of estradiol during fetal development induces masculinization, like testosterone, while injection of a non aromatizable form of testosterone (dihydrotestosterone) fails to induce the differentiation (see McCarthy, 2008). The organizational period is critical in the sense that it happens early in the ontogeny and is necessary for the display of behaviours impacting the fitness of individuals. During this period, sexual dimorphism mainly involves tissues' differentiation and notably the brain. Later in life, steroid hormones secreted from gonads and adrenal glands activate sex differences in behaviours and morphology, among others. This period is called the 'activational period' where steroid hormones activate neural circuits and subsequent behaviours in a sex-specific manner, with reversible effects. In rats for instance, gonadectomized females do not display lordosis, a back arching behaviour indicative of females' sexual receptivity, but the behaviour is restored after the injection of estradiol and progesterone (Arnold & Breedlove, 1985).

1 Neural circuits are neuronal networks, connections between neurons in regions of the brain underpinning a function, or behaviour.

2 paradoxically, the 'female hormone' which is involved in females' reproductive cycle and behaviours

The action of steroid hormones rely on their binding to androgen (AR) and estrogen (ER) receptors regulating downstream gene expression at the basis of behaviours, as well as other sexually dimorphic traits. This is illustrated by testosterone regulating plumage colouration in male red-backed fairywrens (*Malurus melanocephalus*) (Khalil et al., 2020) or skin chemical signalling in male gartner snakes (Rockwell & Mason, 2014). In some frog species, both testosterone and estradiol regulate colour patterns (Sever & Staub, 2011).

The uncovering of the role of testosterone by Phoenix et al. (1959) has since led to a myriad of studies focusing on steroid hormones only to explain sexual dimorphism. This painted an hormone-based view of sexual differentiation, completely neglecting the role of sex chromosomes. Yet, not all sexually dimorphic phenotypes fit the organizational-activational effects of gonadal hormones. In zebra finches for instance, only male sings, which was thought to be the result of differences in steroid hormones. However, females treated with an estrogen inhibitor early in ontogeny, which induces the development of functional testicular tissues, still do not sing (Wade & Arnold, 1996). This suggests that gonadal hormones are not the primary basis for song dimorphism, but genetic factors might. In addition, it has been shown that sex differences (e.g. gene expression, developmental rate) arise prior the differentiation gonads and thus, before hormones are secreted (Burgoyne et al., 1995; Dewing et al., 2003). On that basis, for the last twenty years, researchers have shed light on the role of sex chromosomes in shaping sexual dimorphism, either directly through the expression of sex-linked genes and regulating the expression of autosomes, or indirectly by influencing hormonal levels. Not to mention the fact that the evolution of sex chromosomes and their pattern of inheritance already made them appealing candidates.

Most of the work on vertebrates comes from mammals and birds, but there are studies supporting a direct influence of sex chromosomes (through sex-linked genes) on sexual differentiation in squamates (Yoshimoto et al., 2010), and in fish (Lindholm & Breden, 2002; Winge, 1922). It has even been shown to influence phenotypic divergences between species in closely related fish species (Kitano et al., 2007; Kitano & Peichel, 2012). In contrast, in amphibians, sexual dimorphism seems to reflect gonadal status, and thus the role of hormones rather than sex chromosomes (Ma et al., 2018; Perrin, 2021).

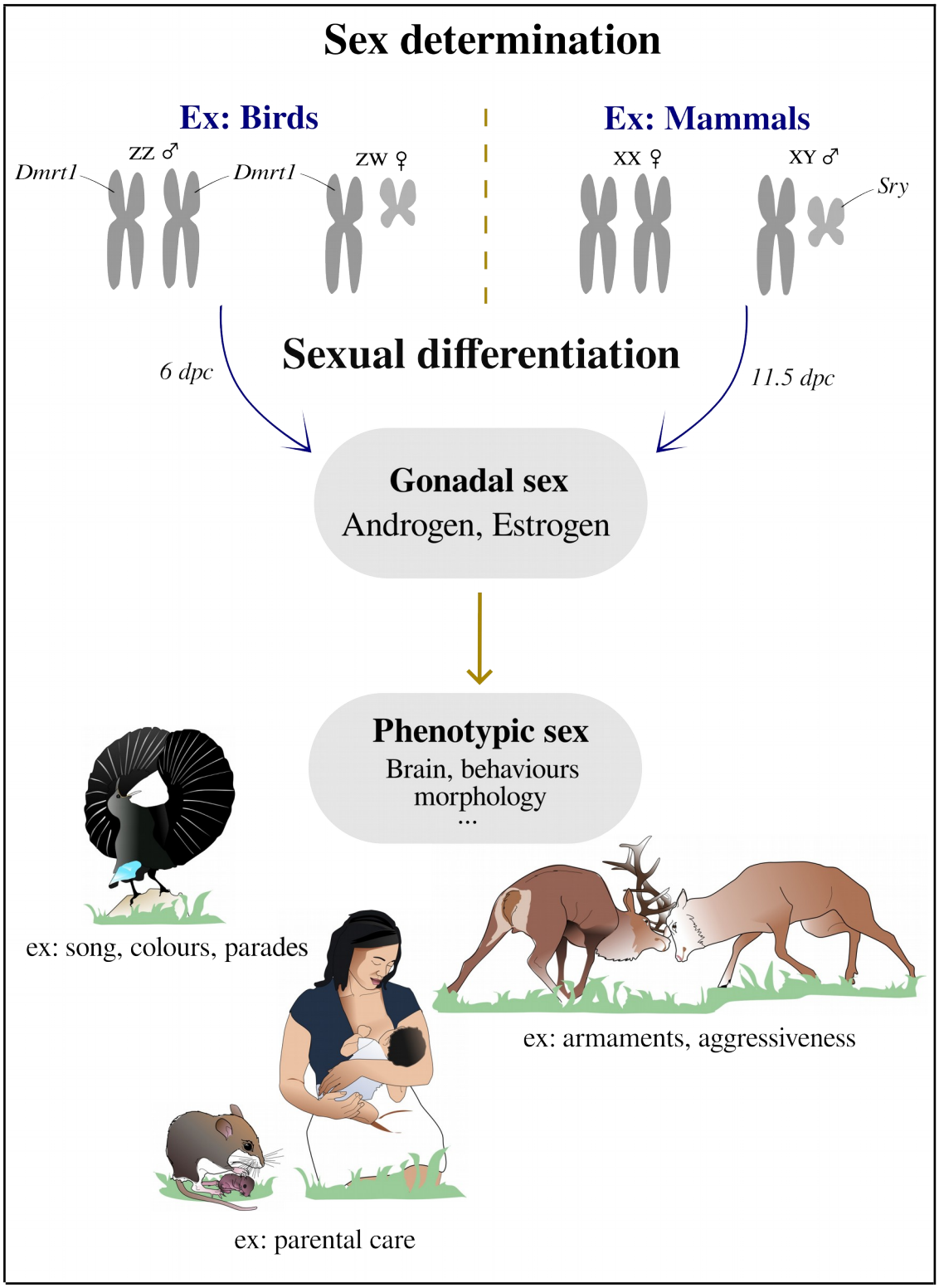

Figure 3. The standard view of sexual differentiation in vertebrates, with the example of birds and mammals. Sex chromosomes[3] and especially a sex determining locus influence the differentiation of gonads (starts ad 6 days *post coitum (dpc)* in birds, 11.5 *dpc* in mammals), which then drive differences in morphology (ornements and armaments), brain and subsequent behaviours (parental care, male-male competition) between the sexes. ©Laurence Meslin

3 Some W chromosome in birds are more similar in size to the Z : reduced size of the W is not a rule of thumb.

2.2 The role of sex chromosomes

2.2.1 Why sex chromosomes ?

In species with a genetic sex determination system involving male heterogamety (XX/XY) or female heterogamety (ZZ/ZW), one chromosome is sex-specific and always at the heterogametic state (Y or W), and the other is present in different copies between the sexes (X and Z chromosomes). These two chromosomes can be highly differentiated, i.e., heteromorphic[4], such as in mammals, or completely homomorphic as in many squamate and amphibian species (Ezaz et al., 2009; Miura, 2017; Vicoso et al., 2013). Although undifferentiated sex chromosomes can participate to sex differences in brain and behaviours (i.e., pleiotropic effects of the sex determining locus), highly differentiated sex chromosomes are expected to be key drivers. In the canonical model of heteromorphic sex chromosomes' evolution, once a sex determining gene evolves, any locus linked to it will decrease in frequency in the sex that do not carry to sex determining allele (Beukeboom & Perrin, 2014a; Bull, 1983; Charlesworth, 1991; Rice, 1987). This linkage is especially advantageous for sexually antagonistic loci, as it increases their chance of being transmitted to the sex they are beneficial to. These loci accumulate on the sex-specific chromosome, and selection should favour the arrest of recombination between them and the sex determining region, hence forming a supergene. In theory, this triggers the progressive arrest of recombination between the X (or Z) and the Y (or W), further accumulation of sexually antagonistic genes, and an enrichment of genes with a sex-biased expression (including sex-limited expression) on the sex chromosomes[5]. We may note that recent models have been developed using neutral processes (accumulation of divergence near the sex determining gene) or by regulatory evolution (silencing of genes with unstable cis-regulatory elements due to divergence), without necessary sexual antagonism, to explain the arrest of recombination and further degeneration of the Y (or W) (Jay et al., 2022; Jeffries et al., 2021; Lenormand et al., 2020). These models predict an impact on gene expression as well, which could also influence sexual dimorphism but with, perhaps, a non adaptive or neutral prospect.

2.2.2 X and Z chromosomes implications

When sex chromosomes are differentiated, dosage compensation evolves to restore the balance of X and Z-linked genes between the sexes. In mammals for instance, the X chromosome is up-regulated in both sexes and one X is inactivated in females so that males and females have equal expression of X-linked genes, and at comparable levels to autosomes (Cooper et al., 1993; Disteche, 2012). In birds, dosage compensation of the Z chromosome seems to occur on a gene-by-gene basis but most

4 Usually, in species with heteromoprhic sex chromosomes, sex determination systems are highly conserved albeit a few exceptions, while many transitions occurs in species with homomorphic sex chromosomes (e.g. Saunders & Veyrunes, 2021; Pokorna & Kratochvil, 2009; Beukeboom & Perrin, 2014).

5 And participate in resolving sexual conflict

importantly, it is incomplete (Mank & Ellegren, 2009; Sigeman et al., 2018). Because the Z chromosome is enriched in genes regulating reproductive functions (Bellott et al., 2010; Disteche, 2012; Sigeman et al., 2018), it is also likely to influence sexual phenotypes. In many other species, such as the platypus (*Ornithorhynchus anatinus*) or the parasitic trematode (*Schistosoma mansoni*), dosage compensation is also incomplete (Cooper et al., 1993; Deakin et al., 2008; Disteche, 2012; Vicoso et al., 2013). Even in mammals, some genes escape inactivation leading to dosage imbalance in sex-linked genes (Berletch et al., 2011, 2015; Disteche, 2012; Fang et al., 2019): ~15% of X-linked genes escape inactivation in humans, and 3-8% in mice (Berletch et al., 2011). Considering that the X chromosome is enriched in neurodevelopmental, cognitive and reproduction-related genes, X-escapees are likely to drive sex differences in brain and behaviours. Experiments on female mice with one X chromosome (Turner syndrome) and males with two or more X chromosomes (Klinefelter syndrome) have shown that X dosage influence the differentiation of neural circuits involved in social behaviours (Arnold et al., 2016; K. H. Cox et al., 2014, 2015). In humans, females with Turner syndrome can be infertile or develop impaired cognitive abilities (Gravholt, 2004), which are thought to reflect haploinsufficiency (i.e., dosage sensitive genes expressed in one copy only). Furthermore, it has been shown that the number of X chromosome influences the expression of hundreds of autosomal genes in mice (Wijchers et al., 2010), likely to contribute to sex differences as well.

Secondly, in mammals, X inactivation can be skewed towards paternal or maternal alleles, referred to as parental imprinting. In humans, females with Turner syndrome expressing the paternal X have a greater intelligence quotient and females expressing the maternal X have higher memory skills (Bishop et al., 2000; Skuse et al., 1997). In genetically modified mouse, females carrying only a maternal X chromosome (X^mO) appear to be less plastic in reversal learning tasks[6] relative to mice expressing the paternal X (X^pO). In birds, there are some evidence for parental imprinting based on studies in chickens, albeit controversial and not on sex chromosomes (Frésard et al., 2013; Tuiskula-Haavisto & Vilkki, 2007, 2007; Wang et al., 2015). All things considered, parental imprinting on the X chromosome is likely to impact sex differences in brain and behaviours.

6 Reversal learning task is a test of cognitive flexibility: individuals must learn to discriminate two conditions and be able to switch they learning when we change the paradigm. For example, a black mark is associate with ‘food rewards’ and a red mark is associated with ‘no reward’. Individuals learn to choose the black mark with the food. Then, we switch the colour associate to the food (i.e., red becomes the ‘reward’ colour) and we measure if individuals reverse their choice or not, and how much time does it take for them to switch and choose the red colour.

2.2.3 Y and W implications

In mammals, the Y chromosome is male specific and its evolution led to a considerable loss of genes, with the remaining being highly specialized in male specific functions (Graves, 2006; Graves & Waters, 2004; Hughes & Page, 2015; Mueller et al., 2013). The Y chromosome lost ~97% of its ancestral content in humans, with ~45 genes remaining[7] (see Graves & Waters, 2004), and in lab mice (2% remaining). In mice though, there has been extensive duplications leading to now 700 protein coding genes present on the Y (Soh et al., 2014). These genes do not have homologs on the X chromosome and some of them are expressed in the brain, where they may contribute to the display of male-specific behaviours (Lahr et al., 1995; Mayer et al., 2000; J. Xu et al., 2002). An interesting example is the sex determining gene, *Sry*, which regulates dopamine levels, a neurotransmitter well known for its implication in the reward system but also influencing sexually dimorphic social behaviours, such as aggression and parental care (e.g. Czech et al., 2012; Dewing et al., 2006; Mahadevia et al., 2021; Scott et al., 2015). In birds, the W chromosome is female-specific and retained between 43%-100% of their ancestral gene content depending on the species, and there is no enrichment in female-biased genes nor in genes with female specific functions (Xu & Zhou, 2020). Therefore, studies do not seem to support a role for the W chromosome, but it might also reflect the fewer number of studies in birds. Indeed, there is a considerable bias towards mammals when it comes to investigate the sexual differentiation of the brain, with the Y chromosome and the sex determining gene whose roles extend further sex determination and the differentiation of gonads.

3 Genetically modified mice to assess sexual differentiation of the brain: a powerful tool but to a certain extent

The brain is fascinating as it controls reproductive phenotypes, from behaviours to some life history traits (e.g. reproductive cycle), which are prime targets of sexual selection and sexually antagonistic selection. As illustrated above, sex differences in brain were long thought to be driven by gonadal hormones only, but there has been increasing evidence for the direct role of sex chromosomes as well. This breakthrough relies on the study of genetically modified rodent species (see Arnold, 2020; Dumas et al., 2000; McCarthy & Arnold, 2011).

A wide range of mouse models have helped identify the impact of sex chromosomes on the sexual differentiation of the brain (see Arnold, 2009a), and disentangle between genetic and hormonal bases of such differences: mice lacking gonads, or mice with turner syndrome, among others. But probably

7 In contrast, the X chromosome kept ~98% of its ancestral content in mammals (Ross et al., 2005)

the most interesting model is the “four core genotype” (FCG) mouse model, which has brought a great leap forward in our knowledge of sexual differentiation (Arnold & Chen, 2009; De Vries et al., 2002).

The FCG model is based on the deletion of the *Sry* gene from the Y chromosome (Y⁻) and the insertion of a *Sry* transgene on an autosome (De Vries et al., 2002). XY⁻ individuals, with the deletion of *Sry,* develop as females, and individuals with both the deletion and the transgene (XY⁻*Sry*) develop as males. Hence, mating an XY⁻ female with an XY⁻*Sry* male produces offspring with four possible sex chromosome complements : XX, XY⁻, XX*Sry* and XY⁻*Sry*. The two former are females and the two latter are males. The power of this system, is that it allows to disentangle the effect of sex chromosomes from gonadal hormones (both organizational and activational effects), by controlling hormonal levels. For instance, the activational effect of hormones can be removed by gonadectomy, or by gonadectomy and equal injection of gonadal hormones. In that case, differences in phenotype can be attributed to genotypic or gonadal sex (organizational effect). The FCG and other mouse models have shown that gonadal sex is the main factor influencing brain and behaviours (e.g., investigation of conspecifics, cortical thickness), but the sex chromosome complement can also influence a few social behaviours (e.g. maternal behaviours, aggression) and many phenotypes related to human diseases (e.g. Alzheimer’s) (reviewed in Arnold, 2020a; Arnold & Chen, 2009).

Yet, the FCG and other mouse models have some limitations and probably one major issue is that a genetically modified model will never replace a natural system shaped by natural and sexual selection. Furthermore, they may not encompass the complexity of interactions between endocrine, genetic and environmental factors. This is emphasized by a fixed[8] genetic background which may have a profound impact on phenotypic responses (Barthold, 2004; Bućan & Abel, 2002; Lipp & Wolfer, 1998, 2003). In addition, genetic modifications may have pleiotropic effects, which can blur signals and interpretations as illustrated by a lower fertility of individuals when compared to wild types (e.g. Vasudevan et al., 2010). On that instance, species with naturally occurring sex reversal, with transitions in sex determination systems, or with bizarre sex chromosomes could bring strong insight into the proximate bases of sex differences in brain and behaviours, while considering the evolutionary processes behind.

In mammals, although sex determination is highly conserved, there are a dozen of rodent species that escape from the rule (see Saunders & Veyrunes, 2021). Some species have lost the Y chromosome, such as in the transcaucasian mole voles (*Ellobius lutescens*) where males and females are both X0/X0.

8 Not completely as genetic drift will induce variation

In others, females carry a Y chromosome, and it is notably the case of the fascinating African pygmy mouse, *Mus minutoides.*

4 The African pygmy mouse

The African pygmy mouse is a wild mouse species and one of the smallest mammals on earth, with an average length of 6 cm and an average weight of 8g (Fig. 4). Although most of this species' ecology is unknown, its distribution extends throughout sub-Saharan Africa and in a wide range of habitats (e.g. forest, grasslands, steppes and deserts) (Veyrunes et al., 2004). *Mus minutoides* belongs to the subgenus *Nannomys,* in which there are 19 species with similar morphologies but which experienced extensive chromosomal rearrangement between and within species (Musser & Carleton, 1993): there have been multiple robertsonian translocations between autosomes, as well as between autosomes and sex chromosomes (Britton-Davidian et al., 2012; Veyrunes et al., 2004, 2007; Veyrunes et al., 2010a; Veyrunes et al., 2014). Consequently, the *Nannomys* group shows a great diversity of karyotypes such as a 2n=36 karyotype in *M. mattheyi* and a 2n=18 to 34 karyotype in *M. minutoides*. However, the most striking chromosomal evolution concerns sex chromosomes in *M. triton* and *M. minutoides.* The former species lost the Y and one X chromosome, i.e., males and females are X0, with a still unknown sex determining locus (Jotterand-Bellomo, 1988). In *M. minutoides*, there are three sex chromosomes (X, X* and Y), multiple neo-sex chromosomes (neo-X, neo-X* and neo-Y) and two sex determining loci (i.e., *Sry* and an unknown mutation on the X* chromosome at the origin of a sex reversal) (Veyrunes, et al., 2010b).

(a)

(b)

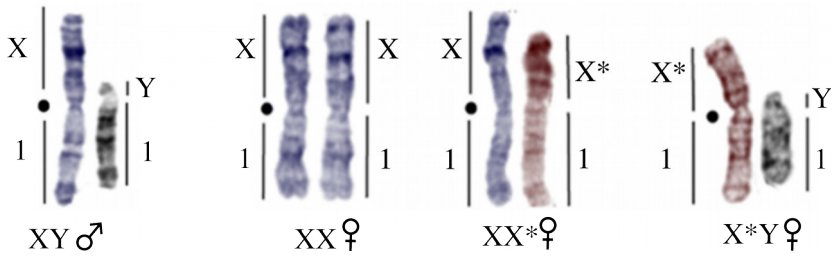

Figure 4. The African pygmy mouse. (a) *Mus minutoides*. © Quentin Martinez. (b) sex and neo-sex chromosomes in the four genotypes : XY, XX, XX* and X*Y from left to right. All sex chromosomes are fused to autosome 1 : neo-X, neo-X* and neo-Y chromosomes except in one population where there has been further chromosomal rearrangement (a whole arm reciprocal translocation) between the neo-X* and a pair of fused autosomes (autosomes 13 and 16; see Veyrunes et al., 2007). Adapted from Veyrunes et al., 2010b.

In *M. minutoides,* the X* chromosome originates from a mutation on the X about 0.9 million years ago (Veyrunes et al., 2013) and overrides the effect of *Sry* by inducing sex reversal in X*Y individuals. Hence, there are four genotypes in natural populations : the classic XX female and XY male genotypes, as well as two new female genotypes, XX* and X*Y. Cytogenomic studies have shown considerable rearrangements between the X and the X* with distinct G-banding patterns, differences in chromosome length (the X is larger than the X*) and with signs of inversions as well as ampliconic sequences (unpublished data). Though the mutation itself is still unknown, expression patterns of key genes during fetal development suggest that the sex reversal mutation involves a gene that act extremely early in the sex determining cascade (close to the *Sry/Sox9* gene network, the two genes at the top of the cascade[9]).

One of the main hypothesis for the emergence of the X* chromosome is a response to a male meiotic drive and the preferential transmission of the Y chromosome leading to a male-biased sex-ratio in populations (Saunders et al., 2022). In breeding conditions, the sex ratio is balanced at the population level but, interestingly, it is not balanced looking at litters of each female genotype specifically. Depending on with whom the male is mating, there is a conditional sex-ratio in the progeny. For instance, if the male mates with a XX female, the Y is preferentially transmitted (mechanisms are still unknown) and 80% of the offspring are males (Saunders et al., 2022). Similarly, males transmit more the Y chromosome when they mate with XX* females, but only 37% of the offspring are males due to the feminizing effect of the X* chromosome. Finally, if a male mates with a X*Y female, the X is preferentially transmitted leading to a slightly biased female sex ratio as well (58% of the progeny are females). While these data support a role for a meiotic drive in the emergence of the X*, it does not explain its maintenance considering the costs due to a XY genotype in a female environment.

In mammals, sex reversal with XY females is detrimental with usually sterile phenotypes, owing to the loss of YY embryos and meiotic disruptions (Lavery et al., 2011; Sakashita et al., 2019). In *M. minutoides*, sex-reversed X*Y females are fully fertile. Previous histology investigations showed similar adult ovarian tissues between the three female genotypes and the absence of testicular tissues in X*Y females (Rahmoun et al., 2014). In addition, ovaries are functional but most surprisingly, X*Y females even have a greater reproductive success than XX and XX* females: they have an early sexual maturity, a greater ovulation rate and bigger litter sizes, which all indicate a greater reproductive output throughout their lifetime breeding period (Saunders et al., 2014). All things being equal, the greater reproductive success of X*Y females is the main hypothesis to explain the maintenance of the system considering the expected associated costs.

9 *Sry* is expressed in females but not *Sox9.*

More interestingly, when you look at behaviours or performance, X*Y females considerably differ from the other females and they even show some male-typical traits. For instance, X*Y females display reduced anxiety-related behaviours as found in males, enhanced territorial aggression and have a greater bite strength in contrast to XX and XX* (Ginot et al., 2017; Saunders et al., 2016). Taken together, the dichotomy between the complete gonad feminization and the display of masculinized traits suggest that sex chromosomes impact the sexual differentiation of the brain in the African pygmy mouse, either directly through sex-linked genes' expression or by regulating autosomal expression, or indirectly through the control of hormonal levels.

5 Research questions

In this thesis, I aimed to investigate consequences of the emergence of the X* chromosome on the sexual differentiation of the brain in the African pygmy mouse, and to reconsider the underestimated role of sex chromosomes in shaping sex differences in brain and behaviours. I was thus interested in the proximate bases (hormonal and genetic) of sexual phenotypes and to clarify these points, I encompassed an integrative framework combining behaviours, neurobiology and transcriptomic analyses.

I first investigated the consequences of sex reversal on two highly sexually dimorphic behaviours in mammals : parental care and territorial aggression, which both have decisive impact on individuals' fitness. For parental care, I was interested on maternal investment specifically, as well as their underlying neural circuits. Two sides are addressed here : maternal behaviours and lactation. For territorial aggression, a previous study had already shown differences in behaviours between female genotypes. Therefore, I investigated whether territorial aggression in X*Y females reflects differences in hormonal levels or the expression of sex-linked genes, to disentangle the role of both factors.

Because the expression of phenotypes correlates with gene expression, I assessed, in a second part, the consequences of sex reversal on the whole brain transcriptome of individuals. This part not only aimed to evaluate the consequences of sex reversal on the brain genetic architecture but also to identify potential candidate genes at the basis of sexual phenotypes.

Finally, the evolution of sex chromosomes can involve sexual antagonism but also degeneration, which could also impact phenotypes. In this last section, I was interested in the evolution of gene expression on sex and neo-sex chromosomes to identify patterns of degeneration. I focused on another organ (the

kidney) but parallels are made with the brain and unfortunately, liver data were unusable. This is a small part of a side project about sex and neo-sex chromosomes' evolution.

I was also involved in a paper focusing on gonadal hormones, which can bring support to the first part on maternal behaviours and territorial aggression. This paper can be found in Annexe.

Part 1: Social and parental behaviours

Chapter 1

Genotypic sex shapes maternal care in the African pygmy mouse, *Mus minutoides*

Heitzmann, L., Challe, M., Perez, J., Castell, L., Galibert, E., Martin, A., Valjent, E., and Veyrunes, F. (2022). Genotypic sex shapes maternal care in the African Pygmy mouse, Mus minutoides. BioRxiv. https://doi.org/10.1101/2022.04.05.487174

Recommended by PCI : https://doi.org/10.24072/pci.evolbiol.100152

bioRxiv preprint doi: https://doi.org/10.1101/2022.04.05.487174; this version posted September 16, 2022. The copyright holder for this preprint (which was not certified by peer review) is the author/funder, who has granted bioRxiv a license to display the preprint in perpetuity. It is made available under aCC-BY-NC-ND 4.0 International license.

Genotypic sex shapes maternal care in the African Pygmy mouse, *Mus minutoides*

Louise D. Heitzmann[1], Marie Challe[1], Julie Perez[1], Laia Castell[2], Evelyne Galibert[2], Agnès Martin[2], Emmanuel Valjent[2] & Frédéric Veyrunes[1]

[1] Institut des Sciences de l'Evolution de Montpellier, Université de Montpellier, CNRS, France

[2] Institut de Génomique Fonctionnelle, Université de Montpellier, CNRS, INSERM, Montpellier, France

abstract

Sexually dimorphic behaviours, such as parental care, have long been thought to be driven mostly, if not exclusively, by gonadal hormones. In the past two decades, a few studies have challenged this view, highlighting the direct influence of the sex chromosome complement (XX vs XY or ZZ vs ZW). The African pygmy mouse, *Mus minutoides*, is a wild mouse species with naturally occurring XY sex reversal induced by a third, feminizing X* chromosome, leading to three female genotypes: XX, XX* and X*Y. Here, we show that sex reversal in X*Y females shapes a divergent maternal care strategy from both XX and XX* females, rather than altering care quality. In addition, we show that sex reversal may also impact the dopaminergic system in the anteroventral periventricular nucleus of the hypothalamus, consistent with one component of maternal care: pup retrieval. Combining behavioural ecology and neurobiology in a rodent subject to natural selection, we evaluate potential candidates for the neural basis of maternal behaviours and strengthen the underestimated role of the sex chromosomes in shaping sex differences in brain and behaviours. All things considered, we further highlight the emergence of a third sexual phenotype, challenging the binary view of phenotypic sexes.

Keywords: Maternal care, natural sex reversal, third sexual phenotype

bioRxiv preprint doi: https://doi.org/10.1101/2022.04.05.487174; this version posted September 16, 2022. The copyright holder for this preprint (which was not certified by peer review) is the author/funder, who has granted bioRxiv a license to display the preprint in perpetuity. It is made available under aCC-BY-NC-ND 4.0 International license.

Introduction

Parental care, though not universal across the animal kingdom, is fundamental in many species for offspring' survival and thus, reproductive success. In mammals, parental care is skewed towards females with an obligatory lactation and greater investments, making it one of the most sexually dimorphic behaviour (see Royle et al., 2012). Male care for offspring is rare (5-10% of mammalian species), mainly observed in monogamous species and always associated with biparental care (Clutton-Brock, 1991; Lukas & Clutton-Brock, 2013). On a proximate scale, this dimorphism as well as other sexually dimorphic traits, was long thought to be a product of gonadal steroid hormones only, acting to shape brain neural circuits (Arnold & Gorski, 1984; Breedlove et al., 1999). In the past two decades, several studies have challenged this view, providing increasing evidence for the direct role of the sex chromosome complement (XX or XY) on sexually dimorphic phenotypes (Arnold, 2004; Gatewood et al., 2006; Mank, 2009; Ngun et al., 2011; Skuse, 2006; Rice, 1984). More precisely, genetically modified mice have allowed to dissociate individuals' gonadal and genotypic sexes such as in the four core genotypes (FCG) model, where the *Sry* gene has been deleted and translocated on an autosome (XX and XY$^-$ females, XX*Sry* and XY$^-$*Sry* males) (see Arnold, 2020). These advances have been crucial to decipher the direct role of both hormones and sex chromosomes on social behaviours (De Vries et al., 2002; Gatewood et al., 2006; Kopsida et al., 2013; Ngun et al., 2014; Skuse, 2006). However, very few studies have examined how sex chromosomes shape parental care and underlying brain neural circuits (Gatewood et al., 2006).

In rodents for instance, males tend to have more cell bodies and greater fiber densities of vasopressin expressing neurons, a neuropeptide involved in crouching over the pups or maternal aggression among others, likely to result from an imbalance in X chromosome number between the sexes (Crenshaw et al., 1992; De Vries & Miller, 1998; De Vries et al.,

bioRxiv preprint doi: https://doi.org/10.1101/2022.04.05.487174; this version posted September 16, 2022. The copyright holder for this preprint (which was not certified by peer review) is the author/funder, who has granted bioRxiv a license to display the preprint in perpetuity. It is made available under aCC-BY-NC-ND 4.0 International license.

2002; Gatewood et al., 2006; Bosch & Neumann, 2012; Cox et al., 2015; Miller et al., 1989;Rood et al., 2008; Rood et al., 2013). Closely related to vasopressin, oxytocin is another substantial neuropeptide for parental care, well-known for its involvement in lactation, but also for enhancing pup retrieval and maternal aggression in females (Gimpl & Fahrenholz, 2001; Pedersen et al., 2006; Okabe et al., 2017; Scott et al., 2015; Bosch & Neumann, 2012). However, the impact of the sex chromosome complement on oxytocin in a parental context in the FCG or other mouse model has never been investigated. While the FCG has been a breakthrough in pointing out the value of the sex complement on parental behaviours, the common view of the system is far from complete considering the complexity of parenting behaviours as well as the various underlying neural pathways. Additionally, studies have only focused on genetically modified animals so far -which may have some limitations (e.g. absence of Sry in XY- females)-, where naturally occurring sex reversal systems subject to natural selection could bring insightful information especially in terms of brain and behaviours' evolution.

In natura, a handful of rodent species display atypical sex determination systems with loss of the Y chromosome in males, or females carrying a Y chromosome (Saunders & Veyrunes, 2021). Among them, the African pygmy mouse, *Mus minutoides*, is peculiarly interesting: a third sex chromosome, called X*, has evolved from a mutation on the X chromosome, and induces sex reversal of X*Y individuals (Veyrunes et al., 2010a). Thus, there are three distinct female genotypes in populations, XX, XX* and X*Y, while all males are XY . Sex-reversed X*Y females are fully fertile (Rahmoun et al., 2014), and have a higher reproductive success than XX and XX* females in laboratory conditions (Saunders et al., 2014). In addition, when compared to XX and XX* females, X*Y females are more aggressive towards intruders, display reduced anxiety, similar to that of males, and have a greater bite force, also comparable to males (Saunders et al., 2016; Ginot et al., 2017).

bioRxiv preprint doi: https://doi.org/10.1101/2022.04.05.487174; this version posted September 16, 2022. The copyright holder for this preprint (which was not certified by peer review) is the author/funder, who has granted bioRxiv a license to display the preprint in perpetuity. It is made available under aCC-BY-NC-ND 4.0 International license.

These male-typical behaviours observed in X*Y individuals, which are unlikely to be testosterone dependant (Veyrunes et al., 2022), suggest that the Y chromosome and/or dosage imbalance in X chromosomes masculinize some neural circuits in the brain of *M. minutoides*. The highly contrasted phenotypes between female genotypes thus represent a tremendous opportunity to understand the neural bases of sexually dimorphic behaviours. Furthermore, the dissociation of gonadal and genotypic sexes makes the African pygmy mouse a key species to investigate the effect of sex chromosomes on sex differences in brain and behaviours. In this study, we used an integrative approach to investigate the effect of genotypic sex on maternal care in *M. minutoides,* from behaviours to candidate brain neural circuits (Fig. 1). Because we show, here, that sex reversal in *M. minutoides* influences pup retrieval, maternal aggression, and nest building behaviours, we focused neural investigations on neurons expressing oxytocin and vasopressin in the paraventricular nucleus of the hypothalamus (PVN), a region and neuropeptides regulating these behaviours (Bendesky et al., 2017, Pedersen et al., 2006; Okabe et al., 2017; Scott et al., 2015; Bosch & Neumann, 2012). Since oxytocin neurons in the PVN are modulated by dopamine neurons in the anteroventral periventricular nucleus of the hypothalamus (AVPV) (Scott et al., 2015) and that dopamine levels can be positively correlated with *Sry* expression in the brain (Milsted et al., 2004; Dewing et al., 2006; Rosenfeld, 2017), we also investigated neurons expressing tyrosine hydroxylase (Th), the rate limiting enzyme for dopamine synthesis, in the AVPV. According to maternal behaviours and the link between sex chromosomes and vasopressin or Th expression in the brain, we expected a greater number of oxytocin, vasopressin and Th expressing neurons in the PVN and AVPV of X*Y females, respectively.

Material & Methods

Animals, genotype identification and study environment

bioRxiv preprint doi: https://doi.org/10.1101/2022.04.05.487174; this version posted September 16, 2022. The copyright holder for this preprint (which was not certified by peer review) is the author/funder, who has granted bioRxiv a license to display the preprint in perpetuity. It is made available under aCC-BY-NC-ND 4.0 International license.

Behavioural experiments were conducted in accordance with European guidelines and with the approval of the French Ethical Committee on animal care and use (No. CEEA-LR-12170) in our laboratory colony (CECEMA facilities of Montpellier University) established from wild-caught animals from Caledon Nature Reserve (South Africa). Approximately 24 generations of mice were bred in our colony. Individuals are reared in large (38 L x 26 W x 24 H cm) or medium cages (31 L x 21 W x 21 H cm) filled with woodchips' bedding, in a room held at 23 °C and with a 15:9 h light-dark cycle. They are supplied with food (mixed bird seeds) and water *ad libitum.* At weaning (i.e., six weeks post-parturition), virgin females are housed in groups of 5-6 in large cages. In our study, either females remained virgins or they were paired with a male at 2-10 months old in a medium cage for breeding and subsequent behavioural assays. Female genotype was identified whether by PCR of *Sry* using total genomic DNA extracted from tail tip biopsies with DNeasy blood and tissue kit (Qiagen) and following Veyrunes et al. (2010a) protocol or by karyotyping using bone marrow of yeast-stimulated individuals as previously described (Veyrunes et al., 2010b). We included X*Y and XX* females which were both littermated of either XX* or X*Y females, and XX females that were littermated of XX or XX* females.

Behavioural assays

We tested primiparous females (i.e. first litter) aged 5.5 months old on average. Tests were conducted during the day, between 10.00 am and 6.30 pm, by an experimenter blind to females' genotype. Each assay was filmed for subsequent analysis, with the exception of the parental care strategy test, which was scored by one-off observations in the cage. When individuals were assessed in more than one assay, we conducted experiments sequentially by increasing magnitude of stress: we first tested females for pup retrieval, followed by mother-pup interactions and then, nest building, with a 15 hours gap at least

bioRxiv preprint doi: https://doi.org/10.1101/2022.04.05.487174; this version posted September 16, 2022. The copyright holder for this preprint (which was not certified by peer review) is the author/funder, who has granted bioRxiv a license to display the preprint in perpetuity. It is made available under aCC-BY-NC-ND 4.0 International license.

between each test. Behavioural data were analysed blindly regarding females' genotype, using Observer v5.0.31 and Observer XT softwares (Noldus).

Pup retrieval experiments were carried out in home cage between 2-10 days post-parturition (dpp). The father and mother were removed while pup(s) (i.e., whole litter) were placed at the opposite corner of the shelter with the nest. An assay started once the female was put back under the shelter and recorded until the first pup was retrieved to account for litter size differences. If no pup had been retrieved within 10 minutes, the assay was ended. A total of 101 females (31 XX, 35 XX* & 35 X*Y) were assessed on both first approach latency and retrieval probability.

Mother-pup interactions experiments were carried out in a new cage (38 x 26 x 24 cm) filled with the individuals' own bedding. We tested females between 2-10 dpp. We placed only one pup at the centre of the cage to account for litter size differences between females. We then placed the mother at a corner of the cage and recorded grooming, crouching and carrying behavioural responses during 10 minutes. We assessed 75 females (25 per genotype) on whether they displace/carry their pup, as well as on duration of grooming, huddling and crouching behaviours.

Nesting tests were performed in home cage, early evening and nest were scored in the following morning after 12 hours of experimentation for 90 females (34 X*Y, 27 XX and 29 XX*). Females were tested between 2-10 dpp. The father was removed from the cage as well as food, water, and all environmental enrichments except bedding. We added one nestlet (5x5 cm of compressed cellulose; Serlab, D00009) to provide nesting materials. Individuals received the same nestlet prior to experiment (post-parturition) for habituation. Nest scoring was assessed from 0 to 5 according to Gaskill *et al.* (2013) graduation: 0-

bioRxiv preprint doi: https://doi.org/10.1101/2022.04.05.487174; this version posted September 16, 2022. The copyright holder for this preprint (which was not certified by peer review) is the author/funder, who has granted bioRxiv a license to display the preprint in perpetuity. It is made available under aCC-BY-NC-ND 4.0 International license.

cellulose unused and no nest, 1- no nest site, 2- flat nest, 3- slightly curved nest, 4- nest with walls, 5- fully enclosed nest. We scored the nest accordingly to the graduation above but with more flexibility allowing intermediary scores as well (e.g. 3.5 or 4.5). We also recorded the percentage of nestlet used by females as they do not necessarily use it to build the nest (i.e., they can use their bedding).

Parental care strategy, or whether mice display biparental care *versus* maternal care only, was investigated for 105 females (29 XX, 37 X*Y and 39 XX*) in home cage. We assessed strategies by characterizing fathers' involvement with pup(s), the latter reflecting females' behaviour towards them (i.e., fathers included or excluded from parental care). We made repeated one-off observations of their position in the cage and possible physical injuries, from birth to 14 dpp (before pup(s) start(s) to explore outside the shelter) and every 2-3 days. We rated fathers' involvement gradually and increasingly, from 1 to 6: 1= father killed or removed for severe injuries, 2= chased, with aggression stigmata, 3= always in a different lodge, not tolerated in the shelter with the pup(s), 4= tolerated inside the shelter but in the opposite corner, 5= under the same shelter, next to the mother and 6= paternal care observed: huddling, carrying, crouching. Score measurements were not repeated if the father was killed or removed (i.e., score 1 or 2, referred to as high level of maternal aggression).

Immunohistochemistry

We sampled virgin individuals only as no experimentations leading to death can be made on mothers. Eighteen virgin mice (3-5 per genotype including males as a control group) were euthanised with isoflurane 4% anaesthesia followed by decapitation. Brains were collected in 4% PFA and stored for at least 48 hours at 4°C. Brains were sliced at 30 µm using a vibratome (Leica Microsystems) and coronal sections were collected into a PBS-

bioRxiv preprint doi: https://doi.org/10.1101/2022.04.05.487174; this version posted September 16, 2022. The copyright holder for this preprint (which was not certified by peer review) is the author/funder, who has granted bioRxiv a license to display the preprint in perpetuity. It is made available under aCC-BY-NC-ND 4.0 International license.

filled container. Floating brain slices were then put in 4x3 well plates (4 wells per individual) and washed three times with Phosphate Buffer Saline (PBS) before staining. We sliced and stained the whole brain to account for any potential divergence from *M. musculus* in the brain anatomy (no data were available on the brain of *M. minutoides*). Brain slices were first incubated for 24h at 4°C or two hours at room temperature (RT) with a Goat coupled Fab anti-mouse IgG blocking buffer (1:1000, Abliance) diluted in PBS with 0.1% Triton 100X (PBS.T) and ~1% BSA to prevent nonspecific binding. Then, slices were incubated for 24-48h at 4°C with mouse anti-Neurophysin I (1:2000, Merck Millipore, marker for Oxytocin), rabbit anti-vasopressin (1:1000, Immunostar) and sheep anti-Th (1:1000, abcam) diluted in PBS.T and BSA, followed by secondary antibodies : Cy3 coupled Donkey anti-mouse IgG antibody (1:1000, Jackson Laboratories), Cy5 coupled Donkey anti-rabbit IgG (1:1000,Jackson Laboratories) and A488 coupled Donkey anti-sheep IgG (1:1000,Jackson Laboratories) diluted in PBS.T and BSA, for 24-48 hours at 4°C. Slices were finally incubated for 3-6 minutes with DAPI (1:10 000, Invitrogen) diluted in PBS and mounted on Polysine® Slides stored at 4°C until imaging.

Imaging and cell counts

Brain slices including the PVN and AVPV were identified based on the mouse brain atlas from Franklin and Paxinos (2001). Selected slices were processed with a scanner (Zeiss Axioscan) or confocal microscopy (Zeiss, LSM 780) and cell counts were done blindly and manually on imageJ, for entire nuclei. We also quantified neurons on a few brain slices using Imaris v9.8 software to compare with manual counts (only for oxytocin as the software did not perform well for vasopressin neurons). Oxytocin and vasopressin cell counts as well as their distribution across the whole PVN nucleus were investigated to account for potential differences in localization between genotypes.

bioRxiv preprint doi: https://doi.org/10.1101/2022.04.05.487174; this version posted September 16, 2022. The copyright holder for this preprint (which was not certified by peer review) is the author/funder, who has granted bioRxiv a license to display the preprint in perpetuity. It is made available under aCC-BY-NC-ND 4.0 International license.

208 Statistical analysis

209 All statistical analyses were conducted on R v4.1.2 (R Core Team, 2021) using *lme4,*
210 *stanarm, ordinal* and *multgee* packages. Pup retrieval was investigated with bayesian
211 (generalized) linear mixed models, incorporating individuals' age as a random effect on the
212 intercept. We fit our models to assess retrieval probability and visit latency using a
213 log(x+1)-transformation to correct for a right-skewed distribution (many latencies at 600s).
214 We ran four Markov chains of 2000 iterations each, removed the first 1000 (warm-up) and
215 kept the second half to estimate our parameters. Both our models checked convergence
216 recommendations ($\hat{R}$<1.1). Post-hoc comparisons were made using *emmeans* package to
217 contrast each genotype. Point estimates reported per genotype are medians (back
218 transformed from the log (x+1) scale) and median-based contrasts with 89% Highest
219 Posterior Density intervals (HPD) excluding one were considered as truly different. Mother-
220 pup interactions were also analysed with Bayesian (generalized) linear mixed models with
221 individuals' age as a random effect and following the same steps as stated above. We
222 log(x+1)-transformed duration responses to correct for a left-skewed distribution (many
223 durations at 0s) and post-hoc comparisons were made to contrast genotypes. Nesting
224 scores were analysed with a cumulative logit model (clm) and probabilities for nest quality
225 per genotype were retrieved accordingly. XX was set as the reference group and we made
226 multiple pairwise comparisons (*emmeans*) with adjusted p-value to assess each genotype
227 effect. Parental care strategy was assessed with a population-averaged ordinal model to
228 account for repeated measures and possible correlation between observations using the
229 ordLORgee() function from *multgee* package (Touloumis, 2015). Probabilities were then
230 retrieved using a back-transformation of parameters estimation according to a cumulative
231 logit link. Cell counts for immunostaining assays were analysed using the non-parametric
232 Kruskal Wallis test for multiple group comparisons.

233

bioRxiv preprint doi: https://doi.org/10.1101/2022.04.05.487174; this version posted September 16, 2022. The copyright holder for this preprint (which was not certified by peer review) is the author/funder, who has granted bioRxiv a license to display the preprint in perpetuity. It is made available under aCC-BY-NC-ND 4.0 International license.

Results

Higher retrieval efficiency in X*Y females

During pup retrieval experiments, X*Y females approached their pup(s) significantly faster than XX and XX* females (Fig. 2a, Fig. S1, table S1), with a median visit latency at 51.7s [33.6-73.8 89% HPD] versus 156.5s [94.5-223.3 89% HPD] for XX and 112s [71.5-158.6 89% HPD] for XX* females. Interestingly, 35.5 % of XX females did not visit their pup(s) while only 17.1% of XX* females and 11.4% of X*Y did not respond (table S2). To confirm that differences were not driven by the absence of response, we reanalysed latencies only on females visiting their pup(s), and we found the same results (Fig S2). Additionally, X*Y females were significantly more likely to retrieve their pup(s) when compared to XX and XX* females, with an estimated retrieval probability of 0.87 [0.77, 0.95 89% HPD], while XX and XX* had a respective probability of 0.47 [0.32, 0.63 89% HPD] and 0.55 [0.42, 0.70 89% HPD] only (Fig. 2b, tableS1). Hence, X*Y females are more efficient at pup retrieval than XX and XX* females.

Poor nest quality in X*Y females

All females showed nesting behaviours as no nest score below 3 was recorded. However, X*Y females were more likely to build poor nest quality in contrast to both XX (Fig. 2c, z= -3.09, p=0.006) and XX* females (z=-4.61, p< 0.001). They had a probability of 0.35 (highest probability) for building a slightly curved nest (i.e. score 3) while they had a 0.17 probability, for making a fully enclosed nest (i.e. score 5). Conversely, XX and especially XX* individuals were more likely to build high quality nests, with a respective probability of 0.47 and 0.71 for a fully enclosed nest. This also indicates a relatively high consistency in nest-building behaviour for XX* females. Though XX* had a higher probability than XX individuals for building high quality nests, they show similar behavioural trends (Fig. 2c, z= -1.82, p= 0.16). Interestingly, most X*Y females did not use the nestlet to build a nest (88.2

bioRxiv preprint doi: https://doi.org/10.1101/2022.04.05.487174; this version posted September 16, 2022. The copyright holder for this preprint (which was not certified by peer review) is the author/funder, who has granted bioRxiv a license to display the preprint in perpetuity. It is made available under aCC-BY-NC-ND 4.0 International license.

%) in contrast to 48.1 % for XX and 41.4% for XX*. We therefore tested for a relationship between nest quality and nestlet usage (i.e. disinterest for the nestlet or poor learning) in X*Y females and did not find any correlation (χ^2 =10.05, p=0.19). X*Y females are thus less efficient at nest building when compared to XX and XX* females.

Genotypic sex does not impact mother-pup interactions

Most females interacted with their pup and there were no significant differences in interaction durations nor probabilities (table S3, Fig. S3-4). X*Y, XX and XX* females spent in median 7.9s [3.07-13.2 89% HPD], 11.2s [4.65-18.8 89% HPD] and 15.9s [7.03-25.8 89% HPD] crouching over the pup, 7.17s [3.48-11.36 89% HPD], 4.96s [2.26-7.97 89% HPD] and 7.30s [3.58-11.64 89% HPD] huddling with the pup, 3.18s [1.36-4.99 89% HPD], 4.87s [8.49-7.46 89% HPD] and 5.79s [2.89-8.70 89% HPD] grooming the pup, respectively. In addition, they had respective probabilities of 0.68 [0.42-0.9 89% HPD], 0.76 [0.5-0.93 89% HPD] and 0.67 [0.4-0.87 89% HPD] to displace their pup.

Genotypic sex influences female parental strategy

X*Y females were on average more likely to show maternal aggression than XX and XX* females, which inversely, were more likely to be involved in biparental care (Fig. 2d, X*Y vs XX, z=-2.81, p=0.005; X*Y vs XX*, z=-2.87, p=0.004). Indeed, X*Y females had a highest probability at 0.33 to severely aggress or kill males (i.e., score 1) in contrast to a 0.19 probability to display biparental care (i.e., score 6). Inversely, XX and XX* females had highest probabilities at 0.46 and 0.43 respectively for biparental care in comparison to 0.12 and 0.13 probabilities for maternal aggression. Strikingly, XX and XX* females' curves almost overlay with quite similar probabilities in each category highlighting identical parental care strategy in XX and XX* females.

Hypothalamic neural circuits of maternal care

bioRxiv preprint doi: https://doi.org/10.1101/2022.04.05.487174; this version posted September 16, 2022. The copyright holder for this preprint (which was not certified by peer review) is the author/funder, who has granted bioRxiv a license to display the preprint in perpetuity. It is made available under aCC-BY-NC-ND 4.0 International license.

We did not find evidence for difference in the global neuroanatomy of *M. minutoides* PVN in comparison to *M. musculus* (Gimpl & Fahrenholz, 2001; Franklin & Paxinos, 2001; Madrigal & Jurado, 2021). Vasopressin is expressed in both parvo- and magnocellular neurons, mostly in intermediate regions of the PVN where it is expressed dorsolaterally (Fig. S5, S7-S10) and oxytocin is mostly expressed in magnocellular neurons and more homogeneously across the nucleus than vasopressin (midline and rostro-caudal axis; Fig. S6-S10). We did not have enough power to statistically compare oxytocin and vasopressin neuron distributions across genotypes but there were no overall striking differences (Fig. S5-S6), with high variabilities in count data due to inter-individual variability and small sample sizes. In addition, there were no differences in oxytocin neurons number between genotypes (Fig. 3a,c-S6, $\chi^2 = 0.89$, $p= 0.83$). We did not find differences in the number of vasopressin expressing neurons either (Fig. 3b,c, $\chi^2=0.82$, $p= 0.84$) but there is a tendency for lower number in X*Y females driven mostly by the lower number of vasopressin neurons in anterior regions (Fig. S5). Finally, there were no differences in the neuroanatomy of the AVPV in comparison to *M. musculus* (Franklin & Paxinos, 2001; Simerly et al., , 1985; Semaan & Kauffman, 2010). Since there is evidence for a sexual dimorphism in the nucleus size in *M. musculus* (Bleier et al., 1982; Semaan & Kauffman, 2010), we weighted the number of Th expressing neurons by the area of the nucleus and did not find differences in the density of Th neurons between genotypes ($\chi^2=2$, $p= 0.57$), though a tendency for a greater density in X*Y females (Fig. 4).

Discussion

The African pygmy mouse is a species with a naturally occurring sex reversal system, involving a dissociation between phenotypic and genotypic sexes in X*Y females. This fascinating system represents a great opportunity to shed light on the impact of the sex chromosomes on sexually dimorphic behaviours such as parental care. By focusing on

bioRxiv preprint doi: https://doi.org/10.1101/2022.04.05.487174; this version posted September 16, 2022. The copyright holder for this preprint (which was not certified by peer review) is the author/funder, who has granted bioRxiv a license to display the preprint in perpetuity. It is made available under aCC-BY-NC-ND 4.0 International license.

maternal phenotypes specifically, we show that sex reversal in *M. minutoides* influences pup retrieval, maternal aggression, nest building behaviours and may also impact the maternal dopaminergic circuit in the AVPV nucleus. Our study confirms and further extends evidence on the influence of the sex chromosome complement on parental behaviours and brings promising prospects for its impact on the neurobiology of parenting.

X*Y females are more efficient at pup retrieval than both XX and XX* females. They first approached their pup faster and showed more consistent retrieval, while XX and XX* showed delayed latencies to first approach and retrieve their pup about one out of two times. Moreover, in a reproductive context, X*Y mothers were highly aggressive towards males, whereas XX and XX* females were more likely to share parental care. Previous results showed that non-reproductive X*Y females are more aggressive than other female genotypes towards intruder males (Saunders et al., 2016). Here, we show this enhanced aggressiveness further extends towards the pup's own father (as male partners were killed or needed to be removed for 43.2% of X*Y females (i.e., 16 out of 37)), suggesting that X*Y females are more likely to be solitary mothers. Furthermore, X*Y females built poor quality nests (slightly curved), while XX and especially XX* females performed better with fully enclosed nests. It was surprising that almost all X*Y females did not use the nestlet, and the lack of correlation between nestlet usage and nest quality strongly suggests a disinterest for the nestlet in X*Y females. Because nest building is an essential component of maternal care especially in altricial species, to protect the young from potential threats for instance, this would thus suggest maladaptation in X*Y females. However, we show here that X*Y females can assure pups protection through agonistic behaviours (i.e. maternal aggression), which might thus make the nest quality less essential for these females. Hence, the divergent behavioural patterns between X*Y and XX / XX* females reflect two distinct maternal strategies shaped by the sex chromosome complement in *M.*

bioRxiv preprint doi: https://doi.org/10.1101/2022.04.05.487174; this version posted September 16, 2022. The copyright holder for this preprint (which was not certified by peer review) is the author/funder, who has granted bioRxiv a license to display the preprint in perpetuity. It is made available under aCC-BY-NC-ND 4.0 International license.

minutoides. Although there is an unequivocal effect of the sex chromosome complement on some maternal behaviours, there were no differences in mother-pup interactions suggesting that it does not modulate all component of maternal care.

It is very striking that X*Y females displayed -quite consistently-, divergent maternal behaviours from XX and XX* females: they showed a greater retrieval efficiency, high level of maternal aggression but also poor nesting skills as found in males suggesting masculinization (data not shown; Topilko et al., 2022). Interestingly, this pattern of co-occurrence of both feminized and masculinized traits in *M. minutoides* X*Y females was already found in previous studies. While X*Y females have functional ovaries and show moreover, a greater reproductive success than both XX and XX* females (e.g. higher ovulation rate, bigger litter sizes) (Rahmoun et al., 2014; Saunders et al., 2014), they also display male-like reduced anxiety behaviours, they are more aggressive, and have a greater bite strength than XX and XX* females (Saunders et al., 2016; Ginot et al., 2017). All things considered, the constant divergence between X*Y on one side and XX and XX* females on the other side highlights that the association of a feminizing X* and a male-specific Y chromosome has given birth to a third sexual phenotype in the African pygmy mouse.

The differences of maternal care behaviours between female genotypes raise questions concerning the genetic bases of maternal strategies in *M. minutoides.* Several hypotheses are discussed here. First, the divergent behaviours of the X*Y females suggest an influence of the Y chromosome and one prime candidate among this gene-poor chromosome is *Sry*, which is expressed in the brain of X*Y females (Rahmoun et al., 2014). Secondly, there could also be an influence of the female specific X* chromosome. However, since XX* females behave like XX females, this would imply maternal X*-biased

bioRxiv preprint doi: https://doi.org/10.1101/2022.04.05.487174; this version posted September 16, 2022. The copyright holder for this preprint (which was not certified by peer review) is the author/funder, who has granted bioRxiv a license to display the preprint in perpetuity. It is made available under aCC-BY-NC-ND 4.0 International license.

chromosome inactivation (X*CI), or parental imprinting of X-linked genes (Gregg et al., 2010; Raefski & O'Neil, 2005), with preferential expression of the paternal X alleles. There is no evidence for skewed X*CI in *M. minutoides* based on cytological investigations of embryos fibroblast cell cultures (Veyrunes & Perez, 2018), but next generation sequencing technologies with a special focus on allele-specific expression in the brain would be necessary to confirm or refute this finding, and therefore help clarify hypotheses. Thirdly, another hypothesis to correlate with divergent maternal strategies is X dosage (i.e., copy number of X chromosomes). In mice, a thousands of autosomal genes are under the influence of X dosage (Wijchers et al., 2010) such as vasopressin, involved in nesting behaviours (Bendesky et al., 2017; De Vries et al., 2002; Gatewood et al., 2006; Cox et al., 2015). In addition, a few X-linked genes, such as Kdm6a involved in gene expression regulation, escape inactivation in mice and have also been suggested to influence sexual phenotypes (3-8%; Tsuchiya & Willard, 2000; Ngun et al., 2014; Arnold, 2020). Finally, on might also suppose an epistasis interaction between the X* and the Y chromosome. In *Drosophila melanogaster* for instance, it has been shown that a few X-linked genes involved in pheromone detection are regulated by the Y chromosome, which is likely to impact reproductive phenotypes (Jiang et al., 2010). Interestingly, some of our behavioural observations are in contradiction with previous findings on the FCG, which may give insight into the genetic bases. Contrary to X*Y females in *M. minutoides*, sex-reversed XY-females in the FCG displayed similar nesting behaviours to XX females but impaired retrieval capabilities: they retrieved less pups and belatedly when compared to XX females (Gatewood et al., 2006). Considering nest building, because the authors controlled for gonadal hormones, this suggested that the *Sry* gene and/or male gonadal hormones acting perinatally to masculinize brain neural circuits, were responsible for the poor nesting skills in males (Gatewood et al., 2006). In our case, X*Y females built poor quality nests while they do not have differences in gonadal/adrenal hormonal levels compared to the

bioRxiv preprint doi: https://doi.org/10.1101/2022.04.05.487174; this version posted September 16, 2022. The copyright holder for this preprint (which was not certified by peer review) is the author/funder, who has granted bioRxiv a license to display the preprint in perpetuity. It is made available under aCC-BY-NC-ND 4.0 International license.

391 other female genotypes (testosterone and estradiol; Veyrunes et al., 2022) but they do
392 express *Sry* in their brain (Rahmoun et al., 2014). Therefore, *Sry* may also influence
393 nesting behaviours in the African pygmy mouse. Considering pup retrieval, results in the
394 FCG suggested that the Y chromosome and/or X dosage imbalance was necessary to
395 alter retrieval phenotypes. Here, we show that X*Y females perform better at pup retrieval
396 even though they have one copy of the X* chromosome, a Y chromosome, and express
397 *Sry* in their brain (Rahmoun et al., 2014). Therefore, either Y-linked genes including *Sry*
398 act distinctly on neural pathways between FCG mice and this wild mouse species, either it
399 is an X* chromosome effect or an epistasis interaction between the X* and the Y
400 chromosome. Although the genetic bases with the relative part of X, X* and Y
401 chromosomes in driving these divergent maternal behaviours requires further
402 investigations, our results show that sex reversal in the African pygmy mouse does not
403 seem to alter maternal care quality, contrary to expectations based on the FCG. This
404 discrepancy further illustrates the need to consider not only genetically modified laboratory
405 mice but also non-model species with alternative phenotypes shaped by natural selection -
406 such as observed in *M. minutoides*-, to better understand the genetic and neural bases of
407 behaviours.
408
409 In mammals, oxytocin and vasopressin are crucial neuropeptides that intervene in the
410 initiation and maintenance of parental care (Zilkha et al., 2017). In rodents, oxytocin
411 expression in the PVN induces pup retrieval and maternal aggression (Neumann et al.,
412 2005 ; Pedersen et al., 2006; Scott et al., 2015; Okabe et al., 2017; Bosch & Neumann,
413 2012) while vasopressin, which can also mediate maternal aggression, has been shown to
414 inhibit nest building (Bendesky et al., 2017; Bosch & Neumann, 2012). Moreover,
415 vasopressin has been shown to be influenced by X chromosome number, with greater
416 expression in individuals with a single X chromosome (De Vries et al., 2002; Gatewood et

bioRxiv preprint doi: https://doi.org/10.1101/2022.04.05.487174; this version posted September 16, 2022. The copyright holder for this preprint (which was not certified by peer review) is the author/funder, who has granted bioRxiv a license to display the preprint in perpetuity. It is made available under aCC-BY-NC-ND 4.0 International license.

al., 2006, Cox et al., 2015). Hence, oxytocin and vasopressin were prime candidates to explain the divergent maternal behaviours in *M. minutoides*, and a greater number of vasopressin and oxytocin neurons in the PVN of X*Y females in comparison to XX and XX* females could have been expected (Fig. 1). However, we did not find such differences between females nor with males, emphasized by high variability in count data (i.e. indicative of low power; Fig. 3a,b). The lack of differences in oxytocinergic and vasopressinergic systems global anatomy in the PVN suggests no differences in oxytocin and vasopressin levels. Nonetheless, larger sample sizes and the functionality of the neuroendocrine networks as well as the hormonal output should be tested to confirm or refute this hypothesis (e.g. quantification of gene and protein expression in the PVN, blood hormonal levels measured over time) (Cox et al., 2015; Scott et al., 2015; Bendesky et al., 2017). In addition, we tested virgin females while parental neural circuits are known to evolve with sexual experience (Lopatina et al., 2011; Scott et al., 2015; Okabe et al., 2017; Zilkha, Scott & Kimchi, 2017). It is thus likely that differences in oxytocin and/or vasopressin between females arise at first pregnancy.

Another interesting brain region to look at was the AVPV. It has been shown that neurons expressing Tyrosine hydroxylase (Th) in the AVPV ($AVPV^{Th}$) stimulate oxytocin expressing neurons in the PVN and consequently pup retrieval in females (Scott et al., 2015). Moreover, these neurons are sexually dimorphic with a greater number in females than males already in virgin individuals (Semaan & Kauffman, 2010; Scott et al., 2015). Our results do not support the sexual dimorphism described in *M. musculus*, however we show a tendency for a greater density of Th neurons in X*Y females, which is also supported by preliminary results on Th mRNA expression levels (RNAseq and RT-qPCR) in the whole brain of *M. minutoides* (unpublished data), as well as with the link between *Sry* and Th (Milsted et al., 2004; Dewing et al., 2006; Rosenfeld, 2017). Therefore, the tendency for Th may also be consistent with pup retrieval results. Though not significant, it brings new

bioRxiv preprint doi: https://doi.org/10.1101/2022.04.05.487174; this version posted September 16, 2022. The copyright holder for this preprint (which was not certified by peer review) is the author/funder, who has granted bioRxiv a license to display the preprint in perpetuity. It is made available under aCC-BY-NC-ND 4.0 International license.

443 perspectives on the link between sex chromosomes and the dopaminergic system as well
444 as between dopamine and parenting.
445 Finally, it is noteworthy that parenting is a complex behaviour that is regulated by diverse
446 neural pathways and neuromodulators. In rats for instance, it has been shown that
447 overexpression of the neuropeptide Y, which is sexually dimorphic, correlates with
448 impaired nesting behaviours (Nahvi & Sabban, 2020 ; Corder et al., 2020). It is thus not
449 unlikely that the sex chromosome complements in *M. minutoides* act on various neural
450 circuits to shape maternal behaviours, and future studies should integrate other brain
451 regions and neuromodulators, to help understand the neural basis of maternal strategies.
452 Because we work on a wild non-model species, we are facing interpretation issues due to
453 small sample sizes, the use of virgin individuals, and technical limitations (stereotaxic
454 surgery has never been performed on this species), which restrain the establishment of a
455 causal link between brain nucleus, peptides and behaviours. Nonetheless, primary
456 investigations on the neuroanatomy are essential to describe and further understand the
457 evolution of the brain and behaviours as illustrated here in a wild species with highly
458 contrasted phenotypes.
459
460 Combining behavioural ecology and the neuroanatomy of parenting, we highlight the
461 emergence of a third sexual phenotype in a wild species. While the relative impact of each
462 sex chromosome on maternal behaviours is yet to be determined, our results bring exciting
463 advances to research on both the neural basis and the impact of the sex chromosomes on
464 natural behaviours. Furthermore, research on multiple sexual phenotypes in other wild
465 species with unusual sex determination system as described here, in the African pygmy
466 mouse, could help strengthen the challenge of rethinking the stereotypical dichotomous
467 view of sexes.

468 **Acknowledgements**

bioRxiv preprint doi: https://doi.org/10.1101/2022.04.05.487174; this version posted September 16, 2022. The copyright holder for this preprint (which was not certified by peer review) is the author/funder, who has granted bioRxiv a license to display the preprint in perpetuity. It is made available under aCC-BY-NC-ND 4.0 International license.

We thank Dr Paul Saunders for insightful comments, advices, and review on the manuscript; Dr Stanislav Cherepanov for oxytocin antibody and insight on the study ; Anne Guillou for interesting discussions on the study and the model. We thank Caroline Hu, Marion Anne-Lise Picard and an anonymous reviewer for fruitful reviews and comments on the manuscript. We thank the animal breeding facility of the University of Montpellier (CECEMA), the imaging facility MRI and Laurence Meslin for the illustration.This work was supported by the French National Research Agency (ANR grant SEXREV 18-CE02-0018-01).

References

Arnold AP. 2004. Sex chromosomes and brain gender. Nat. Rev. Neurosci. **5**, 701–708. (doi:10.1038/nrn1494)

Arnold AP, Gorski RA. 1984. Gonadal steroid induction of structural sex differences in the central nervous system. Annu. Rev. Neurosci. **7**, 413–442. (doi:10.1146/annurev.ne.07.030184.002213)

Arnold AP. 2020. Four Core Genotypes and XY* mouse models: Update on impact on SABV research. Neurosci. Biobehav. Rev. **119**, 1–8. (doi:10.1016/j.neubiorev.2020.09.021)

Bendesky A, Kwon YM, Lassance JM, Lewarch CL, Yao S, Peterson BK, He MX, Dulac C, Hoekstra HE. 2017. The genetic basis of parental care evolution in monogamous mice. Nature **544**, 434–439. (doi:10.1038/nature22074)

Bleier, R., Byne, W., and Siggelkow, I. 1982. Cytoarchitectonic Sexual Dimorphisms of the Medial Preoptic and Anterior Hypothalamic Areas in Guinea Pig, Rat, Hamster, and Mouse. J. Comp. Neurol. **212**, 118-130

Bosch OJ, Meddle SL, Beiderbeck DI, Douglas AJ, Neumann ID. 2005. Brain oxytocin correlates with maternal aggression: link to anxiety. J. Neurosci. **25**, 6807–6815. (doi:10.1523/JNEUROSCI.1342-05.2005)

Bosch OJ, Neumann ID. 2012. Both oxytocin and vasopressin are mediators of maternal care and aggression in rodents: From central release to sites of action. Horm. Behav. **61**, 293–303. (doi:10.1016/j.yhbeh.2011.11.002)

Breedlove, S.M., Cooke, B.M., and Jordan, C.L. 1999. The Orthodox View of Brain Sexual Differentiation. Brain. Behav. Evol. **54**, 8–14.

Clutton-Brock TH. 1991. The Evolution of Parental Care. Princeton University Press.

Corder KM, Li Q, Cortes MA, Bartley AF, Davis TR, Dobrunz LE. 2020. Overexpression of neuropeptide Y decreases responsiveness to neuropeptide Y. Neuropeptides **79**, 101979. (doi:10.1016/j.npep.2019.101979)

Cox KH, Quinnies KM, Eschendroeder A, Didrick PM, Eugster EA, Rissman EF, Rissman EF. 2015 Number of X-chromosome genes influences social behavior and vasopressin gene expression in mice. Psychoneuroendocrinology **51**, 271–281. (doi:10.1016/j.psyneuen.2014.10.010)

bioRxiv preprint doi: https://doi.org/10.1101/2022.04.05.487174; this version posted September 16, 2022. The copyright holder for this preprint (which was not certified by peer review) is the author/funder, who has granted bioRxiv a license to display the preprint in perpetuity. It is made available under aCC-BY-NC-ND 4.0 International license.

Crenshaw, B.J., de Vries, G.J., and Yahr, P. 1992. Vasopressin innervation of sexually dimorphic structures of the gerbil forebrain under various hormonal conditions. J. Comp. Neurol. **322**, 589–598.

De Vries GJ, Miller MA. 1998. Anatomy and function of extrahypothalarnic vasopressin systems in the brain. Prog. Brain Res. **119**, 3–20.

De Vries GJ et al. 2002. A model system for study of sex chromosome effects on sexually dimorphic neural and behavioral traits. J. Neurosci. **22**, 9005–9014. (doi:10.1523/JNEUROSCI.22-20-09005.2002)

Dewing, P., Chiang, C.W.K., Sinchak, K., Sim, H., Fernagut, P.O., Kelly, S., Chesselet, M.F., Micevych, P.E., Albrecht, K.H., Harley, V.R., et al. 2006. Direct regulation of adult brain function by the male-specific factor SRY. Curr. Biol. **16**, 415–420. (doi:10.1016/j.cub.2006.01.017)

Gaskill BN, Karas AZ, Garner JP, Pritchett-Corning KR. 2013. Nest Building as an Indicator of Health and Welfare in Laboratory Mice. J. Vis. Exp. **82**, e51012. (doi:10.3791/51012)

Gatewood JD, Wills A, Shetty S, Xu J, Arnold AP, Burgoyne PS, Rissman EF. 2006. Sex chromosome complement and gonadal sex influence aggressive and parental behaviors in mice. J. Neurosci. **26**, 2335–2342. (doi:10.1523/JNEUROSCI.3743-05.2006)

Gimpl G, Fahrenholz F. 2001. The oxytocin receptor system: Structure, function, and regulation. Physiol. Rev. **81**, 629–683. (doi:10.1152/physrev.2001.81.2.629)

Ginot S, Claude J, Perez J, Veyrunes F. 2017. Sex reversal induces size and performance differences among females of the African pygmy mouse, Mus minutoides. J. Exp. Biol. **220**, 1947–1951. (doi:10.1242/JEB.157552)

Gregg C, Zhang J, Butler JE, Haig D, Dulac C. 2010. Sex-Specific Parent-of-Origin Allelic expression in the Mouse Brain. Science. **329**, 682–685.

Kopsida, E., Lynn, P.M., Humby, T., Wilkinson, L.S., and Davies, W. 2013. Dissociable Effects of Sry and Sex Chromosome Complement on Activity, Feeding and Anxiety-Related Behaviours in Mice. PLoS One **8**, 1–15.

Lopatina O, Inzhutova A, Pichugina YA, Okamoto H, Salmina AB, Higashida H. 2011. Reproductive Experience Affects Parental Retrieval Behaviour Associated with Increased Plasma Oxytocin Levels in Wild-Type and Cd38-Knockout Mice. J. Neuroendocrinol. **23**, 1125–1133. (doi:10.1111/J.1365-2826.2011.02136.X)

Lukas D, Clutton-Brock TH. 2013. The evolution of social monogamy in mammals. Science. **341**, 526–530. (doi:10.1126/SCIENCE.1238677)

Mank JE. 2009. Sex chromosomes and the evolution of sexual dimorphism: Lessons from the genome. Am. Nat. **173**, 141–150. (doi:10.1086/595754)

bioRxiv preprint doi: https://doi.org/10.1101/2022.04.05.487174; this version posted September 16, 2022. The copyright holder for this preprint (which was not certified by peer review) is the author/funder, who has granted bioRxiv a license to display the preprint in perpetuity. It is made available under aCC-BY-NC-ND 4.0 International license.

549 Miller, M.A., Vician, L., Clifton, D.K., and Dorsa, D.M. 1989. Sex differences in vasopressin
550 neurons in the bed nucleus of the stria terminalis by in situ hybridization. Peptides
551 **10**, 615–619.

552 Milsted, A., Serova, L., Sabban, E.L., Dunphy, G., Turner, M.E., and Ely, D.L. 2004.
553 Regulation of tyrosine hydroxylase gene transcription by Sry. Neurosci. Lett. **369**,
554 203–207. (doi:10.1016/j.neulet.2004.07.052)
555
556 Nahvi RJ, Sabban EL. 2020. Sex differences in the neuropeptide Y system and
557 implications for stress related disorders. Biomolecules **10**, 1–21.
558 (doi:10.3390/BIOM10091248)

559 Ngun TC et al. 2014. Feminized behavior and brain gene expression in a novel mouse
560 model of Klinefelter Syndrome. Arch. Sex. Behav. **43**, 1043–1057.
561 (doi:10.1007/s10508-014-0316-0)

562 Ngun TC, Ghahramani N, Sánchez FJ, Bocklandt S, Vilain E. 2011. The genetics of sex
563 differences in brain and behavior. Front. Neuroendocrinol. **32**, 227–246.
564 (doi:10.1016/j.yfrne.2010.10.001)

565 Okabe S et al. 2017. Pup exposure facilitates retrieving behavior via the oxytocin neural
566 system in female mice. Psychoneuroendocrinology **79**, 20–30.
567 (doi:10.1016/j.psyneuen.2017.01.036)

568 Paxinos G, Franklin KBJ. 2001. The mouse brain in stereotaxic coordinates. Elsevier.

569 Pedersen CA, Vadlamudi S V, Boccia ML, Amico JA, Pedersen CA. 2006. Maternal
570 behavior deficits in nulliparous oxytocin knockout mice. Genes, Brain Behav. **5**, 274–
571 281. (doi:10.1111/j.1601-183X.2005.00162.x)

572 Pilar Madrigal, M., and Jurado, S. 2021. Specification of oxytocinergic and
573 vasopressinergic circuits in the developing mouse brain. Commun. Biol. **4**, 586.
574 (doi:10.1038/s42003-021-02110-4)
575
576 R core Team. 2021. R: A Language and Environment for Statistical Computing.

577 Raefski AS, O'Neill MJ. 2005. Identification of a cluster of X-linked imprinted genes in
578 mice. Nat. Genet. **37**, 620–624. (doi:10.1038/ng1567)

579 Rahmoun M, Perez J, Saunders PA, Boizet-Bonhoure B, Wilhelm D, Poulat F, Veyrunes F.
580 2014. Anatomical and molecular analyses of XY ovaries from the african pygmy
581 mouse Mus minutoides. Sex. Dev. **8**, 356–363. (doi:10.1159/000368664)

582 Rice, W.R. 1984. Sex Chromosomes and the Evolution of Sexual Dimorphism. Evolution
583 **38**, 735–742.

584 Rood BD, Murray EK, Laroche J, Yang MK, Blaustein JD, De Vries GJ. 2008. Absence of
585 progestin receptors alters distribution of vasopressin fibers but not sexual
586 differentiation of vasopressin system in mice. Neuroscience **154**, 911–321.
587 (doi:10.1016/J.NEUROSCIENCE.2008.03.087)

bioRxiv preprint doi: https://doi.org/10.1101/2022.04.05.487174; this version posted September 16, 2022. The copyright holder for this preprint (which was not certified by peer review) is the author/funder, who has granted bioRxiv a license to display the preprint in perpetuity. It is made available under aCC-BY-NC-ND 4.0 International license.

588 Rood B., Stott RT, You S, Smith CJW, Woodbury ME, De Vries GJ. 2013. Site of Origin of
589 and Sex Differences in the Vasopressin Innervation of the Mouse (Mus musculus)
590 Brain. J. Comp. Neurol. **521**, 2321–2358. (doi:10.1002/cne.23288)

591 Rosenfeld, C.S. 2017. Brain sexual differentiation and requirement of SRY: Why or Why
592 Not? Front. Neurosci. **11**, 1–14. (doi:10.3389/fnins.2017.00632)
593
594 Royle NJ, Smiseth PT, Kölliker M. 2012. The Evolution of Parental Care. Oxford University
595 Press. (doi:10.1093/ACPROF:OSO/9780199692576.001.0001)

596 Saunders, P.A., Perez, J., Rahmoun, M., Ronce, O., Crochet, P.A., and Veyrunes, F. 2014.
597 XY Females do better than the XX in the African PYGMY mouse, MUS minutoides.
598 Evolution **68**, 2119–2127.

599 Saunders PA, Franco T, Sottas C, Maurice T, Ganem G, Veyrunes F. 2016. Masculinised
600 Behaviour of XY Females in a Mammal with Naturally Occuring Sex Reversal. Sci.
601 Rep. **6**, 1–9. (doi:10.1038/srep22881)

602 Saunders PA, Veyrunes F. 2021. Unusual Mammalian Sex Determination Systems: A
603 Cabinet of Curiosities. Genes. **12**, 1770. (doi:10.3390/GENES12111770)

604 Scott N, Prigge M, Yizhar O, Kimchi T. 2015. A sexually dimorphic hypothalamic circuit
605 controls maternal care and oxytocin secretion. Nature **525**, 519–522.
606 (doi:10.1038/nature15378)

607 Semaan SJ, Kauffman AS. 2010. Sexual Differentiation and Development of Forebrain
608 Reproductive Circuits. Curr. Opin. Neurobiol. **20**, 424–431.
609 (doi:10.1016/J.CONB.2010.04.004)

610 Simerly, R.B., Swanson, L.W., Handa, R.J., and Gorski, R.A. 1985. Influence of perinatal
611 androgen on the sexually dimorphic distribution of tyrosine hydroxylase-
612 immunoreactive cells and fibers in the anteroventral periventricular nucleus of the
613 rat. Neuroendocrinology **40**, 501–510. (doi:10.1159/000124122)
614
615 Skuse DH. 2006. Sexual dimorphism in cognition and behaviour: The role of X-linked
616 genes. Eur. J. Endocrinol. **155**, 99–106. (doi:10.1530/eje.1.02263)

617 Topilko T, Diaz SL, Pacheco CM, Deleuze C, Gaspar P, Renier N. 2022. Edinger-Westphal
618 peptidergic neurons enable maternal preparatory nesting. Neuron **110**, 1–15.
619 (doi:10.1016/j.neuron.2022.01.012)

620 Touloumis A. 2015. R package multgee: A generalized estimating equations solver for
621 multinomial responses. J. Stat. Softw. **64**, 1–14. (doi:10.18637/jss.v064.i08)

622 Tsuchiya, K.D., and Willard, H.F. 2000. Chromosomal domains and escape from X
623 inactivation: comparative X inactivation analysis in mouse and human. Mamm.
624 Genome **11**, 849–854. (doi:10.1007/s003350010175)
625
626 Veyrunes F, Chevret P, Catalan J, Castiglia R, Watson J, Dobigny G, Robinson TJ, Britton-
627 Davidian J. 2010a. A novel sex determination system in a close relative of the house
628 mouse. Proc. R. Soc. B Biol. Sci. **277**, 1049–1056. (doi:10.1098/rspb.2009.1925)

bioRxiv preprint doi: https://doi.org/10.1101/2022.04.05.487174; this version posted September 16, 2022. The copyright holder for this preprint (which was not certified by peer review) is the author/funder, who has granted bioRxiv a license to display the preprint in perpetuity. It is made available under aCC-BY-NC-ND 4.0 International license.

629 Veyrunes F, Catalan J, Tatard C, Cellier-Holzem E, Watson J, Chevret P, Robinson TJ,
630 Britton-Davidian J. 2010b. Mitochondrial and chromosomal insights into karyotypic
631 evolution of the pygmy mouse, Mus minutoides, in South Africa. Chromosom. Res.
632 **18**, 563–574. (doi:10.1007/s10577-010-9144-9)

633 Veyrunes F, Perez J. 2018. X inactivation in a mammal species with three sex
634 chromosomes. Chromosoma **127**, 261–267. (doi:10.1007/s00412-017-0657-2)

635 Veyrunes, F., Perez, J., Heitzmann, L.D., Saunders, P. A., Givalois, L. 2022. Separating
636 the effects of sex hormones and sex chromosomes on behavior in the African pygmy
637 mouse *Mus minutoides,* a species with XY female sex reversal. *bioRxiv*
638 https://doi.org/10.1101/2022.07.11.499546

639 Zilkha N, Scott N, Kimchi T. 2017. Sexual Dimorphism of Parental Care: From Genes to
640 Behavior. Annu. Rev. Neurosci. **40**, 273–305. (doi:10.1146/annurev-neuro-072116-
641 031447)

bioRxiv preprint doi: https://doi.org/10.1101/2022.04.05.487174; this version posted September 16, 2022. The copyright holder for this preprint (which was not certified by peer review) is the author/funder, who has granted bioRxiv a license to display the preprint in perpetuity. It is made available under aCC-BY-NC-ND 4.0 International license.

Figures

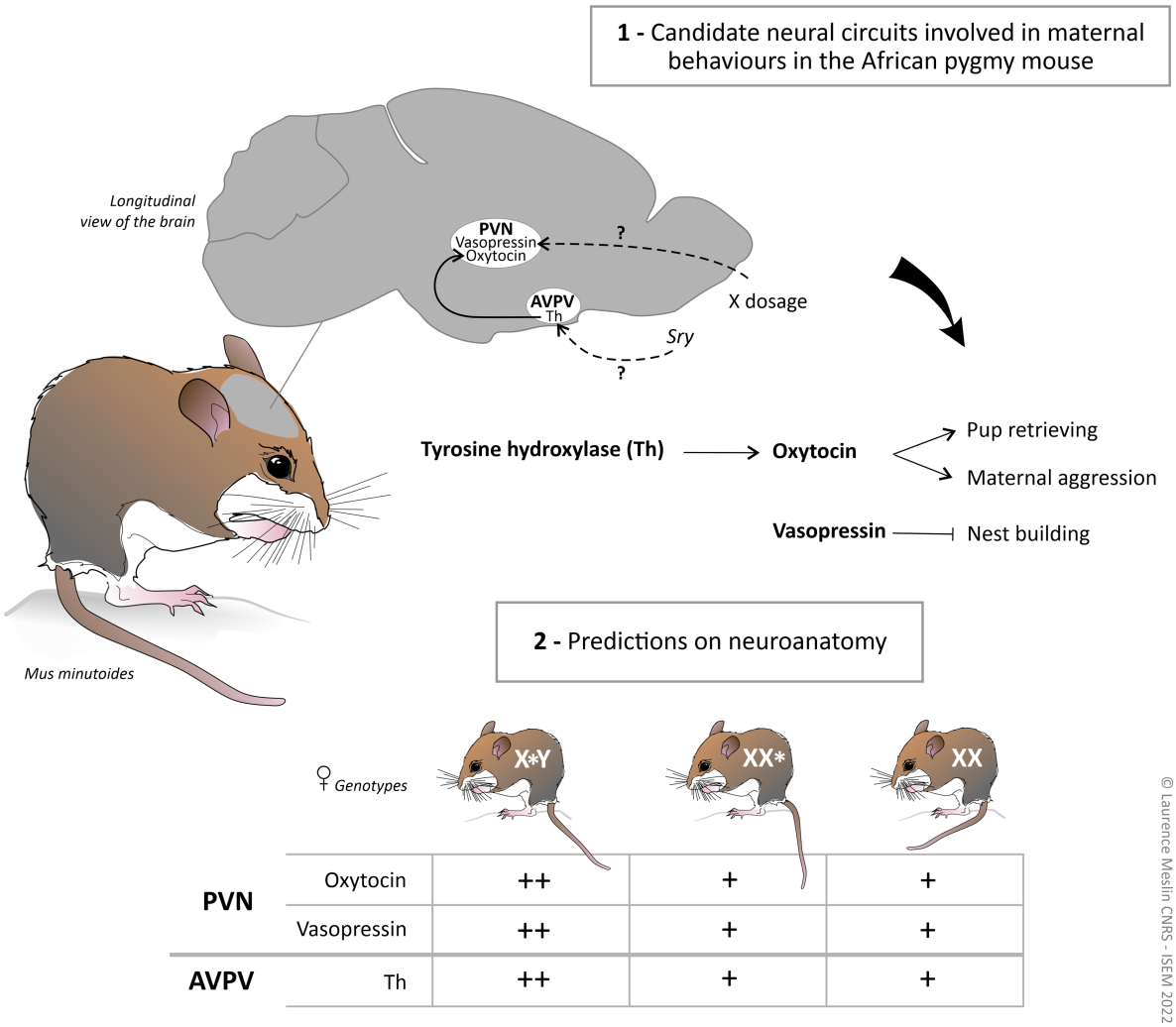

Figure 1. Neural investigations and predictions based on maternal behaviours in the African pygmy mouse as well as on the direct influence of sex chromosome on neuropeptides and neurotransmitters. Maternal behaviour experiments showed that sex-reversal in *M. minutoides* influenced pup retrieval, maternal aggression and nest building, with X*Y females being different from both XX and XX* females for each behaviour. We investigated potential candidates for the neural basis of these behaviours based on *M. musculus* studies: the paraventricular nucleus (PVN) of the hypothalamus where the expression of oxytocin triggers pup retrieval and maternal aggression (i.e. positive correlation) (Scott et al., 2015; Bosch & Neumann, 2012; Okabe et al., 2017; Pedersen et al., 2006) while vasopressin expression inhibits nesting behaviours (i.e., negative correlation) (Bendesky et al., 2017). We also investigated Th neurons (i.e., dopaminergic system) in the anteroventral periventricular nucleus (AVPV) of the hypothalamus, which have been shown to enhance retrieval behaviours through the regulation of oxytocin neurons in the PVN (Scott et al., 2015). Moreover, it has been shown that Th neurons can be regulated by the sex determining gene, *Sry* (e.g. Dewing et al., 2006) and that vasopressin can be influenced by X dosage (e.g. Gatewood et al., 2006). We thus predicted greater oxytocin, vasopressin and Th cell numbers / density in the PVN and AVPV of X*Y females, respectively. © Laurence Meslin CNRS - ISEM 2022

bioRxiv preprint doi: https://doi.org/10.1101/2022.04.05.487174; this version posted September 16, 2022. The copyright holder for this preprint (which was not certified by peer review) is the author/funder, who has granted bioRxiv a license to display the preprint in perpetuity. It is made available under aCC-BY-NC-ND 4.0 International license.

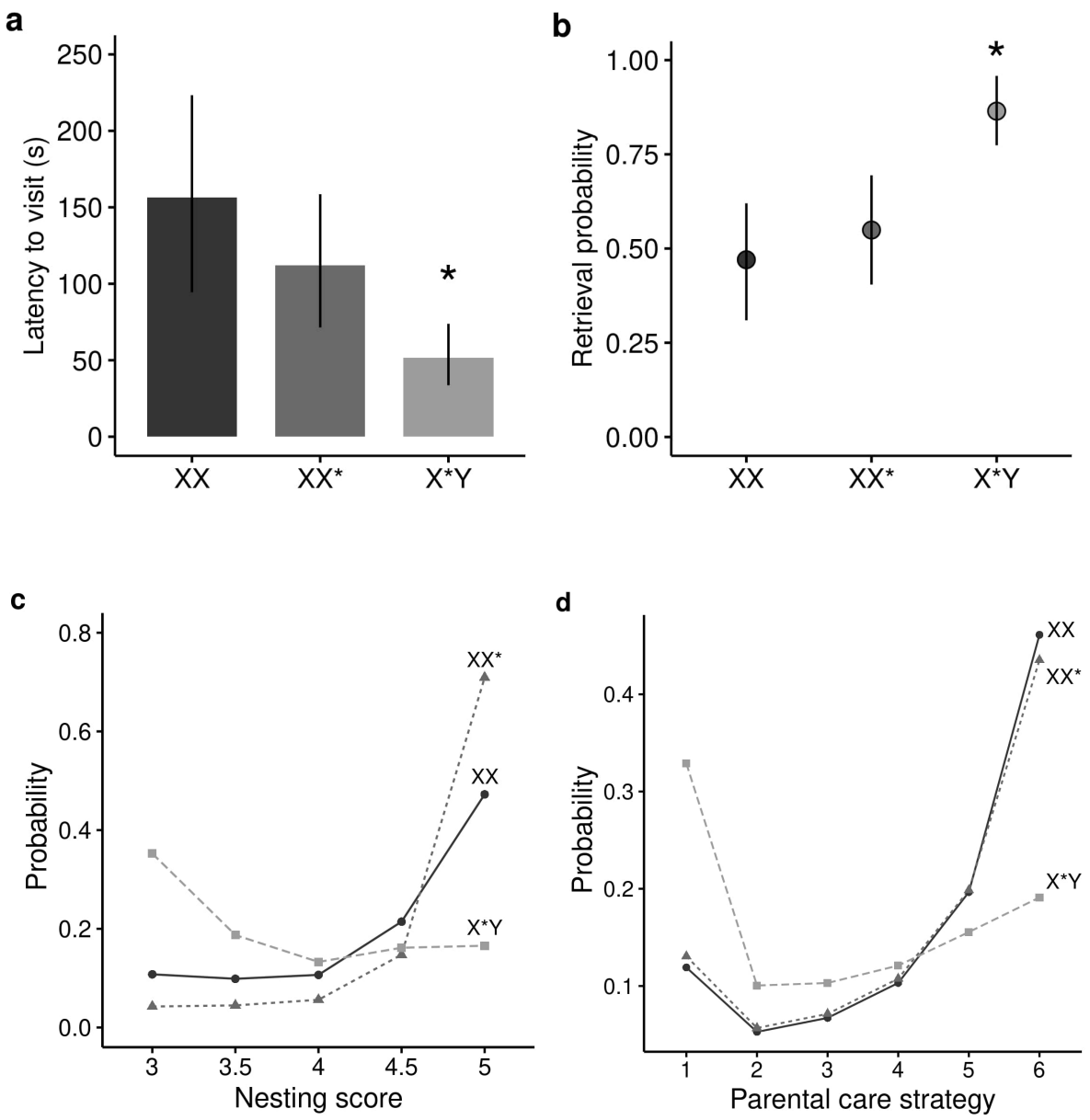

Figure 2. The sex chromosome complement shapes maternal behaviours in the African pygmy mouse. **a,b**, Pup retrieval. Estimates of first visit latency and retrieval probability per genotype. Values are medians with 89% HPD intervals. Latency to first visit and probabilities are retrieved from a back-transformation of our parameters. *Asterisks indicate significance of the genotype effect : X*Y females show a significantly reduced visit latency and a higher retrieval probability in contrast to XX as well as to XX* females (median-based contrasts with 89% HPD intervals are shown in table S2). n_{XX}=31 , n_{XX^*}=35, n_{X^*Y}=35 **c,** Likelihood curves of nest quality depending on females' genotype. Nest quality estimates range from 3 (slightly curved nest) to 5 (fully enclosed nest) as no values below 3 were recorded. X*Y females build poorer quality nest than both XX (p=0.002) and XX* females (p<.0001). n_{XX}=27 , n_{XX^*}=29, n_{X^*Y}=34 **d,** Likelihood curves of parental care strategies regarding fathers involvement inside the nest from 1 : no involvement of fathers and high level of maternal aggression to 6 : biparental care. n_{XX}=29 , n_{XX^*}=39, n_{X^*Y}=37. X*Y females are more likely to display maternal aggression than both XX (p=0.005) and XX* females (p=0.004), which likely share care with males.

bioRxiv preprint doi: https://doi.org/10.1101/2022.04.05.487174; this version posted September 16, 2022. The copyright holder for this preprint (which was not certified by peer review) is the author/funder, who has granted bioRxiv a license to display the preprint in perpetuity. It is made available under aCC-BY-NC-ND 4.0 International license.

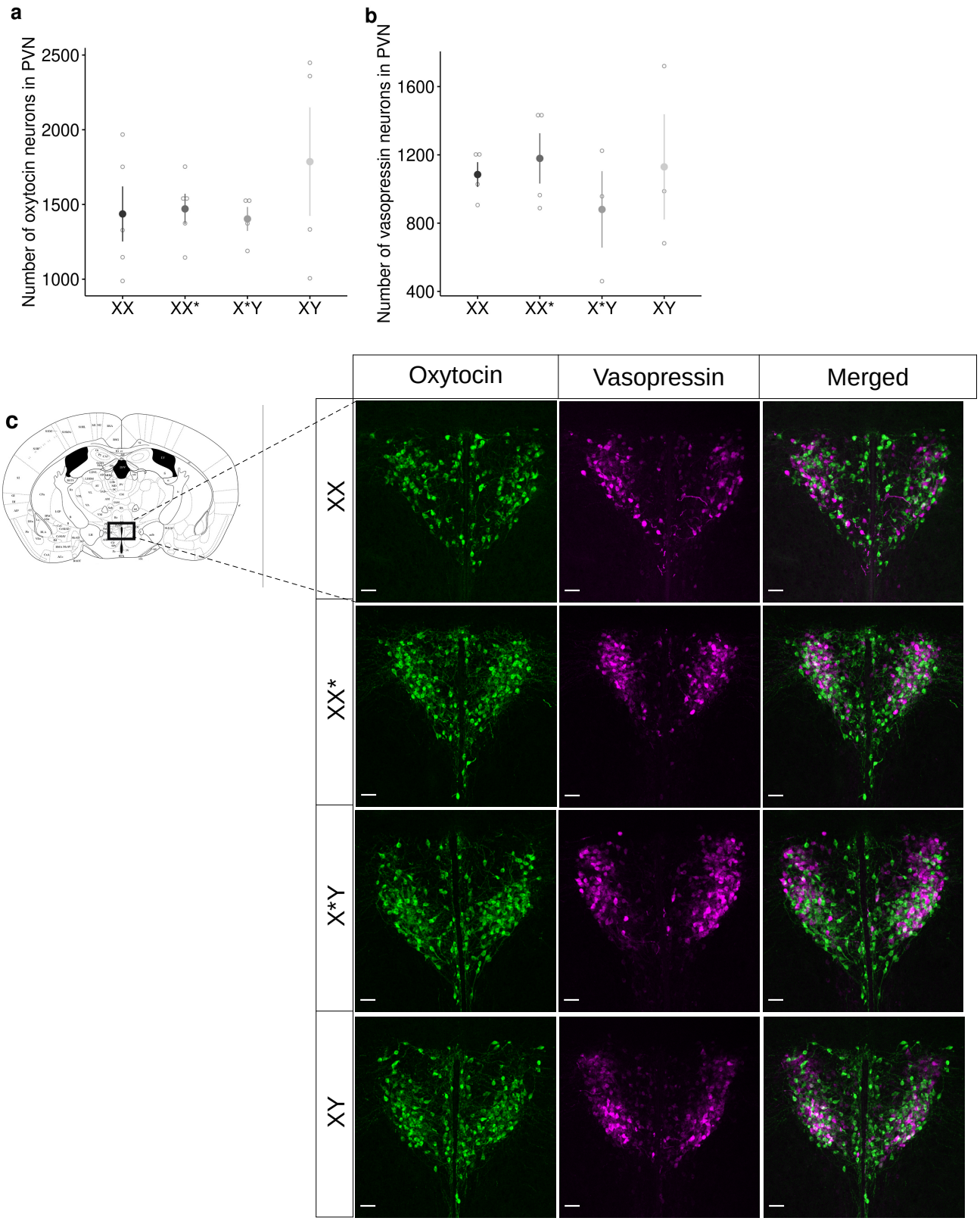

Figure 3. No genotypic sex effect on oxytocin and vasopressin neurons' number in the PVN of virgin individuals. **a,b**, Total number of oxytocin and vasopressin expressing neurons in the PVN of virgin XX, XX*, X*Y females and XY males. Oxytocin : n_{XX}=5 , n_{XX^*}=5, n_{X^*Y}=4, n_{XY}=4. Vasopressin : n_{XX}=4 , n_{XX^*}=4, n_{X^*Y}=3, n_{XY}=3. Data are means ± s.e.m and raw counts are also represented by empty dots. **c,** Oxytocin and vasopressin staining in the PVN of virgin African pygmy mice and associated *M.musculus* brain slice reference (black rectangle represents the PVN area, modified from Franklin & Paxinos, 2001) . Scale bars 50 µm.

bioRxiv preprint doi: https://doi.org/10.1101/2022.04.05.487174; this version posted September 16, 2022. The copyright holder for this preprint (which was not certified by peer review) is the author/funder, who has granted bioRxiv a license to display the preprint in perpetuity. It is made available under aCC-BY-NC-ND 4.0 International license.

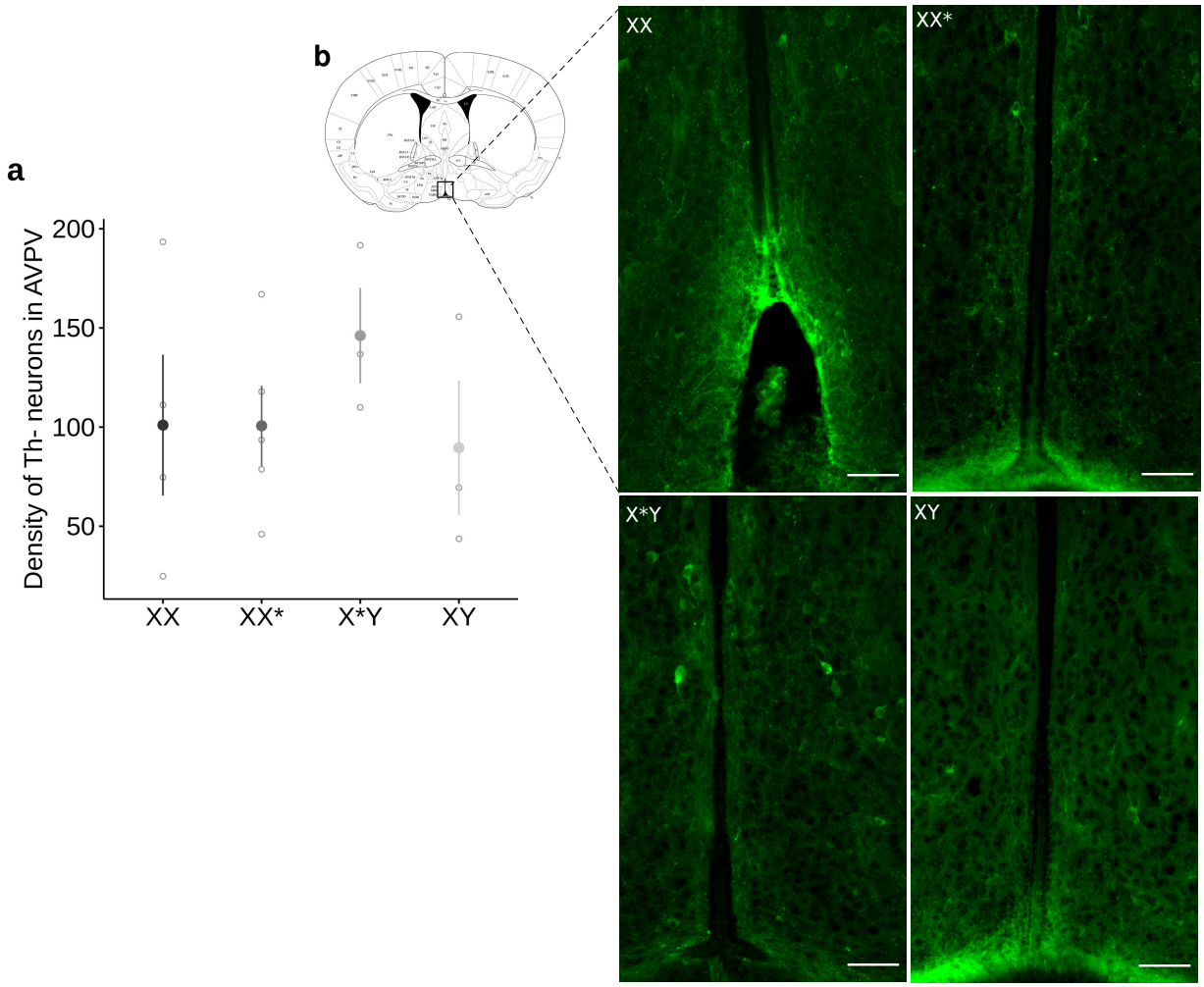

Figure 4. Tendency for greater Th neuron density in the AVPV of X*Y females. **a,** Density of Th- expressing neurons in PVN of virgin XX, XX*, X*Y females and XY males: number of total Th neurons weighted by the sum of the area (mm2). n_{XX}=4 , n_{XX^*}=5, n_{X^*Y}=3, n_{XY}=3. Data are means ± s.e.m and raw counts are also represented by empty dots. **b,** Th staining in the AVPV of virgin African pygmy mice and associated *M.musculus* brain slice reference (black rectangle represents the AVPV area, modified from Franklin & Paxinos, 2001) . Scale bars 50 µm.

Chapter 2

Impact of sex reversal on maternal care: focus on lactation

Louise D. Heitzmann, Anne Guillou, Evelyne Galibert, Marie Challe, Agnes O. Martin[1] & Frederic[1] Veyrunes

[1] Equal contribution

Foreword

In this section, we focused on one specific component of maternal care : lactation, a complex female-specific trait crucial for offspring survival. Lactation, i.e., milk production and ejection from the mammary gland, is induced by Prolactin (PRL), an hormone secreted in the pituitary gland (production), and oxytocin (ejection), a neuropeptide regulating a wide range of social behaviours (e.g., maternal care, pair bonding). We specifically focused on prolactin, as oxytocin was developed in the previous section and no differences were found between females. The aim of this project is to combine three aspects of lactation : neuronal control of prolactin through the hypothalamo-pituitary axis, quantification of circulating prolactin levels and a survey of pups' weight as a proxy of lactation quality. Data presented here are mainly methods that are still being optimized (especially for prolactin quantification) and a few preliminary results of an ongoing investigation. This project is particularly interesting because prolactin is regulated by dopamine, which is likely to be influenced by sex chromosomes : there have been several reports of differences in dopamine levels due to the expression of *Sry,* which is known to be expressed in the brain of X*Y females. Accordingly, greater lactation levels in X*Y would bring exciting new prospects on the consequence of sex reversal in the African pygmy mouse; this could bring further support for the increased fitness in X*Y females and the maintenance of the system due to adaptive phenotypes.

Introduction

Lactation, decisive for the development and survival of offspring, is the prior determinant at the origin of a female-skewed parental care in mammals. On a hormonal basis, these differences involve changes in prolactin (PRL) levels, the hormone necessary for milk production, though its role extends to the regulation of maternal behaviours as well (Neville, 2006). PRL is secreted by the lactotroph cells in the anterior pituitary, or adenohypophysis, from where it is released into the bloodstream, and will then induce milk secretion in the mammary gland (Dobolyi et al., 2020; Neville, 2006). Interestingly, PRL is the only hormone that is under an inhibitory regulation of hypothalamic neurons secreting dopamine (DA) (Arbogast & Voogt, 1996; Ben-Jonathan & Hnasko, 2001). More precisely, tuberoinfundibular dopamine (TIDA) neurons of the arcuate nucleus (Arc) project to the median eminence where DA is released into the blood capillaries of the hypophysial portal system. Dopamine then binds to its receptor (D2) on lactotroph cells of the anterior pituitary, preventing PRL release. During lactation, prolactin release requires the inhibition of TIDA neurons (Arbogast & Voogt, 1996; Le Tissier et al., 2015; Lyons et al., 2012; Lyons & Broberger, 2014; Pérez et al., 2020; Romanò et al., 2013), which can be maintained with suckling stimuli (Berghorn et al., 2001).

In mammals, sex reversal has been shown to have a detrimental impact on female reproductive phenotypes (Vaiman & Pailhoux, 2000). Yet, there are a few wild species with naturally occurring sex reversal that do not fit these observations (see Saunders & Veyrunes, 2021). The African pygmy mouse, for instance, is a wild mouse species with sex-reversed XY females, due to a feminizing X chromosome, called X*. Females in the African pygmy mouse are either XX, XX* or X*Y and there is one male genotype: XY. Interestingly, while we would have expected an impaired reproductive output as well as maternal quality due to the presence of the Y chromosome and the loss of YY embryos, previous studies have shown that X*Y females have a greater reproductive success than the other females (e.g. greater ovulation rate, Saunders et al., 2014), they are more efficient at pup retrieving, and display high levels of maternal aggression (Heitzmann et al., 2022). All things considered, the impact of sex reversal on females' behaviour and reproductive phenotypes raises new questions, such as lactation in X*Y females and whether it can participate to the greater reproductive success previously highlighted. In addition, it has been shown that *Sry,* which is expressed in the brain of X*Y females (Rahmoun et al., 2014), regulates tyrosine hydroxylase (Th), the enzyme necessary for dopamine synthesis (Czech et al., 2012; Dewing et al., 2006). Interestingly, previous neuroanatomical investigations brought promising avenues to explore regarding a potential stimulatory influence of sex reversal on Th levels in X*Y females (Heitzmann et al., 2022; Rahmoun et al., 2014). Therefore, one might suggest that X*Y females have more TIDA neurons than the other females, underlying differences in lactation potential. To answer these questions, we investigate here the neural

pathways involved in prolactin release (i.e., TIDA neurons through the expression of Th, and lactotroph cells in the pituitary), quantify circulating prolactin levels in lactating females and monitor the weight gain of litters during the first week following birth.

Methods

Animals

Animals are reared in our breeding colony (CECEMA, University of Montpellier) established from wild caught animals in a South African population (Caledon Nature Reserve). All experimentations are performed with the approval of the French Ethical Committee on animal care and use (No. CEEA-LR-1270), and following European guidelines. Individuals are housed in a room held at 23°C under a 15:9h light-dark cycle and provided with food and water *ad libitum*. We use 12 virgin females (4 XX, 5 XX* and 3 X*Y) aged between 4-10 months and 4 males aged between (5-18 months). Lactating females are aged between 2-10 months. Females' genotype is identified by PCR of *Sry* (Veyrunes et al., 2010) or by PCR of X/X* chromosome using a combination the following primers: SC328.2.R: 5'-AAGCCTTGACCCAGCCTTCT-3' and SC328.2L1: 5'-TGAAGGACAGGACAGG AACACT-3', which amplified bands of different sizes on the X and X* chromosomes : 553bp and 595 bp, respectively.

Immunostaining

We focused neural investigations on virgin females as using mothers would have implied the loss of the litter and because some genotypes are harder to breed (Saunders et al., 2014; Saunders et al., 2022). Males are included as a control group. We used the same individuals from immunochemistry investigations in Heitzmann et al., (2022) since the whole brain had been stained for Th. These individuals had been injected intra-peritoneally with 150 µl of Domperidone (0.4 mg/kg), a dopamine receptor antagonist, to induce prolactin release and assess lactation capabilities (i.e., secretion potential) in each female genotype. Injections were done 15 minutes before euthanasia using isoflurane 4% followed by decapitation. Brains and pituitaries were collected simultaneously and stored at 4°C in 4% PFA for at least 48 hours. The pituitaries are very thin and small in *M. minutoides*, which led to the loss of a few tissues while sampling. The whole blood was also collected and stored at -20°C. Coronal brain slices of 30 µm were obtained using a vibratome (Leica Microsystems). Brain slices were first incubated using a sheep anti-Th (1:1000, abcam) antibody for 24-48h at 4°C and then using A488 coupled Donkey anti-sheep IgG (1:1000, Jackson Laboratories) secondary antibody for another 24-48h at 4°C (see Heitzmann et al., 2022). Slices were then incubated with DAPI for 3-6 minutes (1:10000, Invitrogen), mounted on Polysine® Slides and stored at 4°C until imaging. We collected brain slices that contained the arcuate nucleus to investigate the number of TIDA neurons for each

genotype. In contrast, because pituitaries are very thin in the African pygmy mouse, we performed staining on the whole structure without slicing. Pituitaries were incubated with rabbit, or Guinea Pig, anti-PRL (1:1000) for 24-48 hours at 4°C followed by Cy3 coupled Donkey anti-rabbit, or anti-Guinea Pig, IgG (1:1000, Jackson Laboratories) for 48 hours at 4°C. Stained tissues were mounted on Polysine® Slides and stored at 4°C until imaging.

Imaging

Pituitary and brain slices (identified using Franklin and Paxinos Atlas) were processed using confocal microscopy (Zeiss, LSM 780). We performed imaging of the arcuate nucleus in regions that contained the median eminence, indicative of the presence of TIDA neurons (Ben-Jonathan & Hnasko, 2001). Cell counts need to be performed.

Survey of litters' weight gain : on-going

Pup(s)' weight is measured at 4 time points with two days between each time point. We weight the whole litter and standardize the weight by the number of pups to account for litter size differences between females. Because litters are not always directly detected (i.e., at birth, P0), but either at one (P1) or two days (P2) post-parturition (dpp), this yields data measurements from birth to eight dpp per genotype. We also score pup(s)' survival.

Tail-tip blood sampling of lactating females : on-going

We collect blood from the tail tips of females either 3 or 4 dpp to avoid extreme disturbance at birth while still being in the PRL secretion surges (Rodriguez-Gonzalez et al., 2020). Because tails are extremely thin, we could not use a needle; we either cut or make a notch at the end of the tail using a scalpel blade. Therefore, each female is sampled only once for animal welfare. We sample between 1.5-6 µl of blood. This high variability in sampling reflects limitations especially due to the small sizes of animals. The whole blood was first diluted at 1:20 (optimal dilution for *M.musculus*, Guillou et al., 2015) in 0.05% PBS-Tween and then 1:40 in 0.05% PBS-Tween, which seems to be our optimal dilution factor (Fig S1).

Prolactin assay : on-going

Prolactin levels are quantified on both lactating and virgin females using the whole blood. We first tested a few virgin individuals injected with domperidone to estimate an optimal dilution factor among the following dilutions of 1:2, 1:10, 1:20, 1:30, 1:40, and selected accordingly an optimal dilution factor of 1:40 (Fig S1). Virgin individuals injected with domperidone were also used to estimate prolactin secretion capacities per genotype. Circulating prolactin levels of virgin and lactating females

are quantified by ELISA and following the customized protocol of Guillou et al., (2015). Measures are duplicated within an assay when we have enough material, and repeated over time to include an 'assay' effect. Repeated measures are averaged per individual.

Preliminary results & perspectives

a) Lactotroph cells in the anterior pituitary

Both rabbit and guinea pig anti-bodies worked. PRL is stored in the cytoplasm of lactotroph cells. The staining helped to confirm that anti-bodies can detect PRL for the immunoenzymatic assay as well. Since PRL levels are quantified by ELISA and because we lost a few tissue samples, the staining of lactotroph cells will be used to illustrate the neuroanatomy of the PRL pathway. XX and XY individuals will be stained as well to complete the four genotypes.

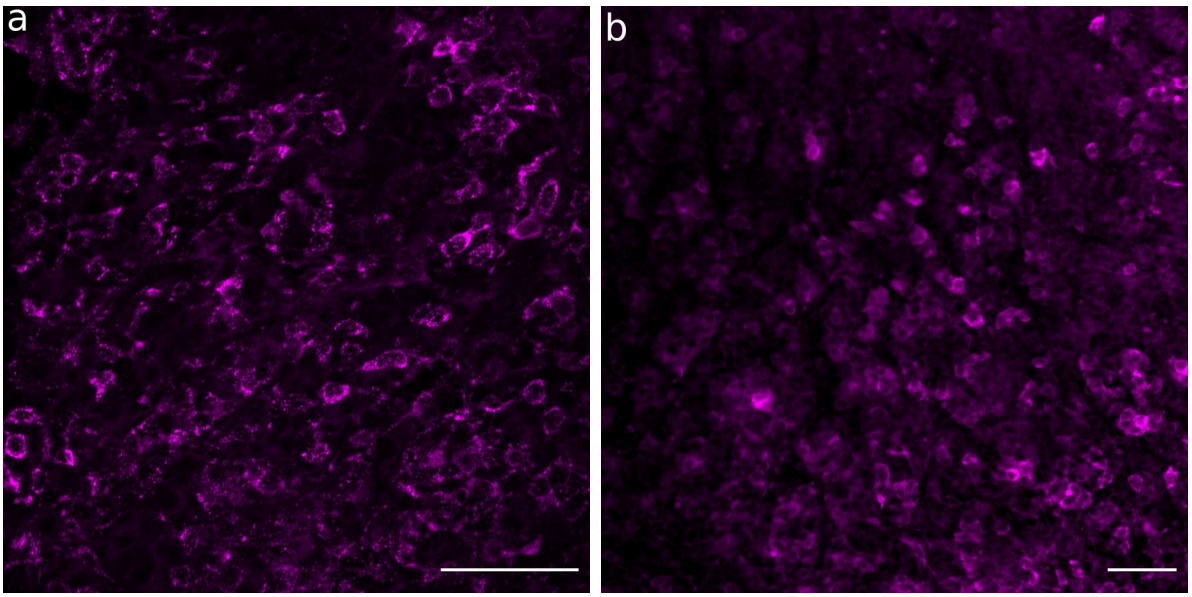

Figure 1. Lactotroph cells in the anterior pituitary. a, X*Y female. b, XX* female. Scale bars represent 50 μm.

b) Dopaminergic neurons in the arcuate nucleus

There are two populations of dopaminergic neurons in the arcuate nucleus: TIDA neurons and periventricular-hypophysial dopamine neurons (PHDA). Here, we are only interested in TIDA neurons, which regulate PRL release. TIDA neurons are located in the dorsomedial part of the arcuate nucleus recognizable by the presence of the median eminence and the 'triangle' shape of the third ventricle (Fig 2). We thus focus on Th expressing neurons in this region, as a proxy for TIDA neurons.

Interestingly, on images, X*Y and XX* females seem more similar with more Th expressing neurons than XX and XY individuals, a pattern that needs to be statistically tested with cell counts.

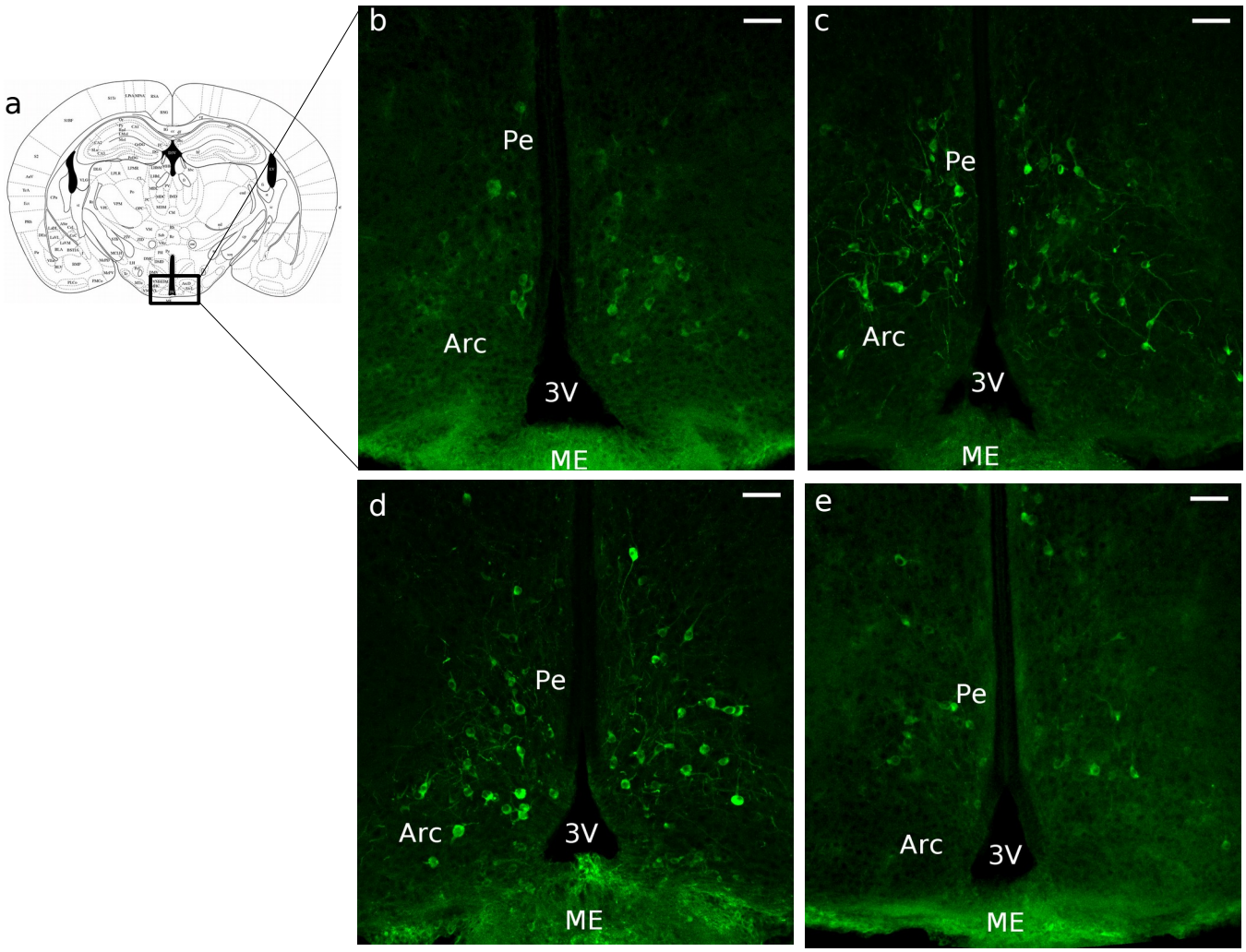

Figure 2. Th expressing neurons in the arcuate nucleus of the African pygmy mouse. Th/dopaminergic neurons in the arcuate nucleus are divided into tuberoinfundibular dopamine (TIDA) neurons and periventricular-hypophysial dopamine (PHDA) neurons. TIDA neurons regulate PRL release and are mainly distributed on the dorsomedial part of the arcuate nucleus (Arc) characterized by the presence of the median eminence (ME) (see Ben-Jonathan & Hnasko, 2001). TIDA neurons project to the external layer of the median eminence where they release dopamine, which is transported through the hypophysial portal vessels to the anterior pituitary. Dopamine inhibits PRL release by binding to its D2 receptor on lactotroph cells, an inhibitory regulation attenuated during lactation. **a,** Localization of the dorsomedial Arc (black rectangle) on a *M.musculus* brain coronal slice. Modified from Paxinos & Franklin, 2001**.** **b**, XX female. **c**, XX* female. **d**, X*Y female. **e**, XY male. Arc = arcuate nucleus, ME= median eminence, Pe= periventricular nucleus ; 3V= third ventricle. Scale bars represent 50 µm. n_{XX}=4, n_{XX*}=5, n_{X*Y}=3, n_{XY}=4.

c) PRL levels in virgin and lactating females.

Results on virgin females injected with domperidone show tendencies for greater PRL levels in XX* and X*Y females (Fig. 3), and most lactating females did not pass the detection threshold (i.e., 2 ng/ml). However, results were not consistent between assays for two XX* females, highlighting methodological limitations and unreliable interpretations (Fig. S1). This inconsistency can result from the formation of a PRL macromolecule (i.e., agglomeration of PRL and immunoglobulin G) (Ahlquist et al., 1998; Fahie-Wilson, 2003; Vaishya et al., 2010) or from interferences with blood components using the whole blood. A first solution is to use the serum instead of the whole blood, to prevent a 'blood' effect. If the problem persists, we will consider methods that have been developed to detect and deal with macroprolactin (e.g, precipitation with polyethylene glycol, PEG) (Vaishya et al., 2010). This should also help improve detection of PRL in lactating females.

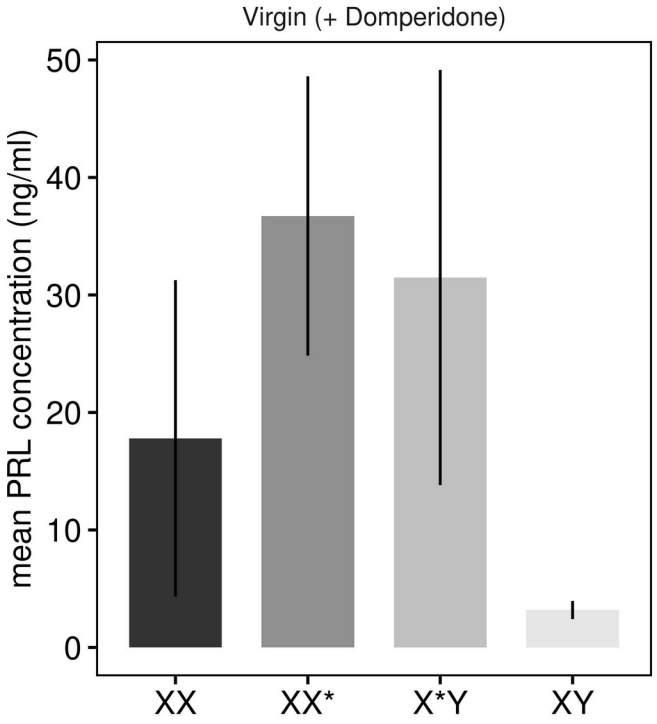

Figure 3. Circulating PRL levels in virgin and lactating females. Virgin females and males were injected with domperidone to trigger prolactin release. We averaged repeated measures per individual. n_{XX}=3, n_{XX*}=4, n_{X*Y}=4, n_{XY}=4. Lactating females were tested at day 3 post-parturition (i.e., L3). n_{XX}=6, n_{XX*}=1, n_{X*Y}=3. Almost all lactating females failed to pass the detection threshold (2 ng/ml) underlying unreliable results for these females. Values are mean ± s.e.m.

d) Litters' weight

At the moment, we followed 18 females (11 XX, 3XX*, 4 X*Y), with 59 observations collected, in total. Some females did not have 4 measurements due to the death of the litter or because some survey

had not been done. This explains why the averaged weight of litters (per genotype) does not follow a strict positive correlation with the time of survey, from P0 to P8 (Fig. 4a,b). X*Y females curve for litters' weight is above XX and XX* females, a pattern that disappear once we average the weight by litter sizes (X*Y seem similar to XX females and XX* females are a bit above). This reflects the bigger litter sizes in X*Y females (Fig. 4c) (Saunders et al., 2014). Pup(s) or litters that did not survive were found in litters of XX females only (Fig. 4d). Moreover, because the genotype of the litter can also influence pup(s)' own development though offspring competition, we might undertake a cross fostering experiment to disentangle the effect of the mothers' genotype from that of the offspring.

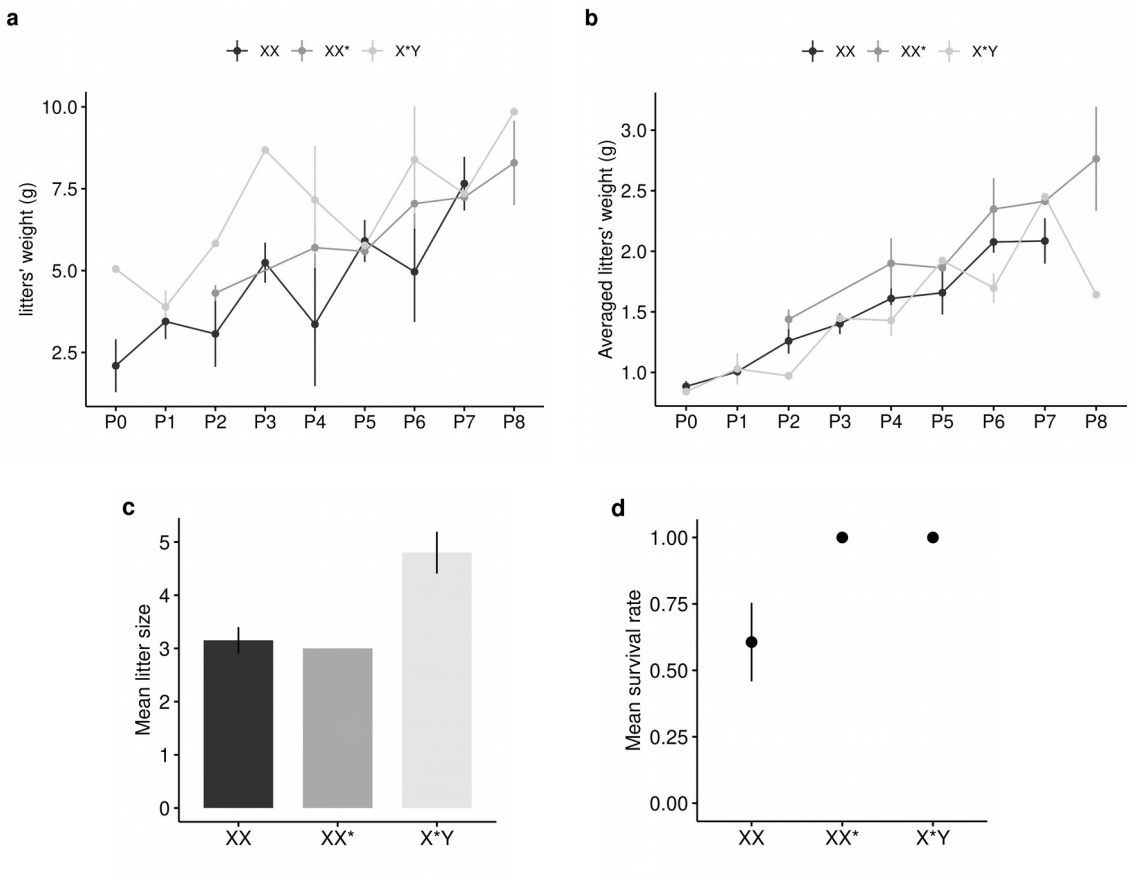

Figure 4. Survey of litters' from birth (P0) to 8 days post-parturition (P8). Litters' weight are measured 4 times with a gap of 2 days between measurements. **a**, litters' weight. Values are mean ± s.e.m. **b**, litters' weight averaged by litter sizes. Values are mean ± s.e.m. **c,** mean litter size per genotype. **d**, mean litters' survival rate (number of pup(s) alive / litter size) per genotype. n_{XX}=11, n_{XX*}=3, n_{X*Y}=4.

Conclusions

PRL is a key hormone for offspring survival and thus for the reproductive success of females as well. Investigations of the PRL pathway represent an exciting project to test for adaptive, or not, consequences of sex reversal on female phenotypes in *M. minutoides*. Preliminary methods and data emphasize the necessity to optimize methods, especially for the quantification of circulating PRL levels (interpretations are unreliable due to inconsistent results), before making any interpretation. Here is a list of what remains to be done in this study :

- Staining of XX and XY pituitaries with a PRL antibody.
- perform cell counts of Th expressing neurons in the arcuate nucleus and analyse the data.
- (Re-)perform ELISA tests :
    * add samples of virgin females injected with domperidone and split samples to test on both serum and whole blood (and repeat measures). This should help us determine whether macroprolactin is responsible for inconsistencies and adjust methods accordingly (e.g. PEG treatment).
    * sampling blood at the tip of the tail of lactating females : get both whole blood and serum samples.
- continue to monitor the weight of litters.

References

Ahlquist, J. A., Fahie-Wilson, M. N., & Cameron, J. (1998). Variable detection of macroprolactin: A cause of apparent change in serum prolactin levels. *Clinical Endocrinology*, *48*(1), 123–124. https://doi.org/10.1046/j.1365-2265.1998.0429a.x

Arbogast, L. A., & Voogt, J. L. (1996). The Responsiveness of Tuberoinfundibular Dopaminergic Neurons to Prolactin Feedback Is Diminished between Early Lactation and Midlactation in the Rat*. *The Endacrmc Soacty*, *1*, 47–54.

Ben-Jonathan, N., & Hnasko, R. (2001). Dopamine as a prolactin (PRL) inhibitor. *Endocrine Reviews*, *22*(6), 724–763. https://doi.org/10.1210/edrv.22.6.0451

Berghorn, K. A., Le, W.-W., Sherman, T. G., & Hoffman, G. E. (2001). Baker and Farbman. In *J. Comp. Neurol 438*, 423–432).

Czech, D. P., Lee, J., Sim, H., Parish, C. L., Vilain, E., & Harley, V. R. (2012). The human testis-determining factor SRY localizes in midbrain dopamine neurons and regulates multiple components of catecholamine synthesis and metabolism. *Journal of Neurochemistry*, *122*(2), 260–271. https://doi.org/10.1111/j.1471-4159.2012.07782.x

Dewing, P., Chiang, C. W. K., Sinchak, K., Sim, H., Fernagut, P. O., Kelly, S., Chesselet, M. F., Micevych, P. E., Albrecht, K. H., Harley, V. R., & Vilain, E. (2006). Direct regulation of adult brain function by the male-specific factor SRY. *Current Biology*, *16*(4), 415–420. https://doi.org/10.1016/j.cub.2006.01.017

Dobolyi, A., Oláh, S., Keller, D., Kumari, R., Fazekas, E. A., Csikós, V., Renner, É., & Cservenák, M. (2020). Secretion and Function of Pituitary Prolactin in Evolutionary Perspective. *Frontiers in Neuroscience, 14*, 621 https://doi.org/10.3389/fnins.2020.00621

Fahie-Wilson, M. (2003). In Hyperprolactinemia, Testing for Macroprolactin Is Essential. *Clinical Chemistry*, *49*(9), 1434–1436. https://doi.org/10.1373/49.9.1434

Guillou, A., Romanò, N., Steyn, F., Abitbol, K., Le Tissier, P., Bonnefont, X., Chen, C., Mollard, P., & Martin, A. O. (2015). Assessment of lactotroph axis functionality in mice: Longitudinal monitoring of PRL secretion by ultrasensitive-ELISA. *Endocrinology*, *156*(5), 1924–1930. https://doi.org/10.1210/en.2014-1571

Heitzmann, L., Challe, M., Perez, J., Castell, L., Galibert, E., Martin, A., Valjent, E., & Veyrunes, F. (2022). Genotypic sex shapes maternal care in the African Pygmy mouse, Mus minutoides. *BioRxiv*. https://doi.org/10.1101/2022.04.05.487174

Le Tissier, P. R., Hodson, D. J., Martin, A. O., Romanò, N., & Mollard, P. (2015). Plasticity of the prolactin (PRL) axis: Mechanisms underlying regulation of output in female mice. *Advances in Experimental Medicine and Biology*, *846*, 139–162. https://doi.org/10.1007/978-3-319-12114-7_6

Lyons, D. J., & Broberger, C. (2014). TIDAL WAVES: Network mechanisms in the neuroendocrine control of prolactin release. *Frontiers in Neuroendocrinology*, *35*(4), 420–438. https://doi.org/10.1016/j.yfrne.2014.02.001

Lyons, D. J., Hellysaz, A., & Broberger, C. (2012). Prolactin Regulates Tuberoinfundibular Dopamine Neuron Discharge Pattern: Novel Feedback Control Mechanisms in the Lactotrophic Axis. *Journal of Neuroscience, 32*(23), 8074-8083 https://doi.org/10.1523/JNEUROSCI.0129-12.2012

Neville, M. C. (2006). CHAPTER 57—Lactation and Its Hormonal Control. In J. D. Neill (Ed.), *Knobil and Neill's Physiology of Reproduction (Third Edition)* (pp. 2993–3054). Academic Press. https://doi.org/10.1016/B978-012515400-0/50062-2

Paxinos, G., & Franklin, K. B. J. (2001). *The mouse brain in stereotaxic coordinates* (Academic Press, Ed.; p. 264). Elsevier.

Pérez, C. T., Ferraris, J., Lunteren, J. A. van, Hellysaz, A., Iglesias, M. J., & Broberger, C. (2020). Adaptive Resetting of Tuberoinfundibular Dopamine (TIDA) Network Activity during Lactation in Mice. *Journal of Neuroscience*, *40*(16), 3203–3216. https://doi.org/10.1523/JNEUROSCI.1553-18.2020

Rahmoun, M., Perez, J., Saunders, P. A., Boizet-Bonhoure, B., Wilhelm, D., Poulat, F., & Veyrunes, F. (2014). Anatomical and molecular analyses of XY ovaries from the african pygmy mouse Mus minutoides. *Sexual Development*, *8*(6), 356–363. https://doi.org/10.1159/000368664

Rodríguez-González, G. L., Bautista, C. J., Rojas-Torres, K. I., Nathanielsz, P. W., & Zambrano, E. (2020). Importance of the lactation period in developmental programming in rodents. *Nutrition Reviews*, *78*, 32–47. https://doi.org/10.1093/nutrit/nuaa041

Romanò, N., Yip, S. H., Hodson, D. J., Guillou, A., Parnaudeau, S., Kirk, S., Tronche, F., Bonnefont, X., Le Tissier, P., Bunn, S. J., Grattan, D. R., Mollard, P., & Martin, A. O. (2013). Plasticity

of hypothalamic dopamine neurons during lactation results in dissociation of electrical activity and release. *Journal of Neuroscience*, *33*(10), 4424–4433. https://doi.org/10.1523/JNEUROSCI.4415-12.2013

Saunders, P. A., Perez, J., Rahmoun, M., Ronce, O., Crochet, P. A., & Veyrunes, F. (2014). XY Females do better than the XX in the African PYGMY mouse, Mus minutoides. *Evolution*, *68*(7), 2119–2127. https://doi.org/10.1111/evo.12387

Saunders, P. A., & Veyrunes, F. (2021). Unusual Mammalian Sex Determination Systems: A Cabinet of Curiosities. *Genes*, *12*(11), 1770–1770. https://doi.org/10.3390/GENES12111770

Vaiman, D., & Pailhoux, E. (2000). Mammalian sex reversal and intersexuality: Deciphering the sex-determination cascade. *Trends in Genetics*, *16*(11), 488–494. https://doi.org/10.1016/S0168-9525(00)02126-0

Vaishya, R., Gupta, R., & Arora, S. (2010). Macroprolactin; A Frequent Cause of Misdiagnosed Hyperprolactinemia in Clinical Practice. *Journal of Reproduction & Infertility*, *11*(3), 161–167.

Veyrunes, F., Chevret, P., Catalan, J., Castiglia, R., Watson, J., Dobigny, G., Robinson, T. J., & Britton-Davidian, J. (2010). A novel sex determination system in a close relative of the house mouse. *Proceedings of the Royal Society B: Biological Sciences*, *277*(1684), 1049–1056. https://doi.org/10.1098/rspb.2009.1925

Chapter 3

Disentangling between hormonal and sex-linked genetic bases of territorial aggression in sex-reversed X*Y females

Louise D. Heitzmann, Marc Fichter, Julie Perez, Xavier Hautecoeur, Theo Deremarque & Frederic Veyrunes

Abstract

Sex differences in social aggression are common across the animal kingdom, with males usually being more aggressive than females. Proximate causes of this sexual dimorphism involve steroid hormones and especially testosterone, but also sex chromosomes with imbalance in sex-linked genes. However, the direct influence of sex chromosomes is far from being understood as studies are few, and because we usually cannot distinguish the relative contribution of sex-linked genes from hormones (i.e., genotypic and gonadal sexes are indissociable). The African pygmy mouse is a wild mouse species with a dissociation between gonadal and genotypic sex. Due to a sex reversal mutation on the X chromosome at the origin of a third sex chromosome, called X*, there are three female genotypes in natural populations : XX, XX* and X*Y, while all males are XY. Interestingly, a previous study has shown that X*Y females are more aggressive than XX and XX* females. Hence, to decipher the relative contribution of sex-linked genes and hormones in driving this aggressiveness, we re-conducted the same agonistic behavioural assay in females of the same African pygmy mouse population. Following assays, we measured females' testosterone levels and quantified the expression of sex-linked genes known to regulate aggressiveness, which we correlated with aggressiveness levels. Even though our results are preliminary and need further investigations, we showed that sex-linked genes rather than steroid hormones are more likely to drive aggressiveness in X*Y females. All things considered, species with unusual sex determination system shaped by evolution, such as in the African pygmy mouse, can provide considerable help to shed light on the direct role of sex-linked genes in driving sex differences in brain and behaviours.

Introduction

Aggression is a complex social behaviour widespread across the animal kingdom. In many species, social aggression is highly sexually dimorphic, prevalent in males competing for territories and mates, while female aggression mainly involves pup protection (Darwin, 1871; Pandolfi et al., 2021). This sexual dimorphism arises from differences in steroid hormones levels, especially testosterone, but also from sex chromosomes and imbalance in sex-linked genes, though their role has been considerably neglected (Book et al., 2001; Gatewood et al., 2006; Giammanco et al., 2005; Lovell-Badge, 2005; Pandolfi et al., 2021; Rose et al., 1971; Saunders et al., 2016; Sluyter et al., 1996; Wu et al., 2009; Xu et al., 2012). Moreover, it is still not clear whether sex chromosomes influence hormones, or whether sex-linked genes directly impact brain neural pathways underpinning aggressiveness.

Perinatally and at adulthood, testosterone and aromatization of testosterone to estradiol are essential to masculinize brain neural circuits underlying male-specific behaviours (Arnold, 2009; Arnold & Breedlove, 1985; Breedlove et al., 1999; Phoenix, 2009; Phoenix et al., 1959; Wu et al., 2009). These two periods are referred as the organizational (perinatal) period, with permanent effects of testosterone, and the activational (adulthood) period, with reversible effects. Therefore, testosterone appeared as a key factor for the initiation and maintenance of aggressive behaviours in males and interestingly, testosterone has also been linked to female aggression in many vertebrate species (Albert et al., 1989; Cantarero et al., 2015; Denson et al., 2018; Gill et al., 2007; Woodley & Moore, 1999). However, the effect of testosterone is not a rule of thumb (Compaan et al., 1993; Denson et al., 2018; Everts et al., 1997; Hashikawa et al., 2017; Mahadevia et al., 2021; Oliveira et al., 2021), and there has been increasing evidence for the direct influence of sex chromosomes on aggressive behaviours (Gatewood et al., 2006; Guillot et al., 1995; Mortaud et al., 2010; Saunders et al., 2016).

The Y chromosome is a prime candidate to investigate the genetic basis of sex differences in aggressiveness. In humans, there have been multiple reports of violent and incarcerated males with an extra Y chromosome (47, XYY), in favour of a link between the Y chromosome and aggression (reviewed in Re & Birkhoff, 2015). These results were highly debated due to inconsistencies, notably with many XYY males that did not show patterns of aggressive behaviours. Nevertheless, one Y-linked gene appeared as a strong candidate : the sex determining gene, *Sry*. In mice for instance, *Sry* is expressed in some regions of the brain where it regulates dopamine levels, a neurotransmitter involved in social behaviours, including aggression (Czech et al., 2012; Dewing et al., 2006; Godar et al., 2016; Korzan et al., 2006; Kudryavtseva et al., 2017; Mahadevia et al., 2021; van Erp & Miczek, 2000; Yamaguchi & Lin, 2018). More specifically, *Sry* stimulates the expression of tyrosine hydroxylase (*Th*), the enzyme necessary for dopamine synthesis, leading to higher levels of dopamine, which are

positively correlated with aggressiveness. Interestingly, a X-linked gene is also involved in the dopaminergic pathway: monoamine oxydase A, *MaoA*, coding an enzyme that degrades dopamine (Shih et al., 1999). In mice, a knock-out in *MaoA* has been related to enhanced aggressiveness, and low expression levels have also been found in humans displaying highly aggressive behaviours (Cases et al., 1995; Godar et al., 2016; Kudryavtseva et al., 2017; Scott et al., 2008). All things considered, sex-linked genes may have a non-negligible influence on territorial aggression. However, their contribution in shaping brain neural circuits underpinning aggressive behaviours is usually hard to disentangle from steroid hormones. This is due to the fact that genotypic sexes are indissociable from gonadal sexes in most species.

Genetically modified mouse models have brought considerable help to highlight the influence of the sex chromosomes on sexually dimorphic behaviours such as aggression (Gatewood et al., 2006; Guillot et al., 1995). In the four core genotype mouse model for instance, gonadal and genotypic sexes are separated (XX, XY- females and XY-*Sry*, XX*Sry* males) and sex-reversed XY- females are more aggressive than XX females even though they have comparable hormonal levels (Gatewood et al., 2006). Similarly in Nile tilapia, sex-reversed XY females are more aggressive than XX females, which is independent of testosterone levels (Gennotte et al., 2017). However, those studies have some limitations, such as the absence of *Sry* expression in the brain of XY- mice, or because sex reversal is induced by hormonal treatment as in Nile tilapia, in which, moreover, the relative contribution of sex-linked genes and hormones remains unclear. Yet, there are a few species with naturally occurring sex reversal that could help disentangle between these factors (see Saunders & Veyrunes, 2021). The African pygmy mouse for instance is a wild mouse species in which sex-reversed XY females are found. About 1 million years ago, there was a mutation on the X chromosome that gave birth to a third sex chromosome, called X*, which induces sex reversal in X*Y individuals (Veyrunes et al., 2010a). Three female genotypes are found in natural populations XX, XX* and X*Y, while all males are XY. Although these females have functional ovaries (Rahmoun et al., 2014), they have a different female phenotype from the other females, with divergences in maternal care (Heitzmann et al., 2022), in performance (Ginot et al., 2017) and they are also more aggressive than the other females (Saunders et al., 2016). While there is evidence for a sex-chromosome effect to shape this aggressive phenotype, the relative contribution of hormones and sex-linked genes is unknown. Here, we reproduced an assay on agonistic behaviours from Saunders et al., (2016) to investigate the hormonal and genetic basis of territorial aggression in X*Y females. We evaluated testosterone as well as expression levels of sex-linked genes in the three female genotypes following agonistic assays, and correlated expression levels with aggressiveness levels. Quantification of gene expression levels were focused on sex-linked genes involved in the dopaminergic system: *Sry* (on the Y chromosome), *MaoA*

(on the X), as well as *Th* which is also sex-linked in the African pygmy mouse, being located on an autosome fused to the sex chromosomes (i.e., neo-sex chromosomes; Veyrunes et al., 2010b; Veyrunes et al., 2006).

Material & Methods

Animals

Individuals were reared in a room held at 23°C with a 15:9 light-dark cycle in our breeding facility at the University of Montpellier (CECEMA). Virgin females were kept in groups of 5-6 individuals in cages (38 x 26 x 24 cm) filled with woodchips bedding, with constant food and water supply. In our study, males were grouped by two or isolated in small cages (32 x 45 cm). We genotyped females by PCR of *Sry* (Veyrunes et al., 2010a) and using X/X* markers with the following primers : SC328.2.R 5'- AAGCCTTGACCCAGCCTTCT-3' and SC328.2L1 5'-TGAAGGACAGGACAGG AACACT-3'. The primers amplified one band for XX females (553 bp), two bands for XX* females (553 and 595 bp) and one band for X*Y females (595 bp). Animal experimentations were performed with the approval of the French Ethical Committee on animal care and use (No. CEEA-LR-1270), and following European guidelines.

Resident-intruder assay

Tests were conducted following the same procedures as in Saunders et al. (2016). Virgin females aged between 7-10 months were placed in large plexiglass cages (40 L x 30 W x 30 H cm) with females' own bedding and enrichment for 48 hours, in order to establish the resident status. We placed females at estrus stage to make sure they would not be sexually receptive by the time of experimentations (i.e., 48 hours later), which is likely to influence aggression (Hyde & Sawyer, 1977). Prior the assay, males were placed in a side cage (10 x 10 x 10 cm) with a trap door leading to the experimental environment. An assay started once the male entered the female environment and female-male interactions were then recorded for 10 minutes. Each experiment was analysed by one rater blind to females' genotype. We measured the number of attacks (bite attempts), intimidations (females stand on their hind legs with an offensive posture) as well as chasing duration. The number of attacks and intimidations were corrected by the overall number of interactions to account for differences in female-male encounters between assays. Aggressive behaviours were cumulated to determine an aggressiveness level : we added attack frequency to intimidation frequency, and to the percent of time females spent chasing the male (i.e., chasing duration over experiment duration). At the end of each assay, females were anaesthetized and then decapitated. Blood and brain were instantaneously collected for hormonal dosage and RNA quantification of candidate genes. Overall, we tested 11 X*Y

females, 3 XX and 3 XX* females. XX and XX* females were considered as one control group with a low level of aggression (Saunders et al., 2016).

Testosterone dosage assay

The whole blood collected after females' euthanasia was left to clot for approximately 45-60 minutes. Samples were then centrifuged for 10 minutes at 4500 rpm and serum were collected into new tubes and stored at -20°C until processing. Testosterone levels were quantified by immuno-enzymatic assay using IBL International ELISA kit (#RE52151) and following manufacturer's instructions. We measured samples only once due to insufficient serum volumes for duplicates and because testosterone measurements in females cannot be diluted due to low hormonal levels (Veyrunes et al., 2022). All but one female (X*Y) passed the detection threshold.

RNA extraction , reverse transcription and RT-qPCR of Th, MaoA and Sry

Brains collected were immediately placed in RNAlater®, maintained at 4°C for 48 hours and then stored at -80 °C until further use. Whole brain RNA was extracted using RNeasy® Plus Mini Kit (QIAgen). Tissues were first grounded in liquid nitrogen using a mortar and a pestle under a sterile environment. We added a lysis buffer to homogenize materials and because we used the whole tissue, we adjusted volumes to four times volume recommendations (4 x 6 µL of β-mercapto and 4 x 600 µL of RLT buffer). This gave us four tubes per sample. RNA was purified for two tubes following manufacturer's protocol and the remaining two tubes were stored at -80°C. Extracted RNA was eluted in 50 µL of RNase free water and stored at -80°C until further use. We also included RNA samples of 3 females per genotype that did not perform behavioural assays to control for the treatment effect on expression levels (i.e., quantification of baseline *Th*, *Sry* and *MaoA* expression levels). These females were previously used for next generation sequencing (unpublished data). Before real-time PCR quantifications (RT-qPCR), samples were first treated with DNase (TurboDNA-free™, Invitrogen) followed by reverse transcription of 1 µg of samples converted into cDNA using SuperScript IV Reverse Transcriptase kit (Invitrogen) and following provided protocol. qPCR were performed on a LightCycler 480 (Roche) and using SensiFAST™ SYBR® No-ROX kit (Meridian). We used *Rps29* as a reference gene, which had previously been used (see Rahmoun et al., 2014). Expression levels of *Th*, *MaoA*, *Sry*, and *Rps29* were measured in triplicates in one assay. Primers are shown in table 1. Relative expression levels were measured on LightCycler 480 software v 1.5 (Roche). Because RT-qPCR did not perform well on *Sry* -probably due to the presence of multiple divergent copies with variable sizes, which may have dampen amplification efficiency-, we did not include *Sry* results in the analysis. Three X*Y and one XX* females from the resident-intruder assay were excluded due to amplification failures for both *Th* and *MaoA* quantification. One XX and one XX* female were

removed from baseline *MaoA* quantification as well as one XX* and one X*Y female for *Th* baseline quantification.

Statistical analyses

All statistical analyses were performed on R v4.2.1 (R core Team 2022). Data for XX and XX* females were grouped to form the control group. Behavioural responses were analysed with non parametric Wilcoxon tests. Testosterone levels were compared between females with a Student test and positive correlations between testosterone and aggressiveness levels were made by a Spearman correlation test. *MaoA* and *Th* expression levels were compared between females with (resident-intruder assay) and without (baseline) the treatment by a two-way ANOVA using genotype and treatment as grouping factors and including an interaction term. Pairwise post-hoc comparisons were made using *emmeans* package and p.values were adjusted for multiple testing using a Benjamini-Hochberg correction. Correlations between gene expression levels and aggressive behaviours were performed by Spearman correlation tests. Because of their known effect on behaviours, we tested *Th* and testosterone for a positive correlation, and *MaoA* for a negative correlation.

Results

Agonistic behaviours

There were no significant differences between X*Y females and XX/XX* females in attack frequency (Fig 1a, Wilcoxon test, W=26, p =0.5), intimidation frequency (Fig 1b, Wilcoxon test, W=21, p=0.18) nor chasing duration (Fig 1c, Wilcoxon test, W=28.5, p=0.62) between females, although we found tendencies for greater levels of aggressiveness in X*Y females.

Testosterone levels

There were no difference in testosterone levels between X*Y and XX/XX* females (Fig 2a, Student test, t=0.04, df=11.4, p=0.97) and we did not find a positive correlation between testosterone levels and aggressiveness levels in X*Y (Fig 2b, Spearman test, S=210.6, p=0.44) nor in XX/XX* females (Spearman test, S=25.4, p=0.6).

Candidate gene expression

X*Y females had a significantly lower baseline expression level of *MaoA* than XX/XX* females (Fig 3a, Post-hoc comparison, p=0.0002), while we did not find a difference between females that experimented the resident-intruder assay (Post-hoc comparison, p=0.15). Interestingly, we found a significant difference in *MaoA* expression levels between baseline and following the agonistic assay in XX/XX* females (Post-hoc comparison, p=0.0002) but not in X*Y females (Post-hoc comparison,

p=0.65). However, we did not find a significant negative correlation between *MaoA* expression and aggressiveness levels in X*Y females (Fig 3b, S=35.7, p=0.9) nor in XX/XX* females (S=6.66, p=0.89). We did not find a significant difference in baseline *Th* expression levels between X*Y and XX/XX* females (Fig3,c Post-hoc comparison, p=0.1) nor after the resident-intruder experiments (Post-hoc comparison, p=0.44). However, *Th* expression levels were significantly lower following the resident-intruder experiments for both groups (Post-hoc comparison, X*Y, p=0.006; XX+XX*, p=0.02), when compared to baseline. We did not find a significant positive correlation between *Th* expression levels and aggressiveness in X*Y (Fig 3d, S=45.1 p=0.12) nor in XX/XX* females (S=6.66, p=0.11).

Discussion

Gonadal hormones and sex chromosomes interact to shape brain neural circuits underlying behaviours. Looking at aggression specifically, the role of steroid hormones and especially testosterone has been widely investigated and the latter has been defined as a key factor for this male-biased behaviour (e.g. Giammanco et al., 2005; Wu et al., 2009; Xu et al., 2012). However, there has been increasing evidence for the influence of sex chromosomes, with the expression of sex-linked genes or through the regulation of autosomal expression (Cases et al., 1995; Compaan et al., 1993; Everts et al., 1997; Gatewood et al., 2006; Godar et al., 2016; Kudryavtseva et al., 2017; Scott et al., 2008). Here, we encompassed an integrative framework correlating behaviours, hormonal levels and gene expression to understand the molecular bases of territorial aggression in X*Y females of the African pygmy mouse. Although our results reflect a lack of statistical power with only tendencies for an enhanced aggressiveness in X*Y females, our results showed that steroid hormones are unlikely to be responsible for territorial aggression in X*Y females conversely to sex-linked genes involved in the dopaminergic system, which appeared as strong candidates worth investigating further.

In this study, we reproduced the resident-intruder assay from a behavioural study by Saunders et al., (2016), where they showed that sex-reversed X*Y females were more aggressive than XX and XX* females. We did not find the same outcome with no significant differences between X*Y and XX/XX* females. In addition, our results showed that the effect size for aggressive behaviours in X*Y females was not as strong as the one reported eight years ago (experimentations were carried out in 2014), with a greater variance. Because we used individuals from the same colony, the lower aggressiveness level may reflect an artificial selection of highly aggressive X*Y females, which were harder to breed (i.e., males were killed and females were removed from breeding cages). In birds, it has been shown that one generation of captive breeding is sufficient for the loss of anti-predatory behaviours (Carrete & Tella, 2015). In our case, there has been a gap of about eight years between experimentations, with

approximately two generations per year (males and females remain together for *ca* 6 months in our breeding colony). It is thus likely that highest levels of aggressiveness were artificially selected against in our breeding facility. Consequently, the lack of significance may reflect a combination of a lower effect size and a lower sample size (i.e., low statistical power), especially considering the strong tendencies observed, and because one XX female drove the pattern in XX/XX* females.

One prime candidate to relate with territorial aggression in X*Y females was the male-biased hormone, testosterone. Testosterone is a key factor for the masculinization of brain neural pathways, either directly or through the aromatization of testosterone to estrogen (Han & De Vries, 2003; Phoenix, 2009; Phoenix et al., 1959; Wu et al., 2009). More precisely, testosterone has been shown to regulate social aggression in males, but also in females as illustrated in some bird species, rats and humans (Cantarero et al., 2015; Denson et al., 2018; Giammanco et al., 2005; Gill et al., 2007; Rose et al., 1971; Wu et al., 2009). Here, we did not find differences in testosterone levels between females. This pattern was also found in a recent study on baseline testosterone levels in *M. minutoides* and with comparable concentrations (i.e., ~ 1.5 ng/mL; Veyrunes et al., 2022). Furthermore, we did not find a correlation between testosterone and aggressiveness levels for X*Y females nor for XX/XX* females. A few hypotheses could explain the lack of correlation. First of all, it is likely that testosterone is not involved in females' territorial aggression in the African pygmy mouse. In the barred buttonquails (*Turnix suscitator*) for example, females are territorial and display aggressive behaviours, which are independent of testosterone secretions (Muck & Goymann, 2019). Secondly, the action of testosterone depends on its receptor, the androgen receptor (AR) (see Cunningham et al., 2012): testosterone binds to AR in specific regions of the brain, such as the ventromedial hypothalamus (VMH) tightly linked to female aggression (Hashikawa et al., 2017), where it modulates gene expression (Cunningham et al., 2012) and subsequent behaviours. Hence, similar testosterone levels does not rule out an effect of testosterone through an interaction with its receptor. It is also noteworthy that the *Ar* gene is on the X chromosome and therefore likely to be influenced by differences in sex chromosome complements between females (e.g., X dosage, divergence between X and X* copies). It would thus be necessary to quantify *Ar* expression levels in the brain and specific regions involved in females' aggressiveness to confirm or infirm the role of steroid hormones. Finally, female territorial aggression can depend on other steroid hormones. For instance, it has been shown that the ratio of testosterone over corticosterone was a more reliable measure to correlate with aggressiveness than testosterone itself (Montoya et al., 2012; Terburg et al., 2009). Interestingly, X*Y females have a lower basal level of corticosterone than XX and XX* females, but this difference disappears in stressful conditions (Veyrunes et al., 2022). Thus, the ratio testosterone:corticosterone is unlikely to be responsible for aggression as exposure to a male intruder is presumed to induces stress in a female

resident. On another hand, estrogens have also been shown to regulate female aggression in mice and humans (Denson et al., 2018; Hashikawa et al., 2017; Woodley & Moore, 1999), and aromatization of testosterone to estradiol is also a key factor in the masculinization of brain neural pathways (Wu et al., 2009). Though we did not investigate estradiol specifically in the brain, a recent investigation highlighted no differences in estradiol concentrations between female genotypes (Veyrunes et al., 2022). Because females do not show differences in concentration at adulthood, we assume they do not have differences in steroid hormone levels during fetal development as well, albeit it remained to be tested. On that note, it has been shown that the intrauterine hormonal environment could also influence aggressiveness, where females developing between two males are more aggressive than females developing with adjacent females (Ryan & Vandenbergh, 2002). However, in our case, it would imply that XX females are the most aggressive, as they are more likely to be subjected to androgens *in utero* (80% of offspring in XX litters are males; Saunders et al., 2022), which is not supported by our observations (i.e., X*Y females are the most aggressive). Thus, taken together, our results do not support a hormonal basis for territorial aggression in X*Y females.

A few sex-linked genes were also good candidates to correlate with differences in aggression between females. A prime candidate, though its influence is controversial (Gatewood et al., 2006; Lee & Harley, 2012; Lovell-Badge, 2005), was *Sry,* which is expressed in the brain of X*Y females (Rahmoun et al., 2014). We also assessed *Th* and *MaoA*, which regulate dopamine synthesis and degradation respectively, and which are known to control aggressive behaviours (Czech et al., 2012; Dewing et al., 2006; Korzan et al., 2006; Mahadevia et al., 2021). Furthermore*, MaoA* is in the non-recombining region between X and X* chromosomes, and is present in multiple copies on the X chromosome only (unpublished data), suggesting lower levels in X*Y females. It is also interesting to note that *Sry* has been shown to regulate *Th* and *MaoA*, albeit with both inhibitory and stimulating effect depending on the region of the brain for the latter (Lee et al., 2019; Lee & Harley, 2012; Wu et al., 2009). All things considered, *Sry*, *MaoA*, and *Th* were strong candidates to help identify the genetic basis of X*Y females' enhanced aggressiveness. Although we did not quantify *Sry* expression, *MaoA* and *Th* expression levels may support the role of the dopaminergic system: we found strong tendencies, some significant, for greater *Th* and lower *MaoA* levels in X*Y females, regardless of whether females experienced the behavioural assay or not. Our results corroborate the lower number of *MaoA* copies on the X* chromosome that suggested lower expression levels, and point towards greater levels of dopamine in X*Y females. This is in line with a previous study on the neural basis of parental behaviours in the African pygmy mouse, where dopamine seemed positively influenced by sex reversal as well (Heitzmann et al., 2022). Nevertheless, we did not find significant correlations between *MaoA*, *Th* and aggressiveness levels. It was also very striking that *MaoA* and *Th* expression

levels dropped drastically, between baseline and following the agonistic assay. While lower levels of *MaoA* were expected and were consistent with females displaying aggressive behaviours under stressful conditions, we would have expected, on the other hand, an increase of *Th* expression levels. This result could partly explain the difference in aggressiveness levels between X*Y females in our study and those from Saunders et al., (2016), and confirms the partial loss of highly aggressive phenotypes in our breeding colony. It also showed that we cannot differentiate between the treatment (i.e., agonistic assay) and a breeding facility effect in correlating *MaoA*/*Th* expression levels with aggressiveness. This strengthens the necessity to increase sample sizes and include control individuals of similar generation to compare phenotypic traits. Furthermore, combined with *in situ* hybridization in regions of the brain controlling aggression (e.g. VMH), further investigations should help unravel the role of the dopaminergic system and sex-linked genes in controlling aggressive behaviours in the African pygmy mouse.

Gonadal hormones have dominated the view of sex differences in brain and behaviours for centuries, especially the role of testosterone at young developmental stages and adulthood (see Arnold, 2009; Breedlove et al., 1999). However, it is now well stated that sex chromosomes and sex-linked genes have a direct influence on sexual dimorphism as well. Our results seem to support the influence of sex chromosomes and suggest that sex-linked genes rather than steroid hormones are likely to regulate and shape X*Y females' territorial aggression in the African pygmy mouse. This fascinating system, along with other unusual sex determination systems, offer great opportunities to investigate the genetic basis of sexual phenotypes and to disentangle the direct role of sex chromosomes and gonadal hormones in shaping sexual dimorphism.

Acknowledgements

We thank the CECEMA for the housing of animals and Marie Challe for her assistance on the maintenance of the breeding colony. We also than the Genseq Platform for allowing us to perform RT-qPCR and Philippe Clair for his assistance on RT-qPCR as well as on data analysis on the LightCycler 480 software.

References

Albert, D. J., Jonik, R. H., Walsh, M. L., & Petrovic, D. M. (1989). Testosterone supports hormone-dependent aggression in female rats. *Physiology & Behavior*, *46*(2), 185–189. https://doi.org/10.1016/0031-9384(89)90253-9

Arnold, A. P. (2009). The organizational-activational hypothesis as the foundation for a unified theory of sexual differentiation of all mammalian tissues. *Hormones and Behavior*, *55*(5), 570–578. https://doi.org/10.1016/j.yhbeh.2009.03.011

Arnold, A. P., & Breedlove, S. M. (1985). Organizational and activational effects of sex steroids on brain and behavior: A reanalysis. *Hormones and Behavior*, *19*(4), 469–498. https://doi.org/10.1016/0018-506X(85)90042-X

Book, A. S., Starzyk, K. B., & Quinsey, V. L. (2001). The relationship between testosterone and aggression: A meta-analysis. *Aggression and Violent Behavior*, *6*(6), 579–599. https://doi.org/10.1016/S1359-1789(00)00032-X

Breedlove, S. M., Cooke, B. M., & Jordan, C. L. (1999). The Orthodox View of Brain Sexual Differentiation. *Brain, Behavior and Evolution*, *54*(1), 8–14. https://doi.org/10.1159/000006607

Cantarero, A., Laaksonen, T., Järvistö, P. E., Gil, D., López-Arrabé, J., Redondo, A. J., & Moreno, J. (2015). Nest Defence Behaviour and Testosterone Levels in Female Pied Flycatchers. *Ethology*, *121*(10), 946–957. https://doi.org/10.1111/eth.12407

Carrete, M., & Tella, J. L. (2015). Rapid loss of antipredatory behaviour in captive-bred birds is linked to current avian invasions. *Scientific Reports*, *5*(1), 18274. https://doi.org/10.1038/srep18274

Cases, O., Seif, I., Grimsby, J., Gaspar, P., Chen, K., Pournin, S., Müller, U., Aguet, M., Babinet, C., Shih, J. C., & De Maeyer, E. (1995). Aggressive Behavior and Altered Amounts of Brain Serotonin and Norepinephrine in Mice Lacking MAOA. *Science*, *268*(5218), 1763–1766. https://doi.org/10.1126/science.7792602

Compaan, J. C., Buijs, R. M., Pool, C. W., De Ruiter, A. J. H., & koolhaas, J. M. (1993). Differential lateral septal vasopressin innervation in aggressive and nonaggressive male mice. *Brain Research Bulletin*, *30*(1–2), 1–6. https://doi.org/10.1016/0361-9230(93)90032-7

Cunningham, R. L., Lumia, A. R., & McGinnis, M. Y. (2012). Androgen Receptors, Sex Behavior, and Aggression. *Neuroendocrinology*, *96*(2), 131–140. https://doi.org/10.1159/000337663

Czech, D. P., Lee, J., Sim, H., Parish, C. L., Vilain, E., & Harley, V. R. (2012). The human testis-determining factor SRY localizes in midbrain dopamine neurons and regulates multiple components of catecholamine synthesis and metabolism. *Journal of Neurochemistry*, *122*(2), 260–271. https://doi.org/10.1111/j.1471-4159.2012.07782.x

Darwin, C. (1871). *The Descent of Man and Selection in Relationship to Sex*. London, UK: John Murray

Denson, T. F., O'Dean, S. M., Blake, K. R., & Beames, J. R. (2018). Aggression in Women: Behavior, Brain and Hormones. *Frontiers in Behavioral Neuroscience*, *12*, 81. https://doi.org/10.3389/fnbeh.2018.00081

Dewing, P., Chiang, C. W. K., Sinchak, K., Sim, H., Fernagut, P. O., Kelly, S., Chesselet, M. F., Micevych, P. E., Albrecht, K. H., Harley, V. R., & Vilain, E. (2006). Direct regulation of adult brain function by the male-specific factor SRY. *Current Biology*, *16*(4), 415–420. https://doi.org/10.1016/j.cub.2006.01.017

Everts, H. G. J., De Ruiter, A. J. H., & Koolhaas, J. M. (1997). Differential Lateral Septal Vasopressin in Wild-type Rats: Correlation with Aggression. *Hormones and Behavior*, *31*(2), 136–144. https://doi.org/10.1006/HBEH.1997.1375

Gatewood, J. D., Wills, A., Shetty, S., Xu, J., Arnold, A. P., Burgoyne, P. S., & Rissman, E. F. (2006). Sex chromosome complement and gonadal sex influence aggressive and parental behaviors in mice. *Journal of Neuroscience*, *26*(8), 2335–2342. https://doi.org/10.1523/JNEUROSCI.3743-05.2006

Gennotte, V., Akonkwa, B., Mélard, C., Denoël, M., Cornil, C. A., & Rougeot, C. (2017). Do sex reversal procedures differentially affect agonistic behaviors and sex steroid levels depending on the sexual genotype in Nile tilapia? *Journal of Experimental Zoology Part A: Ecological and Integrative Physiology*, *327*(4), 153–162. https://doi.org/10.1002/jez.2080

Giammanco, M., Tabacchi, G., Giammanco, S., Di Majo, D., & La Guardia, M. (2005). Testosterone and aggressiveness. *Medical Science Monitor: International Medical Journal of Experimental and Clinical Research*, *11*(4), RA136-145.

Gill, S. A., Alfson, E. D., & Hau, M. (2007). Context matters: Female aggression and testosterone in a year-round territorial neotropical songbird (Thryothorus leucotis). *Proceedings of the Royal Society B: Biological Sciences*, *274*, 2187–2194. https://doi.org/10.1098/rspb.2007.0457

Ginot, S., Claude, J., Perez, J., & Veyrunes, F. (2017). Sex reversal induces size and performance differences among females of the African pygmy mouse, Mus minutoides. *Journal of Experimental Biology*, *220*(11), 1947–1951. https://doi.org/10.1242/JEB.157552

Godar, S. C., Fite, P. J., Mcfarlin, K. M., & Bortolato, M. (2016). The role of monoamine oxidase A in aggression: Current translational developments and future challenges HHS Public Access. *Prog Neuropsychopharmacol Biol Psychiatry*, *69*, 90–100. https://doi.org/10.1016/j.pnpbp

Guillot, P. V., Carlier, M., Maxson, S. C., & Roubertoux, P. L. (1995). Intermale aggression tested in two procedures, using four inbred strains of mice and their reciprocal congenics: Y chromosomal implications. *Behavior Genetics*, *25*(4), 357–360. https://doi.org/10.1007/BF02197285

Han, T. M., & De Vries, G. J. (2003). Organizational effects of testosterone, estradiol, and dihydrotestosterone on vasopressin mRNA expression in the bed nucleus of the stria terminalis. *Journal of Neurobiology*, *54*(3), 502–510. https://doi.org/10.1002/neu.10157

Hashikawa, K., Hashikawa, Y., Tremblay, R., Zhang, J., Feng, J. E., Sabol, A., Piper, W. T., Lee, H., Rudy, B., & Lin, D. (2017). Esr1+ cells in the ventromedial hypothalamus control female aggression. *Nature Neuroscience*, *20*(11), 1580–1590. https://doi.org/10.1038/nn.4644

Heitzmann, L., Challe, M., Perez, J., Castell, L., Galibert, E., Martin, A., Valjent, E., & Veyrunes, F. (2022). Genotypic sex shapes maternal care in the African Pygmy mouse, Mus minutoides. *BioRxiv*. https://doi.org/10.1101/2022.04.05.487174

Hyde, J. S., & Sawyer, T. F. (1977). Estrous cycle fluctuations in aggressiveness of house mice. *Hormones and Behavior*, *9*(3), 290–295. https://doi.org/10.1016/0018-506X(77)90064-2

Korzan, W. J., Forster, G. L., Watt, M. J., & Summers, C. H. (2006). Dopaminergic activity modulation via aggression, status, and a visual social signal. *Behavioral Neuroscience*, *120*(1), 93–102. https://doi.org/10.1037/0735-7044.120.1.93

Kudryavtseva, N. N., Smagin, D. A., Kovalenko, I. L., Galyamina, A. G., Vishnivetskaya, G. B., Babenko, V. N., & Orlov, Y. L. (2017). Serotonergic genes in the development of

anxiety/depression-like state and pathology of aggressive behavior in male mice: RNA-seq data. *Molecular Biology*, *51*(2), 251–262. https://doi.org/10.1134/S0026893317020133

Lee, J., & Harley, V. R. (2012). The male fight-flight response: A result of SRY regulation of catecholamines? *BioEssays*, *34*(6), 454–457. https://doi.org/10.1002/bies.201100159

Lee, J., Pinares-Garcia, P., Loke, H., Ham, S., Vilain, E., & Harley, V. R. (2019). Sex-specific neuroprotection by inhibition of the Y-chromosome gene, SRY, in experimental Parkinson's disease. *Proceedings of the National Academy of Sciences of the United States of America*, *116*(33), 16577–16582. https://doi.org/10.1073/pnas.1900406116

Lovell-Badge, R. (2005). Aggressive behaviour: Contributions from genes on the Y chromosome. *Novartis Foundation Symposium*, *268*, 20–33. https://doi.org/10.1002/0470010703.ch3

Mahadevia, D., Saha, R., Manganaro, A., Chuhma, N., Ziolkowski-Blake, A., Morgan, A. A., Dumitriu, D., Rayport, S., & Ansorge, M. S. (2021). Dopamine promotes aggression in mice via ventral tegmental area to lateral septum projections. *Nature Communications*, *12*(1). https://doi.org/10.1038/S41467-021-27092-Z

Montoya, E. R., Terburg, D., Bos, P. A., & van Honk, J. (2012). Testosterone, cortisol, and serotonin as key regulators of social aggression: A review and theoretical perspective. *Motivation and Emotion*, *36*(1), 65–73. https://doi.org/10.1007/s11031-011-9264-3

Mortaud, S., Nicolas, L., Pinoteau, W., Tordjman, S., Carlier, M., & Roubertoux, P. L. (2010). Brain pathways mediating the pro-aggressive effect of the steroid sulfatase (Sts) gene. *Behavior Genetics*, *40*(2), 211–219. https://doi.org/10.1007/s10519-010-9340-6

Muck, C., & Goymann, W. (2019). Exogenous testosterone does not modulate aggression in sex-role-reversed female Barred Buttonquails, Turnix suscitator. *Journal of Ornithology*, *160*(2), 399–407. https://doi.org/10.1007/s10336-018-1615-3

Oliveira, V. E. deMoura, Lukas, M., Wolf, H. N., Durante, E., Lorenz, A., Mayer, A.-L., Bludau, A., Bosch, O. J., Grinevich, V., Egger, V., De Jong, T. R., & Neumann, I. D. (2021). Oxytocin and vasopressin within the ventral and dorsal lateral septum modulate aggression in female rats. *Nature Communications*, *12*, 2900. https://doi.org/10.1038/s41467-021-23064-5

Pandolfi, M., Scaia, M. F., & Paz, M. F. (2021). Sexual Dimorphism in Aggression: Sex-Specific Fighting Strategies Across Species. *Frontiers in Behavioural Neuroscience*, *15,* 659615. https://doi.org/10.3389/fnbeh.2021.659615

Phoenix, C. H. (2009). Organizing action of prenatally administered testosterone propionate on the Tissues mediating mating behavior in the female guinea pig. *Hormones and Behavior*, *55*(5), 566–566. https://doi.org/10.1016/j.yhbeh.2009.01.004

Phoenix, C. H., Goy, R. W., Gerall, A. A., & Young, W. C. (1959). Organizing action of prenatally administered testosterone propionate on the tissues mediating mating behavior in the female guinea pig. *Endocrinology*, *65*, 369–382. https://doi.org/10.1210/endo-65-3-369

Rahmoun, M., Perez, J., Saunders, P. A., Boizet-Bonhoure, B., Wilhelm, D., Poulat, F., & Veyrunes, F. (2014). Anatomical and molecular analyses of XY ovaries from the african pygmy mouse Mus minutoides. *Sexual Development*, *8*(6), 356–363. https://doi.org/10.1159/000368664

R core Team. (2022). *R: A Language and Environment for Statistical Computing*. R Foundation for Statistical Computing. https://www.r-project.org/

Re, L., & Birkhoff, J. M. (2015). The 47,XYY syndrome, 50 years of certainties and doubts: A systematic review. *Aggression and Violent Behavior*, *22*, 9–17. https://doi.org/10.1016/J.AVB.2015.02.003

Rose, R. M., Holaday, J. W., & Bernstein, I. S. (1971). Plasma Testosterone, Dominance Rank and Aggressive Behaviour in Male Rhesus Monkeys. *Nature*, *231*(5302), 366–368. https://doi.org/10.1038/231366a0

Ryan, B. C., & Vandenbergh, J. G. (2002). Intrauterine position effects. *Neuroscience & Biobehavioral Reviews, 26*(6), 665-678. https://doi.org/10.1016/S0149-7634(02)00038-6

Saunders, P. A., Franco, T., Sottas, C., Maurice, T., Ganem, G., & Veyrunes, F. (2016). Masculinised Behaviour of XY Females in a Mammal with Naturally Occuring Sex Reversal. *Scientific Reports*, *6*, 1–9. https://doi.org/10.1038/srep22881

Saunders, P. A., Perez, J., Ronce, O., & Veyrunes, F. (2022). Multiple sex chromosome drivers in a mammal with three sex chromosomes. *Current Biology*, *32*(9), 2001-2010.e3. https://doi.org/10.1016/j.cub.2022.03.029

Saunders, P. A., & Veyrunes, F. (2021). Unusual Mammalian Sex Determination Systems: A Cabinet of Curiosities. *Genes*, *12*(11), 1770–1770. https://doi.org/10.3390/GENES12111770

Scott, A. L., Bortolato, M., Chen, K., & Shih, J. C. (2008). Novel monoamine oxidase A knock out mice with human-like spontaneous mutation. *Neuroreport*, *19*(7), 739–739. https://doi.org/10.1097/WNR.0B013E3282FD6E88

Shih, J. C., Chen, K., & Ridd, M. J. (1999). Role of MAO A and B in neurotransmitter metabolism and behavior. *Polish Journal of Pharmacology*, *51*(1), 25–29.

Sluyter, F., Van Oortmerssen, G. A., De Ruiter, A. J. H., & Koolhaas, J. M. (1996). Aggression in wild house mice: Current state of affairs. *Behavior Genetics*, *26*(5), 489–496. https://doi.org/10.1007/BF02359753

Terburg, D., Morgan, B., & van Honk, J. (2009). The testosterone–cortisol ratio: A hormonal marker for proneness to social aggression. *International Journal of Law and Psychiatry*, *32*(4), 216–223. https://doi.org/10.1016/J.IJLP.2009.04.008

van Erp, A. M. M., & Miczek, K. A. (2000). Aggressive Behavior, Increased Accumbal Dopamine, and Decreased Cortical Serotonin in Rats. *The Journal of Neuroscience*, *20*(24), 9320–9325. https://doi.org/10.1523/JNEUROSCI.20-24-09320.2000

Veyrunes, F., Chevret, P., Catalan, J., Castiglia, R., Watson, J., Dobigny, G., Robinson, T. J., & Britton-Davidian, J. (2010a). A novel sex determination system in a close relative of the house mouse. *Proceedings of the Royal Society B: Biological Sciences*, *277*(1684), 1049–1056. https://doi.org/10.1098/rspb.2009.1925

Veyrunes, F., Catalan, J., Tatard, C., Cellier-Holzem, E., Watson, J., Chevret, P., Robinson, T. J., & Britton-Davidian, J. (2010b). Mitochondrial and chromosomal insights into karyotypic evolution of the pygmy mouse, Mus minutoides, in South Africa. *Chromosome Research*, *18*(5), 563–574. https://doi.org/10.1007/s10577-010-9144-9

Veyrunes, F., Dobigny, G., Yang, F., O'Brien, P. C. M., Catalan, J., Robinson, T. J., & Britton-Davidian, J. (2006). Phylogenomics of the genus Mus (Rodentia; Muridae): Extensive genome repatterning is not restricted to the house mouse. *Proceedings of the Royal Society B: Biological Sciences*, *273*(1604), 2925–2934. https://doi.org/10.1098/rspb.2006.3670

Veyrunes, F., Perez, J., Heitzmann, L., Saunders, P. A., & Givalois, L. (2022). Separating the effects of sex hormones and sex chromosomes on behavior in the African pygmy mouse *Mus minutoides,* a species with XY female sex reversal [Preprint]. Evolutionary Biology. https://doi.org/10.1101/2022.07.11.499546

Woodley, S. K., & Moore, M. C. (1999). Female territorial aggression and steroid hormones in mountain spiny lizards. *Animal Behaviour*, *57*(5), 1083–1089. https://doi.org/10.1006/anbe.1998.1080

Wu, M. V., Manoli, D. S., Fraser, E. J., Coats, J. K., Tollkuhn, J., Honda, S. I., Harada, N., & Shah, N. M. (2009). Estrogen Masculinizes Neural Pathways and Sex-Specific Behaviors. *Cell*, *139*(1), 61–72. https://doi.org/10.1016/j.cell.2009.07.036

Xu, X., Coats, J. K., Yang, C. F., Wang, A., Ahmed, O. M., Alvarado, M., Izumi, T., & Shah, N. M. (2012). Modular genetic control of sexually dimorphic behaviors. *Cell*, *148*(3), 596–607. https://doi.org/10.1016/j.cell.2011.12.018

Yamaguchi, T., & Lin, D. (2018). Functions of medial hypothalamic and mesolimbic dopamine circuitries in aggression. *Current Opinion in Behavioral Sciences*, *24*, 104–112. https://doi.org/10.1016/J.COBEHA.2018.06.011

Figures

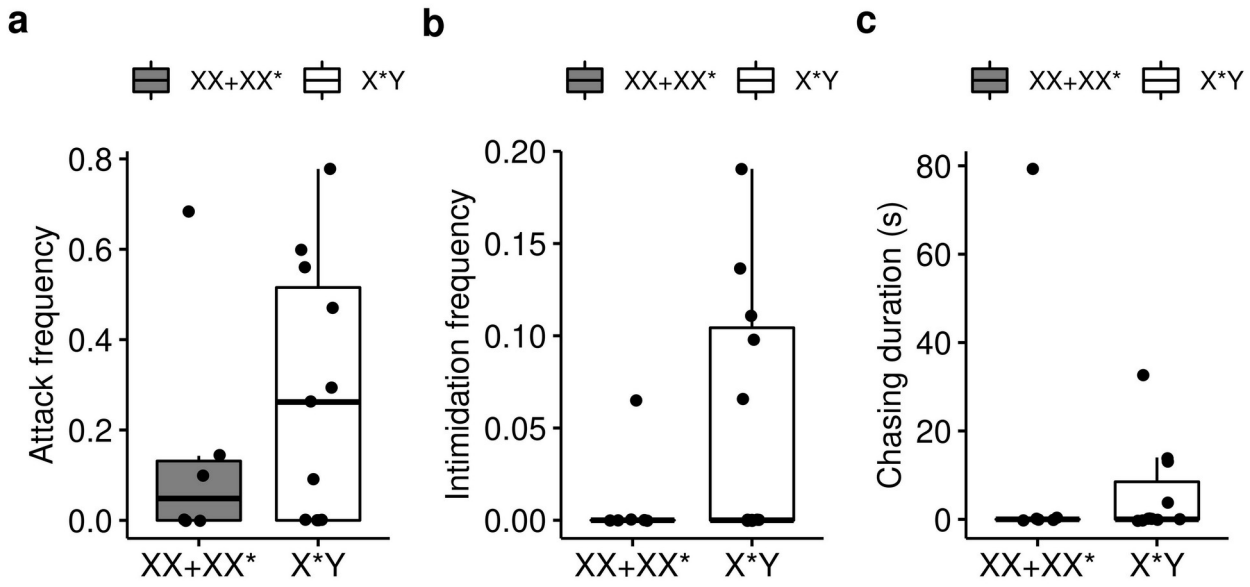

Figure 1. Tendency for enhanced aggressiveness in X*Y females. **a,b,** Frequency of attacks and intimidations towards a male intruder : number of attacks or offensive postures standardized by the overall number of female-male interactions. **c,** Cumulated chasing duration in seconds. XX and XX* females formed the control group with low aggressiveness (Saunders et al., 2016). Black dots represent raw data. N_{XX+XX*}=6 and n_{X*Y}=11.

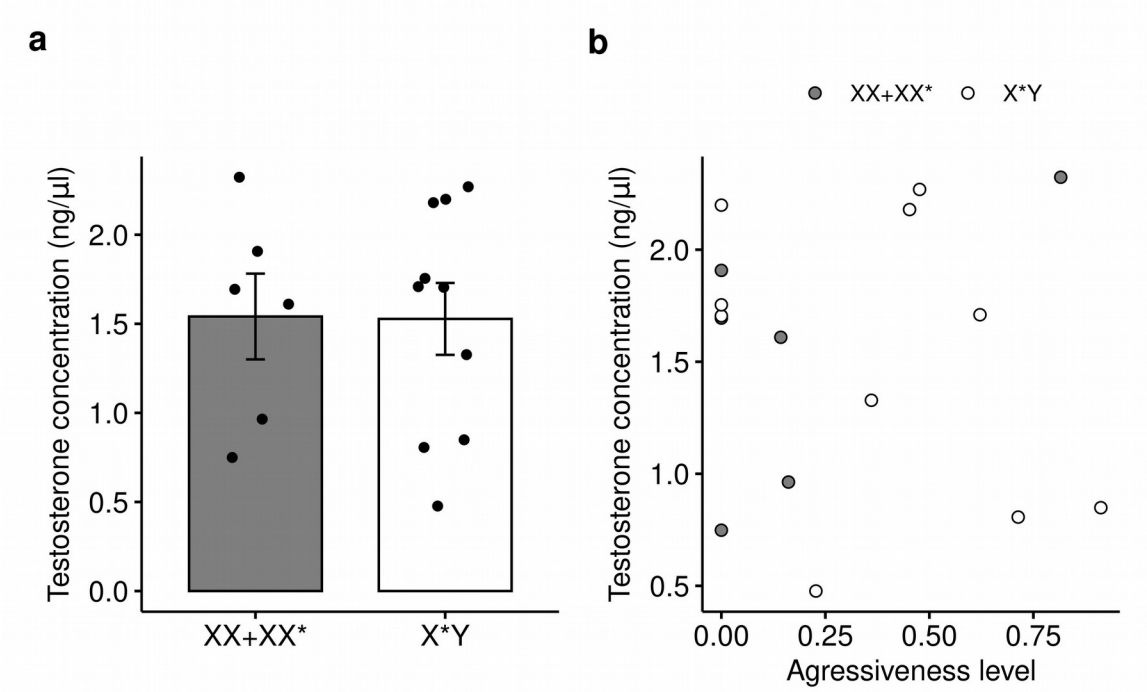

Figure 2. No correlation between testosterone and aggressiveness levels. **a,** Serum testosterone concentrations in X*Y and XX/XX* females following the resident-intruder test. Bars are mean ± s.e.m and black dots represent raw data. **b,** Correlation between aggressiveness and testosterone levels. XX and XX* females formed the control group with low aggressiveness (Saunders et al., 2016). N_{XX+XX*}=6 and n_{X*Y}=10.

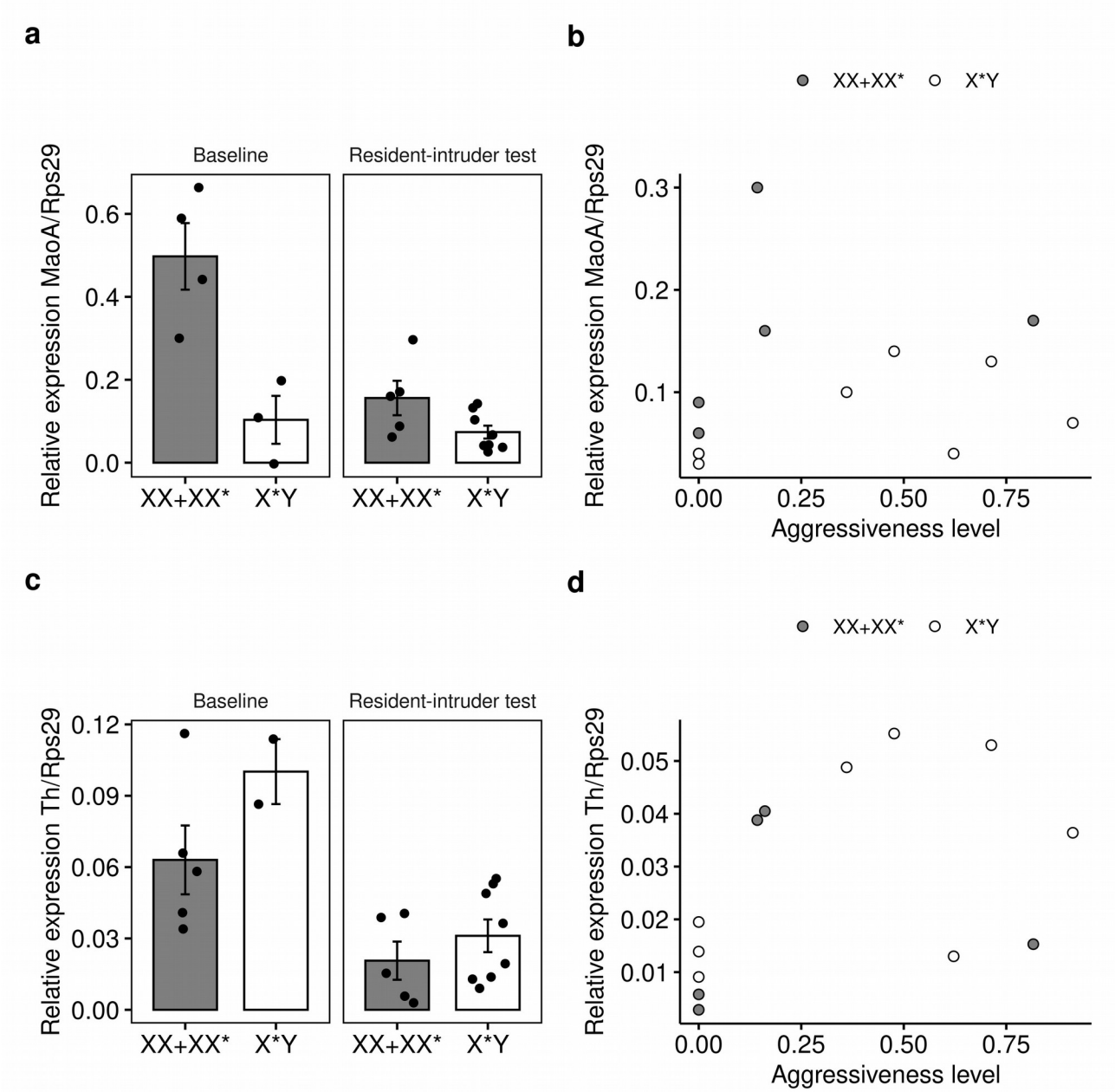

Figure 3. No correlation between *Th*, *MaoA* and aggressiveness levels. **a,c** Relative expression of *MaoA* (**a**) and *Th* (**c**) in X*Y and XX/XX* females at baseline and after the resident-intruder test. Bars are mean ± s.e.m and black dots represent raw data. **b,d**, Correlation between aggressiveness and *MaoA* (**b**) or *Th* (**d**) levels. XX and XX* females formed the control group with low aggressiveness (Saunders et al., 2016). *MaoA,* baseline N_{XX+XX*}=4 and n_{X*Y} =3 ; resident-intruder assay, N_{XX+XX*}= 5 and n_{X*Y} =8 ; *Th,* baseline N_{XX+XX*}=5 and n_{X*Y} =2 ; resident-intruder, N_{XX+XX*}= 5 and n_{X*Y} =8.

Gene name		Primer sequence (5'-3')	Annealing temperature	Product size
Sry	Forward	TTCCAGGAGGCACAGAGACT	60°C	333 bp
	Reverse	GTGTTGGAACTCGTGCTGAA		
Th	Forward	AGTGCACACAGTACATCCGTCATGC	60°C	Unknown
	Reverse	AATGTCCTGGGAGAACTGGGCAAATG		
MaoA	Forward	GGGCTGTCATCAAGTGCATG	60°C	Unknown
	Reverse	TGAAATTGGAGCCTCCTCATCA		

Table 1. Sequences of primers used for RT-qPCR.

Part 2: Sexual differentiation of the brain transcriptome

Chapter 4

Brain transcriptomic architecture of a wild mouse species with sex reversal: a three sex chromosome orchestra

Louise D. Heitzmann, Paul A. Saunders, Julie Perez, Pierre Boursot* & Frederic Veyrunes*

* equal contribution

Foreword

In this section, we i) investigate the consequences of sex reversal on the brain transcriptome, ii) seek for candidate genes at the molecular bases of the different female phenotypes highlighted in the previous sections as well as before this thesis, and iii) discuss the relative contributions of sex and neo-sex chromosomes in driving the differentiation of the brain transcriptome and sex-linked phenotypes. Some of our analyses are based on the work done by Dr. Paul Saunders in another study on sex and neo-sex chromosomes' evolution (see chapter 5): genome assembly, anchoring on *Mus musculus* genome to identify genomic regions, analysis of orthology with *M. musculus* to retrieve gene names, identification of non-recombining regions, SNP calling to detect allelic variants and masking the reference genome. Because these data are not published yet, we referred to them as "(Saunders et al., in prep)" in the main text. The study of Saunders et al., will be published prior to this work.

Brain transcriptomic architecture of a wild mouse species with sex reversal: a three sex chromosome orchestra

Louise D. Heitzmann, Paul A. Saunders, Julie Perez, Pierre Boursot & Frederic Veyrunes

Institut des Sciences de l'Evolution de Montpellier (ISEM), Université de Montpellier / CNRS / IRD, France

Gonadal hormones and sex chromosomes drive sex differences in the brain and subsequent phenotypes. However, the relative contribution of both factors has remained elusive because gonadal and genotypic sex are usually confounded. The African pygmy mouse, *Mus minutoides*, has a polygenic sex determination system involving a dissociation between gonadal and genotypic sexes. In natural populations, there is one male genotype, XY, but three female genotypes: XX, XX* and X*Y, due to a feminizing X* chromosome. In addition, all sex chromosomes are fused to autosomes, generating neo-X, neo-X* and neo-Y sex chromosomes. X*Y females display striking phenotypic divergences when compared to the other females: a greater ovulation rate, divergent maternal behaviours and enhanced aggressiveness. These phenotypes suggest underlying divergences in the brain transcriptome, that would thus be influenced by the sex chromosome complement (through the direct expression of sex-linked genes and the regulation of autosomal expression, or via hormones). Here, we compare the brain transcriptome of the four sexual genotypes in *M. minutoid*es. We report that, although the brain transcriptome mainly reflects gonadal sex (83% of differentially expressed genes), sex chromosomes have a pervasive interacting influence as well, which is predominant for a significant proportion (17%) of genes, whose expression patterns corroborate the different female phenotypes. These differentially expressed genes are enriched on sex and neo-sex chromosomes, suggesting a direct role of the sex chromosome complement, and an evolutionary dynamic triggered by the new mode of transmission of sex chromosomes. Furthermore, our analysis sheds light on several candidate genes to correlate with phenotypic variations observed between females: genes involved in reproductive functions (e.g. *Amhr2*), or social behaviours through the dopaminergic pathway (e.g. *MaoA*). Finally, we found a preferential expression of X over X* alleles, suggesting a skewed inactivation of the X* chromosome in the brain of XX* females. All things considered, we show that the sex determination system has profoundly impacted the brain transcriptome, which brings exciting prospects on the molecular bases of sexual dimorphism and the resolution of sexual conflict.

Key-words: Gonadal sex, sex chromosomes, sex reversal, third sexual phenotype, brain transcriptome, sexual conflicts

Introduction

Sex differences in brain and behaviours are commonly assumed to be driven by gonadal hormones, which influence the brain transcriptome, i.e., gene expression and, subsequently, various phenotypes. Although males and females share most or even their entire genome, they show sex-specific patterns of gene expression likely to influence behavioural and reproductive phenotypes (Nishida et al., 2005; Pointer et al., 2013; Ellegren & Parsch, 2007; Rayner et al., 2019; Ngun et al., 2014). One main hypothesis to explain such differences is related to the divergence in males and females' optimum for fitness-related traits that depend on the same genes. Accordingly, divergences of phenotypic optima between the sexes lead to sex-specific selective pressures and, possibly, to intra-locus sexual conflicts, that can be mitigated or solved through sex-biased gene expression (Ellegren & Parsch, 2007; Mank, 2017; Wright et al., 2018; Lichilín et al., 2021). On that note, heteromorphic sex chromosomes found in many species are thought to play a substantial role in sexual differentiation: their sex-specific transmission pattern allows their specialisation to optimise phenotypes of one, or the other sex (Graves, 2006; Mank, 2009a; Mueller et al., 2013; Rice, 1984), although equivocal (see Dean & Mank, 2014). This is especially expected for non-recombining sex chromosomes (Y or W) because they are transmitted by one sex only in comparison to recombining sex chromosomes (X or Z), for which there is an interplay between sex-biased transmission (e.g the X is more often transmitted by females) and sex-linked ploidy (which affects the efficacy of selection depending on dominance) (Mank, 2009b, Rice, 1984; Trivers, 1988). Sex chromosomes are thus expected to be enriched for genes with a sex-biased expression, which can impact brain sexual differentiation, either directly (sex-linked gene expression and through the regulation of autosomal genes), or indirectly by influencing hormones, which in turn, control gene expression (Wijchers et al., 2010; Blencowe et al., 2022). This state-of-art has led to many researches evaluating the genetic bases of sexual dimorphism and sexual conflicts, as well as contributing to disentangle the relative part of gonadal hormones and sex chromosomes on brain sexual differentiation.

In vertebrates with genetic sex determination (GSD), and especially with differentiated sex chromosomes, sexual differentiation of the brain is known to be influenced by gonadal hormones, but

the role of sex chromosomes has been widely neglected (Han & De Vries, 2003; Van Nas et al., 2009; Blencowe et al., 2022; Peterson et al., 2013; Wu et al., 2009; Arnold, 2020; Konkle & McCarthy; 2011; Wostenholme et al., 2013; Breedlove et al., 2009). During the perinatal period (i.e., organizational period) and at adulthood (i.e., activational period), surges of testosterone and aromatization of testosterone to estrogen act to masculinize brain neural circuits, as witnessed by patterns of gene expression (Han & De Vries, 2003; Morris et al., 2004; Arnold, 2009; Konkle & McCarthy, 2011; Peterson et al., 2013; Blencowe et al., 2022). However, it must be noted that sex-biased expression arises before gonadal differentiation and thus, hormonal secretions (Hale et al., 2011; Ayers et al., 2013; Arnold, 2004: Ma et al., 2018), illustrating the incompleteness of the hormone-centered view of brain sexual differentiation (Breedlove et al., 1999; Carruth et al., 2002; Arnold, 2009). This also suggests that sex chromosomes play a role in the sexual differentiation of the brain, early in ontogeny. However, in most studies, hormones and sex chromosomes are so intrinsically confounded that it is hard to decipher the relative contribution of both factors.

A handful of studies have investigated the relative influence of sex chromosomes and gonads on the transcriptional architecture of non-gonadal tissues, highlighting a prevalent effect of gonads, and thus, hormones (Blencowe et al., 2022; Ma et al., 2018; Ortega et al., 2019). Some of these studies relied on genetically modified mouse models, and interpretations should be done with caution due to, for instance, pleiotropic effects of mutations, or due to a fixed genetic background, which can influence phenotypes as well (Barthold, 2004; Blencowe et al., 2022; Bućan & Abel, 2002). On the other hand, the few studies on non-model species with naturally occurring sex reversal showed no phenotypic variation, depicting a relatively small contribution of sex chromosomes in driving sexual differentiation (Ma et al., 2018; Veltsos et al., 2019). The African pygmy mouse, *Mus minutoides*, naturally possesses three sex chromosomes: the classical X and Y plus a feminizing X* chromosome. The latter originates from a still unknown feminizing mutation on the X chromosome, that overrides the effect of *Sry* (Veyrunes et al., 2013). The X* stopped recombining with the X chromosome over 2/3 of the length of the X chromosome. Moreover, in this species, all sex chromosomes fused to autosomes (i.e., neo-

sex chromosomes), with non-recombining regions between neo-X, neo-X* and neo-Y genomic regions as well (fig.1). The emergence of the X* has led to three female genotypes in natural populations: XX, XX* and X*Y, while males are XY. Interestingly, X*Y adult females have functional gonads with a typical ovarian structure (Rahmoun et al., 2014). However, previous studies showed that X*Y females diverge from the other females in terms of reproductive traits (e.g. they have a greater ovulation rate; Saunders et al., 2014), social and parental behaviours (Saunders et al., 2016; Heitzmann et al., 2022) as well as bite performance and skull morphology (Ginot et al., 2017). They also display some traits that are considered as male-typical: anxiety-related behaviours, aggressiveness and corticosterone levels (Saunders et al., 2016; Ginot et al., 2017; Veyrunes et al., 2022). These differences have shed light on a new sexual phenotype shaped by sex chromosomes, and likely to reflect differences in gene expression between genotypes. In this study, we evaluated the influence of sex chromosomes (including neo-sex chromosomes) on the brain transcriptomic architecture of the four genotypes. We aim to understand whether gene expression reflects gonadal (i.e., male or female) or genotypic sex defined by the sex chromosome complement (i.e., XX, XX*, X*Y and XY). Furthermore, using overall and allele-specific expression of genes, we pinpoint potential candidates for the molecular bases of female phenotypical divergences, and discuss the relative part of each sex chromosome in shaping the three sexual phenotypes in *M.minutoides*.

Material & Methods

a) Animals and sampling

Animals were bred in our breeding colony at the university of Montpellier (CECEMA facilities). The colony was established from wild caught animals in the Caledon Nature reserve, in South Africa (Veyrunes et al., 2010; see Heitzmann et al,. 2022 for further details on rearing conditions). In this study, we sampled the whole brain of 20 virgin individuals (5 per genotype: XX, XX*, X*Y and XY) aged between 5-9 months old. Females were genotyped by PCR of *Sry* using gDNA extracted from tail tip biopsies following Veyrunes et al. (2010a) or by karyotyping using bone marrow of yeast-stimulated individuals (see Veyrunes et al., 2010b). We used unrelated individuals when possible, but

some related animals (siblings) have been included both within and between genotypic groups. Mice were euthanized by cervical dislocation and whole brains were collected and preserved in 2 mL tubes with RNAlater® (ThermoFisher). Samples were maintained at 4°C for 48 hours and then stored at -80°C until processing. Whole brain RNA was extracted under a sterile environment following RNeasy® Plus Mini Kit (Qiagen) protocol for animal tissue, with three steps: tissue disruption, homogeneization and RNA purification. Brains were grounded into a fine powder in liquid nitrogen using a pestle and a mortar to assure cell membranes' disruption. Tissue were then homogenized with a lysis buffer consisting of 24 µL of β-mercapto added to 2400 µL of RLT Plus (4x volume recommendations for 20-30 mg of tissue). After homogenization, we split the lysate into four tubes to prevent columns' clogging during RNA purification. We purified two tubes per sample following the manufacturer's provided protocol and stored the other two at -80°C. Total RNA was eluted in 50 µL of RNase-free water and stored at -80°C until further use.

b) Sequencing and mapping

Stranded RNA-seq libraries preparation and cDNA sequencing were performed by Fasteris SA (Switzerland) using an Illumina HiSeq 3000/4000. Sequencing generated ~13-20 millions of 150 pb paired-end reads per sample. We assessed quality control of the samples using FastQC v0.11.5. Reads were filtered and trimmed using cutadapt v1.15 to keep reads with a minimal quality of 30, a minimal length of 75 pb and to remove adapters as well as N flanking bases (*-q 30 -m 75 -a AGATCGGAAGAGC -A AGATCGGAAGAGC –trim-n*). Trimmed reads were then mapped on our XX reference genome (https://www.ncbi.nlm.nih.gov/data-hub/genome/GCA_902729485.2/), which was masked for fixed SNPs between sex chromosomes (i.e., sequence divergence) to account for mapping bias using STAR software v2.5. We used the XX reference genome to avoid further mapping issues due to a chimeric assembly of the X*Y genome. We allowed for 3 mismatch in 150 pb paired-end reads, marked duplicated as well as multi-mapper reads, and sorted reads by coordinates using the command lines *--outFilterMismatchNoverLmax 0.02 --bamRemoveDuplicatesType UniqueIdentical --outSAMtype BAM SortedByCoordinate*. We then performed gene quantification using the

featureCounts software from the subread v1.6 package, for reverse stranded data, at the exon level and with a minimum mapping quality score of 10 (*-f exon -Q 10 -s 2*). The latter returned a text file per sample, including read counts for each gene annotated on the XX reference genome.

c) Differential expression analysis

Read counts were filtered to keep genes with a minimal coverage of 10 reads in at least 5 individuals (i.e., size of each genotypic group) and subsequent gene expression analysis was performed using EdgeR. We made multiple pairwise comparisons between the four genotypes (i.e., 6 contrasts, e.g. XX *vs* X*Y) to detect genes that were differentially expressed between at least one contrast of genotype, with a Benjamini-Hochberg correction for multiple testing. Genes with a fold-change value greater or equal 1.5, and with a false discovery rate (FDR) below or equal 5% were considered as differentially expressed (DE). Unbiased and DE genes in *M.minutoides* were then log normalized using the TMM normalization method in edgeR to account for differences in read depth and library sizes between samples (cpm function in edgeR). We further scaled and centered the expression of each gene to a mean of 0, and a standard deviation of 1 across samples. This allows to make graphical comparisons of gene expression between samples and thus, between genotypes.

d) Gene expression clustering

Sex-biased genes were grouped according to their expression pattern by an unsupervised hierarchical clustering method using the Weighted Gene Correlation Network Analysis (WGCNA) software v.1.68 (Zhang & Horvath, 2005). WGCNA group genes whose expression are highly correlated (co-expressed genes) into modules (i.e., clusters). We used a bidweight midcorrelation with a maximum percentile outlier of 0.05 following authors' recommendations. We chose a soft thresholding power of 13 based on the scale-free topology fit indices (R^2 values > 0.8 and slope close to 1) to detect 'signed' modules of co-expressed genes (signed modules distinguish between mirror clusters). We allowed for a minimal module size of 5 genes and merged modules with a threshold height of 0.21 on the clustering dendrogram (i.e., similar clusters). We identified sex-biased expression categories (e.g.

genes whose expression is influenced by gonadal sex) graphically and using the module-biological trait correlation function of WGCNA (table 1).

e) Scaffolds assignment to chromosomes and DE gene distribution

Scaffolds from *M.minutoides* genome were anchored on *M. musculus* genome (scaffolds that did not anchor were defined as "unassigned" genomic regions). Then, we corrected for chromosome homologies between the two species (Veyrunes et al., 2005). In our population, sex chromosomes are fused to different autosomes leading to neo-X, neo-Y sex chromosomes, which involve autosome 1 ($1^{Neo\text{-}X}$ and $1^{Neo\text{-}Y}$), and neo-X* chromosomes involving autosomes 1 ($1^{Neo\text{-}X*}$), 13 ($13^{Neo\text{-}X*}$), and 16 (entirely recombining and thus considered as autosomal) (fig. 1, see supplemental methods) (Veyrunes et al., 2004; Veyrunes et al., 2007; Baudat et al., 2019). These neo-sex chromosomes have both non-recombining (NR) and recombining (R) regions (Baudat et al., 2019; Saunders et al., in prep). Similarly, some regions of X and X* chromosomes stopped recombining as well (fig. 1). We thus separated the genome in different genomic compartments to investigate DE gene distributions, depending of their origin and recombination pattern: autosomes, X/X* chromosomes wit both R and NR regions, and neo-sex chromosomes: chromosome 1 (chr1) and chromosome 13 (chr13), which both have R and NR regions. We combined data for chr1 and chr13 into a "neo-sex" chromosome category while considering their recombination status (R or NR).

f) Allele-specific expression

We used the ASEReadCounter command from GATK v4.1 to retrieve reference and alternative allele counts at the SNP level for sex and all neo-sex chromosomes. We filtered mapped reads for mapping quality, base quality and the minimum number of bases that pass filters with the following parameters: *--min-mapping-quality 10 --min-base-quality 10 -min-depth 10*. Allele counts at the gene level were then obtained using the ASEReadCounter* pipeline (Mendelevich et al., 2020). Prior to imbalance analyses, we removed sex and neo-sex linked genes for which we found two alleles in XX females or when an X allele was found in X*Y females (i.e., misdiagnosed SNP: shared polymorphism between

chromosomes). We also filtered genes with a minimal count of 10 reads in at least 5 allelic counts out of the 10 (2 alleles x 5 sample replicates). We focused on allele-specific expression in females to correlate with phenotypic divergences and tested XX* and X*Y individuals only because XX females are presumed to be homozygous at each loci. XX* and X*Y females were tested separately due to different allelic comparisons. We modelled allele-specific expression fitting a negative-binomial distribution, using gene ID and alleles' origin as fixed effects and with an interaction term. Post-hoc pairwise comparisons between reference and alternate alleles for each gene were made applying a Benjamini-Hochberg correction for multiple testing. Genes that passed the 5% FDR threshold were considered to have a true allelic imbalance. Finally, random X/X* chromosome inactivation was assessed with allele-specific expression of X/X*-linked genes in XX* females.

g) Gene ontology, candidate genes & enrichment analysis

We used a gene by gene approach to investigate the biological processes of genes in clusters showing a 'genotypic sex' bias and for genes showing allele-specific expression. This allows to identify candidate genes for the previously described phenotypic divergences between genotypes (Saunders et al., 2014; Saunders et al., 2016; Ginot et al., 2017; Heitzmann et al., 2022; Veyrunes et al., 2022). We added gene ontology (GO) terms based on the online tool amiGO (https://geneontology.org). Furthermore, an enrichment analysis per cluster was performed using the clusterProfiler v4.0 software. We used all genes detected in *M.minutoides* as a background to test for enrichment and applied an adjusted p.value threshold of 0.05 (Benjamini-Hochberg correction for multiple testing) to detect significant enrichments.

h) Statistical analyses

Overall gene differential expression, hierarchical clustering, allele-specific expressio and clusters' enrichment in GO terms analyses were performed on R v3.6 (R core Team, 2022). Distributions of DE genes were tested for enrichment on sex and neo-sex chromosomes by comparing frequencies of DE genes on sex and neo-sex chromosomes to that of autosomes for each cluster using Pearson χ^2 test

(one-sided hypothesis) and with permutation tests. For the latter, we sampled genes from the genome (the number of genes sampled is the number of genes in the genomic compartment we are interested in) a 1000 times, and compared expected frequencies of DE genes in each cluster category to the ones observed. In other words, we randomly reassigned genes on neo-sex (NR and R), sex chromosomes (NR and R) and autosomes, from genes in the whole genome, and checked whether we found the same or greater proportions of DE genes that belong to a specific cluster. P.values were determined by the number of times expected frequencies were greater or even to observed frequencies over the 1000 iterations. Genomic regions enriched in DE genes identified by both methods were considered as truly enriched.

Results

Differential gene expression

We sequenced the whole brain transcriptome of *M. minutoides* for 5 individuals of each genotypic sex (XX, XX*, X*Y females and XY males) bred in captivity. We detected 13286 expressed genes, among which 1310 were differentially expressed (DE) in at least one contrast from the four sexual genotypes. The $\log_2$ fold-changes for each contrast are presented in supplemental information S1. We used WGCNA methods to define clusters of genes based on their joint expression patterns across the four genotypes. Among the 1310 DE genes, 1307 were thus split into 8 clusters (fig. 2). The remaining 3 genes were not attributed to any cluster due to low a correlation with the module eigengene. For one cluster of 709 genes (~54% of DE genes), the dominant pattern was a male-biased expression (MB cluster). However, a significant contribution of the Y chromosome was detected independently of gonadal status (fig. 2, fig. S1). Conversely, a group of 374 genes (~39% of DE genes) was mainly characterized by a female-biased expression pattern (FB cluster). The method divided this set into three clusters due to different interactions with the sexual genotype (fig. 2, fig. S1): female-biased but with variance between the three genotypes (FB1 cluster, 18 genes), female-biased with greater expression levels in X*-carrying individuals (FB2 cluster, 176 genes), and female-biased with

underexpression in X*Y females (FB3 cluster, 180 genes). Patterns of the four remaining clusters mainly reflected an influence of genotypic rather than gonadal sex (17% of DE genes). Two of them revealed an influence of the presence of the Y chromosome, with 53 genes overexpressed and 102 genes underexpressed in individuals carrying a Y chromosome, i.e., both X*Y and XY individuals (YB and -YB clusters, respectively; fig. 2, fig. S1). In another cluster, 31 genes displayed a gradient of expression level: highest in XX females, followed by XX* and XY individuals, and then X*Y females, highlighting an influence of the number of X chromosome (X dose cluster; fig. 2, fig. S1). Lastly, a cluster of 38 genes underexpressed in XX* and X*Y females indicated an influence of the presence of the X* chromosome on gene expression (-X*B cluster; fig. 2, fig. S1). We then examined the distribution of the genes in each cluster among genomic regions with different sex-linked transmission properties (autosomes, X/X* and neo-sex chromosomes). We found that female-biased genes were enriched on X/X* chromosomes only, while no enrichment was found for male-biased genes (fig. 2b, table 2). Genes whose expression was influenced by genotypic sex were enriched on X/X* and neo-sex chromosomes (fig. 2b, table 2).

Gene ontology and function of DE genes

Male biased genes were enriched in mitochondrial function GO terms (supplemental information S2) and female-biased genes in axon development GO terms (supplemental information S3). There was no significant enrichment of GO terms in clusters showing a genotype effect. Looking at ontologies gene-by-gene, we found a few genes DE between females, which are known to control social behaviours: *MaoA*, *Th*, *Sts* (Scott et al., 2008; Mahadevia et al., 2021; Scott et al., 2015; Mortaud et al., 2010), as well as reproductive traits: *Amhr2* and *Lhb* (Cimino et al., 2016; Huhtaniemi et al., 2006), or known to escape X inactivation in *M. musculus*: Kdm6a, Ddx3x and Eif2s3x (Yang et al., 2010) (table S1-S2, supplemental information S1).

Allele specific expression in XX females*

We were interested in studying allele-specific expression in the non-recombining regions of X/X* and neo-sex chromosomes. Whole genome resequencing of wild-derived samples (Saunders et al., in prep) allowed us to detect a number of diagnostic SNPs (i.e., fixed SNPs) in coding regions for that purpose. In XX* females, we detected 97 genes with such allelic variation, of which 74 between X and X* chromosomes, and 23 genes located in the non-recombining regions of neo-sex chromosomes (fig. 3a). Interestingly, 65 X/X*-linked genes (out of 74) showed a significant bias towards X alleles' expression, and the remaining 9 showed no significant bias (table S3, supplementary file S4). This pattern was consistent across all individuals and regardless of the overall expression pattern of these genes, i.e., the cluster they belong to (fig. S2, table S3, supplementary file S4). Among these 65 genes, 55 had a *M. musculus* ortholog (see table S3) that we could include in the ontology analysis. They were mainly involved in the development of the nervous system and RNA processing (e.g. transcription, splicing, methylation; table S3). In contrast, only one of the 23 genes on the neo-sex chromosomes showed a true allelic imbalance, located in the non-recombining region of chr13 ($13^{Neo\text{-}X^*}$), with a preferential expression of the autosomal copy (fig. 3a, fig. S2, table S3, supplementary file S4).

*Allele specific expression in X*Y females*

We applied the same approach as above to X*Y females. In this case, the relevant genomic regions used are the non-recombining regions of chr13 (comparison of $13^{Neo\text{-}X^*}$and 13^{Aut} alleles) and chr1 (comparison of $1^{Neo\text{-}X^*}$ and $1^{Neo\text{-}Y}$ alleles). We found 253 genes with diagnostic SNPs on chr1, while there were only 10 genes with diagnostic SNPs on chr13 (fig. 3b, fig. S3, supplemental information 5). There was an overall tendency for the overexpression of autosomal (13^{aut}) over neo-X* ($13^{Neo\text{-}X^*}$) alleles for chr13, and $1^{Neo\text{-}X^*}$ over $1^{Neo\text{-}Y}$ alleles for chr1, albeit to a lesser extent (fig. 3b, fig. S3). However, only 14 genes showed a true allelic imbalance, and they were on chr1 ($1^{Neo\text{-}X^*}$ vs $1^{Neo\text{-}Y}$). Five and nine genes showed a preferential expression of $1^{Neo\text{-}Y}$ and $1^{Neo\text{-}X^*}$ alleles, respectively (table S4, see supplementary file S5). Orthologies and ontologies of these genes are presented in table S4.

Discussion

The African pygmy mouse is a species with a polygenic sex determination system involving a dissociation between phenotypic and genotypic sexes, with the presence of three female genotypes and including females carrying the Y chromosome. Previous studies have shown striking divergences in behaviours and life history traits between the different females, thus revealing the role of sex chromosomes and their mode of transmission in shaping sex-linked phenotypes. We found that gonadal sex is predominant in shaping the brain transcriptome of *M. minutoides.* However, for a non-negligible proportion of genes, i.e., 17% of DE genes, expression was mostly influenced by genotypic sex; X*Y females being either similar to males or different from the other sexual genotypes. This first instance highlighted that sex reversal has profoundly impacted the transcriptome of X*Y females. Moreover, the impacted genes were peculiarly enriched in the non-recombining regions of X/X* and neo-sex chromosomes (fig. 2b). Thus, these genomic regions with a new mode of transmission drive the brain transcriptional architecture of the four genotypes in *M.minutoides,* and seemingly, subsequent phenotypic divergences between females. Finally, allele-specific expression analyses pointed towards the preferential inactivation of the X* chromosome (which is always maternal), in the brain of XX* females. This striking result is however concordant with the observation of similar phenotypes between XX* and XX females (Saunders et al., 2014; Saunders et al., 2016; Heitzmann et al., 2022; Veyrunes et al., 2022).

a) The brain transcriptome reflects an influence of the sexual genotypes.

In common frogs (*Rana temporaria)*, with naturally occurring sex-reversed males (XX) and females (XY°, where ° refers to a proto-Y chromosome), a whole-body transcriptome study showed that gonadal sex was the main factor influencing gene expression (Ma et al., 2018). Recently, the same result was found in the FCG mouse model, with sex-reversed XY- females lacking *Sry* and XX*Sry* males, using liver and adipose tissue transcriptomes (Blencowe et al., 2022). More precisely, only 0.06% of DE genes showed a genotype effect in common frogs, and ~0.01-0.02% of DE genes in the FCG model (~10 genes whose expression is influenced by the genotype in comparison to ~500-1000

DE genes influenced by the activational effect of gonadal hormones). In our study, we used the brain transcriptome of a mouse species with three female genotypes (XX, XX* and X*Y) and one male genotype (XY), and found ~83% of DE genes that group females together against males. Although these genes showed variance in expression according to the genotype -especially for female-biased genes-, our results are consistent with a transcriptional architecture that mainly reflects gonadal sex. Nonetheless, in contrast to the FCG mouse model or the common frog, a considerable proportion of genes (~17%) was influenced by the sex chromosome complement. Approximately two thirds of these genes grouped X*Y and XY individuals together against XX and XX* females. This result demonstrate a Y chromosome effect and/or an effect of X/X* chromosome number, but also suggests that X and X* chromosomes have a similar influence on these genes. The remaining third of the genes separated X*Y females from the other genotypes, suggesting a X* and/or a X chromosome effect (e.g. X dose), with different impacts on gene expression between X and X* chromosomes. These genes were overrepresented in the non-recombining regions of sex and neo-sex chromosomes, and a similar pattern was found on the kidney transcriptome (Saunders et al., in prep). Consequently, the three sex chromosomes (X, X* and Y) and neo-sex chromosomes play a substantial role in shaping the brain transcriptome of *M. minutoides* and in driving the divergent female phenotypes.

b) Candidate genes for the molecular bases of the different female phenotypes.

Previous studies showed that X*Y females differ from both XX and XX* females on many traits. For instance, X*Y females breed earlier and have an ovulation rate 1.5x greater than the other females (Saunders et al., 2014), they are more aggressive towards intruders (Saunders et al., 2016) and they are more efficient at pup retrieval (Heitzmann et al., 2022). Interestingly, we found a few genes differentially expressed according to the genotype that can be correlated with some of these phenotypes. For instance, the Anti-Mullerian Hormone Receptor 2 (*Amhr2*) gene present on autosome 15 and the Luteinizing hormone subunit beta (*Lhb*) gene present in the non-recombining region of neo-X, neo-X* and neo-Y chromosomes, are both essential for gonadal functions (Coss, 2018; Huhtaniemi et al., 2006). More precisely, the Anti-Mullerian Hormone (AMH) positively

influences gonadotropin releasing hormone (GnRH) neurons in the hypothalamus, which influence the secretion of Luteinizing hormone (LH) and Follicle stimulating hormone (FSH) in the pituitary and regulating females' cycle (Coss, 2018; Huhtaniemi et al., 2006). An overexpression of AMH/*Amhr2* and LH was found in females having polycystic ovary syndrom (PCOS), with impaired ovulation and follicle maturation (Cimino et al., 2016). Here, *Amhr2* and *Lhb* (though not in the pituitary) are underexpressed in X*Y females in comparison to XX, XX* and XY individuals, consistent with differences in ovulation rate and thus, reproductive success between females (Saunders et al., 2014). We further found two candidate genes known to regulate aggressiveness: monoamine oxydase A (*MaoA*), present in the non-recombining region of X/X*, and Steroid sulfatase (*Sts*), also sex-linked but because the gene is present on a scaffold that did not map on *M. musculus* genome, we do not know if it is in the recombining or the non-recombining region (Mortaud et al., 2010; Scott et al., 2008). However, *Sts* is unlikely to explain differences in aggressiveness between females because it is underexpressed in X*Y females (and in males) when compared to XX and XX* females, while it has been shown that it is an overexpression that triggers aggressive behaviours (Mortaud et al., 2010). In contrast, the down-regulation of *MaoA,* an enzyme involved in dopamine degradation, has been related to enhanced aggressiveness (Scott et al., 2008), and the gene is underexpressed in X*Y females. This result corroborates the genomic data showing a duplication of this gene on the X chromosome, while it remains in a single copy on the X* (Saunders et al., in prep). Moreover, we found another gene involved in the dopaminergic system, Tyrosine hydroxylase (*Th,* the rate limiting enzyme for dopamine synthesis, present in the recombining region of chr1), known to stimulate both aggressive and maternal behaviours in laboratory mice (Mahadevia et al., 2021; Scott et al., 2015). Though *Th* belongs to the female-biased cluster, it is significantly overexpressed in X*Y females when compared to XX, XX* and XY individuals. Taken together, our results highlight two sex-linked genes from the dopaminergic pathway that are strong candidates to correlate with divergences in social and parental behaviour in *M. minutoides.*

Another interesting candidate gene is the lysine demethylase 6a, *Kdm6a*, an X-linked gene escaping X chromosome inactivation (XCI) in laboratory mice (Yang et al., 2010). *Kdm6a* regulates neurons' sexual differentiation in the ventromedial hypothalamus (Cabrera Zapata et al., 2021), and the paraventricular nucleus of the hypothalamus (Xu et al., 2008), regions involved in sex differences in social, reproductive and parental behaviours (Bayless & Shah, 2016; Scott et al., 2015; Hashikawa et al., 2017; Musatov et al., 2006). Here, XX and XX* females had a greater expression level of *Kdm6a* when compared to X*Y and XY individuals. This first suggests that *Kdm6a* also escape inactivation in *M. minutoides,* and theorizes that it could regulate the expression of genes involved in social/parental behaviours at the origin of phenotypic divergences between females. On that note, our results suggest that *Ddx3x* and *Eif2s3x* escape inactivation in *M. minutoides* as they do in *M. musculus,* since we found greater expression levels in XX and XX* females. In light of these findings, we were able to identify several candidate genes for the molecular basis of the different sexual phenotypes in the African pygmy mouse. Further investigations with RT-qPCR would be necessary to confirm gene expression differences, and *in situ* hybridization in specific regions of the brain, such as in the hypothalamus, could help confirm or infirm the correlation (although not causality) between these genes and phenotypic divergences among XX, XX* and X*Y females.

c) Allele-specific expression and X/X* chromosome inactivation in XX* females

Then, we were also interested on whether allele-specific expression in non-recombining regions of sex and neo-sex chromosomes could also be related to phenotypical divergences. We did not find striking evidence for allelic imbalance between neo-sex chromosomes for XX* females and a few genes showed imbalance between $1^{\text{Neo-X*}}$ and $1^{\text{Neo-Y}}$ alleles in X*Y females. These genes have no known effect on sexual phenotypes as described in *M. minutoides* (fig. 3, fig. s2-s3, table S3-S4, supplemental information S4-S5; Saunders et al., 2014; Saunders et al., 2016; Heitzmann et al., 2022; Veyrunes et al., 2022). Strikingly though, concerning X/X*-linked genes, we showed that XX* females preferentially expressed X alleles for 65 out of the 74 (i.e., 87.8%) genes showing allelic variation (fig. 3a, fig. s2). Since this pattern was found for both unbiased and DE genes and consistent across

individuals, it strongly suggests a chromosome-wide effect and thus, the preferential partial inactivation of the X* chromosome (X*CI) in the brain of XX* females. This could explain similar overall gene expression patterns found here between XX* and XX females but most importantly, it is in line with their similar behavioural and fertility phenotypes. This result however contrasts with the random XCI previously found using embryo fibroblast cultures or the sequencing of the kidney transcriptome in *M.minutoides* (Veyrunes & Perez, 2018; Saunders et al., 2022), as well as an overall random XCI in eutherian mammals. In fact, a very limited number of studies have reported evidence for a skewed XCI in mammals, but it mainly involves the inactivation of the paternal X, as shown in Marsupials (Cooper et al., 1993) or in the brain of neonatal mice (Wang et al., 2010). Conversely, our result rather points towards the preferential inactivation of the maternal X* in the brain of *M. minutoides.* Hence, in the future, it could be worthy to investigate genes involved in X chromosome inactivation (e.g. *Xist* or its antisense gene, *Tsix*), or use methods such as bisulfite-converted DNA sequencing assessing methylation patterns to confirm or infirm this pattern.

In the following section, we discuss two main hypotheses to explain X* preferential inactivation involving i) X* chromosome degeneration, and ii) X-linked genomic imprinting (i.e., preferential expression of the paternal allele) in response to intra-locus sexual conflicts. Regarding the first hypothesis, the X* chromosome is female specific and about 2/3 of the chromosome does not recombine with the X chromosome (Saunders et al., in prep). Because of the absence of recombination, the X* could accumulate mutations in cis-regulatory elements, that have deleterious effects on the level of expression (supposing that expression level is under stabilising selection). Preferential expression of X alleles (which recombine and can more easily purge deleterious mutations) in XX* females could thus mitigate this effect. Accordingly, selection should favour a decrease in expression and even complete silencing of deleterious alleles on the X*, as predicted by models of degeneration by loss of expression due to the accumulation of deleterious mutations (Lenormand et al., 2020; Lenormand & Roze, 2022). However, in X*Y females, the X* is hemyzygous and faces an already degenerated Y chromosome, exposing it to a strong purifying

selection. Hence, the X* is unlikely to degenerate, or at least to a very limited extent and with the evolution of trans-regulatory factors in X*Y females to approach optimal levels. Nevertheless, because there is no evidence for the preferential expression of X alleles in the kidney (Saunders et al., in prep), this strongly suggests that skewed X*CI in the brain of XX* females is unlikely to be a response to X* chromosome degeneration.

The second hypothesis, X-linked genomic imprinting with preferential expression of paternal X alleles, has been suggested (on theoretical grounds) to evolve under polygamy, or under sex-specific selection (Iwasa & Pomiankowski, 2001; Day & Bonduriansky, 2004). In the first scenario (i.e., polygamy), females mate with multiple males, which will impact the relatedness between males and sons, and increase intra-locus sexual conflicts over maternal investment: paternally inherited alleles favour increased maternal investment into males' own offspring, while maternal inherited alleles favour a decrease in investment (Iwasa & Pomiankowski, 2001). Furthermore, because X-linked genes do not have Y homologs, complete silencing of the maternal X does not evolve otherwise there would be no expression in males. In the second scenario (i.e., sex-specific selection), selection favours greater expression levels of X-linked genes in females, but because males express the maternal X, it implies that the regulation occurs on the paternal X (Iwasa & Pomiankowski, 2001; Day & Bonduriansky, 2004). However, we may note that this scenario is based on a classical XX/XY system with a shared X, while in our case, it involves a female-specific chromosome (X*): if selection favours greater expression in females, we could expect that both the maternal X* and paternal X are likely to be expressed in XX* females. Another possible scenario is that because the emergence of the X* has led to new inheritance patterns of sex chromosomes, the latter presumably have new evolutionary trajectories, which will thus influence how they react to sexual conflicts. For example, because the X* is female-specific, transmitted exclusively from mothers to daughters, gene expression should be free to evolve towards a female phenotypical optimum. On the other hand, the X chromosome spends more time in a male environment in comparison to what prevails in an XX/XY system (Saunders et al., 2022). This may generate new conflicts and lay ground for the masculinization of the X chromosome. Therefore, the new evolutionary trajectories of X and X* could drive new sexual

conflicts, with divergent interests between chromosomes and at the basis of X* preferential inactivation in XX* females. Future theoretical models of X-linked genomic imprinting integrating polygenic sex determination systems could help us understand the ultimate causes behind the preferential expression of the paternal X.

Conclusion

The African pygmy mouse is a peculiar species with three sex chromosomes: the classical X and Y, and a feminizing X* chromosome. In this work, we have demonstrated that the new sex chromosome architecture as well as their mode of transmission profoundly affect the brain transcriptome, which reflects females' phenotypic divergences and thus, the third sexual phenotype highlighted in previous studies (Saunders et al., 2014; Saunders et al., 2016; Heitzmann et al., 2022; Veyrunes et al., 2022). Moreover, we were able to found several candidate genes that could underpin sex-linked phenotypes, directly and indirectly related to the brain (e.g. maternal behaviours, ovulation). All things being equal, our results emphasize that the evolution of sex and neo-sex chromosomes in the African pygmy mouse has opened avenues to sexual conflicts, as well as to their resolution.

References

Arnold, A. P. (2009). The organizational-activational hypothesis as the foundation for a unified theory of sexual differentiation of all mammalian tissues. *Hormones and Behavior*, 55(5), 570–578. https://doi.org/10.1016/j.yhbeh.2009.03.011

Arnold, A. P. (2004). Sex chromosomes and brain gender. *Nature Reviews Neuroscience*, 5(9), 701–708. https://doi.org/10.1038/nrn1494

Arnold, A. P. (2020). Sexual differentiation of brain and other tissues: Five questions for the next 50 years. *Hormones and Behavior*, 120, 104691. https://doi.org/10.1016/j.yhbeh.2020.104691

Arnold, A. P., Reue, K., Eghbali, M., Vilain, E., Chen, X., Ghahramani, N., Itoh, Y., Li, J., Link, J. C., Ngun, T., & Williams-Burris, S. M. (2016). The importance of having two X chromosomes. *Philosophical Transactions of the Royal Society B: Biological Sciences*, 371(1688). https://doi.org/10.1098/rstb.2015.0113

Ayers, K. L., Davidson, N. M., Demiyah, D., Roeszler, K. N., Grützner, F., Sinclair, A. H., Oshlack, A., & Smith, C. A. (2013). RNA sequencing reveals sexually dimorphic gene expression before

gonadal differentiation in chicken and allows comprehensive annotation of the W-chromosome. *Genome Biology*, 14, R26. https://doi.org/10.1186/gb-2013-14-3-r26

Barthold, S. W. (2004). Genetically altered mice : Phenotypes, no phenotypes, and Faux phenotypes. *Genetica*, 122, 75-88.

Baudat, F., de Massy, B., & Veyrunes, F. (2019). Sex chromosome quadrivalents in oocytes of the African pygmy mouse Mus minutoides that harbors non-conventional sex chromosomes. *Chromosoma*, 128(3), 397-411. https://doi.org/10.1007/s00412-019-00699-4

Bayless, D. W., & Shah, N. M. (2016). Genetic dissection of neural circuits underlying sexually dimorphic social behaviours. Philosophical Transactions of the Royal Society B: Biological *Sciences*, 371, 20150109. https://doi.org/10.1098/rstb.2015.0109

Blencowe, M., Chen, X., Zhao, Y., Itoh, Y., McQuillen, C. N., Han, Y., Shou, B. L., McClusky, R., Reue, K., Arnold, A. P., & Yang, X. (2022). Relative contributions of sex hormones, sex chromosomes, and gonads to sex differences in tissue gene regulation. *Genome Research*, 32, 807–824. https://doi.org/10.1101/GR.275965.121

Breedlove, S. M., Cooke, B. M., & Jordan, C. L. (1999). The orthodox view of brain sexual differentiation. *Brain, Behavior and Evolution*, 54(1), 8–14. https://doi.org/10.1159/000006607

Bućan, M., & Abel, T. (2002). The mouse : Genetics meets behaviour. Nature Reviews. *Genetics*, 3(2), 114-123. https://doi.org/10.1038/nrg728

Cabrera Zapata, L. E., Cisternas, C. D., Sosa, C., Luis, ·, Garcia-Segura, M., Arevalo, M. A., María, ·, & Cambiasso, J. (2021). X-linked histone H3K27 demethylase Kdm6a regulates sexually dimorphic differentiation of hypothalamic neurons. *Cellular and Molecular Life Science*, 78, 7043–7060. https://doi.org/10.1007/s00018-021-03945-0

Cimino, I., Casoni, F., Liu, X., Messina, A., Parkash, J., Jamin, S. P., Catteau-Jonard, S., Collier, F., Baroncini, M., Dewailly, D., Pigny, P., Prescott, M., Campbell, R., Herbison, A. E., Prevot, V., & Giacobini, P. (2016). Novel role for anti-Müllerian hormone in the regulation of GnRH neuron excitability and hormone secretion. *Nature Communications*, 7. https://doi.org/10.1038/NCOMMS10055

Cooper, D. W., Johnston, P. G., Watson, J. M., & Graves, J. A. M. (1993). X-inactivation in marsupials and monotremes. *Seminars in Developmental Biology*, 4(2), 117–128. https://doi.org/10.1006/SEDB.1993.1014

Coss, D. (2017). Regulation of reproduction via tight control of gonadotropin hormone levels. *Molecular and Cellular Endocrinology*, 463, 116–130. https://doi.org/10.1016/j.mce.2017.03.022

Day, T., & Bonduriansky, R. (2004). Intralocus Sexual Conflict Can Drive the Evolution of Genomic Imprinting. *Genetics*, 167, 1537–1546. https://doi.org/10.1534/genetics.103.026211

Dean, R., & Mank, J. E. (2014). The role of sex chromosomes in sexual dimorphism : Discordance between molecular and phenotypic data. *Journal of Evolutionary Biology*, 27(7), 1443-1453. https://doi.org/10.1111/jeb.12345

Ellegren, H., & Parsch, J. (2007). The evolution of sex-biased genes and sex-biased gene expression. *Nature Reviews Genetics*, 8(9), 689–698. https://doi.org/10.1038/nrg2167

Fang, H., Disteche, C. M., & Berletch, J. B. (2019). X Inactivation and Escape: Epigenetic and Structural Features. *Frontiers in Cell and Developmental Biology*, 7, 219. https://doi.org/10.3389/FCELL.2019.00219/FULL

Gil-Fernández, A., Ribagorda, M., Martín-Ruiz, M., López-Jiménez, P., Laguna, T., Gómez, R., Parra, M. T., Viera, A., Veyrunes, F., & Page, J. (2021). Meiotic Behavior of Achiasmate Sex Chromosomes in the African Pygmy Mouse Mus mattheyi Offers New Insights into the Evolution of Sex Chromosome Pairing and Segregation in Mammals. *Genes*, 12, 1434. https://doi.org/10.3390/genes12091434

Ginot, S., Claude, J., Perez, J., & Veyrunes, F. (2017). Sex reversal induces size and performance differences among females of the African pygmy mouse, Mus minutoides. *Journal of Experimental Biology*, 220(11), 1947–1951. https://doi.org/10.1242/JEB.157552

Graves, J. A. M. (2006). Sex chromosome specialization and degeneration in mammals. *Cell*, 124(5), 901–914. https://doi.org/10.1016/J.CELL.2006.02.024

Hale, M. C., Xu, P., Scardina, J., Wheeler, P. A., Thorgaard, G. H., & Nichols, K. M. (2011). Differential gene expression in male and female rainbow trout embryos prior to the onset of gross morphological differentiation of the gonads Matthew. *BMC Genomics,* 12, 404-404. https://doi.org/10.1186/1471-2164-12-404

Han, T. M., & De Vries, G. J. (2003). Organizational Effects of Testosterone, Estradiol, and Dihydrotestosterone on Vasopressin mRNA Expression in the Bed Nucleus of the Stria Terminalis. *J Neurobiol*, 54, 502–510. https://doi.org/10.1002/neu.10157

Hashikawa, K., Hashikawa, Y., Tremblay, R., Zhang, J., Feng, J. E., Sabol, A., Piper, W. T., Lee, H., Rudy, B., & Lin, D. (2017). Esr1+ cells in the ventromedial hypothalamus control female aggression. *Nature Neuroscience*, 20(11), 1580–1590. https://doi.org/10.1038/nn.4644

Heitzmann, L., Challe, M., Perez, J., Castell, L., Galibert, E., Martin, A., Valjent, E., & Veyrunes, F. (2022). Genotypic sex shapes maternal care in the African Pygmy mouse, Mus minutoides. *bioRxiv*. https://doi.org/10.1101/2022.04.05.487174

Huhtaniemi, I., Ahtiainen, P., Pakarainen, T., Rulli, S. B., Zhang, F. P., & Poutanen, M. (2006). Genetically modified mouse models in studies of luteinising hormone action. *Molecular and Cellular Endocrinology*, 252(1–2), 126–135. https://doi.org/10.1016/J.MCE.2006.03.026

Huynh, K. D., & Lee, J. T. (2001). Imprinted X inactivation in eutherians: a model of gametic execution and zygotic relaxation. *Current Opinion in Cell Biology*, 13(6), 690–697. https://doi.org/10.1016/S0955-0674(00)00272-6

Huynh, K. D., & Lee, J. T. (2005). X-chromosome inactivation: a hypothesis linking ontogeny and phylogeny. *Nature Reviews Genetics* 2005 6:5, 6(5), 410–418. https://doi.org/10.1038/nrg1604

Iwasa, Y., & Pomiankowski, A. (2001). The Evolution of X-Linked Genomic Imprinting creating patterns of X-linked imprinting. *Genetics*, 158, 1801–1809.

Konkle, A. T. M., & McCarthy, M. M. (2011). Developmental time course of estradiol, testosterone, and dihydrotestosterone levels in discrete regions of male and female rat brain. *Endocrinology*, 152(1), 223–235. https://doi.org/10.1210/en.2010-0607

Lenormand, T., Fyon, F., Sun, E., & Correspondence, D. R. (2020). Sex Chromosome Degeneration by Regulatory Evolution. *Current Biology*, 30, 3001-3006.e5. https://doi.org/10.1016/j.cub.2020.05.052

Lenormand, T., & Roze, D. (2022). Y recombination arrest and degeneration in the absence of sexual dimorphism. *Science*, 375(6581), 663-666. https://doi.org/10.1126/SCIENCE.ABJ1813/SUPPL_FILE/SCIENCE.ABJ1813_MDAR_REPRODUCIBILITY_CHECKLIST.PDF

Lichilín, N., Taher, A. El, & Böhne, A. (2021). Sex-biased gene expression and recent sex chromosome turnover. *Philosophical Transactions of the Royal Society B: Biological Sciences*, 376, 20200107. https://doi.org/10.1098/rstb.2020.0107

Ma, W. J., Veltsos, P., Sermier, R., Parker, D. J., & Perrin, N. (2018). Evolutionary and developmental dynamics of sex-biased gene expression in common frogs with proto-Y chromosomes. *Genome Biology*, 19(1), 1–17. https://doi.org/10.1186/s13059-018-1548-4

Mahadevia, D., Saha, R., Manganaro, A., Chuhma, N., Ziolkowski-Blake, A., Morgan, A. A., Dumitriu, D., Rayport, S., & Ansorge, M. S. (2021). Dopamine promotes aggression in mice via ventral tegmental area to lateral septum projections. *Nature Communications*, 12, 6796. https://doi.org/10.1038/s41467-021-27092-z

Mank, J. E. (2009a). Sex chromosomes and the evolution of sexual dimorphism : Lessons from the genome. *American Naturalist*, 173(2), 141-150. https://doi.org/10.1086/595754

Mank, J. E. (2009b). The evolution of heterochiasmy : The role of sexual selection and sperm competition in determining sex-specific recombination rates in eutherian mammals. *Genetics Research*, 91(5), 355-363. https://doi.org/10.1017/S0016672309990255

Mank, J. E. (2017). The transcriptional architecture of phenotypic dimorphism. *Nature Ecology and Evolution*, 1(1), 1-7. https://doi.org/10.1038/s41559-016-0006

Morris, J. A., Jordan, C. L., & Breedlove, S. M. (2004). Sexual differentiation of the vertebrate nervous system. *Nature Neuroscience*, 7(10), 1034–1039. https://doi.org/10.1038/nn1325

Mortaud, S., Nicolas, L., Pinoteau, W., Tordjman, S., Carlier, M., & Roubertoux, P. L. (2010). Brain pathways mediating the pro-aggressive effect of the steroid sulfatase (Sts) gene. *Behavior Genetics*, 40(2), 211–219. https://doi.org/10.1007/s10519-010-9340-6

Mueller, J. L., Skaletsky, H., Brown, L. G., Zaghlul, S., Rock, S., Graves, T., Auger, K., Warren, W. C., Wilson, R. K., & Page, D. C. (2013). Independent specialization of the human and mouse X chromosomes for the male germ line. *Nature Genetics*, 45(9), 1083-1087. https://doi.org/10.1038/ng.2705

Musatov, S., Chen, W., Pfaff, D. W., Kaplitt, M. G., & Ogawa, S. (2006). RNAi-mediated silencing of estrogen receptor α in the ventromedial nucleus of hypothalamus abolishes female sexual behaviors. *PNAS*, 103(27), 10456–10460. https://doi.org/10.1073/PNAS.0603045103

Ngun, T. C., Ghahramani, N. M., Creek, M. M., Williams-Burris, S. M., Barseghyan, H., Itoh, Y., Sánchez, F. J., McClusky, R., Sinsheimer, J. S., Arnold, A. P., & Vilain, E. (2014). Feminized behavior and brain gene expression in a novel mouse model of Klinefelter Syndrome. *Archives of Sexual Behavior*, 43(6), 1043–1057. https://doi.org/10.1007/s10508-014-0316-0

Nishida, Y., Yoshioka, M., & St.-Amand, J. (2005). Sexually dimorphic gene expression in the hypothalamus, pituitary gland, and cortex. *Genomics*, 85(6), 679–687. https://doi.org/10.1016/j.ygeno.2005.02.013

Ortega, M. T., Bivens, N. J., Jogahara, T., Kuroiwa, A., Givan, S. A., & Rosenfeld, C. S. (2019). Sexual dimorphism in brain transcriptomes of Amami spiny rats (Tokudaia osimensis): A rodent species where males lack the y chromosome. *BMC Genomics*, 20(1), 1–17. https://doi.org/10.1186/s12864-019-5426-6

Peterson, M. P., Rosvall, K. A., Choi, J.-H., Ziegenfus, C., & Tang, H. (2013). Testosterone Affects Neural Gene Expression Differently in Male and Female Juncos: A Role for Hormones in Mediating Sexual Dimorphism and Conflict. *PLoS ONE*, 8(4), 61784. https://doi.org/10.1371/journal.pone.0061784

Pointer, M. A., Harrison, P. W., Wright, A. E., & Mank, J. E. (2013). Masculinization of Gene Expression Is Associated with Exaggeration of Male Sexual Dimorphism. *PLoS Genetics*, 9(8), e1003697. https://doi.org/10.1371/journal.pgen.1003697

Rahmoun, M., Perez, J., Saunders, P. A., Boizet-Bonhoure, B., Wilhelm, D., Poulat, F., & Veyrunes, F. (2014). Anatomical and molecular analyses of XY ovaries from the african pygmy mouse Mus minutoides. *Sexual Development,* 8(6), 356–363. https://doi.org/10.1159/000368664

Rayner, J. G., Pascoal, S., & Bailey, N. W. (2019). Release from intralocus sexual conflict? Evolved loss of a male sexual trait demasculinizes female gene expression. *Proceedings of the Royal Society B: Biological Sciences*, 286(1901), 20190497. https://doi.org/10.1098/rspb.2019.0497

Rice, W. R. (1984). Sex Chromosomes and the Evolution of Sexual Dimorphism. *Evolution*, 38(4), 735-742.

Salido, E. C., Li, X. M., Yen, P. H., Martin, N., Mohandas, T. K., & Shapiro, L. J. (1996). Cloning and expression of the mouse pseudoautosomal steroid sulphatase gene (Sts). *Nature Genetics*, 13(1), 83–86. https://doi.org/10.1038/NG0596-83

Saunders, P. A., Franco, T., Sottas, C., Maurice, T., Ganem, G., & Veyrunes, F. (2016). Masculinised Behaviour of XY Females in a Mammal with Naturally Occuring Sex Reversal. *Scientific Reports*, 6, 1–9. https://doi.org/10.1038/srep22881

Saunders, P. A., Perez, J., Rahmoun, M., Ronce, O., Crochet, P. A., & Veyrunes, F. (2014). XY Females do better than the XX in the African Pygmy mouse, Mus minutoides. *Evolution*, 68(7), 2119–2127. https://doi.org/10.1111/evo.12387

Saunders, P. A., & Veyrunes, F. (2021). Unusual Mammalian Sex Determination Systems: A Cabinet of Curiosities. *Genes*, 12(11), 1770. https://doi.org/10.3390/GENES12111770

Scott, A. L., Bortolato, M., Chen, K., & Shih, J. C. (2008). Novel monoamine oxidase A knock out mice with human-like spontaneous mutation. *Neuroreport*, 19(7), 739. https://doi.org/10.1097/WNR.0B013E3282FD6E88

Scott, N., Prigge, M., Yizhar, O., & Kimchi, T. (2015). A sexually dimorphic hypothalamic circuit controls maternal care and oxytocin secretion. *Nature*, 525(7570), 519–522. https://doi.org/10.1038/nature15378

Trivers, R. (1988). Sex differences in rates of recombination and sexual selection. In The evolution of sex : An examination of current ideas (p. 270-286). Sinauer Associates, Incorporated.

Van Nas, A., Guhathakurta, D., Wang, S. S., Yehya, N., Horvath, S., Zhang, B., Ingram-Drake, L., Chaudhuri, G., Schadt, E. E., Drake, T. A., Arnold, A. P., & Lusis, A. J. (2009). Elucidating the role of gonadal hormones in sexually dimorphic gene coexpression networks. *Endocrinology*, 150(3), 1235–1249. https://doi.org/10.1210/EN.2008-0563

Veltsos, A. (2019). No evidence that Y-chromosome differentiation affects male fitness in a Swiss population of common frogs. *Journal of Evolutionary Biology*, 33, 401-409.

Veyrunes, F., Catalan, J., Sicard, B., Robinson, T. J., Duplantier, J.-M., Granjon, L., Dobigny, G., & Britton-Davidian, J. (2004). Autosome and sex chromosome diversity among the African pygmy mice, subgenus Nannomys (Murinae; Mus). *Chromosome Research*, 12, 369–382.

Veyrunes, F., Chevret, P., Catalan, J., Castiglia, R., Watson, J., Dobigny, G., Robinson, T. J., & Britton-Davidian, J. (2010a). A novel sex determination system in a close relative of the house mouse. *Proceedings of the Royal Society B: Biological Sciences*, 277(1684), 1049–1056. https://doi.org/10.1098/rspb.2009.1925

Veyrunes, F., Catalan, J., Tatard, C., Cellier-Holzem, E., Watson, J., Chevret, P., Robinson, T. J., & Britton-Davidian, J. (2010b). Mitochondrial and chromosomal insights into karyotypic evolution of the pygmy mouse, Mus minutoides, in South Africa. *Chromosome Research*, 18(5), 563–574. https://doi.org/10.1007/s10577-010-9144-9

Veyrunes, F., Dobigny, G., Yang, F., O'brien, P. C. M., Catalan, J., Robinson, T. J., & Britton-Davidian, J. (2006). Phylogenomics of the genus Mus (Rodentia; Muridae): extensive genome repatterning is not restricted to the house mouse. *Proceedings of the Royal Society B: Biological Sciences*, 273, 2925–2934. https://doi.org/10.1098/rspb.2006.3670

Veyrunes, F., & Perez, J. (2018). X inactivation in a mammal species with three sex chromosomes. *Chromosoma*, 127(2), 261–267. https://doi.org/10.1007/s00412-017-0657-2

Veyrunes, F., Perez, J., Paintsil, S. N. C., Fichet-Calvet, E., & Britton-Davidian, J. (2013). Insights into the evolutionary history of the X-linked sex reversal mutation in mus minutoides : Clues from sequence analyses of the Y-linked sry gene. *Sexual Development*, 7(5), 244-252. https://doi.org/10.1159/000351223

Veyrunes, F., Perez, J., Heitzmann, L., Saunders, P. A., & Givalois, L. (2022). Separating the effects of sex hormones and sex chromosomes on behavior in the African pygmy mouse Mus minutoides, a species with XY female sex reversal. *BioRxiv*. https://doi.org/10.1101/2022.07.11.499546

Veyrunes, F., Watson, J., Robinson, T. J., & Britton-Davidian, J. (2007). Accumulation of rare sex chromosome rearrangements in the African pygmy mouse, Mus (Nannomys) minutoides: A whole-arm reciprocal translocation (WART) involving an X-autosome fusion. *Chromosome Research*, 15(2), 223–230. https://doi.org/10.1007/s10577-006-1116-8

Wang, X., Soloway, P. D., & Clark, A. G. (2010). Paternally biased X inactivation in mouse neonatal brain. *Genome Biology*, 11(7), 1–15. https://doi.org/10.1186/GB-2010-11-7-R79/FIGURES/5

Wijchers, P. J., Yandim, C., Panousopoulou, E., Ahmad, M., Harker, N., Saveliev, A., Burgoyne, P. S., & Festenstein, R. (2010). Sexual dimorphism in mammalian autosomal gene regulation is

determined not only by sry but by sex chromosome complement as well. *Developmental Cell*, 19(3), 477–484. https://doi.org/10.1016/J.DEVCEL.2010.08.005

Wolstenholme, J. T., Rissman, E. F., & Bekiranov, S. (2013). Sexual differentiation in the developing mouse brain : Contributions of sex chromosome genes. *Genes, Brain and Behavior*, 12(2), 166-180. https://doi.org/10.1111/gbb.12010

Wright, A. E., Fumagalli, M., Cooney, C. R., Bloch, N. I., Vieira, F. G., Buechel, S. D., Kolm, N., & Mank, J. E. (2018). Male-biased gene expression resolves sexual conflict through the evolution of sex-specific genetic architecture. *Evolution Letters*, 2(2), 52–61. https://doi.org/10.1002/evl3.39

Wu, M. V., Manoli, D. S., Fraser, E. J., Coats, J. K., Tollkuhn, J., Honda, S. I., Harada, N., & Shah, N. M. (2009). Estrogen Masculinizes Neural Pathways and Sex-Specific Behaviors. *Cell*, 139(1), 61–72. https://doi.org/10.1016/j.cell.2009.07.036

Xu, J., Deng, X., Watkins, R., & Disteche, C. M. (2008). Behavioral/Systems/Cognitive Sex-Specific Differences in Expression of Histone Demethylases Utx and Uty in Mouse Brain and Neurons. *The Journal of Neuroscience*, 28, 4521–4527. https://doi.org/10.1523/JNEUROSCI.5382-07.2008

Yang, F., Babak, T., Shendure, J., & Disteche, C. M. (2010). Global survey of escape from X inactivation by RNA-sequencing in mouse. *Genome Research*, 20(5), 614–622. https://doi.org/10.1101/GR.103200.109

Figures

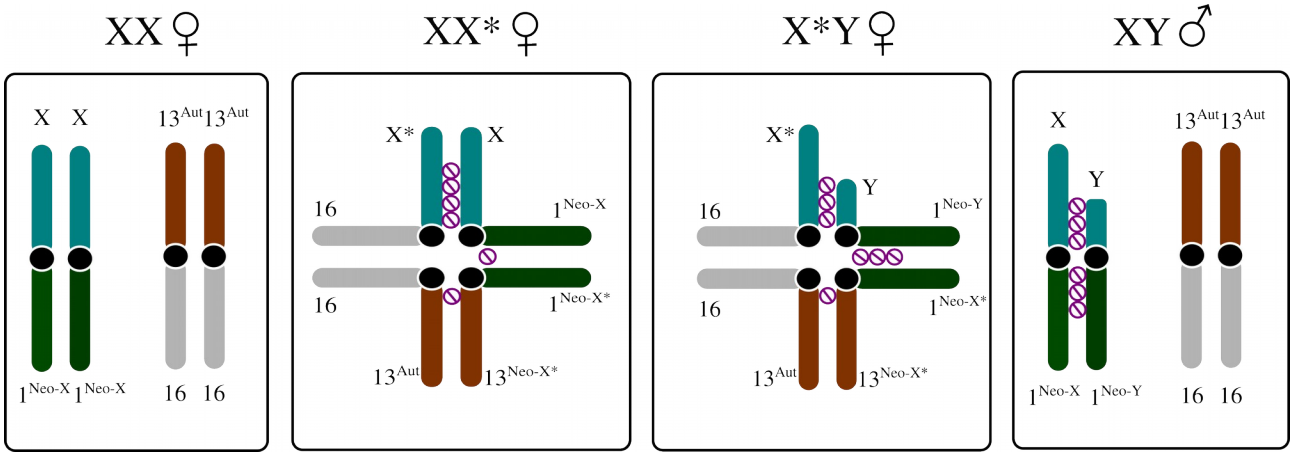

Figure 1. **Scheme of meiotic configurations of sex and neo-sex chromosomes in the four genotypes of the African pygmy mouse**. Autosome 1 is fused to chromosome X and Y, and autosome 16 is fused to chromosome X*, following a whole arm reciprocal translocation between neo-sex chromosome X*.1 and autosome 13.16 (see Veyrunes et al., 2007; Baudat et al., 2019). XX females are (X.1)(X.1) and males are (X.1)(Y.1). Both are homozygous for the autosomal pair (13.16). X*Y and XX* females are heterozygous for chromosome 13: they both have an autosomal copy (linked to autosome 16): 13^{Aut} and a sex-linked copy (linked to autosome 1): $13^{Neo\text{-}X*}$. Some regions of sex and neo-sex chromosomes have stopped recombining (Saunders et al., in prep) and are represented by purple prohibited symbols.

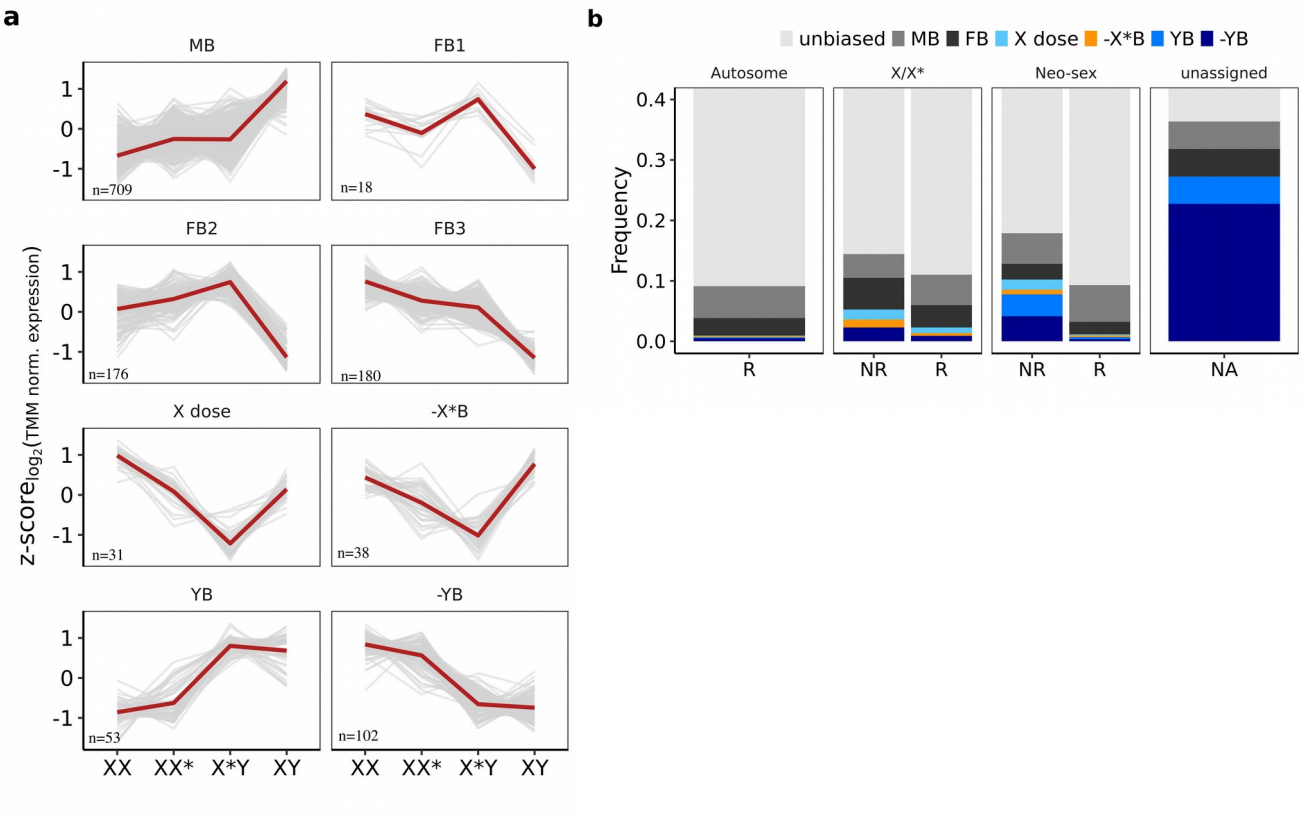

Figure 2. Brain transcriptional architecture in the African pygmy mouse. **a,** Clustering of the 1310 differentially expressed genes in the brain of *M. minutoides*. Each graph corresponds to a module of genes with similar expression patterns identified by the WGCNA software. Grey lines correspond to the average expression of each gene in the four genotypes and dark red lines correspond to the average expression of all genes. Expression values are z-scores : TMM-normalized expression data are $\log_2$ transformed followed by scaling and centering. We detected 8 clusters : MB= genes with a male-biased expression pattern; FB1= female-biased expression with variance across genotype ; FB2= female-biased with overexpression in individuals carrying an X* chromosome ; FB3= female-biased with underexpression in X*Y females ; X dose= underexpression in individuals with a single copy of the X chromosome and even more in X*Y females ; -X*B= underexpression in individuals with the X* chromosome ;YB= overexpression in individuals with a Y chromosome ; -YB= underexpression in individuals with a Y chromosome. 3 genes were not assigned to any modules. The number of genes in each cluster are represented on each graph. **b,** Distribution of differentially expressed (DE) genes across genomic regions. The three female-biased clusters were grouped together as gonadal sex was the main effect (fig. S1). The 'unassigned' category corresponds to regions of the *M. minutoides* genome that did not anchor to the *M. musculus* genome. Enrichment analyses are presented in table 1. Autosomes = 9 799 genes; X/X* (R) = 218 genes, X/X* (NR) = 305 genes, neo-sex (R) = 2167; neo-sex (NR) = 772 genes; unassigned = 22 genes.

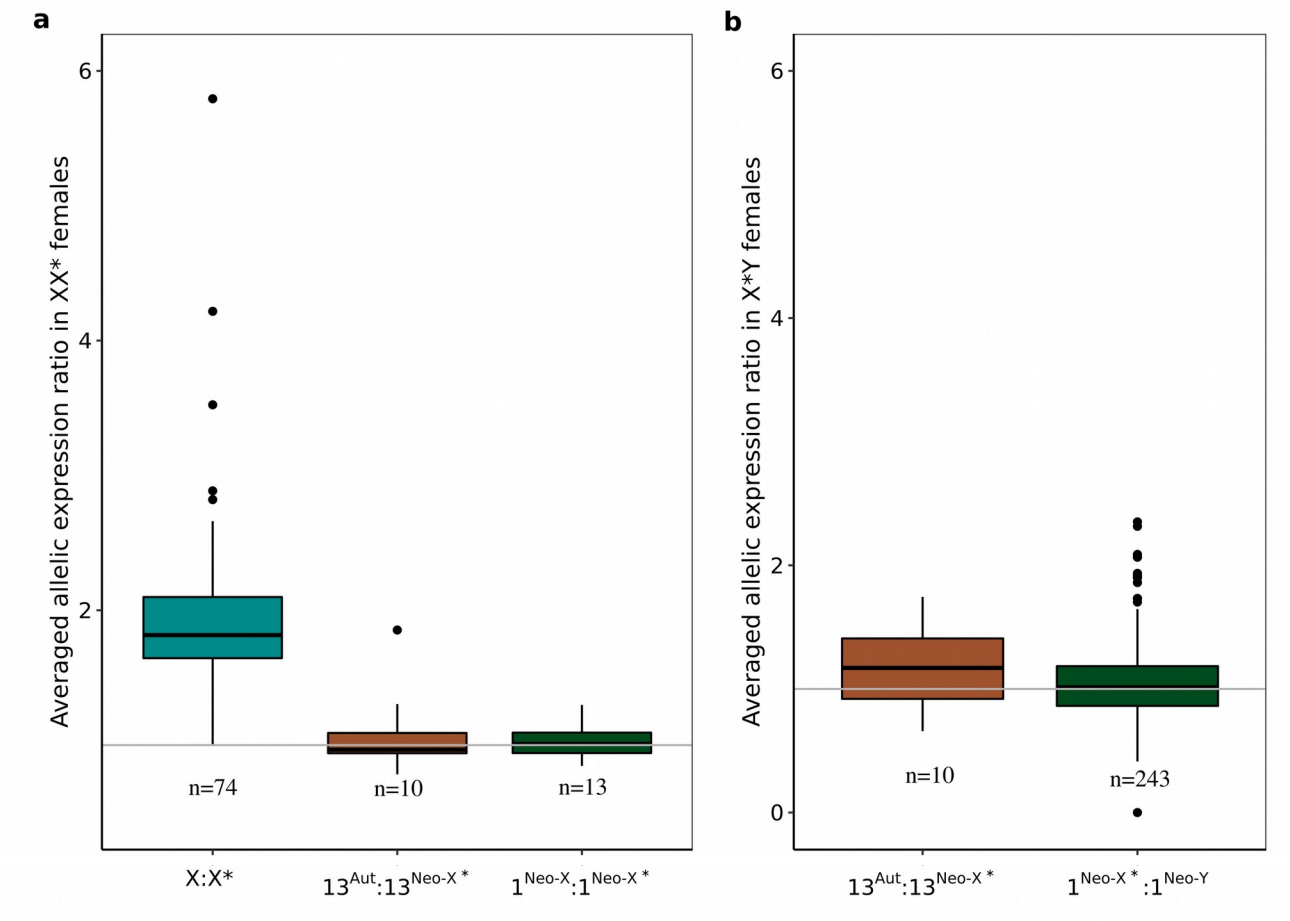

Figure 3. Allele-specific expression in the brain of XX* and X*Y females. a, Averaged allelic expression ratios of (neo-)sex-linked alleles in XX* females. **b,** Averaged expression ratios of neo-sex-linked alleles in X*Y females. Values in boxplots represent ratios averaged across the five individuals, for each X/X*-linked and/or neo-sex-linked genes. We split neo-sex chromosomes into whether they involve chr1 or chr13. Grey lines indicate ratios of 1 with equal expression of both alleles. All genes showing allelic variation are represented. Genes with true allelic imbalance for which we found a *M. musculus* ortholog are shown in table S3 and table S4 for XX* and X*Y females, respectively. Allelic expression ratios per individuals within XX* and X*Y females are represented in fig. S3 and fig. S4.

	Autosomes		Neo-sex (R)			Neo-sex (NR)			X/X* (NR)			X/X* (R)		
Clusters	N ($Freq_{obs}$)	Permutation test p.value	N ($Freq_{obs}$)	Pearson χ^2 p.value	Permutation test p.value	N ($Freq_{obs}$)	Pearson χ^2 p.value	Permutation test p.value	N ($Freq_{obs}$)	Pearson χ^2 p.value	Permutation test p.value	N ($Freq_{obs}$)	Pearson χ^2 p.value	Permutation test p.value
FB	284 (0.03)	0.19	45 (0.02)	0.98	0.29	20 (0.03)	0.65	0.69	16 (0.05)	**0.01 ****	**0.02***	8 (0.04)	0.32	0.29
MB	515 (0.05)	0.78	131 (0.06)	0.08	0.62	39 (0.05)	0.56	0.67	12 (0.04)	0.81	0.9	11 (0.05)	0.5	0.62
X dose	7 (0.0007)	1	4 (0.002)	0.12	0.76	13 (0.02)	**<0.0001*****	**0.0009*****	5 (0.02)	**<0.0001*****	**0.0009*****	2 (0.009)	0.001	0.09
-X*B	21 (0.002)	0.99	6 (0.003)	0.38	0.46	6 (0.008)	**0.004****	**0.02***	4 (0.01)	**<0.0001*****	**0.01****	1 (0.005)	0.49	0.46
YB	17 (0.002)	1	7 (0.003)	0.13	0.8	28 (0.04)	**<0.0001*****	**0.0009*****	0	0.51	0.71	0	0.5	0.58
-YB	48 (0.005)	1	8 (0.004)	0.72	0.5	32 (0.04)	**<0.0001*****	**0.0009*****	7 (0.02)	**<0.0001*****	**0.01****	2 (0.009)	0.34	0.5
Unbiased	8909 (0.91)	-	1967 (0.91)	-	-	634 (0.82)	-	-	261 (0.86)	-	-	194 (0.89)	-	-

Table 1. **Distribution of DE genes and enrichment analysis**. Observed frequencies ($Freq_{obs}$) of DE genes on sex and neo-sex chromosomes were compared to that of autosomes using Pearson χ^2 tests (one sided hypothesis). N values refer to the number of genes in each category. Enrichment on sex and neo-sex chromosomes were also tested using permutation tests. We considered regions enriched in DE genes when significance thresholds were passed in both methods. The three female-biased clusters were grouped together. Asterisks indicate the significance level.*** $p \leq 0.001$, **$p \leq 0.01$,*$p \leq 0.05$ and significant p.values are in bold. Enrichment results were consistent across methods and showed an enrichment in DE genes with a genotype effect on sex and neo-sex chromosomes. MB= male-biased ; FB= female-biased; X dose = genes overexpressed in XX females, followed by XX* and XY individuals, and then X*Y; -X*B= genes underexpressed in X*-carrying females; YB= genes overexpressed in Y-carrying individuals; -YB= genes underexpressed in Y-carrying individuals.

Chapter 5

The evolution of gene expression on sex and neo-sex chromosomes: detecting signs of degeneration ?

Louise D. Heitzmann, Paul A. Saunders, Julie Perez, Pierre Boursot* & Frédéric Veyrunes*

* equal contribution

Foreword

This chapter is based on a side project on sex and neo-sex chromosomes' evolution in the African pygmy mouse, in collaboration with Dr. Paul Saunders. In this project, I undertake similar analyses that I developed on the brain transcriptome, to evaluate the evolution of gene expression in sex-linked non-recombining regions (e.g. differential expression, clustering and allele-specific expression analyses). Because X/X* and neo-sex chromosomes have stopped recombining, these methods could help detect signs of degeneration at the gene expression level. Data presented here are based on analyses that are still in progress, and our plan will be to publish these results alongside Paul's work describing the arrest of recombination and the evolution of sequences in non-recombining regions. These results, although they are a part of a different project, can nevertheless bring insights on whether sex chromosomes' degeneration can also induce phenotypic divergences between females, and thus describe another axis of the genotype-phenotype relationship.

Besides my work on brain sexual differentiation, I took part in a big project on the investigation of sex and neo-sex chromosomes' evolution in the African pygmy mouse, using the kidney transcriptome. As I participated in the brain sampling (RNA extraction) and did the analyses (from quality control of sequencing data to gene/allelic expression), I could thus bring my skills to the project. We also have the liver transcriptome but preliminary analyses show these data are unusable.

The system in *M. minutoides* is young with a feminizing X* and multiple neo-sex chromosomes, especially in our population study, that emerged less than a million years ago (e.g. Veyrunes et al., 2004; Veyrunes et al., 2007; Veyrunes et al., 2013). Sex and neo-sex chromosomes have different ancestries (Fig 1A) and each show patterns of recombination suppression potentially leading to their degeneration (Fig 1B). Hence, the system in *M. minutoides* is one of a kind example to test theoretical models of sex chromosomes' evolution. However, in Paul's analyses, we did not find signs of degeneration based on sequence analyses (i.e., no large deletions, no accumulation of transposable elements, no accumulation of detrimental mutations in coding sequences, etc). This might be due to the fact that recombination suppression is recent (<1Mya), so that signs of degeneration have not had time to evolve. We thus tested whether we could observe degeneration at the gene expression level, as suggested by recent models of sex chromosomes' evolution (e.g Lenormand et al., 2020; Lenormand & Roze, 2022). I thus implemented the skills and methods developed in the previous chapter on the brain transcriptome to detect such signs (methods are described in supplementary methods): we assumed that chromosome degeneration was associated with down-regulation of gene expression in individuals with non-recombining regions (in the absence of dosage compensation) and/or down-regulation of non-recombining alleles (e.g. Lenormand et al., 2020; Lenormand & Roze, 2022).

As a reminder, we have four different genomic compartments according to their sex-linkage and recombination patterns: autosomes, X/X* chromosomes chromosome 1 (chr1; $1^{Neo\text{-}X}$, $1^{Neo\text{-}X*}$ and $1^{Neo\text{-}Y}$ copies) and chromosome 13 (chr13; 13^{Aut} and $13^{Neo\text{-}X*}$ copies). Some region of the X* does not recombine with the X chromosome (Fig 1B). This non-recombining region is referred to as NR in contrast to the recombining region: R. The three possible copies of chr1: $1^{Neo\text{-}X}$, $1^{Neo\text{-}X*}$ and $1^{Neo\text{-}Y}$ (Fig 1B), have different recombination patterns (Fig 1B): there is a large region (and probably the most ancient) on the $1^{Neo\text{-}Y}$ that do not recombine with the other two copies of chr1 ($1^{Neo\text{-}X/X*}$), which we called NRY. Another small region does not recombine between the three copies, this region is referred to as NR within chr1. Finally, there is a small non-recombining region on chr13: $13^{Neo\text{-}X*}$ copy does not recombine with the autosomal copy. Non-recombining and recombining regions are referred to as NR and R, within chr13.

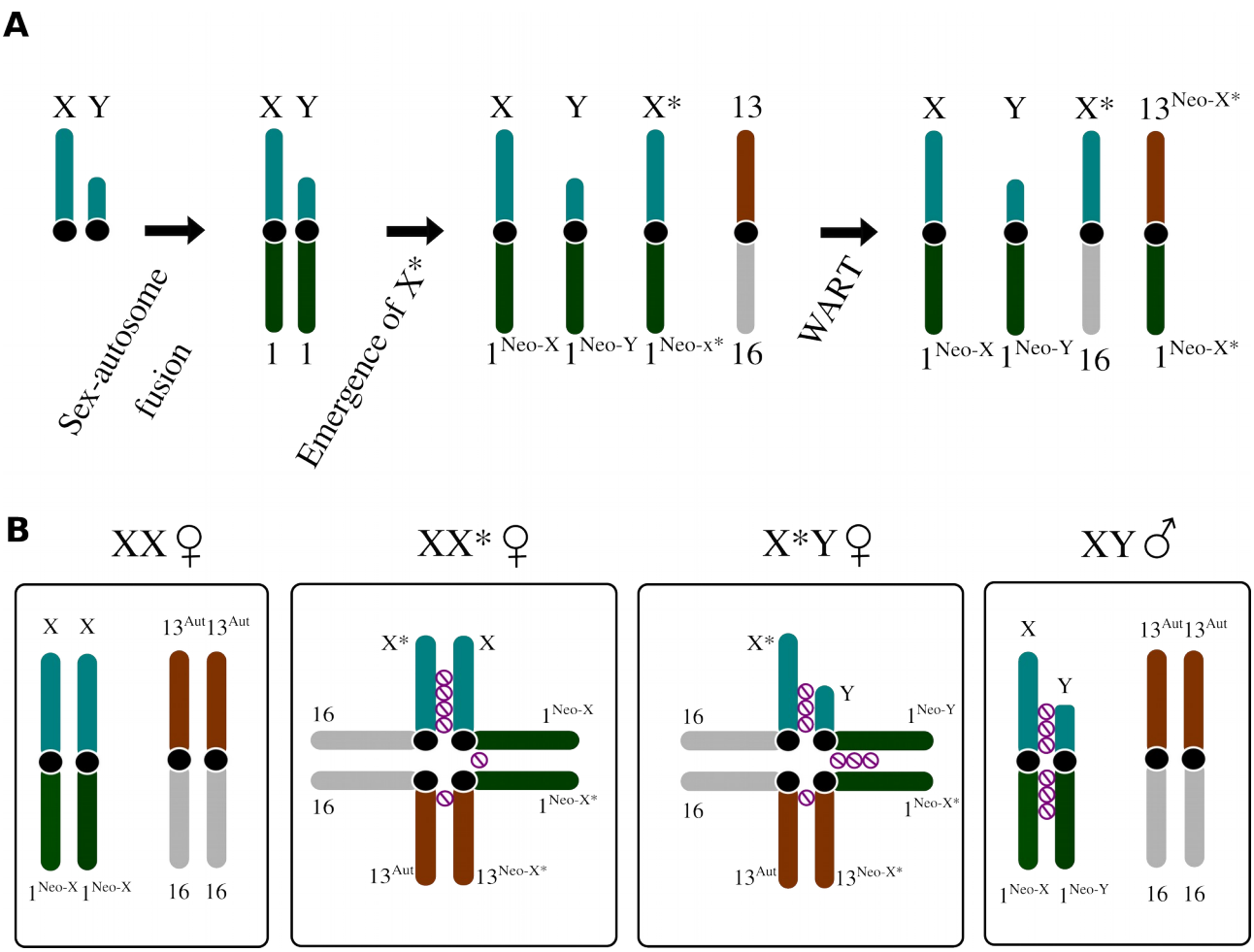

Figure 1. Evolution and configurations (at meiosis) of sex and neo-sex chromosomes in the African pygmy mouse, with patterns of recombination. **A,** Timeline of events leading to the three sex chromosomes and the multiple neo-sex chromosomes. Here, we presumed that the sex-autosome fusion predates the emergence of the X*. WART= whole arm reciprocal translocation. **B,** Recombination status between each gametologs in each genotype. Recombination suppression is indicated by purple prohibited symbols. Adapted from P. Saunders.

A few predictions can be made: the X* carries a large non-recombining region, potentially prone to degeneration, but because the X* is hemizygous in X*Y females (it is facing an already highly degenerated Y chromosome in X*Y females), we hypothesized that X* degeneration is unlikely or restricted: mild deleterious effects that can be compensated with X* preferential silencing in XX* females, and trans-regulatory factors in X*Y females to restore optimal expression levels (assuming expression is under strong stabilising selection). For chr1, predictions of degeneration differ between NR and NRY regions. NRY region is free to degenerate as the $1^{Neo\text{-}Y}$ always faces a recombining -homolog ($1^{Neo\text{-}X}$ in males and $1^{Neo\text{-}X*}$ in X*Y females). In the NR region, $1^{Neo\text{-}X}$ recombines in XX females so degeneration is not expected, and degeneration of $1^{Neo\text{-}X*}$ and $1^{Neo\text{-}Y}$ depends on the status of

its homologous partner, i.e., one can degenerate only if the other copy is functional because expressing two deleterious copies will be counter-selected. We defined it as alternative degeneration. In contrast, because autosome 13 recombines in XX and XY individuals, we hypothesized that the NR region of $13^{Neo\text{-}X*}$ is free to degenerate.

1. Detecting genes with an overall expression pattern consistent with degeneration (and no dosage compensation)

We first investigated gene differential expression, to test whether we find the same patterns of expression in the kidney as in the brain (gene expression influenced by both gonadal and genotypic sex), and among which some could fit patterns of degeneration: lower expression levels in individuals carrying NR regions, and thus suggesting also the lack of dosage compensation. We were thus interested in genes underexpressed in X*Y and XY individuals (test for $1^{Neo\text{-}Y}$ degeneration), or X*Y and XX* (test for $1^{Neo\text{-}X*}$, $13^{Neo\text{-}X*}$ and X* degeneration). Among the 13430 genes expressed in the kidney, 352 were found to be differentially expressed (DE), with expression patterns highly similar to what we found on the brain (Fig 2a). Based on a clustering analysis (k-means), we found 114 genes under the influence of gonads (male or female-biased, 85 and 29 genes, respectively), 64 with an influence of both gonads and sex chromosomes, and the remaining 174 were mainly influenced by sex chromosomes (Fig 2a). Among the 174 DE genes, 43 genes were underexpressed in X*-carrying females (-X*B cluster), 24 genes were underexpressed in X*Y and XY individuals (-YB cluster), and 27 genes had the lowest expression level in X*Y females, followed by XX* and males (XX females had the highest level of expression; X dose cluster). After identifying genes with a pattern of expression we were interested in, we needed to retrieve genes that were in the sex-linked NR regions of sex and neo-sex chromosomes and in fact, we found a significant enrichment of X dose genes along the X/X* chromosomes (both in NR and R regions), and a significant enrichment of X dose and -YB genes along the NR and NRY regions of chr1 (Fig 2b, tables S1 and S2).

(figure below)

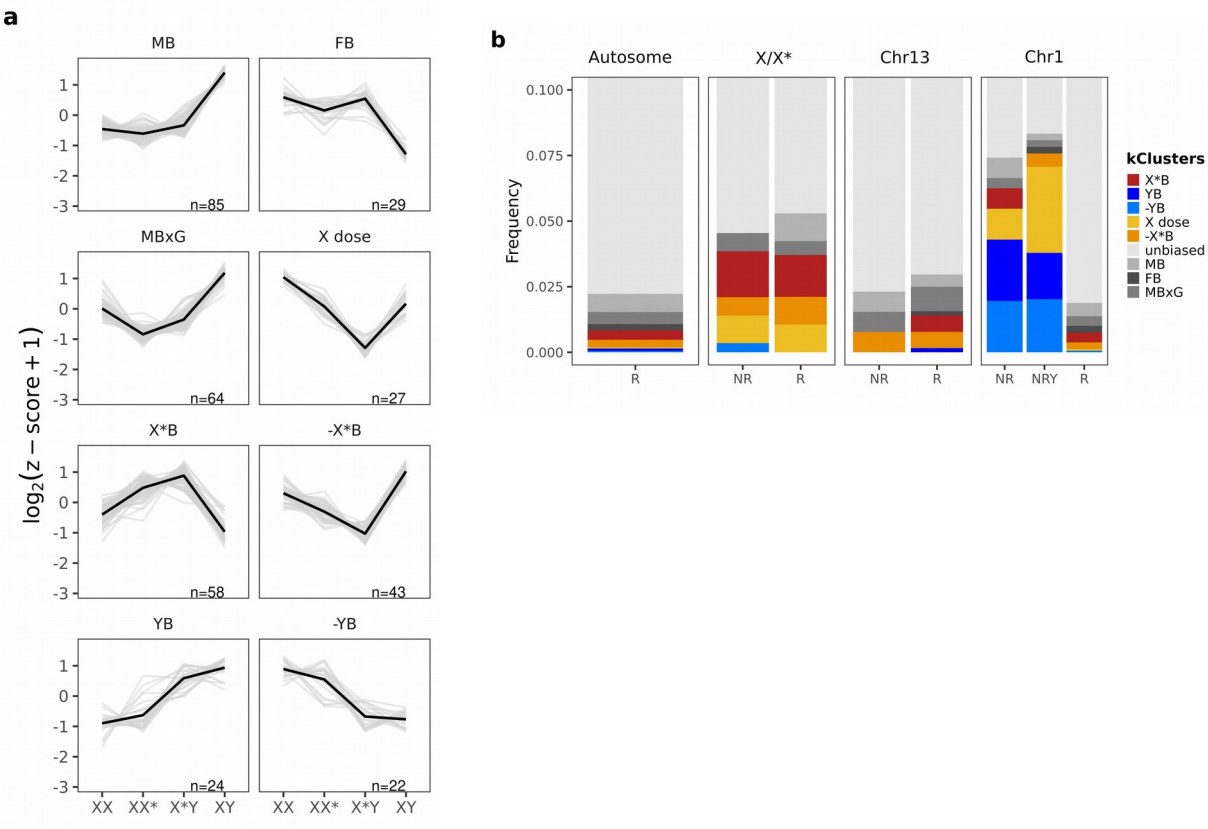

Figure 2. Differential expression and distribution of differentially expressed genes (DEG). **a,** Clustering (k-means) of DEG detected by multiple pairwise comparisons. Values are z-scores of normalized expression data (TMM) on the $\log_2$ scale. The number of genes in each cluster are represented on each graph. Gray lines represent average expression of genes and the black lines represent the averaged expression of all genes (which defines the clusters' expression pattern). **b,** Distribution of DEG in each genomic compartment. Chr1 was split in NR (non-recombining region between $1^{\text{Neo-X}}$, $1^{\text{Neo-X*}}$ and $1^{\text{Neo-Y}}$) and NRY regions (non-recombining between $1^{\text{Neo-X/X*}}$ and $1^{\text{Neo-Y}}$). Sample sizes and enrichment are represented in table S1. FB= female-biased; MB= male-biased; MBxG= male-biased with variance between female genotypes; X dose = influence of the number of X chromosome: overexpression in XX followed by XX* and XY, and then X*Y; X*B= overexpression in individuals carrying a X* chromosome, i.e., X*-biased; -X*B= underexpression in individuals carrying a X* chromosome; YB= overexpression in individuals carrying a Y chromosome, i.e., Y-biased; -YB= underexpression in individuals carrying a Y chromosome.

2. Orientation of gene expression changes in NR regions.

Because differential expression of the genes highlighted above could be due to a down-regulation of gene expression in these genotypes, or an up-regulation of gene expression in the other genotypes, we then compared overall gene expression to an outgroup, *M. mattheyi* (a closely related species that belong to the same subgenus *Nannomys,* we thus assumed it is the ancestral state). We could thus orientate changes of expression in NR regions. Based on this investigation, we did not see clear signs of degeneration (without dosage compensation), with only a few sex-linked genes that were underexpressed in individuals carrying the non-recombining copy (Fig 3). Moreover, most of the changes involved an up-regulation in other genotypes. A very few were down-regulated and the most concerned genomic region was the NR region of the $1^{Neo\text{-}Y}$ chromosome: 5 genes were down-regulated in X*Y and XY individuals compared to *M. mattheyi*.

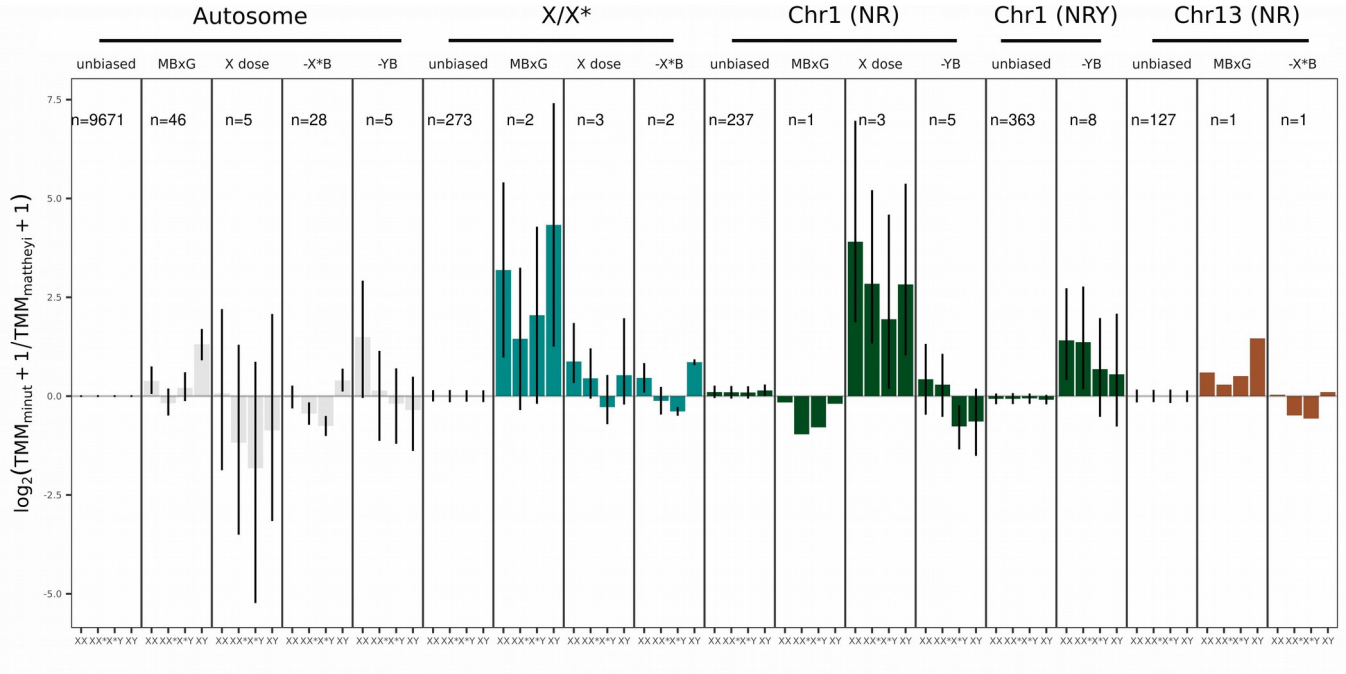

Figure 3. Expression changes of underexpressed genes in NR regions and autosomes. Values are mean normalized expression ratios (*M.minutoides / M. mattheyi)* on the $\log_2$ scale, ± 95% confidence intervals. 0 indicates no difference in expression levels between species (grey lines). Unbiased genes represent the control group. The number of genes in each category are represented on each graph. Genotypes in each panel are from left to right: XX, XX* and X*Y and XY.

3. Allele-specific expression in NR regions

In a second time, we assessed allele-specific expression of genes that carry known fixed differences in NR regions of X/X* and neo-sex chromosomes (see supplemental methods). Assuming degeneration is associated with a down-regulation of non-recombining alleles, there were no signs of global degeneration in these regions: expression between the recombining and non-recombining gametologs was balanced overall (Fig 4a). Concerning X and X* specifically, this suggests a random X/X* inactivation, which contrasts results on the brain and strengthens the preferential X* chromosome inactivation and/or imprinting found on the brain only. Nevertheless, we did find a pattern for the 1^{Neo-Y}: 31 (out of 219) genes significantly deviated from a balanced expression between 1^{Neo-Y} and $1^{Neo-X/X*}$ in XY and X*Y individuals. Expression levels of the 1^{Neo-Y} allele were lower for 21 of these genes. We included informations on the overall expression pattern (unbiased, differentially expressed) and comparisons with the outgroup to test for dosage compensation. We assumed that unbiased genes (i.e., similar expression levels between the four genotypes) but with greater expression of recombining alleles indicate dosage compensation, and similarly if genes had an expression level close to the outgroup (although debatable). The outgroup was presumed to partially indicate the direction of the change as well. On that instance, most of the genes for which 1^{Neo-Y} alleles were underexpressed (15 out of 21) were unbiased in their overall expression between the four genotypes (Fig 4b), and with an expression close to, or greater than *M. mattheyi.* This suggests both down-regulation of 1^{Neo-Y} alleles and up-regulation of 1^{Neo-X} and 1^{Neo-X*} alleles in X*Y and XY individuals and thus, potential dosage compensation. This is consistent with the theory of simultaneous dosage compensation to 1^{Neo-Y} degeneration in NR regions.

(figure below)

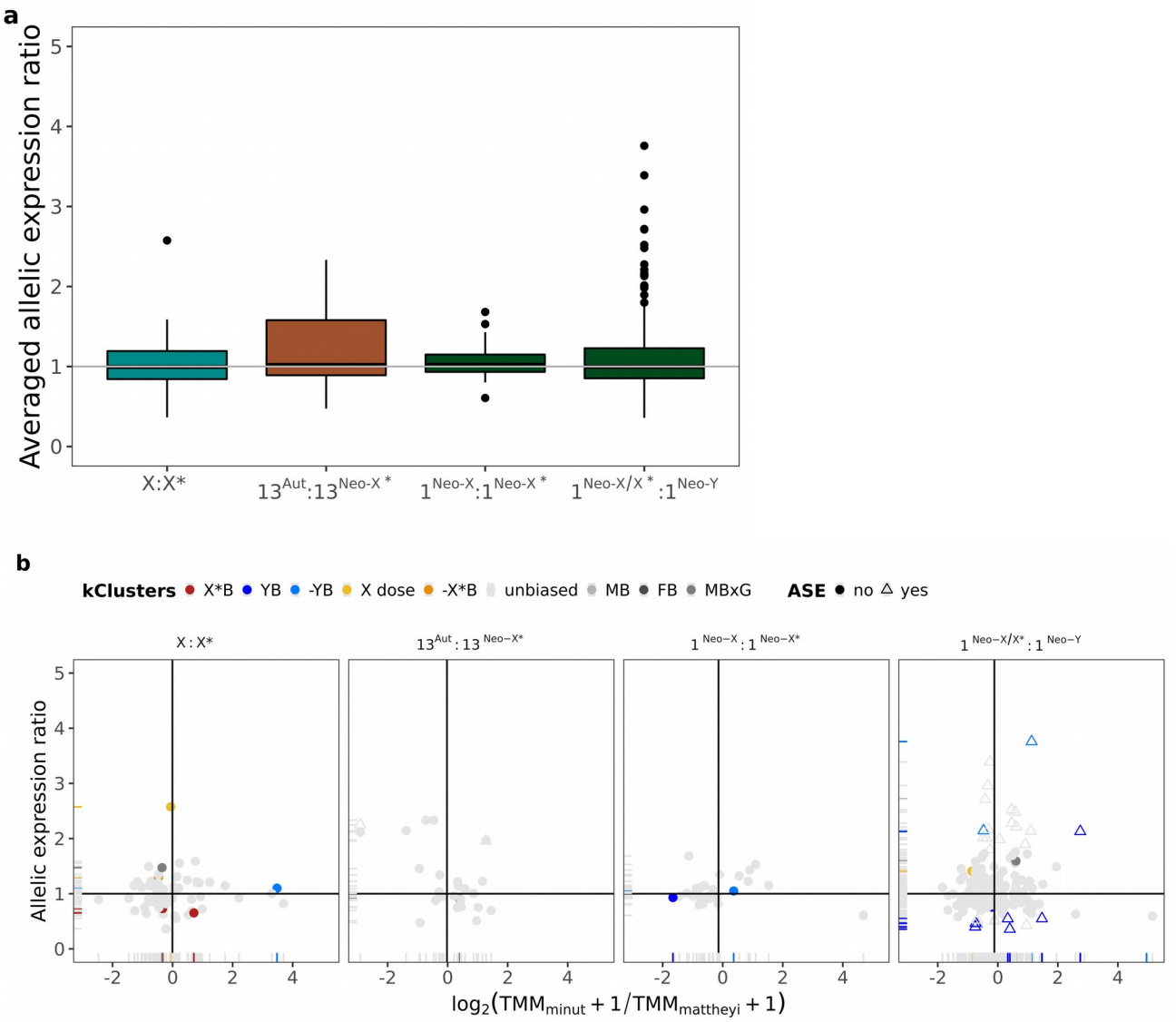

Figure 4. Allele-specific expression in NR regions. 13^{Aut}:$13^{Neo\text{-}X*}$ allelic expression ratios were assessed using XX* and X*Y females, $1^{Neo\text{-}X}$:$1^{Neo\text{-}X*}$ and X:X* alleles were assessed using XX* females, and $1^{Neo\text{-}X/X*}$:$1^{Neo\text{-}Y}$ alleles were assessed using X*Y and XY individuals. Allelic ratio values were averaged between genotypes, except for X/X* alleles. **a,** Global allelic expression in each NR region. **b,** **A**llelic expression as a function of expression changes in *M. minutoides*. The y-axis represents averaged allelic ratios and the x-axis represents overall normalized expression ratios (*minutoides/mattheyi*) on the $\log_2$ scale: expression values for *M. minutoides* were averaged between genotypes used. Solid vertical lines correspond to mean overall expression ratios and horizontal lines correspond to allelic ratios of 1 (i.e., equal expression of recombining and non-recombining alleles).Alleles with true allelic imbalance are represented with triangles. $n_{X/X*}$=64, $n_{13Aut/13Neo\text{-}X*}$=26, $n_{1Neo\text{-}X/1Neo\text{-}X*}$= 26 ,$n_{1Neo\text{-}X/X*/1Neo\text{-}Y}$= 219.

Conclusion and perspectives

Using similar methods to the one used on the brain transcriptome, we found similar results on the kidney (with the exception of X/X* inactivation and imprinting), which show the conspicuous effect of the new architecture of the sex chromosomes in driving tissue's differentiation. Although there is no striking evidence of degeneration, we do show some subtle signs in the NR region of the $1^{Neo\text{-}Y}$ chromosome, which carry a large and probably the most ancient non-recombining region: we found evidence for the down-regulation of alleles in the non-recombining region of the $1^{Neo\text{-}Y}$ copy, and dosage compensation for most of them. The different ancestries are likely to drive the dynamic of sex and neo-sex chromosomes' differentiation. Moreover, these results in favour of an ongoing degeneration could broaden our views on the different sexual phenotypes found in *M. minutoides*. We shed light on another potential evolutionary mechanism driving phenotypic divergences, and perhaps maladaptation depicting the genotype-phenotype relationship. However, this is just the tip of the icerberg and in order to complete this part on the evolution of gene expression, further investigations must be undertaken, notably:

*Comparing allele-specific expression on the $1^{Neo\text{-}Y}$ chromosome to the expression of the outgroup directly, *M. Mattheyi*) and running allele-specific expression on *M. mattheyi* which could help us further orientate allelic expression changes.

* Investigating the function of genes that fit degeneration patterns.

* Use both our reference genomes (XX and X*Y) to strengthen analyses and investigate the Y chromosome (no assembly available yet)

* Investigate sex-biased expression in *M. mattheyi* and compare expression levels with the four genotypes in *M. minutoides* to test the impact of the new mode of sex chromosomes' transmission on the evolution of gene expression: (de)-feminization, (de)-masculinization.

References

Lenormand, T., Fyon, F., Sun, E., & Correspondence, D. R. (2020). Sex Chromosome Degeneration by Regulatory Evolution. *Current Biology*, *30*, 3001-3006.e5. https://doi.org/10.1016/j.cub.2020.05.052

Lenormand, T., & Roze, D. (2022). Y recombination arrest and degeneration in the absence of sexual dimorphism. *Science*, *375*(6581), 663-666. https://doi.org/10.1126/SCIENCE.ABJ1813/SUPPL_FILE/SCIENCE.ABJ1813_MDAR_REPRODUCIBILITY_CHECKLIST.PDF

Veyrunes, F., Catalan, J., Sicard, B., Robinson, T. J., Duplantier, J.-M., Granjon, L., Dobigny, G., & Britton-Davidian, J. (2004). Autosome and Sex Chromosome Diversity Among the African Pygmy Mice, Subgenus Nannomys (Murinae; Mus). *Chromosome Research*, *12*(4), 369–382. https://doi.org/10.1023/B:CHRO.0000034098.09885.e6

Veyrunes, F., Watson, J., Robinson, T. J., & Britton-Davidian, J. (2007). Accumulation of rare sex chromosome rearrangements in the African pygmy mouse, Mus (Nannomys) minutoides : A whole-arm reciprocal translocation (WART) involving an X-autosome fusion. *Chromosome Research*, *15*(2), 223-230. https://doi.org/10.1007/s10577-006-1116-8

Veyrunes, F., Perez, J., Paintsil, S. N. C., Fichet-Calvet, E., & Britton-Davidian, J. (2013). Insights into the evolutionary history of the X-linked sex reversal mutation in mus minutoides: Clues from sequence analyses of the Y-linked sry gene. *Sexual Development*, *7*(5), 244–252. https://doi.org/10.1159/000351223

General discussion

Sexual dimorphism is usually associated with sexual selection (e.g. mate choice, intra-sexual competition) as well as the resolution -or partial resolution-, of sexual conflicts stemming from sex differences in phenotypic optima for a trait, or between interacting traits under sex-specific selection. In vertebrates, the proximate biological factor at the basis of sexual dimorphism was long thought to be gonadal steroid hormones, influencing the expression of genes and subsequent phenotypes. This paradigm is even more accurate for sex differences in brain and behaviours, where studies have focused on hormones only to seek and explain sexual dimorphism (e.g. Breedlove et al., 1999; Phoenix et al., 1959). Yet, sex chromosomes can be conducive to sexual conflicts (and their resolution) on one hand, and it has been shown that differences between the sexes arise before gonadal differentiation (Arnold, 2004; Ayers et al., 2013; Hale et al., 2011; Ma et al., 2018), supporting a role for sex chromosomes. For over the past two decades, several studies, mostly using genetically modified mice, have shown that sex chromosomes can have a direct influence on the sexual differentiation of the brain, hence impacting fitness-related phenotypes (Arnold, 2020b; De Vries et al., 2002; Gatewood et al., 2006). However, the role of sex chromosomes is far from being understood and most studies rely on genetically modified mice, which may have some limitations especially when you are interested in phenotypes shaped by natural and sexual selection.

For the past ten years, a wild mouse species, the African pygmy mouse (*Mus minutoides*), has proved to be a fascinating species, that can help us tackle these questions. In *M. minutoides*, there are three sex chromosomes and multiple neo-sex chromosomes at the origin of three different female genotypes: XX, XX* and X*Y, with a special emphasis on the latter implying females with a Y chromosome. Not only females have different genotypes but they also display different phenotypes, where X*Y females were found to have a greater reproductive success than XX and XX* females (Saunders et al., 2014), but had some masculinized traits: enhanced aggressiveness, higher bite strength, reduced anxiety (Ginot et al., 2017; Saunders et al., 2016). This highlight a dichotomy between gonadal and phenotypic sex, with X*Y females being different from the other females, and questions about the differentiation of the brain in this species as well as the role of sex chromosomes in shaping sex differences in brain and behaviours. Throughout my thesis, I worked on the African pygmy mouse and encompassed an integrative framework combining behavioural , neurobiological and transcriptomic approaches, to study the consequences of this atypical system on the differentiation of the brain and behaviours. Hence, this is a collaborative work that included many people from various domains in biology, which have helped contribute to disentangle from the hormonal and

genetic bases of brain sexual differentiation. Overall, this collaborative work showed that the new sex chromosome architectures have profoundly impacted phenotypes, with the accumulation of divergence in fitness-related traits.

The depiction of a genotype-phenotype relationship is not unequivocal, and studies examining the genetic bases of complex phenotypes remain rare (Bendesky et al., 2017; Elipot et al., 2014; Metz et al., 2017; Moore et al., 2022). The African pygmy mouse, with four genotypes and various phenotypes represent a tremendous opportunity to describe this relationship. By combining diverse approaches, we have been able to relate behaviours with potential underlying proximate mechanisms (e.g. candidate gene expression, neural pathways), and discuss the evolutionary causes behind the different female phenotypes.

Overall, we found that the brain transcriptome of *M.minutoides* reflects the different phenotypes observed, as illustrated by the relatively high proportion of genes (17%), for which X*Y females were either similar to males or different from all individuals. Even genes that were male or female-biased, and especially the latter, showed an influence of the X* and/or the Y chromosome. This result contrasted previous studies based on genetically modified mouse or wild species with naturally occurring sex reversal, but with no phenotypic variation (e.g. Blencowe et al., 2022.; Ma et al., 2018). In the latter, genotypic sex had a minor influence on the phenotypes (less than 1%), with a major influence of gonadal sex and thus, steroid hormones. We found that differentially expressed genes were enriched on sex and neo-sex chromosomes, which highlight their direct role in driving the sexual differentiation of the brain in *M. minutoides*. These patterns were also found on the kidney transcriptome (chapter 5), supporting the role of sex and neo-sex chromosomes in shaping the differentiation of non gonadal tissues and subsequent phenotypes. Looking at allele-specific expression, we found a preferential expression of X over X* alleles in the non-recombining region of the X/X* chromosome in XX* females. Because the pattern was global, it pointed towards a chromosome-wide effect and thus, the skewed inactivation of the X* chromosome. Interestingly, we did not find this pattern looking at the kidney[10] (chapter 5), which suggested random inactivation, in line with previous results based on embryo fibroblast cell cultures (Veyrunes & Perez, 2018). Therefore, non-random inactivation of the X* chromosome is only found in the brain so far, which raises questions about the evolutionary processes it must stem from. But most importantly, this singular result underpins and could thus explain the constant phenotypic similarities between XX and XX* females. This also contributes to the identification of the genetic basis of female phenotypes.

10 We have data for the liver ,which suggest random inactivation as well, but preliminary investigations on the transcriptome reflected sequencing issues. We thus did not use these data.

Indeed, it had been previously shown that XX and XX* females display similar behavioural and morphological traits related to aggressiveness, anxiety and reproduction (Ginot et al., 2017; Saunders et al., 2014, 2016). Here, we further extend similarities to parental behaviours and to the genetic/ hormonal input. We found that the sex chromosome complement shapes maternal behaviours: with X*Y females being more efficient at pup retrieval, displaying greater levels of maternal aggression, but they are less efficient at building nests than the other females. Because nests are critical to assure pups' protection from potential threats, we suggest that X*Y females can compensate protection with maternal aggression. On that instance, sex chromosomes do not seem to alter maternal care quality but rather shape two distinct parental strategy (chapter 1), where X*Y females diverge from both XX and XX* females. Because females do not display differences in testosterone and estradiol (see Annexe), it suggests that these differences either reflect a direct impact of sex-linked genes' expression, or their influence on autosomal expression. Neural circuits investigations were inconclusive but we still found an interesting candidate : the neo-sex-linked gene tyrosine hydroxylase (*Th*), coding the enzyme stimulating dopamine synthesis, and known to stimulate pup retrieval in laboratory mice, through the regulation of oxytocin (N. Scott et al., 2015). Because *Th* can be under the positive influence of the *Sry* gene, which is expressed in the brain of X*Y females (Rahmoun et al., 2014), and considering it is located in the recombining region of the Neo-X*/neo-Y copies of chromosome 1, it was a strong candidate to correlate with behaviours. However, we only found a tendency for a greater density of neurons expressing *Th* in the anteroventral periventricular nucleus of the hypothalamus in X*Y females, when compared to XX and XX* females (and males). Interestingly, *Th* also came up when investigating the molecular basis of enhanced territorial aggression in X*Y females (chapter 3). In the latter study, we re-investigated testosterone concentrations as in the study in Annexe but in a post-aggression context, and found that circulating testosterone was unlikely to drive territorial aggression in females. We however highlighted another gene regulating dopamine levels, in addition to *Th*, the sex-linked gene monoamine oxydase A (*MaoA*), whose expression levels were consistent with an overall enhanced aggressiveness in X*Y females (Scott et al., 2008). In fact, *Th* and *MaoA* genes were also found looking at the whole brain transcriptome (chapter 4), with expression levels reflecting the phenotypes observed. Therefore, sex chromosomes are likely to directly drive the divergence in social and maternal behaviours found in *M. minutoides,* through sex-linked genes expression rather than through the regulation of steroid hormones. One of their potential actors that came out as a strong candidate and which needs further investigations is the dopaminergic system.

Interestingly, we further found candidate genes that are related to fertility, separating X*Y females from both XX and XX* females (chapter 4). More precisely, we found two genes : *Amhr2* (autosomal) and *Lhb* (neo-sex linked), which are involved in the regulation of folliculogenesis (i.e.,

ovarian follicle maturation) and ovulation. When overexpressed, these genes impair reproductive functions by preventing follicle maturation due to a high ratio luteinizing hormone (LH) over follicle stimulating hormone (FSH), a characteristic found in polycystic ovary syndrome (Cimino et al., 2016; Huhtaniemi et al., 2006). Because both are underexpressed in X*Y females (similar expression in XX, XX* and males), they thus represent good candidates at the genetic basis of the greater reproductive success in X*Y females (Saunders et al., 2014). Not only we found candidate genes, but we were also able to discriminate and refute some, narrowing the potential genetic bases of phenotypes. This is the case for the steroid sulfatase gene, for which an overexpression is positvively related to aggression (Mortaud et al., 2010), inconsistent with our observations on the brain transcriptome (underexpressed in Y-bearers). We did not find other striking genes that correspond to behaviours or other traits observed among individuals, but an in-depth analysis of genes in each cluster compared to the literature could help suggest new phenotypes that have not been outlined yet.

Combining the brain transcriptome, neural investigations and behaviours, we showed that sex chromosomes contribute to the differentiation of the brain and behaviours in *M. minutoides*. It is noteworthy though that we only confronted the effects of gonadal hormones at adulthood (i.e., activational effect of steroid hormones) to that of sex chromosomes, and we did not include the potential effect of hormones during fetal development (i.e., organizational effect). Because we did not find evidence for differences in hormones among adults, we assumed that hormonal levels do not differ perinatally as well, albeit this needs to be be experimentally tested. On that note, we have been collecting for over a year the brains of embryos, from ~8.5 days *post-coitum* (dpc) to birth, including the 11.5 dpc period where gonads start to differentiate. For example, we could test for a differential expression of androgen and estrogen receptors, or whether *Sry* is expressed in the brain during early stages of development. These data could help us investigate the ontogeny of sex differences in brain and the biological factors involved : sex chromosomes and hormones.

Taken together, we emphasize that the emergence of the X* chromosome has redesigned the evolutionary trajectories of sex-linked genomic regions (according to their mode of transmission), which in turn drive the sexual phenotypes in the African pygmy mouse. Interestingly, similar results were found in a recent study on the African cichlid fish *Metriaclima mbenjii*, with a polygenic sex determination system, where there are three female genotypes (ZZXX, ZWXX, ZWXY) and one male genotype (ZZXY) (Moore et al., 2022). In this species, genotypic sex has been shown to influence morphology (e.g mass, body shape, anogenital distance), behaviours (e.g. grooming) of the three types of females, and could also influence reproductive phenotypes (differences in genital size). Their result implied that the evolution of a new sex determining gene opened avenues to multiple

sexual phenotypes, in line with our findings following the emergence of the X*. Thus, we challenge here the long-standing view of brain sexual differentiation triggered by steroid hormones, and underline the necessity to investigate system subject to natural and sexual selection to understand the role of sex chromosome in shaping sexual dimorphism/polymorphism.

The divergent phenotypes and their genetic bases -especially the preferential expression of X alleles (underpinning X*-biased inactivation)-, raised questions about the evolutionary forces driving these patterns. The new architecture of sex and neo-sex chromosomes drives divergent evolutionary trajectories between sex-linked regions, which may generate new sexual conflicts and influence how they cope with them. In the following is discussed the potential role of each sex chromosome (and neo-sex chromosomes).

One one hand, there is the male-specific Y chromosome, which is now found in a female environment. We could expect that the expression of Y-linked alleles, which have been tight to a male context for over 166 My and are involved in male-specific phenotypes, is thus disadvantageous for X*Y females. For example, Y-linked genes, such as *Sry*, have been related or suggested to trigger aggressiveness, increase susceptibility to Parkinson's disease (Arnold, 2020a; Lee et al., 2019), and impair parental behaviours (Gatewood et al., 2006). In the brain transcriptome, we found a few Y-linked genes expressed in the brain of X*Y females, but *Sry* was not detected. However, we know from another study that it is expressed in the brain of X*Y females (Rahmoun et al., 2014) and hence, could alter and masculinize female phenotypes. Accordingly, we found that X*Y females do not build good quality nests (which theoretically, could alter pup survival) (chapter 1), a pattern found in males (unpublished data), whichcould thus suggest maladaptation due to the presence of the Y. Moreover, we found that 12% of differentially expressed genes (which is the majority of genes under the influence of genotypic sex: 17% previously shown) were expressed at similar levels in the brain of X*Y females and males. However, these genes were mostly found in the non-recombining region of the neo-Y chromosome, which has a more recent evolution (Veyrunes et al., 2004, 2007, 2013). This reflects a greater evolutionary dynamic following the arrest of recombination on the neo-Y, which is likely to drive maladaptive phenotypes. Indeed, once chromosomes stop recombining, selection efficiency is dampen and deleterious mutation can accumulate and drive the loss of optimal gene expression, the loss of genes and the accumulation of transposable elements (TEs) underpinning chromosome degeneration (e.g. (B. Charlesworth & Charlesworth, 2000; Graves, 2006). Interestingly, in *Drosophila* for example, it has been shown that the formation of heterochromatin that allows for the silencing of TEs and repeats is less efficient in males, and this process decreases drastically in old males in comparison to females (Nguyen & Bachtrog, 2021). The subsequent overexpression of TEs

has been hypothesized to explain reduced lifespan and fertility in males in many species, and is referred to as the 'Y/W' toxic effect[11] (see Marais et al., 2018; Nguyen & Bachtrog, 2021). Similarly, in male plants, degeneration of the Y chromosome has been suggested to alter fertility and longevity (see Charlesworth, 2018) because of hemizygosity and expression of recessive mutations (selection is less efficient at removing slightly deleterious mutations impacting fitness). Although there is no evidence for TEs enrichment on the neo-Y chromosome, we however shed light on the subtle degeneration of Y-linked alleles using the kidney transcriptome of *M. minutoides* (allele-specific expression and comparison of overall expression to an outgroup : *M. mattheyi,* the presumed ancestral state) (chapter 5). Allele-specific expression results indicated dosage compensation for most of the genes concerned, albeit we also found a couple of genes down-regulated in Y-bearers (with and without allelic variation), suggesting the lack or incomplete dosage compensation. Interestingly, in the brain, we found both instance of preferential expression of Neo-X* and neo-Y alleles in X*Y females (with and without a bias in expression), which support the degeneration of neo-Y alleles but also imprinting, with the preferential expression of one allele over the other probably due to sexual conflicts. Altogether, the presence of the neo-Y chromosome in X*Y females is likely to drive phenotypic divergence in X*Y females (both adaptive and/or non-adaptive), albeit we did not find a direct link with observed phenotypes (chapter 4). As for the Y chromosome, which is already degenerated and enriched in repeated sequences, its future assembly will help us test for allele-specific expression of homologs between the X* and the Y chromosome, and for the direct effect of Y-linked genes in X*Y females. Because we have the X*Y reference genome as well (though assembly is chimeric between neo-sex chromosomes), it will also be interesting to combine both method to assess the role of Y-linked genes and strengthen the analyses presented in this thesis.

On the other hand, there is the X chromosome, hemizygous in males, and thus directly subjected to selection: recessive mutations beneficial to males but detrimental to females can accumulate, while dominant mutations will be purged in females due to recombination. The interplay between inheritance (including effective population size), mutation, allelic dominance, recombination and sex-specific selection can thus influence the dynamic of X evolution, as illustrated by the "faster-X effect" (i.e., greater rate of evolution on the X chromosome; Meisel & Connallon, 2013). However, in our case, the X chromosome spends more time in a male context: in our study population, X*Y females are found in greater proportions (e.g. ~75% of females are X*Y) and 80% of offspring in XX litters are males (XX are the rare sex) (Saunders et al., 2022). Hence, one could suggest a greater accumulation of male-beneficial genes on the X chromosome, leading to its "masculinization".

11 Interestingly, preliminary investigations show that there is a negative correlation between aging and X*Y females litter sizes, sharper than in XX and XX* females. This work is currently being carried out in collaboration with JF. Lemaitre & Y. Voituron

Eventually, the propagation of male beneficial alleles will impact the expression in females as well, generating an intra-locus sexual conflict. Consequently, differential expression or parental imprinting would be favoured by selection to solve or mitigate such conflicts. This is exemplified by the enrichment of genes on the X/X* chromosomes, that are underexpressed in the brain and kidney of X*Y females (and XX* to a lesser extent) (chapter4-5). Moreover, we found that the majority of differences between the X and the X* were driven by changes on the X chromosome (chapter 5), and some of them are probably due to gene duplications (e.g *MaoA*; Saunders et al., in prep*)*, which are not found on the X* chromosome (likely to be at the ancestral state). Hence, genes underexpressed in X*Y females due to the divergence of the X chromosome (similar expression levels between XX, XX* and XY individuals) (chapter 4), could support a process of "masculinization", and its potential contribution to maladaptive phenotypes in XX/XX* females. For instance, genes regulating fertility: *Amhr2* and *Lhb* are equally expressed between XX, XX* and males, with patterns of expression that correlate the divergent phenotypes. However, *Amhr2* is autosomal and *Lhb* is in the non-recombining region of chromosome 1, suggesting either an impact of X alleles on neo-sex alleles and/or autosomes, or a direct influence of neo-sex alleles. On that instance, adaptive phenotypes and notably the greater reproductive success in X*Y females could reflect a reduced fertility in XX/XX* females (maladaptation) due to changes on the X chromosome, which deviates from its female optimum. However, to confirm masculinization of the X chromosome, we would need to test whether expression levels for specific genes are beneficial to male phenotypes (e.g. QTL analysis).

Finally (and X corollary), there is the X*, a female specific chromosome directly subject to selection in X*Y females due to hemizygosity, which makes it favourable for females to reach their phenotypical optima. This hypothesis could explain the greater reproductive success in X*Y females, and investigations on lactation could also point towards an effect of the X* (chapter 2): preliminary results are not usable but it seemed **at first sight** that XX* and X*Y were both different from XX females, in favour of a beneficial effect of X* on lactation efficiency (e.g. more dopamine neurons regulating prolactin and greater levels of prolactin). However, methods in this study need to be optimized and explored further before concluding on the adaptive role of the X* chromosome on lactation. Moreover, X* stopped recombining with a large portion of the X chromosome (two thirds), which favours divergence in this genomic region. However, because the X* faces an already degenerated Y chromosome, the X* is likely to be under strong purifying selection. Therefore, differential expression between X/X* chromosomes could reflect (partially) solved sexual conflicts, rather than genetic degeneration of the X* chromosome. This is supported by allele-specific expression analysis showing no preference of X over X* alleles in the kidney. However, in the brain, we found that X alleles are overexpressed (X* seems to be preferentially inactivated), highlighting X-

linked genomic imprinting probably due to underlying sexual conflict as suggested above (Day & Bonduriansky, 2004; Iwasa & Pomiankowski, 2001). Finally, genomic regions linked to the X* chromosome, also show signs of differentiation between copies. For instance, the *Lhb* gene, which contributes to the regulation of ovulation and represents an appealing candidate to correlate with the greater ovulation rate in X*Y females is located in the non-recombing region of chromosome 1 (i.e., no recombination between $1^{Neo\text{-}X}$, $1^{Neo\text{-}X*}$ and $1^{Neo\text{-}Y}$). Hence, X* and the different versions of neo-X* chromosomes could all contribute to the adaptative phenotypes in X*-carriers.

Although questions persist and many more have been raised (e.g. sexual conflict at the basis of X* preferential inactivation),all things being equal, the new sex chromosome architecture in *M. minutoides* seem to have laid grounds for new sexual conflicts, Accordingly, it is possible that differences in gene expression at the basis of the new sexual phenotypes emerged from these conflicts.

In this thesis, we did not test whether sexual selection could influence the different phenotypes as well, but females do not show extravagant sexual dimorphism in morphology and previous studies were rather unfavourable to male preference for a female genotype among the three (Saunders et al., 2016). Considering the propensity of X*Y females on being more aggressive, we could hypothesize a female-female competition over a mate, but there is no evidence for inter-female aggression in our breeding colony (in cages of females) that could suggest otherwise. Nevertheless, it would be interesting to observe mice behaviours in a natural or semi-natural environment: assess social interactions and their mating system. This could support, or not, a role for sexual selection, as well as confirm behaviours observed here, in a controlled environment.

In conclusion, we have seen that not only sex and neo-sex chromosomes influence the sexual differentiation of the brain in the African pygmy mouse, but their combination in a polygenic sex determination system has broadened the dimensions of sexual dimorphism, and rather depicts a sexual polymorphism. And it is on that note that I would like to end this work by a short parallel with social sciences, and what can we learn from the African pygmy mouse about sex and gender.

The brain, more than just a reflection of gonadal sex : implications for social sciences

"I'm just a woman with a penis" In one person, John Irving

Sex differences in brain and behaviours have retained most of our attention for centuries, trying to depict the very own singularities of male and female phenotypes in humans. Some of these studies have been helpful to understand inequalities in terms of disease susceptibility for instance, which can in turn help predict and treat these diseases (e.g. Alzheimer's and Parkison's diseases are more prevalent in males (see Arnold, 2020a for review; Davis et al., 2020; Lee et al., 2019)), or to investigate the evolution of sexual dimorphism, in relation to sexual conflicts for instance (e.g. in the present thesis). Others have been misused and have been the motor of a distinction between a male and a female brain, i.e., neurosexism (Eliot, 2019). These studies have helped shape two sexual categories with each, specific characteristics and roles anchored into society. On that basis any deviation from the category would be considered as pathological or abnormal[12]. These classes have justified the settlement of a hierarchy based on patriarchy in many societies, where males are dominant, the strong sex and geniuses, while females are submissive, dependent, maternal and less smart (Bian et al., 2018; Kortenhaus & Demarest, 1993). For instance, it was over a century ago, in 1879, that Gustave Le Bon (see Gould, 1980) wrote :

> "All psychologists which have studied the intelligence of women, as well as poets and novelists, recognize today that they represent the most inferior forms of human evolution and that they are closer to children and savages than to an adult, civilized man. They excel in fickleness, inconstancy, absence of thought and logic, and incapacity to reason."

Even Darwin, when he conceptualized his fascinating theory of sexual selection to describe sexual dimorphism (which has been a breakthrough for the scientific community), he was focused on males as the sexy and combative sex, while females are choosy and present traits mainly involved in parental care (Darwin, 1871). His work has led to further study biases. Yet, they are many counter-examples where females are the combative sex like in hyenas, or with brighter colours such as on the face of rhesus macaques (see Clutton-Brock & Huchard, 2013 for review). All in all, there has been a constant dichotomy between what a male or a female phenotype is and must be, delineating a

12 e.g. the depathologization of transgender persons has been declared in 2019 by the World Health Organization (Castro-Peraza et al., 2019)

stereotypical view of sexual phenotypes[13]. Because the distinction of both rely on the gonadal status of an individual (i.e., ovaries or testes), it creates a confusion between sex as a function, and gender that encompasses all secondary sexual characteristics including brain and behaviours in social sciences[14].

Yet, while gonadal sex is defined by the presence of ovaries or testes that defines a female or a male in their reproductive function respectively, there is no one typical female or male brain, and both phenotype and genotype can be uncoupled. In the African pygmy mouse, there are three different female genotypes : they all have ovaries and each present brain similarities and divergences to each other, as well as to males. Thus, our results emphasize that phenotypic sex is not dichotomic, it varies and takes many shapes; its reflects an interaction of hormones and sex chromosomes in a specific environment, and any change in one of these factors is likely to influence the phenotype. It is even more true in human societies where experiences and culture are dominant parts of our lives that interact with our biological factors to shape how we think, behave and react to situations.

13 This is illustrated in our society by the market of children's toys that is starkly divided between "girls" and "boys" toys (e.g. household activities, beauty and child care for girls, cars, soldiers and legos for boys) (Hand, 2017)

14 Gender in social sciences is a social construction based on traits, roles and norms specific to each sex, including interactions between the sexes and their inclusion into a hierarchical society (mainly patriarchal).

Cited references

Abbott, J. K. (2011). Intra-locus sexual conflict and sexually antagonistic genetic variation in hermaphroditic animals. *Proceedings of the Royal Society B: Biological Sciences*, *278*(1703), 161-169. https://doi.org/10.1098/rspb.2010.1401

Afonso, A. S., Cantareli, C. V., Levy, R. P., & Veras, L. B. (2016). Evasive mating behaviour by female nurse sharks, *Ginglymostoma cirratum* (Bonnaterre, 1788), in an equatorial insular breeding ground. *Neotropical Ichthyology*, *14*. https://doi.org/10.1590/1982-0224-20160103

Alexander, R. D., Hoogland, J. L., Howard, R. D., Noonan, K. M., & Sherman, P. W. (1979). *Sexual dimorphisms and breeding systems in pinnipeds, ungulates, primates, and humans*. 402-435.

Arnold, A. P. (2004). Sex chromosomes and brain gender. *Nature Reviews Neuroscience*, *5*(9), 701-708. https://doi.org/10.1038/nrn1494

Arnold, A. P. (2009a). Mouse Models for Evaluating Sex Chromosome Effects that Cause Sex Differences in Non-Gonadal Tissues. *Journal of Neuroendocrinology*, *21*(4), 377-386. https://doi.org/10.1111/j.1365-2826.2009.01831.x

Arnold, A. P. (2009b). The organizational-activational hypothesis as the foundation for a unified theory of sexual differentiation of all mammalian tissues. *Hormones and Behavior*, *55*(5), 570-578. https://doi.org/10.1016/j.yhbeh.2009.03.011

Arnold, A. P. (2017). A general theory of sexual differentiation. *Journal of Neuroscience Research*, *95*(1-2), 291-300. https://doi.org/10.1002/jnr.23884

Arnold, A. P. (2020a). Four Core Genotypes and XY* mouse models : Update on impact on SABV research. *Neuroscience and Biobehavioral Reviews*, *119*, 1-8. https://doi.org/10.1016/j.neubiorev.2020.09.021

Arnold, A. P. (2020b). Sexual differentiation of brain and other tissues : Five questions for the next 50 years. *Hormones and Behavior*, *120*, 104691. https://doi.org/10.1016/j.yhbeh.2020.104691

Arnold, A. P., & Breedlove, S. M. (1985). Organizational and activational effects of sex steroids on brain and behavior : A reanalysis. *Hormones and Behavior*, *19*(4), 469-498. https://doi.org/10.1016/0018-506X(85)90042-X

Arnold, A. P., & Chen, X. (2009). What does the « four core genotypes » mouse model tell us about sex differences in the brain and other tissues? *Frontiers in Neuroendocrinology*, *30*(1), 1-9. https://doi.org/10.1016/j.yfrne.2008.11.001

Arnold, A. P., Reue, K., Eghbali, M., Vilain, E., Chen, X., Ghahramani, N., Itoh, Y., Li, J., Link, J. C., Ngun, T., & Williams-Burris, S. M. (2016). The importance of having two X chromosomes. *Philosophical Transactions of the Royal Society B: Biological Sciences*, *371*(1688). https://doi.org/10.1098/RSTB.2015.0113

Arnqvist, G., & Rowe, L. (1995). Sexual conflict and arms races between the sexes : A morphological adaptation for control of mating in a female insect. *Proceedings of the Royal Society of London. Series B: Biological Sciences*, *261*(1360), 123-127. https://doi.org/10.1098/rspb.1995.0126

Ashman, T.-L. (2009). Sniffing out patterns of sexual dimorphism in floral scent. *Functional Ecology*, *23*(5), 852-862. https://doi.org/10.1111/j.1365-2435.2009.01590.x

Ayers, K. L., Davidson, N. M., Demiyah, D., Roeszler, K. N., Grützner, F., Sinclair, A. H., Oshlack, A., & Smith, C. A. (2013). RNA sequencing reveals sexually dimorphic gene expression before gonadal differentiation in chicken and allows comprehensive annotation of the W-chromosome. In *Genome Biology* (Vol. 14, p. R26-R26). https://doi.org/10.1186/gb-2013-14-3-r26

Bachtrog, D., Mank, J. E., Peichel, C. L., Kirkpatrick, M., Otto, S. P., Ashman, T.-L., Hahn, M. W., Kitano, J., Mayrose, I., Ming, R., Perrin, N., Ross, L., Valenzuela, N., Vamosi, J. C., & Consortium, T. T. of S. (2014). Sex Determination : Why So Many Ways of Doing It? *PLOS Biology*, *12*(7), e1001899. https://doi.org/10.1371/journal.pbio.1001899

Barrett, S. C. H., & Hough, J. (2013). Sexual dimorphism in flowering plants. *Journal of Experimental Botany*, *64*(1), 67-82. https://doi.org/10.1093/jxb/ers308

Barthold, S. W. (2004). Genetically altered mice : Phenotypes, no phenotypes, and Faux phenotypes. *Genetica*, *122*, 75-88.

Bateman, A. J. (1948). Intra-sexual selection in Drosophila. *Heredity*, *2*(3), 349-368. https://doi.org/10.1038/hdy.1948.21

Bedhomme, S., Bernasconi, G., Koene, J. M., Lankinen, Å., Arathi, H. S., Michiels, N. K., & Anthes, N. (2009). How does breeding system variation modulate sexual antagonism? *Biology Letters*, *5*(5), 717-720. https://doi.org/10.1098/rsbl.2009.0401

Bedhomme, S., & Chippindale, A. K. (2007). Irreconcilable differences : When sexual dimorphism fails to resolve sexual conflict. In D. J. Fairbairn, W. U. Blanckenhorn, & T. Székely (Éds.), *Sex, Size and Gender Roles : Evolutionary Studies of Sexual Size Dimorphism* (p. 0). Oxford University Press. https://doi.org/10.1093/acprof:oso/9780199208784.003.0021

Bell, G. (1978). The evolution of anisogamy. *Journal of Theoretical Biology*, *73*(2), 247-270. https://doi.org/10.1016/0022-5193(78)90189-3

Bellott, D. W., Skaletsky, H., Pyntikova, T., Mardis, E. R., Graves, T., Kremitzki, C., Brown, L. G., Rozen, S., Warren, W. C., Wilson, R. K., & Page, D. C. (2010). Convergent evolution of chicken Z and human X chromosomes by expansion and gene acquisition. *Nature*, *466*(7306), 612-616. https://doi.org/10.1038/nature09172

Bendesky, A., Kwon, Y. M., Lassance, J. M., Lewarch, C. L., Yao, S., Peterson, B. K., He, M. X., Dulac, C., & Hoekstra, H. E. (2017). The genetic basis of parental care evolution in monogamous mice. *Nature*, *544*(7651), 434-439. https://doi.org/10.1038/nature22074

Berletch, J. B., Ma, W., Yang, F., Shendure, J., Noble, W. S., Disteche, C. M., & Deng, X. (2015). Escape from X Inactivation Varies in Mouse Tissues. *PLOS Genetics*, *11*(3), e1005079-e1005079. https://doi.org/10.1371/JOURNAL.PGEN.1005079

Berletch, J. B., Yang, F., Xu, J., Carrel, L., & Disteche, C. M. (2011). Genes that escape from X inactivation. *Human Genetics*, *130*(2), 237-245. https://doi.org/10.1007/s00439-011-1011-z

Beukeboom, L. W., & Perrin, N. (2014a). The evolution of sex chromosomes. In L. W. Beukeboom & N. Perrin (Éds.), *The Evolution of Sex Determination* (p. 0). Oxford University Press. https://doi.org/10.1093/acprof:oso/9780199657148.003.0005

Beukeboom, L. W., & Perrin, N. (2014b). What are sexes, and why are there sexes? In L. W. Beukeboom & N. Perrin (Éds.), *The Evolution of Sex Determination* (p. 0). Oxford University Press. https://doi.org/10.1093/acprof:oso/9780199657148.003.0001

Bian, L., Leslie, S.-J., & Cimpian, A. (2018). Evidence of bias against girls and women in contexts that emphasize intellectual ability. *American Psychologist*, *73*, 1139-1153. https://doi.org/10.1037/amp0000427

Billiard, S., López-Villavicencio, M., Devier, B., Hood, M. E., Fairhead, C., & Giraud, T. (2011). Having sex, yes, but with whom? Inferences from fungi on the evolution of anisogamy and mating types. *Biological Reviews of the Cambridge Philosophical Society*, *86*(2), 421-442. https://doi.org/10.1111/j.1469-185X.2010.00153.x

Bishop, D. V. M., Canning, E., Elgar, K., Morris, E., Jacobs, P. A., & Skuse, D. H. (2000). Distinctive patterns of memory function in subgroups of females with Turner syndrome : Evidence for imprinted loci on the X-chromosome affecting neurodevelopment. *Neuropsychologia*, *38*(5), 712-721. https://doi.org/10.1016/S0028-3932(99)00118-9

Blencowe, M., Chen, X., Zhao, Y., Itoh, Y., McQuillen, C. N., Han, Y., Shou, B. L., McClusky, R., Reue, K., Arnold, A. P., & Yang, X. (2022). Relative contributions of sex hormones, sex chromosomes, and gonads to sex differences in tissue gene regulation. *Genome Research*, *32*, 807-824. https://doi.org/10.1101/GR.275965.121

Breedlove, S. M., Cooke, B. M., & Jordan, C. L. (1999). The Orthodox View of Brain Sexual Differentiation. *Brain, Behavior and Evolution*, *54*, 8-14. https://doi.org/10.1159/000006607

Britton-Davidian, J., Robinson, T. J., & Veyrunes, F. (2012). Systematics and evolution of the African pygmy mice, subgenus Nannomys : A review. *Acta Oecologica*, *42*, 41-49. https://doi.org/10.1016/j.actao.2012.01.001

Bućan, M., & Abel, T. (2002). The mouse : Genetics meets behaviour. *Nature Reviews Genetics*, *3*(2), 114-123. https://doi.org/10.1038/nrg728

Bull, J. J. (1983). Evolution of sex determining mechanisms. *Evolution of Sex Determining Mechanisms.* https://www.cabdirect.org/cabdirect/abstract/19840180646

Burgoyne, P. S., Thornhill, A. R., Boudrean, S. K., Darling, S. M., Bishop, C. E., & Evans, E. P. (1995). The genetic basis of XX-XY differences present before gonadal sex differentiation in the mouse. *Philosophical Transactions of the Royal Society of London. Series B, Biological Sciences*, *350*(1333), 253-260. https://doi.org/10.1098/rstb.1995.0159

Castro-Peraza, M. E., García-Acosta, J. M., Delgado, N., Perdomo-Hernández, A. M., Sosa-Alvarez, M. I., Llabrés-Solé, R., & Lorenzo-Rocha, N. D. (2019). Gender Identity : The Human Right of Depathologization. *International Journal of Environmental Research and Public Health*, *16*(6), 978. https://doi.org/10.3390/ijerph16060978

Chailakhyan, M. Kh. (1979). Genetic and Hormonal Regulation of Growth, Flowering, and Sex Expression in Plants. *American Journal of Botany*, *66*(6), 717-736. https://doi.org/10.2307/2442417

Charlesworth, B. (1991). The evolution of sex chromosomes. *Science (New York, N.Y.)*, *251*(4997), 1030-1033. https://doi.org/10.1126/science.1998119

Charlesworth, B., & Charlesworth, D. (2000). The degeneration of Y chromosomes. *Philosophical Transactions of the Royal Society B: Biological Sciences*, *355*(1403), 1563-1572.

Charlesworth, D. (2018). Does sexual dimorphism in plants promote sex chromosome evolution? *Environmental and Experimental Botany*, *146*, 5-12. https://doi.org/10.1016/j.envexpbot.2017.11.005

Chue, J., & Smith, C. A. (2011). Sex determination and sexual differentiation in the avian model. *The FEBS Journal*, *278*(7), 1027-1034. https://doi.org/10.1111/j.1742-4658.2011.08032.x

Cimino, I., Casoni, F., Liu, X., Messina, A., Parkash, J., Jamin, S. P., Catteau-Jonard, S., Collier, F., Baroncini, M., Dewailly, D., Pigny, P., Prescott, M., Campbell, R., Herbison, A. E., Prevot, V., & Giacobini, P. (2016). Novel role for anti-Müllerian hormone in the regulation of GnRH neuron excitability and hormone secretion. *Nature Communications*, *7*. https://doi.org/10.1038/NCOMMS10055

Clutton-Brock, T. H. (1982). The Functions of Antlers. *Behaviour*, *79*(2/4), 108-125.

Clutton-Brock, T. H. (1985). Size, Sexual Dimorphism, and Polygyny in Primates. In W. L. Jungers (Éd.), *Size and Scaling in Primate Biology* (p. 51-60). Springer US. https://doi.org/10.1007/978-1-4899-3647-9_4

Clutton-Brock, T. H. (1991). *The Evolution of Parental Care* (p. 352). Princeton University Press.

Clutton-Brock, T. H., & Huchard, E. (2013). Social competition and selection in males and females. *Philosophical Transactions of the Royal Society B: Biological Sciences*, *368*(1631), 20130074. https://doi.org/10.1098/rstb.2013.0074

Cooper, D. W., Johnston, P. G., Watson, J. M., & Graves, J. A. M. (1993). X-inactivation in marsupials and monotremes. *Seminars in Developmental Biology*, *4*(2), 117-128. https://doi.org/10.1006/SEDB.1993.1014

Cox, K. H., Bonthuis, P. J., & Rissman, E. F. (2014). Mouse model systems to study sex chromosome genes and behavior : Relevance to humans. *Frontiers in Neuroendocrinology*, *35*(4), 405-419. https://doi.org/10.1016/j.yfrne.2013.12.004

Cox, K. H., Quinnies, K. M., Eschendroeder, A., Didrick, P. M., Eugster, E. A., Rissman, E. F., & Rissman, E. F. (2015). Number of X-chromosome genes influences social behavior and vasopressin gene expression in mice. *Psychoneuroendocrinology*, *51*, 271-281. https://doi.org/10.1016/j.psyneuen.2014.10.010

Cox, R. M., & Calsbeek, R. (2009). Sexually Antagonistic Selection, Sexual Dimorphism, and the Resolution of Intralocus Sexual Conflict. *The American Naturalist*, *173*(2), 176-187. https://doi.org/10.1086/595841

Czech, D. P., Lee, J., Sim, H., Parish, C. L., Vilain, E., & Harley, V. R. (2012). The human testis-determining factor SRY localizes in midbrain dopamine neurons and regulates multiple components of catecholamine synthesis and metabolism. *Journal of Neurochemistry*, *122*(2), 260-271. https://doi.org/10.1111/j.1471-4159.2012.07782.x

Darwin, C. (1871). *The Descent of Man and Selection in Relationship to Sex*.

Davies, N. B., Krebs, J. R., & West, S. A. (2012). *An Introduction to Behavioural Ecology, 4th Edition | Wiley* (4th éd.).

Davis, E. J., Broestl, L., Abdulai-Saiku, S., Worden, K., Bonham, L. W., Miñones-Moyano, E., Moreno, A. J., Wang, D., Chang, K., Williams, G., Garay, B. I., Lobach, I., Devidze, N., Kim, D., Anderson-Bergman, C., Yu, G.-Q., White, C. C., Harris, J. A., Miller, B. L., … Dubal, D. B. (2020). A second X chromosome contributes to resilience in a mouse model of Alzheimer's disease. *Science Translational Medicine*, *12*(558), eaaz5677. https://doi.org/10.1126/scitranslmed.aaz5677

Day, T., & Bonduriansky, R. (2004). Intralocus Sexual Conflict Can Drive the Evolution of Genomic Imprinting. *Genetics*, 167, 1537-1546. https://doi.org/10.1534/genetics.103.026211

De Vries, G. J., Rissman, E. F., Simerly, R. B., Yang, L. Y., Scordalakes, E. M., Auger, C. J., Swain, A., Lovell-Badge, R., Burgoyne, P. S., & Arnold, A. P. (2002). A model system for study of sex chromosome effects on sexually dimorphic neural and behavioral traits. *Journal of Neuroscience*, *22*(20), 9005-9014. https://doi.org/10.1523/JNEUROSCI.22-20-09005.2002

Deakin, J. E., Hore, T. A., Koina, E., & Marshall Graves, J. A. (2008). The status of dosage compensation in the multiple X chromosomes of the platypus. *PLoS Genetics*, *4*(7), e1000140. https://doi.org/10.1371/journal.pgen.1000140

Derks, M. F. L., Smit, S., Salis, L., Schijlen, E., Bossers, A., Mateman, C., Pijl, A. S., de Ridder, D., Groenen, M. A. M., Visser, M. E., & Megens, H.-J. (2015). The Genome of Winter Moth (Operophtera brumata) Provides a Genomic Perspective on Sexual Dimorphism and Phenology. *Genome Biology and Evolution*, *7*(8), 2321-2332. https://doi.org/10.1093/gbe/evv145

Dewing, P., Chiang, C. W. K., Sinchak, K., Sim, H., Fernagut, P. O., Kelly, S., Chesselet, M. F., Micevych, P. E., Albrecht, K. H., Harley, V. R., & Vilain, E. (2006). Direct regulation of adult brain function by the male-specific factor SRY. *Current Biology*, *16*(4), 415-420. https://doi.org/10.1016/j.cub.2006.01.017

Dewing, P., Shi, T., Horvath, S., & Vilain, E. (2003). Sexually dimorphic gene expression in mouse brain precedes gonadal differentiation. *Brain Research. Molecular Brain Research*, *118*(1-2), 82-90. https://doi.org/10.1016/s0169-328x(03)00339-5

Disteche, C. M. (2012). Dosage Compensation of the Sex Chromosomes. *Annual review of genetics*, *46*, 537-560. https://doi.org/10.1146/annurev-genet-110711-155454

Dumas, P., Pausová, Z., Kren, V., Krenová, D., Pravenec, M., Dumont, M., Ely, D., Turner, M., Sun, Y., Tremblay, J., & Hamet, P. (2000). Contribution of autosomal loci and the Y chromosome to the stress response in rats. *Hypertension*, *35*(2), 568-573. https://doi.org/10.1161/01.HYP.35.2.568

Eliot, L. (2019). Neurosexism : The myth that men and women have different brains. *Nature*, *566*(7745), 453-454. https://doi.org/10.1038/d41586-019-00677-x

Elipot, Y., Hinaux, H., Callebert, J., Launay, J.-M., Blin, M., & Rétaux, S. (2014). A mutation in the enzyme monoamine oxidase explains part of the Astyanax cavefish behavioural syndrome. *Nature Communications*, *5*(1), 3647. https://doi.org/10.1038/ncomms4647

Ezaz, T., Sarre, S. D., O'Meally, D., Graves, J. A. M., & Georges, A. (2009). Sex Chromosome Evolution in Lizards : Independent Origins and Rapid Transitions. *Cytogenetic and Genome Research*, *127*(2-4), 249-260. https://doi.org/10.1159/000300507

Fang, H., Disteche, C. M., & Berletch, J. B. (2019). X Inactivation and Escape : Epigenetic and Structural Features. *Frontiers in Cell and Developmental Biology*, *7*, 219-219. https://doi.org/10.3389/FCELL.2019.00219/FULL

Frank, L. G. (1986). Social organization of the spotted hyaena Crocuta crocuta. II. Dominance and reproduction. *Animal Behaviour*, *34*(5), 1510-1527. https://doi.org/10.1016/S0003-3472(86)80221-4

Frésard, L., Morisson, M., Brun, J.-M., Collin, A., Pain, B., Minvielle, F., & Pitel, F. (2013). Epigenetics and phenotypic variability : Some interesting insights from birds. *Genetics, Selection, Evolution: GSE*, *45*, 16. https://doi.org/10.1186/1297-9686-45-16

Gans, C. (1996). An Overview of Parental Care among the Reptilia. In J. S. Rosenblatt & C. T. Snowdon (Éds.), *Advances in the Study of Behavior* (Vol. 25, p. 145-157). Academic Press. https://doi.org/10.1016/S0065-3454(08)60332-0

Gatewood, J. D., Wills, A., Shetty, S., Xu, J., Arnold, A. P., Burgoyne, P. S., & Rissman, E. F. (2006). Sex chromosome complement and gonadal sex influence aggressive and parental behaviors in mice. *Journal of Neuroscience*, *26*(8), 2335-2342. https://doi.org/10.1523/JNEUROSCI.3743-05.2006

Ginot, S., Claude, J., Perez, J., & Veyrunes, F. (2017). Sex reversal induces size and performance differences among females of the African pygmy mouse, Mus minutoides. *Journal of Experimental Biology*, *220*(11), 1947-1951. https://doi.org/10.1242/JEB.157552

Girard, M. B., & Endler, J. A. (2014). Peacock spiders. *Current Biology*, *24*(13), R588-R590. https://doi.org/10.1016/j.cub.2014.05.026

Gould, S. J. (1980). *Women's Brains*.

Graves, J. A. M. (2006). Sex chromosome specialization and degeneration in mammals. *Cell*, *124*(5), 901-914. https://doi.org/10.1016/J.CELL.2006.02.024

Graves, J. A. M., & Waters, P. D. (2004). Mammalian Sex Chromosome Evolution—The Rise and Fall of the Y Chromosome. In M. Schmid & I. Nanda (Éds.), *Chromosomes Today* (p. 3-14). Springer Netherlands. https://doi.org/10.1007/978-94-017-1033-6_1

Gravholt, C. H. (2004). Epidemiological, endocrine and metabolic features in Turner syndrome. *European Journal of Endocrinology*, *151*(6), 657-687. https://doi.org/10.1530/eje.0.1510657

Hale, M. C., Xu, P., Scardina, J., Wheeler, P. A., Thorgaard, G. H., & Nichols, K. M. (2011). Differential gene expression in male and female rainbow trout embryos prior to the onset of gross morphological differentiation of the gonads Matthew. *BMC Genomics*, *12*, 404-404. https://doi.org/10.1186/1471-2164-12-404

Hamilton, W. D., & Zuk, M. (1982). Heritable True Fitness and Bright Birds : A Role for Parasites? *Science*, *218*(4570), 384-387. https://doi.org/10.1126/science.7123238

Hand, C. (2017). *Everything You Need to Know About Sexism*. The Rosen Publishing Group, Inc.

Hopkins, B. R., & Kopp, A. (2021). Evolution of sexual development and sexual dimorphism in insects. *Current Opinion in Genetics & Development*, *69*, 129-139. https://doi.org/10.1016/j.gde.2021.02.011

Hughes, J. F., & Page, D. C. (2015). The Biology and Evolution of Mammalian Y Chromosomes. *Annual Review of Genetics*, *49*, 507-527. https://doi.org/10.1146/annurev-genet-112414-055311

Huhtaniemi, I., Ahtiainen, P., Pakarainen, T., Rulli, S. B., Zhang, F. P., & Poutanen, M. (2006). Genetically modified mouse models in studies of luteinising hormone action. *Molecular and Cellular Endocrinology*, *252*(1-2), 126-135. https://doi.org/10.1016/J.MCE.2006.03.026

Iwasa, Y., & Pomiankowski, A. (2001). The evolution of X-linked genomic imprinting. *Genetics*, *158*(4), 1801-1809. https://doi.org/10.1093/genetics/158.4.1801

Jay, P., Tezenas, E., Véber, A., & Giraud, T. (2022). Sheltering of deleterious mutations explains the stepwise extension of recombination suppression on sex chromosomes and other supergenes. *PLOS Biology*, *20*(7), e3001698. https://doi.org/10.1371/journal.pbio.3001698

Jeffries, D. L., Gerchen, J. F., Scharmann, M., & Pannell, J. R. (2021). A neutral model for the loss of recombination on sex chromosomes. *Philosophical Transactions of the Royal Society B: Biological Sciences*, *376*(1832), 20200096. https://doi.org/10.1098/rstb.2020.0096

Jotterand-Bellomo, M. (1988). Chromosome analysis of five specimens of Mus bufo-triton (Muridae) from Burundi (Africa) : Three cytogenetic entities, a special type of chromosomal sex determination, taxonomy, and phylogeny. *Cytogenetic and Genome Research*, *48*(2), 88-91. https://doi.org/10.1159/000132596

Khalil, S., Welklin, J. F., McGraw, K. J., Boersma, J., Schwabl, H., Webster, M. S., & Karubian, J. (2020). Testosterone regulates CYP2J19-linked carotenoid signal expression in male red-backed fairywrens (Malurus melanocephalus). *Proceedings of the Royal Society B: Biological Sciences*, *287*(1935), 20201687. https://doi.org/10.1098/rspb.2020.1687

Kitano, J., Mori, S., & Peichel, C. L. (2007). Sexual Dimorphism in the External Morphology of the Threespine Stickleback (Gasterosteus Aculeatus). *Copeia*, *2007*(2), 336-349. https://doi.org/10.1643/0045-8511(2007)7[336:SDITEM]2.0.CO;2

Kitano, J., & Peichel, C. L. (2012). Turnover of sex chromosomes and speciation in fishes. *Environmental Biology of Fishes*, *94*(3), 549-558. https://doi.org/10.1007/s10641-011-9853-8

Kokko, H., & Jennions, M. D. (2008). Parental investment, sexual selection and sex ratios. *Journal of Evolutionary Biology*, *21*(4), 919-948. https://doi.org/10.1111/J.1420-9101.2008.01540.X

Kortenhaus, C. M., & Demarest, J. (1993). Gender role stereotyping in children's literature : An update. *Sex Roles*, *28*(3), 219-232. https://doi.org/10.1007/BF00299282

Lahr, G., Maxson, S. C., Mayer, A., Just, W., Pilgrim, C., & Reisert, I. (1995). Transcription of the Y chromosomal gene, Sry, in adult mouse brain. *Molecular Brain Research*, *33*(1), 179-182. https://doi.org/10.1016/0169-328X(95)00136-G

Lavery, R., Lardenois, A., Ranc-Jianmotamedi, F., Pauper, E., Gregoire, E. P., Vigier, C., Moreilhon, C., Primig, M., & Chaboissier, M.-C. (2011). XY Sox9 embryonic loss-of-function mouse mutants show complete sex reversal and produce partially fertile XY oocytes. *Developmental Biology*, *354*(1), 111-122. https://doi.org/10.1016/j.ydbio.2011.03.029

Le Boeuf, B. J., & Mesnick, S. (1991). Sexual Behavior of Male Northern Elephant Seals : I. Lethal Injuries to Adult Females. *Behaviour*, *116*(1/2), 143-162.

Lee, J., Pinares-Garcia, P., Loke, H., Ham, S., Vilain, E., & Harley, V. R. (2019). Sex-specific neuroprotection by inhibition of the Y-chromosome gene, SRY, in experimental Parkinson's disease. *Proceedings of the National Academy of Sciences of the United States of America*, *116*(33), 16577-16582. https://doi.org/10.1073/pnas.1900406116

Lehtonen, J., Kokko, H., & Parker, G. A. (2016). What do isogamous organisms teach us about sex and the two sexes? *Philosophical Transactions of the Royal Society B: Biological Sciences*, *371*(1706), 20150532. https://doi.org/10.1098/rstb.2015.0532

Lehtonen, J., & Parker, G. A. (2014). Gamete competition, gamete limitation, and the evolution of the two sexes. *Molecular Human Reproduction*, *20*(12), 1161-1168. https://doi.org/10.1093/molehr/gau068

Lenormand, T., Fyon, F., Sun, E., & Correspondence, D. R. (2020). Sex Chromosome Degeneration by Regulatory Evolution. *Current Biology*, *30*, 3001-3006.e5. https://doi.org/10.1016/j.cub.2020.05.052

Lindholm, A., & Breden, F. (2002). Sex chromosomes and sexual selection in poeciliid fishes. *The American Naturalist*, *160 Suppl 6*, S214-224. https://doi.org/10.1086/342898

Lipp, H.-P., & Wolfer, D. P. (1998). Genetically modified mice and cognition. *Current Opinion in Neurobiology*, *8*(2), 272-280. https://doi.org/10.1016/S0959-4388(98)80151-7

Lipp, H.-P., & Wolfer, D. P. (2003). Genetic background problems in the analysis of cognitive and neuronal changes in genetically modified mice. *Clinical Neuroscience Research*, *3*(4), 223-231. https://doi.org/10.1016/S1566-2772(03)00096-3

Liu, J., Chen, L.-Y., Zhou, P., Liao, Z., Lin, H., Yu, Q., & Ming, R. (2021). Sex biased expression of hormone related genes at early stage of sex differentiation in papaya flowers. *Horticulture Research*, *8*(1), 1-13. https://doi.org/10.1038/s41438-021-00581-4

Ma, W. J., Veltsos, P., Sermier, R., Parker, D. J., & Perrin, N. (2018). Evolutionary and developmental dynamics of sex-biased gene expression in common frogs with proto-Y chromosomes. *Genome Biology*, *19*(1), 1-17. https://doi.org/10.1186/s13059-018-1548-4

Ma, W. J., Veltsos, P., Toups, M. A., Rodrigues, N., Sermier, R., Jeffries, D. L., & Perrin, N. (2018). Tissue specificity and dynamics of sex-biased gene expression in a common frog population with differentiated, yet homomorphic, sex chromosomes. *Genes*, *9*(6), 12-15. https://doi.org/10.3390/genes9060294

Marais, G. A. B., Gaillard, J.-M., Vieira, C., Plotton, I., Sanlaville, D., Gueyffier, F., & Lemaitre, J.-F. (2018). Sex gap in aging and longevity : Can sex chromosomes play a role? *Biology of Sex Differences*, *9*, 33. https://doi.org/10.1186/s13293-018-0181-y

Mahadevia, D., Saha, R., Manganaro, A., Chuhma, N., Ziolkowski-Blake, A., Morgan, A. A., Dumitriu, D., Rayport, S., & Ansorge, M. S. (2021). Dopamine promotes aggression in mice via ventral tegmental area to lateral septum projections. *Nature Communications*, *12*(1). https://doi.org/10.1038/S41467-021-27092-Z

Mank, J. E., & Ellegren, H. (2009). All dosage compensation is local : Gene-by-gene regulation of sex-biased expression on the chicken Z chromosome. *Heredity*, *102*(3), 312-320. https://doi.org/10.1038/hdy.2008.116

Mank, J. E., Hultin-Rosenberg, L., Zwahlen, M., & Ellegren, H. (2008). Pleiotropic constraint hampers the resolution of sexual antagonism in vertebrate gene expression. *American Naturalist*, *171*(1), 35-43. https://doi.org/10.1086/523954

Mank, J. E., Wedell, N., & Hosken, D. J. (2013). Polyandry and sex-specific gene expression. *Philosophical Transactions of the Royal Society B: Biological Sciences*, *368*(1613), 20120047. https://doi.org/10.1098/rstb.2012.0047

Mayer, A., Mosler, G., Just, W., Pilgrim, C., & Reisert, I. (2000). Developmental profile of Sry transcripts in mouse brain. *Neurogenetics*, *3*(1), 25-30. https://doi.org/10.1007/s100480000093

McCarthy, M. M. (2008). Estradiol and the Developing Brain. *Physiological reviews*, *88*(1), 91-124. https://doi.org/10.1152/physrev.00010.2007

McCarthy, M. M., & Arnold, A. P. (2011). Reframing sexual differentiation of the brain. *Nature Neuroscience*, *14*(6), 677-683. https://doi.org/10.1038/nn.2834

McPherson, F. J., & Chenoweth, P. J. (2012). Mammalian sexual dimorphism. *Animal Reproduction Science*, *131*(3), 109-122. https://doi.org/10.1016/j.anireprosci.2012.02.007

Meisel, R. P., & Connallon, T. (2013). The faster-X effect : Integrating theory and data. *Trends in genetics : TIG*, *29*(9), 537-544. https://doi.org/10.1016/j.tig.2013.05.009

Metz, H. C., Bedford, N. L., Pan, Y. L., & Hoekstra, H. E. (2017). Evolution and Genetics of Precocious Burrowing Behavior in Peromyscus Mice. *Current Biology*, *27*(24), 3837-3845.e3. https://doi.org/10.1016/j.cub.2017.10.061

Miura, I. (2017). Sex Determination and Sex Chromosomes in Amphibia. *Sexual Development*, *11*(5-6), 298-306. https://doi.org/10.1159/000485270

Moore, E. C., Ciccotto, P. J., Peterson, E. N., Lamm, M. S., Albertson, R. C., & Roberts, R. B. (2022). Polygenic sex determination produces modular sex polymorphism in an African cichlid fish. *Proceedings of the National Academy of Sciences*, *119*(14), e2118574119. https://doi.org/10.1073/pnas.2118574119

Mortaud, S., Nicolas, L., Pinoteau, W., Tordjman, S., Carlier, M., & Roubertoux, P. L. (2010). Brain pathways mediating the pro-aggressive effect of the steroid sulfatase (Sts) gene. *Behavior Genetics*, *40*(2), 211-219. https://doi.org/10.1007/s10519-010-9340-6

Mueller, J. L., Skaletsky, H., Brown, L. G., Zaghlul, S., Rock, S., Graves, T., Auger, K., Warren, W. C., Wilson, R. K., & Page, D. C. (2013). Independent specialization of the human and mouse X chromosomes for the male germ line. *Nature Genetics*, *45*(9), 1083-1087. https://doi.org/10.1038/ng.2705

Musser, G. G., & Carleton, M. D. (1993). Family Muridae. In *Mammal species of the world. Ataxonomic and geographic reference* (Wilson DE, Reeder DM). ashington andLondon: Smithsonian Institution Press.

Niitsu, S., Toga, K., Tomizuka, S., Maekawa, K., Machida, R., & Kamito, T. (2014). Ecdysteroid-Induced Programmed Cell Death Is Essential for Sex-Specific Wing Degeneration of the Wingless-Female Winter Moth. *PLOS ONE*, *9*(2), e89435. https://doi.org/10.1371/journal.pone.0089435

Nguyen, A. H., & Bachtrog, D. (2021). Toxic Y chromosome : Increased repeat expression and age-associated heterochromatin loss in male Drosophila with a young Y chromosome. *PLoS Genetics*, *17*(4), e1009438. https://doi.org/10.1371/journal.pgen.1009438

Parker, G. A. (1982). Why are there so many tiny sperm? Sperm competition and the maintenance of two sexes. *Journal of Theoretical Biology*, *96*(2), 281-294. https://doi.org/10.1016/0022-5193(82)90225-9

Parker, G. A., Baker, R. R., & Smith, V. G. F. (1972). The origin and evolution of gamete dimorphism and the male-female phenomenon. *Journal of Theoretical Biology*, *36*(3), 529-553. https://doi.org/10.1016/0022-5193(72)90007-0

Pélissié, B., Jarne, P., & David, P. (2012). Sexual Selection Without Sexual Dimorphism : Bateman Gradients in a Simultaneous Hermaphrodite. *Evolution*, *66*(1), 66-81. https://doi.org/10.1111/j.1558-5646.2011.01442.x

Perrin, N. (2021). Sex-chromosome evolution in frogs : What role for sex-antagonistic genes? *Philosophical Transactions of the Royal Society B: Biological Sciences*, *376*(1832), 20200094. https://doi.org/10.1098/rstb.2020.0094

Phoenix, C. H., Goy, R. W., Gerall, A. A., & Young, W. C. (1959). Organizing action of prenatally administered testosterone propionate on the tissues mediating mating behavior in the female guinea pig. *Endocrinology*, *65*, 369-382. https://doi.org/10.1210/endo-65-3-369

Pointer, M. A., Harrison, P. W., Wright, A. E., & Mank, J. E. (2013). Masculinization of Gene Expression Is Associated with Exaggeration of Male Sexual Dimorphism. *PLoS Genetics*, *9*(8), e1003697-e1003697. https://doi.org/10.1371/journal.pgen.1003697

Quirola, D. R., Mármol, A., Torres-Carvajal, O., Narváez, A. E., Ayala-Varela, F., & Moore, I. T. (2017). Use of a rostral appendage during social interactions in the Ecuadorian Anolis proboscis. *Journal of Natural History*, *51*(27-28), 1625-1638. https://doi.org/10.1080/00222933.2017.1332790

Rahmoun, M., Perez, J., Saunders, P. A., Boizet-Bonhoure, B., Wilhelm, D., Poulat, F., & Veyrunes, F. (2014). Anatomical and molecular analyses of XY ovaries from the african pygmy mouse Mus minutoides. *Sexual Development*, *8*(6), 356-363. https://doi.org/10.1159/000368664

Rayner, J. G., Pascoal, S., & Bailey, N. W. (2019). Release from intralocus sexual conflict ? Evolved loss of a male sexual trait demasculinizes female gene expression. *Proceedings of the Royal Society B: Biological Sciences*, *286*(1901), 20190497-20190497. https://doi.org/10.1098/rspb.2019.0497

Rey, R., Josso, N., & Racine, C. (2000). Sexual Differentiation. In K. R. Feingold, B. Anawalt, A. Boyce, G. Chrousos, W. W. de Herder, K. Dhatariya, K. Dungan, J. M. Hershman, J. Hofland, S. Kalra, G. Kaltsas, C. Koch, P. Kopp, M. Korbonits, C. S. Kovacs, W. Kuohung, B. Laferrère, M. Levy, E. A. McGee, … D. P. Wilson (Éds.), *Endotext*. MDText.com, Inc. http://www.ncbi.nlm.nih.gov/books/NBK279001/

Rice, W. R. (1987). The Accumulation of Sexually Antagonistic Genes as a Selective Agent Promoting the Evolution of Reduced Recombination between Primitive Sex Chromosomes. *Evolution*, *41*(4), 911-914. https://doi.org/10.2307/2408899

Rockwell, P. M., & Mason, R. T. (2014). A novel mechanism regulating a sexual signal : The testosterone-based inhibition of female sex pheromone expression in garter snakes. *Hormones and Behavior*, *66*(3), 509-516. https://doi.org/10.1016/j.yhbeh.2014.07.007

Rönn, J., Katvala, M., & Arnqvist, G. (2007). Coevolution between harmful male genitalia and female resistance in seed beetles. *Proceedings of the National Academy of Sciences*, *104*(26), 10921-10925. https://doi.org/10.1073/pnas.0701170104

Rowe, L., & Day, T. (2006). Detecting sexual conflict and sexually antagonistic coevolution. *Philosophical Transactions of the Royal Society B: Biological Sciences*. https://doi.org/10.1098/rstb.2005.1788

Sagi, A., Snir, E., & Khalaila, I. (1997). Sexual differentiation in decapod crustaceans : Role of the androgenic gland. *Invertebrate Reproduction & Development*, *31*(1-3), 55-61. https://doi.org/10.1080/07924259.1997.9672563

Sakashita, A., Wakai, T., Kawabata, Y., Nishimura, C., Sotomaru, Y., Alavattam, K. G., Namekawa, S. H., & Kono, T. (2019). XY oocytes of sex-reversed females with a Sry mutation deviate from the normal developmental process beyond the mitotic stage. *Biology of Reproduction*, *100*(3), 697-710. https://doi.org/10.1093/biolre/ioy214

Saunders, P. A., Franco, T., Sottas, C., Maurice, T., Ganem, G., & Veyrunes, F. (2016). Masculinised Behaviour of XY Females in a Mammal with Naturally Occuring Sex Reversal. *Scientific Reports*, *6*, 1-9. https://doi.org/10.1038/srep22881

Saunders, P. A., Perez, J., Rahmoun, M., Ronce, O., Crochet, P. A., & Veyrunes, F. (2014). XY Females do better than the XX in the African PYGMY mouse, MUS minutoides. *Evolution*, *68*(7), 2119-2127. https://doi.org/10.1111/evo.12387

Saunders, P. A., Perez, J., Ronce, O., & Veyrunes, F. (2022). Multiple sex chromosome drivers in a mammal with three sex chromosomes. *Current Biology*, *32*(9), 2001-2010.e3. https://doi.org/10.1016/j.cub.2022.03.029

Saunders, P. A., & Veyrunes, F. (2021). Unusual Mammalian Sex Determination Systems : A Cabinet of Curiosities. *Genes*, *12*(11), 1770-1770. https://doi.org/10.3390/GENES12111770

Scott, A. L., Bortolato, M., Chen, K., & Shih, J. C. (2008). Novel monoamine oxidase A knock out mice with human-like spontaneous mutation. *Neuroreport*, *19*(7), 739-739. https://doi.org/10.1097/WNR.0B013E3282FD6E88

Scott, N., Prigge, M., Yizhar, O., & Kimchi, T. (2015). A sexually dimorphic hypothalamic circuit controls maternal care and oxytocin secretion. *Nature*, *525*(7570), 519-522. https://doi.org/10.1038/nature15378

Scotti, I., & Delph, L. F. (2006). Selective trade-offs and sex-chromosome evolution in Silene latifolia. *Evolution; International Journal of Organic Evolution*, *60*(9), 1793-1800.

Sever, D. M., & Staub, N. L. (2011). Chapter 5—Hormones, Sex Accessory Structures, and Secondary Sexual Characteristics in Amphibians. In D. O. Norris & K. H. Lopez (Éds.),

Hormones and Reproduction of Vertebrates (p. 83-98). Academic Press. https://doi.org/10.1016/B978-0-12-374931-4.10005-7

Sigeman, H., Ponnikas, S., Videvall, E., Zhang, H., Chauhan, P., Naurin, S., & Hansson, B. (2018). Insights into Avian Incomplete Dosage Compensation : Sex-Biased Gene Expression Coevolves with Sex Chromosome Degeneration in the Common Whitethroat. *Genes*, *9*(8), 373. https://doi.org/10.3390/genes9080373

Skuse, D. H., James, R. S., Bishop, D. V. M., Coppin, B., Dalton, P., Aamodt-Leeper, G., Bacarese-Hamilton, M., Creswell, C., McGurk, R., & Jacobs, P. A. (1997). Evidence from Turner's syndrome of an imprinted X-linked locus affecting cognitive function. *Nature*, *387*(6634), 705-708. https://doi.org/10.1038/42706

Smith, J. M. (1978). *The Evolution of Sex*. CUP Archive.

Smith, J. M. (1982). *Evolution and the Theory of Games*. Cambridge University Press. https://doi.org/10.1017/CBO9780511806292

Soh, Y. Q. S., Alföldi, J., Pyntikova, T., Brown, L. G., Graves, T., Minx, P. J., Fulton, R. S., Kremitzki, C., Koutseva, N., Mueller, J. L., Rozen, S., Hughes, J. F., Owens, E., Womack, J. E., Murphy, W. J., Cao, Q., de Jong, P., Warren, W. C., Wilson, R. K., … Page, D. C. (2014). Sequencing the mouse Y chromosome reveals convergent gene acquisition and amplification on both sex chromosomes. *Cell*, *159*(4), 800-813. https://doi.org/10.1016/j.cell.2014.09.052

Trivers, T. (1972). Parental investment and sexual selection. *Sexual Selection & the Descent of Man, Aldine de Gruyter, New York*, 136-179.

Tuiskula-Haavisto, M., & Vilkki, J. (2007). Parent-of-origin specific QTL--a possibility towards understanding reciprocal effects in chicken and the origin of imprinting. *Cytogenetic and Genome Research*, *117*(1-4), 305-312. https://doi.org/10.1159/000103192

Vasudevan, K., Raber, J., & Sztein, J. (2010). Fertility comparison between wild type and transgenic mice by in vitro fertilization. *Transgenic research*, *19*(4), 587-594. https://doi.org/10.1007/s11248-009-9336-2

Veyrunes, F., Catalan, J., Sicard, B., Robinson, T. J., Duplantier, J.-M., Granjon, L., Dobigny, G., & Britton-Davidian, J. (2004). Autosome and Sex Chromosome Diversity Among the African Pygmy Mice, Subgenus Nannomys (Murinae; Mus). *Chromosome Research*, *12*(4), 369-382. https://doi.org/10.1023/B:CHRO.0000034098.09885.e6

Veyrunes, F., Catalan, J., Tatard, C., Cellier-Holzem, E., Watson, J., Chevret, P., Robinson, T. J., & Britton-Davidian, J. (2010). Mitochondrial and chromosomal insights into karyotypic evolution of the pygmy mouse, Mus minutoides, in South Africa. *Chromosome Research*, *18*(5), 563-574. https://doi.org/10.1007/s10577-010-9144-9

Veyrunes, F., Chevret, P., Catalan, J., Castiglia, R., Watson, J., Dobigny, G., Robinson, T. J., & Britton-Davidian, J. (2010). A novel sex determination system in a close relative of the house mouse. *Proceedings of the Royal Society B: Biological Sciences*, *277*(1684), 1049-1056. https://doi.org/10.1098/rspb.2009.1925

Veyrunes, F., & Perez, J. (2018). X inactivation in a mammal species with three sex chromosomes. *Chromosoma*, *127*(2), 261-267. https://doi.org/10.1007/s00412-017-0657-2

Veyrunes, F., Perez, J., Borremans, B., Gryseels, S., Richards, L. R., Duran, A., Chevret, P., Robinson, T. J., & Britton-Davidian, J. (2014). A new cytotype of the African pygmy mouse Mus minutoides in Eastern Africa. Implications for the evolution of sex-autosome translocations. *Chromosome Research*, *22*(4), 533-543. https://doi.org/10.1007/s10577-014-9440-x

Veyrunes, F., Perez, J., Paintsil, S. N. C., Fichet-Calvet, E., & Britton-Davidian, J. (2013). Insights into the evolutionary history of the X-linked sex reversal mutation in mus minutoides : Clues from sequence analyses of the Y-linked sry gene. *Sexual Development*, *7*(5), 244-252. https://doi.org/10.1159/000351223

Veyrunes, F., Watson, J., Robinson, T. J., & Britton-Davidian, J. (2007). Accumulation of rare sex chromosome rearrangements in the African pygmy mouse, Mus (Nannomys) minutoides : A whole-arm reciprocal translocation (WART) involving an X-autosome fusion. *Chromosome Research*, *15*(2), 223-230. https://doi.org/10.1007/s10577-006-1116-8

Vicoso, B., Emerson, J. J., Zektser, Y., Mahajan, S., & Bachtrog, D. (2013). Comparative Sex Chromosome Genomics in Snakes : Differentiation, Evolutionary Strata, and Lack of Global Dosage Compensation. *PLOS Biology*, *11*(8), e1001643. https://doi.org/10.1371/journal.pbio.1001643

Wade, J., & Arnold, A. P. (1996). Functional testicular tissue does not masculinize development of the zebra finch song system. *Proceedings of the National Academy of Sciences*, *93*(11), 5264-5268. https://doi.org/10.1073/pnas.93.11.5264

Wang, Q., Li, K., Zhang, D., Li, J., Xu, G., Zheng, J., Yang, N., & Qu, L. (2015). Next-Generation Sequencing Techniques Reveal that Genomic Imprinting Is Absent in Day-Old Gallus gallus domesticus Brains. *PLOS ONE*, *10*(7), e0132345. https://doi.org/10.1371/journal.pone.0132345

Wijchers, P. J., Yandim, C., Panousopoulou, E., Ahmad, M., Harker, N., Saveliev, A., Burgoyne, P. S., & Festenstein, R. (2010). Sexual dimorphism in mammalian autosomal gene regulation is determined not only by sry but by sex chromosome complement as well. *Developmental Cell*, *19*(3), 477-484. https://doi.org/10.1016/J.DEVCEL.2010.08.005

Winge, Ö. (1922). A peculiar mode of inheritance and its cytological explanation. *Journal of Genetics*, *12*(2), 137-144. https://doi.org/10.1007/BF02983077

Wong, J. W. Y., Meunier, J., & Kölliker, M. (2013). The evolution of parental care in insects : The roles of ecology, life history and the social environment. *Ecological Entomology*, *38*(2), 123-137. https://doi.org/10.1111/een.12000

Xu, J., Burgoyne, P. S., Arnold, A. P., Kuschel, B., Auranen, A., McBride, S., Novik, K. L., Antoniou, A., Lipscombe, J. M., Day, N. E., Easton, D. F., Ponder, B. A. J., Pharoah, P. D. P., & Dunning, A. (2002). Sex differences in sex chromosome gene expression in mouse brain. *Human Molecular Genetics*, *11*(12), 1409-1419. https://doi.org/10.1093/hmg/11.12.1409

Xu, L., & Zhou, Q. (2020). The Female-Specific W Chromosomes of Birds Have Conserved Gene Contents but Are Not Feminized. *Genes*, *11*(10), 1126. https://doi.org/10.3390/genes11101126

Yoshimoto, S., Ikeda, N., Izutsu, Y., Shiba, T., Takamatsu, N., & Ito, M. (2010). Opposite roles of DMRT1 and its W-linked paralogue, DM-W, in sexual dimorphism of Xenopus laevis : Implications of a ZZ/ZW-type sex-determining system. *Development*, *137*(15), 2519-2526. https://doi.org/10.1242/dev.048751

Zahavi, A. (1975). Mate selection—A selection for a handicap. *Journal of Theoretical Biology*, *53*(1), 205-214. https://doi.org/10.1016/0022-5193(75)90111-3

Zemp, N., Tavares, R., Muyle, A., Charlesworth, D., Marais, G. A. B., & Widmer, A. (2016). Evolution of sex-biased gene expression in a dioecious plant. *Nature Plants*, *2*(11). https://doi.org/10.1038/nplants.2016.168

Supplemental Information

S.1 Genotypic sex shapes maternal care in the African pygmy mouse, *Mus minutoides*

Supplementary Material

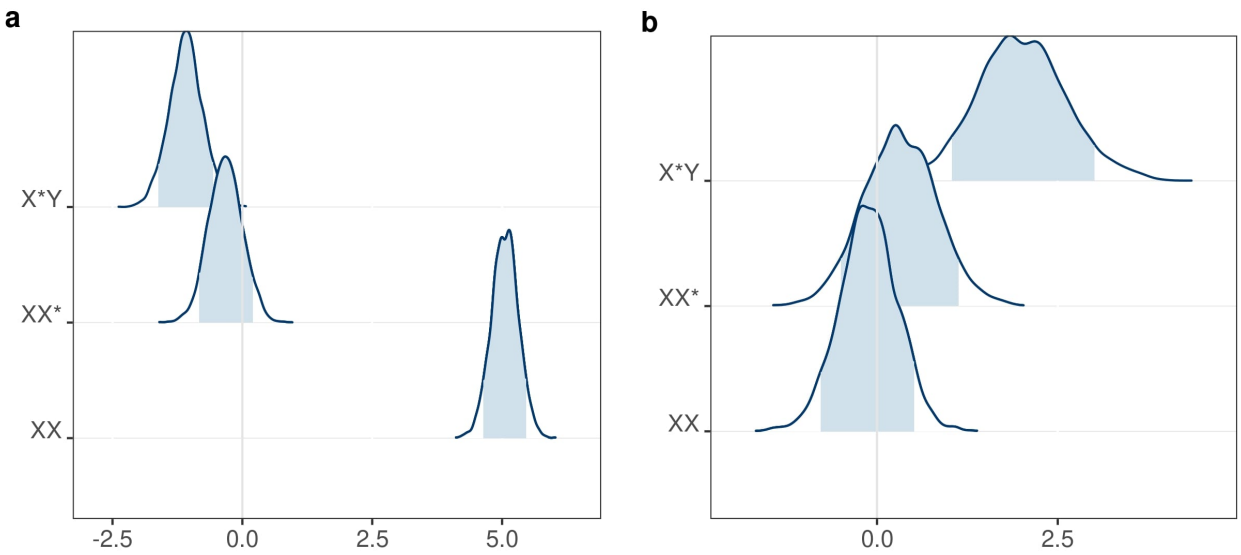

Figure S1. Posterior density interval estimates of genotype effect on pup retrieval. **a,b,** latency to first visit and retrieval probability respectively. XX females are defined as the reference population and slope estimates are represented for XX* and X*Y females effects. Estimates are on the log (x+1) and logit scale (**a** and **b** respectively). Shaded areas represent 89% Highest Posterior Density intervals (HPD) and groups whose HPD intervals cross the vertical grey line are considered as not significantly different from the reference group (XX).

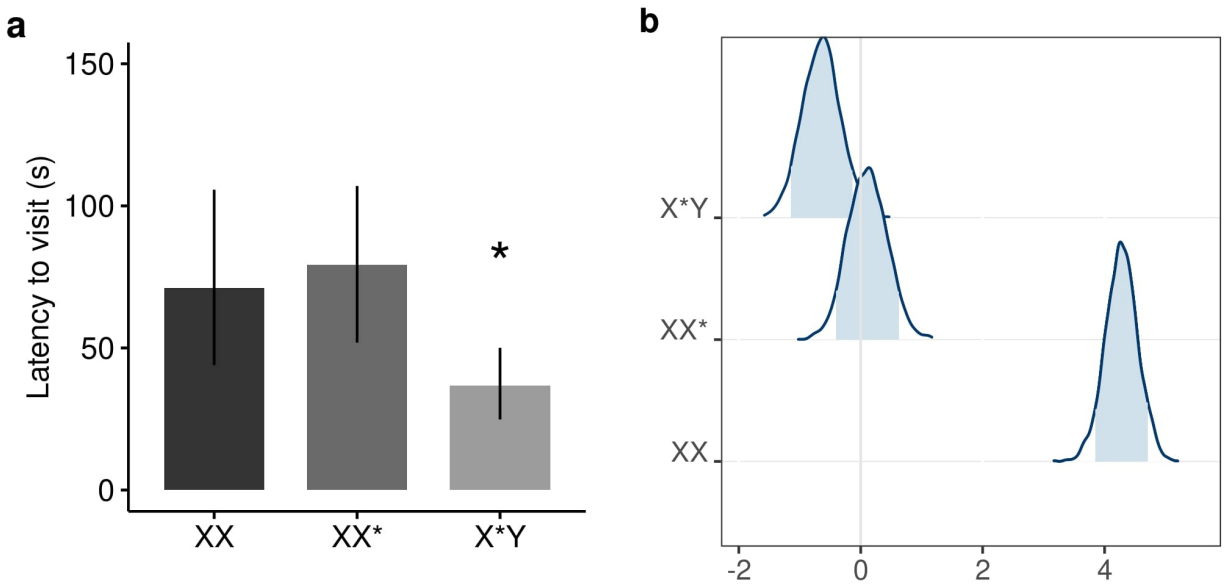

Figure S2. Visit latencies for females responding only. **a,** Estimates of first visit latency per genotype. Values are medians ± 89% HPD intervals. Estimates are retrieved from a back-transformation of models' parameters. *Asterisk indicate significance of the genotype effect. **b**, Posterior density interval estimates of genotype effect. XX females are defined as the reference population and slope estimates are represented for XX* and X*Y female effects. Estimates are on the log (x+1) scale. Shaded areas represent 89% Highest Posterior Density intervals (HPD) and group whose HPD intervals cross the vertical grey line are considered as not significantly different from the reference group (XX).n_{XX}=20 , n_{XX*}=29, n_{X*Y}=31.

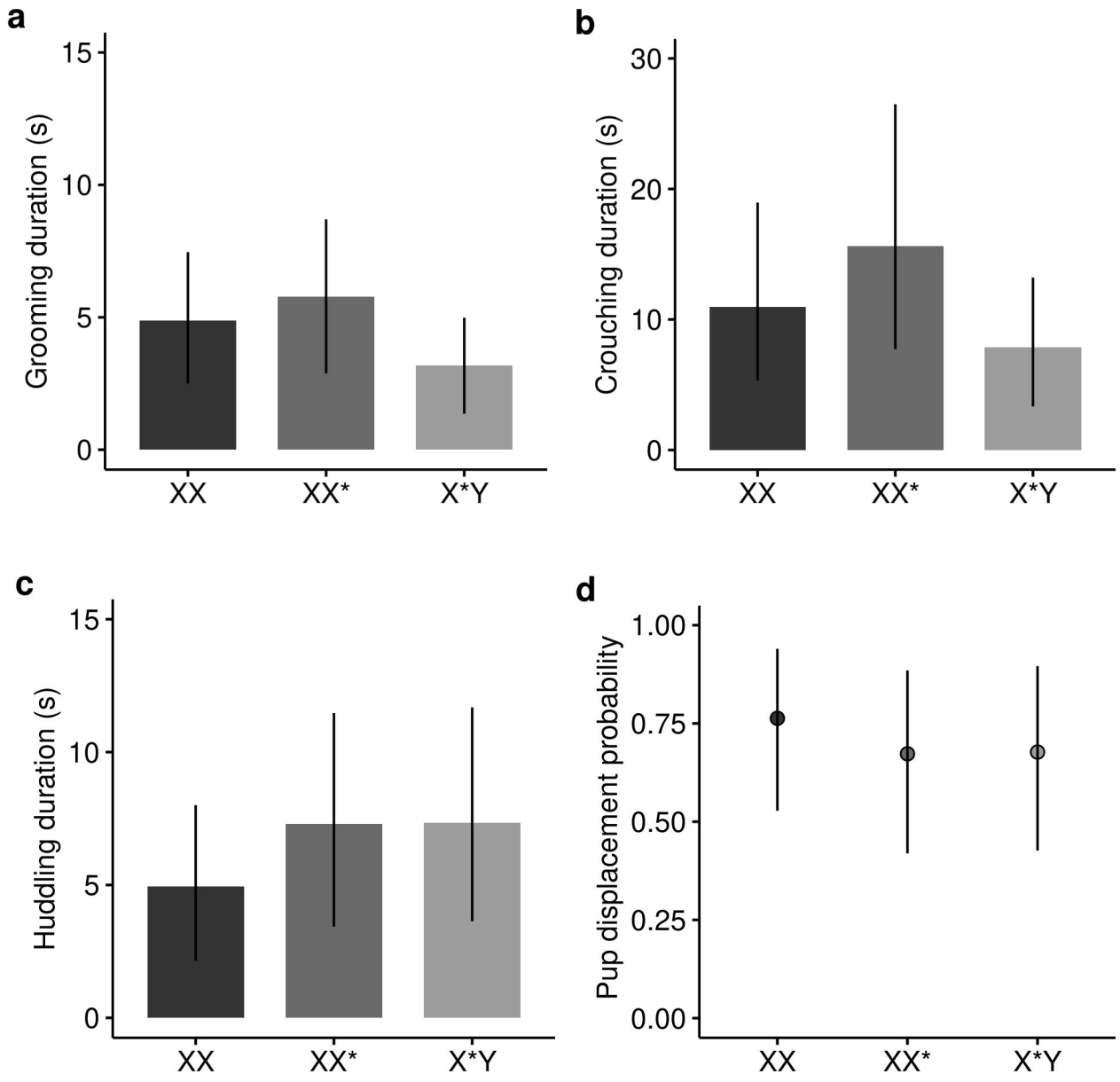

Figure S3. The sex chromosome complement does not influence direct mother-pup interactions in the African pygmy mouse. Values are medians ± 89% HPD intervals. Estimates are retrieved from a back-transformation of models' parameters. n=25 per genotype.

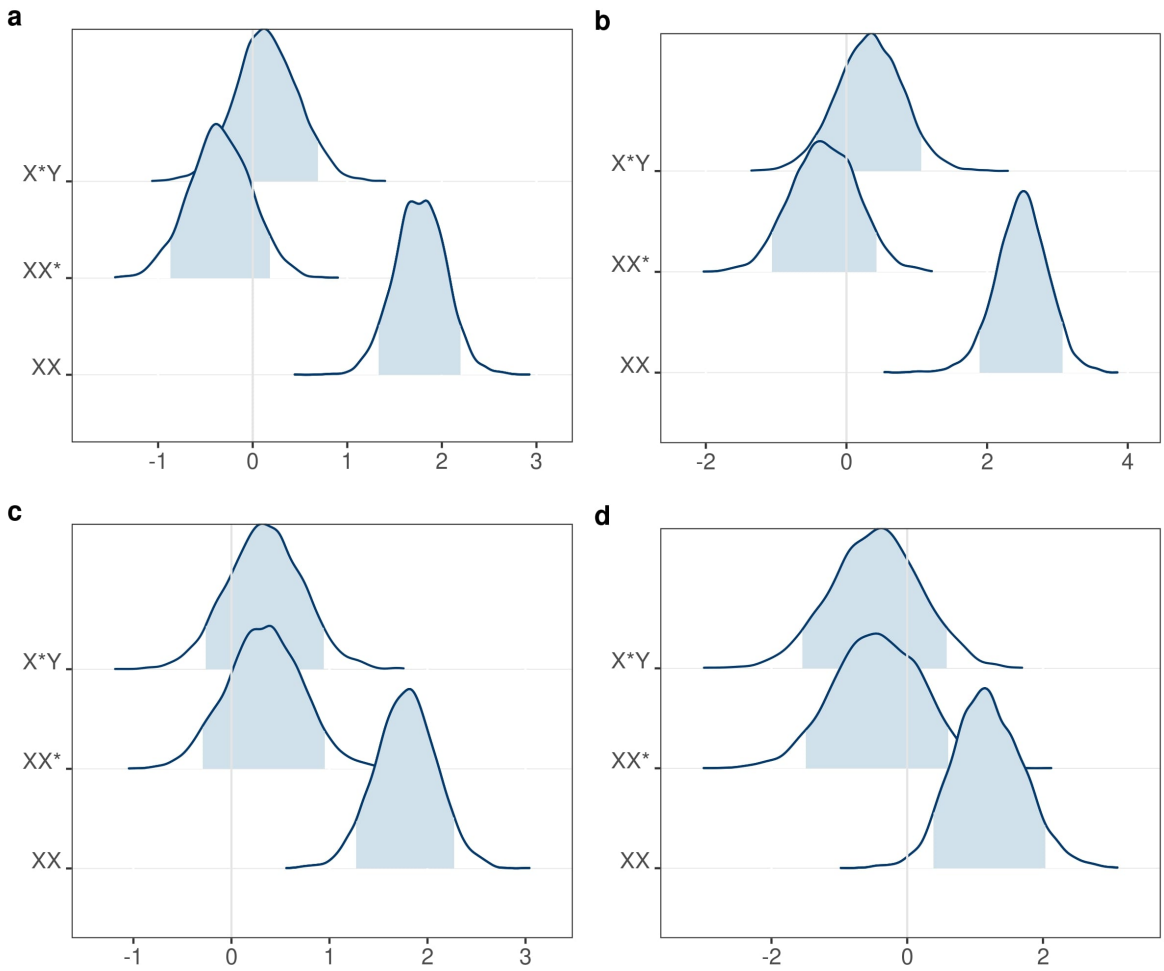

Figure S4. Posterior density interval estimates of genotype effect on mother-pup interactions. **a,** grooming duration. **b,** crouching duration. **c,** huddling duration. **d,** pup displacement in the cage probability. XX females are defined as the reference population and slope estimates are represented for XX* and X*Y females effects. Estimates are on the log (x+1) and logit scale (**a,b,c** and **d** respectively). Shaded areas represent 89% Highest Posterior Density intervals (HPD) and group whose HPD intervals cross the vertical grey line are considered as not significantly different from the reference group (XX). n=25 per genotype.

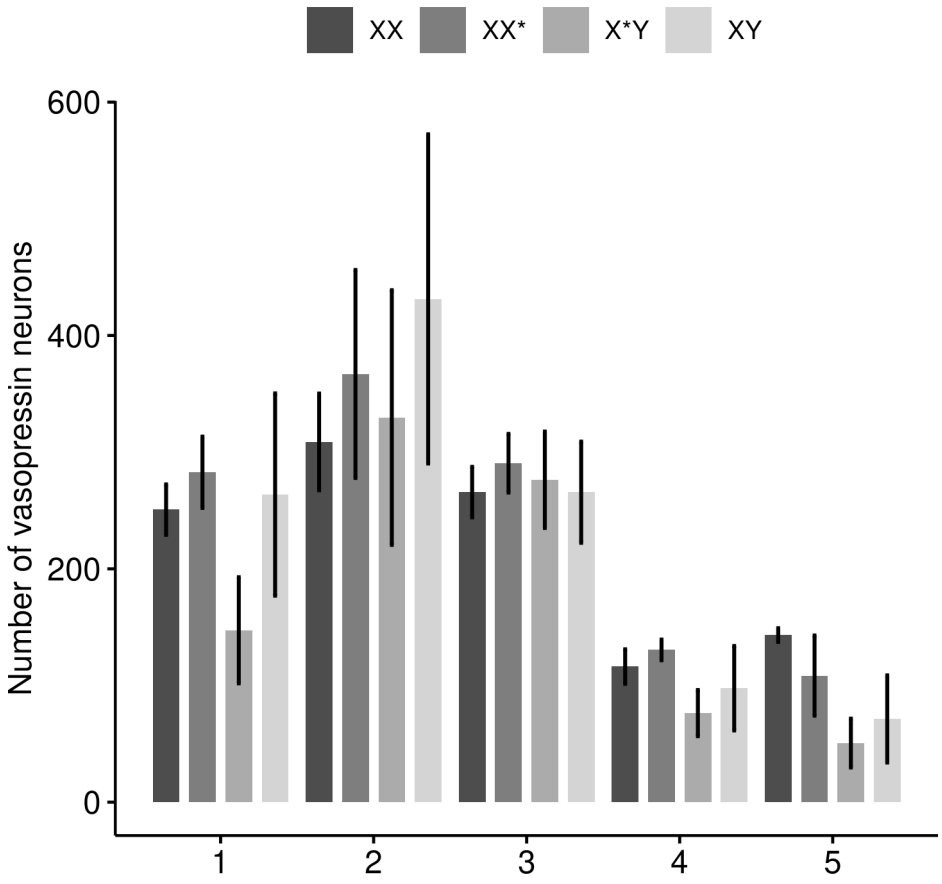

Figure S5. Vasopressin neurons distribution across the PVN. Values are mean ± s.e.m. We removed one X*Y female due to staining issues on few brain slices. Regions (1-5) are illustrated in Fig S7-S10. n_{XX}=4 , n_{XX^*}=4, n_{X^*Y}=2, n_{XY}=3. Males tend to have greater vasopressin neurons in region 2 (early intermediate region) and X*Y females tend to have lower vasopressin neurons in region 1 (anterior region).

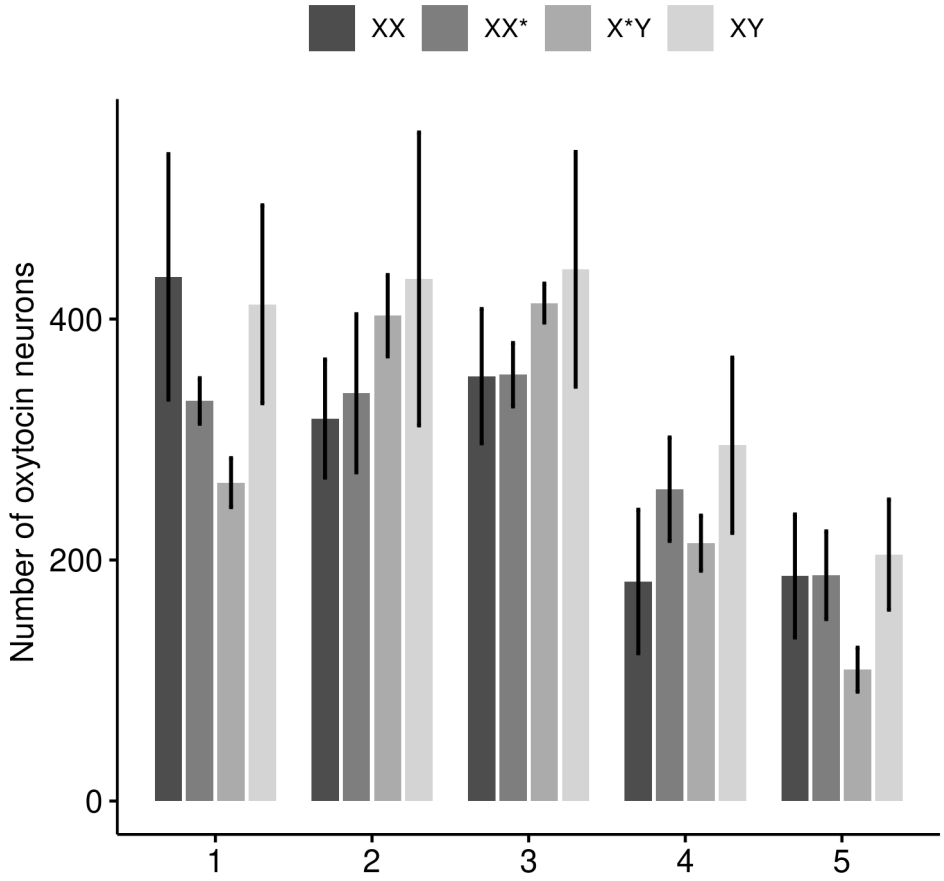

Figure S6. Oxytocin neurons distribution across the PVN. Values are mean ± s.e.m. Regions (1-5) are illustrated in Fig S7-S10. n_{XX}=5 , n_{XX^*}=5, n_{X^*Y}=4, n_{XY}=4.There is a tendency for a left skewed oxytocin distribution in XX females with a greater neuron number in anterior regions, while in intermediate regions for X*Y females and both regions for XX* and XY individuals. X*Y females tend to have a lower number of oxytocin neurons in region 1 and 5 in comparison to other individuals.

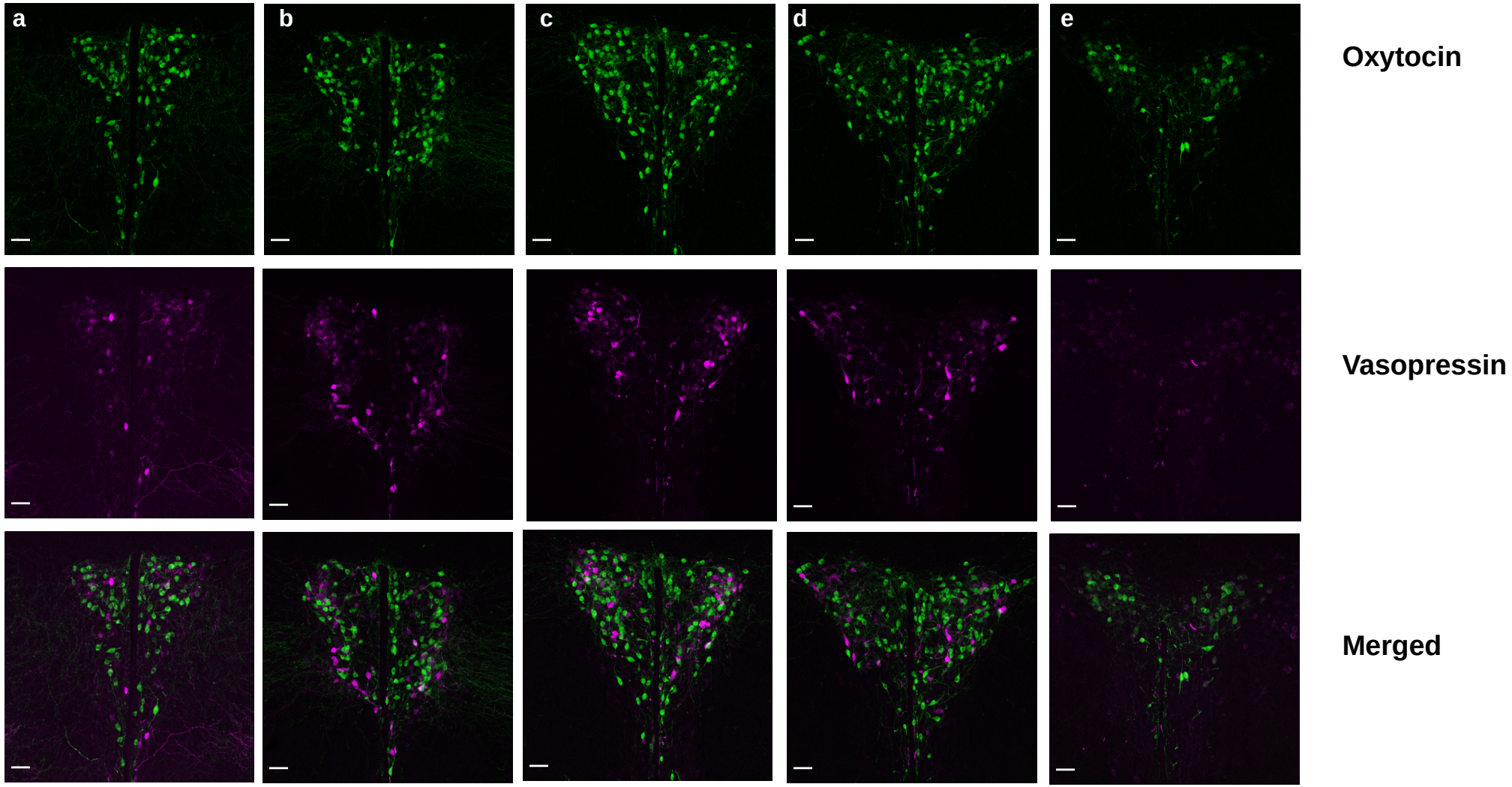

Figure S7. Oxytocin and vasopressin neurons' expression across the PVN in XX females. **a,** region 1 : anterior. **b,c**, regions 2 and 3 : intermediate. **d,e,** regions 4 and 5 : posterior.

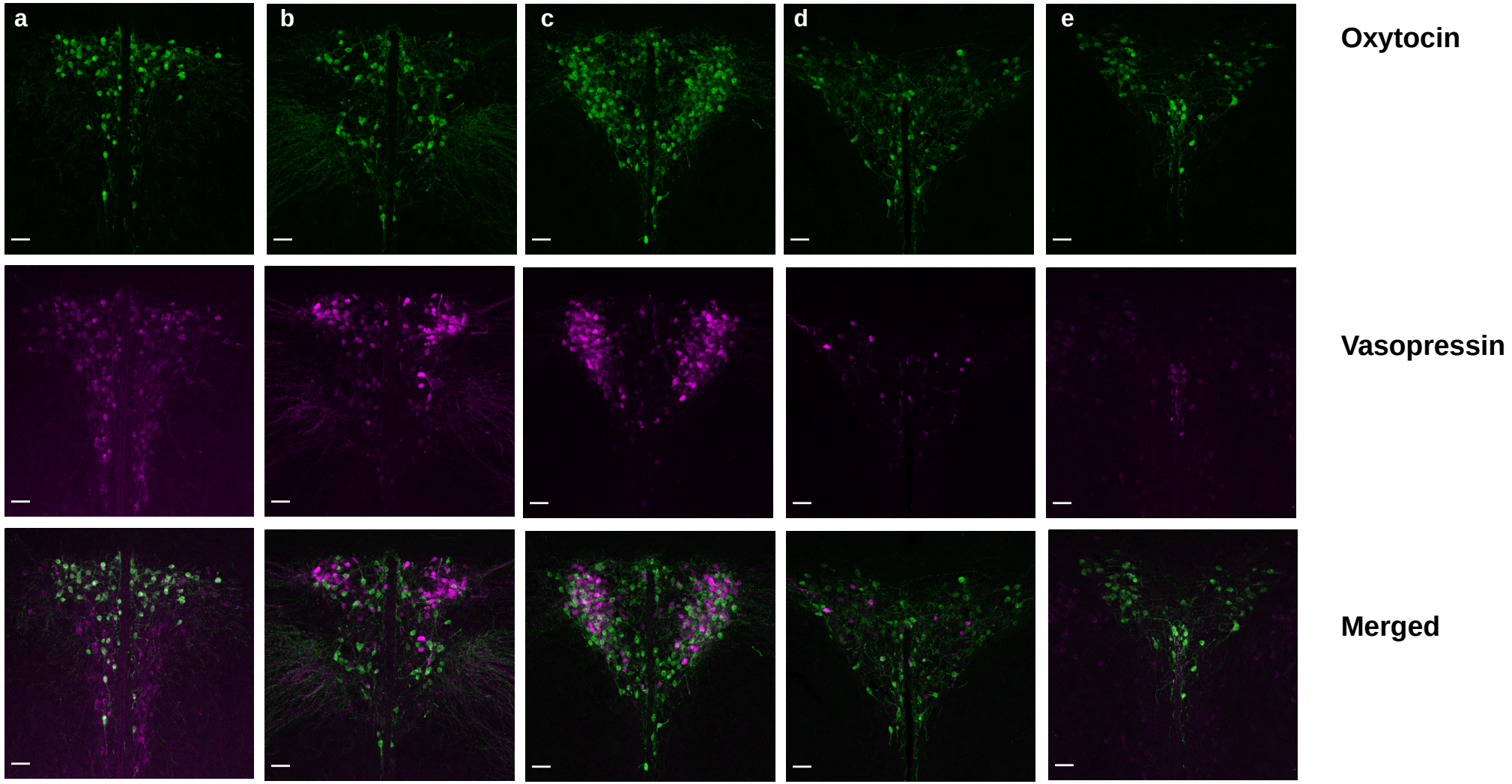

Figure S8. Oxytocin and vasopressin neurons' expression across the PVN in XX* females. **a,** region 1 : anterior. **b,c**, regions 2 and 3 : intermediate. **d,e,** regions 4 and 5 : posterior.

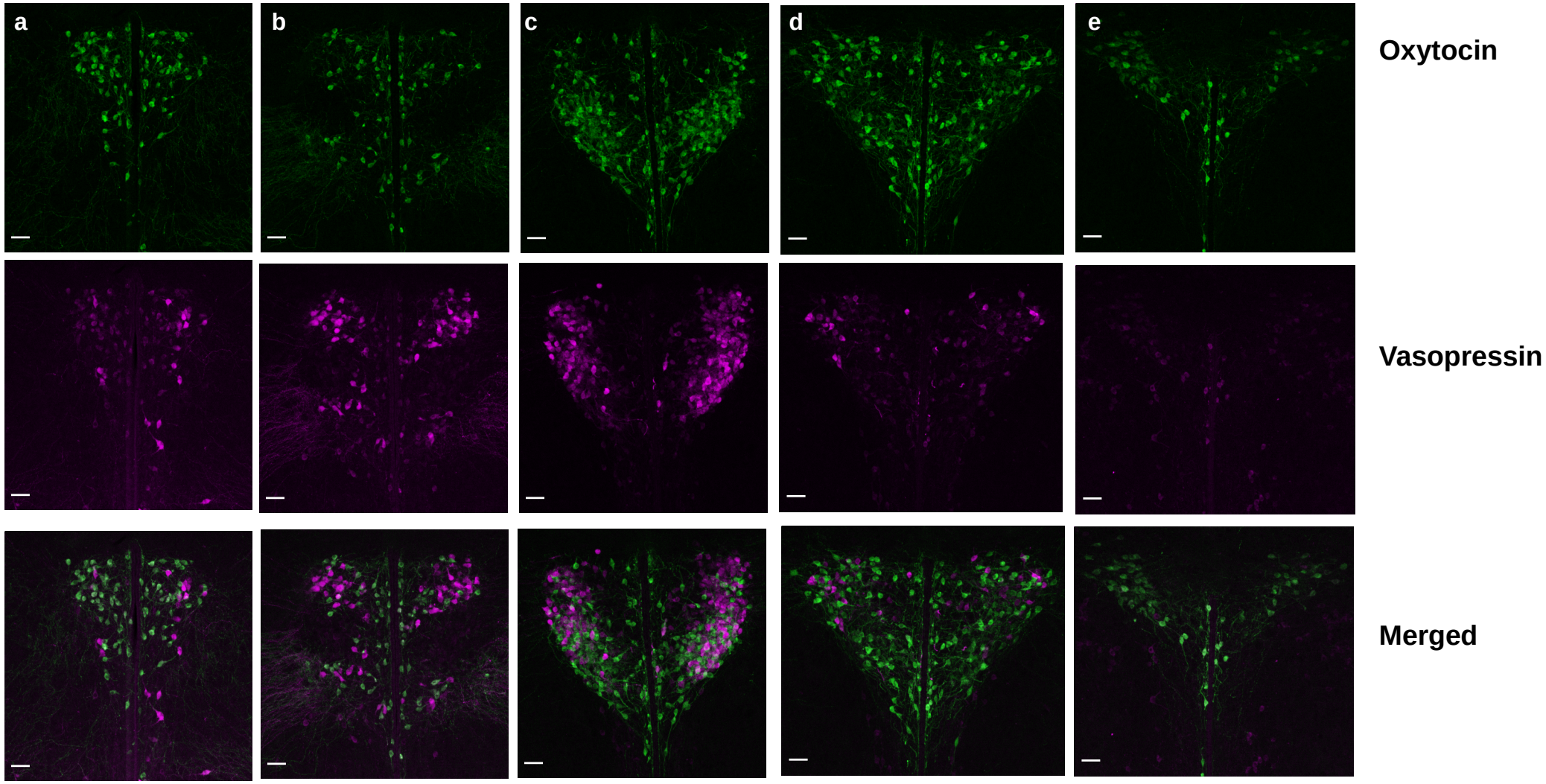

Figure S9. Oxytocin and vasopressin neurons' expression across the PVN in X*Y females. **a,** region 1 : anterior. **b,c**, regions 2 and 3 : intermediate. **d,e,** regions 4 and 5 : posterior.

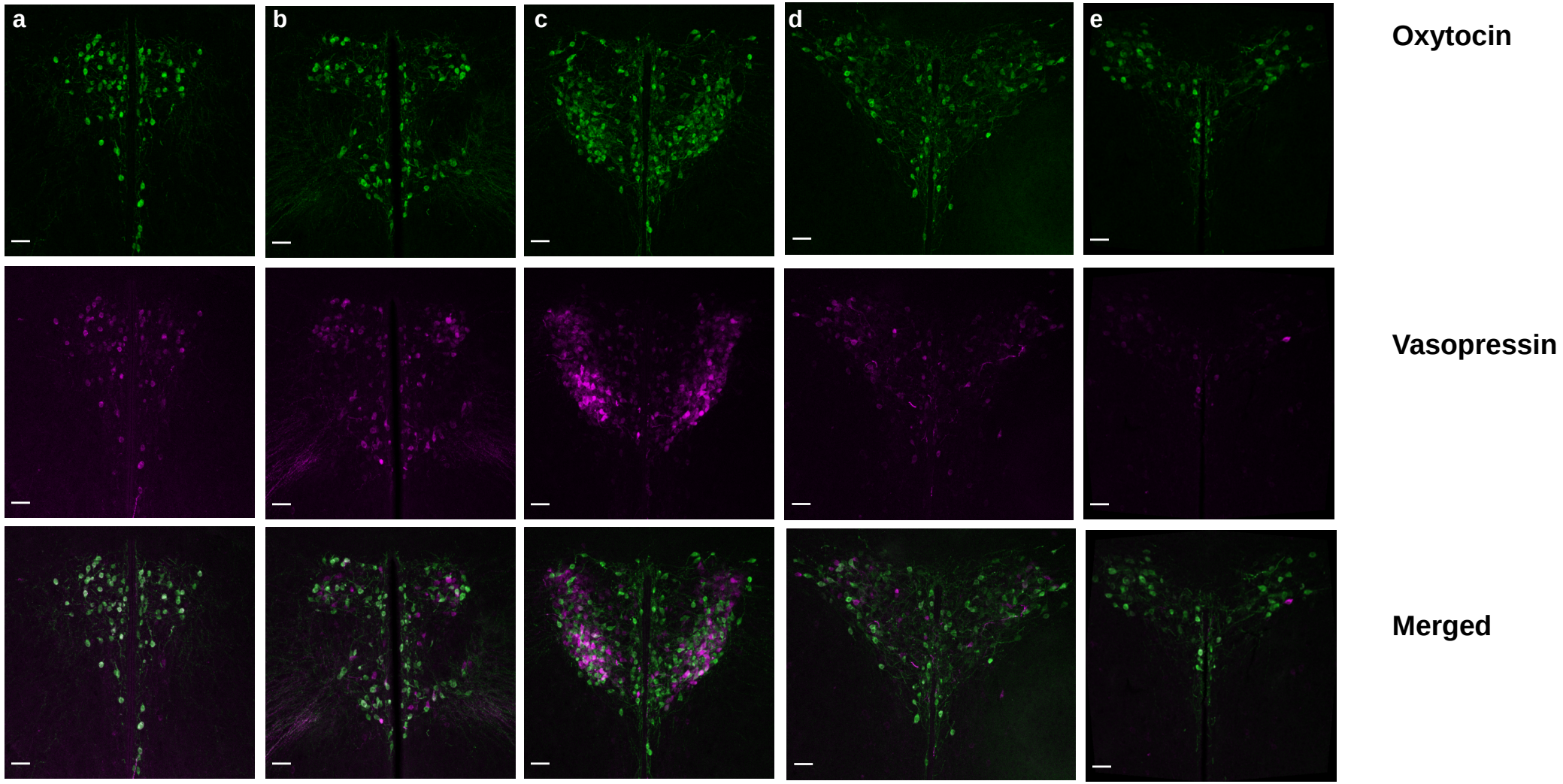

Figure S10. Oxytocin and vasopressin neurons' expression across the PVN in XY males. **a,** region 1 : anterior. **b,c**, regions 2 and 3 : intermediate. **d,e,** regions 4 and 5 : posterior.

	Latency to visit (s)		Retrieval probability	
	Estimates	*HPD (89%)*	*Estimates*	*HPD (89%)*
XX	156.5	94.5 –223.3	0.47	0.32 –0.63
XX*	112	71.5– 158.6	0.55	0.42 –0.70
X*Y	51.7	33.6– 73.8	0.87	0.77 –0.95
Contrasts	*ratio*	*HPD (89%)*	*Odd ratio*	*HPD (89%)*
XX / X*Y	2.97	1.57-4.65	0.14	0.03–0.30
XX / XX*	1.4	0.7-2.1	0.74	0.23–1.4
XX* / X*Y	2.1	1.09-3.31	0.19	0.04-0.4

Table S1. Median estimates and median-based contrast estimates for pup retrieval experiments. Contrast estimates with 89% HPD including 1 are considered as not significantly different. An odd-ratio above one (or near 0) indicates a higher (or lower) behavioural likelihood in the first group of the contrast, an odd-ratio around 1 indicates no group-effect. Probabilities and latencies (s) are retrieved using a back-transformation of the model parameters. n_{XX}=31 , n_{XX^*}=35, n_{X^*Y}=35.

	Pup retrieval			Mother-pup interactions				
Genotype	***N***	**Visit response (%)**	**Retrieval response (%)**	**N**	**Carrying (%)**	**Grooming (%)**	**Crouching (%)**	**Huddling (%)**
XX	31	20 (64.5)	15 (48.4)	25	19 (0.76)	20 (0.8)	23 (0.92)	18 (0.72)
XX*	35	29 (82.9)	19 (54.3)	25	17 (0.68)	22 (0.88)	22 (0.88)	21 (0.84)
X*Y	35	31 (88.6)	30 (85.7)	25	17 (0.68)	18 (0.72)	20 (0.8)	22 (0.88)

Table S2. Group sample sizes and proportions of individuals showing a response for pup retrieval and mother-pup interactions experiments.

	Grooming Duration (s)		Crouching duration (s)		Huddling duration (s)		Pup displacement probability	
	Estimates	*HPD (89%)*	*Estimates*	*HPD (89%)*	*Estimates*	*HPD (89%)*	*Estimates*	*HPD (89%)*
XX	4.87	2.49-7.46	10.98	5.32-19	4.95	2.15-8	0.76	0.53-0.94
XX*	5.79	2.89-8.70	15.61	7.73-26.5	7.30	3.43-11.5	0.67	0.42-0.89
X*Y	3.18	1.36-4.99	7.89	3.34-13.2	7.33	3.63-11.7	0.68	0.43-0.9
Contrasts	*ratio*	*HPD (89%)*	*ratio*	*HPD (89%)*	*ratio*	*HPD (89%)*	*Odd ratio*	*HPD (89%)*
XX / X*Y	1.42	0.75-2.21	1.36	0.52-2.52	0.71	0.32-1.21	1.54	0.24-5.93
XX / XX*	0.87	0.44-1.33	0.71	0.27–1.34	0.71	0.32-1.2	1.58	0.25-6.37
XX*/ X*Y	1.64	0.86-2.57	1.88	0.66-3.43	1	0.42-1.62	0.96	0.12-3.47

Table S3. Median estimates and median-based contrast estimates for mother-pup interaction investigations Contrast estimates with 89% HPD including 1 are considered as not significantly different. An odd-ratio above one (or near 0) indicates a higher (or lower) behavioural likelihood in the first group of the contrast, an odd-ratio around 1 indicates no group-effect. Probabilities and durations (s) are retrieved using a back-transformation of the model parameters. n=25 per genotype.

S.2 Impact of sex reversal on maternal care: focus on lactation

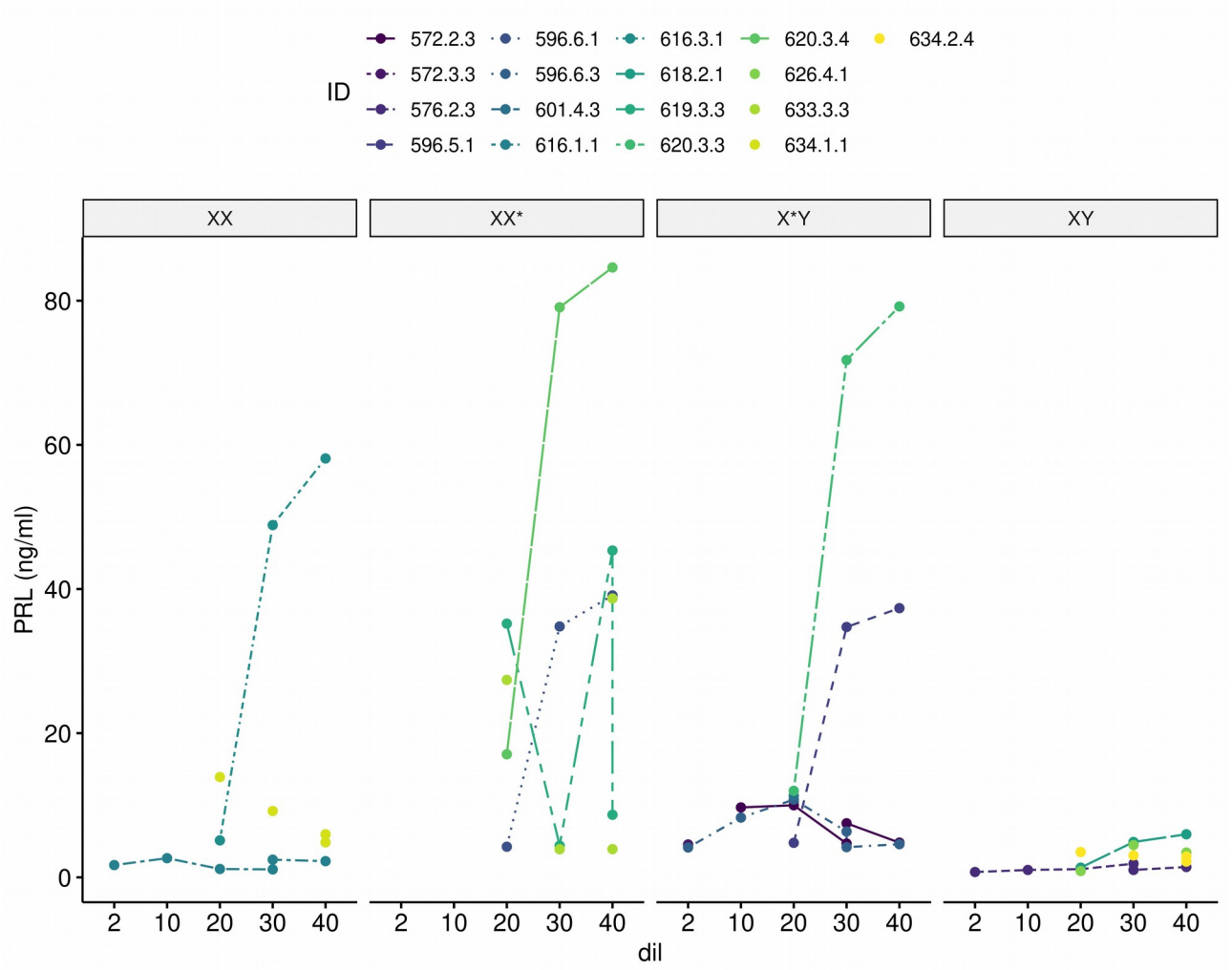

Figure S1. Circulating PRL levels in males and virgin females. Virgin females and males were injected with domperidone to trigger prolactin release. Each curve corresponds to PRL concentrations at each dilution factor for an individual, including repeated measures. Measures were inconsistent for two XX* females (633.3.3 and 620.3.4) raising questions about methodological issues. n_{XX}=3, n_{XX^*}=4, n_{X^*Y}=4, n_{XY}=4.

S.3 Brain transcriptomic architecture of a wild mouse species with sex reversal: a three sex chromosome orchestra

Supplemental information

Supplemental methods

Neo-sex chromosomes evolution and genomic regions' assignment

In the African pygmy mouse, there are multiple Robertsonian fusions between autosomes but also between sex chromosomes and autosome 1, leading to neo-sex chromosomes (X.1), (X*.1) and (Y.1) (Veyrunes et al., 2004). Moreover, our study population is characterized by a whole arm reciprocal translocation (WART) between neo-sex chromosome (X*.1) and the fused autosomes (13.16) that gave rise to new neo-sex chromosomes variants (X*.16) and (1.13) (Veyrunes et al., 2007). This rearrangement impacts XX* and X*Y females only (Baudat et al. 2019). Thus, XX females and XY males are (X.1)(X.1) and (X.1)(Y.1) respectively, with both the autosomal pair (13.16). In contrast, XX* females are (X.1)(X*.16), X*Y females are (X*.16)(Y.1), and both have the (1.13)(13.16) neo-sex/autosomal copies (Fig 1). Sex-linked chromosomes 1, 13 and 16 do not show patterns of inactivation in the four genotypes, both copies are expressed (Veyrunes & Perez, 2018).

The sex-linked region of chromosome 13 (chr13) was defined as $13^{Neo\text{-}X^*}$ and started to stop recombining with the autosomal copy of chr13 (13^{Aut}) (Fig 1). The non-recombining region was referred to as NR. Because sex-linked and autosomal regions of chromosome 16 recombine, we classified this chromosome as 'autosomal'. Finally, there are three copies of chromosome 1 (chr1): Neo-Y ($1^{Neo\text{-}Y}$), neo-X($1^{Neo\text{-}X}$) and neo-X* ($1^{Neo\text{-}X^*}$). The larger non-recombining region of chr1 involves $1^{Neo\text{-}X/X^*}$ and $1^{Neo\text{-}Y}$, and there is also a small region where recombination is lacking between the three copies of chromosome 1 (NR). Distributions of DE genes were then explored using the following genomic compartments with each recombination pattern: autosome (R) , X/X* (R, NR) and neo-sex (R, NR) that includes chr1 and chr13. We did not include the Y chromosome as there is no assembly for it yet.

Supplemental Figures

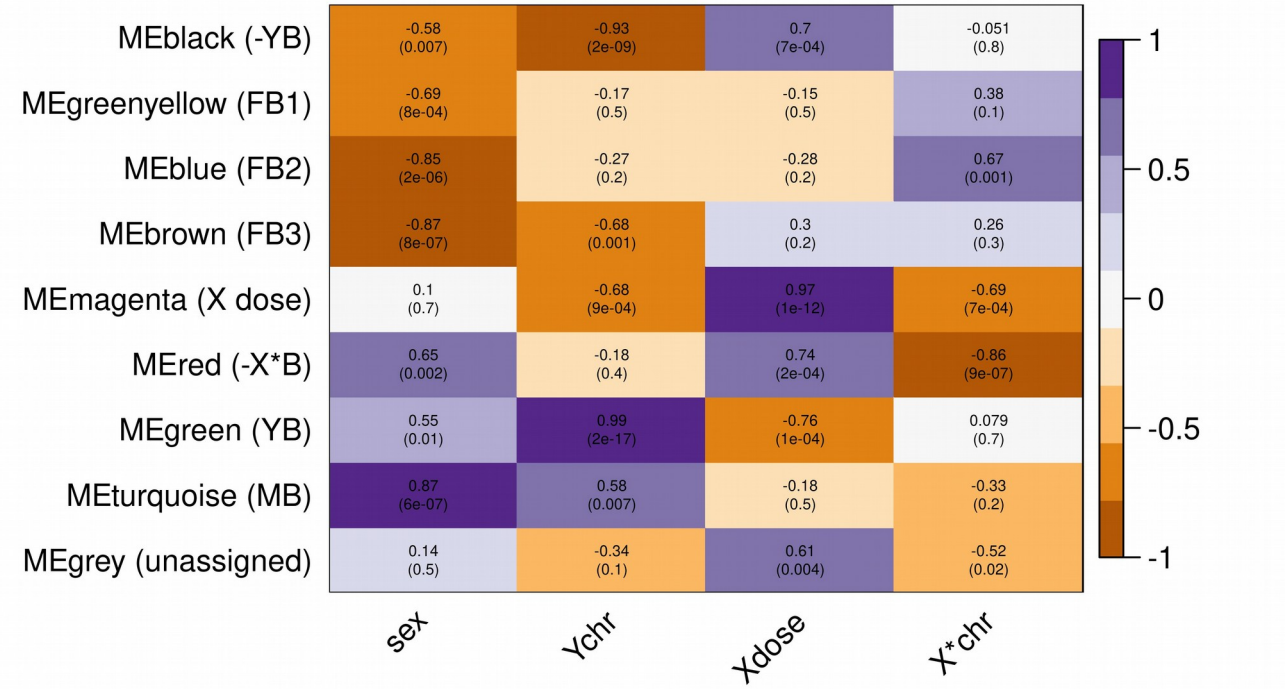

Figure S1. Module-biological trait correlations. 'MEcolor' correspond to module eigengenes of co-expressed gene modules (i.e., clusters) identified in the clustering analysis. Biological traits represented on the x-axis are: 'sex': female or male (XX=0 XX*=0, X*Y=0, XY=1); 'Ychr': presence of the Y chromosome / one copy of the X(*) chromosome (XX=0, XX*=0, X*Y=1, XY=1) ; 'Xdose: X chromosome copy number (XX=2, XX*=1, X*Y=1, XY=0) ; 'X*chr': presence of the X* chromosome (XX=0, XX*=1, X*Y=1, XY=0). Values represent pearson correlation coefficients ranging from -1 to 1 and calculated from WGCNA software. P.values are shown in brackets. Significance of the correlation allow to detect which biological trait drives expression patterns for each module. Correspondence between module colors and cluster names used in this study are shown in supplementary file S1. Turquoise= male-biased genes (MB), greenyellow, blue and brown= female-biased genes (FB1, FB2 and FB3 respectively) ; magenta= underexpressed in individuals with a single copy of the X chromosome (X dose) ; red= down-regulation in individuals with a X* chromosome (-X*B) ; green and black= under- and overexpressed genes in individuals carrying a Y chromosome.

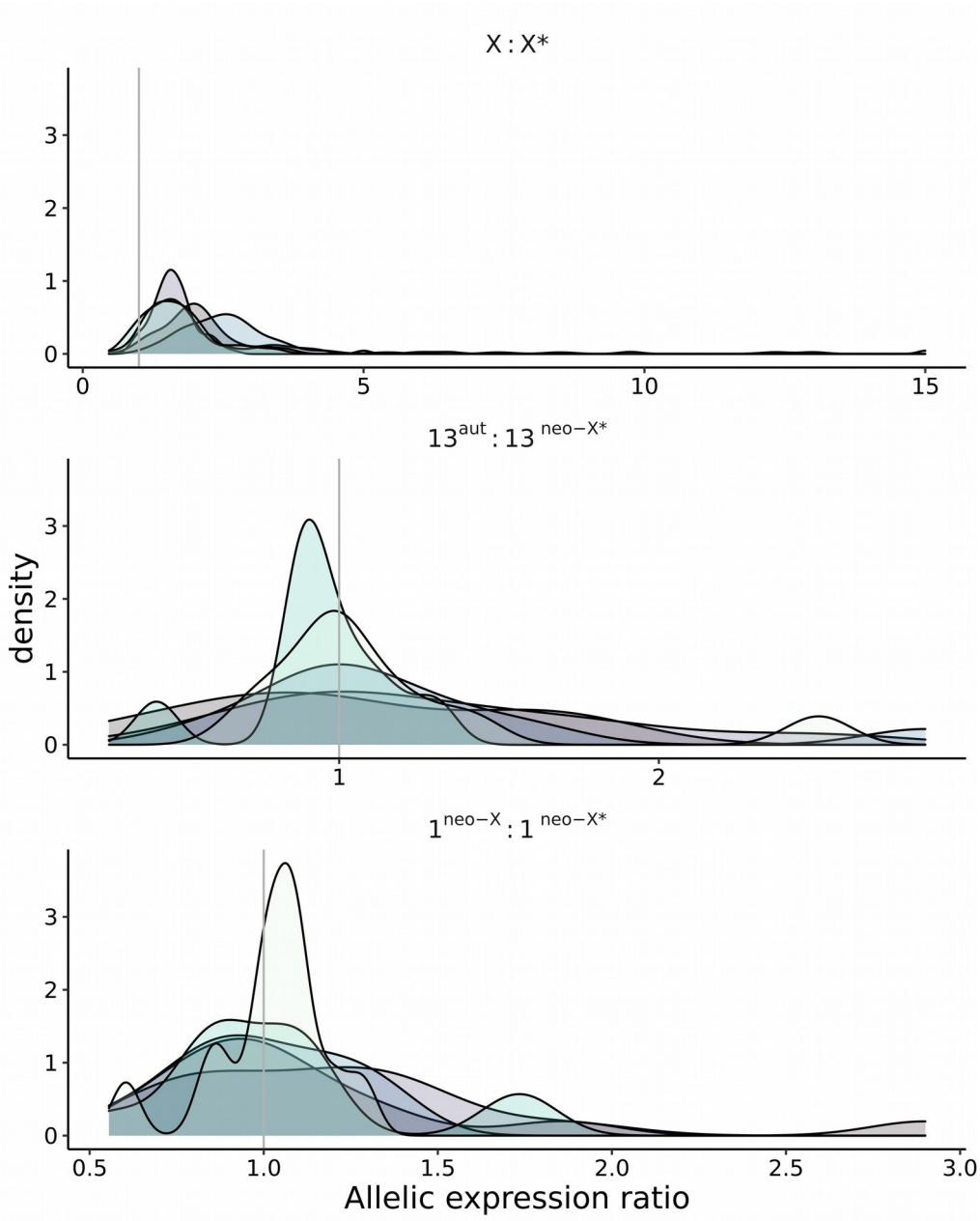

Figure S2. Distribution of allelic expression ratios in the five XX* females. Each colour correspond to a specific female. Grey lines indicate a ratio of 1 and thus equal expression of both alleles. Ratios are outlined above graphics (X over X* alleles, 13^{Aut} over $13^{Neo\text{-}X*}$ alleles, and $1^{Neo\text{-}X}$ over $1^{Neo\text{-}X*}$ alleles). $n_{X/X*}$=74, $n_{13Aut/13Neo\text{-}X*}$=10, $n_{1Neo\text{-}X/1Neo\text{-}X*}$=13.

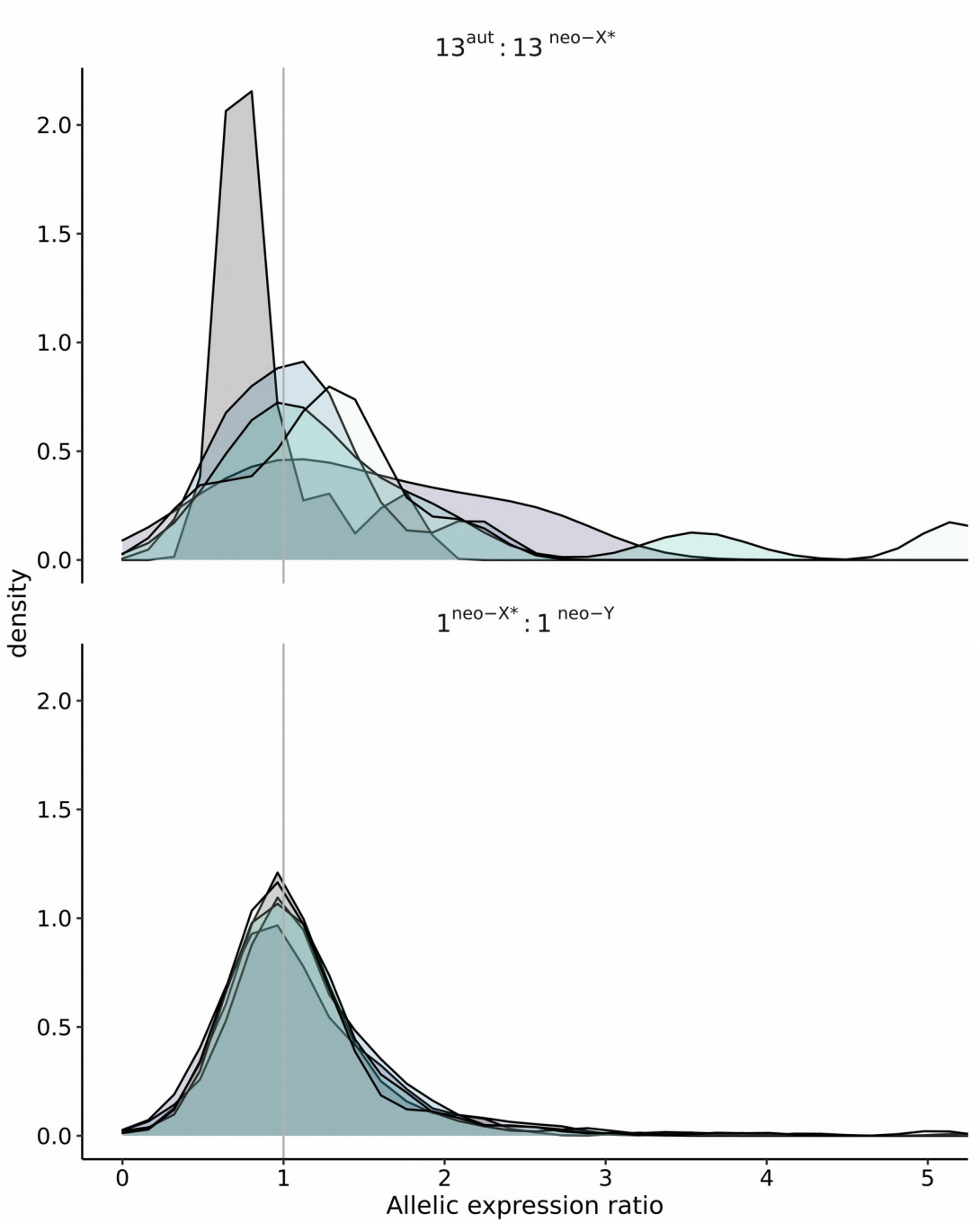

Figure S3. Distribution of allelic expression ratios in the five X*Y females. Each colour correspond to a specific female. Grey lines indicate a ratio of 1 and thus equal expression of both alleles. Ratios are outlined above graphics (13^{Aut} over $13^{Neo\text{-}X*}$ alleles, and $1^{Neo\text{-}X*}$ over $1^{Neo\text{-}Y}$ alleles) $n_{13Aut/13Neo\text{-}X*}$=10, $n_{1Neo\text{-}X*/1Neo\text{-}Y}$=243.

Supplemental Tables

List of tables

Table S1. Ontologies (biological process) of genes in clusters with an effect of genotypic sex on gene expression. Gene names were retrieved from an orthology analysis (Saunders et al., in prep). ENSEMBL IDs matching to multiple gene names / orthologs are separated with semi-colons and synonym names of genes are in brackets. Ontologies were retrieved using the amiGO web tool for gene ontology (https://geneontology.org). Contributors are database sources for ontology terms presented. We were not able to assign *Sts* to a recombining or non-recombining region between X and X* chromosomes (i.e., *Sts* is on a scaffold that did not anchor on *M. musculus* genome).
† indicates genes known to escape inactivation in *M. musculus* and/or likely to escape inactivation in *M. minutoides.*
* indicates candidate genes for phenotypic divergences observed in previous studies on the consequences of sex reversal in *M. minutoides*

Table S2. Candidate genes for phenotypic divergences highlighted in *M. minutoides*, based on *M. musculus* studies.

Table S3. Ontologies of sex-linked and neo-X/neo-X*-linked genes showing allelic imbalance in the brain of XX* females, and overlap with clusters. All sex-linked genes showed a bias towards the expression of X alleles. The unique gene showing allelic imbalance on neo-sex chromosomes was biased towards the expression of the neo-X allele. We found 55 gene names, out of the 65 sex-linked genes, using orthologies with *M. musculus* (Saunders et al., in prep). Ontologies were retrieved with the amiGO web tool for gene ontology (https://geneontology.org). Contributors are database sources for ontology terms presented.
† indicates genes known to escape inactivation in *M. musculus* and/or likely to escape inactivation in *M. minutoides.*

Table S4. Ontologies of neo-X*/neo-Y-linked genes showing allelic imbalance in the brain of X*Y females. Gene names were found using orthologies with *M. musculus* (Saunders et al., in prep). Ontologies were retrieved with the amiGO web tool for gene ontology (https://geneontology.org). Contributors are database sources for ontology terms presented.

Table S1. Ontologies (biological process) of genes in clusters with a genotypic sex effect on gene expression

† genes known to escape inactivation in *M. musculus* and/or likely to escape inactivation in *M. minutoides.*
* candidate genes for phenotypic divergences observed in previous studies on the consequences of sex reversal in *M. minutoides*

Cluster	***Gene name***	***Gene ontology***	***Contributor***	**Genomic compartment**
YB	*1700028J19Rik*	Biological process	MGI	chr1 (NR)
	2410002F23Rik	Biological process	MGI	chr1 (NR)
	Aldh3b3	Cellular aldehyde metabolic process	GO_Central	chr1 (R)
	Alox5	Leukocyte chemotaxis involved in inflammatory response	MGI	Autosome
	BC049352 (Smim 35)	Biological process	MGI	chr13 (R)
	Catsperg1;Catsperg 2	Biological process / spermatogenesis	MGI/Uniprot	chr1 (NR)
	Ccdc61	Cell projection organization	Uniprot	chr1 (NR)
	Cd70	Immune response	Uniprot	chr1 (R)
	Crtam	Positive regulation of cytokine production	MGI	chr13 (NR)
	Derl3	Protein N-linked glycosylation via aspatagine	MGI	Autosome
	Dll3	Skeletal system development	MGI	chr1 (NR)
	Dpy19l3	Protein C-linked glycosylation via 2'-alpha-mannosyl-L-tryptophan	GO_Central	chr1 (NR)
	Dsc2	Cell adhesion	Uniprot	Autosome
	Eif3k	Translation initiation	MGI	Autosome
	Exo5	DNA repair	Uniprot	Autosome
	Fam71e1(Garin5a)	Innate immune response	Uniprot	chr1 (NR)

Table S1 (Continued)

Cluster	*Gene name*	*Gene ontology*	*Contributor*	**Genomic compartment**
YB	*Fxyd3*	Ion transport	Uniprot	chr1 (NR)
	Hddc3	-	-	chr1 (NR)
	Htatip2	Apoptotic process	Uniprot	chr1 (NR)
	Il16	Chemotaxis	Uniprot	chr1 (NR)
	Kcnj14	Ion transport	Uniprot	chr1 (NR)
	Kptn	Actin filament organization	Uniprot	chr1 (NR)
	Lpin3	Lipid metabolic process	Uniprot	Autosome
	Lsr	Regulation of lipid metabolic process	MGI	chr1 (NR)
	Myd88	Immune system process	Uniprot	chr13 (R)
	Nfyc	Regulation of histone acetylation	MGI	Autosome
	Nudt19	Coenzyme A catabolic process	Uniprot	chr1 (NR)
	Pex11a	Regulation of peroxisome size	MGI	chr1 (NR)
	Plekha4	Positive regulation of canonical Wnt signaling pathway	MGI	chr1 (NR)
	Psma1	Immune system process	Uniprot	Autosome
	Rhod	Actin filament organization	GO_Central	chr1 (R)
	Rlbp1	Visual perception	Uniprot	chr1 (NR)
	Snrpd2	mRNA splicing, via spliceosome	MGI	Autosome
	Stab2	Cell adhesion	Uniprot	Autosome
	Trmt10b	Methylation	Uniprot	Autosome

Table S1 (Continued)

Cluster	*Gene name*	*Gene ontology*	*Contributor*	**Genomic compartment**
YB	*Upk1a*	Epithelial cell differentiation	MGI	chr1 (NR)
	Zc3h4	Negative regulation of DNA-templated transcription, elongation	MGI	Autosome
	Zfp51	Regulation of transcritpion by RNA polymerase II	GO_Central	chr1 (NR)
	Zfp524; Gm44973	Regulation of transcritpion by RNA polymerase II	GO_Central	chr1 (NR)
	Zfp59	-	-	chr1 (NR)
	Zfp760	Regulation of transcritpion by RNA polymerase II	GO_Central	chr1 (NR)
	Zfp78	Regulation of transcritpion by RNA polymerase II	GO_Central	chr1 (NR)
	Zfp82	Regulation of transcritpion by RNA polymerase II	GO_Central	chr1 (NR)
-YB	*9530053A07Rik*	Biological process	MGI	chr1 (NR)
	Aadat	Biosynthetic process	Uniprot	Autosome
	Aars2	tRNA modification	Uniprot	chr1 (R)
	Ado			Autosome
	Adrb1	Glycogen catabolic process	MGI	chr1 (R)
	AI987944	Regulation of transcritpion by RNA polymerase II	GO_Central	chr1 (NR)
	Asah2	Lipid metabolic process	Uniprot	chr1 (R)
	B630019K06Rik	Biological process	MGI	X/X* (NR)
	Bard1	DNA repair	ComplexPortal	Autosome
	C5ar1	Chemotaxis	UniProt	chr1 (NR)

Table S1 (Continued)

Cluster	*Gene name*	*Gene ontology*	*Contributor*	**Genomic compartment**
-YB	*Caps2*	-	-	Autosome
	Ceacam1;Ceacam2	Cell adhesion	MGI	chr1 (NR)
	Cep89	Chemical synaptic transmission	Uniprot	chr1 (NR)
	Chrdl1	Cell differentiation	UniProt	X/X* (R)
	Chst3	Carbohydrate metabolic process	UniProt	Autosome
	Cks2	Cell division	Uniprot	Autosome
	Clcf1	Positive regulation of cell population proliferation	MGI	chr1 (R)
	Clcn1	Ion transport	Uniprot	Autosome
	Cpm	Proteolysis	Uniprot	Autosome
	Creb5	Regulation of transcritpion by RNA polymerase II	GO_Central	Autosome
	Ddx3x †	Regulation of translation	Uniprot	X/X*(NR)
	Dhx34	Nuclear transcribed mRNA catabolic process	MGI	chr1 (NR)
	Eps8l1	Rho protein signal transduction	MGI	chr1 (NR)
	Ercc2	Transcription by RNA polymerase II	MGI	chr1 (NR)
	Fam161a	Cell projection organization	Uniprot	Autosome
	Fbxl14	Ubiquitin-dependent protein catabolic process	MGI	Autosome
	Fkrp	Protein processing	MGI	chr1 (NR)
	Gbx2	Regulation of nervous system development	GO_Central	Autosome
	Gh	Positive regulation of neurogenesis	MGI	Autosome

Table S1 (Continued)

Cluster	*Gene name*	*Gene ontology*	*Contributor*	**Genomic compartment**
-YB	*Gm21983;Mia*	Extracellular matrix organization /	GO_Central	chr1 (NR)
	Gm773	Meiotic cell cycle	GO_Central	X/X* (R)
	Grrp1 (Fam110d)	Biological process	MGI	Autosome
	Hnrnpa0	3'-UTR-mediated mRNA stabilization	UniProt	Autosome
	Hsd17b14	Steroid catabolic process	MGI	chr1 (NR)
	Ier5l	Biological process	MGI	Autosome
	Irf2bpl	Nervous system development	MGI	Autosome
	Irgq	Biological process	MGI	chr1 (NR)
	Kdm6a*†	Regulation of gene expression	GO_Central	X/X* (NR)
	Klf16	Regulation of transcription by RNA polymerase II	MGI	Autosome
	Klhl15	Protein ubiquitination	UniProt	X/X* (NR)
	Lin28b	miRNA catabolic process	MGI	Autosome
	Lratd1	Cell morphogenesis	MGI	Autosome
	Mafb	Regulation of DNA-templated transcription	MGI	Autosome
	Man2b2	Metabolic process	UniProt	Autosome (R)
	Mex3d	mRNA catabolic process	MGI	Autosome
	Mn1	Multicellular organism development	UniProt	Autosome (R)
	Mob3a	Signal transduction	GO_Central	Autosome
	Mybpc2	Cell adhesion	Uniprot	chr1 (NR)

Table S1 (Continued)

Cluster	*Gene name*	*Gene ontology*	*Contributor*	**Genomic compartment**
-YB	*Nfic*	Regulation of DNA-templated transcription	UniProt	Autosome
	Nova2	Regulation of alternative mRNA splicing, via spliceosome	Uniprot	chr1 (NR)
	Nrarp	Notch signaling pathway	MGI	Autosome
	Nucb1	Regulation of protein targeting	MGI	chr1 (NR)
	P2rx3	Neuronal action potential	MGI	Autosome
	P3h2	Collagen metabolic process	MGI	Autosome
	Pak4	Phosphorylation	Uniprot	chr1 (NR)
	Pou3f4	Regulation of DNA-templated transcription	UniProt	X/X* (NR)
	Ppp1r12c	Signal transduction	UniProt	Autosome
	Prom2	Positive regulation of protein phosphorylation	MGI	Autosome
	Samd4b	Regulation of mRNA stability	UniProt	chr1 (NR)
	Samhd1	DNA replication	Uniprot	Autosome
	Saxo2	-	-	chr1 (NR)
	Scrt2	Regulation of neuron migration	MGI	Autosome
	Sdad1	Protein transport	Uniprot	Autosome (R)
	Sox1	Nervous system development	Uniprot	Autosome
	Sox12	Regulation of transcription by RNA polymerase II	Uniprot	Autosome
	St8sia2	Protein glycosylation	MGI	chr1 (NR)
	Sts*†	*Steroid metabolic process*	UniProt	Unassigned (X)

Table S1 (Continued)

Cluster	*Gene name*	*Gene ontology*	*Contributor*	**Genomic compartment**
-YB	*Tdp2*	DNA repair	Uniprot	Autosome
	Tdrd12	Male meiotic nuclear division	Uniprot	chr1 (NR)
	Tmem158	Biological process	MGI	chr13 (R)
	Tnfrsf10b	Signal transduction	Uniprot	Autosome
	Ubald1	Biological process	MGI	chr1 (R)
	Vgf	Regulation of neuronal synaptic plasticity	MGI	Autosome (R)
	Wipf2	Actin filament-based movement	GO_Central	Autosome
	Xrcc1	Single strand break repair	Uniprot	chr1 (NR)
	Zbtb45	Nervous system development	UniProt	chr1 (NR)
	Zfp36l1	MAPK cascade	MGI	Autosome
	Zfp503	Negative regulation of gene expression	MGI	Autosome
	Zfp541	Protein sumoylation	MGI	chr1 (NR)
	Zfp758	Regulation of transcritpion by RNA polymerase II	GO_Central	chr1 (NR)
	Zfp788	Regulation of transcritpion by RNA polymerase II	GO_Central	chr1 (NR)
	Zfp943	Regulation of transcritpion by RNA polymerase II	GO_Central	chr1 (NR)
	Zfp944	Regulation of transcritpion by RNA polymerase II	GO_Central	chr1 (NR)
	Zfp983	Regulation of transcritpion by RNA polymerase II	GO_Central	chr1 (NR)
	Zfp995; Zfp947	Regulation of transcritpion by RNA polymerase II	GO_Central	chr1 (NR)

Table S1 (Continued)

Cluster	***Gene name***	***Gene ontology***	***Contributor***	**Genomic compartment**
X dose	*1110051M20Rik*	-	-	Autosome
	Aldh3b1	Lipid metabolic process	Uniprot	chr1 (R)
	Alpk3	Protein phosphorylation	Uniprot	chr1 (NR)
	Apln	Feeding behaviour/signal transduction	MGI/uniprot	X/X* (R)
	Ccdc186	Vesicle cytoskeletal trafficking	MGI	chr1 (R)
	Cd300ld2;Cd300ld4;Cd300ld5;Cd300ld3	Biological process / Immune system process	MGI / Uniprot	Autosome
	D16Ertd472e	Cerebral cortex neuron differentiation	Uniprot	Autosome
	Eif2s3x †	Translation	Uniprot	X/X* (NR)
	Fam174b	Golgi organization	MGI	chr1 (NR)
	Ldha	Lactate metabolic process	MGI	chr1 (NR)
	*Lhb**	Progesterone biosynthetic process	MGI	chr1 (NR)
	Lrrc28	-	-	chr1 (NR)
	*MaoA**	Catecholamine metabolic process	Uniprot	X/X* (NR)
	Mef2a	Mitochondrial genome maintenance	Uniprot	chr1 (NR)
	Pde8a	Positive regulation of protein phosphorylation	MGI	chr1 (NR)
	Prr33	Response to wounding	MGI	chr1 (R)
	Slc28a1	Nucleoside transmembrane transport	GO_Central	chr1 (NR)
	Srpx	Response to endoplasmic reticulum stress	MGI	X/X* (NR)

Table S1 (Continued)

Cluster	***Gene name***	***Gene ontology***	***Contributor***	**Genomic compartment**
X dose	*Synm*	Intermediate filament cytoskeleton organization	Uniprot	chr1 (NR)
	Taf1	Histone acetylation	Uniprot	X/X* (NR)
	Tdrd1	Meiotic cell cycle	Uniprot	chr1 (R)
	Tec	Protein phosphorylation	Uniprot	Autosome (R)
	Trim55	Protein ubiquitination	GO_Central	Autosome
	Ttc23	Positive regulation of smoothened signaling pathway	Uniprot	chr1 (NR)
	Uba2	Protein sumoylation	MGI	chr1 (NR)
	Wdr93	Electron transport chain	Uniprot	chr1 (NR)
	Whamm	Endoplasmic reticulum to Golgi vesicle-mediated transport	MGI	chr1 (NR)
-X*B	*2610318N02Rik*	Biological process	MGI	Autosom
	Acot10;Acot9	Acyl-CoA metabolic process	GO_Central	X/X* (NR)
	*Amhr2**	Anti-Mullerian hormone signalling pathway	MGI	Autosome
	Bmx	Protein phosphorylation	Uniprot	X/X* (NR)
	Cd101	Positive regulation of myeloid leukocyte differentiation	MGI	Autosome
	Fau	Cytoplasmic translation	ComplexPortal	chr1 (NR)
	Folh1	Protein catabolic process	MGI	chr1 (R)
	Gm28042;Pla2g4b	Glycerophospholipid catabolic process	GO_Central	Autosome
	Gm45808	D-xylose catabolic process	GO_central	chr1 (NR)

Table S1 (Continued)

Cluster	*Gene name*	*Gene ontology*	*Contributor*	**Genomic compartment**
-X*B	*Gnb3*	Signal transduction	Uniprot	Autosome
	H4c11;H4c12;H4c17;H4c18;H4c9;H4c8;H4c6;H4c4;H4c3;H4c2;H4c1;H4c14;H4f16	Nucleosome assembly	GO_Central	Autosome
	Hemk1	Methylation	Uniprot	chr1 (R)3
	Kif19a	Axonemal microtubule depolymerization	UniProt	Autosome
	Mesp1	Neurogenesis	MGI	chr1 (NR)
	Mfap2	Embryonic eye morphogenesis	GO_Central	Autosome
	Mgarp	Regulation of mitochrondrial organization	UniProt	Autosome
	Myo18b	Actomyosin structure organization	GO_Central	Autosome (R)
	Paqr5	Cell differentiation	Uniprot	chr13 (R)
	Pde6g	Visual perception	Uniprot	Autosome
	Pi16	Negative regulation of peptidase activity	Uniprot	chr1 (R)
	Plekhf1	Endosome organization	MGI	chr1 (NR)
	Pop4	RNA processing	Uniprot	chr1 (NR)
	Prdx4	Cell redox homeostasis	GO_Central	X/X* (NR)
	Rhpn2	Signal transduction	Uniprot	chr1 (NR)

Table S1 (Continued)

Cluster	*Gene name*	*Gene ontology*	*Contributor*	**Genomic compartment**
-X*B	*Riox2*	Ribosome biogenesis	Uniprot	Autosome
	Rps13	Translation	Uniprot	Autosome
	Slc38a5	Glutamine transport	MGI	X/X* (NR)
	Snap23	Protein transport	MGI	Autosome
	Spocd1	DNA methylation	Uniprot	Autosome
	Tmem128	Biological process	MGI	Autosome (R)
	Tmem191c	Biological process	MGI	Autosome
	Traf3ip2	Humoral immune response	GO_Central	Autosome
	Wdr27	Biological process	MGI	chr1 (R)

Table S2. Candidate genes for phenotypic divergences highlighted in *M. minutoides,* based on *M. musculus* studies.

Cluster	Gene name	Genomic compartment	Known expression influence on M. musculus phenotypes
X dose	MaoA	X/X* (NR)	Knock-out in *MaoA* is associated with enhanced aggressiveness (Scott et al., 2008)
X dose	*Lhb*	Chr1 (NR)	Overexpression in pituitary is associated with impaired ovulation (Huhtaniemi et al., 2006)
-X*B	*Amhr2*	Autosome	Overexpression in some hypothalamic nuclei is associated with impaired ovulation and polycistic ovary syndrom (PCOS) (Cimino et al., 2016)
-YB	*Sts*	X/X*	Aggressive individuals have greater expression levels of *Sts* (Mortaud et al., 2010)
-YB	*Kdm6a*	X/X* (NR)	Gene escaping inactivation with an impact on brain sexual differentiation (e.g. differentiation of hypothalamic neurons ; Cabrera Zapata et al., 2021)
FB1	Th	Chr1 (R)	*Th* stimulates dopamine production, which is positively correlated with aggressiveness or maternal care depending on the region of the brain (Mahadevia et al., 2021 ; Scott et al., 2015)

Table S3. Ontologies of X/X*-linked and $1^{Neo\text{-}X}/1^{Neo\text{-}X*}$-linked genes showing allelic imbalance in the brain of XX* females, and overlap with clusters.

† genes known to escape inactivation in *M. musculus* and/or likely to escape inactivation in *M. minutoides.*

Alleles	Gene name	Gene ontology	Contributor	Cluster
X/X* alleles	*Armcx3*	Axonal transport of mitochondrion	MGI	Unbiased
	Armcx4	Biological process	MGI	Unbiased
	Atp6ap2	Central nervous system maturation	UniProt	Unbiased
	Bex1	Nervous system development	UniProt	Unbiased
	Ccdc120	microtubule anchoring at centrosome	MGI	Unbiased
	Cdkl5	Neuron migration	MGI	Unbiased
	Chm	Intracellular protein transport	Uniprot	Unbiased
	Cnksr2	Regulation of signal transduction	Uniprot	Unbiased
	Dlg3	receptor localization to synapse	GO_Central	Unbiased
	Drp2	Synapse organization	MGI	Unbiased
	Eif2s3x †	Translation	Uniprot	X dose
	Frmpd4	Postsynaptic actin cytoskeleton organization	MGI	Unbiased
	Ftsj1	RNA methylation	GO_Central	Unbiased
	Gpm6b	Protein transport	UniProt	Unbiased
	Hdac6	Chromatin organization	UniProt	Unbiased
	Huwe1	DNA repair	UniProt	FB2
	Iqsec2	Modulation of chemical synaptic transmission	MGI	Unbiased
	Itm2a	Immunoglobulin production	MGI	Unbiased

Table S3 (Continued)

Alleles	Gene name	Gene ontology	Contributor	Cluster
X/X* alleles	*Maged1*	Regulation of circadian rythm	UniProt	Unbiased
	Magee1	Negative regulation of transcription by RNA polymerase II	GO_Central	Unbiased
	Magt1	Magnesion ion transport	MGI	Unbiased
	Map7d2	Microtubule cytoskeleton organizaton	GO_Central	Unbiased
	Nap1l3	Nucleosome assembly	GO_Central	Unbiased
	Nono	Immune system process	MGI	Unbiased
	Ogt	Glucosamine metabolic process	MGI	Unbiased
	Ophn1	Postsynaptic actin cytoskeleton organization	MGI	Unbiased
	Pbdc1	Biological process	MGI	Unbiased
	Pcsk1n	Neuropeptide signaling pathway	UniProt	Unbiased
	Pcytb	Respiratory electron transport chain	UniProt	Unbiased
	Pdha1	Carbohydrate metabolic process	UniProt	Unbiased
	Phka1	Carbohydrate metabolic process	UniProt	Unbiased
	Pim2	Protein phosphorylation	UniProt	Unbiased
	Porcn	Protein lipidation	UniProt	Unbiased
	Pqbp1	Alternative mRNA splicing via spliceosome	MGI	Unbiased
	Rragb	Regulation of TOR signaling	MGI	Unbiased
	Sh3bgrl	Biological process	MGI	Unbiased
	Sh3kbp1	Endocytosis	UniProt	Unbiased
	Slc16a2	Thyroid hormone transport	MGI	Unbiased

Table S3 (Continued)

Alleles	Gene name	Gene ontology	Contributor	Cluster
X/X* alleles	*Slc35a2*	Carbohydrate transport	UniProt	Unbiased
	Slc9a7	Ion transport	UniProt	Unbiased
	Smc1a	DNA repair	UniProt	Unbiased
	Stard8	Signal transduction	UniProt	Unbiased
	Suv39h1	Chromatim organization	MGI	Unbiased
	Syn1	Neurotransmitter secretion	MGI	Unbiased
	Taf1	RNA polymerase II preinitiation complex assembly	GO_Central	X dose
	Taf9b	Negative regulation of transcription by RNA polymerase II	MGI	Unbiased
	Tceal5	-	-	Unbiased
	Tmem47	Cell-cell adhesion	GO_Central	Unbiased
	Tro	Negative regulation of transcription by RNA polymerase II	GO_Central	Unbiased
	Tspyl2	Chromatin organization	UniProt	Unbiased
	Wdr13	Negative regulation of type B pancreatic cell proliferation	MGI	Unbiased
	Wdr45	Cellular response to starvation	MGI	Unbiased
	Xk	Amino acid transport	UniProt	Unbiased
	Yipf6	Intestinal epithelial cell development	MGI	Unbiased
	Zmym3	Cytoskeleton organization	MGI	Unbiased
Neo-X/Neo-X*alleles	*Dcps*	mRNA processing	Uniprot	MB

Table S4. Ontologies of $1^{Neo\text{-}X^*}/1^{Neo\text{-}Y}$-linked genes showing allelic imbalance in the brain of X*Y females.

Gene name	Gene ontology	Contributor	Cluster	Allele bias
Chrna7	Synaptic transmissiom, cholinergic	MGI	Unbiased	Neo-Y> Neo-X*
Fkrp	Protein processing	MGI	-YB	Neo-X* > Neo-Y
Hsd17b14	Steroid catabolic process	MGI	-YB	Neo-X* > Neo-Y
Kcnj14	Ion transport	Uniprot	YB	Neo-Y > Neo-X*
Kptn	Actin filament organization	Uniprot	YB	Neo-Y > Neo-X*
Ldha	Carbohydrate metabolic process	Uniprot	X dose	Neo-X* > Neo-Y
Lsr	Regulation of lipid metabolic process	MGI	YB	Neo-Y > Neo-X*
Ndufa3	Mitochondrial respiratory chain complex I assembly	MGI	MB	Neo-Y > Neo-X*
Ppp1r14a	Regulation of phosphorylation	UniProt	unbiased	Neo-X* > Neo-Y
Rps11	Translation	UniProt	MB	Neo-X* > Neo-Y
Sergef	Negative regulation of protein secretion	MGI	unbiased	Neo-X* > Neo-Y
U2af2	mRNA splicing, via spliceosome	MGI	unbiased	Neo-X* > Neo-Y
Xrcc1	Single strand break repair	Uniprot	-YB	Neo-X* > Neo-Y
Zfp541	Spermatogenesis	Uniprot	-YB	Neo-X* > Neo-Y

Supplemental references

Baudat, F., de Massy, B., & Veyrunes, F. (2019). Sex chromosome quadrivalents in oocytes of the African pygmy mouse Mus minutoides that harbors non-conventional sex chromosomes. *Chromosoma*, 128(3), 397-411. https://doi.org/10.1007/s00412-019-00699-4

Cabrera Zapata, L. E., Cisternas, C. D., Sosa, C., Luis, ·, Garcia-Segura, M., Arevalo, M. A., María, ·, & Cambiasso, J. (2021). X-linked histone H3K27 demethylase Kdm6a regulates sexually dimorphic differentiation of hypothalamic neurons. *Cellular and Molecular Life Science*, 78, 7043–7060. https://doi.org/10.1007/s00018-021-03945-0

Cimino, I., Casoni, F., Liu, X., Messina, A., Parkash, J., Jamin, S. P., Catteau-Jonard, S., Collier, F., Baroncini, M., Dewailly, D., Pigny, P., Prescott, M., Campbell, R., Herbison, A. E., Prevot, V., & Giacobini, P. (2016). Novel role for anti-Müllerian hormone in the regulation of GnRH neuron excitability and hormone secretion. *Nature Communications*, 7. https://doi.org/10.1038/NCOMMS10055

Huhtaniemi, I., Ahtiainen, P., Pakarainen, T., Rulli, S. B., Zhang, F. P., & Poutanen, M. (2006). Genetically modified mouse models in studies of luteinising hormone action. *Molecular and Cellular Endocrinology,* 252(1–2), 126–135. https://doi.org/10.1016/J.MCE.2006.03.026

Mahadevia, D., Saha, R., Manganaro, A., Chuhma, N., Ziolkowski-Blake, A., Morgan, A. A., Dumitriu, D., Rayport, S., & Ansorge, M. S. (2021). Dopamine promotes aggression in mice via ventral tegmental area to lateral septum projections. *Nature Communications*, 12, 6796. https://doi.org/10.1038/s41467-021-27092-z

Mortaud, S., Nicolas, L., Pinoteau, W., Tordjman, S., Carlier, M., & Roubertoux, P. L. (2010). Brain pathways mediating the pro-aggressive effect of the steroid sulfatase (Sts) gene. *Behavior Genetics*, 40(2), 211–219. https://doi.org/10.1007/s10519-010-9340-6

Scott, A. L., Bortolato, M., Chen, K., & Shih, J. C. (2008). Novel monoamine oxidase A knock out mice with human-like spontaneous mutation. *Neuroreport*, 19(7), 739. https://doi.org/10.1097/WNR.0B013E3282FD6E88

Scott, N., Prigge, M., Yizhar, O., & Kimchi, T. (2015). A sexually dimorphic hypothalamic circuit controls maternal care and oxytocin secretion. Nature, 525(7570), 519–522. https://doi.org/10.1038/nature15378

Veyrunes, F., Catalan, J., Sicard, B., Robinson, T. J., Duplantier, J.-M., Granjon, L., Dobigny, G., & Britton-Davidian, J. (2004). Autosome and sex chromosome diversity among the African pygmy mice, subgenus Nannomys (Murinae; Mus). *Chromosome Research*, 12, 369–382.

Veyrunes, F., & Perez, J. (2018). X inactivation in a mammal species with three sex chromosomes. *Chromosoma*, 127(2), 261–267. https://doi.org/10.1007/s00412-017-0657-2

Veyrunes, F., Watson, J., Robinson, T. J., & Britton-Davidian, J. (2007). Accumulation of rare sex chromosome rearrangements in the African pygmy mouse, Mus (Nannomys) minutoides: A whole-arm reciprocal translocation (WART) involving an X-autosome fusion. *Chromosome Research*, 15(2), 223–230. https://doi.org/10.1007/s10577-006-1116-8

Supplemental information S1-S5

Supplemental information S1

Log_2FC for the 1310 genes differentially expressed (DEG) between two genotypes at least, in the African pygmy mouse (edgeR results). Results are based on multiple pairwise comparisons (four genotypes = six possible comparisons), with a FDR threshold set at 0.05. Clusters in which genes were placed by the WGCNA software are included as well as corresponding names used in the main text (based on module-trait correlations, see fig s1). Bold values indicate an absolute FC greater or equal 1.5. Lines highlighted in yellow represent candidate genes for sexual phenotypes (*) or likely to escape inactivation (†). A Vienn diagram represents overlap of DEG between each genotypic comparison. Ensemble IDs and gene names are also indicated (when available).

Supplemental information S2

Enrichment in GO terms in the male-biased cluster. The top10 GO terms are represented.

Supplemental information S3

Enrichment in GO terms in the female-biased cluster. The top10 GO terms are represented.

Supplemental information S4

Allelic imbalance results in XX* females. All genes showing allelic variation (i.e. diagnostic SNPs found in coding sequences between gametologs) are represented. Genes showing true allelic imbalance are highlighted and in bold. Values represent results from post-hoc comparisons of allelic expression (following the negative binomial model). Genomic regions concerned are indicated as well as the name of the clusters to which genes were assigned in the WGCNA analysis (see supplemental information S1). Ensemble IDs and gene names are also indicated (when available).

Supplemental information S5

Allelic imbalance results in X*Y females. All genes showing allelic variation (i.e. diagnostic SNPs found in coding sequences between gametologs). Genes showing true allelic imbalance are highlighted and in bold. Values represent results from post-hoc comparisons of allelic expression (following the negative binomial model). Genomic regions concerned are indicated as well as the name of the clusters to which genes were assigned in the WGCNA analysis (see supplemental information S1). Ensemble IDs and gene names are also indicated (when available).

gene_id	module	cluste	chr	gene name	logFC.XX_XY	logFC.XX*_XY	logFC.X*Y_XY	logFC.XX_X*Y	logFC.XX_XX*	LogFC.XX*_X*Y
ENSMSEG00005002	red	-X*B	Autosome	Mfap2	0.0468701539149502	**-0.630620443317649**	-0.499632070443614	0.546502224358564	**0.677490597232599**	-0.130988372874035
ENSMSEG00005006	red	-X*B	Autosome	Pde6g	**0.861523529817042**	**-1.07423398422074**	**-0.924260582308641**	**1.78578411212568**	**1.93575751403778**	-0.149973401912099
ENSMSEG00005006	red	-X*B	Autosome	Gnb3	0.300563223679078	**-1.09018894338794**	**-0.93014443140013**	**1.23070765507921**	**1.39075216706702**	-0.160044511987815
ENSMSEG00005009	red	-X*B	Autosome		-0.574850964647708	**-0.780624448486674**	**-1.73506521587534**	**1.16021425122763**	0.205773483838967	-0.230378624751142
ENSMSEG00005002	red	-X*B	Autosome	Kif19a	0.0692518685464306	**-0.956004746146501**	-0.218865520361252	0.288117388907682	**1.02525661469293**	**-0.737139225785249**
ENSMSEG00005007	red	-X*B	Autosome	Mgarp	-0.0652702591091001	-0.581813831450674	**-0.63735516004665**	0.57208490093755	0.516543572341574	0.0555413285959763
ENSMSEG00005014	red	-X*B	Autosome	Riox2	0.0292880207257807	-0.509567418532782	**-0.634617111185217**	**0.663905131910998**	0.538855439258563	0.125049692652435
ENSMSEG00005007	red	-X*B	Autosome	Traf3ip2	-0.277713185757953	-0.428640412415279	**-0.627777535051966**	0.350064349294012	0.150927226657325	0.199137122636687
ENSMSEG00005021	red	-X*B	Autosome	Gm28042	-0.0462275872922414	-0.396384251541143	**-0.770253622235782**	**0.724026034943541**	0.350156664248902	0.373869370694639
ENSMSEG00005002	red	-X*B	Autosome	Cd101	-0.56889726778677	**-0.650655752706518**	**-1.09528454904957**	0.526387281262805	0.0817584849197481	0.444628796343056
ENSMSEG00005000	red	-X*B	Autosome	Snap23	-0.328651354869841	-0.213866049205907	**-0.666619242991275**	0.337967888121434	-0.114785305663934	0.452753193785369
ENSMSEG00005009	red	-X*B	Autosome		-0.33398833493184	**-1.06221290488626**	**-1.53518223146126**	**1.20119389652942**	**0.728224569954417**	0.472969326575004
ENSMSEG00005010	red	-X*B	Autosome	Tmem191c	-0.335124298045102	-0.31077050457115	**-0.960558745496595**	**0.625434447451493**	-0.0243537934739511	**0.649788240925444**
ENSMSEG00005000	red	-X*B	Autosome	Tmem128	-0.316355548620367	-0.230276760546196	**-0.897049444850744**	0.580693896230376	-0.086078788074171	**0.666772684304548**
ENSMSEG00005003	red	-X*B	Autosome	Spocd1	-0.0159594941794805	-0.309105192756207	**-1.02656571478457**	**1.01060622060509**	0.293145698576726	**0.717460522028361**
ENSMSEG00005014	red	-X*B	Autosome	**Amhr2* °**	0.0455102405494597	0.0405453059948541	**-0.737216382407586**	**0.782726622957045**	0.00496493455460566	**0.77776168840244**
ENSMSEG00005007	red	-X*B	Autosome		-0.343019125181617	**-1.31593519984671**	**-1.08555657509557**	**0.742537449913951**	**0.972916074665093**	**0.954440767388661**
ENSMSEG00005022	red	-X*B	Autosome	Myo18b	**-0.978708673601616**	**-1.60638626476075**	**-2.68900660914484**	**1.71029793554323**	**0.62767759115913**	**1.0826203443841**
ENSMSEG00005006	red	-X*B	Autosome	H4c11	-0.464247834712444	-0.44489570962663	**-1.66110550600582**	**1.19685767129338**	-0.0193521250858143	**1.21620979637919**
ENSMSEG00005019	red	-X*B	Autosome	Rps13	-0.294213557761188	0.368630154422762	**-1.10486111746554**	**0.81064755970435**	**-0.662843712183949**	**1.4734912718883**
ENSMSEG00005008	red	-X*B	Autosome	2610318N02R	-0.29232994355484	-0.474663042751847	**-2.06135780732952**	**1.76902786377468**	0.182333099197007	**1.58669476457768**
ENSMSEG00005006	red	-X*B	chr1 (NR)	Gm45808	-0.157468380549028	**-1.02060107686332**	**-0.796070788560313**	**0.638602408011285**	**0.86313269631429**	-0.224530288303005
ENSMSEG00005003	red	-X*B	chr1 (NR)	Fau	**-0.600670666985635**	**-0.921174582683642**	**-1.18320619299395**	0.582535526008317	0.320503915698007	0.262031610310311
ENSMSEG00005022	red	-X*B	chr1 (NR)	Pop4	-0.0449387080598325	-0.287460597383186	**-0.787731002391862**	**0.74279229433203**	0.242521889323353	0.500270405008677
ENSMSEG00005022	red	-X*B	chr1 (NR)	Rhpn2	0.117662420598952	-0.500872629194006	**-1.1438132781994**	**1.26147569879835**	**0.618535049792958**	**0.642940649005394**
ENSMSEG00005019	red	-X*B	chr1 (NR)	Plekhf1	-0.145043992378423	**-0.617866380255866**	**-1.87527345252456**	**1.73022946014613**	0.472822387877443	**1.25740707226869**
ENSMSEG00005019	red	-X*B	chr1 (NR)	Mesp1	0.161420756595883	**-0.907150607695376**	**-2.49383355470568**	**2.65525431130156**	**1.06857136429126**	**1.5866829470103**
ENSMSEG00005014	red	-X*B	X/X* (R)		-0.280886725993863	**-0.779375706310205**	**-3.43126221529708**	**3.15037548930321**	0.498488980316341	**2.65188650898687**
ENSMSEG00005006	red	-X*B	chr1 (R)		-0.228855522335461	-0.520333057347809	**-0.69751605146038**	0.468660529124918	0.291477535012347	0.177182994112571
ENSMSEG00005020	red	-X*B	chr1 (R)	Pi16	-0.216245402160811	-0.440103425885361	**-0.663742034650166**	0.447496632489355	0.22385802372455	0.223638608764805
ENSMSEG00005008	red	-X*B	chr1 (R)	Folh1	-0.199186044440878	-0.120365094493932	**-0.703353376747154**	0.504167332306276	-0.0788209499469462	0.582988282253222
ENSMSEG00005016	red	-X*B	chr1 (R)	Wdr27	-0.149978315925671	-0.311133704684974	**-0.919200612443844**	**0.769222296518173**	0.161155388759303	**0.608066907758871**
ENSMSEG00005018	red	-X*B	chr13 (R)	Paqr5	-0.350081458880432	**-1.1883666716601**	**-1.17676155021661**	**0.826680091336179**	**0.83828521277967**	-0.0116051214434904
ENSMSEG00005019	red	-X*B	chr13 (R)	Hemk1	0.0402535762475386	-0.407570574874642	**-0.659434829876979**	**0.699688406124517**	0.44782415112218	0.251864255002337
ENSMSEG00005022	red	-X*B	X/X* (NR)	Slc38a5	0.174221711649102	-0.425105188511915	-0.51159711613342	**0.685818827782523**	**0.599326900161018**	0.0864919276215051
ENSMSEG00005023	red	-X*B	X/X* (NR)	Bmx	-0.48752450915294	**-0.707304827753108**	**-1.29205991799467**	**0.804535408841726**	0.219780318600167	0.584755090241559
ENSMSEG00005004	red	-X*B	X/X* (NR)	Acot10	-0.426519616191697	**-0.718337520373002**	**-1.4624743706113**	**1.0359547544196**	0.291817904181305	**0.744136850238295**
ENSMSEG00005021	red	-X*B	X/X* (NR)	Prdx4	**-0.648313180469998**	**-0.858684858625909**	**-2.49383230698869**	**1.84551912651869**	0.210371678155911	**1.63514744836278**
ENSMSEG00005022	black	-YB	Autosome	Prom2	**1.00290525654698**	0.316148053984209	0.397378745476881	**0.605526511070103**	**0.686757202562774**	-0.0812306914926715
ENSMSEG00005019	black	-YB	Autosome	Gh	**2.31708567490919**	**-2.00426665094683**	**5.11549936742834**	**-2.79841369251915**	**4.32135232585602**	**-7.11976601837517**
ENSMSEG00005009	black	-YB	Autosome		0.480407338958495	**0.745957293063212**	-0.395014377419009	**0.875421716377504**	-0.265549954104717	0.0609612464311618
ENSMSEG00005021	black	-YB	Autosome	Vgf	**1.01054850933069**	0.430698349915925	0.265681456719875	**0.744867052610811**	0.579850159414761	0.16501689319605
ENSMSEG00005019	black	-YB	Autosome	Irf2bpl	**0.734604452676463**	0.563515782714189	0.395115403457467	0.339489049218996	0.171088669962274	0.168400379256723
ENSMSEG00005020	black	-YB	Autosome	Sdad1	**0.638234726593188**	0.49327830637179	0.294096955088395	0.344137771504793	0.144956420221398	0.199181351283395
ENSMSEG00005013	black	-YB	Autosome	Grrp1	**0.867446922957193**	0.0718614801726449	-0.144290312053222	**1.01173723501042**	**0.795585442784548**	0.216151792225867
ENSMSEG00005007	black	-YB	Autosome	Nfic	**0.699833488532473**	**0.587148289496777**	0.367570526413173	0.3322629621193	0.112685199035696	0.219577763083603

ENSMSEG00005005(	black	-YB	Autosome	Wipf2	**0.718106510899851**	0.572474853521179	0.344428835117845	0.373677675782006	0.145631657378671	0.228046018403335
ENSMSEG00005014(	black	-YB	Autosome	Gbx2	0.479620566807379	-0.0117799367540029	-0.269421595914493	**0.749042162721872**	0.491400503561382	0.25764165916049
ENSMSEG00005005<	black	-YB	Autosome	Ado	**0.627304509732336**	0.392805538315946	0.116656732965238	0.510647776767098	0.23449897141639	0.276148805350708
ENSMSEG00005007(	black	-YB	Autosome	Bard1	**1.18964908853434**	0.238108249623331	-0.0393936581433496	**1.22904274667769**	**0.951540838911013**	0.27750190776668
ENSMSEG00005016(	black	-YB	Autosome	Samhd1	**0.808733069353161**	0.271434095415472	-0.0428469721963983	**0.851580041549559**	0.537298973937688	0.314281067611871
ENSMSEG00005018(	black	-YB	Autosome	Zfp503	**1.10253307731884**	**0.831894871198386**	0.513625999420725	**0.588907077898114**	0.270638206120452	0.318268871777661
ENSMSEG00005013(	black	-YB	Autosome	Mex3d	**0.715951436177409**	**0.594117711332567**	0.254237385988106	0.461714050189303	0.121833724844843	0.339880325344461
ENSMSEG00005020(	black	-YB	Autosome	Mn1	**0.91238271616249**	**0.677514280338593**	0.328903380488272	0.583479335674218	0.234868435823897	0.348610899850322
ENSMSEG00005021(	black	-YB	Autosome	Klf16	**0.773969605839588**	0.554522896842127	0.184020863784263	**0.589948742055326**	0.219446708997461	0.370502033057865
ENSMSEG00005013(	black	-YB	Autosome	Man2b2	0.405002095027982	0.0987622810550571	-0.273030540237015	**0.678032635264997**	0.306239813972925	0.371792821292072
ENSMSEG00005006(	black	-YB	Autosome	Lratd1	**0.60486835299481**	0.57372297849013	0.187620033255688	0.417248319739122	0.0311453745046791	0.386102945234443
ENSMSEG00005002(	black	-YB	Autosome	Zfp36l1	**0.814633266623215**	0.561822033063405	0.159282727476591	**0.655350539146624**	0.25281123355981	0.402539305586814
ENSMSEG00005005(	black	-YB	Autosome	Chst3	**0.999587804982809**	0.427711455080401	0.0152195528484473	**0.984368252134362**	0.571876349902409	0.412491902231953
ENSMSEG00005001<	black	-YB	Autosome	Cpm	**0.876685074666453**	0.242614658088844	-0.181502976742558	**1.05818805140901**	**0.634070416577608**	0.424117634831402
ENSMSEG00005020(	black	-YB	Autosome	Fbxl14	**0.832585702220078**	0.57641684184037	0.142206714803837	**0.690378987416241**	0.256168860379708	0.434210127036533
ENSMSEG00005002(	black	-YB	Autosome	Nrarp	**0.907138694983882**	**0.992943608560322**	0.538242028243044	0.368896666740838	-0.0858049135764406	0.454701580317278
ENSMSEG00005001(	black	-YB	Autosome	Lin28b	**1.20912931015209**	**0.958616112383666**	0.478730493446419	**0.730398816705674**	0.250513197768427	0.479885618937247
ENSMSEG00005007(	black	-YB	Autosome		**1.16811118756947**	**1.07860993973893**	**0.588087249733967**	0.580023937835506	0.0895012478305441	0.490522690004962
ENSMSEG00005008(	black	-YB	Autosome	Scrt2	**1.25208371501872**	**0.685409290026661**	0.189509005004509	**1.06257471001421**	0.566674424992063	0.495900285022151
ENSMSEG00005021(	black	-YB	Autosome	Tdp2	0.570999686980895	0.362337810840057	-0.152170386587392	**0.723170073568286**	0.208661876140838	0.514508197427449
ENSMSEG00005008<	black	-YB	Autosome	Asah2	**0.709801321336497**	**0.694396518594048**	0.177619403953105	0.532181917383392	0.0154048027424493	0.516777114640943
ENSMSEG00005017(	black	-YB	Autosome	Mafb	**1.25932779002046**	**1.01282777207671**	0.495972510918414	**0.763355279102047**	0.246500017943756	0.516855261158291
ENSMSEG00005020(	black	-YB	Autosome		**0.640343902183931**	0.574709972934568	-0.0121654813546605	**0.652509383538591**	0.0656339292493623	0.550611135768018
ENSMSEG00005018(	black	-YB	Autosome	Sox12	**0.78374620083506**	**0.750265757719416**	0.174526034929628	**0.609220165905432**	0.0334804431156446	0.575739722789788
ENSMSEG00005013(	black	-YB	Autosome	Hnrnpa0	**1.32178205981889**	**1.02186171706306**	0.44400872152362	**0.877773338295271**	0.299920342755827	0.577852995539444
ENSMSEG00005000(	black	-YB	Autosome		**0.857130329399556**	0.561199268175496	0.500238021744334	0.356892307655222	0.29593106122406	**0.586875454289229**
ENSMSEG00005005(	black	-YB	Autosome	Ppp1r12c	**0.71260368995784**	**0.73841847645471**	0.130448477630827	0.582155212327013	-0.02581478649687	**0.607969998823883**
ENSMSEG00005012<	black	-YB	Autosome	Fam161a	**1.10625069953016**	**0.738772237122857**	0.127582787977991	**0.978667911552168**	0.367478462407302	**0.611189449144866**
ENSMSEG00005009(	black	-YB	Autosome	Aadat	0.213851991109891	0.550342504736071	-0.12297188327211	0.336823874382002	-0.336490513626179	**0.673314388008181**
ENSMSEG00005000(	black	-YB	Autosome	P2rx3	0.34605503842093	0.149250778132893	-0.54023146714877	**0.8862865055697**	0.196804260288037	**0.689482245281663**
ENSMSEG00005015(	black	-YB	Autosome		**1.77221527634334**	**1.6159457703179**	**0.911881294082807**	**0.860333982260535**	0.156269506025441	**0.704064476235093**
ENSMSEG00005014(	black	-YB	Autosome	Mob3a	0.338280413884652	0.230816326368123	-0.47368522558345	**0.811965639468102**	0.107464087516529	**0.704501551951573**
ENSMSEG00005013(	black	-YB	Autosome	Adrb1	**0.818026503725393**	**0.780693704803772**	0.07140871988957	**0.746617783835823**	0.037332798921621	**0.709284984914202**
ENSMSEG00005001(	black	-YB	Autosome	Sox1	**1.14801693541765**	**1.05935784459961**	0.349908785394503	**0.798108150023148**	0.0886590908180402	**0.709449059205108**
ENSMSEG00005020(	black	-YB	Autosome	Ier5l	**0.991617349127597**	**0.84326981755321**	0.116217551864955	**0.875399797262642**	0.148347531574387	**0.727052265688255**
ENSMSEG00005018(	black	-YB	Autosome	Tnfrsf10b	**1.19339509144028**	**1.18162590117134**	0.436191899780569	**0.757203191659712**	0.0117691902689405	**0.745434001390771**
ENSMSEG00005001(	black	-YB	Autosome	Creb5	**0.671938446124404**	**0.879727194608678**	0.105299906861217	0.566638539263187	-0.207788748484274	**0.774427287747461**
ENSMSEG00005006<	black	-YB	Autosome	Caps2	0.380201424423868	0.475029482337055	-0.347056642692684	**0.727258067116551**	-0.0948280579131869	**0.822086125029738**
ENSMSEG00005018(	black	-YB	Autosome	Clcf1	-0.24224201803959	0.376948614036499	-0.513353546290197	0.271111528250607	**-0.619190632076089**	**0.890302160326696**
ENSMSEG00005018(	black	-YB	Autosome	P3h2	**1.29230150124252**	**0.832333822592123**	-0.199114162131144	**1.49141566337367**	0.459967678650401	**1.03144798472327**
ENSMSEG00005000(	black	-YB	Autosome	Cks2	0.576903624708403	**0.678270545611467**	-0.37450015190704	**0.951403776615442**	-0.101366920903064	**1.05277069751851**
ENSMSEG00005002(	black	-YB	Autosome		**0.739012268980715**	**0.687569967136199**	-0.382825737736404	**1.12183800671712**	0.0514423018445162	**1.0703957048726**
ENSMSEG00005003(	black	-YB	Autosome	Clcn1	0.56356846016933	**1.06676626294795**	-0.0322316590237896	**0.59580011919312**	-0.503197802778624	**1.09899792197174**
ENSMSEG00005004(	black	-YB	Autosome		**0.94846785615865**	**0.807569342947511**	0.256958207179493	**0.691509648979157**	0.140898513211139	**1.14097167048222**
ENSMSEG00005016(	black	-YB	chr1 (NR)	Nova2	**0.657218001261045**	0.431894552840989	0.284131720351031	0.373086280910013	0.225323448420056	0.147762832489958
ENSMSEG00005019(	black	-YB	chr1 (NR)	Samd4b	**0.604158047488586**	0.415850660418134	0.180498815738847	0.423659231749739	0.188307387070452	0.235351844679287
ENSMSEG00005011(	black	-YB	chr1 (NR)	Zbtb45	**0.605841691489289**	0.408576103229608	0.164974458803216	0.440867232686073	0.197265588259681	0.243601644426391

ENSMSEG00005014	black	-YB	chr1 (NR)	Irgq	**0.696959616999134**	**0.602423919648653**	0.315035331244703	0.381924285754431	0.0945356973504815	0.28738858840395
ENSMSEG00005006	black	-YB	chr1 (NR)	Nucb1	**0.618460748408657**	0.491029744275886	0.119089028720564	0.499371719688093	0.127431004132771	0.371940715555321
ENSMSEG00005019	black	-YB	chr1 (NR)	Pak4	**0.589720692956821**	0.481645277766027	0.0942120979329519	0.495508595023869	0.108075415190794	0.387433179833075
ENSMSEG00005006	black	-YB	chr1 (NR)	Hsd17b14	**0.651895219188284**	0.383657165843158	-0.130259389298061	**0.782154608486345**	0.268238053345126	0.513916555141219
ENSMSEG00005014	black	-YB	chr1 (NR)	Xrcc1	0.514262328758813	0.344785984889974	-0.176141824714495	**0.690404153473308**	0.169476343868839	0.520927809604469
ENSMSEG00005022	black	-YB	chr1 (NR)	AI987944	0.553376438835367	**0.71842798170161**	0.158872385484631	0.394504053350736	-0.165051542866244	0.559555596216979
ENSMSEG00005019	black	-YB	chr1 (NR)	Fkrp	**1.04241560827501**	**0.872317266262601**	0.268180398123402	**0.774235210151607**	0.170098342012408	**0.604136868139198**
ENSMSEG00005012	black	-YB	chr1 (NR)	Eps8l1	0.422522681689445	0.385680526700948	-0.228340679294033	**0.650863360983478**	0.0368421549884969	**0.614021205994981**
ENSMSEG00005008	black	-YB	chr1 (NR)	Ercc2	**0.697619246395837**	0.512808488083419	-0.128210011519706	**0.825829257915544**	0.184810758312418	**0.641018499603125**
ENSMSEG00005018	black	-YB	chr1 (NR)	C5ar1	0.333577351863302	0.34355752981397	-0.310425601553675	**0.644002953416977**	-0.00998017795066739	**0.653983131367644**
ENSMSEG00005012	black	-YB	chr1 (NR)	Saxo2	**0.633600777030216**	**0.618476798972022**	-0.0471273127090489	**0.680728089739265**	0.0151239780581934	**0.665604111681071**
ENSMSEG00005018	black	-YB	chr1 (NR)	Dhx34	**1.15340216355444**	**0.978049408327245**	0.271800456926936	**0.881601706627501**	0.175352755227192	**0.706248951400309**
ENSMSEG00005022	black	-YB	chr1 (NR)		**1.06052525972077**	**1.19318181338971**	0.0322266050092112	**1.02829865471156**	-0.132656553668938	**0.813035631466396**
ENSMSEG00005019	black	-YB	chr1 (NR)	Gm21983	0.294747701498293	0.389468428326142	-0.426392958532595	**0.721140660030888**	-0.0947207268278486	**0.815861386858737**
ENSMSEG00005014	black	-YB	chr1 (NR)	Zfp944	**0.749779566268537**	**0.84900483477064**	0.0289563763543597	**0.720823189914178**	-0.0992252685021029	**0.82004845841628**
ENSMSEG00005014	black	-YB	chr1 (NR)	St8sia2	**1.5708558409337**	**0.882695399431295**	0.0395573471208003	**1.5312984938129**	**0.688160441502407**	**0.843138052310495**
ENSMSEG00005022	black	-YB	chr1 (NR)	Cep89	**0.774515459368433**	**0.748422183506135**	-0.100112861281992	**0.874628320650425**	0.0260932758622977	**0.848535044788127**
ENSMSEG00005022	black	-YB	chr1 (NR)	Zfp788	**0.864807145611447**	**0.928753994919946**	0.060787947089829	**0.804019198521618**	-0.0639468493084983	**0.867966047830117**
ENSMSEG00005019	black	-YB	chr1 (NR)	Zfp541	**0.753031184820481**	**0.741135345755788**	-0.142130182875378	**0.895161367695859**	0.0118958390646936	**0.883265528631165**
ENSMSEG00005000	black	-YB	chr1 (NR)	Mybpc2	0.565909134697835	0.425744358490744	-0.470807123713316	**1.03671625841115**	0.14016477620709	**0.89655148220406**
ENSMSEG00005020	black	-YB	chr1 (NR)	9530053A07R	**1.01632406996299**	**0.927869287621283**	-0.000693403815136514	**1.01701747377813**	0.0884547823417096	**0.928562691436419**
ENSMSEG00005014	black	-YB	chr1 (NR)	Zfp758	**1.18953328839894**	**1.15646362398644**	0.110679566721035	**1.07885372167791**	0.0330696644125049	**1.0457840572654**
ENSMSEG00005023	black	-YB	chr1 (NR)	Zfp983	**0.793134247695698**	**1.00990132200235**	-0.0725040255045944	**0.865638273200292**	-0.216767074306655	**1.08240534750695**
ENSMSEG00005008	black	-YB	chr1 (NR)	Zfp943	**0.860841464708444**	**1.12282773317225**	0.00851214141953261	**0.852329323288912**	-0.261986268463802	**1.11431559175271**
ENSMSEG00005013	black	-YB	chr1 (NR)		**1.33573241963656**	**0.977528935998143**	**-1.26606180860345**	**2.60179422824001**	0.358203483638416	**1.1609552083805**
ENSMSEG00005008	black	-YB	chr1 (NR)	Zfp995	**1.40728242003331**	**1.64590076880318**	0.361800886304811	**1.0454815337285**	-0.238618348769872	**1.28409988249837**
ENSMSEG00005021	black	-YB	chr1 (NR)	Ceacam1	**0.882490532668761**	**0.96389162287975**	-0.4395669691277	**1.32205750179646**	-0.0814010902109883	**1.40345859200745**
ENSMSEG00005022	black	-YB	chr1 (NR)	Tdrd12	**0.955802164149658**	**0.82752888388252**	**-0.622131205928586**	**1.57793337007824**	0.128273280267137	**1.44966008981111**
ENSMSEG00005020	black	-YB	chr1 (NR)		**0.64763660131688**	**0.665092351553249**	-0.147943279913148	**0.795579881230027**	-0.0174557502363689	**2.2435907446016**
ENSMSEG00005019	black	-YB	X/X* (R)	Chrdl1	**0.883056741587504**	**0.72888411060361**	0.299296119120226	0.583760622467278	0.154172630983894	0.429587991483384
ENSMSEG00005009	black	-YB	X/X* (R)	Gm773	**7.35405002618531**	**8.41840940949145**	**4.54157604011973**	**2.81247398606557**	**-1.06435938330614**	**3.87683336937171**
ENSMSEG00005016	black	-YB	chr1 (R)	Ubald1	**0.598898430632108**	0.388950827540536	0.0793519806169629	0.519546450015145	0.209947603091572	0.309598846923573
ENSMSEG00005009	black	-YB	chr1 (R)	Aars2	0.449280032094855	0.147321071517892	-0.240443041794783	**0.689723073889638**	0.301958960576963	0.387764113312675
ENSMSEG00005022	black	-YB	chr1 (R)		**0.630366951833105**	**1.02392420934342**	-0.0653206247050074	**0.695687576538113**	-0.393557257510311	**1.08924483404842**
ENSMSEG00005004	black	-YB	chr13 (R)	Tmem158	**0.872692325244736**	**1.06471909225593**	-0.0694388763095146	**0.94213120155425**	-0.192026767011198	**1.13415796856545**
ENSMSEG00005007	black	-YB	X/X* (NR)	Pou3f4	**0.673557154447691**	0.273503343880886	0.0939172870238123	0.579639867423879	0.400053810566805	0.179586056857074
ENSMSEG00005005	black	-YB	X/X* (NR)	Klhl15	**0.635607313703159**	0.508952348103796	0.304945586565841	0.330661727137319	0.126654965599364	0.204006761537955
ENSMSEG00005001	black	-YB	X/X* (NR)	**Ddx3x †**	0.580817702520811	**0.600472261880672**	0.229169259158545	0.351648443362267	-0.0196545593598605	0.371303002722127
ENSMSEG00005016	black	-YB	X/X* (NR)	**Kdm6a *†**	**0.715401527859416**	**0.748599165282872**	0.339582822290498	0.375818705568918	-0.0331976374234563	0.409016342992375
ENSMSEG00005012	black	-YB	X/X* (NR)	B630019K06R	**0.598037339953611**	0.45628823465252	-0.145475052476243	**0.743512392429854**	0.141749105301091	**0.601763287128763**
ENSMSEG00005017	black	-YB	X/X* (NR)		0.313975529751928	0.387878837092122	-0.356629287236686	**0.670604816988614**	-0.0739033073401939	**0.744508124328808**
ENSMSEG00005017	black	-YB	X/X* (NR)		**1.45221490702091**	**1.14095650156359**	0.143425186354672	**1.30878972066624**	0.311258405457321	**0.997531315208915**
ENSMSEG00005005	black	-YB	unassigned		**1.56746356892368**	**1.14206355561796**	0.11975440704963	**1.44770916187405**	0.42540001330572	0.554840031446536
ENSMSEG00005005	black	-YB	unassigned		**1.85543274989322**	**1.63837869934091**	**0.670911512791502**	**1.18452123710172**	0.217054050552312	**0.967467186549408**
ENSMSEG00005005	black	-YB	unassigned		**1.06826986947549**	**1.0715007915002**	0.516660760053666	0.551609109421828	-0.00323092202470765	**1.02230914856833**
ENSMSEG00005005	black	-YB	unassigned		**0.893100955096417**	**0.743528210413763**	-0.288336384484772	**1.18143733958119**	0.149572744682654	**1.03186459489854**
ENSMSEG00005005	black	-YB	unassigned	**Sts * °(†)**	**1.69087592456525**	**1.3809394711505**	0.213295494645844	**1.4775804299194**	0.309936453414753	**1.16764397650465**

ENSMSEG00005017	greenyello	FB	Autosome	Myo5b	**0.637065698970608**	0.552904019263733	**0.623922335152941**	0.0131433638176666	0.0841616797068751	-0.0710183158892085
ENSMSEG00005010	greenyello	FB	Autosome	Dlx5	**1.02940527081127**	**0.672033461419177**	**0.832470846131776**	0.196934424679494	0.357371809392093	-0.1604373847126
ENSMSEG00005022	greenyello	FB	Autosome	Scube1	**0.851972566365721**	0.565254819510778	**0.728019347080234**	0.123953219285487	0.286717746854943	-0.162764527569456
ENSMSEG00005010	greenyello	FB	Autosome	Sema3c	**0.632084386272149**	0.495136008750666	**0.69793501224541**	-0.0658506259732607	0.136948377521483	-0.202799003494744
ENSMSEG00005018	greenyello	FB	Autosome	Lama3	0.310677734331701	0.451213391706	**0.657100594027632**	-0.346422859695931	-0.140535657374298	-0.205887202321632
ENSMSEG00005015	greenyello	FB	Autosome	Prkca	0.403273521676618	0.345815425485472	**0.587819896813293**	-0.184546375136676	0.0574580961911461	-0.242004471327822
ENSMSEG00005014	greenyello	FB	Autosome	Pbx3	0.431894627438713	0.239366992655481	**0.605839595079977**	-0.173944967641264	0.192527634783232	-0.366472602424496
ENSMSEG00005014	greenyello	FB	Autosome	Syt10	**0.743103704569506**	**0.842935856827904**	**1.21335119332036**	-0.470247488750859	-0.0998321522583985	-0.370415336492461
ENSMSEG00005011	greenyello	FB	Autosome	Kcnb2	0.541969711823657	0.306226744079595	**0.688468436530017**	-0.14649872470636	0.235742967744062	-0.382241692450422
ENSMSEG00005001	greenyello	FB	Autosome	Tshz1	**0.654384459457597**	0.353796048443619	**0.758234997052078**	-0.103850537594481	0.300588411013978	-0.404438948608459
ENSMSEG00005006	greenyello	FB	Autosome	Map3k1	0.471594128712396	0.291674150216904	**0.70553013972111**	-0.233936011008714	0.179919978495492	-0.413855989504206
ENSMSEG00005008	greenyello	FB	Autosome	Dlx2	**1.5277290931334**	**0.867754713113587**	**1.39074396903758**	0.136985124095828	**0.659974380019816**	-0.522989255923988
ENSMSEG00005016	greenyello	FB	Autosome	Myo16	**0.821118227799835**	0.401952541099212	**0.954637422093809**	-0.133519194293973	0.419165686700623	-0.552684880994597
ENSMSEG00005003	greenyello	FB	Autosome	Myo16	**0.915841910287812**	0.571744384165032	**1.15199571426763**	-0.236153803979819	0.34409752612278	-0.580251330102599
ENSMSEG00005009	greenyello	FB	Autosome	Ptpro	0.447265901978743	0.309120713954398	**0.925254975732236**	-0.477989073753493	0.138145188024345	**-0.616134261777838**
ENSMSEG00005013	greenyello	FB	Autosome	Aga	0.339605968953388	-0.202977492658812	0.439490031145293	-0.0998840621919057	0.5425834616122	**-0.642467523804105**
ENSMSEG00005014	greenyello	FB	Autosome	Sp7	**1.70332188550429**	**0.868794509620109**	**1.76723030950348**	-0.063908423999188	**0.83452737588418**	**-0.898435799883368**
ENSMSEG00005009	greenyello	FB	chr1 (R)	**Th* °**	0.12507966593738	-0.136982010112496	**0.88896886059138**	**-0.763889194654001**	0.262061676049875	**-1.02595087070388**
ENSMSEG00005008	blue	FB2	Autosome	Mef2c	0.506734379810265	**0.614133581376327**	**0.630634870192211**	-0.123900490381945	-0.107399201566062	-0.0165012888158836
ENSMSEG00005009	blue	FB2	Autosome	Rc3h2	0.510079045867748	0.565406420253924	**0.586859746579535**	-0.076780700711787	-0.0553273743861756	-0.0214533263256113
ENSMSEG00005021	blue	FB2	Autosome	Shroom3	0.535488797895022	**0.663916089827845**	**0.68986206613328**	-0.154373268238259	-0.128427291932823	-0.0259459763054352
ENSMSEG00005010	blue	FB2	Autosome	Ptpn4	0.43837539774363	0.583016088626806	**0.613115159283252**	-0.174739761539622	-0.144640690883176	-0.0300990706564457
ENSMSEG00005018	blue	FB2	Autosome	Sema3a	**0.596549949376386**	**0.666213974301248**	**0.714416176092543**	-0.117866226716157	-0.0696640249248622	-0.0482022017912952
ENSMSEG00005022	blue	FB2	Autosome		-0.0578524200308975	-0.0761051835491514	**0.6696361407582**	**-0.727488560789098**	0.0182527635182538	-0.0490767409213818
ENSMSEG00005016	blue	FB2	Autosome	Cntnap5a	0.424936696416276	**0.628537735277909**	**0.68479814324221**	-0.259861446825934	-0.203601038861633	-0.0562604079643009
ENSMSEG00005010	blue	FB2	Autosome	Plxna2	0.442094639782375	0.532764736390886	**0.592244293200031**	-0.150149653417656	-0.0906700966085109	-0.0594795568091448
ENSMSEG00005013	blue	FB2	Autosome	Fam135b	0.442270494052346	0.531907209381104	**0.591828102712109**	-0.149557608659763	-0.0896367153287585	-0.0599208933310042
ENSMSEG00005020	blue	FB2	Autosome	Ino80d	**0.608941662644394**	**0.688770958422383**	**0.750841050412513**	-0.141899387768119	-0.0798292957779891	-0.0620700919901298
ENSMSEG00005003	blue	FB2	Autosome		0.462966165632712	**0.72360582021489**	0.533672732560282	-0.0707065669275697	-0.260639654582178	-0.0711866369360778
ENSMSEG00005019	blue	FB2	Autosome	Sod3	**0.58555731035682**	**0.814176144330313**	**0.887203880051828**	-0.301646569695008	-0.228618833973493	-0.0730277357215144
ENSMSEG00005008	blue	FB2	Autosome	Usp13	0.546025266671517	0.526174186433736	**0.600338693418241**	-0.0543134267467238	0.0198510802377814	-0.0741645069845052
ENSMSEG00005018	blue	FB2	Autosome	Dgkh	0.451306134397665	**0.590667911348835**	**0.666762906620574**	-0.215456772222909	-0.13936177695117	-0.0760949952717388
ENSMSEG00005005	blue	FB2	Autosome	Notch1	0.498784142483488	0.561773262301232	**0.643157461587366**	-0.144373319103877	-0.0629891198177436	-0.0813841992861338
ENSMSEG00005008	blue	FB2	Autosome	Lrp1	**0.604682136185386**	**0.66288846186947**	**0.74435437613488**	-0.139672239949493	-0.0582063256840833	-0.0814659142654101
ENSMSEG00005001	blue	FB2	Autosome	Lrp1b	0.54377776557237	**0.859159087346617**	**0.940816912938063**	-0.397039147365693	-0.315381321774248	-0.0816578255914457
ENSMSEG00005020	blue	FB2	Autosome	Zfhx4	0.52182249100368	0.531323463749714	**0.615204217482747**	-0.0933817264790668	-0.00950097274603358	-0.0838807537330332
ENSMSEG00005015	blue	FB2	Autosome	Scn8a	0.506100526909549	0.544215795695474	**0.63027011895717**	-0.124165925047622	-0.0381152687859254	-0.0860543232616963
ENSMSEG00005007	blue	FB2	Autosome	Trmt44	-0.0797401618389493	**0.66836600723158**	**0.755383059636282**	**-0.835123221475232**	**-0.74810616907053**	-0.0870170524047022
ENSMSEG00005000	blue	FB2	Autosome	Cep350	0.439204460227006	0.532710459646244	**0.62974932049412**	-0.190544860267114	-0.0935059994192383	-0.0970388608478761
ENSMSEG00005013	blue	FB2	Autosome	Plxna4	0.490856782157985	0.534567088734592	**0.636235524655144**	-0.145378742497159	-0.0437103065766073	-0.101668435920552
ENSMSEG00005012	blue	FB2	Autosome	Sema3e	**1.00731967212443**	**1.10960738207639**	**1.21360977551278**	-0.206290103388348	-0.102287709951962	-0.104002393436387
ENSMSEG00005018	blue	FB2	Autosome	Arfgef3	0.475516040925815	**0.611374416205262**	**0.721600717499915**	-0.2460846765741	-0.135858375279447	-0.110226301294653
ENSMSEG00005019	blue	FB2	Autosome	Adamts3	0.414386357088601	0.558895213395303	**0.676670861957311**	-0.262284504868711	-0.144508856306702	-0.117775648562008
ENSMSEG00005011	blue	FB2	Autosome	Pou2f1	**0.729016280172904**	**0.654754914509596**	**0.773589933701011**	-0.0445736535281076	0.0742613656633076	-0.118835019191415
ENSMSEG00005010	blue	FB2	Autosome	Soga1	**0.590058258647579**	0.580795199519286	**0.70534069801729**	-0.11528243936971	0.00926305912829354	-0.124545498498004
ENSMSEG00005019	blue	FB2	Autosome	Tnr	**0.638791147162728**	0.534467434177845	**0.659670573824621**	-0.0208794266618933	0.104323712984884	-0.125203139646777
ENSMSEG00005006	blue	FB2	Autosome	Abca1	0.275366454724742	0.47854406286495	**0.606616479370113**	-0.331250024645371	-0.203177608140208	-0.128072416505163

ENSMSEG00005015(	blue	FB2	Autosome	Tanc2	0.525582694113176	0.556412742890145	**0.684809593143467**	-0.159226899030291	-0.0308300487769695	-0.128396850253322
ENSMSEG00005003	blue	FB2	Autosome	Tnks	0.45046525500764	0.469225457630474	**0.598777227085094**	-0.148311972077454	-0.0187602026228337	-0.12955176945462
ENSMSEG00005019	blue	FB2	Autosome	Bmpr2	0.410931693397205	0.511781472217041	**0.642773971991771**	-0.231842278594566	-0.100849778819837	-0.130992499774729
ENSMSEG00005005	blue	FB2	Autosome	Cacna2d1	0.376206582516729	0.52840621531728	**0.660855902814055**	-0.284649320297326	-0.152199632800551	-0.132449687496775
ENSMSEG00005013	blue	FB2	Autosome	Wdfy3	0.383657886581357	0.482357505042427	**0.614892643110741**	-0.231234756529384	-0.0986996184610705	-0.132535138068313
ENSMSEG00005009	blue	FB2	Autosome	Erbb4	0.428815609510024	**0.610043538284559**	**0.743068579352383**	-0.314252969842359	-0.181227928774536	-0.133025041067823
ENSMSEG00005013	blue	FB2	Autosome		0.331396146502917	**0.965531878918841**	**1.03671851585492**	**-0.705322369352002**	**-0.634135732415924**	-0.133571232071286
ENSMSEG00005003	blue	FB2	Autosome	Prrc2c	**0.692809694220708**	0.582757489801676	**0.719610554199317**	-0.0268008599786094	0.110052204419032	-0.136853064397641
ENSMSEG00005013	blue	FB2	Autosome	Grin2a	0.341843803205453	0.540125115854582	**0.67913839154728**	-0.337294588341827	-0.198281312649129	-0.139013275692698
ENSMSEG00005010	blue	FB2	Autosome	Fgd4	0.377136509310818	0.488045169943447	**0.62806636538499**	-0.250929856074172	-0.11090866063263	-0.140021195441543
ENSMSEG00005006	blue	FB2	Autosome		0.34650723607219	**0.984185356158698**	**1.31602286777681**	**-0.969515631704623**	**-0.637678120086508**	-0.141685887478695
ENSMSEG00005006	blue	FB2	Autosome		0.458280221403487	0.436366073897109	**0.594610120139531**	-0.136329898736044	0.0219141475063774	-0.143078004491043
ENSMSEG00005016	blue	FB2	Autosome		0.505911142607731	0.443122184485977	**0.593595804376944**	-0.087684661769213	0.0627889581217542	-0.144020045994694
ENSMSEG00005016	blue	FB2	Autosome	Atp13a5	0.018989583917989	0.562599303577891	**0.70780033817764**	**-0.688810754259651**	-0.543609719659902	-0.145201034599749
ENSMSEG00005022	blue	FB2	Autosome	Gpr158	0.497428371664101	0.52157360476901	**0.669787309714652**	-0.172358938050551	-0.0241452331049088	-0.148213704945642
ENSMSEG00005016(	blue	FB2	Autosome		**0.614797412569197**	**1.96269179919934**	**2.49028915832104**	**-1.87549174575185**	**-1.34789438663014**	-0.150473619890967
ENSMSEG00005002	blue	FB2	Autosome	Nrcam	0.490895107248468	0.447518433075381	**0.598609419478215**	-0.107714312229747	0.0433766741730878	-0.151090986402834
ENSMSEG00005017	blue	FB2	Autosome		**0.843404748070083**	**0.912975010009761**	**0.962051750931143**	-0.118647002861059	-0.0695702619396773	-0.151773958374088
ENSMSEG00005011	blue	FB2	Autosome	Fut9	0.349626501681423	0.468332027040217	**0.623099159624744**	-0.273472657943322	-0.118705525358795	-0.154767132584527
ENSMSEG00005012	blue	FB2	Autosome	Asxl3	0.484942931673414	0.489320221563754	**0.644159860782135**	-0.159216929108721	-0.00437728989033926	-0.154839639218382
ENSMSEG00005002	blue	FB2	Autosome		0.0830338549691572	0.206525254300575	**0.658183676834033**	-0.575149821864876	-0.123491399331418	-0.158244046242421
ENSMSEG00005012	blue	FB2	Autosome	Nfat5	0.385541237820673	0.498205178033588	**0.656810814588219**	-0.271269576767546	-0.112663940212915	-0.15860563655463
ENSMSEG00005003	blue	FB2	Autosome	Limch1	0.385342170544698	0.518173399537298	**0.677391241748324**	-0.292049071203626	-0.1328312289926	-0.159217842211026
ENSMSEG00005017	blue	FB2	Autosome	Nfib	0.376988943245049	0.455425719933552	**0.615566478636842**	-0.238577535391794	-0.0784367766885038	-0.16014075870329
ENSMSEG00005008	blue	FB2	Autosome	Usf3	0.347722932056603	0.435279564581747	**0.596304883164111**	-0.248581951107508	-0.0875566325251435	-0.161025318582364
ENSMSEG00005003	blue	FB2	Autosome	Csmd3	**0.703369168356625**	**0.600369929997638**	**0.765800970335439**	-0.0624318019788139	0.102999238358987	-0.165431040337801
ENSMSEG00005007	blue	FB2	Autosome	Phc3	**0.625601032130771**	0.51933265893538	**0.686949865805897**	-0.0613488336751256	0.106268373195392	-0.167617206870517
ENSMSEG00005021	blue	FB2	Autosome	Fnip2	0.37081949969169	0.446487495181634	**0.622497548711216**	-0.251678049019527	-0.0756679954899445	-0.176010053529582
ENSMSEG00005013	blue	FB2	Autosome	Trrap	0.363896406087346	0.422778728974048	**0.598963384789617**	-0.235066978702272	-0.0588823228867027	-0.176184655815569
ENSMSEG00005006	blue	FB2	Autosome	Nwd2	0.408712590472718	0.576018663802136	**0.754313341195522**	-0.345600750722804	-0.167306073329418	-0.178294677393386
ENSMSEG00005015	blue	FB2	Autosome	Helz	0.343928846839934	0.435155553819588	**0.615138795144731**	-0.271209948304797	-0.0912267069796541	-0.179983241325143
ENSMSEG00005022	blue	FB2	Autosome	Med13	0.359626149005068	0.438626795080325	**0.62199482719118**	-0.262368678186112	-0.0790006460752569	-0.183368032110855
ENSMSEG00005009	blue	FB2	Autosome	Tnrc6b	0.454236104662485	0.540160422796745	**0.723761019209549**	-0.269524914547064	-0.0859243181342594	-0.183600596412805
ENSMSEG00005000(	blue	FB2	Autosome	Thsd7a	**0.638115581228173**	**0.720950436634347**	**0.906225073913239**	-0.268109492685067	-0.082834855406174	-0.185274637278893
ENSMSEG00005012(	blue	FB2	Autosome	Pclo	0.498034894290164	**0.769421924348193**	**0.958375248553855**	-0.460340354263691	-0.271387030058028	-0.188953324205663
ENSMSEG00005008(	blue	FB2	Autosome	Lrp1	0.486572441619996	**0.759779090272435**	**0.949695941535208**	-0.463123499915212	-0.273206648652439	-0.189916851262773
ENSMSEG00005021	blue	FB2	Autosome	Nos1	0.482517687361304	0.426507436677444	**0.618114236309825**	-0.135596548948521	0.0560102506838595	-0.191606799632381
ENSMSEG00005000(	blue	FB2	Autosome	Tenm3	0.521010767602759	0.542048620859017	**0.742692477636702**	-0.221681710033944	-0.0210378532562588	-0.200643856777685
ENSMSEG00005002(	blue	FB2	Autosome	Chrm2	0.452722851569041	0.407004460189633	**0.611344444617121**	-0.15862159304808	0.0457183913794083	-0.204339984427488
ENSMSEG00005019	blue	FB2	Autosome	Eml5	**0.615203035879807**	0.48563495716915	**0.691248455638108**	-0.0760454197583013	0.129568078710657	-0.205613498468958
ENSMSEG00005009	blue	FB2	Autosome	Gprin3	**0.649580616653263**	**0.658957496042241**	**0.864613297162027**	-0.215032680508763	-0.00937687938897805	-0.205655801119785
ENSMSEG00005001	blue	FB2	Autosome	Cacna1e	0.407652502308967	0.565545626165081	**0.774432402255756**	-0.366779899946789	-0.157893123856114	-0.208886776090675
ENSMSEG00005013	blue	FB2	Autosome	Map1b	0.481290734474503	0.443517974163127	**0.661442963768214**	-0.180152229293711	0.037772760311376	-0.217924989605087
ENSMSEG00005001(	blue	FB2	Autosome	Tbc1d32	**0.589162726912306**	0.468919019258021	**0.688477253942496**	-0.0993145270301902	0.120243707654286	-0.219558234684476
ENSMSEG00005003(	blue	FB2	Autosome	Cdh6	0.271593063663735	0.454854930734246	**0.674603250165322**	-0.403010186501587	-0.183261867070511	-0.219748319431075
ENSMSEG00005017	blue	FB2	Autosome	Fat1	0.340455886085511	0.494223566264199	**0.742883244028962**	-0.402427357943451	-0.153767680178688	-0.248659677764763
ENSMSEG00005017(	blue	FB2	Autosome	Cpd	**0.619386001052189**	0.443647716090634	**0.698555785050723**	-0.0791697839985345	0.175738284961555	-0.254908068960089

ENSMSEG00005013[illegible]	blue	FB2	Autosome	Erich3	0.198064126703732	0.338706709688652	**0.593905212686851**	-0.39584108598312	-0.14064258298492	-0.2551985029982
ENSMSEG00005012[illegible]	blue	FB2	Autosome	Xkr6	0.049740913710092	**0.838311260032419**	**1.09713520930111**	**-1.04739429559102**	**-0.788570346322327**	-0.258823949268695
ENSMSEG00005010[illegible]	blue	FB2	Autosome	Lrrc55	0.562289210136811	0.41543049789345	**0.6760649525085**	-0.113775742371689	0.146858712243361	-0.26063445461505
ENSMSEG00005019[illegible]	blue	FB2	Autosome		0.385294725336382	0.466863739014913	**0.609941743505956**	-0.224647018169574	-0.0815690136785312	-0.261280416561396
ENSMSEG00005007[illegible]	blue	FB2	Autosome	Lama4	0.539313223223473	0.321559214600959	**0.585384296615483**	-0.0460710733920103	0.217754008622513	-0.263825082014524
ENSMSEG00005007[illegible]	blue	FB2	Autosome	Akap9	0.499846988370191	**0.634916796598494**	**0.902886621344087**	-0.403039632973896	-0.135069808228303	-0.267969824745594
ENSMSEG00005004[illegible]	blue	FB2	Autosome	Rest	0.550581899960257	0.479607072186577	**0.748192933375954**	-0.197611033415697	0.0709748277736798	-0.268585861189377
ENSMSEG00005013[illegible]	blue	FB2	Autosome	Myh11	0.273815774594436	0.317013350338562	**0.590153345200976**	-0.316337570606539	-0.0431975757441254	-0.273139994862414
ENSMSEG00005015[illegible]	blue	FB2	Autosome	Pcdhb16	**0.6952493814423**	**0.767386572535713**	**1.04521879701383**	-0.349969415571525	-0.072137191093413	-0.277832224478112
ENSMSEG00005016[illegible]	blue	FB2	Autosome	Tbck	0.543450636131785	0.362963916388141	**0.640936859537356**	-0.0974862234055715	0.180486719743644	-0.277972943149216
ENSMSEG00005007[illegible]	blue	FB2	Autosome	Kdr	0.46844017604011	0.387753488380885	**0.667337056534164**	-0.198896880494053	0.0806866876592248	-0.279583568153278
ENSMSEG00005014[illegible]	blue	FB2	Autosome	Cacna1c	0.484869611943112	0.539876763828002	**0.819789706741799**	-0.334920094798687	-0.0550071518848899	-0.279912942913797
ENSMSEG00005000[illegible]	blue	FB2	Autosome	Cnot6l	**0.732556666820354**	**0.725068735142858**	**1.01122309649282**	-0.278666429672463	0.00748793167749536	-0.286154361349958
ENSMSEG00005020[illegible]	blue	FB2	Autosome	Kcnh7	0.425614264614204	0.546178037063832	**0.833656114397103**	-0.4080418497829	-0.120563772449629	-0.287478077333271
ENSMSEG00005005[illegible]	blue	FB2	Autosome	Zswim6	0.447241623019628	0.342308414382898	**0.632258924984953**	-0.185017301965325	0.10493320863673	-0.289950510602055
ENSMSEG00005017[illegible]	blue	FB2	Autosome	Cd93	0.307077131489229	0.411379964362847	**0.701678917448363**	-0.394601785959134	-0.104302832873618	-0.290298953085516
ENSMSEG00005017[illegible]	blue	FB2	Autosome	Ryr2	0.473370220104567	0.430635979299895	**0.721319653459897**	-0.247949433355331	0.0427342408046721	-0.290683674160003
ENSMSEG00005019[illegible]	blue	FB2	Autosome	Kcnh5	0.290389203910252	0.419666454645875	**0.714645013275313**	-0.424255809365061	-0.129277250735624	-0.294978558629437
ENSMSEG00005007[illegible]	blue	FB2	Autosome		0.303952847963686	0.503476531084175	**0.814219413410673**	-0.510266565446987	-0.199523683120489	-0.310742882326498
ENSMSEG00005006[illegible]	blue	FB2	Autosome	Cspg4b	**0.630474418301954**	0.563213815495553	**0.883491384919946**	-0.253016966617992	0.0672606028064017	-0.320277569424394
ENSMSEG00005015[illegible]	blue	FB2	Autosome	Igsf10	0.451649481498451	0.515753321195458	**0.837122503852364**	-0.385473022353913	-0.0641038396970075	-0.321369182656905
ENSMSEG00005004[illegible]	blue	FB2	Autosome		**0.642128558088558**	**0.728682213436325**	**0.989962629997721**	-0.347834071909163	-0.0865536553477669	-0.331837511618115
ENSMSEG00005005[illegible]	blue	FB2	Autosome	Lmln	0.290236579661552	0.348808942362769	**0.681417127194734**	-0.391180547533182	-0.0585723627012173	-0.332608184831965
ENSMSEG00005016[illegible]	blue	FB2	Autosome	Grin2b	0.341195655570234	0.554136876144073	**0.902451667307567**	-0.561256011737333	-0.212941220573839	-0.348314791163494
ENSMSEG00005006[illegible]	blue	FB2	Autosome	Il17rd	**0.952836477463941**	**0.974312502462602**	**1.32301094786931**	-0.370174470405369	-0.0214760249986615	-0.348698445406708
ENSMSEG00005005[illegible]	blue	FB2	Autosome	Bmp3	**0.742034847093695**	**0.627445093746468**	**0.976794620099618**	-0.234759773005923	0.114589753347227	-0.34934952635315
ENSMSEG00005002[illegible]	blue	FB2	Autosome	Xkr4	0.533560639795596	0.396429899327255	**0.775077194935378**	-0.241516555139782	0.13713074046834	-0.378647295608122
ENSMSEG00005021[illegible]	blue	FB2	Autosome	Gpld1	0.24881489215377	0.389756366372122	**0.791399022854049**	-0.542584130700279	-0.140941474218352	-0.401642656481927
ENSMSEG00005020[illegible]	blue	FB2	Autosome	Itga4	0.390359723687444	**0.793768940700256**	**1.22641527421664**	**-0.836055550529199**	-0.403409217012812	-0.432646333516387
ENSMSEG00005021[illegible]	blue	FB2	Autosome		0.471239897339478	0.504085533228443	**0.648105579223137**	-0.17686568188366	-0.0328456358889654	-0.451658422533458
ENSMSEG00005014[illegible]	blue	FB2	Autosome	Lpp	**0.644845994580693**	**0.595687451920764**	**1.05690085570736**	-0.412054861126662	0.0491585426599294	-0.461213403786592
ENSMSEG00005009[illegible]	blue	FB2	Autosome	Rnf213	0.134532145249979	0.318976945876211	**0.793877977254179**	**-0.6593458320042**	-0.184444800626232	-0.474901031377967
ENSMSEG00005008[illegible]	blue	FB2	Autosome	Egflam	0.348043075472295	0.126920760256181	**0.607408054906611**	-0.259364979434316	0.221122315216114	-0.48048729465043
ENSMSEG00005008[illegible]	blue	FB2	Autosome	Fat2	0.170713557968794	0.136363565143724	**0.634673601601649**	-0.463960043632855	0.0343499928250704	-0.498310036457925
ENSMSEG00005019[illegible]	blue	FB2	Autosome	Reln	0.293685848638043	0.297223623368705	**0.800221385297268**	-0.506535536659225	-0.00353777473066195	-0.502997761928563
ENSMSEG00005000[illegible]	blue	FB2	Autosome	Fam184b	0.570341125338868	0.352224633027819	**0.859351388147679**	-0.289010262808811	0.218116492311049	-0.50712675511986
ENSMSEG00005001[illegible]	blue	FB2	Autosome		0.23223367686726	**0.926823733362752**	**0.904208749824238**	**-0.671975072956978**	**-0.694590056495493**	-0.527597359121703
ENSMSEG00005021[illegible]	blue	FB2	Autosome	Ifih1	-0.13367884458415	0.28993223848798	**0.846826177158555**	**-0.980505021742705**	-0.42361108307213	-0.556893938670575
ENSMSEG00005012[illegible]	blue	FB2	Autosome	Parp14	-0.0546981395531284	0.382376593821867	**0.984550844103257**	**-1.03924898365639**	-0.437074733374996	**-0.60217425028139**
ENSMSEG00005016[illegible]	blue	FB2	Autosome	Ubxn8	**0.620113707031447**	0.152160087482024	**0.762770285813531**	-0.142656578782084	0.467953619549423	**-0.610610198331506**
ENSMSEG00005014[illegible]	blue	FB2	Autosome		**1.06075919555168**	**0.927332990705612**	**1.06901887818431**	-0.00825968263262715	0.133426204846068	**-0.745741324307352**
ENSMSEG00005000[illegible]	blue	FB2	Autosome	Matn4	-0.093687545663377	0.107878009368941	**0.882943547104619**	**-0.976631092767996**	-0.201565555032318	**-0.775065537735678**
ENSMSEG00005012[illegible]	blue	FB2	Autosome	Lamc2	**0.740018543278857**	-0.0223109598299912	**1.04618913890575**	-0.306170595626892	**0.762329503108848**	**-1.06850009873574**
ENSMSEG00005007[illegible]	blue	FB2	Autosome	Fmn1	**0.597824110461505**	**0.660884099229154**	**0.659652033521215**	-0.0618279230597102	-0.0630599887676495	0.00123206570793937
ENSMSEG00005003[illegible]	blue	FB2	Autosome	Dgkb	**0.601001302361776**	0.521238435621595	0.50963592178733	0.0913653805744461	0.0797628667401808	0.0116025138342654
ENSMSEG00005009[illegible]	blue	FB2	Autosome	Brca2	0.288233158460993	**0.630636155331841**	**0.614773546390187**	-0.326540387929194	-0.342402996870848	0.0158626089416533
ENSMSEG00005014[illegible]	blue	FB2	Autosome		0.437854276099647	0.45866230882198	**0.592233540893266**	-0.154379264793619	-0.0208080327223327	0.0226149835385145

ENSMSEG00005012[illegible]	blue	FB2	Autosome	Fryl	**0.688979124784181**	**0.622759252042942**	**0.598298674448949**	0.0906804503352321	0.066219872741239	0.0244605775939931
ENSMSEG00005004[illegible]	blue	FB2	Autosome	Tnik	**0.587825034901362**	**0.598447167637388**	0.568725246910354	0.0190997879910081	-0.0106221327360254	0.0297219207270334
ENSMSEG00005003[illegible]	blue	FB2	Autosome	Trhde	0.534322719285844	**0.668858114403477**	**0.633581010412051**	-0.0992582911262069	-0.134535395117633	0.0352771039914261
ENSMSEG00005003[illegible]	blue	FB2	Autosome	Tnrc6c	**0.680659234368809**	**0.588599976936395**	0.551286993286673	0.129372241082136	0.0920592574324142	0.0373129836497223
ENSMSEG00005012[illegible]	blue	FB2	Autosome	Grik3	**0.611224897493991**	0.537656882027	0.499940826705449	0.111284070788542	0.0735680154669906	0.0377160553215515
ENSMSEG00005010[illegible]	blue	FB2	Autosome	Hic2	0.565537783208635	**0.774575275156174**	**0.73398995151356**	-0.168452168304925	-0.209037491947539	0.0405853236426142
ENSMSEG00005015[illegible]	blue	FB2	Autosome	Rictor	**0.699646819271841**	**0.755064438398541**	**0.712968452812925**	-0.0133216335410839	-0.0554176191266998	0.0420959855856159
ENSMSEG00005016[illegible]	blue	FB2	Autosome	Hecw1	0.521954359269276	**0.620020922639872**	0.559258258514277	-0.0373038992450005	-0.0980665633705957	0.0607626641255952
ENSMSEG00005006[illegible]	blue	FB2	Autosome	Fbn1	**0.605706550727362**	**0.618810392380482**	0.557148236977853	0.0485583137495096	-0.0131038416531199	0.0616621554026295
ENSMSEG00005011[illegible]	blue	FB2	Autosome	Hgf	0.507436415225662	**0.745212354179131**	**0.676110569544508**	-0.168674154318846	-0.237775938953469	0.0691017846346224
ENSMSEG00005007[illegible]	blue	FB2	Autosome	Nyap2	**0.702112860564805**	**0.769247761395831**	**0.695479890446966**	0.00663297011783904	-0.0671349008310264	0.0737678709488654
ENSMSEG00005022[illegible]	blue	FB2	Autosome	Oprm1	**0.928009133666879**	**1.03579629093513**	**0.960933418046546**	-0.0329242843796665	-0.107787157268249	0.074862872888583
ENSMSEG00005006[illegible]	blue	FB2	Autosome	Trps1	0.364915392525154	**0.652353238773542**	0.537496300136669	-0.172580907611515	-0.287437846248389	0.114856938636874
ENSMSEG00005003[illegible]	blue	FB2	Autosome		0.401743085202268	0.466351166634388	**0.618125125008475**	-0.216382039806208	-0.0646080814321199	0.189933087654609
ENSMSEG00005016[illegible]	blue	FB2	Autosome	Cdh9	0.58441977164406	**0.743028556784767**	0.545175825344471	0.039243946299589	-0.158608785140707	0.197852731440296
ENSMSEG00005010[illegible]	blue	FB2	Autosome	Igfn1	-0.310407510849435	**0.968982424936952**	**0.604172410996899**	**-0.914579921846334**	**-1.27938993578639**	0.364810013940053
ENSMSEG00005021[illegible]	blue	FB2	Autosome	Gbgt1	-0.118005568614236	**0.66644967855807**	0.240756918720996	-0.358762487335232	**-0.784455247172306**	0.425692759837074
ENSMSEG00005012[illegible]	blue	FB2	chr1 (NR)		-0.149047379405787	0.325507907177449	0.437562508892764	**-0.586609888298551**	-0.474555286583236	-0.112054601715315
ENSMSEG00005022[illegible]	blue	FB2	chr1 (NR)	Zfp619	-0.0439445627635908	0.0695457254585816	0.541964789144657	**-0.585909351908248**	-0.113490288222172	-0.472419063686076
ENSMSEG00005010[illegible]	blue	FB2	chr1 (NR)	Zfp940	-0.103618971447914	0.565957264518415	0.478478420303178	-0.582097391751092	**-0.669576235966329**	0.0874788442152367
ENSMSEG00005018[illegible]	blue	FB2	chr1 (NR)		0.336024751798676	**0.934295994519137**	0.561928682494495	-0.225903930695819	**-0.598271242720461**	0.372367312024642
ENSMSEG00005007[illegible]	blue	FB2	chr1 (NR)	Fut2	0.248314477795521	**2.52995776986895**	**1.95264370771218**	**-1.70432922991665**	**-2.28164329207342**	0.57731406215677
ENSMSEG00005002[illegible]	blue	FB2	chr13 (NR)	Vwa5a	0.130429375017309	**0.734809554741383**	0.583090502602113	-0.452661127584804	**-0.604380179724074**	0.15171905213927
ENSMSEG00005018[illegible]	blue	FB2	X/X* (R)	Tenm1	0.317744842136857	0.431807507642453	**0.636645923854463**	-0.318901081717606	-0.114062665505596	-0.204838416212011
ENSMSEG00005019[illegible]	blue	FB2	X/X* (R)	Pak3	**0.588891041252271**	0.538872446724073	0.476302072488089	0.112588968764181	0.0500185945281971	0.062570374235984
ENSMSEG00005017[illegible]	blue	FB2	chr1 (R)	Tenm4	0.531064288046651	0.481848162815234	**0.616779741906066**	-0.0857154538594147	0.0492161252314174	-0.134931579090832
ENSMSEG00005016[illegible]	blue	FB2	chr1 (R)	Zfp871	0.357274591565503	0.408310030036596	**0.630427007389445**	-0.273152415823942	-0.0510354384710928	-0.22211697735285
ENSMSEG00005010[illegible]	blue	FB2	chr1 (R)		**0.629355083048531**	0.417690573917449	**0.741288780297411**	-0.11193369724888	0.211664509131083	-0.323598206379962
ENSMSEG00005016[illegible]	blue	FB2	chr1 (R)	Slc8a1	**0.606656456276364**	0.454397668188096	**0.794167865607433**	-0.187511409331069	0.152258788088269	-0.339770197419337
ENSMSEG00005001[illegible]	blue	FB2	chr1 (R)	Pgm2l1	0.448880183016287	**0.596937960221753**	0.437470537726832	0.0114096452894552	-0.148057777205466	0.159467422494921
ENSMSEG00005012[illegible]	blue	FB2	chr13 (R)	Fam76b	0.549051407612539	**0.637280054616304**	**0.646891383532858**	-0.0978399759203192	-0.0882286470037653	-0.00961132891655394
ENSMSEG00005013[illegible]	blue	FB2	chr13 (R)	Zc3h12c	**0.649652958278657**	**0.645300723922807**	**0.701328188636583**	-0.0516752303579256	0.00435223435585081	-0.0560274647137764
ENSMSEG00005011[illegible]	blue	FB2	chr13 (R)	Phip	0.505071678178805	**0.6147425697196**	**0.73272761957397**	-0.227655941395165	-0.109670891540796	-0.11798504985437
ENSMSEG00005001[illegible]	blue	FB2	chr13 (R)	Rfx7	0.447904742863822	0.450654888594658	**0.632596682231829**	-0.184691939368006	-0.00275014573083611	-0.18194179363717
ENSMSEG00005005[illegible]	blue	FB2	chr13 (R)	Ctdspl	**0.752202683840194**	0.521056236649178	**0.714220297172276**	0.0379823866679187	0.231146447191016	-0.193164060523097
ENSMSEG00005016[illegible]	blue	FB2	chr13 (R)	Xrn1	0.481755039777742	0.489024881859627	**0.776767454032395**	-0.295012414254653	-0.00726984208188522	-0.287742572172768
ENSMSEG00005018[illegible]	blue	FB2	chr13 (R)	Rplp1	**-1.13536295466555**	**1.58080709802881**	**1.89845575942272**	**-3.03381871408827**	**-2.71617005269436**	-0.317648661393909
ENSMSEG00005005[illegible]	blue	FB2	chr13 (R)		**1.07762357200879**	**0.662218409066801**	**1.04030502913517**	0.0373185428736296	0.415405162941994	-0.378086620068364
ENSMSEG00005011[illegible]	blue	FB2	chr13 (R)	Cyp11a1	0.0423599946725588	0.383929166067457	**1.14095284356507**	**-1.09859284889251**	-0.341569171394899	**-0.75702367749761**
ENSMSEG00005018[illegible]	blue	FB2	X/X* (NR)		**1.25757452003898**	**2.42857240134659**	**3.581081287791**	**-2.32350676775202**	**-1.17099788130761**	-0.0905997580270357
ENSMSEG00005000[illegible]	blue	FB2	X/X* (NR)	Usp9x	0.430414733930195	0.475704232757822	**0.624314010505106**	-0.193899276574911	-0.0452894988276265	-0.148609777747284
ENSMSEG00005023[illegible]	blue	FB2	X/X* (NR)	Nlgn3	0.545471262984101	0.565985104293374	**0.724685462023707**	-0.179214199039606	-0.0205138413092729	-0.158700357730333
ENSMSEG00005018[illegible]	blue	FB2	X/X* (NR)	Huwe1	0.329687838152585	0.36814072478793	**0.620169742095827**	-0.290481903943242	-0.0384528866353454	-0.252029017307896
ENSMSEG00005023[illegible]	blue	FB2	X/X* (NR)	Adgrg2	0.0100271095458908	0.356263094600601	**0.615419909508562**	**-0.605392799962671**	-0.34623598505471	-0.259156814907961
ENSMSEG00005023[illegible]	blue	FB2	X/X* (NR)	Nhsl2	0.405137901687297	0.34822278883869	**0.638862897895989**	-0.233724996208692	0.0569151128486067	-0.290640109057299
ENSMSEG00005022[illegible]	blue	FB2	X/X* (NR)		0.415212084318275	0.521780376852827	**0.612380134879863**	-0.197168050561588	-0.106568292534552	-0.301020332256488
ENSMSEG00005006[illegible]	blue	FB2	X/X* (NR)	Atrx	0.563641723967242	0.530469388438458	**0.926285198401663**	-0.362643474434421	0.0331723355287838	-0.395815809963205

ENSMSEG00005023[blue	FB2	X/X* (NR)	Piga	0.149828194403547	0.391581489535522	**0.884047851849085**	**-0.734219657445538**	-0.241753295131975	-0.492466362313564
ENSMSEG00005010[blue	FB2	X/X* (NR)	Cybb	0.138927006897249	**1.10555776405959**	**1.67325386134467**	**-1.53432685444742**	**-0.966630757162342**	-0.567696097285082
ENSMSEG00005023[blue	FB2	X/X* (NR)		0.520186818949279	**0.714798711528193**	0.545635702700426	-0.0254488837511477	-0.194611892578914	**-1.1525088864444**
ENSMSEG00005005[blue	FB2	X/X* (NR)	Diaph2	**0.586989126133736**	**0.656386815249947**	0.540765229582777	0.0462238965509593	-0.0693976891162116	0.115621585667171
ENSMSEG00005007[blue	FB2	X/X* (NR)		0.40034581493072	0.387434513960426	**0.688454846216914**	-0.288109031286194	0.012911300970294	0.169163008827766
ENSMSEG00005014[blue	FB2	unassigned	1500009L16Ri	**0.981849328681558**	**1.46144188135512**	**1.14449079883425**	-0.16264147015269	-0.479592552673563	0.316951082520872
ENSMSEG00005012[brown	FB3	Autosome	Ror1	**0.862779290014779**	0.457008342043227	0.458408492136082	0.404370797878697	0.405770947971552	-0.00140015009285472
ENSMSEG00005000[brown	FB3	Autosome	Shh	**1.11464394853454**	**0.653854512597075**	**0.664772095613736**	0.449871852920804	0.460789435937465	-0.0109175830166612
ENSMSEG00005004[brown	FB3	Autosome	Adamtsl1	**0.720101413683007**	**0.749664371010379**	**0.764479872789917**	-0.0443784591069097	-0.029562957327372	-0.0148155017795377
ENSMSEG00005010[brown	FB3	Autosome		0.576624257351155	0.457445228575315	**0.632993430842877**	-0.0563691734917221	0.11917902877584	-0.0203360184511673
ENSMSEG00005014[brown	FB3	Autosome	Rbm20	**0.829909269133007**	**0.797080682082777**	**0.82476058992983**	0.00514867920317751	0.0328285870502302	-0.0276799078470526
ENSMSEG00005020[brown	FB3	Autosome	Tet3	**0.704491807194513**	**0.585016707799564**	**0.617178170168644**	0.0873136370258694	0.119475099394949	-0.0321614623690801
ENSMSEG00005000[brown	FB3	Autosome	Arl5b	**0.984050286354167**	**0.884574906573319**	**0.923864706268111**	0.0601855800860559	0.0994753797808477	-0.0392897996947917
ENSMSEG00005005[brown	FB3	Autosome	Heyl	**0.895556196382842**	0.476180625092158	0.52496326405586	0.370592932326982	0.419375571290684	-0.0487826389637021
ENSMSEG00005003[brown	FB3	Autosome	Tacr1	**0.819397290712702**	0.421668606364184	0.475673053298769	0.343724237413933	0.397728684348518	-0.0540044469345848
ENSMSEG00005011[brown	FB3	Autosome	Zfp462	**0.595616375394438**	0.481453545090316	0.535966657811731	0.0596497175827071	0.114162830304122	-0.0545131127214148
ENSMSEG00005003[brown	FB3	Autosome	Ogfod1	**0.640956643743468**	0.347184030826962	0.402234000079473	0.238722643663995	0.293772612916505	-0.0550499692525105
ENSMSEG00005008[brown	FB3	Autosome	Xkr7	**0.836537322980594**	0.455838066592133	0.513802861556245	0.322734461424348	0.380699256388461	-0.0579647949641124
ENSMSEG00005005[brown	FB3	Autosome	Ppid	**1.71519878694428**	-0.0490199978621 52	0.0126007132038748	**1.70259807374041**	**1.76421878480643**	-0.0616207110660269
ENSMSEG00005007[brown	FB3	Autosome	Sema6a	**0.612120259673986**	0.383767737430441	0.448011032929448	0.164109226744537	0.228352522243544	-0.0642432954990068
ENSMSEG00005010[brown	FB3	Autosome	Ppargc1b	**0.693575862364321**	0.581760187940808	**0.647632415397194**	0.0459434469671273	0.111815674423513	-0.0658722274563856
ENSMSEG00005000[brown	FB3	Autosome	Gpr158	**0.706416338103344**	**0.65358065615675**	**0.723760591387388**	-0.0173442532840439	0.0528356819465949	-0.0701799352306389
ENSMSEG00005010[brown	FB3	Autosome	Nid2	**0.976723524537145**	**0.768286281084097**	**0.841222192777902**	0.135501331759244	0.208437243453049	-0.0729359116938048
ENSMSEG00005009[brown	FB3	Autosome	Cacna1i	**0.710625750074981**	**0.607559080346662**	**0.681922252709379**	0.0287034973656016	0.103066669728318	-0.0743631723627168
ENSMSEG00005022[brown	FB3	Autosome	Card11	**1.05431772311371**	0.489570057914277	0.564840566869619	0.489477156244094	0.564747665199436	-0.0752705089553417
ENSMSEG00005014[brown	FB3	Autosome	Tiam1	**0.58529990744125**	0.354263253809741	0.429964367141481	0.155335540299769	0.231036653631509	-0.0757011133317394
ENSMSEG00005022[brown	FB3	Autosome	Lingo4	**0.913142745339937**	**0.828283477797882**	**0.907396912790773**	0.00574583254916387	0.0848592675420551	-0.0791134349928912
ENSMSEG00005015[brown	FB3	Autosome	Nfasc	**0.655674846364548**	0.448695414349994	0.553488414797994	0.102186431566554	0.206979432014554	-0.104793000448
ENSMSEG00005004[brown	FB3	Autosome	Ncan	**0.805332012770062**	**0.607645895682364**	**0.71686493749278**	0.0884670752772828	0.197686117087699	-0.109219041810416
ENSMSEG00005020[brown	FB3	Autosome	Pcdh17	**0.612899904517226**	0.479858176716845	**0.589215330213862**	0.0236845743033643	0.133041727800381	-0.109357153497016
ENSMSEG00005002[brown	FB3	Autosome	Srgap1	**0.610696525685261**	0.437111964523695	0.547210777109896	0.0634857485753648	0.173584561161565	-0.110098812586201
ENSMSEG00005018[brown	FB3	Autosome	Spry4	**1.11600670093257**	**0.673646308210369**	**0.797135887208377**	0.318870813724192	0.442360392722199	-0.123489578998008
ENSMSEG00005018[brown	FB3	Autosome	Npas4	**2.42361266108951**	**1.35224778480388**	**1.48171016269881**	**0.941902498390704**	**1.07136487628564**	-0.129462377894932
ENSMSEG00005010[brown	FB3	Autosome	Peg10	**0.73010023391301**	**0.600087627855004**	0.559884117299068	0.170216116613942	0.130012606058006	-0.136906065415207
ENSMSEG00005000[brown	FB3	Autosome	Fras1	**0.594020032523956**	0.422998346794938	0.562689604789112	0.0313304277348438	0.171021685729018	-0.139691257994174
ENSMSEG00005012[brown	FB3	Autosome	Dsp	**1.56922013386417**	**0.826121688204543**	**0.96733605675013**	**0.601884077114045**	**0.743098445659632**	-0.141214368545587
ENSMSEG00005010[brown	FB3	Autosome	Traf6	**0.663710473667324**	0.234358378732264	0.386562085620343	0.277148388046982	0.429352094935061	-0.152203706888079
ENSMSEG00005015[brown	FB3	Autosome		**0.635693958133761**	0.520361553642191	0.434089213236438	0.201604744897323	0.11533240449157	-0.163940745176818
ENSMSEG00005020[brown	FB3	Autosome		**0.72416074109633**	**0.669575450698888**	0.577459738871843	0.146701002224487	0.0545852903974419	-0.166992828941494
ENSMSEG00005001[brown	FB3	Autosome	Kcnk13	**1.73101256218121**	**1.02412615529902**	**1.19809128925373**	0.532921272927482	**0.706886406882193**	-0.173965133954711
ENSMSEG00005014[brown	FB3	Autosome		0.568635111394024	0.468119949542909	**0.632060694719727**	-0.063425583325703	0.100515161851115	-0.175548202267562
ENSMSEG00005017[brown	FB3	Autosome	Trib1	**0.75103455538998**	0.276833691192307	0.459604517582041	0.291430037807939	0.474200864197674	-0.182770826389734
ENSMSEG00005020[brown	FB3	Autosome	Plagl1	**0.657140900414085**	0.513537860893681	**0.700135175499885**	-0.0429942750858008	0.143603039520403	-0.186597314606204
ENSMSEG00005011[brown	FB3	Autosome	Tmem245	**0.606840131408849**	0.491456385716143	**0.699088855224007**	-0.0922487238151581	0.115383745692705	-0.207632469507864
ENSMSEG00005015[brown	FB3	Autosome		**1.50109453899135**	**1.02073506907832**	**0.679872921887314**	**0.821221617104034**	0.480359469913031	-0.217337848091529
ENSMSEG00005013[brown	FB3	Autosome	Syn3	**0.808779585707919**	0.338820037319284	0.565996313007059	0.242783272700861	0.469959548388635	-0.227176275687775
ENSMSEG00005005[brown	FB3	Autosome	Slc4a8	**0.690722193079304**	0.286086175583708	0.514589571725274	0.176132621354031	0.404636017495596	-0.228503396141566

ENSMSEG00005006	brown	FB3	Autosome	Notch2	0.557187094541867	0.436232732518719	**0.667606016952001**	-0.110418922410134	0.120954362023147	-0.231373284433282
ENSMSEG00005017	brown	FB3	Autosome	Kcnn3	**0.585890706048345**	0.355327410302177	**0.592744204483845**	-0.00685349843549947	0.230563295746168	-0.237416794181667
ENSMSEG00005012	brown	FB3	Autosome	Niban1	**1.28263959406902**	**0.841212879800711**	**1.09145647708439**	0.191183116984626	0.441426714268305	-0.250243597283679
ENSMSEG00005012	brown	FB3	Autosome	Lamc1	0.472955626390802	0.302078476400376	**0.606490467843109**	-0.133534841452307	0.170877149990426	-0.304411991442733
ENSMSEG00005000	brown	FB3	Autosome		**0.60864386760405**	0.558279279438997	0.483802090123833	0.124841777480218	0.0503645881650527	-0.404908892849556
ENSMSEG00005010	brown	FB3	Autosome	Susd1	**1.02787431704973**	0.356143465476892	**0.930891624982579**	0.0969826920671489	**0.671730851572835**	-0.574748159505686
ENSMSEG00005002	brown	FB3	Autosome	Ankrd52	**0.683509589608403**	0.369063080083496	0.35815041535518	0.325359174253223	0.314446509524906	0.0109126647283166
ENSMSEG00005010	brown	FB3	Autosome	Mfhas1	**0.611182734706567**	0.437832784881633	0.426568794773869	0.184613939932698	0.173349949824934	0.0112639901077641
ENSMSEG00005014	brown	FB3	Autosome		**0.650630749302043**	0.44221728175912	0.462553300210287	0.188077449091755	0.208413467542923	0.0127710914985
ENSMSEG00005010	brown	FB3	Autosome	Aldh1b1	**1.18603598403558**	0.285606525945932	0.272811629803252	**0.913224354232327**	**0.900429458089647**	0.01279489614268
ENSMSEG00005008	brown	FB3	Autosome	Plagl2	**0.651580921264651**	**0.64505780215149**	**0.630647307143683**	0.0209336141209676	0.00652311911316039	0.0144104950078072
ENSMSEG00005006	brown	FB3	Autosome	Bcl11b	**0.588505824165013**	0.412573544182836	0.394725675615475	0.193780148549538	0.175932279982177	0.0178478685673611
ENSMSEG00005022	brown	FB3	Autosome	Runx1t1	**0.637909601246772**	0.444791069581384	0.425720877840842	0.21218872340593	0.193118531665388	0.0190701917405422
ENSMSEG00005013	brown	FB3	Autosome	Midn	**0.64979494965748**	0.248817481658823	0.229367731966154	0.420427217691326	0.400977467998657	0.019449749692669
ENSMSEG00005001	brown	FB3	Autosome	Adam19	**0.599915993960877**	0.300382112580484	0.2781802052192	0.321735788741677	0.299533881380393	0.0222019073612841
ENSMSEG00005001	brown	FB3	Autosome	Svep1	**0.757490754411615**	**0.705628274867424**	**0.682053193922227**	0.0754375604893874	0.0518624795441908	0.0235750809451967
ENSMSEG00005014	brown	FB3	Autosome	Slit1	**0.698416022168162**	0.528225459741277	0.501098366711306	0.197317655456856	0.170190562426886	0.0271270930299701
ENSMSEG00005021	brown	FB3	Autosome	Tnrc18	**0.585569953609751**	0.518764885499274	0.490111401119607	0.0954585524901446	0.0668050681104767	0.0286534843796679
ENSMSEG00005005	brown	FB3	Autosome	Egr2	**1.78761781542657**	**0.991797897629493**	**0.954218515432045**	**0.833399299994528**	**0.795819917797081**	0.0375793821974478
ENSMSEG00005018	brown	FB3	Autosome		0.50652709465181	**0.651505058441149**	0.386998269185373	0.119528825466437	-0.14497796378934	0.0389630223570911
ENSMSEG00005010	brown	FB3	Autosome	Peg10	**0.677085764574126**	0.525590494709927	**0.662496560125134**	0.0145892044489921	0.151495269864199	0.0402035105559361
ENSMSEG00005017	brown	FB3	Autosome	Galr1	**1.44500045303944**	**1.08145573078402**	**1.03686768820508**	0.408132764834367	0.363544722255423	0.0445880425789435
ENSMSEG00005012	brown	FB3	Autosome	Sh3pxd2b	**0.635679885624771**	0.51404632676484	0.464522969506799	0.171156916117972	0.121633558859931	0.0495233572580409
ENSMSEG00005011	brown	FB3	Autosome	Creb3l2	**0.59182073710822**	**0.636938577251747**	**0.586660988832035**	0.00515974827618475	-0.0451178401435273	0.0502775884197121
ENSMSEG00005018	brown	FB3	Autosome	Cpeb3	**0.737074707221165**	**0.637862943138559**	0.583755640967315	0.15331906625385	0.0992117640826061	0.0541073021712438
ENSMSEG00005013	brown	FB3	Autosome	Trappc9	**0.593968470826346**	0.443876605033879	0.388043417955007	0.205925052871339	0.150091865792467	0.0558331870788725
ENSMSEG00005000	brown	FB3	Autosome	Glra1	**0.986625515290023**	**0.859370386107327**	**0.802109122189697**	0.184516393100326	0.127255129182697	0.0572612639176297
ENSMSEG00005003	brown	FB3	Autosome	Sertad2	**0.736260751538006**	**0.665825799003848**	**0.60556606971323**	0.130694681824776	0.0704349525341582	0.0602597292906177
ENSMSEG00005002	brown	FB3	Autosome		**0.598025755318084**	0.513212333757437	0.474249311400346	0.123776443917738	0.0848134215606474	0.0606294345478585
ENSMSEG00005008	brown	FB3	Autosome		0.519011560439034	0.541834002416853	**0.708826831358347**	-0.189815270919313	-0.0228224419778186	0.0744771893151649
ENSMSEG00005022	brown	FB3	Autosome	Radil	**0.701410469644806**	0.459310332123915	0.381736902821773	0.319673566823033	0.24210013752089	0.0775734293021422
ENSMSEG00005007	brown	FB3	Autosome	Mideas	**0.715571279650038**	0.520946686601351	0.441750072956072	0.273821206693966	0.194624593048687	0.0791966136452789
ENSMSEG00005005	brown	FB3	Autosome	Prr36	**0.604349186087164**	0.51278585293863	0.431861265613048	0.172487920474115	0.0915633331485342	0.0809245873255812
ENSMSEG00005013	brown	FB3	Autosome	Arc	**1.76030423155695**	**1.04587644042109**	**0.963534594634791**	**0.796769636922163**	**0.714427791135868**	0.0823418457862947
ENSMSEG00005013	brown	FB3	Autosome	Ccn1	**1.34428898479494**	**0.767769079837667**	**0.68339916308854**	**0.660889821706404**	0.576519904957277	0.0843699167491266
ENSMSEG00005021	brown	FB3	Autosome		**0.698089785405283**	0.570873868103404	0.326489011327641	0.371600774077642	0.12721591730188	0.0862723404057526
ENSMSEG00005006	brown	FB3	Autosome		**0.674685437242188**	0.310968489866472	**0.715877382716028**	-0.0411919454738401	0.363716947375716	0.0921157118270452
ENSMSEG00005009	brown	FB3	Autosome		**0.727026953914343**	**0.659260374203422**	**0.598630939655564**	0.12839601425878	0.067766579710921	0.0923391984261286
ENSMSEG00005006	brown	FB3	Autosome	Kif24	**0.79515394475944**	**0.635432931065749**	0.543000280851352	0.252153663908088	0.159721013693691	0.092432650214397
ENSMSEG00005003	brown	FB3	Autosome	Mast3	**0.650453750013249**	0.423487932107871	0.327978991111097	0.322474758902152	0.226965817905378	0.0955089409967738
ENSMSEG00005010	brown	FB3	Autosome	Ccdc177	**1.02708213015492**	**0.847040139736465**	**0.750027587714743**	0.277054542440176	0.180041990418455	0.0970125520217215
ENSMSEG00005015	brown	FB3	Autosome	Kif26a	**0.701881738776117**	0.507757317879324	0.406272799320463	0.295608939455654	0.194124420896793	0.101484518558861
ENSMSEG00005018	brown	FB3	Autosome		**0.776706494545242**	**0.808188104606**	**0.684234920681662**	0.0924715738635802	-0.0314816100607577	0.105713159188279
ENSMSEG00005015	brown	FB3	Autosome	Mbd6	**0.588740218834525**	0.371548157652707	0.265414581279878	0.323325637554647	0.217192061181818	0.106133576372829
ENSMSEG00005011	brown	FB3	Autosome	Cachd1	**0.700435720034737**	0.429326186866347	0.322760391677621	0.377675328357115	0.27110953316839	0.106565795188726
ENSMSEG00005013	brown	FB3	Autosome	Plce1	**0.818247596308665**	**0.590161054555531**	0.48278619017131	0.335461406137355	0.228086541753134	0.107374864384221
ENSMSEG00005020	brown	FB3	Autosome	Ahdc1	**0.736361230778115**	0.534268427917557	0.426227920397524	0.310133310380591	0.202092802860557	0.108040507520033

ENSMSEG00005010[illegible]	brown	FB3	Autosome	Phlda1	**0.653997103339899**	0.211358872794083	0.100839919753456	0.553157183586444	0.442638230545817	0.110518953040627
ENSMSEG00005007[illegible]	brown	FB3	Autosome	Fam222b	**0.796522695934065**	0.571854584360431	0.452865558689519	0.343657137244546	0.224668111573633	0.118989025670913
ENSMSEG00005019[illegible]	brown	FB3	Autosome	Rc3h1	**0.705615191093795**	**0.675472759218581**	0.555975685057404	0.149639506036391	0.0301424318752143	0.119497074161176
ENSMSEG00005010[illegible]	brown	FB3	Autosome	Cracd	**0.70065551042097**	0.578184099051761	0.455156444813248	0.245499065607722	0.122471411369209	0.123027654238513
ENSMSEG00005001[illegible]	brown	FB3	Autosome		**0.678484233648206**	0.436484910203419	0.33077175101514	0.347712482633066	0.241999323444787	0.123953183924338
ENSMSEG00005019[illegible]	brown	FB3	Autosome	Egr1	**1.43499697407334**	**0.776563273118611**	**0.652216929998264**	**0.782780044075079**	**0.658433700954731**	0.124346343120348
ENSMSEG00005020[illegible]	brown	FB3	Autosome	Dusp6	**0.606559975843584**	0.394534743010161	0.264806193812273	0.341753782031311	0.212025232833423	0.129728549197888
ENSMSEG00005016[illegible]	brown	FB3	Autosome	Foxp2	**0.831909963715765**	**0.740725955503762**	**0.610947655624967**	0.220962308090798	0.0911840082120034	0.129778299878795
ENSMSEG00005010[illegible]	brown	FB3	Autosome	Sh3pxd2a	**0.679418512053148**	0.535129319108136	0.405326369526141	0.274092142527006	0.144289192945012	0.129802949581994
ENSMSEG00005018[illegible]	brown	FB3	Autosome	Apc2	**0.612134452364428**	0.524159264282999	0.389005722524213	0.223128729840215	0.0879751880814292	0.135153541758786
ENSMSEG00005010[illegible]	brown	FB3	Autosome	Grm1	**0.610846567439471**	0.504664299700086	0.367760322477245	0.243086244962226	0.106182267739385	0.136903977222841
ENSMSEG00005003[illegible]	brown	FB3	Autosome	Crocc	**0.719399468104506**	0.339900409658741	0.195706408735985	0.523693059368521	0.379499058445765	0.144194000922755
ENSMSEG00005002[illegible]	brown	FB3	Autosome	Grip1	**0.816463387301527**	0.519113113370684	0.37166388946881	0.444799497832717	0.297350273930843	0.147449223901874
ENSMSEG00005002[illegible]	brown	FB3	Autosome	Sobp	**0.626610394128411**	0.54499881594297	0.394061303667804	0.232549090460607	0.0816115781854414	0.150937512275165
ENSMSEG00005008[illegible]	brown	FB3	Autosome		**0.684805464830711**	**0.628897463570416**	0.536558265144287	0.148247199686424	0.0559080012602951	0.152130200203626
ENSMSEG00005009[illegible]	brown	FB3	Autosome	Col1a1	**1.46421485229294**	**0.95933019233431**	**0.806066756083695**	**0.658148096209241**	0.504884659958627	0.153263436250615
ENSMSEG00005015[illegible]	brown	FB3	Autosome	Inf2	**0.617387755889311**	0.376828742658899	0.214849585989865	0.402538169899447	0.240559013230412	0.161979156669034
ENSMSEG00005009[illegible]	brown	FB3	Autosome	Pld5	**0.605732014344831**	0.342598450857597	0.178753899659529	0.426978114685301	0.263133563487234	0.163844551198067
ENSMSEG00005020[illegible]	brown	FB3	Autosome	Sfmbt2	**0.834403010110336**	**0.770132175644015**	**0.603808243940694**	0.230594766169641	0.0642708344663202	0.166323931703321
ENSMSEG00005001[illegible]	brown	FB3	Autosome	Sox9	**0.978019686920548**	**0.692986350104451**	0.523951390529008	0.454068296391541	0.285033336816097	0.169034959575443
ENSMSEG00005022[illegible]	brown	FB3	Autosome	Fam222a	**0.674231681760409**	0.366158957190674	0.184830305396513	0.489401376363896	0.308072724569735	0.181328651794161
ENSMSEG00005015[illegible]	brown	FB3	Autosome	Klf5	**0.716675762511952**	**0.593342843218328**	0.411128153304119	0.305547609207833	0.123332919293624	0.182214689914208
ENSMSEG00005009[illegible]	brown	FB3	Autosome	Htr4	**0.807392805587048**	**0.691320305885705**	0.508495578162085	0.298897227424963	0.116072499701343	0.18282472772362
ENSMSEG00005012[illegible]	brown	FB3	Autosome	Nckap5l	**0.775754183760547**	0.570096770885806	0.372537699303951	0.403216484456596	0.205657412874741	0.197559071581855
ENSMSEG00005011[illegible]	brown	FB3	Autosome	Auts2	**0.796028970992712**	0.533600366523645	0.333066201159518	0.462962769833194	0.262428604469067	0.200534165364127
ENSMSEG00005006[illegible]	brown	FB3	Autosome	Inafm2	**1.10488773676714**	**0.848300978868771**	**0.645961222197832**	0.458926514569306	0.256586757898367	0.202339756670939
ENSMSEG00005017[illegible]	brown	FB3	Autosome	Arhgap26	0.568795012220771	**0.614693675639695**	0.411371459738554	0.157423552482217	-0.0458986634189235	0.20332221590114
ENSMSEG00005010[illegible]	brown	FB3	Autosome	Vash2	0.474664770241616	**0.767873023779314**	0.543819783408845	-0.0691550131672292	-0.293208253537699	0.22405324037047
ENSMSEG00005021[illegible]	brown	FB3	Autosome	Ier2	**1.51769461824772**	**0.942839629672771**	**0.713750649433952**	**0.803943968813772**	0.574854988574954	0.229088980238819
ENSMSEG00005008[illegible]	brown	FB3	Autosome	Zdhhc21	0.397336751578143	**0.663113799638067**	0.432340170455828	-0.0350034188776849	-0.265777048059924	0.230773629182239
ENSMSEG00005008[illegible]	brown	FB3	Autosome	Fstl4	**0.917481061124376**	**0.706435563691232**	0.47186476099729	0.445616300127086	0.211054497433144	0.234570802693942
ENSMSEG00005008[illegible]	brown	FB3	Autosome	Kctd12	**0.975109832269255**	**0.668262548445609**	0.432244444044592	0.542865388224664	0.306847283823647	0.236018104401017
ENSMSEG00005021[illegible]	brown	FB3	Autosome		**0.875038238000747**	0.436538993193627	**0.653876841285156**	0.221161396715591	0.43849924480712	0.244384856775763
ENSMSEG00005018[illegible]	brown	FB3	Autosome		**0.598199170672843**	0.263378671263252	0.250607579764752	0.347591590908091	0.334820499409591	0.264506789255777
ENSMSEG00005002[illegible]	brown	FB3	Autosome	Jun	**0.868088939755621**	**0.794675152018533**	0.527401566791337	0.340687372964284	0.0734137877370882	0.267273585227196
ENSMSEG00005019[illegible]	brown	FB3	Autosome	Arid3a	**0.855485168607822**	0.412893652980184	0.127796442267496	**0.727688726340326**	0.442591515627638	0.285097210712689
ENSMSEG00005020[illegible]	brown	FB3	Autosome	Adat1	**0.736235069247031**	**0.94595175670942**	**0.649316337799406**	0.0869187314476244	-0.20971668746239	0.296635418910014
ENSMSEG00005012[illegible]	brown	FB3	Autosome	Slc7a11	0.513594355184993	**0.751037088134992**	0.422534812709112	0.0910595424758809	-0.237442732949999	0.32850227542588
ENSMSEG00005018[illegible]	brown	FB3	Autosome	Fos	**1.8902564923572**	**1.28353571138129**	**0.944778967264222**	**0.945477525092976**	**0.606720780975904**	0.338756744117072
ENSMSEG00005008[illegible]	brown	FB3	Autosome		**0.610074590302693**	0.478972939070456	0.32684273886683	0.283231851435862	0.131101651232237	0.340862147191003
ENSMSEG00005022[illegible]	brown	FB3	Autosome	Egr4	**1.70252926039397**	**1.25065363236098**	**0.892323247655373**	**0.810206012738601**	0.451875628032991	0.35833038470561
ENSMSEG00005009[illegible]	brown	FB3	Autosome	Fyb2	**1.04409509670226**	**1.73420614717651**	**1.36490600544251**	-0.320810908740256	**-0.690111050474248**	0.369300141733992
ENSMSEG00005000[illegible]	brown	FB3	Autosome	Zbtb41	0.422728335019687	**0.641155468083906**	0.258009476242938	0.164718858776749	-0.218427133064219	0.383145991840968
ENSMSEG00005012[illegible]	brown	FB3	Autosome	Hs6st3	**0.722101262874232**	**0.842519052927552**	0.323818566155667	0.398282696718565	-0.12041779005332	0.518700486771885
ENSMSEG00005019[illegible]	brown	FB3	Autosome	Osr1	**0.609415997229184**	**0.95334339713179**	0.42592584473962	0.183490152489564	-0.343927399902606	0.52741755239217
ENSMSEG00005016[illegible]	brown	FB3	Autosome	Slc18a1	**2.70715827527128**	**2.94448108600517**	**2.4005022071832**	0.306656068088081	-0.23732281073389	0.543978878821971
ENSMSEG00005013[illegible]	brown	FB3	Autosome	Nr4a3	**0.985533600977685**	**0.919588225850036**	0.369050584593379	**0.616483016384306**	0.0659453751276491	0.550537641256657

ENSMSEG00005000(brown	FB3	Autosome	Spta1	**1.51367765211573**	**0.871204142921825**	0.311163363686918	**1.20251428842881**	**0.642473509193902**	0.560040779234907
ENSMSEG00005021(brown	FB3	Autosome	Junb	**1.72300854491338**	**1.23524821232416**	**0.641154082150137**	**1.08185446276324**	0.487760332589214	**0.594094130174027**
ENSMSEG00005019(brown	FB3	chr1 (NR)	Acan	**0.854542651522635**	0.573207407967587	**0.719301133007099**	0.135241518515536	0.281335243555047	-0.146093725039512
ENSMSEG00005018(brown	FB3	chr1 (NR)	Nav2	0.524134026203814	0.413140571668379	**0.689088467538769**	-0.164954441334955	0.110993454535434	-0.27594789587039
ENSMSEG00005020(brown	FB3	chr1 (NR)	Prr12	**0.624259531168442**	0.427625819415979	0.379450131096492	0.244809400071951	0.196633711752464	0.0481756883194869
ENSMSEG00005018(brown	FB3	chr1 (NR)	Pnmal2	**0.72181268951406**	0.527243521730804	0.378125390354362	0.343687299159698	0.194569167783256	0.149118131376442
ENSMSEG00005018(brown	FB3	chr1 (NR)	Slc6a5	**0.913878137729616**	**0.889630247307665**	**0.740154750195626**	0.17372338753399	0.0242478904219513	0.149475497112038
ENSMSEG00005017(brown	FB3	chr1 (NR)	Zfp526	**0.677143287580251**	0.374682971734468	0.220652545836351	0.4564907417439	0.302460315845783	0.154030425898117
ENSMSEG00005005(brown	FB3	chr1 (NR)	Lmtk3	**0.651632744675269**	0.432482043546409	0.248013875514861	0.403618869160408	0.219150701128859	0.184468168031549
ENSMSEG00005020(brown	FB3	chr1 (NR)	Ggn	**0.716414849365303**	0.376439301163673	0.189074555151353	0.527340294213951	0.33997554820163	0.18736474601232
ENSMSEG00005011(brown	FB3	chr1 (NR)		**1.03184917430694**	**1.21678954269**	**1.00578818662571**	0.0260609876812328	-0.184940368383061	0.211001356064293
ENSMSEG00005011(brown	FB3	chr1 (NR)	Zswim9	**0.69798315451089**	**0.633365008929201**	0.355205472811595	0.342777681699294	0.0646181455816887	0.278159536117606
ENSMSEG00005017(brown	FB3	chr1 (NR)	Nccrp1	**0.749683126282786**	**0.661548436610182**	0.360561990744703	0.389121135538084	0.0881346896726041	0.30098644586548
ENSMSEG00005011(brown	FB3	chr1 (NR)	Leng8	0.479428829473325	0.243256257675494	-0.146525420596732	**0.625954250070057**	0.236172571797831	0.389781678272225
ENSMSEG00005016(brown	FB3	chr1 (NR)	Zfp583	**0.865737564784112**	**0.665934109011127**	0.251539826700298	**0.614197738083814**	0.199803455772985	0.414394282310828
ENSMSEG00005014(brown	FB3	chr1 (NR)	Zfp575	**1.14491849321385**	**1.44397997399816**	**0.595145210952096**	0.549773282261752	-0.299061480784312	**0.848834763046064**
ENSMSEG00005006(brown	FB3	X/X* (R)	Rtl4	**0.890325494717519**	0.464559315668102	**0.68057130802102**	0.209754186696499	0.425766179049417	-0.216011992352917
ENSMSEG00005019(brown	FB3	X/X* (R)	Hs6st2	**0.775459654897007**	**0.739402720429589**	**0.691110925926885**	0.0843487289701214	0.0360569344674178	0.0482917945027036
ENSMSEG00005018(brown	FB3	X/X* (R)	Aff2	0.583403293476219	**0.680503011599841**	0.566513306708534	0.0168899867676842	-0.0970997181236222	0.113989704891306
ENSMSEG00005005(brown	FB3	X/X* (R)	Smim10l2a	**1.98547606382458**	**1.3765424435208**	**1.18767272496517**	**0.797803338859403**	**0.608933620303778**	0.188869718555625
ENSMSEG00005001(brown	FB3	X/X* (R)		**0.622200405425729**	0.524036564436418	0.326319540475809	0.29588086494992	0.0981638409893108	0.197717023960609
ENSMSEG00005012(brown	FB3	X/X* (R)	Irs4	**0.733946355510114**	**0.611876004958331**	0.253362022942199	0.480584332567916	0.122070350551783	0.358513982016132
ENSMSEG00005017(brown	FB3	chr1 (R)		**0.723671245828085**	0.422844047842437	0.458256426678053	0.265414819150031	0.300827197985648	-0.0354123788356167
ENSMSEG00005021(brown	FB3	chr1 (R)	Sec14l5	**0.765683662281987**	0.44106425746941	0.494387463596166	0.27129619868582	0.324619404812577	-0.0533232061267564
ENSMSEG00005015(brown	FB3	chr1 (R)		**0.623957633070311**	0.493478591659639	0.554400036923407	0.0695575961469041	0.130479041410673	-0.0609214452637686
ENSMSEG00005015(brown	FB3	chr1 (R)	Brd4	**0.594525465746053**	0.329068125482304	0.391116375278462	0.203409090467591	0.265457340263749	-0.0620482497961582
ENSMSEG00005017(brown	FB3	chr1 (R)	Slc5a7	**0.882244230321168**	0.575681096541999	**0.647797928989043**	0.234446301332126	0.30656313377917	-0.0721168324470439
ENSMSEG00005020(brown	FB3	chr1 (R)	Ankrd42	**0.721216603436196**	**0.645591690850252**	0.559147176689979	0.162069426746217	0.0756249125859442	0.086444514160273
ENSMSEG00005016(brown	FB3	chr1 (R)	Sik1	**0.898153889851291**	0.571835121703365	0.426096568214276	0.472057321637015	0.326318768147926	0.145738553489089
ENSMSEG00005017(brown	FB3	chr1 (R)	Cckbr	**0.776094455289014**	0.500193913262652	0.315098888115533	0.460995567173481	0.275900542026362	0.185095025147119
ENSMSEG00005003(brown	FB3	chr1 (R)		**0.675695874945438**	**0.667042680953444**	0.477153449230575	0.198542425714863	0.00865319399199402	0.189889231722869
ENSMSEG00005005(brown	FB3	chr1 (R)	Gpr26	0.472791211562289	**0.662246149318802**	0.441263103816171	0.0315281077461181	-0.189454937756513	0.220983045502631
ENSMSEG00005004(brown	FB3	chr13 (R)	Car12	**0.728865996592465**	0.352877891421109	0.353025249059803	0.375840747532662	0.375988105171355	-0.000147357638693323
ENSMSEG00005010(brown	FB3	chr13 (R)	Bcl9l	**0.599108426827352**	0.402618601152773	0.406890483475968	0.192217943351383	0.196489825674579	-0.00427188232319566
ENSMSEG00005005(brown	FB3	chr13 (R)	Scn5a	**0.593879208235806**	0.423517898402639	0.428279084131503	0.165600124104304	0.170361309833167	-0.00476118572886356
ENSMSEG00005020(brown	FB3	chr13 (R)	Bsn	0.546945654305554	**0.585406599572104**	**0.590350186057802**	-0.043404531752248	-0.0384609452665508	-0.0049435864856972
ENSMSEG00005011(brown	FB3	chr13 (R)	Minar1	**0.652608441825477**	0.485573697919255	**0.601837210972713**	0.0507712308527637	0.167034743906222	-0.116263513053458
ENSMSEG00005008(brown	FB3	chr13 (R)	Hcn4	**0.796933806224223**	0.230994848262181	0.525010250703536	0.271923555520687	0.565938957962042	-0.294015402441355
ENSMSEG00005011(brown	FB3	chr13 (R)	Vps13c	**0.914742034019226**	**0.759235456028924**	**1.16022600077511**	-0.245483966755885	0.155506577990302	-0.400990544746187
ENSMSEG00005008(brown	FB3	chr13 (R)	Amotl2	**0.710730707026328**	0.539987486559931	0.362450772072778	0.34827993495355	0.170743220466397	0.177536714487153
ENSMSEG00005010(brown	FB3	chr13 (R)		**1.33980502033104**	**1.36281906677031**	**1.13699710208349**	0.202807918247551	-0.0230140464392646	0.225821964686816
ENSMSEG00005014(brown	FB3	chr13 (R)	Al593442	**0.704926743367907**	**0.690573538316742**	0.438584519134735	0.266342224233173	0.0143532050511656	0.251989019182007
ENSMSEG00005022(brown	FB3	X/X* (NR)		**0.707136165768295**	0.535197211468708	0.522359759688263	0.184776406080032	0.171938954299587	0.0128374517804452
ENSMSEG00005013(brown	FB3	X/X* (NR)		**1.65676172061473**	**1.53135703676351**	**1.24550732940888**	0.41125439120585	0.125404683851222	0.285849707354628
ENSMSEG00005023(brown	FB3	X/X* (NR)	Dmd	0.398348451518338	**0.647200499499027**	0.287937016261552	0.110411435256786	-0.248852047980689	0.359263483237475
ENSMSEG00005022(grey	grey	Autosome	Mpz	**1.49736150524135**	-0.200204514422283	-0.374730747647661	**1.87209225288901**	**1.69756601966363**	0.174526233225378
ENSMSEG00005007(grey	grey	Autosome	Arhgap15	-0.378491470930841	0.233846051078744	-0.516462644869617	0.137971173938776	**-0.612337522009585**	**0.750308695948361**

ENSMSEG00005004{	grey	grey	chr13 (R)	Zkscan7	-0.431657622049928	0.487835484938103	0.522834389302591	**-0.954492011352519**	**-0.919493106988031**	-0.0349989043644882
ENSMSEG00005020]	turquoise	MB	Autosome	Atpif1	**-0.676874260186675**	-0.544474722570357	-0.543637902499496	-0.133236357687179	-0.132399537616318	-0.000836820070861054
ENSMSEG00005011[	turquoise	MB	Autosome	Uqcrfs1	**-0.658738242374322**	-0.452245957705568	-0.451378401079019	-0.207359841295303	-0.206492284668754	-0.000867556626548825
ENSMSEG00005020]	turquoise	MB	Autosome	Mrps14	**-0.646186021090857**	-0.362033278777695	-0.360613188365318	-0.285572832725539	-0.284152742313162	-0.00142009041237774
ENSMSEG00005000[	turquoise	MB	Autosome	Itgb1bp1	**-0.593359391107745**	-0.464256363875279	-0.461960701032953	-0.131398690074793	-0.129103027232466	-0.00229566284232626
ENSMSEG00005019:	turquoise	MB	Autosome	Rps15	**-0.81476221662347**	**-0.763545735282753**	**-0.760296107163773**	-0.0544661094596974	-0.0512164813407176	-0.0032496281189798
ENSMSEG00005015<	turquoise	MB	Autosome	Tmem179b	**-0.598809588053076**	-0.426924106094922	-0.423551369835766	-0.17525821821731	-0.171885481958153	-0.00337273625915673
ENSMSEG00005020<	turquoise	MB	Autosome	Psma7	**-0.839366442720791**	**-0.664879598575617**	**-0.660279084829771**	-0.17908735789102	-0.174486844145173	-0.00460051374584663
ENSMSEG00005007J	turquoise	MB	Autosome	Pfdn1	**-0.615040762844228**	-0.469213551611663	-0.464098933395272	-0.150941829448955	-0.145827211232565	-0.00511461821639076
ENSMSEG00005019:	turquoise	MB	Autosome	Rplp0	**-0.644979191243972**	**-0.59638624821497**	**-0.590693563708759**	-0.0542856275352131	-0.0485929430290017	-0.00569268450621144
ENSMSEG00005008<	turquoise	MB	Autosome	Ppih	**-0.830778752180394**	-0.544492148191014	-0.537088281840816	-0.293690470339577	-0.286286603989379	-0.00740386635019772
ENSMSEG00005022(	turquoise	MB	Autosome	Psmb4	**-0.645697417073691**	-0.554165777777301	-0.544193392917141	-0.10150402415655	-0.0915316392963899	-0.00997238486015975
ENSMSEG00005013[	turquoise	MB	Autosome	Eef1g	**-0.6287057888634**	-0.559566624319543	-0.548325886129319	-0.0803799027340812	-0.0691391645438574	-0.0112407381902237
ENSMSEG00005006:	turquoise	MB	Autosome	Rpain	**-0.954031629603332**	**-0.729741820349131**	**-0.71743073764914**	-0.236600891954192	-0.224289809254201	-0.0123110826999912
ENSMSEG00005002[	turquoise	MB	Autosome	Chchd7	**-0.752845275336239**	-0.450216710299357	-0.43787017824958	-0.314975097086659	-0.302628565036882	-0.0123465320497771
ENSMSEG00005020[	turquoise	MB	Autosome	Rpp38	**-0.744809595649561**	-0.449915146637497	-0.436969445627218	-0.307840150022343	-0.294894449012064	-0.012945701010279
ENSMSEG00005016[	turquoise	MB	Autosome	Rpl17	**-1.11711255335419**	**-0.924451610876923**	**-0.9106571962944**	-0.20645535705979	-0.192660942477267	-0.0137944145825234
ENSMSEG00005015[	turquoise	MB	Autosome		-0.50897780196507	-0.404707181148478	**-0.910798383433633**	0.401820581468563	-0.104270620816592	-0.0140513701882584
ENSMSEG00005009[	turquoise	MB	Autosome	S100a13	**-0.742084165189405**	-0.534965417611232	-0.520745649304356	-0.221338515885049	-0.207118747578173	-0.0142197683068759
ENSMSEG00005015<	turquoise	MB	Autosome		**-1.35235055530746**	**-0.630133673637708**	**-1.41546686423106**	0.063116308923595	**-0.722216881669756**	-0.0145126098090053
ENSMSEG00005014[	turquoise	MB	Autosome	Spcs1	**-0.61392434991183**	-0.463227434347314	-0.446492696246295	-0.167431653665535	-0.150696915564516	-0.0167347381010191
ENSMSEG00005018[	turquoise	MB	Autosome	Sfxn4	**-0.936262508555492**	**-0.724105060850148**	**-0.706646621000116**	-0.229615887555375	-0.212157447705343	-0.0174584398500321
ENSMSEG00005000[	turquoise	MB	Autosome	Rpp25l	**-0.608533846910738**	-0.544033480862856	-0.526524780072406	-0.0820090668383316	-0.0645003660478825	-0.0175087007904492
ENSMSEG00005017[	turquoise	MB	Autosome	Rgcc	**-0.722246702793963**	**-0.771991937619549**	**-0.754235073245089**	0.0319883704511255	0.0497452348255856	-0.0177568643744601
ENSMSEG00005001[	turquoise	MB	Autosome	Ovca2	**-0.619395033142091**	-0.514605984754254	-0.495639466604346	-0.123755566537745	-0.104789048387837	-0.0189665181499085
ENSMSEG00005006J	turquoise	MB	Autosome		**-1.20827662869801**	**-0.985759155283784**	**-1.09069788157914**	-0.117578747118872	-0.222517473414227	-0.0191383639587469
ENSMSEG00005004:	turquoise	MB	Autosome	Mrpl50	**-0.774718625033583**	-0.455339807557328	-0.434614563961786	-0.340104061071796	-0.319378817476254	-0.020725243595542
ENSMSEG00005014[	turquoise	MB	Autosome	Plekhj1	**-0.671730594335611**	-0.542893563819544	-0.521969198436438	-0.149761395899173	-0.128837030516068	-0.0209243653831057
ENSMSEG00005007{	turquoise	MB	Autosome		**-0.865912452379608**	**-0.661978472563103**	**-0.73628287367137**	-0.129629578708237	-0.203933979816505	-0.021353215897717
ENSMSEG00005010]	turquoise	MB	Autosome	Nsa2	**-0.604981262663756**	-0.544687185853743	-0.523050004393211	-0.081931258270545	-0.0602940768100126	-0.0216371814605325
ENSMSEG00005015]	turquoise	MB	Autosome	Polr2g	**-0.699611039596829**	-0.51153458196858	-0.489839975880447	-0.209771063716381	-0.188076457628249	-0.0216946060881325
ENSMSEG00005017[	turquoise	MB	Autosome	Rps27	**-1.16849449703379**	**-0.926520246683582**	**-0.904615647001001**	-0.263878850032785	-0.241974250350204	-0.021904599682581
ENSMSEG00005009(	turquoise	MB	Autosome	Psma6	**-0.608236571905537**	-0.519271594113134	-0.496388300141317	-0.11184827176422	-0.0889649777924035	-0.0228832939718166
ENSMSEG00005011]	turquoise	MB	Autosome	Ccdc113	**-1.08299352106003**	**-0.89280968870993**	**-0.869483442421521**	-0.213510078638507	-0.190183832350097	-0.0233262462884093
ENSMSEG00005003(	turquoise	MB	Autosome		-0.58114642806955	**-0.959057112085705**	-0.218372768318621	-0.362773659750929	0.377910684016155	-0.0241336744109317
ENSMSEG00005020]	turquoise	MB	Autosome	Xbp1	**-0.633136794832489**	-0.564043887172829	-0.539527572677158	-0.0936092221553307	-0.0690929076596599	-0.0245163144956708
ENSMSEG00005006[	turquoise	MB	Autosome		**-0.789818679317211**	-0.581473856714464	**-0.62609042844111**	-0.1637282508761	-0.208340322602747	-0.0249842635150579
ENSMSEG00005012[	turquoise	MB	Autosome	Psph	**-0.649291965633773**	-0.554683679191562	-0.529461474371572	-0.119830491262201	-0.0946082864422106	-0.0252222048199902
ENSMSEG00005003{	turquoise	MB	Autosome	Cox14	**-0.652748251708379**	-0.541516849033153	-0.515925310634331	-0.136822941074048	-0.111231402675226	-0.0255915383988226
ENSMSEG00005018[	turquoise	MB	Autosome	Cox7c	**-0.801432610953959**	**-0.815551238788215**	**-0.789703641212194**	-0.0117289697417653	0.0141186278342558	-0.0258475975760212
ENSMSEG00005001:	turquoise	MB	Autosome	Iah1	**-0.729282254832237**	-0.551629383550294	-0.524862612769111	-0.204419642063126	-0.177652871281943	-0.0267667707811829
ENSMSEG00005000]	turquoise	MB	Autosome	Spatc1	**-0.773016017080088**	**-1.28643055649957**	**-1.25890284324459**	0.485886826164506	0.513414539419487	-0.0275277132549803
ENSMSEG00005017[	turquoise	MB	Autosome		**-0.808294023562261**	**-0.74234415994166**	**-0.790760650942712**	-0.0175333726195489	-0.0659498636206014	-0.0278977387935528
ENSMSEG00005003]	turquoise	MB	Autosome	Fabp3	**-0.746008097702858**	-0.463894721951943	-0.43278334593318	-0.313224751769678	-0.282113375750915	-0.0311113760187629
ENSMSEG00005012]	turquoise	MB	Autosome		**-0.819230360773146**	-0.161691249945321	0.172231941353423	**-0.991462302126569**	**-0.657539110827825**	-0.0312624626075798
ENSMSEG00005012[	turquoise	MB	Autosome		-0.174992370432769	**-0.972584569407071**	**-0.756432566136367**	0.581440195703598	**0.797592198974302**	-0.0320649832651093
ENSMSEG00005012:	turquoise	MB	Autosome	Fam162a	**-0.665560495718672**	-0.505245532039808	-0.472826059158493	-0.192734436560179	-0.160314963678864	-0.0324194728813146

ENSMSEG00005007	turquoise	MB	Autosome	Hyi	**-0.716285344986985**	-0.473490646273703	-0.440900002859636	-0.27538534212735	-0.242794698713283	-0.0325906434140671
ENSMSEG00005000	turquoise	MB	Autosome		**-0.850437008016051**	**-1.14377938769247**	**-0.745164942793188**	-0.105272065222863	0.293342379676414	-0.0327441173329522
ENSMSEG00005015	turquoise	MB	Autosome	Rps23	**-0.840993070508561**	**-0.787078890361335**	**-0.963192221160692**	0.122199150652131	-0.053914180147226	-0.0329049163083438
ENSMSEG00005003	turquoise	MB	Autosome		**-1.19696991988462**	-0.0296267379695089	-0.0386958016573367	**-1.15827411822728**	**-1.16734318191511**	-0.0342315893725593
ENSMSEG00005014	turquoise	MB	Autosome	Ninj1	**-0.601784968945636**	-0.455146299271521	-0.419085790766457	-0.182699178179179	-0.146638669674116	-0.0360605085050636
ENSMSEG00005009	turquoise	MB	Autosome	Stx8	**-0.593721017114544**	-0.46127504893227	-0.422516540604125	-0.171204476510419	-0.132445968182274	-0.038758508328145
ENSMSEG00005006	turquoise	MB	Autosome	Polr2h	**-0.73348602318653**	-0.454506233340487	-0.415275822173315	-0.318210201013215	-0.278979789846044	-0.0392304111671713
ENSMSEG00005020	turquoise	MB	Autosome	Pop5	**-0.822335073510666**	**-0.968396359275086**	**-0.92755582998497**	0.105220756474304	0.14606128576442	-0.0408405292901161
ENSMSEG00005002	turquoise	MB	Autosome	Atp5h	**-0.654226059419875**	**-0.596407588515268**	-0.555289384031057	-0.0989366753888184	-0.057818470904607	-0.0411182044842114
ENSMSEG00005008	turquoise	MB	Autosome	Atp23	-0.584537698729859	**-0.588607688591805**	-0.546434328851306	-0.0381033698785522	0.00406998986194684	-0.042173359740499
ENSMSEG00005022	turquoise	MB	Autosome	Gtf3a	**-0.752704070239552**	**-0.685648162947481**	**-0.64344208849916**	-0.109261981740391	-0.0670559072920707	-0.0422060744483208
ENSMSEG00005004	turquoise	MB	Autosome	Rps6	**-0.940748784102568**	**-0.861603753040531**	**-0.818088101069335**	-0.122660683033233	-0.0791450310620367	-0.043515651971196
ENSMSEG00005016	turquoise	MB	Autosome		**-0.611972994744436**	-0.480561245332731	-0.446329655960172	-0.165643338784264	-0.131411749411705	-0.0442868791363769
ENSMSEG00005009	turquoise	MB	Autosome	Mrpl20	**-0.61459483077702**	-0.525841090413726	-0.481275019720196	-0.133319811056823	-0.0887537403632935	-0.0445660706935298
ENSMSEG00005012	turquoise	MB	Autosome		-0.568239465572721	**-0.702191292604103**	-0.427180888865111	-0.14105857670761	0.133951827031382	-0.0446208361948253
ENSMSEG00005010	turquoise	MB	Autosome		**-0.703063355614136**	**-0.585885818690187**	-0.56674745473144	-0.136315900882696	-0.11717753692395	-0.0449810939290912
ENSMSEG00005005	turquoise	MB	Autosome	Commd6	**-0.682920646298163**	-0.534391462890791	-0.489330599120741	-0.193590047177421	-0.148529183407372	-0.0450608637700499
ENSMSEG00005018	turquoise	MB	Autosome	Slc25a5	-0.263735433120888	**-0.703775344568739**	**-0.657749989793504**	0.394014556672616	0.440039911447851	-0.0460253547752346
ENSMSEG00005022	turquoise	MB	Autosome	Brk1	**-0.728581751419314**	-0.555789171974863	-0.50899934287234	-0.219582408546974	-0.172792579444451	-0.0467898291025225
ENSMSEG00005010	turquoise	MB	Autosome	Nit2	**-0.738444271953487**	-0.524564624559487	-0.47776518766469	-0.260679084288796	-0.213879647394	-0.0467994368947962
ENSMSEG00005016	turquoise	MB	Autosome	Ggact	**-0.587169398321803**	-0.519981230054828	-0.472247028701108	-0.114922369620695	-0.067188168266975	-0.0477342013537195
ENSMSEG00005003	turquoise	MB	Autosome	Mrps21	**-0.694644335397901**	-0.456807405064166	-0.408455890873845	-0.286188444524056	-0.237836930333736	-0.0483515141903204
ENSMSEG00005017	turquoise	MB	Autosome	Mrps33	**-0.602953367569234**	-0.490351581895157	-0.441035306638679	-0.161918060930555	-0.112601785674076	-0.0493162752564785
ENSMSEG00005000	turquoise	MB	Autosome		**-1.19650710023196**	**-0.938500110828825**	**-0.974663900639389**	-0.221843199592572	-0.258006989403136	-0.0497911051169103
ENSMSEG00005012	turquoise	MB	Autosome	2700062C07R	**-0.703659836274675**	-0.495193013677207	-0.444126959948302	-0.259532876326373	-0.208466822597468	-0.0510660537289053
ENSMSEG00005018	turquoise	MB	Autosome	Ostc	**-0.659344599716917**	**-0.615781939177689**	-0.563453444004328	-0.0958911557125885	-0.0435626605392279	-0.0523284951733606
ENSMSEG00005003	turquoise	MB	Autosome		**-0.782234501843531**	**-0.607674171506688**	-0.562693077577596	-0.219541424265935	-0.174560330336844	-0.053367846639253
ENSMSEG00005003	turquoise	MB	Autosome	Mrps7	**-0.628662307295414**	-0.555887780002624	-0.50118742620968	-0.127474881085734	-0.0727745272927899	-0.0547003537929444
ENSMSEG00005005	turquoise	MB	Autosome	Tmem141	**-0.673083035893686**	-0.535882759465533	-0.47982895349269	-0.193254082400996	-0.137200276428153	-0.0560538059728433
ENSMSEG00005004	turquoise	MB	Autosome	Ndufs4	**-0.752595364390001**	**-0.590992665632892**	-0.533850039562142	-0.218745324827858	-0.161602698757108	-0.0571426260707499
ENSMSEG00005016	turquoise	MB	Autosome	Katnal2	**-1.49948842796782**	-0.25715384423618	-0.199325514855277	**-1.30016291311255**	**-1.24233458373164**	-0.0578283293809039
ENSMSEG00005018	turquoise	MB	Autosome		**-0.678536152211547**	-0.519300424814823	-0.406469117267599	-0.272067034943948	-0.159235727396724	-0.0595654635241249
ENSMSEG00005018	turquoise	MB	Autosome	Cd63	**-0.62614629711932**	-0.46055069080683	-0.400340044332995	-0.225806252786325	-0.16559560631249	-0.0602106464738354
ENSMSEG00005015	turquoise	MB	Autosome	Commd8	**-0.589100205841259**	-0.387244562134046	-0.326642595849057	-0.262457609992202	-0.201855643707213	-0.0606019662849885
ENSMSEG00005002	turquoise	MB	Autosome	Cmbl	**-0.910711151252245**	**-0.588373314654762**	-0.52756131723398	-0.383149834018264	-0.322337836597483	-0.0608119974207817
ENSMSEG00005018	turquoise	MB	Autosome	Use1	**-0.869605599735371**	**-0.827766240977441**	**-0.766660551381485**	-0.102945048353886	-0.0418393587579298	-0.0611056895959559
ENSMSEG00005010	turquoise	MB	Autosome	Pmf1	**-0.675462258009199**	-0.495629275469571	-0.430769008818705	-0.244693249190494	-0.179832982539628	-0.0648602666508662
ENSMSEG00005003	turquoise	MB	Autosome	S100a11	**-0.691901630894631**	-0.43371889656678	-0.368766446549323	-0.323135184345308	-0.258182734327851	-0.0649524500174571
ENSMSEG00005000	turquoise	MB	Autosome	Anxa3	**-0.808702450816341**	**-0.654440628932489**	**-0.587200080446913**	-0.221502370369429	-0.154261821883853	-0.0672405484855761
ENSMSEG00005015	turquoise	MB	Autosome	Tmem258	**-0.598548173357088**	-0.544338829159067	-0.476944000188179	-0.121604173168908	-0.0542093441980211	-0.0673948289708874
ENSMSEG00005017	turquoise	MB	Autosome	Isca2	**-0.651371322276467**	-0.545743429983479	-0.478129998061849	-0.173241324214618	-0.105627892292988	-0.0676134319216301
ENSMSEG00005016	turquoise	MB	Autosome	Crip1	**-0.929184124972697**	**-1.02635769944503**	**-0.957865181667782**	0.0286810566950843	0.0971735744723322	-0.0684925177772479
ENSMSEG00005018	turquoise	MB	Autosome	Hax1	**-0.585216058932886**	-0.546968916757953	-0.47747374530526	-0.107742313627626	-0.0382471421749331	-0.0694951714526933
ENSMSEG00005017	turquoise	MB	Autosome	Eif3e	**-0.596325953485002**	-0.515472263304011	-0.443834007278475	-0.152491946206527	-0.0808536901809911	-0.071638256025536
ENSMSEG00005015	turquoise	MB	Autosome	Lexm	**-0.792650198100979**	-0.173644262362943	-0.100623226060934	**-0.692026972040045**	**-0.619005935738036**	-0.0730210363020091
ENSMSEG00005016	turquoise	MB	Autosome		**-0.86117706249302**	**-0.754399431645769**	-0.492022010063252	-0.369155052429769	-0.106777630847251	-0.0735868250230461
ENSMSEG00005003	turquoise	MB	Autosome	Mrpl19	**-0.6747514521662**	-0.306588695366918	-0.232922278548011	-0.441829173618189	-0.368162756799281	-0.0736664168189078

ENSMSEG00005002(	turquoise	MB	Autosome	Fggy	**-0.611252961661465**	-0.506261731334736	-0.432305836365425	-0.17894712529604	-0.104991230326729	-0.0739558949693108
ENSMSEG00005010'	turquoise	MB	Autosome		**-0.952186761830463**	**-0.805970495988938**	**-0.954094593240546**	0.00190783141008349	-0.146216265841525	-0.0748627638751436
ENSMSEG00005002$	turquoise	MB	Autosome	Mrpl13	**-0.625631820084833**	-0.505807432075977	-0.43078924555936	-0.194842574525472	-0.119824388008856	-0.0750181865166166
ENSMSEG00005000(	turquoise	MB	Autosome	Serf2	**-0.640860327318465**	-0.518212579935024	-0.442981697787177	-0.197878629531287	-0.12264774738344	-0.0752308821478469
ENSMSEG00005009$	turquoise	MB	Autosome	Tmem52	**-0.643007573138545**	**-1.08726279643317**	**-1.01185920282643**	0.368851629687889	0.444255223294626	-0.075403593606737
ENSMSEG00005008(	turquoise	MB	Autosome		-0.456042048292046	**-0.593898173981894**	-0.461960560761951	0.00591851246990488	0.137856125689848	-0.0761656659194316
ENSMSEG00005001$	turquoise	MB	Autosome		**-0.722303756735805**	**-0.605036664431428**	-0.499346404621199	-0.222957352114605	-0.117267092304377	-0.0764505493332023
ENSMSEG00005018;	turquoise	MB	Autosome	Gng11	**-0.600639222743187**	**-0.63361572383125**	-0.556482881074282	-0.0441563416689053	0.0329765010880622	-0.0771328427569676
ENSMSEG00005003]	turquoise	MB	Autosome	Pecr	**-0.672477595324364**	**-0.685605103915559**	**-0.605053641047636**	-0.0674239542767277	0.0131275085911948	-0.0805514628679225
ENSMSEG00005004;	turquoise	MB	Autosome	Ndufs3	**-0.58953412130142**	-0.362076777358291	-0.277997978281565	-0.311536143019855	-0.22745734394313	-0.0840787990767255
ENSMSEG00005016<	turquoise	MB	Autosome	Nol12	**-0.746028268716544**	**-0.624136289248098**	-0.537866952036615	-0.208161316679929	-0.121891979468446	-0.0862693372114828
ENSMSEG00005008(	turquoise	MB	Autosome	Ctxn2	**-0.684223620145952**	**-0.590651163893473**	-0.501173510667287	-0.183050109478665	-0.0935724562524788	-0.0894776532261857
ENSMSEG00005014;	turquoise	MB	Autosome	Nts	**-0.734809981782026**	-0.458807760128498	-0.368771255068227	-0.366038726713799	-0.276002221653528	-0.0900365050602708
ENSMSEG00005004$	turquoise	MB	Autosome	Mien1	**-0.773624420121735**	-0.517172384663014	-0.426819188669561	-0.346805231452175	-0.256452035458722	-0.090353195993453
ENSMSEG00005007(	turquoise	MB	Autosome	Dipk1c	**-0.781644155123222**	-0.544696453040215	-0.454121937927691	-0.327522217195531	-0.236947702083006	-0.0905745151125244
ENSMSEG00005005$	turquoise	MB	Autosome		**-1.09543117178015**	**-0.822246191872301**	**-1.0379575221554**	-0.0574736496247495	-0.273184979907849	-0.0919699250487138
ENSMSEG00005010$	turquoise	MB	Autosome	Atp5j	**-1.99481345873058**	-0.525147550484065	-0.433089018890945	**-1.56172443983964**	**-1.46966590824652**	-0.0920585315931201
ENSMSEG00005011'	turquoise	MB	Autosome	Tmem208	**-0.868953248469244**	**-0.694851515139225**	**-0.602583313837632**	-0.266369934631612	-0.174101733330019	-0.0922682013015927
ENSMSEG00005022$	turquoise	MB	Autosome	Fgfbp3	**-0.937031669658479**	**-1.0623430348002**	**-0.968939480876683**	0.0319078112182044	0.125311365141722	-0.0934035539235171
ENSMSEG00005000?	turquoise	MB	Autosome	Rac3	**-0.619037698373262**	**-0.647654894841714**	-0.553715409394543	-0.0653222889787187	0.028617196468452	-0.0939394854471708
ENSMSEG00005018]	turquoise	MB	Autosome	Blvra	**-0.696066351987338**	**-0.909515547092317**	**-0.813093893416123**	0.117027541428785	0.213449195104978	-0.0964216536761934
ENSMSEG00005005<	turquoise	MB	Autosome		**-0.871456827098016**	**-0.703832786156688**	**-0.742466870562204**	-0.128989956535812	-0.167624040941327	-0.0978878594641912
ENSMSEG00005021$	turquoise	MB	Autosome	Slc30a10	**-0.697913880888441**	-0.46075367115379	-0.36049588535393	-0.33741799553451	-0.23716020973465	-0.10025778579986
ENSMSEG00005003$	turquoise	MB	Autosome		**-0.93744948236771**	**-1.16070826207375**	**-2.3179135389276**	**1.38046405655989**	0.22325877970604	-0.101872458977145
ENSMSEG00005017'	turquoise	MB	Autosome	Nsmce2	**-0.669549431538157**	-0.555752510229427	-0.453320689774883	-0.216228741763274	-0.11379692130873	-0.102431820454544
ENSMSEG00005005$	turquoise	MB	Autosome	Ybey	**-0.860704189520844**	**-0.586036692165304**	-0.482477660944212	-0.378226528576631	-0.27466749735554	-0.103559031221091
ENSMSEG00005020(	turquoise	MB	Autosome		**-0.763087427695291**	-0.563053803336982	**-0.687889063819098**	-0.0751983638761936	-0.200033624358309	-0.10462320620155
ENSMSEG00005002(	turquoise	MB	Autosome		**-0.770578919473557**	**-0.694400349884589**	**-0.620813524861543**	-0.149765394612013	-0.0761785695889673	-0.105690259810228
ENSMSEG00005014;	turquoise	MB	Autosome	Selenof	**-1.04336891872538**	**-0.675041131173274**	-0.569310615886511	-0.474058302838868	-0.368327787552105	-0.105730515286764
ENSMSEG00005004$	turquoise	MB	Autosome	Mettl23	**-0.841846603832269**	**-0.725809538011334**	**-0.619828307765027**	-0.222018296067242	-0.116037065820934	-0.105981230246307
ENSMSEG00005007&	turquoise	MB	Autosome	Mterf1a	**-0.889526243141978**	**-0.829039992288194**	**-0.721545729012213**	-0.167980514129764	-0.060486250853784	-0.10749426327598
ENSMSEG00005008<	turquoise	MB	Autosome	Ap4s1	**-1.08747131969694**	**-0.796549539676542**	**-0.688701790525704**	-0.398769529171233	-0.290921780020395	-0.107847749150837
ENSMSEG00005002<	turquoise	MB	Autosome	Washc3	**-0.593338851007495**	-0.420988071852221	-0.310127899291559	-0.283210951715936	-0.172350779155274	-0.110860172560662
ENSMSEG00005009?	turquoise	MB	Autosome	E2f5	**-0.631307796042341**	-0.305491560951415	-0.193856713671416	-0.437451082370926	-0.325816235090926	-0.111634847279999
ENSMSEG00005016<	turquoise	MB	Autosome	Gm10320	**-0.83977842709905**	**-0.672506672104125**	-0.55970931106682	-0.28006911603223	-0.167271754994925	-0.112797361037305
ENSMSEG00005009(	turquoise	MB	Autosome		-0.566041086780834	**-0.681119137605671**	-0.410011539376716	-0.156029547404118	0.115078050824836	-0.112831307547224
ENSMSEG00005005(	turquoise	MB	Autosome	Dph7	**-0.661841838915349**	**-0.621150756502153**	-0.507607764961235	-0.154234073954115	-0.0406910824131966	-0.113542991540918
ENSMSEG00005021?	turquoise	MB	Autosome	Scp2	**-0.969301100323826**	-0.524452508545756	-0.410784723916299	-0.558516376407526	-0.444848591778069	-0.113667784629457
ENSMSEG00005009&	turquoise	MB	Autosome	Gm43738	**-0.645342699835342**	-0.533011297375298	-0.416517091749186	-0.228825608086157	-0.112331402460044	-0.116494205626112
ENSMSEG00005004<	turquoise	MB	Autosome	Ptpmt1	**-0.700532645560329**	**-0.70593201056688**	**-0.589413360558609**	-0.11111928500172	0.0053993650065505	-0.116518650008271
ENSMSEG00005002&	turquoise	MB	Autosome	Galnt15	**-0.915936606984067**	**-0.66531498522317**	-0.547346451899925	-0.368590155084142	-0.250621621760897	-0.117968533323245
ENSMSEG00005021&	turquoise	MB	Autosome	Smdt1	**-0.721611564601528**	**-0.605449452039839**	-0.486588875820333	-0.235022688781195	-0.116162112561689	-0.118860576219506
ENSMSEG00005008(	turquoise	MB	Autosome	Ppcs	**-0.686131555455786**	-0.356303324989509	-0.235418672088578	-0.450712883367208	-0.329828230466277	-0.120884652900931
ENSMSEG00005002$	turquoise	MB	Autosome		**-0.850319709089574**	-0.579851998461987	-0.41792785066083	-0.432391858428744	-0.270467710627587	-0.123129427296793
ENSMSEG00005014$	turquoise	MB	Autosome	Hoga1	**-1.04155898596452**	-0.458733042692537	-0.333147162627771	**-0.708411823336745**	-0.58282594327198	-0.125585880064765
ENSMSEG00005004]	turquoise	MB	Autosome	Gng5	-0.574127355682297	**-0.59715143365725**	-0.469655672604343	-0.104471683077954	0.0230240779749532	-0.127495761052907
ENSMSEG00005002?	turquoise	MB	Autosome	Llph	**-0.702373838895645**	**-0.634980575995968**	-0.506090064632793	-0.196283774262851	-0.0673932628996764	-0.128890511363175

ENSMSEG00005008	turquoise	MB	Autosome	**-0.876352521702596**	**-0.681576843878464**	-0.524664391886114	-0.351688129816482	-0.194775677824131	-0.129109360784038
ENSMSEG00005020	turquoise	MB	Autosome	**-1.14660794200994**	**-0.868715389231866**	**-0.766842930254721**	-0.379765011755217	-0.277892552778073	-0.129642242904866
ENSMSEG00005009	turquoise	MB	Autosome S100a16	**-0.690222041742186**	-0.553353074405457	-0.421516331293361	-0.268705710448826	-0.136868967336729	-0.131836743112097
ENSMSEG00005019	turquoise	MB	Autosome	**-0.98156572140887**	**-0.798508193534573**	**-0.753887357339747**	-0.227678364069122	-0.183057527874297	-0.131937613219943
ENSMSEG00005017	turquoise	MB	Autosome Rack1	**-0.62253023913028**	**-0.608116361295749**	-0.475235094363442	-0.147295144766838	-0.0144138778345318	-0.132881266932306
ENSMSEG00005015	turquoise	MB	Autosome Car4	**-0.951022653910584**	**-0.700486885084384**	-0.564898865465674	-0.38612378844491	-0.250535768826199	-0.135588019618711
ENSMSEG00005000	turquoise	MB	Autosome Prodh	-0.217455670441444	**-0.688535126310164**	-0.551558593043308	0.334102922601864	0.47107945586872	-0.136976533266856
ENSMSEG00005014	turquoise	MB	Autosome Pfdn5	**-0.969491427100507**	**-0.692296023310805**	-0.553336024271333	-0.416155402829174	-0.277195403789702	-0.138959999039471
ENSMSEG00005013	turquoise	MB	Autosome Fkbp10	**-0.869747121506621**	**-0.602025870395035**	-0.460536281636782	-0.40921083986984	-0.267721251111586	-0.141489588758254
ENSMSEG00005020	turquoise	MB	Autosome	**-1.26111560975422**	**-0.972580515023732**	**-1.02482254247011**	-0.236293067284109	-0.288535094730486	-0.142058809007526
ENSMSEG00005021	turquoise	MB	Autosome Vip	**-0.67568725921198**	-0.543862210678972	-0.401171402526688	-0.274515856685292	-0.131825048533007	-0.142690808152285
ENSMSEG00005006	turquoise	MB	Autosome Eef1akmt1	**-0.651271104722537**	-0.550890282887618	-0.405468097562495	-0.245803007160042	-0.100380821834919	-0.145422185325122
ENSMSEG00005022	turquoise	MB	Autosome Igfbp3	**-0.641009351941378**	-0.267497493153119	-0.120849786584236	-0.520159565357142	-0.373511858788259	-0.146647706568883
ENSMSEG00005012	turquoise	MB	Autosome Rps11	**-0.950333302799012**	**-0.926729951198632**	**-0.779275830898219**	-0.171057471900792	-0.0236033516003794	-0.147454120300413
ENSMSEG00005000	turquoise	MB	Autosome Btbd19	**-1.00116887151644**	-0.311249683571978	-0.160871210104222	**-0.840297661412218**	**-0.689919187944461**	-0.150378473467757
ENSMSEG00005001	turquoise	MB	Autosome Grk4	-0.109390334352422	**-1.01774316819674**	**-0.86565993925224**	**0.756269604899818**	**0.908352833844313**	-0.152083228944495
ENSMSEG00005010	turquoise	MB	Autosome Mrpl49	**-0.792121331290649**	-0.573918981938188	-0.421748353190363	-0.370372978100285	-0.21820234935246	-0.152170628747825
ENSMSEG00005021	turquoise	MB	Autosome Trappc2l	**-0.703362309914856**	-0.545852775344354	-0.390665014167211	-0.312697295747645	-0.157509534570501	-0.155187761177143
ENSMSEG00005010	turquoise	MB	Autosome	**-1.00562794006536**	**-0.820141029357576**	**-0.697011602060784**	-0.30861633800458	-0.185486910707787	-0.156912451992351
ENSMSEG00005018	turquoise	MB	Autosome Smim7	**-1.02718866764229**	**-0.783460237720376**	**-0.622916533385669**	-0.404272134256622	-0.243728429921915	-0.160543704334707
ENSMSEG00005015	turquoise	MB	Autosome	**-0.650161310737798**	-0.540869641427791	-0.526357031618786	-0.123804279119012	-0.109291669310006	-0.161924147801157
ENSMSEG00005004	turquoise	MB	Autosome Dynlt2b	**-0.673515893436537**	-0.58384351336341	-0.421497274478255	-0.252018618958282	-0.0896723800731265	-0.162346238885155
ENSMSEG00005011	turquoise	MB	Autosome	**-1.33769972678007**	**-1.34121150314464**	**-1.19915269413711**	-0.138547032642952	0.00351177636457417	-0.165643114717948
ENSMSEG00005008	turquoise	MB	Autosome Gabra6	**-0.595138928768066**	-0.448330635972818	-0.281725914835598	-0.313413013932468	-0.146808292795247	-0.16660472113722
ENSMSEG00005013	turquoise	MB	Autosome Sdhaf2	**-0.66529040137988**	-0.439673369980157	-0.272786703914848	-0.392503697465032	-0.225617031399723	-0.166886666065309
ENSMSEG00005022	turquoise	MB	Autosome Ndufb4	**-0.730147933730988**	**-0.694096366457609**	-0.522166481492785	-0.207981452238203	-0.0360515672733787	-0.171929884964824
ENSMSEG00005002	turquoise	MB	Autosome	**-0.889191650474048**	**-0.699535930673039**	**-0.876673236223114**	-0.0125184142509334	-0.189655719801009	-0.171929891429515
ENSMSEG00005010	turquoise	MB	Autosome Cd9	**-0.729695172901628**	**-0.62306261895828**	-0.450545515711016	-0.279149657190612	-0.106632553943348	-0.172517103247264
ENSMSEG00005000	turquoise	MB	Autosome Rarres2	-0.54094500104728	**-0.589201652819008**	-0.416486186532426	-0.124458814514854	0.0482566517717276	-0.172715466286582
ENSMSEG00005013	turquoise	MB	Autosome Lsm10	**-0.734474514858255**	**-0.587661758063334**	-0.412123245972036	-0.322351268886219	-0.146812756794921	-0.175538512091298
ENSMSEG00005009	turquoise	MB	Autosome Fam118a	**-0.641450296366991**	-0.430024440500659	-0.252511728230491	-0.388938568136499	-0.211425855866332	-0.177512712270167
ENSMSEG00005007	turquoise	MB	Autosome Slc19a3	**-0.799387526590154**	**-0.862079531446792**	**-0.681168020740096**	-0.118219505850058	0.0626920048566383	-0.180911510706697
ENSMSEG00005019	turquoise	MB	Autosome	**-0.868571181269357**	**-0.693079448924267**	**-0.616913783004835**	-0.251657398264522	-0.17549173234509	-0.181692755931545
ENSMSEG00005022	turquoise	MB	Autosome Serhl	**-0.788694973160936**	**-0.683436582571489**	-0.500870396142078	-0.287824577018858	-0.105258390589448	-0.18256618642941
ENSMSEG00005018	turquoise	MB	Autosome Lims2	**-0.85333987981614**	**-0.646103448263437**	-0.462780621164548	-0.390559258651592	-0.207236431552703	-0.183322827098889
ENSMSEG00005002	turquoise	MB	Autosome Immp1l	**-0.591519841160723**	-0.58376344821369	-0.3910271331871	-0.200492707973623	-0.00775639294703288	-0.19273631502659
ENSMSEG00005007	turquoise	MB	Autosome	**-1.09923500008468**	**-0.966893575312861**	**-0.913525728673608**	-0.185709271411076	-0.132341424771823	-0.193053836566236
ENSMSEG00005022	turquoise	MB	Autosome Gngt2	**-0.797683234344106**	**-0.71329075804045**	-0.519768879917157	-0.277914354426949	-0.0843924763036553	-0.193521878123294
ENSMSEG00005013	turquoise	MB	Autosome Gstm5	**-0.910297906637263**	**-0.710972235835322**	-0.516902035022921	-0.393395871614342	-0.199325670801941	-0.194070200812401
ENSMSEG00005011	turquoise	MB	Autosome Atp5g2	**-0.659400123921074**	**-0.626468317909495**	-0.428773547722014	-0.230626576199061	-0.032931806011579	-0.197694770187481
ENSMSEG00005016	turquoise	MB	Autosome Npm3	**-0.709630764360277**	**-0.642952254720454**	-0.445216640714959	-0.264414123645319	-0.0666785096398238	-0.197735614005495
ENSMSEG00005021	turquoise	MB	Autosome Gck	**-0.617862720955351**	-0.495854920016989	-0.297767544340492	-0.320095176614859	-0.122007800938362	-0.198087375676497
ENSMSEG00005005	turquoise	MB	Autosome	**-0.60739622807792**	-0.294007376181925	-0.219144612306781	-0.388251615771139	-0.313388851895996	-0.199244141247557
ENSMSEG00005000	turquoise	MB	Autosome Lcmt2	**-1.15588162823198**	**-0.824462334478193**	**-0.623924668405103**	-0.53195695982688	-0.33141929375379	-0.20053766607309
ENSMSEG00005002	turquoise	MB	Autosome	**-0.84469082742632**	**-0.65960209050307**	**-0.74532498231257**	-0.0993658451137495	-0.18508873692325	-0.200903126063146
ENSMSEG00005022	turquoise	MB	Autosome Gpx8	**-1.06124792383511**	**-0.695129089611382**	-0.493485583459927	-0.567762340375179	-0.366118834223724	-0.201643506151454
ENSMSEG00005005	turquoise	MB	Autosome Tspan11	**-0.687439243665148**	-0.459226124792134	-0.25510338236725	-0.432335861297898	-0.228213118873013	-0.204122742424885

ENSMSEG00005016	turquoise	MB	Autosome	Clybl	**-0.588517589680451**	-0.467694703371471	-0.263454625250372	-0.325062964430079	-0.12082288630898	-0.204240078121099
ENSMSEG00005009	turquoise	MB	Autosome	Gmip	-0.453806248030827	**-0.626765535178723**	-0.421246335874844	-0.0325599121559831	0.172959287147895	-0.205519199303878
ENSMSEG00005007	turquoise	MB	Autosome	Ndufc1	**-0.839396153299299**	**-0.770933259997085**	-0.56424611310254	-0.275150040196758	-0.0684628933022137	-0.206687146894544
ENSMSEG00005011	turquoise	MB	Autosome	Lrrc29	**-0.752610333234384**	-0.525677717769102	-0.317337284444057	-0.435273048790327	-0.226932615465282	-0.208340433325045
ENSMSEG00005021	turquoise	MB	Autosome	Arpc4	**-0.623138215484063**	-0.543083196588219	-0.331951375002295	-0.291186840481768	-0.0800550188958434	-0.211131821585924
ENSMSEG00005015	turquoise	MB	Autosome		**-1.23081003925566**	**-0.747917240973334**	**-1.28023843717886**	0.0494283979232006	-0.482892798282323	-0.216152003270704
ENSMSEG00005013	turquoise	MB	Autosome	Galnt12	**-1.17681728408199**	-0.513610863669953	-0.297208351766482	**-0.879608932315504**	**-0.663206420412033**	-0.216402511903472
ENSMSEG00005018	turquoise	MB	Autosome	Mrpl13	**-0.932219708253294**	-0.467396640627653	-0.250212323961057	**-0.682007384292237**	-0.464823067625641	-0.217184316666597
ENSMSEG00005021	turquoise	MB	Autosome	Lix1	**-0.67739453330063**	**-0.616693083386639**	-0.39885008105925	-0.27854445224138	-0.0607014499139913	-0.217843002327388
ENSMSEG00005011	turquoise	MB	Autosome	Lsm3	**-1.11740841470811**	**-0.831717022045177**	**-0.606796862215644**	-0.51061155249247	-0.285691392662937	-0.224920159829534
ENSMSEG00005019	turquoise	MB	Autosome	Gm27027	**-0.863841353058782**	-0.359074897220931	-0.133798587123469	**-0.730042765935313**	-0.504766455837851	-0.225276310097461
ENSMSEG00005014	turquoise	MB	Autosome		**-0.95622494760703**	**-0.635534859933763**	**-0.838738588538745**	-0.117486359068286	-0.320690087673267	-0.225772972320113
ENSMSEG00005010	turquoise	MB	Autosome	Pyurf	**-0.650358879311649**	**-0.593114528525874**	-0.365468902693393	-0.284889976618256	-0.0572443507857745	-0.227645625832481
ENSMSEG00005009	turquoise	MB	Autosome	2700097O09R	**-0.937594185614497**	-0.462589218512014	-0.227296244344311	**-0.710297941270186**	-0.475004967102483	-0.235292974167703
ENSMSEG00005020	turquoise	MB	Autosome	Pet100	**-0.729233153788112**	**-0.720459857981414**	-0.48417505180373	-0.245058101984382	-0.00877329580669787	-0.236284806177684
ENSMSEG00005022	turquoise	MB	Autosome	Niban3	-0.552770057898234	**-0.677307773119901**	-0.440218850880528	-0.112551207017706	0.124537715221667	-0.237088922239373
ENSMSEG00005011	turquoise	MB	Autosome		**-0.814915631553987**	**-0.766640266522373**	**-0.812327373704882**	-0.00258825784910482	-0.0482753650316138	-0.237246637605873
ENSMSEG00005003	turquoise	MB	Autosome	Ly96	-0.567927320956492	**-0.792580292922628**	-0.546743782159183	-0.0211835387973098	0.224652971966136	-0.245836510763446
ENSMSEG00005011	turquoise	MB	Autosome	Gins3	**-1.49788710431192**	**-1.61284107932991**	**-1.36412736911792**	-0.133759735193996	0.114953975017994	-0.248713710211989
ENSMSEG00005019	turquoise	MB	Autosome	Nostrin	**-0.863931486031561**	**-0.630944745211337**	-0.372146595734679	-0.491784890296882	-0.232986740820223	-0.258798149476658
ENSMSEG00005013	turquoise	MB	Autosome	Oma1	**-0.869238124872173**	-0.352749336343557	-0.0939376932299222	**-0.77530043164225**	-0.516488788528616	-0.258811643113634
ENSMSEG00005002	turquoise	MB	Autosome	Rpl24	**-0.744290336007452**	**-0.924561493731182**	**-0.662969497065709**	-0.0813208389417422	0.18027115772373	-0.261591996665473
ENSMSEG00005007	turquoise	MB	Autosome		**-3.37886119796046**	**-1.65904231415754**	**-3.55828017720145**	0.179418979240991	**-1.71981888380292**	-0.262377421582518
ENSMSEG00005005	turquoise	MB	Autosome	Slc47a1	**-0.670954262465987**	-0.454685525647779	-0.188566685440232	-0.482387577025755	-0.216268736818208	-0.266118840207547
ENSMSEG00005020	turquoise	MB	Autosome	Ebpl	**-0.858645737464403**	-0.362902417253909	-0.0919488898475573	**-0.766696847616846**	-0.495743320210494	-0.270953527406352
ENSMSEG00005002	turquoise	MB	Autosome		**-1.04714842988689**	**-0.847353258053303**	**-0.897462715310938**	-0.149685714575952	-0.199795171833587	-0.271107598228954
ENSMSEG00005005	turquoise	MB	Autosome	Ppie	**-0.920163036641085**	**-0.642691917301963**	-0.370305053518045	-0.54985798312304	-0.277471119339122	-0.272386863783918
ENSMSEG00005008	turquoise	MB	Autosome	Gsta3	**-0.686603831597429**	**-1.36847987012575**	**-1.09403729354329**	0.407433461945863	**0.681876038528325**	-0.274442576582462
ENSMSEG00005011	turquoise	MB	Autosome		**-0.866629606695983**	-0.497275966989814	-0.298031825742257	-0.568597780953726	-0.369353639706169	-0.275010403738992
ENSMSEG00005017	turquoise	MB	Autosome	Pcbd2	**-0.77145687772693**	**-0.730973346557851**	-0.446947686004688	-0.324509191722242	-0.0404835311690788	-0.284025660553164
ENSMSEG00005014	turquoise	MB	Autosome	Igfbp6	**-1.67063954741724**	**-0.891850026091222**	**-0.60725254749062**	**-1.06338699992662**	**-0.778789521326022**	-0.284597478600601
ENSMSEG00005016	turquoise	MB	Autosome	Kazald1	**-0.722346094799366**	**-0.715481278208124**	-0.43062767386921	-0.291718420930156	-0.00686481659124204	-0.284853604338914
ENSMSEG00005012	turquoise	MB	Autosome	Nrros	-0.550953062920148	-0.0890976476503219	0.205210308731011	**-0.756163371651159**	-0.461855415269826	-0.294307956381333
ENSMSEG00005015	turquoise	MB	Autosome		**-0.696736769121969**	**-0.642407922834006**	**-0.703061510449017**	0.00632474132704791	-0.0543288462879628	-0.305466772199188
ENSMSEG00005015	turquoise	MB	Autosome	As3mt	**-1.26000903051817**	**-0.839311310825088**	-0.528634327879933	**-0.731374702638232**	-0.420697719693077	-0.310676982945155
ENSMSEG00005013	turquoise	MB	Autosome	Phf7	**-0.774776713146943**	-0.374979429971621	-0.0630421236232873	**-0.711734589523656**	-0.399797283175323	-0.311937306348333
ENSMSEG00005015	turquoise	MB	Autosome	Lrrc10b	**-0.60554880046073**	-0.474865685687109	-0.161554861400334	-0.443993939060396	-0.130683114773622	-0.313310824286774
ENSMSEG00005007	turquoise	MB	Autosome	Tmem140	**-0.772644709205163**	**-0.737659131641902**	-0.422508821151667	-0.350135888053497	-0.0349855775632613	-0.315150310490235
ENSMSEG00005022	turquoise	MB	Autosome	Ufc1	**-0.837159216849404**	-0.575805388636915	-0.244321247531649	**-0.592837969317755**	-0.261353828212489	-0.331484141105266
ENSMSEG00005019	turquoise	MB	Autosome	Gchfr	**-0.77567732037097**	**-0.790143223010172**	-0.457388809275815	-0.318288511095155	0.0144659026392026	-0.332754413734357
ENSMSEG00005010	turquoise	MB	Autosome		**-1.46866865564209**	**-1.12220283966954**	**-1.07241173455263**	-0.396256921089461	-0.346465815972551	-0.333923191298744
ENSMSEG00005007	turquoise	MB	Autosome	Isg15	**-1.09262030824971**	**-0.860780991763603**	-0.52133363003442	-0.571286678215292	-0.231839316486109	-0.339447361729183
ENSMSEG00005000	turquoise	MB	Autosome	Catsper2	**-1.04405400217006**	**-0.844116543719662**	-0.490844772797076	-0.553209229372981	-0.199937458450395	-0.353271770922586
ENSMSEG00005009	turquoise	MB	Autosome	Ccdc190	**-0.699671020714599**	**-0.808225169243017**	-0.454104746452093	-0.245566274262506	0.108554148528418	-0.354120422790924
ENSMSEG00005009	turquoise	MB	Autosome	Cd59b	**-0.848190479627895**	**-1.09673344674207**	**-0.739929138884117**	-0.108261340743777	0.248542967114173	-0.35680430785795
ENSMSEG00005012	turquoise	MB	Autosome	Cd38	-0.331612079789691	-0.0776624538361251	0.288934402513167	**-0.620546482302858**	-0.253949625953566	-0.366596856349292
ENSMSEG00005011	turquoise	MB	Autosome		**-0.685513045637301**	**-0.724009845354681**	-0.498236873034568	-0.187276172602733	0.0384967997173802	-0.367810603810829

ENSMSEG00005000{	turquoise	MB	Autosome	Wfdc2	**-0.836787148883142**	-0.387864921126892	-0.0044652840389427	**-0.832321864844199**	-0.44892222775625	-0.383399637087949
ENSMSEG00005005(	turquoise	MB	Autosome	Ecscr	**-0.840736611497754**	**-0.593999644038245**	-0.210308809700985	**-0.630427801796769**	-0.246736967459509	-0.38369083433726
ENSMSEG00005007{	turquoise	MB	Autosome		**-0.61670794320702**	-0.557983389211881	-0.569826497165446	-0.0468814460415736	-0.0587245539951391	-0.398614444899277
ENSMSEG00005008(	turquoise	MB	Autosome	Ecrg4	**-0.895161164819168**	**-0.844125438306917**	-0.412442263625452	-0.482718901193716	-0.0510357265122508	-0.431683174681465
ENSMSEG00005017{	turquoise	MB	Autosome	Fhit	**-0.667997527365629**	**-1.00396029367465**	-0.560681771381579	-0.10731575598405	0.335962766309016	-0.443278522293066
ENSMSEG00005007{	turquoise	MB	Autosome	Lao1	**-1.7684075834776**	**-0.725779604688759**	-0.262915202696335	**-1.50549238078127**	**-1.04262797878884**	-0.462864401992424
ENSMSEG00005020(	turquoise	MB	Autosome	Upp1	**-1.09484009729644**	-0.53656371656135	-0.0577354522722864	**-1.03710464502415**	-0.55827638073509	-0.478828264289064
ENSMSEG00005014{	turquoise	MB	Autosome	Ifi44l	**-1.24530780489309**	**-0.912173642507922**	-0.433319795784968	**-0.811988009108121**	-0.333134162385167	-0.478853846722954
ENSMSEG00005005{	turquoise	MB	Autosome	Grhpr	**-1.20005719869295**	**-0.99390974539335**	-0.492574612995311	**-0.707482585697637**	-0.206147453299598	-0.50133513239804
ENSMSEG00005002{	turquoise	MB	Autosome		**-0.728346135917934**	-0.464411454570668	-0.581106976865705	-0.147239159052228	-0.263934681347265	-0.504419865516672
ENSMSEG00005001{	turquoise	MB	Autosome	Hmgn2	**-0.734029691510737**	**-0.659726370928486**	-0.151146018435022	-0.582883673075715	-0.0743033205822515	-0.508580352493463
ENSMSEG00005009(	turquoise	MB	Autosome	Clec2g	**-0.97854233157773**	**-0.855815810087797**	-0.33639412326937	**-0.64214820830836**	-0.122726521489933	-0.519421686818427
ENSMSEG00005012{	turquoise	MB	Autosome	Col20a1	-0.25033423159976	**-0.914892110530479**	-0.345258264905881	0.0949240333061201	**0.664557878930718**	-0.569633845624598
ENSMSEG00005008{	turquoise	MB	Autosome		**-0.961594673487017**	**-0.985128810460636**	**-0.784225684397491**	-0.177368989089526	0.0235341369736193	-0.570746717272659
ENSMSEG00005020{	turquoise	MB	Autosome	C330018D20R	**-0.660583512246449**	**-0.907196905114907**	-0.302826602544762	-0.357756909701687	0.246613392868458	**-0.604370302570145**
ENSMSEG00005016{	turquoise	MB	Autosome	Tmem216	**-0.989023684171307**	**-0.926088752054004**	-0.216104684038954	**-0.772919000132353**	-0.0629349321173027	**-0.70998406801505**
ENSMSEG00005015(	turquoise	MB	Autosome		**-0.663491360441818**	-0.547854857593592	**-0.597525204136744**	-0.0659661563050745	-0.115636502848226	**-0.740684343767084**
ENSMSEG00005008{	turquoise	MB	Autosome		**-0.904705552492152**	**-0.823604897787576**	**-0.651675006358061**	-0.253030546134092	-0.0811006547045762	**-0.875989044028854**
ENSMSEG00005020(	turquoise	MB	Autosome	Grifin	-0.49376936231806	-0.559960841838968	0.485621993359228	**-0.979391355677288**	0.066191479520908	**-1.0455828351982**
ENSMSEG00005017(	turquoise	MB	Autosome	Casq1	**-0.884723059512897**	**-1.76018340183667**	-0.388861666361187	-0.49586139315171	**0.875460342323772**	**-1.37132173547548**
ENSMSEG00005022{	turquoise	MB	Autosome	Rnf212	**-1.55628142893978**	**-1.65603086359191**	-0.0562217403676635	**-1.50005968857212**	0.0997494346521229	**-1.59980912322424**
ENSMSEG00005000{	turquoise	MB	Autosome	Tmem243	**-0.677386953143284**	-0.566236297360569	-0.566645858149496	-0.110741094993788	-0.111150655782715	0.000409560788926777
ENSMSEG00005005{	turquoise	MB	Autosome	Psmb6	**-0.741211433234698**	**-0.638018264217824**	**-0.640525454606918**	-0.10068597862778	-0.103193169016874	0.00250719038909387
ENSMSEG00005018{	turquoise	MB	Autosome	Fastkd2	**-0.631501259800371**	-0.449463231809206	-0.452061054189575	-0.179440205610796	-0.182038027991166	0.0025978223803696
ENSMSEG00005022(	turquoise	MB	Autosome	Alkbh2	**-0.752907517259173**	-0.574153279496357	-0.579016653902254	-0.17389086335692	-0.178754237762817	0.00486337440589729
ENSMSEG00005015{	turquoise	MB	Autosome	Cox4i1	**-0.837746125839855**	**-0.693892926885016**	**-0.699296741959033**	-0.138449383880822	-0.143853198954839	0.00540381507401749
ENSMSEG00005016(	turquoise	MB	Autosome	Naa20	**-0.697581273292904**	-0.539156652360865	-0.54489280191598	-0.152688471376924	-0.158424620932039	0.00573614955511522
ENSMSEG00005015{	turquoise	MB	Autosome	Psmb5	**-0.659964772246714**	-0.584809411846973	**-0.590802333911594**	-0.0691624383351205	-0.0751553603997415	0.00599292206462095
ENSMSEG00005001{	turquoise	MB	Autosome		**-2.22618553440864**	**-1.15460306818217**	-0.278614024153317	**-1.94757151025533**	**-1.07158246622647**	0.00843784191092201
ENSMSEG00005009{	turquoise	MB	Autosome	Tbca	**-0.683671667856301**	-0.475266283293406	-0.483904389132785	-0.199767278723516	-0.208405384562895	0.00863810583937863
ENSMSEG00005008(	turquoise	MB	Autosome		**-0.762636798943325**	**-0.643076641741093**	**-0.75491413537727**	-0.0077226635660544	-0.119560157202232	0.00906906368782788
ENSMSEG00005013(	turquoise	MB	Autosome	Rpl37a	**-0.96696648019602**	**-0.79529248004038**	**-0.804926739005831**	-0.162039741190189	-0.17167400015564	0.00963425896545072
ENSMSEG00005007{	turquoise	MB	Autosome		**-3.05314642967721**	-0.296014474662463	**-1.45766220382368**	**-1.59548422585353**	**-2.75713195501475**	0.00968114909236675
ENSMSEG00005007{	turquoise	MB	Autosome	Hspb11	-0.492100243600297	**-0.701888065796312**	**-0.711636805613874**	0.219536562013577	0.209787822196015	0.0097487398175616
ENSMSEG00005009(	turquoise	MB	Autosome	S100a1	**-0.660815025123965**	-0.5019266313649	-0.511678187749106	-0.14913683737486	-0.158888393759066	0.00975155638420624
ENSMSEG00005004{	turquoise	MB	Autosome	Paxx	**-0.784535045541536**	**-0.61873811659328**	**-0.630216841624561**	-0.154318203916974	-0.165796928948255	0.0114787250312807
ENSMSEG00005006(	turquoise	MB	Autosome		**-0.775921592501491**	**-0.60336032147424**	-0.543794857950115	-0.232126734551376	-0.172561271027251	0.0118431079535655
ENSMSEG00005002{	turquoise	MB	Autosome	Atpsckmt	**-0.744589845140053**	-0.427773797586143	-0.440368627759049	-0.304221217381004	-0.31681604755391	0.0125948301729062
ENSMSEG00005006{	turquoise	MB	Autosome	Gsap	-0.544404200399319	**-0.650494972344343**	**-0.663256015249915**	0.118851814850596	0.106090771945024	0.0127610429055724
ENSMSEG00005004(	turquoise	MB	Autosome	Psmg3	**-0.702297707621607**	-0.474731779366661	-0.4875181980106	-0.214779509611007	-0.227565928254946	0.0127864186439388
ENSMSEG00005007{	turquoise	MB	Autosome	Rpl27	**-0.832534180461751**	**-0.705565802283281**	**-0.71897127031936**	-0.113562910142391	-0.12696837817847	0.0134054680360795
ENSMSEG00005019(	turquoise	MB	Autosome	Serp2	**-0.632515732177876**	-0.526920404797957	-0.54141435304244	-0.0911013791354355	-0.105595327379919	0.0144939482444835
ENSMSEG00005002{	turquoise	MB	Autosome	Stard3nl	**-0.657969501966649**	-0.550069220587473	-0.565936915208655	-0.0920325867579934	-0.107900281379176	0.0158676946211827
ENSMSEG00005013(	turquoise	MB	Autosome	Leprot	**-0.852871758144094**	-0.406930313848058	-0.42294549337745	-0.429926264766644	-0.445941444296036	0.0160151795293919
ENSMSEG00005007{	turquoise	MB	Autosome	Naa38	**-0.759519744543941**	**-0.605537160145666**	**-0.621839811617526**	-0.137679932926415	-0.153982584398275	0.0163026514718593
ENSMSEG00005012(	turquoise	MB	Autosome	Gpx4	**-0.748260187474033**	**-0.608625242013364**	**-0.624930694811242**	-0.123329492662791	-0.139634945460669	0.0163054527978782
ENSMSEG00005013{	turquoise	MB	Autosome	Rasd1	**-0.644397898930098**	**-0.605973376359007**	**-0.623138427566968**	-0.0212594713631297	-0.0384245225710904	0.0171650512079608

ENSMSEG00005014	turquoise	MB	Autosome	Smim26	**-0.957893300588693**	-0.517017703710935	-0.53529151328797	-0.422601787300723	-0.440875596877758	0.018273809577035
ENSMSEG00005009	turquoise	MB	Autosome	Id1	**-0.633310547631821**	**-0.733948300365992**	**-0.752338053933846**	0.119027506302025	0.100637752734171	0.0183897535678539
ENSMSEG00005019	turquoise	MB	Autosome	Rpl5	**-0.900264773516804**	**-0.734611868599278**	**-0.753230941357952**	-0.147033832158851	-0.165652904917526	0.0186190727586742
ENSMSEG00005018	turquoise	MB	Autosome	Nat8f7	-0.352767872254335	**-0.638920162692813**	**-0.659144058083847**	0.306376185829512	0.286152290438479	0.0202238953910337
ENSMSEG00005008	turquoise	MB	Autosome	Dhrs11	**-0.587869529754248**	-0.534555537063065	-0.555155284455192	-0.0327142452990553	-0.0533139926911825	0.0205997473921273
ENSMSEG00005008	turquoise	MB	Autosome	Lamtor4	**-0.765638463897521**	-0.569273271328878	**-0.590071994123936**	-0.175566469773585	-0.196365192568642	0.0207987227950575
ENSMSEG00005005	turquoise	MB	Autosome	Rad1	**-1.10680303829319**	-0.157769762590944	-0.179230795896399	**-0.927572242396788**	**-0.949033275702243**	0.0214610333054544
ENSMSEG00005020	turquoise	MB	Autosome	Aprt	**-0.598957465890079**	-0.497479223757318	-0.520740418365131	-0.0782170475249481	-0.101478242132761	0.0232611946078131
ENSMSEG00005017	turquoise	MB	Autosome	Naca	**-0.770228637889542**	**-0.646837487423064**	**-0.670715890773446**	-0.0995127471160955	-0.123391150466477	0.0238784033503818
ENSMSEG00005011	turquoise	MB	Autosome	Rpl23	**-0.714228882669349**	-0.558661280926766	-0.582699882142935	-0.131529000526414	-0.155567601742583	0.0240386012161687
ENSMSEG00005010	turquoise	MB	Autosome	Erh	**-0.620787039125053**	-0.572154012971773	**-0.597632666696175**	-0.0231543724288782	-0.0486330261532798	0.0254786537244016
ENSMSEG00005005	turquoise	MB	Autosome	Bri3	**-0.596488574289393**	-0.429003423705961	-0.454944001425074	-0.141544572864318	-0.167485150583431	0.0259405777191131
ENSMSEG00005021	turquoise	MB	Autosome	Acot13	**-0.626578181335081**	-0.520437792339769	-0.546430023950525	-0.080148157384556	-0.106140388995312	0.0259922316107561
ENSMSEG00005000	turquoise	MB	Autosome	Dgcr6	**-0.647462546267676**	**-0.593238716461317**	**-0.619495333631703**	-0.0279672126359731	-0.0542238298063593	0.0262566171703862
ENSMSEG00005012	turquoise	MB	Autosome	Snrnp25	**-0.636467223192604**	-0.535607991195735	-0.562294778244624	-0.0741724449479801	-0.10085923199687	0.0266867870488895
ENSMSEG00005000	turquoise	MB	Autosome		**-1.14997259000062**	-0.566154593670719	**-0.709781645329581**	-0.440190944671034	-0.583817996329897	0.0268276057356171
ENSMSEG00005003	turquoise	MB	Autosome	Rpl7	**-0.636320667899897**	-0.560672731920005	**-0.588857124218319**	-0.0474635436815778	-0.0756479359798921	0.0281843922983144
ENSMSEG00005001	turquoise	MB	Autosome	Rpl32	**-0.96886290824064**	**-0.78843430250159**	**-0.817827600365976**	-0.151035307874663	-0.18042860573905	0.0293932978643866
ENSMSEG00005007	turquoise	MB	Autosome	Ntan1	**-0.612827192810926**	-0.496613667926308	-0.526947939426908	-0.0858792533840183	-0.116213524884618	0.0303342715005998
ENSMSEG00005013	turquoise	MB	Autosome	Nkain4	**-0.768029456933308**	-0.447289625079648	-0.478498111953572	-0.289531344979736	-0.32073983185366	0.0312084868739239
ENSMSEG00005020	turquoise	MB	Autosome	Mrpl15	**-0.666421635414274**	-0.447744974738462	-0.479110046269989	-0.187311589144286	-0.218676660675812	0.0313650715315268
ENSMSEG00005005	turquoise	MB	Autosome	Rnf139	**-0.793976238144058**	**-0.635486781385143**	**-0.666935937378485**	-0.127040300765573	-0.158489456758915	0.031449155993342
ENSMSEG00005014	turquoise	MB	Autosome	Slc25a33	**-0.667445581061184**	-0.521750075475078	-0.55367399555737	-0.113771585503814	-0.145695505586106	0.0319239200822919
ENSMSEG00005010	turquoise	MB	Autosome	Atp5e	**-1.06402289088856**	**-0.852507461003064**	**-0.884768525947794**	-0.179254364940765	-0.211515429885496	0.0322610649447302
ENSMSEG00005021	turquoise	MB	Autosome	Surf1	**-0.753803892734802**	**-0.619255707886777**	**-0.652958472061983**	-0.10084542067282	-0.134548184848025	0.0337027641752057
ENSMSEG00005005	turquoise	MB	Autosome	Rpl19	**-0.858085486598024**	**-0.680987862651382**	**-0.715161045399233**	-0.142924441198791	-0.177097623946642	0.034173182747851
ENSMSEG00005018	turquoise	MB	Autosome	Slc25a34	**-1.48744598495824**	-0.566367238072586	**-0.600649641229192**	**-0.88679634372905**	**-0.921078746885657**	0.0342824031566065
ENSMSEG00005015	turquoise	MB	Autosome	Cops9	**-0.97778351704174**	**-0.650772080940461**	**-0.685912859272587**	-0.291870657769153	-0.327011436101279	0.0351407783321267
ENSMSEG00005003	turquoise	MB	Autosome		**-0.593664184213824**	-0.529691986346483	-0.453241437013281	-0.140422747200543	-0.0639721978673412	0.0361637898105637
ENSMSEG00005022	turquoise	MB	Autosome		**-0.589082401271015**	-0.459984896196955	-0.435851221786023	-0.153231179484992	-0.12909750507406	0.0364614008415811
ENSMSEG00005000	turquoise	MB	Autosome	Fkbp11	-0.573481263943416	-0.580837081470143	**-0.617899625410605**	0.044418361467189	0.00735581752672696	0.037062543940462
ENSMSEG00005022	turquoise	MB	Autosome	Stmn1	**-0.632304873581315**	-0.41942848514008	-0.456525357407048	-0.175779516174267	-0.212876388441234	0.0370968722669678
ENSMSEG00005014	turquoise	MB	Autosome	Emc7	**-0.588792286393958**	-0.42408551242383	-0.461693727889322	-0.127098558504637	-0.164706773970128	0.0376082154654915
ENSMSEG00005007	turquoise	MB	Autosome	Rnd2	**-0.635273292224482**	-0.490543980321522	-0.528932470711509	-0.106340821512973	-0.14472931190296	0.0383884903899864
ENSMSEG00005012	turquoise	MB	Autosome		**-0.897241249128388**	**-0.749888185786344**	**-0.913889600879592**	0.0166483517512041	-0.147353063342045	0.0386340844055158
ENSMSEG00005010	turquoise	MB	Autosome	Abcg2	**-0.716810003637021**	-0.529716052290116	-0.569378767883628	-0.147431235753394	-0.187093951346905	0.0396627155935114
ENSMSEG00005010	turquoise	MB	Autosome	Nr1h3	-0.366782864507397	**-0.626699660476659**	**-0.666607258847827**	0.29982439434043	0.259916795969263	0.0399075983711672
ENSMSEG00005008	turquoise	MB	Autosome	Prdx1	**-0.737005442467546**	-0.5273578337138	-0.568829620000079	-0.168175822467466	-0.209647608753746	0.0414717862862798
ENSMSEG00005011	turquoise	MB	Autosome	Sec61g	**-0.986337118889432**	**-0.733930880776722**	**-0.775423905884157**	-0.210913213005275	-0.25240623811271	0.0414930251074348
ENSMSEG00005012	turquoise	MB	Autosome	Rpl9-ps6	**-1.12185860409895**	**-0.880691899992355**	**-0.92351713635739**	-0.198341467741565	-0.241166704106599	0.0428252363650345
ENSMSEG00005015	turquoise	MB	Autosome	Micos10	**-0.72750219191972**	-0.512785640165967	-0.555677719753837	-0.171824472165883	-0.214716551753752	0.0428920795878699
ENSMSEG00005017	turquoise	MB	Autosome	Smim18	**-0.678067942596589**	-0.523078501332986	-0.566293165908871	-0.111774776687718	-0.154989441263603	0.0432146645758851
ENSMSEG00005007	turquoise	MB	Autosome	Tmem256	**-0.874135386157939**	**-0.684208429663482**	**-0.727428040598972**	-0.146707345558967	-0.189926956494457	0.0432196109354897
ENSMSEG00005014	turquoise	MB	Autosome	Polr2e	-0.549882977075942	-0.573659278569252	**-0.617251697123745**	0.0673687200478033	0.0237763014933103	0.043592418554493
ENSMSEG00005015	turquoise	MB	Autosome		**-0.885414804573981**	**-0.727936409869555**	**-0.754764015605172**	-0.130650788968809	-0.157478394704427	0.0446120717266464
ENSMSEG00005007	turquoise	MB	Autosome	Cyb5a	**-0.756821846113811**	-0.523795436580582	-0.568740026079216	-0.188081820034595	-0.233026409533229	0.0449445894986341
ENSMSEG00005019	turquoise	MB	Autosome		**-1.11167291818982**	**-0.779044480056937**	**-0.93275135545288**	-0.178921562736936	-0.33262843813288	0.045687107182509

ENSMSEG00005002	turquoise	MB	Autosome	Sdhb	**-0.614145714429116**	-0.466851049491699	-0.513319608331036	-0.10082610609808	-0.147294664937417	0.0464685588393367
ENSMSEG00005020	turquoise	MB	Autosome	Txndc9	**-0.629700534115579**	-0.386947497172055	-0.433915253070772	-0.195785281044807	-0.242753036943524	0.0469677558987174
ENSMSEG00005021	turquoise	MB	Autosome	Eif2s2	**-0.606575990578989**	-0.412049585774904	-0.459467468857874	-0.147108521721116	-0.194526404804085	0.0474178830829692
ENSMSEG00005015	turquoise	MB	Autosome	Bad	**-0.585836244077611**	-0.499289911413448	-0.546995556516433	-0.0388406875611781	-0.0865463326641629	0.0477056451029847
ENSMSEG00005000	turquoise	MB	Autosome		**-4.49705004730163**	**-1.2694988642823**	**-3.17436030860425**	**-1.32268973869738**	**-3.22755118301933**	0.0484164910010525
ENSMSEG00005003	turquoise	MB	Autosome		**-1.81221313067091**	-0.473919574501018	**-1.00474285485431**	**-0.807470275816595**	**-1.33829355616989**	0.0485832664034238
ENSMSEG00005003	turquoise	MB	Autosome	Cox7c	**-0.810731584178099**	**-0.640931144287469**	**-0.689715910484476**	-0.121015673693624	-0.16980043989063	0.0487847661970064
ENSMSEG00005008	turquoise	MB	Autosome		**-0.810003460042821**	-0.250123144707796	-0.121013783923758	**-0.688989676119063**	-0.559880315335025	0.049670346543152
ENSMSEG00005011	turquoise	MB	Autosome	Ndufb2	**-1.08672757566543**	**-1.05529106103416**	**-1.10504870751008**	0.0183211318446513	-0.0314365146312703	0.0497576464759215
ENSMSEG00005002	turquoise	MB	Autosome		**-0.65683037118111**	-0.549463540747564	-0.535412170559306	-0.121418200621804	-0.107366830433546	0.0501094572576351
ENSMSEG00005000	turquoise	MB	Autosome		**-0.626747576151548**	-0.394108742267869	-0.366211003474317	-0.260536572677231	-0.232638833883678	0.0502882248128618
ENSMSEG00005015	turquoise	MB	Autosome	Polr3k	**-0.624267588717692**	-0.333995091486881	-0.38452437620455	-0.239743212513142	-0.290272497230811	0.0505292847176692
ENSMSEG00005002	turquoise	MB	Autosome	Slirp	**-0.702076763153572**	**-0.615796649774774**	**-0.666528505899412**	-0.0355482572541602	-0.0862801133787981	0.0507318561246379
ENSMSEG00005012	turquoise	MB	Autosome	Prxl2a	**-0.863795314732112**	**-0.661449065247638**	**-0.712345237982662**	-0.15145007674945	-0.202346249484474	0.0508961727350243
ENSMSEG00005020	turquoise	MB	Autosome	Rpl6	**-0.796045981013072**	**-0.67547657181689**	**-0.726674457115735**	-0.0693715238973363	-0.120569409196182	0.0511978852988458
ENSMSEG00005019	turquoise	MB	Autosome		-0.281635896748375	-0.530587425255846	**-0.648335026082103**	0.366699129333728	0.248951528507471	0.0522420274463768
ENSMSEG00005018	turquoise	MB	Autosome		**-0.894831137835626**	**-0.652695123110352**	**-0.727779787399217**	-0.167051350436409	-0.242136014725274	0.0558377462877545
ENSMSEG00005009	turquoise	MB	Autosome	Gm6993	**-0.596713706783394**	-0.360936526697747	-0.417187946111743	-0.179525760671651	-0.235777180085647	0.0562514194139959
ENSMSEG00005019	turquoise	MB	Autosome	Abracl	**-0.739223364830295**	-0.547714324790012	**-0.604134157615668**	-0.135089207214627	-0.191509040040283	0.0564198328256562
ENSMSEG00005012	turquoise	MB	Autosome	Ndufs5	**-0.834011768247747**	**-0.638383115087893**	**-0.696145410359708**	-0.13786635788804	-0.195628653159854	0.0577622952718146
ENSMSEG00005016	turquoise	MB	Autosome	Med21	**-0.600606293764135**	-0.531981976264857	**-0.591141410312108**	-0.00946488345202763	-0.0686243174992782	0.0591594340472506
ENSMSEG00005017	turquoise	MB	Autosome	Mrpl32	-0.57635665652286	-0.542445952831141	**-0.60236002603101**	0.0260033695081491	-0.0339107036917195	0.0599140731998686
ENSMSEG00005003	turquoise	MB	Autosome	Ten1	**-0.676083524317821**	-0.505279316312681	-0.565677311618986	-0.110406212698835	-0.17080420800514	0.0603979953063056
ENSMSEG00005000	turquoise	MB	Autosome		**-1.63989593110251**	**-1.06283075223935**	**-0.825584114633481**	**-0.814311816469033**	-0.57706517886316	0.0606535876150107
ENSMSEG00005009	turquoise	MB	Autosome	Eif3m	**-0.714574671048443**	-0.579642300750644	**-0.640823399071834**	-0.0737512719766092	-0.134932370297799	0.0611810983211903
ENSMSEG00005010	turquoise	MB	Autosome	Rapsn	**-0.845135277869704**	**-0.747092239443022**	**-0.808846282401563**	-0.0362889954681406	-0.0980430384266814	0.0617540429585408
ENSMSEG00005018	turquoise	MB	Autosome	Gm11808	**-0.839960399284792**	**-0.585863155494413**	**-0.648340356171209**	-0.191620043113584	-0.25409724379038	0.0624772006767961
ENSMSEG00005013	turquoise	MB	Autosome	Lamtor5	**-0.620116127223046**	-0.423743485607269	-0.487725197422986	-0.13239092980006	-0.196372641615777	0.0639817118157173
ENSMSEG00005021	turquoise	MB	Autosome	Castor1	**-0.650240476542903**	-0.448479347161099	-0.513216775285568	-0.137023701257334	-0.201761129381804	0.0647374281244695
ENSMSEG00005019	turquoise	MB	Autosome	Atp5k	**-0.752262080578615**	-0.58311282045293	**-0.648158314934819**	-0.104103765643796	-0.169149260125684	0.0650454944818884
ENSMSEG00005004	turquoise	MB	Autosome	Itpa	**-0.84727779664398**	-0.498863183765082	-0.564150484396115	-0.283127312247866	-0.348414612878898	0.0652873006310324
ENSMSEG00005005	turquoise	MB	Autosome	Egfl7	-0.572103013424423	-0.519832328628468	**-0.585920147050281**	0.0138171336258578	-0.0522706847959553	0.066087818421813
ENSMSEG00005012	turquoise	MB	Autosome	Swi5	**-0.604090592804143**	-0.501425400089605	-0.567666191684186	-0.0364244011199573	-0.102665192714538	0.0662407915945805
ENSMSEG00005016	turquoise	MB	Autosome	Nhp2	**-0.592693070028563**	-0.531129891074196	**-0.597504940238189**	0.00481187020962649	-0.0615631789543673	0.0663750491639938
ENSMSEG00005003	turquoise	MB	Autosome	Tomm7	**-0.809515759919533**	-0.552033276843044	**-0.618461333421098**	-0.191054426498435	-0.257482483076489	0.0664280565780539
ENSMSEG00005008	turquoise	MB	Autosome	Rpl35	**-0.824778052291649**	**-0.680213645143962**	**-0.747350115859802**	-0.0774279364318472	-0.144564407147687	0.0671364707158398
ENSMSEG00005019	turquoise	MB	Autosome	Pradc1	**-0.645626283561731**	-0.43012404110871	-0.498049163275416	-0.147577120286315	-0.215502242453021	0.067925122166706
ENSMSEG00005005	turquoise	MB	Autosome	Fam83d	**-1.47303062765373**	**-1.56824771720672**	**-1.63820570602056**	0.165175078366834	0.0952170895529871	0.0699579888138473
ENSMSEG00005003	turquoise	MB	Autosome	Ndufa13	**-0.71809719494568**	-0.571465795397882	**-0.642887769100705**	-0.0752094258449747	-0.146631399547798	0.0714219737028229
ENSMSEG00005014	turquoise	MB	Autosome	Rpl31	**-1.0225407871602**	**-0.804649492002302**	**-0.878793251652417**	-0.143747535507784	-0.217891295157898	0.0741437596501147
ENSMSEG00005015	turquoise	MB	Autosome		**-0.662281205735683**	-0.48517846239542	**-0.639482038492227**	-0.0227991672434565	-0.177102743340263	0.0743044011082673
ENSMSEG00005018	turquoise	MB	Autosome		**-0.724850514982206**	**-0.763534677370838**	-0.395724073560009	-0.329126441422197	0.0386841623886325	0.0750846642888648
ENSMSEG00005014	turquoise	MB	Autosome	Gm44502	**-0.615692935723129**	-0.418660567266213	-0.495211444184818	-0.120481491538311	-0.197032368456916	0.0765508769186051
ENSMSEG00005003	turquoise	MB	Autosome	Mrpl47	**-0.612658321074603**	-0.442674309006957	-0.519750223903579	-0.0929080971710246	-0.169984012067646	0.0770759148966219
ENSMSEG00005023	turquoise	MB	Autosome	Ndufb7	**-0.592450010285634**	-0.53217794287359	**-0.610685302988504**	0.0182352927028703	-0.0602720674120439	0.0785073601149142
ENSMSEG00005008	turquoise	MB	Autosome	Tefm	**-0.849833860375834**	**-0.598132269583292**	**-0.676974384261546**	-0.172859476114288	-0.251701590792542	0.0788421146782537
ENSMSEG00005022	turquoise	MB	Autosome	Mgst3	**-0.625099232855134**	-0.523179645736192	**-0.602486099315202**	-0.0226131335399319	-0.101919587118942	0.0793064535790104

ENSMSEG00005010	turquoise	MB	Autosome	Nenf	**-0.93230920839868**	**-0.685457606960216**	**-0.76520595154906**	-0.16710325684962	-0.246851601438464	0.0797483445888444
ENSMSEG00005005	turquoise	MB	Autosome	Tomm5	**-0.697933583509422**	-0.561180817987344	**-0.641805380294121**	-0.0561282032153005	-0.136752765522077	0.0806245623067768
ENSMSEG00005008	turquoise	MB	Autosome	Rpl21	**-0.732267376016969**	**-0.597980497246888**	**-0.678647932015553**	-0.053619444001416	-0.134286878770081	0.0806674347686653
ENSMSEG00005020	turquoise	MB	Autosome	Pcp2	**-0.684193123183886**	-0.450115812763557	-0.532127127552869	-0.152065995631017	-0.234077310420329	0.0820113147893117
ENSMSEG00005022	turquoise	MB	Autosome		**-0.59857488874654**	-0.496547584718275	-0.464482601453166	-0.134092287293374	-0.102027304028264	0.0830208110932291
ENSMSEG00005011	turquoise	MB	Autosome	Ndufaf6	**-0.778102522941959**	-0.445264405772226	-0.53066253977072	-0.247439983171239	-0.332838117169733	0.0853981339984937
ENSMSEG00005011	turquoise	MB	Autosome		**-0.711284728399316**	**-0.604100103634006**	-0.512130178585293	-0.199154549814023	-0.10718462476531	0.0857228918095005
ENSMSEG00005005	turquoise	MB	Autosome	Rps14	**-1.10372560198509**	**-0.927042858343731**	**-1.01290527060809**	-0.090820331377	-0.17668274364136	0.0858624122643604
ENSMSEG00005002	turquoise	MB	Autosome	Mrpl41	**-0.710219858437815**	-0.567002176964215	**-0.653459172686143**	-0.0567606857516722	-0.1432176814736	0.0864569957219276
ENSMSEG00005012	turquoise	MB	Autosome	Commd1	-0.558791670797733	-0.510841612673205	**-0.598746609991911**	0.0399549391941779	-0.0479500581245272	0.0879049973187051
ENSMSEG00005018	turquoise	MB	Autosome	Rps26	-0.513410407001642	-0.522467040199526	**-0.611324019158981**	0.09791361215734	0.00905663319788435	0.0888569789594556
ENSMSEG00005019	turquoise	MB	Autosome	Tipin	-0.555597402475525	**-0.597849784057815**	**-0.68872688038868**	0.133129477913155	0.0422523815822892	0.0908770963308657
ENSMSEG00005002	turquoise	MB	Autosome	Rps20	**-1.09400826413331**	**-0.762284452956376**	**-0.853168047286426**	-0.24084021684688	-0.33172381117693	0.0908835943300502
ENSMSEG00005008	turquoise	MB	Autosome	Ndufa4	**-0.776689064642971**	-0.569359694609304	**-0.661587171574628**	-0.115101893068343	-0.207329370033667	0.0922274769653244
ENSMSEG00005010	turquoise	MB	Autosome	Guf1	**-0.650979111010412**	-0.408303852885808	-0.50150738234924	-0.149471728661173	-0.242675258124604	0.0932035294634313
ENSMSEG00005017	turquoise	MB	Autosome	Efcab10	**-0.986267604188063**	**-0.992878311580968**	**-1.08993990146462**	0.103672297276556	0.00661070739290505	0.097061589883651
ENSMSEG00005016	turquoise	MB	Autosome	Gins2	**-0.591360625577968**	-0.54920565759948	**-0.646809374369977**	0.0554487487920089	-0.042154967978488	0.0976037167704969
ENSMSEG00005000	turquoise	MB	Autosome	Mbip	**-0.590658781780038**	-0.41738111190076	-0.515270800410334	-0.075387981369704	-0.173277669879278	0.0978896885095736
ENSMSEG00005006	turquoise	MB	Autosome	Slc18b1	**-0.663294054408367**	-0.269747997377747	-0.367777261899409	-0.295516792508957	-0.393546057030619	0.0980292645216619
ENSMSEG00005016	turquoise	MB	Autosome	Mgp	**-0.799714894925599**	**-0.592250422443711**	**-0.690558620422598**	-0.109156274503001	-0.207464472481888	0.0983081979788875
ENSMSEG00005018	turquoise	MB	Autosome	Tprkb	**-0.977739333031677**	-0.350411965204231	-0.449502193308236	-0.52823713972344	**-0.627327367827445**	0.0990902281040049
ENSMSEG00005001	turquoise	MB	Autosome	Coprs	**-0.614269382922529**	-0.467529070784916	-0.568026057110961	-0.0462433258115685	-0.146740312137613	0.100496986326044
ENSMSEG00005007	turquoise	MB	Autosome	Dtwd1	**-0.671610567455458**	-0.338996380772904	-0.439735472551645	-0.231875094903813	-0.332614186682553	0.10073909177874
ENSMSEG00005015	turquoise	MB	Autosome		**-1.31055094787845**	**-0.79069182713804**	**-1.78751336396604**	0.476962416087594	-0.519859120740411	0.101965361045409
ENSMSEG00005006	turquoise	MB	Autosome	Ccl27a	**-0.709346832169461**	-0.565795370908847	**-0.668938155904516**	-0.040408676264945	-0.143551461260615	0.10314278499567
ENSMSEG00005006	turquoise	MB	Autosome	Psmb10	-0.567280598587036	-0.544697026282958	**-0.649347777465693**	0.0820671788786564	-0.0225835723040786	0.104650751182735
ENSMSEG00005004	turquoise	MB	Autosome		**-0.815030558429097**	**-0.663026390731589**	**-0.69948779157317**	-0.115542766855927	-0.152004167697508	0.104938726295356
ENSMSEG00005009	turquoise	MB	Autosome	Rpa3	**-0.791659477352904**	**-0.609617244643664**	**-0.716620803128311**	-0.0750386742245932	-0.18204223270924	0.107003558484647
ENSMSEG00005011	turquoise	MB	Autosome	Atp6v1f	**-0.655655473188859**	**-0.591960374054877**	**-0.699052514399438**	0.0433970412105789	-0.0636950991339816	0.107092140344561
ENSMSEG00005009	turquoise	MB	Autosome	Gm128	**-0.909066248279756**	-0.504326527559343	**-0.611739477065637**	-0.297326771214119	-0.404739720720413	0.107412949506294
ENSMSEG00005020	turquoise	MB	Autosome	Rpl31	**-0.924294176910463**	**-0.683765509814332**	**-0.79245727883421**	-0.131836898076252	-0.24052866709613	0.108691769019878
ENSMSEG00005020	turquoise	MB	Autosome	Snrpe	**-0.68688321422312**	-0.50118683987921	**-0.61002885116908**	-0.0768543630540403	-0.18569637434391	0.10884201128987
ENSMSEG00005013	turquoise	MB	Autosome	Cartpt	-0.439747019100488	-0.499000239895431	**-0.608435898714542**	0.168688879614055	0.0592532207949433	0.109435658819111
ENSMSEG00005020	turquoise	MB	Autosome	Rps27a	**-0.913531570637954**	**-0.716294364814929**	**-0.826424200165979**	-0.0871073704719743	-0.197237205823025	0.11012983535105
ENSMSEG00005006	turquoise	MB	Autosome	Chchd1	**-0.887183202504199**	**-0.637382926686739**	**-0.747552609020529**	-0.13963059348367	-0.24980027581746	0.11016968233379
ENSMSEG00005018	turquoise	MB	Autosome	Gm20390	**-0.684300604690175**	-0.56443360865114	**-0.675751212883288**	-0.00854939180688676	-0.119866996039035	0.111317604232149
ENSMSEG00005004	turquoise	MB	Autosome		**-0.719447464101503**	-0.524491744416665	-0.480204865280288	-0.239242598821215	-0.194955719684838	0.111837493636177
ENSMSEG00005014	turquoise	MB	Autosome	Cox6c	**-0.80904411569432**	**-0.616919066651979**	**-0.729039964779967**	-0.0800041509143533	-0.192125049042341	0.112120898127988
ENSMSEG00005005	turquoise	MB	Autosome	Rpl26	**-0.775942609732505**	**-0.62943783197924**	**-0.742143856860854**	-0.0337987528716513	-0.146504777753265	0.112706024881614
ENSMSEG00005004	turquoise	MB	Autosome	Snrpd1	**-0.62980913428494**	-0.411963420787471	-0.526277116266058	-0.103532018018882	-0.21784571349747	0.114313695478588
ENSMSEG00005009	turquoise	MB	Autosome	Snrpf	**-0.602228236010564**	-0.453324751336362	-0.567819985048249	-0.0344082509623148	-0.148903484674202	0.114495233711887
ENSMSEG00005015	turquoise	MB	Autosome	Siva1	-0.37293884072897	**-0.660008129459629**	**-0.775010723179626**	0.402071882450656	0.287069288730659	0.115002593719997
ENSMSEG00005007	turquoise	MB	Autosome	Rpl11	**-0.877185497721656**	**-0.699480032875537**	**-0.814819781931649**	-0.0623657157900066	-0.177705464846119	0.115339749056112
ENSMSEG00005006	turquoise	MB	Autosome		**-0.63538531705276**	-0.548609494266824	-0.450721634802633	-0.184663682250127	-0.0867758227859363	0.116695522295037
ENSMSEG00005002	turquoise	MB	Autosome		**-1.10217558254691**	**-1.2490090433148**	**-1.33202985440803**	0.229854271861129	0.1468334607679	0.117747600826257
ENSMSEG00005021	turquoise	MB	Autosome	Adi1	**-0.610300658848736**	-0.376958237772685	-0.496102034442009	-0.114198624406727	-0.233342421076051	0.119143796669324
ENSMSEG00005016	turquoise	MB	Autosome	Wfdc1	**-0.89597088488757**	**-0.614933040795977**	**-0.735016135016487**	-0.160954749871083	-0.281037844091594	0.12008309422051

ENSMSEG00005021	turquoise	MB	Autosome	Mrps28	**-0.60773034181251**	-0.413316184755372	-0.533736239837938	-0.0739941019745715	-0.194414157057138	0.120420055082566
ENSMSEG00005005	turquoise	MB	Autosome	Slc26a10	-0.569613468039441	-0.540061907294337	**-0.664788551226234**	0.0951750831867931	-0.0295515607451034	0.124726643931897
ENSMSEG00005018	turquoise	MB	Autosome		**-0.74878375899877**	**-0.904611484692343**	**-0.738968369974395**	-0.0098153890243749	0.155827725693573	0.124835260482115
ENSMSEG00005011	turquoise	MB	Autosome	Lamtor2	**-0.627838658007556**	-0.482291883738302	**-0.607805758296689**	-0.0200328997108671	-0.145546774269254	0.125513874558387
ENSMSEG00005018	turquoise	MB	Autosome	Hddc2	**-0.98641650369119**	**-0.674176566845496**	**-0.802830241220445**	-0.183586262470746	-0.312239936845695	0.128653674374949
ENSMSEG00005006	turquoise	MB	Autosome	Rps12	**-0.879135453646865**	**-0.692217395878958**	**-0.826633468046917**	-0.0525019855999479	-0.186918057767907	0.134416072167959
ENSMSEG00005012	turquoise	MB	Autosome	Pigx	**-0.663844210793637**	-0.437747848966605	-0.572705793016317	-0.0911384177773203	-0.226096361827032	0.134957944049712
ENSMSEG00005001	turquoise	MB	Autosome	Rps28	**-0.629661723945125**	**-0.65925497287947**	**-0.79603490824438**	0.166373184299256	0.0295932489343453	0.13677993536491
ENSMSEG00005006	turquoise	MB	Autosome	Lrrc23	**-0.64377602774483**	-0.145462512967568	-0.284333122228064	-0.359442905516765	-0.498313514777262	0.138870609260496
ENSMSEG00005017	turquoise	MB	Autosome	Mrnip	**-0.661361229347452**	**-0.591358927754166**	**-0.730433307234011**	0.0690720778865594	-0.070002301593286	0.139074379479845
ENSMSEG00005016	turquoise	MB	Autosome	Ndufb8	**-0.86242755548692**	**-0.593268801919563**	**-0.733363281610015**	-0.129064273876906	-0.269158753567358	0.140094479690452
ENSMSEG00005007	turquoise	MB	Autosome	Rpl22l1	**-1.20970570213845**	**-0.833357275173692**	**-0.973624101474753**	-0.236081600663692	-0.376348426964754	0.140266826301062
ENSMSEG00005004	turquoise	MB	Autosome	Eva1a	**-0.678688931670005**	-0.416368434094034	-0.556787775106742	-0.121901156563263	-0.262320497575971	0.140419341012708
ENSMSEG00005000	turquoise	MB	Autosome		-0.542786221689369	-0.486240042663405	**-0.69174794986016**	0.148961728170791	-0.0565461790259635	0.143627051658862
ENSMSEG00005001	turquoise	MB	Autosome	Ndufb6	**-0.753773815521917**	-0.557620964189059	**-0.701739274623997**	-0.05203454089792	-0.196152851332858	0.144118310434938
ENSMSEG00005022	turquoise	MB	Autosome	Wdr83	-0.520491860548137	-0.505553371156073	**-0.650640660126447**	0.13014879957831	-0.0149384893920636	0.145087288970374
ENSMSEG00005018	turquoise	MB	Autosome	Rwdd1	**-0.609208722025122**	-0.356341708867052	-0.504258455510149	-0.104950266514973	-0.252867013158071	0.147916746643097
ENSMSEG00005009	turquoise	MB	Autosome		**-1.31878718014806**	**-1.06534724868229**	**-1.04036298516723**	-0.278424194980833	-0.253439931465775	0.148124097251608
ENSMSEG00005020	turquoise	MB	Autosome	Rps21	**-0.899591160613237**	**-0.753114049255184**	**-0.902342837149815**	0.00275167653657807	-0.146477111358053	0.149228787894631
ENSMSEG00005018	turquoise	MB	Autosome	Mpv17	-0.482645760606738	-0.4990202601533	**-0.652238267775034**	0.169592507168297	0.0163744995465621	0.153218007621735
ENSMSEG00005010	turquoise	MB	Autosome		**-0.924842760153076**	**-1.06103455906357**	-0.556614693546895	-0.36822806660618	0.136191798910492	0.153706875395944
ENSMSEG00005010	turquoise	MB	Autosome		**-0.754165859344061**	-0.104767583702635	-0.457205687752754	-0.296960171591307	**-0.649398275641426**	0.154303576096807
ENSMSEG00005012	turquoise	MB	Autosome	Rpl8	-0.531216748287164	-0.453461875961797	**-0.607804931189733**	0.0765881829025692	-0.077754872325367	0.154343055227936
ENSMSEG00005004	turquoise	MB	Autosome	Ndufaf5	**-0.701920889596096**	**-0.761873933039066**	**-0.918381609180443**	0.216460719584347	0.0599530434429697	0.156507676141378
ENSMSEG00005010	turquoise	MB	Autosome	Mgst1	**-0.880121336534623**	-0.553311816862061	**-0.711333982540491**	-0.168787353994132	-0.326809519672562	0.15802216567843
ENSMSEG00005010	turquoise	MB	Autosome	Mpc2	**-0.624184327816778**	-0.462958739702756	**-0.623232169239721**	-0.000952158577057115	-0.161225588114022	0.160273429536964
ENSMSEG00005004	turquoise	MB	Autosome	Rpl13	**-1.52953358873813**	**-1.30645485404061**	**-1.79099205712447**	0.261458468386343	-0.223078734697513	0.160320430967752
ENSMSEG00005012	turquoise	MB	Autosome	Mrps18c	**-0.998320955580861**	**-0.716419245481802**	**-0.878568185369225**	-0.119752770211637	-0.28190171009906	0.162148939887423
ENSMSEG00005005	turquoise	MB	Autosome		**-0.910425306285471**	-0.57400721787214	-0.380953381305904	-0.529471924979567	-0.336418088413331	0.164001415093249
ENSMSEG00005004	turquoise	MB	Autosome	Adprhl1	**-1.21853213599923**	0.00502505888772339	-0.161431061073064	**-1.05710107492616**	**-1.22355719488695**	0.166456119960787
ENSMSEG00005015	turquoise	MB	Autosome	1700123O20R	-0.512404973805306	-0.523829224325687	**-0.692396749865521**	0.179991776060216	0.0114242505203817	0.168567525539834
ENSMSEG00005013	turquoise	MB	Autosome	Ido2	**-1.00156284178516**	-0.18834895996738	-0.357271694589186	**-0.64429114719597**	**-0.813213881817776**	0.168922734621806
ENSMSEG00005017	turquoise	MB	Autosome	Acy3	-0.481188841269279	-0.435200563971407	**-0.605015257086007**	0.123826415816729	-0.045988277297872	0.169814693114601
ENSMSEG00005000	turquoise	MB	Autosome	Ndufb1	**-0.913378526023112**	**-0.616685191009009**	**-0.789491447828394**	-0.123887078194717	-0.296693335014102	0.172806256819385
ENSMSEG00005008	turquoise	MB	Autosome	Rps23	**-1.05233811328781**	**-0.86001043017534**	**-0.827105513866996**	-0.225232599420818	-0.192327683112474	0.176113330799357
ENSMSEG00005009	turquoise	MB	Autosome	S100a6	**-1.2658800937816**	**-0.808562367251661**	**-0.985370131284058**	-0.28050996249754	-0.457317726529937	0.176807764032397
ENSMSEG00005016	turquoise	MB	Autosome		**-0.73731828795865**	**-0.653679150406805**	**-0.662116992317727**	-0.075201295640923	-0.083639137551845	0.177137305550076
ENSMSEG00005014	turquoise	MB	Autosome	Tnnc1	**-0.628853442503318**	-0.506108508860601	**-0.684457745578839**	0.0556043030755212	-0.122744933642718	0.178349236718239
ENSMSEG00005010	turquoise	MB	Autosome	Fau	**-0.738269091337753**	**-0.675511149013091**	**-0.85414039090539**	0.115871299567636	-0.062757942324662	0.178629241892298
ENSMSEG00005010	turquoise	MB	Autosome	Rad51ap1	**-0.705796503614124**	0.0192452743227585	-0.159862263785794	-0.54593423982833	**-0.725041777936883**	0.179107538108552
ENSMSEG00005005	turquoise	MB	Autosome	Brix1	**-0.969927033768367**	-0.198233058363628	-0.3792686854713	**-0.590658348297066**	**-0.771693975404739**	0.181035627107672
ENSMSEG00005004	turquoise	MB	Autosome	Tyw5	-0.479530872160121	-0.468860940309404	**-0.650709438795942**	0.171178566635821	-0.0106699318507165	0.181848498486538
ENSMSEG00005017	turquoise	MB	Autosome	Atp5o	**-0.641395676351055**	-0.424245907852156	**-0.608296992532644**	-0.0330986838184108	-0.217149768498899	0.184051084680488
ENSMSEG00005019	turquoise	MB	Autosome	Rpl30	**-0.724773439312925**	**-0.798586450390044**	**-0.986451963255094**	0.261678523942169	0.0738130110771186	0.18786551286505
ENSMSEG00005007	turquoise	MB	Autosome	Sdf2	**-0.764278732609903**	-0.475125249121716	**-0.663217799500115**	-0.101060933109788	-0.289153483488187	0.188092550378399
ENSMSEG00005004	turquoise	MB	Autosome	Ube2t	**-0.768207398147026**	-0.556546090193312	**-0.748926767263332**	-0.019280630883694	-0.211661307953715	0.192380677070021
ENSMSEG00005006	turquoise	MB	Autosome	Snrpd3	**-0.619688379428403**	-0.376206834965499	-0.574711258628512	-0.0449771207998915	-0.243481544462904	0.198504423663013

ENSMSEG00005014	turquoise	MB	Autosome		**-0.958954149550281**	-0.444768064972628	-0.546733426018036	-0.412220723532245	-0.514186084577653	0.203203728604981
ENSMSEG00005015	turquoise	MB	Autosome		**-0.609670219616742**	-0.538308356722673	-0.507045894115093	-0.102624325501649	-0.0713618628940696	0.205507907196755
ENSMSEG00005016	turquoise	MB	Autosome	Haus1	**-0.867489548843513**	-0.323804351080044	-0.533878154211479	-0.333611394632033	-0.543685197763469	0.210073803131435
ENSMSEG00005009	turquoise	MB	Autosome	Rbis	**-1.01867325523675**	**-0.70879778193522**	**-0.91951681261827**	-0.0991564426184811	-0.309875473301531	0.21071903068305
ENSMSEG00005010	turquoise	MB	Autosome		**-0.919288827856292**	**-0.771086043172199**	**-0.821374267985061**	-0.0979145598712304	-0.148202784684092	0.2157113302831
ENSMSEG00005011	turquoise	MB	Autosome	Id3	-0.490117554595053	-0.480004214582975	**-0.701267131484199**	0.211149576889146	-0.0101133400120773	0.221262916901223
ENSMSEG00005008	turquoise	MB	Autosome	Dnajc19	-0.463735982424939	-0.369753082687405	**-0.591991842768623**	0.128255860343683	-0.0939828997375343	0.222238760081218
ENSMSEG00005003	turquoise	MB	Autosome	Fmc1	**-0.626013878130601**	-0.359080473470584	-0.584172625162054	-0.041841252968547	-0.266933404660017	0.22509215169147
ENSMSEG00005019	turquoise	MB	Autosome	Lyrm2	**-0.877578153627825**	-0.217073836224926	-0.442747892254629	-0.434830261373196	**-0.660504317402898**	0.225674056029702
ENSMSEG00005021	turquoise	MB	Autosome	Fabp5	**-0.808196580172931**	-0.488363271425948	**-0.716082071345722**	-0.0921145088272096	-0.319833308746983	0.227718799919774
ENSMSEG00005001	turquoise	MB	Autosome	Ntpcr	**-0.721769917375593**	**-0.61751526068673**	**-0.849764464246073**	0.12799454687048	-0.104254656688862	0.232249203559343
ENSMSEG00005023	turquoise	MB	Autosome	Rph3al	**-0.627154784582267**	-0.47032912533375	**-0.704592023136025**	0.0774372385537584	-0.156825659248517	0.234262897802276
ENSMSEG00005000	turquoise	MB	Autosome	Mrgbp	-0.501087009179999	-0.349909609126449	**-0.586102938153778**	0.0850159289737797	-0.151177400053549	0.236193329027329
ENSMSEG00005013	turquoise	MB	Autosome	Taf13	**-0.736529487145655**	-0.511024987167928	**-0.74833904642683**	0.0118095592811743	-0.225504499977727	0.237314059258901
ENSMSEG00005014	turquoise	MB	Autosome	Pyroxd1	**-0.679855026710728**	-0.135146636497839	-0.373215054258095	-0.306639972452633	-0.54470839021289	0.238068417760256
ENSMSEG00005017	turquoise	MB	Autosome	Ndufs6	**-0.680878750241142**	-0.485351107782588	**-0.723590999012237**	0.0427122487710947	-0.195527642458554	0.238239891229649
ENSMSEG00005022	turquoise	MB	Autosome	Polr1d	-0.506780966880648	-0.344507315111925	**-0.591938979855443**	0.0851580129747945	-0.162273651768723	0.247431664743518
ENSMSEG00005021	turquoise	MB	Autosome	Lsm7	-0.418460581727444	-0.380061439406431	**-0.631774836248581**	0.213314254521137	-0.038399142321013	0.25171339684215
ENSMSEG00005015	turquoise	MB	Autosome	Sag	-0.0672176631433101	**-1.57710703182515**	**-1.83706401119075**	**1.76984634804744**	**1.50988936868184**	0.259956979365593
ENSMSEG00005009	turquoise	MB	Autosome	Apip	**-0.757982874190745**	-0.50614441329095	**-0.772534954351984**	0.0145520801612394	-0.251838460899796	0.266390541061035
ENSMSEG00005022	turquoise	MB	Autosome	Uqcr10	**-0.749759476348102**	-0.531291061348278	**-0.806377157049897**	0.0566176807017944	-0.218468414999824	0.275086095701619
ENSMSEG00005004	turquoise	MB	Autosome	D11Wsu47e	**-0.736086512717014**	-0.12519632439099	-0.410631595320236	-0.325454917396778	**-0.610890188326024**	0.285435270929246
ENSMSEG00005022	turquoise	MB	Autosome	Ndufa6	-0.429948465251354	-0.336300764219958	**-0.62487377866506**	0.194925313413707	-0.0936477010313958	0.288573014445103
ENSMSEG00005013	turquoise	MB	Autosome	Uqcr11	**-0.757399000546531**	-0.516862505609125	**-0.807110086976688**	0.049711086430157	-0.240536494937406	0.290247581367563
ENSMSEG00005008	turquoise	MB	Autosome	Cd300c2	**-0.739413930838889**	-0.265599040226372	-0.55826491356926	-0.181149017269628	-0.473814890612516	0.292665873342888
ENSMSEG00005021	turquoise	MB	Autosome	Ptgr1	**-0.717436728116047**	-0.405031703862622	**-0.706093402215932**	-0.0113433259001155	-0.312405024253425	0.301061698353309
ENSMSEG00005019	turquoise	MB	Autosome	Pfdn4	**-0.594033155396897**	-0.333009352933828	**-0.636729623641146**	0.0426964682442491	-0.261023802463068	0.303720270707317
ENSMSEG00005014	turquoise	MB	Autosome	Avpi1	-0.272731236373111	-0.28957967591207	**-0.593677248347358**	0.320946011974247	0.0168484395389597	0.304097572435287
ENSMSEG00005005	turquoise	MB	Autosome	Pigl	**-0.814118927841755**	**-0.820547259986371**	**-1.12948781755014**	0.315368889708388	0.00642833214461581	0.308940557563772
ENSMSEG00005021	turquoise	MB	Autosome	Rps26	-0.23006659214748	-0.411530713861731	**-0.722843453677692**	0.492776861530211	0.18146412171425	0.311312739815961
ENSMSEG00005002	turquoise	MB	Autosome	Tamm41	-0.522505589223151	-0.352644088995159	**-0.668371925274496**	0.145866336051345	-0.169861500227992	0.315727836279337
ENSMSEG00005001	turquoise	MB	Autosome	Ndufa12	-0.461386364662278	-0.332782927579019	**-0.654215132314973**	0.192828767652695	-0.128603437083259	0.321432204735955
ENSMSEG00005021	turquoise	MB	Autosome	Magoh	-0.395692852220083	-0.332321567100437	**-0.662633472314625**	0.266940620094542	-0.0633712851196461	0.330311905214188
ENSMSEG00005007	turquoise	MB	Autosome	Tex30	-0.472716400685429	-0.286658270420202	**-0.621550504250478**	0.148834103565049	-0.186058130265227	0.334892233830276
ENSMSEG00005001	turquoise	MB	Autosome	AU041133	**-0.89276093577419**	-0.237842208200721	-0.579463671826315	-0.313297263947875	**-0.654918727573469**	0.341621463625594
ENSMSEG00005011	turquoise	MB	Autosome		**-0.730274646461014**	-0.490840676401082	-0.361198433496216	-0.369076212964798	-0.239433970059931	0.352438104050118
ENSMSEG00005018	turquoise	MB	Autosome	Psmg4	**-0.708902237449286**	-0.441091638879015	**-0.799832424972026**	0.09093018752274	-0.267810598570271	0.358740786093011
ENSMSEG00005007	turquoise	MB	Autosome	Fbxo15	**-1.0447752184899**	**-0.769376107710192**	**-1.13194096018861**	0.0871657416987082	-0.275399110779708	0.362564852478416
ENSMSEG00005014	turquoise	MB	Autosome	Gm10778	-0.506508203145861	0.139117264378431	-0.236572513087193	-0.269935690058668	**-0.645625467524293**	0.375689777465624
ENSMSEG00005012	turquoise	MB	Autosome	Fau	**-0.66134343585922**	**-0.684327484201777**	**-1.06424673031034**	0.402903294451122	0.0229840483425569	0.379919246108565
ENSMSEG00005018	turquoise	MB	Autosome	Gal	-0.533496992819636	-0.199731080380152	**-0.585703024197699**	0.0522060313780635	-0.333765912439484	0.385971943817547
ENSMSEG00005013	turquoise	MB	Autosome	Rnase4	**-0.940957787428155**	-0.104067601027043	-0.491608580049794	-0.449349207378361	**-0.836890186401112**	0.387540979022751
ENSMSEG00005018	turquoise	MB	Autosome	Nudt8	-0.484606125932815	-0.362101628731217	**-0.75953936220579**	0.274933236272975	-0.122504497201598	0.397437733474573
ENSMSEG00005022	turquoise	MB	Autosome	Phyhd1	**-0.607230938452278**	-0.377410453315702	**-0.780819884528277**	0.173588946075999	-0.229820485136576	0.403409431212575
ENSMSEG00005022	turquoise	MB	Autosome	Efcab6	-0.38235917264665	-0.203835810708273	**-0.611457500952484**	0.229098328305834	-0.178523361938377	0.407621690244211
ENSMSEG00005021	turquoise	MB	Autosome		**-0.637812110440023**	-0.528087867695682	-0.49534375036273	-0.142468360077293	-0.109724242744341	0.411174777158654
ENSMSEG00005004	turquoise	MB	Autosome	Smim8	-0.542854696379281	0.0456331917007004	-0.376591218270147	-0.166263478109134	**-0.588487888079982**	0.422224409970847

ENSMSEG00005009{	turquoise	MB	Autosome	Ddb2	-0.375824984810435	-0.356200863993253	**-0.787980027678357**	0.412155042867921	-0.0196241208171824	0.431779163685104
ENSMSEG00005007⁴	turquoise	MB	Autosome		**-0.87462949915822**	**-0.638778822583421**	-0.457086066651876	-0.417543432506344	-0.235850676574799	0.432661513557659
ENSMSEG00005012⁷	turquoise	MB	Autosome	Acyp2	-0.520117706440137	-0.173456380691811	**-0.633864399709631**	0.113746693269494	-0.346661325748326	0.46040801901782
ENSMSEG00005016]	turquoise	MB	Autosome	Wfdc18	**-1.49918527949329**	-0.12999592372933	**-0.611539853224069**	**-0.887645426269217**	**-1.36918935576396**	0.481543929494739
ENSMSEG00005009]	turquoise	MB	Autosome	Rpl13	**-0.682367901736151**	-0.532322603843987	**-0.692643034811739**	0.0102751330755875	-0.150045297892164	0.484537203083856
ENSMSEG00005003(	turquoise	MB	Autosome		**-0.790650815940008**	-0.169353580490382	-0.580528357649036	-0.210122458290971	**-0.621297235449626**	0.506091202285155
ENSMSEG00005005]	turquoise	MB	Autosome	Cox19	-0.435892604415781	-0.139241249427962	**-0.647593857775749**	0.211701253359969	-0.296651354987819	0.508352608347787
ENSMSEG00005016⁷	turquoise	MB	Autosome		**-0.75362594841723**	**-0.626752089574388**	**-0.675335355977811**	-0.078290592439419	-0.126873858842843	0.530823280353296
ENSMSEG00005010€	turquoise	MB	Autosome		**-1.77929848616344**	**-1.15949585730539**	**-1.21533360359314**	-0.563964882570299	**-0.619802628858054**	0.532321196205523
ENSMSEG00005007³	turquoise	MB	Autosome	Proca1	**-0.960974275622279**	-0.344591154411317	**-0.898538704974943**	-0.0624355706473359	**-0.616383121210962**	0.553947550563626
ENSMSEG00005016²	turquoise	MB	Autosome	1190005I06Rik	**-1.09929060384403**	-0.513052458804827	**-1.10401439594773**	0.00472379210370431	**-0.586238145039203**	**0.590961937142907**
ENSMSEG00005021£	turquoise	MB	Autosome	Gmnn	**-1.11532334198616**	-0.365105625354329	**-1.01385837148036**	-0.101464970505799	**-0.75021771663183**	**0.648752746126031**
ENSMSEG00005005£	turquoise	MB	Autosome	Gm17455	**-0.841853014430531**	-0.465393021736667	**-1.1193526315702**	0.277499617139668	-0.376459992693864	**0.653959609833532**
ENSMSEG00005004£	turquoise	MB	Autosome	Ucma	**-1.36295090199997**	-0.151206057090725	**-0.869520943381875**	-0.493429958618094	**-1.21174484490924**	**0.71831488629115**
ENSMSEG00005009]	turquoise	MB	Autosome		**-1.47440638489419**	**-0.894895032037508**	**-0.790271825835958**	**-0.684134559058235**	-0.579511352856686	**0.785333190593351**
ENSMSEG00005010£	turquoise	MB	Autosome	Serpind1	**-0.598733106369444**	-0.201071816746267	**-0.991085574147872**	0.392352467778428	-0.397661289623177	**0.790013757401605**
ENSMSEG00005009³	turquoise	MB	Autosome	Ccdc42	**-0.921787640970027**	**-0.603023259858019**	**-1.43560027906839**	0.513812638098362	-0.318764381112009	**0.832577019210371**
ENSMSEG00005018²	turquoise	MB	Autosome		**-1.80271708695632**	**-1.23938900488901**	**-0.668642287616352**	**-1.13407479933996**	-0.563328082067305	**0.996821536828004**
ENSMSEG00005009€	turquoise	MB	Autosome	Ccn5	**-1.05463930278252**	**-1.30508613463861**	**-2.3693274506341**	**1.31468814785158**	0.250446831856094	**1.06424131599549**
ENSMSEG00005010⁴	turquoise	MB	Autosome		**-0.614720895735907**	-0.496083815611124	**-0.928745329168784**	0.314024433432877	-0.118637080124783	**1.15720527685385**
ENSMSEG00005009€	turquoise	MB	Autosome		**-0.833247728426031**	**-0.656425466618713**	**-0.635072250720996**	-0.198175477705035	-0.176822261807318	**1.16164772916122**
ENSMSEG00005001(	turquoise	MB	Autosome	Cfap97d2	**-1.31103092664612**	**-0.881270960277896**	**-2.39235211229503**	**1.08132118564891**	-0.429759966368223	**1.51108115201714**
ENSMSEG00005017⁴	turquoise	MB	Autosome		**-0.608560876837801**	-0.436983330942388	-0.446664480034755	-0.161896396803046	-0.171577545895413	**1.89923786304391**
ENSMSEG00005000⁴	turquoise	MB	Autosome		**-0.711091312766067**	**-0.661846153857833**	-0.356379381658645	-0.354711931107422	-0.0492451589082348	**1.90486144432195**
ENSMSEG00005020£	turquoise	MB	chr1 (NR)	Rpl13a	**-1.0194735610091**	**-0.827279137780756**	**-0.822656827890925**	-0.19681673311818	-0.192194423228349	-0.00462230988983057
ENSMSEG00005020²	turquoise	MB	chr1 (NR)	Mrpl46	**-0.629802208661931**	-0.453743426028772	-0.448583542207388	-0.181218666454543	-0.176058782633159	-0.00515988382138396
ENSMSEG00005017€	turquoise	MB	chr1 (NR)	Tmem147	**-0.740946251462329**	**-0.620090486853437**	**-0.602747630094713**	-0.138198621367616	-0.120855764608891	-0.0173428567587243
ENSMSEG00005010€	turquoise	MB	chr1 (NR)	Psenen	**-0.617695791268963**	-0.503392899062492	-0.43747559149111	-0.180220199777853	-0.114302892206471	-0.0659173075713827
ENSMSEG00005007£	turquoise	MB	chr1 (NR)	Pih1d1	**-0.711368476453415**	**-0.665790253667731**	**-0.599817282361683**	-0.111551194091732	-0.045578222785684	-0.0659729713060482
ENSMSEG00005011⁴	turquoise	MB	chr1 (NR)	Selenos	**-0.748535683212715**	-0.509197540094253	-0.439900991211327	-0.308634692001388	-0.239338143118462	-0.0692965488829259
ENSMSEG00005021£	turquoise	MB	chr1 (NR)	Cd79a	**-0.771430670564135**	-0.559337989876166	-0.48846385407241	-0.282966816491724	-0.212092680687969	-0.0708741358037555
ENSMSEG00005010€	turquoise	MB	chr1 (NR)	Polr2i	**-0.643505666336063**	-0.559397783293639	-0.473373757929808	-0.170131908406255	-0.0841078830424236	-0.0860240253638314
ENSMSEG00005007⁷	turquoise	MB	chr1 (NR)	Rras	**-0.773937466366658**	-0.581684362906766	-0.4925978459688	-0.281339620397858	-0.192253103459892	-0.0890865169379659
ENSMSEG00005016£	turquoise	MB	chr1 (NR)	Ech1	**-0.614405401202781**	-0.531628964199899	-0.438515947103566	-0.175889454099216	-0.0827764370028829	-0.0931130170963328
ENSMSEG00005020²	turquoise	MB	chr1 (NR)	Eif3k	**-0.659722872376051**	**-0.634941621155206**	-0.533752421402655	-0.125970450973396	-0.0247812512208454	-0.101189199752551
ENSMSEG00005002³	turquoise	MB	chr1 (NR)	Klk7	**-0.641285948253184**	0.372910752058094	0.535867501397602	**-1.17715344965079**	**-1.01419670031128**	-0.162956749339508
ENSMSEG00005007⁴	turquoise	MB	chr1 (NR)	Rps11	**-0.862609974724793**	**-0.805608879369709**	**-0.629409702387286**	-0.233200272337507	-0.0570010953550844	-0.176199176982423
ENSMSEG00005002³	turquoise	MB	chr1 (NR)	Klk8	**-0.728074848974387**	-0.297227418652717	-0.100819926108739	**-0.627254922865647**	-0.43084743032167	-0.196407492543978
ENSMSEG00005022€	turquoise	MB	chr1 (NR)	Pdcd2l	**-0.754742377827985**	**-0.748578111035308**	-0.490607631235678	-0.264134746592306	-0.00616426679267706	-0.257970479799629
ENSMSEG00005003§	turquoise	MB	chr1 (NR)	Ndufa3	**-1.02169477533803**	**-0.895080196774029**	**-0.605959740311774**	-0.415735035026256	-0.126614578564002	-0.289120456462255
ENSMSEG00005011£	turquoise	MB	chr1 (NR)	Snrpa1	**-0.914587382935869**	**-0.738750346124616**	-0.440604213946929	-0.47398316898894	-0.175837036811252	-0.298146132177687
ENSMSEG00005019€	turquoise	MB	chr1 (NR)	Aen	-0.55609932719554	**-1.13639757661999**	**-0.810281423289356**	0.254182096093815	0.580298249424453	-0.326116153330638
ENSMSEG00005006£	turquoise	MB	chr1 (NR)	Zfp551	-0.540294939861921	-0.310050634184282	0.0506157180437503	**-0.590910657905671**	-0.230244305677639	-0.360666352228032
ENSMSEG00005016⁴	turquoise	MB	chr1 (NR)	Sars2	-0.584055438825216	**-0.665426238839886**	-0.27958983326566	-0.304465605559556	0.0813708000146708	-0.385836405574227
ENSMSEG00005009€	turquoise	MB	chr1 (NR)	Fxyd5	**-0.618371898656807**	**-0.702850440941935**	-0.29051663420158	-0.327855264455227	0.0844785422851284	-0.412333806740356
ENSMSEG00005020⁴	turquoise	MB	chr1 (NR)	Gm45713	**-0.792737547095217**	**-0.865453643396711**	-0.435169383986292	-0.357568163108925	0.0727160963014934	-0.430284259410418
ENSMSEG00005019⁴	turquoise	MB	chr1 (NR)	Isg20	**-1.38745450647331**	**-0.942676784727167**	0.151853796049684	**-1.539308302523**	-0.444777721746146	**-1.09453058077685**

ENSMSEG00005003	turquoise	MB	chr1 (NR)	Rps9	**-0.954826073943302**	**-0.79483732011539**	**-0.805298177020578**	-0.149527896922724	-0.159988753827912	0.0104608569051879
ENSMSEG00005010	turquoise	MB	chr1 (NR)	Cox6b1	**-0.586824260872035**	-0.495634912862055	-0.511906104027319	-0.074918156844716	-0.0911893480099802	0.0162711911652642
ENSMSEG00005014	turquoise	MB	chr1 (NR)	Rps7	**-1.00365307401558**	**-0.954696524239034**	**-1.00958628182985**	0.00593320781426712	-0.0489565497765492	0.0548897575908163
ENSMSEG00005018	turquoise	MB	chr1 (NR)	Rps16	**-0.894654885539068**	**-0.734224537349836**	**-0.843258517591786**	-0.0513963679472823	-0.160430348189232	0.10903398024195
ENSMSEG00005011	turquoise	MB	chr1 (NR)	Rps5	**-0.888357785423363**	**-0.708824494495572**	**-0.820349053213985**	-0.0680087322093772	-0.17953329092779	0.111524558718413
ENSMSEG00005010	turquoise	MB	chr1 (NR)	Cox7a1	**-1.13171761968577**	**-0.747287099689474**	**-0.871424888042255**	-0.260292731643516	-0.384430519996297	0.124137788352781
ENSMSEG00005008	turquoise	MB	chr1 (NR)	Snrpd2	**-0.714962572775862**	-0.549860812349406	**-0.702056285351244**	-0.0129062874246179	-0.165101760426456	0.152195473001838
ENSMSEG00005015	turquoise	MB	chr1 (NR)	Isoc2b	**-0.723921779608906**	-0.513105540578025	**-0.674450109683031**	-0.0494716699258748	-0.210816239030881	0.161344569105006
ENSMSEG00005020	turquoise	MB	chr1 (NR)	Pafah1b3	-0.539581804835406	-0.446365006900275	**-0.616790541868298**	0.0772087370328916	-0.0932167979351308	0.170425534968022
ENSMSEG00005020	turquoise	MB	chr1 (NR)		**-0.796297425143559**	-0.340197867531777	-0.526972934200404	-0.269324490943155	-0.456099557611782	0.186775066668628
ENSMSEG00005006	turquoise	MB	chr1 (NR)	Bcat2	-0.457127314382518	-0.383652113761625	**-0.668994261827083**	0.211866947444565	-0.0734752006208934	0.285342148065459
ENSMSEG00005023	turquoise	MB	chr1 (NR)	Pdcd5	-0.233280519442148	-0.12279139693697	**-0.645705744009395**	0.412425224567247	-0.110489122505178	0.522914347072425
ENSMSEG00005016	turquoise	MB	chr13 (NR)	Dcps	-0.446037751237477	**-0.648504852811726**	**-0.626162787838315**	0.180125036600838	0.202467101574249	-0.0223420649734112
ENSMSEG00005022	turquoise	MB	chr13 (NR)		**-0.696405060678289**	-0.545996239364952	-0.490564643512694	-0.205840417165595	-0.150408821313337	-0.055431595852258
ENSMSEG00005016	turquoise	MB	chr13 (NR)	Fam118b	**-0.655564968070671**	-0.531507351345138	-0.332988352778242	-0.322576615292429	-0.124057616725533	-0.198518998566895
ENSMSEG00005005	turquoise	MB	chr13 (NR)	Acp5	-0.264741868531904	**-1.12419235697581**	**-0.668141992416284**	0.40340012388438	**0.859450488443903**	-0.456050364559523
ENSMSEG00005007	turquoise	MB	X/X* (R)	Rpl39	**-1.10937324789047**	**-0.826034748974069**	**-0.812808360646155**	-0.296564887244315	-0.283338498916402	-0.0132263883279135
ENSMSEG00005018	turquoise	MB	X/X* (R)	Ssr4	**-0.651975790818202**	-0.537182168759415	-0.502989046955028	-0.148986743863174	-0.114793622058787	-0.0341931218043873
ENSMSEG00005012	turquoise	MB	X/X* (R)	Lage3	**-0.656523133308774**	-0.510517454834811	-0.447769976374577	-0.208753156934197	-0.146005678473963	-0.0627474784602345
ENSMSEG00005000	turquoise	MB	X/X* (R)		-0.481220161176695	**-0.680786676317114**	-0.56817490364478	0.0869547424680846	0.199566515140419	-0.0675397477308086
ENSMSEG00005013	turquoise	MB	X/X* (R)		**-0.621054106503724**	-0.548663676772612	-0.550381787127397	-0.0706723193763268	-0.072390429731112	-0.112611772672334
ENSMSEG00005001	turquoise	MB	X/X* (R)	Tmsb15b1	**-1.05043810578354**	**-0.783004714194348**	**-0.621535081102808**	-0.428903024680734	-0.267433391589193	-0.16146963309154
ENSMSEG00005019	turquoise	MB	X/X* (R)		**-0.850957252747692**	**-0.669186835028566**	**-0.601647087297757**	-0.249310165449935	-0.181770417719126	0.00171811035478516
ENSMSEG00005007	turquoise	MB	X/X* (R)	Ndufa1	**-0.690798896966686**	-0.518299895587164	-0.540493745044928	-0.150305151921758	-0.172499001379522	0.0221938494577639
ENSMSEG00005022	turquoise	MB	X/X* (R)	Hprt	**-0.868386388022617**	**-0.746441282835348**	**-0.772555663643448**	-0.0958307243791687	-0.121945105187269	0.0261143808080999
ENSMSEG00005007	turquoise	MB	X/X* (R)	Rps7	**-1.84590120673212**	**-1.45114205808274**	**-1.88308486001002**	0.037183653277903	-0.39475914864938	0.431942801927283
ENSMSEG00005014	turquoise	MB	X/X* (R)	Rpl13a	**-0.655503684083053**	-0.49705544268687	**-0.941102969750345**	0.285599285667292	-0.158448241396184	0.444047527063476
ENSMSEG00005017	turquoise	MB	chr1 (R)	Metrn	**-0.61859251166501**	-0.278028257642744	-0.277103047187572	-0.341489464477437	-0.340564254022266	-0.000925210455171305
ENSMSEG00005017	turquoise	MB	chr1 (R)	Antkmt	**-0.599656777969596**	-0.536654105361517	-0.535439752235703	-0.0642170257338922	-0.0630026726080786	-0.00121435312581363
ENSMSEG00005015	turquoise	MB	chr1 (R)	Crym	**-0.63260065565028**	-0.3860345065102	-0.381169357909875	-0.251431297740404	-0.246566149140079	-0.00486514860032498
ENSMSEG00005017	turquoise	MB	chr1 (R)		**-0.891031228925198**	-0.537799659979031	-0.46765695190645	-0.423374277018748	-0.353231568946167	-0.0152976278368591
ENSMSEG00005018	turquoise	MB	chr1 (R)	Atp6v0e	**-0.590898393319833**	-0.530880487083935	-0.502712747884423	-0.0881856454354098	-0.0600179062358977	-0.0281677391995121
ENSMSEG00005009	turquoise	MB	chr1 (R)	Psmb1	**-0.893207727272301**	**-0.592942719431959**	-0.563018121755133	-0.330189605517168	-0.300265007840342	-0.0299245976768262
ENSMSEG00005012	turquoise	MB	chr1 (R)	Pycard	**-0.775049654610952**	**-0.829597102827259**	**-0.793498197047073**	0.0184485424361211	0.0545474482163075	-0.0360989057801865
ENSMSEG00005022	turquoise	MB	chr1 (R)	Nupr1	**-0.654867593647431**	-0.485230514466204	-0.448431273853342	-0.206436319794089	-0.169637079181227	-0.036799240612862
ENSMSEG00005015	turquoise	MB	chr1 (R)	Cebpzos	**-0.677631335648932**	-0.410623662905905	-0.36273307652325	-0.314898259125681	-0.267007672743026	-0.0478905863826549
ENSMSEG00005017	turquoise	MB	chr1 (R)		**-1.35313603840526**	**-0.747885239542582**	**-0.768516915684934**	-0.584619122720322	**-0.605250798862674**	-0.0528324393568515
ENSMSEG00005009	turquoise	MB	chr1 (R)	Lsp1	**-0.816529162135964**	**-0.687675262891894**	**-0.633720622924468**	-0.182808539211496	-0.12885389924407	-0.0539546399674267
ENSMSEG00005008	turquoise	MB	chr1 (R)	Micos13	**-0.723674843055796**	-0.530396053667223	-0.475052216955223	-0.248622626100573	-0.193278789388573	-0.0553438367119997
ENSMSEG00005012	turquoise	MB	chr1 (R)		**-0.803519727976892**	**-0.720631494218382**	**-0.72206275578522**	-0.0814569721916725	-0.08288823375851	-0.0694837358893038
ENSMSEG00005021	turquoise	MB	chr1 (R)		**-0.759984891958497**	**-0.592245282136939**	-0.576947654300079	-0.183037237658418	-0.167739609821559	-0.0701427080725809
ENSMSEG00005015	turquoise	MB	chr1 (R)	Tmem159	**-0.640677892743262**	-0.442237561760646	-0.368350638135907	-0.272327254607356	-0.198440330982617	-0.0738869236247392
ENSMSEG00005001	turquoise	MB	chr1 (R)	Rps3	**-0.821038895354415**	**-0.70706594711173**	**-0.623352950872654**	-0.197685944481761	-0.113972948242685	-0.0837129962390756
ENSMSEG00005017	turquoise	MB	chr1 (R)	Nubp2	**-0.649484834922416**	-0.505931420272846	-0.420772671689568	-0.228712163232848	-0.14355341464957	-0.0851587485832786
ENSMSEG00005021	turquoise	MB	chr1 (R)	Eci1	**-0.617664309067344**	**-0.626937338260334**	-0.537886416480522	-0.0797778925868221	0.00927302919299017	-0.0890509217798122
ENSMSEG00005001	turquoise	MB	chr1 (R)	Ccdc167	**-0.616955395445798**	-0.569681589203642	-0.476477836409057	-0.140477559036741	-0.047273806242156	-0.0932037527945847
ENSMSEG00005010	turquoise	MB	chr1 (R)	Polr1c	**-0.700407439881064**	-0.46345695292	-0.369099146937049	-0.331308292944015	-0.236950486961064	-0.0943578059829511

ENSMSEG00005005	turquoise	MB	chr1 (R)	Lst1	**-0.877202185148504**	**-0.699246235716298**	**-0.596982595771286**	-0.280219589377218	-0.177955949432205	-0.102263639945012
ENSMSEG00005016	turquoise	MB	chr1 (R)	Cyp4f40	**-0.675477676040635**	-0.47645186939401	-0.373481049524615	-0.30199662651602	-0.199025806646625	-0.102970819869395
ENSMSEG00005019	turquoise	MB	chr1 (R)	Nsmce1	**-0.687930225211671**	-0.556421579111144	-0.444655163464672	-0.243275061746999	-0.131508646100526	-0.111766415646472
ENSMSEG00005021	turquoise	MB	chr1 (R)	Fkbp5	**-0.628086617279529**	-0.549377054382045	-0.426612404521416	-0.201474212758113	-0.078709562897483	-0.12276464986063
ENSMSEG00005006	turquoise	MB	chr1 (R)	H2-M3	**-0.97637749943747**	-0.465768025020702	-0.334777911366084	**-0.641599588071386**	-0.510609474416768	-0.130990113654618
ENSMSEG00005013	turquoise	MB	chr1 (R)	Marchf2	**-0.759268332406045**	-0.566285031059223	-0.432149205441746	-0.327119126964299	-0.192983301346822	-0.134135825617477
ENSMSEG00005004	turquoise	MB	chr1 (R)	Tspan4	**-0.875936956613328**	**-0.709731243550005**	-0.561121705064178	-0.314815251549149	-0.166205713063323	-0.148609538485827
ENSMSEG00005006	turquoise	MB	chr1 (R)	C2	**-0.812675753297862**	-0.546345967329733	-0.395235156912314	-0.417440596385548	-0.266329785968129	-0.15111081041742
ENSMSEG00005021	turquoise	MB	chr1 (R)	Ggnbp1	**-1.09361458186096**	**-0.831231544158626**	**-0.676010133928359**	-0.417604447932599	-0.262383037702332	-0.155221410230267
ENSMSEG00005016	turquoise	MB	chr1 (R)	Taf10	**-0.596005843575114**	-0.572973893389677	-0.412186228414505	-0.183819615160609	-0.0230319501854364	-0.160787664975173
ENSMSEG00005016	turquoise	MB	chr1 (R)	Ilk	**-0.680288709238121**	-0.563691825916081	-0.395451267152972	-0.284837442085149	-0.11659688332204	-0.168240558763109
ENSMSEG00005006	turquoise	MB	chr1 (R)	Polr1h	**-0.690077895807538**	**-0.63626028757862**	-0.448367980652101	-0.241709915155437	-0.0538176082289184	-0.187892306926519
ENSMSEG00005017	turquoise	MB	chr1 (R)	Taldo1	**-0.629755007920653**	-0.536814764943186	-0.321085086325524	-0.308669921595129	-0.0929402429774669	-0.215729678617662
ENSMSEG00005015	turquoise	MB	chr1 (R)	D7Ertd443e	-0.286141101077306	**-0.596880067194865**	-0.353833896639735	0.0676927955624291	0.310738966117559	-0.24304617055513
ENSMSEG00005008	turquoise	MB	chr1 (R)	Rps13	**-0.944919012454118**	**-0.93110319065717**	**-0.676257656459334**	-0.268661355994784	-0.0138158217969489	-0.254845534197835
ENSMSEG00005006	turquoise	MB	chr1 (R)	Tcf19	**-0.924455966712921**	-0.518887423746975	-0.219156140686017	**-0.705299826026903**	-0.405568542965945	-0.299731283060958
ENSMSEG00005005	turquoise	MB	chr1 (R)	Ager	**-1.85608711456456**	**-0.64543283557317**	-0.110322955614034	**-1.74576415895052**	**-1.21065427899139**	-0.535109879959136
ENSMSEG00005003	turquoise	MB	chr1 (R)	Umodl1	**-1.77830358797335**	**-1.07262533608014**	-0.534229887879423	**-1.24407370009393**	**-0.705678251893211**	-0.538395448200714
ENSMSEG00005001	turquoise	MB	chr1 (R)		**-0.682723394039146**	-0.555548461983638	-0.486064726094334	-0.196658667944811	-0.127174932055507	0.00143126156683749
ENSMSEG00005008	turquoise	MB	chr1 (R)	Sirt3	**-0.623682312631686**	-0.469097192855063	-0.472752432298706	-0.150929880332979	-0.154585119776623	0.0036552394436435
ENSMSEG00005022	turquoise	MB	chr1 (R)		**-0.903984980294066**	**-0.807624069692343**	**-0.754791630335492**	-0.149193349958575	-0.0963609106017231	0.0168013584564996
ENSMSEG00005003	turquoise	MB	chr1 (R)		**-0.73547050043415**	**-0.587831343430039**	**-0.604632701886539**	-0.130837798547611	-0.147639157004111	0.0206316761423521
ENSMSEG00005010	turquoise	MB	chr1 (R)	Mrpl23	**-0.853652146433535**	**-0.785434058327105**	**-0.807550520115508**	-0.0461016263180266	-0.06821808810643	0.0221164617884034
ENSMSEG00005016	turquoise	MB	chr1 (R)	Mrpl17	**-0.748794835673244**	-0.507906720015498	-0.534443214633319	-0.214351621039926	-0.240888115657747	0.0265364946178213
ENSMSEG00005021	turquoise	MB	chr1 (R)		**-0.951980260959958**	**-0.827891095832712**	**-0.951937001246448**	**-4.325971351006640e-05**	-0.124089165127245	0.0395867844259692
ENSMSEG00005021	turquoise	MB	chr1 (R)	Bola2	**-0.747970662960193**	**-0.684627967862642**	**-0.729137202639103**	-0.0188334603210904	-0.0633426950975511	0.0445092347764607
ENSMSEG00005002	turquoise	MB	chr1 (R)	Cript	**-0.609713827327815**	-0.451695521334862	-0.51816725115681	-0.0915465761710046	-0.158018305992952	0.0664717298219477
ENSMSEG00005021	turquoise	MB	chr1 (R)	Gng13	**-1.03343722459829**	**-0.667127463266913**	**-0.733626269864029**	-0.299810954734262	-0.366309761331379	0.0664988065971169
ENSMSEG00005020	turquoise	MB	chr1 (R)	Nthl1	**-0.889973714542611**	-0.535731735443641	**-0.602258805998073**	-0.287714908544537	-0.354241979098969	0.066527070554432
ENSMSEG00005011	turquoise	MB	chr1 (R)	Slc30a6	**-0.623299400710974**	-0.256074125531607	-0.323920549329157	-0.299378851381817	-0.367225275179367	0.0678464237975498
ENSMSEG00005006	turquoise	MB	chr1 (R)	Tmem126a	**-0.682526038127149**	**-0.590735152869265**	**-0.661540394963708**	-0.0209856431634411	-0.0917908852578841	0.0708052420944431
ENSMSEG00005022	turquoise	MB	chr1 (R)	AI413582	-0.540357988777283	-0.527062594612964	**-0.60605306485119**	0.0656950760739066	-0.0132953941643189	0.0789904702382256
ENSMSEG00005010	turquoise	MB	chr1 (R)	Mrps18a	-0.549849954118261	-0.547604477467472	**-0.634607970815245**	0.0847580166969843	-0.00224547665078877	0.087003493347773
ENSMSEG00005017	turquoise	MB	chr1 (R)	Trim21	**-0.729631773499431**	-0.3488520231874	-0.436665661552982	-0.292966111946449	-0.380779750312031	0.0878136383655829
ENSMSEG00005008	turquoise	MB	chr1 (R)	Oard1	**-0.653738541158785**	-0.455912004071043	-0.545849174374082	-0.107889366784703	-0.197826537087742	0.0899371703030393
ENSMSEG00005015	turquoise	MB	chr1 (R)	Rps15a	**-0.733887778520191**	**-0.61334492452203**	**-0.706325161822757**	-0.0275626166974336	-0.120542853998161	0.0929802373007276
ENSMSEG00005013	turquoise	MB	chr1 (R)	Angptl4	**-1.13145084997793**	-0.487295204356548	**-0.591308115185309**	-0.540142734792617	**-0.644155645621378**	0.104012910828761
ENSMSEG00005015	turquoise	MB	chr1 (R)	Bccip	**-0.595659705425915**	-0.290103377683146	-0.395102223995994	-0.20055748142992	-0.305556327742768	0.104998846312848
ENSMSEG00005019	turquoise	MB	chr1 (R)	Msrb1	**-0.614146883556599**	-0.520863914323287	**-0.625969163581877**	0.0118222800252773	-0.0932829692333127	0.10510524925859
ENSMSEG00005008	turquoise	MB	chr1 (R)	Rgs10	**-0.63375360730867**	-0.3971624280838	-0.50916756405848	-0.12458604325019	-0.23659117922487	0.11200513597468
ENSMSEG00005011	turquoise	MB	chr1 (R)		**-0.981178131136147**	**-0.747091639038892**	**-0.786678423464861**	-0.194499707671286	-0.234086492097255	0.124045905413735
ENSMSEG00005008	turquoise	MB	chr1 (R)	Tnnt3	**-1.27062428540685**	**-0.950619693986119**	**-1.07753457879299**	-0.193089706613859	-0.320004591420727	0.126914884806867
ENSMSEG00005018	turquoise	MB	chr1 (R)	Nmral1	-0.453509382756326	**-0.665061229080268**	**-0.823292293109915**	0.369782910353589	0.211551846323941	0.158231064029647
ENSMSEG00005021	turquoise	MB	chr1 (R)	Uqcc2	**-0.941348955830092**	**-0.621567093985456**	**-0.802253076153382**	-0.139095879676711	-0.319781861844636	0.180685982167926
ENSMSEG00005011	turquoise	MB	chr1 (R)	Akip1	**-0.945117222741342**	-0.486324567093414	**-0.690262591436048**	-0.254854631305294	-0.458792655647928	0.203938024342634
ENSMSEG00005017	turquoise	MB	chr1 (R)	Thrsp	**-0.920418956484474**	-0.372750690228374	**-0.611796940512004**	-0.30862201597247	-0.5476682662561	0.239046250283629
ENSMSEG00005008	turquoise	MB	chr1 (R)	Rpl36	-0.572255357942533	-0.541819800592506	**-0.781981494160714**	0.209726136218181	-0.0304355573500271	0.240161693568209

ENSMSEG00005010	turquoise	MB	chr1 (R)	Mydgf	-0.513466062016667	-0.335914801353696	**-0.591709559300856**	0.0782434972841885	-0.177551260662971	0.255794757947159
ENSMSEG00005012	turquoise	MB	chr1 (R)	Ndufb2	**-0.898895259838242**	**-0.624273915485024**	**-0.913084855635853**	0.0141895957976107	-0.274621344353218	0.288810940150829
ENSMSEG00005017	turquoise	MB	chr1 (R)	Flywch2	**-0.62252950809975**	-0.406552016487637	**-0.806974899871454**	0.184445391771703	-0.215977491612113	0.400422883383816
ENSMSEG00005009	turquoise	MB	chr1 (R)	Gucy2d	**-1.63107763289196**	**-1.32297024808735**	**-1.76201108271685**	0.13093344982489	-0.308107384804607	0.439040834629497
ENSMSEG00005019	turquoise	MB	chr1 (R)	Rgs11	**-0.748450522963971**	-0.46605099859303	**-1.14945797212277**	0.401007449158798	-0.282399524370941	**0.683406973529738**
ENSMSEG00005008	turquoise	MB	chr1 (R)	H2-Ob	**-1.91125925595182**	-0.39844439421637	**-1.33685787580666**	-0.574401380145161	**-1.51281486173545**	**0.938413481590287**
ENSMSEG00005004	turquoise	MB	chr13 (R)	Mrap2	-0.512246200315915	**-0.622962505151948**	**-0.621648827334169**	0.109402627018254	0.110716304836033	-0.00131367781777918
ENSMSEG00005020	turquoise	MB	chr13 (R)	Gpx1	**-0.697008487875384**	-0.524740832685738	-0.508724117438127	-0.188284370437258	-0.172267655189646	-0.0160167152476115
ENSMSEG00005004	turquoise	MB	chr13 (R)		**-0.735304895104921**	-0.534124219569072	**-0.724335472925489**	-0.0109694221794319	-0.201180675535849	-0.0229465470666318
ENSMSEG00005000	turquoise	MB	chr13 (R)	Rpl4	**-0.632987053921736**	-0.568391379490923	-0.527706420828765	-0.105280633092971	-0.064595674430813	-0.040684958662158
ENSMSEG00005013	turquoise	MB	chr13 (R)	Zbtb16	**-0.607856606193602**	**-0.78722494676346**	**-0.698617236625135**	0.0907606304315323	0.179368340569857	-0.088607710138325
ENSMSEG00005010	turquoise	MB	chr13 (R)	Naalad2	**-1.88155945388487**	**-1.78458851872387**	**-1.67529193123268**	-0.206267522652184	-0.0969709351609941	-0.10929658749119
ENSMSEG00005019	turquoise	MB	chr13 (R)		**-1.03838165946646**	**-1.43813906353306**	**-1.57905998225301**	0.54067832278655	0.3997574040666	-0.119258307669739
ENSMSEG00005009	turquoise	MB	chr13 (R)	Prss50	**-1.1431966922474**	**-0.871101495087704**	**-0.685904079813913**	-0.45729261243349	-0.272095197159699	-0.185197415273791
ENSMSEG00005019	turquoise	MB	chr13 (R)	Ndufaf3	**-0.590168568256906**	**-0.588209722012142**	-0.394683233703292	-0.195485334553613	-0.00195884624476331	-0.19352648830885
ENSMSEG00005017	turquoise	MB	chr13 (R)	Myzap	**-0.874396932830205**	**-0.904066445384518**	-0.377999033550758	-0.496397899279447	0.0296695125543127	-0.52606741183376
ENSMSEG00005004	turquoise	MB	chr13 (R)		**-0.979350256275077**	**-0.75218086267211**	**-0.729234315605478**	-0.250115940669599	-0.227169393602967	-0.560351450159349
ENSMSEG00005008	turquoise	MB	chr13 (R)	Anapc13	**-0.835730152301405**	**-0.60373494840188**	**-0.632803586994543**	-0.202926565306863	-0.231995203899525	0.0290686385926626
ENSMSEG00005014	turquoise	MB	chr13 (R)	Rwdd2a	**-0.602290596379181**	-0.448715539961162	-0.487675229832361	-0.11461536654682	-0.153575056418019	0.0389596898711991
ENSMSEG00005009	turquoise	MB	chr13 (R)	Rps25	**-1.05476269097609**	**-0.798390619125213**	**-0.841639657248879**	-0.213123033727213	-0.256372071850879	0.0432490381236662
ENSMSEG00005017	turquoise	MB	chr13 (R)	Tcta	**-0.589949331088214**	-0.4297761594288	-0.477771398560375	-0.112177932527839	-0.160173171659414	0.0479952391315753
ENSMSEG00005009	turquoise	MB	chr13 (R)	Ccdc84	**-0.595729549557174**	**-0.672148058237039**	**-0.732743451940941**	0.137013902383768	0.0764185086798654	0.0605953937039024
ENSMSEG00005005	turquoise	MB	chr13 (R)	Rpl14	**-0.901112730290015**	**-0.764537652094112**	**-0.82556683873907**	-0.0755458915509448	-0.136575078195902	0.0610291866449576
ENSMSEG00005012	turquoise	MB	chr13 (R)	Cox7a2	**-0.970760330555683**	**-0.670589075224127**	**-0.735281456556854**	-0.235478873998829	-0.300171255331556	0.0646923813327271
ENSMSEG00005002	turquoise	MB	chr13 (R)	Gm5426	**-0.889801058340205**	-0.57062219681547	**-0.647236793277881**	-0.242564265062324	-0.319178861524735	0.076614596462411
ENSMSEG00005002	turquoise	MB	chr13 (R)	Jaml	**-0.62079575221903**	-0.533839246152548	**-0.614668577128408**	-0.00612717509062212	-0.086956506066482	0.0808293309758599
ENSMSEG00005000	turquoise	MB	chr13 (R)	2310030G06R	**-0.800625247654511**	0.129182683094096	0.0472851159450375	**-0.847910363599548**	**-0.929807930748606**	0.081897567149058
ENSMSEG00005012	turquoise	MB	chr13 (R)	Timm8b	**-0.748332258436679**	-0.548135905639956	**-0.642975752052761**	-0.105356506383918	-0.200196352796723	0.094839846412805
ENSMSEG00005012	turquoise	MB	chr13 (R)	Commd4	**-0.650901499003015**	-0.515331922672811	**-0.642274700476068**	-0.00862679852694774	-0.135569576330205	0.126942777803257
ENSMSEG00005006	turquoise	MB	chr13 (R)		**-0.633817976696183**	**-1.22537553094269**	**-0.665024080783341**	0.0312061040871575	**0.591557554246506**	0.14092091871995
ENSMSEG00005016	turquoise	MB	chr13 (R)	Srprb	**-0.89627519040539**	-0.51289834484596	**-0.676651102460476**	-0.219624087944914	-0.38337684555943	0.163752757614516
ENSMSEG00005012	turquoise	MB	chr13 (R)	Pts	**-0.619008914351315**	-0.441151982423792	**-0.607906815714045**	-0.01110209863727	-0.177856931927522	0.166754833290252
ENSMSEG00005009	turquoise	MB	chr13 (R)		**-0.716571765355408**	**-0.65215265207334**	-0.532894344403601	-0.183677420951807	-0.0644191132820686	0.190211253356417
ENSMSEG00005016	turquoise	MB	chr13 (R)	Gsta4	-0.399245319778104	**-0.70661608697996**	**-0.91166165085404**	0.512416331075936	0.307370767201856	0.20504556387408
ENSMSEG00005005	turquoise	MB	chr13 (R)	Tipin	**-0.652963419206645**	-0.386632814132036	**-0.686879007457208**	0.0339155882505637	-0.266330605074609	0.300246193325172
ENSMSEG00005006	turquoise	MB	chr13 (R)	Cmc1	-0.581696941325308	-0.37368259775168	**-0.751860168536739**	0.170163227211432	-0.208014343573628	0.37817757078506
ENSMSEG00005010	turquoise	MB	chr13 (R)	Ccdc153	-0.581424672364042	**-0.621642755769598**	**-1.01618499786278**	0.434760325498736	0.0402180834055563	0.39454224209318
ENSMSEG00005017	turquoise	MB	chr13 (R)	Nme9	**-1.06002530238593**	**-0.595723785097349**	**-1.02256831378966**	-0.0374569885962755	-0.464301517288585	0.42684452869231
ENSMSEG00005018	turquoise	MB	chr13 (R)	Ppm1m	**-1.61149939496525**	**-1.19127258502664**	**-1.71913868897284**	0.107639294007595	-0.420226809938609	0.527866103946204
ENSMSEG00005021	turquoise	MB	X/X* (NR)		**-0.587069010531535**	-0.434878331498779	-0.207055576065833	-0.380013434465703	-0.152190679032756	-0.0473356847244112
ENSMSEG00005003	turquoise	MB	X/X* (NR)	Rpl36al	**-0.690610204762386**	**-0.660084244465352**	**-0.597283747404877**	-0.0933264573575086	-0.0305259602970331	-0.0628004970604755
ENSMSEG00005022	turquoise	MB	X/X* (NR)	Tmsb4x	**-0.832393303628243**	**-0.631551257654984**	-0.566928057665539	-0.265465245962704	-0.200842045973259	-0.0646231999894454
ENSMSEG00005006	turquoise	MB	X/X* (NR)		**-0.824401865055648**	**-0.7352299640414**	**-0.666021250243895**	-0.158380614811753	-0.0891719010142477	-0.0692087137975055
ENSMSEG00005011	turquoise	MB	X/X* (NR)	Hsd17b10	-0.553410630634341	**-0.595709565672949**	-0.480630192219559	-0.0727804384147823	0.0422989350386079	-0.11507937345339
ENSMSEG00005023	turquoise	MB	X/X* (NR)		**-0.643669948900275**	-0.531771344387088	-0.484435659662677	-0.159234289237598	-0.111898604513186	-0.227822755432947
ENSMSEG00005004	turquoise	MB	X/X* (NR)	Tceal8	**-0.617020813778547**	-0.415223277595926	-0.46181397355654	-0.155206840222007	-0.20179753618262	0.0465906959606134
ENSMSEG00005007	turquoise	MB	X/X* (NR)	Cox7b	**-0.610375437675982**	-0.483507879080167	-0.554069882297435	-0.0563055553785478	-0.126867558595815	0.0705620032172672

ENSMSEG00005023(	turquoise	MB	X/X* (NR)	Cited1	**-0.673210290154444**	-0.548061589555794	**-0.677138549984387**	0.0039282598299427	-0.12514870059865	0.129076960428593
ENSMSEG00005000(	turquoise	MB	X/X* (NR)	Rbm3	**-0.793217402033617**	-0.540268017000188	**-0.731152334765572**	-0.0620650672680447	-0.252949385033429	0.190884317765384
ENSMSEG00005003(	turquoise	MB	X/X* (NR)	Sytl4	**-1.09601070210756**	**-1.07588916672434**	**-1.34624422374347**	0.250233521635908	-0.0201215353832182	0.270355057019126
ENSMSEG00005004(	turquoise	MB	X/X* (NR)	Timm8a1	-0.433834665656783	-0.308291423731357	**-0.715842298893644**	0.282007633236861	-0.125543241925426	0.407550875162287
ENSMSEG00005015(	turquoise	MB	unassigne(	Mrps21	**-0.669285517754011**	-0.481735570103129	-0.546851163876822	-0.122434353877189	-0.187549947650882	0.0651155937736927
ENSMSEG00005013(	magenta	X dose	Autosome	Trim55	**0.593354029360541**	**-0.746146187872622**	-0.328005733788021	**0.921359763148562**	**1.33950021723316**	-0.418140454084601
ENSMSEG00005008(	magenta	X dose	Autosome	Cd300ld2	**1.2600860530743**	**-1.4338421428374**	**-0.770695350321599**	**2.0307814033959**	**2.6939281959117**	**-0.663146792515801**
ENSMSEG00005000(	magenta	X dose	Autosome	D16Ertd472e	0.288591646585855	-0.129211102383419	-0.470089017234021	**0.758680663819876**	0.417802748969274	0.340877914850602
ENSMSEG00005010(	magenta	X dose	Autosome	1110051M20R	0.254738554446592	-0.213993752637498	-0.558082037055137	**0.812820591501729**	0.46873230708409	0.344088284417639
ENSMSEG00005022(	magenta	X dose	Autosome	Tec	**0.650920971527114**	0.0345264100303947	-0.381398028492665	**1.03231900001978**	**0.61639456149672**	0.41592443852306
ENSMSEG00005010(	magenta	X dose	Autosome		0.134113039592089	-0.179347573056471	**-0.700125825986078**	**0.834238865578166**	0.313460612648559	0.520778252929607
ENSMSEG00005019(	magenta	X dose	Autosome	Aldh3b1	0.497451675119619	0.228903724420636	-0.295229374834014	**0.792681049953632**	0.268547950698983	0.524133099254649
ENSMSEG00005018(	magenta	X dose	Autosome	Tdrd1	**0.976502801954455**	-0.0560917275251865	**-1.06652093684384**	**2.0430237387983**	**1.03259452947964**	**1.01042920931865**
ENSMSEG00005019(	magenta	X dose	Autosome	Ccdc186	**0.846566469241335**	0.175490635183655	**-1.11128515411149**	**1.95785162335282**	**0.67107583405768**	**1.28677578929514**
ENSMSEG00005019(	magenta	X dose	Autosome		**0.845527169560165**	0.161456951876419	**-1.22543658634416**	**2.07096375590432**	**0.684070217683746**	**1.38689353822058**
ENSMSEG00005006(	magenta	X dose	chr1 (NR)	**Lhb* °**	0.475605482150218	-0.262196291004923	-0.581154964413555	**1.05676044656377**	**0.737801773155141**	0.318958673408632
ENSMSEG00005022(	magenta	X dose	chr1 (NR)	Mef2a	**0.726067849116557**	0.290443041437668	-0.273572419589541	**0.999640268706098**	0.435624807678889	0.564015461027209
ENSMSEG00005020(	magenta	X dose	chr1 (NR)	Wdr93	0.5579810333885	0.0397094705010782	-0.579583200133248	**1.13756423352175**	0.518271562887422	**0.619292670634326**
ENSMSEG00005014(	magenta	X dose	chr1 (NR)	Fam174b	0.536906186122873	0.134051412846018	-0.511067825090819	**1.04797401121369**	0.402854773276855	**0.645119237936838**
ENSMSEG00005022(	magenta	X dose	chr1 (NR)	Uba2	0.571702616174177	0.0635110160218316	**-0.664336077601006**	**1.23603869377518**	0.508191600152345	**0.727847093622838**
ENSMSEG00005012(	magenta	X dose	chr1 (NR)	Whamm	0.474189364304611	-0.104550722558638	**-0.835636043152284**	**1.30982540745689**	0.578740086863249	**0.731085320593646**
ENSMSEG00005005(	magenta	X dose	chr1 (NR)	Ldha	0.257362473444944	-0.223547715869081	**-1.06669051053183**	**1.32405298397678**	0.480910189314025	**0.843142794662753**
ENSMSEG00005022(	magenta	X dose	chr1 (NR)	Lrrc28	**0.627379892920733**	0.0402273145435367	**-1.26868387873858**	**1.89606377165931**	**0.587152578377197**	**1.30891119328211**
ENSMSEG00005011(	magenta	X dose	chr1 (NR)	Alpk3	**0.785458288574176**	-0.414271353566744	**-1.88010761666038**	**2.66556590523456**	**1.19972964214092**	**1.46583626309364**
ENSMSEG00005022(	magenta	X dose	chr1 (NR)	Ttc23	0.276553880350187	-0.266780759323314	**-1.74157533084116**	**2.01812921119134**	0.543334639673501	**1.47479457151784**
ENSMSEG00005011(	magenta	X dose	chr1 (NR)	Pde8a	**1.27328040420622**	0.461325395172131	**-1.12011401700104**	**2.39339442120726**	**0.811955009034089**	**1.58143941217317**
ENSMSEG00005011(	magenta	X dose	chr1 (NR)	Synm	**1.17786300788641**	0.281756345719219	**-1.80415419752818**	**2.98201720541459**	**0.896106662167189**	**2.0859105432474**
ENSMSEG00005011(	magenta	X dose	chr1 (NR)	Slc28a1	**1.63997232769272**	**0.638617535069074**	**-2.01586406354628**	**3.65583639123899**	**1.00135479262364**	**2.65448159861535**
ENSMSEG00005002(	magenta	X dose	X/X* (R)	Apln	0.25279769885332	-0.0253317426769041	-0.377872535309095	**0.630670234162415**	0.278129441530224	0.352540792632191
ENSMSEG00005013(	magenta	X dose	X/X* (R)		0.128572725254639	**-5.84876303772204**	**-6.33504169443174**	**6.46361441968638**	**5.97733576297668**	0.486278656709702
ENSMSEG00005009(	magenta	X dose	chr1 (R)	Prr33	-0.0351580374720089	0.196349911667971	**-1.02224417410401**	**0.987086136632003**	-0.23150794913998	**1.21859408577198**
ENSMSEG00005010(	magenta	X dose	X/X* (NR)	Srpx	0.582921710976552	-0.0840498145201122	**-0.646676102299182**	**1.22959781327573**	**0.666971525496664**	0.56262628777907
ENSMSEG00005022(	magenta	X dose	X/X* (NR)	Taf1	0.21038056589554	-0.0745391086883599	**-0.753460529469993**	**0.963841095365532**	0.284919674583899	**0.678921420781633**
ENSMSEG00005004(	magenta	X dose	X/X* (NR)	**Eif2s3x †**	0.474644601632184	0.249326928748968	-0.556979856373072	**1.03162445800526**	0.225317672883216	**0.80630678512204**
ENSMSEG00005009(	magenta	X dose	X/X* (NR)	**Maoa * °**	0.0430070769853006	-0.307030989476428	**-1.86766786610959**	**1.91067494309489**	0.350038066461729	**1.56063687663316**
ENSMSEG00005004(	magenta	X dose	X/X* (NR)		-0.234826795006813	**-0.836451291030891**	**-4.76243634130683**	**4.52760954630001**	**0.601624496024078**	**3.92598505027593**
ENSMSEG00005006(	green	YB	Autosome	Trmt10b	**-0.595338656985512**	-0.330170213904076	-0.0841230827288011	-0.511215574256711	-0.265168443081436	-0.246047131175275
ENSMSEG00005001(	green	YB	Autosome		**-1.58759896599667**	**-2.1461258158143**	-0.0618332694141349	**-1.52576569658254**	0.558526849817622	-0.273296939578103
ENSMSEG00005010(	green	YB	Autosome	Nfyc	-0.254246554392408	0.0599174618707349	0.381703179359345	**-0.635949733751754**	-0.314164016263143	-0.321785717488611
ENSMSEG00005010(	green	YB	Autosome	Exo5	**-1.94581211227449**	-0.338944594224317	0.135123205858972	**-2.08093531813347**	**-1.60686751805018**	-0.474067800083289
ENSMSEG00005010(	green	YB	Autosome	Lpin3	**-0.805992453278436**	-0.564704385931618	0.0282253963021876	**-0.834217849580624**	-0.241288067346818	**-0.592929782233806**
ENSMSEG00005006(	green	YB	Autosome	Derl3	**-0.65920249071456**	-0.331597868364642	0.406239643445913	**-1.06544213416047**	-0.327604622349918	**-0.737837511810554**
ENSMSEG00005021(	green	YB	Autosome		**-3.39225148509921**	**-3.25711217030566**	-0.373935547624355	**-3.01831593747485**	-0.135139314793548	**-0.73800912091566**
ENSMSEG00005017(	green	YB	Autosome	Alox5	**-0.674819366529402**	**-0.824101210881813**	-0.0680060616304564	**-0.606813304898946**	0.149281844352411	**-0.756095149251356**
ENSMSEG00005019(	green	YB	Autosome	Aldh3b3	**-1.07047537683838**	-0.324218941689791	**0.638793170172367**	**-1.70926854701075**	**-0.746256435148588**	**-0.963012111862158**
ENSMSEG00005018(	green	YB	Autosome	Stab2	-0.50420793044112	-0.287726070729577	**0.714909568900866**	**-1.21911749934199**	-0.216481859711543	**-1.00263563963044**
ENSMSEG00005018(	green	YB	Autosome	Rhod	**-1.05662642629755**	**-1.16788524503839**	-0.093110336538213	**-0.963516089759334**	0.111258818740844	**-1.07477490850018**

ENSMSEG00005011	green	YB	Autosome	Dsc2	**-0.966760016004651**	**-0.885285581571043**	0.31270567343514	**-1.27946568943979**	-0.0814744344336078	**-1.19799125500618**
ENSMSEG00005022	green	YB	Autosome		**-1.05527241782831**	**-1.29764836434818**	-0.000966063698395969	**-1.05430635412991**	0.242375946519874	**-1.29668230064978**
ENSMSEG00005009	green	YB	Autosome	Psma1	**-3.64390564688637**	**-1.08712627070238**	**0.85320384892246**	**-4.49710949580883**	**-2.556779376184**	**-1.94033011962484**
ENSMSEG00005003	green	YB	Autosome		**-1.46601709026841**	**-1.45959653973458**	**-0.721587418818919**	**-0.744429671449493**	-0.00642055053383307	**-2.08429254640016**
ENSMSEG00005022	green	YB	Autosome		-0.405300608183874	0.000742014371586991	0.27403895394969	**-0.679339562133565**	-0.406042622555461	**-2.8831766226813**
ENSMSEG00005002	green	YB	Autosome	Zc3h4	**-1.90331900882884**	**-2.64855480337049**	0.400336078918369	**-2.30365508774721**	**0.745235794541647**	**-3.04889088228886**
ENSMSEG00005007	green	YB	Autosome	Snrpd2	**-4.23916762255241**	**-3.86758798248731**	**-0.63820388503439**	**-3.60096373751802**	-0.371579640065101	**-3.22938409745292**
ENSMSEG00005016	green	YB	Autosome	Eif3k	**-4.28652333068736**	**-4.6337624206245**	-0.343097864716665	**-3.9434254659707**	0.347239089937143	**-4.29066455590784**
ENSMSEG00005022	green	YB	chr1 (NR)	Nudt19	-0.584407418692832	**-0.589556963143038**	-0.149675818865516	-0.434731599827316	0.00514954445020615	-0.439881144277522
ENSMSEG00005010	green	YB	chr1 (NR)	Zfp82	-0.56880415001537	**-0.595323667417042**	-0.154564275024966	-0.414239874990404	0.0265195174016725	-0.440759392392076
ENSMSEG00005012	green	YB	chr1 (NR)	Zfp524	-0.448064108068291	**-0.603267896275098**	-0.160604690848933	-0.287459417219358	0.155203788206807	-0.442663205426165
ENSMSEG00005017	green	YB	chr1 (NR)	Dll3	**-0.844030832496344**	**-0.701177856682971**	-0.224671275806591	**-0.619359556689754**	-0.142852975813373	-0.476506580876381
ENSMSEG00005019	green	YB	chr1 (NR)	Kptn	**-0.943153846583598**	**-0.759475449009242**	-0.252413298465257	**-0.690740548118341**	-0.183678397574356	-0.507062150543984
ENSMSEG00005006	green	YB	chr1 (NR)	Plekha4	**-1.05355221072701**	-0.186349925918325	0.325122511374566	**-1.37867472210158**	**-0.867202284808684**	-0.511472437292891
ENSMSEG00005007	green	YB	chr1 (NR)	Lsr	-0.532865173627492	**-0.629952419416622**	-0.113285068738481	-0.419580104889012	0.0970872457891301	-0.516667350678142
ENSMSEG00005017	green	YB	chr1 (NR)	Ccdc61	**-0.967216873727782**	**-0.780681577632172**	-0.241885613484827	**-0.725331260242955**	-0.186535296095611	-0.538795964147344
ENSMSEG00005019	green	YB	chr1 (NR)	Pex11a	-0.393614089972021	-0.452791086482683	0.139481016863105	-0.533095106835126	0.0591769965106623	**-0.592272103345788**
ENSMSEG00005018	green	YB	chr1 (NR)	Htatip2	**-0.851662244467828**	**-0.683198496174396**	-0.0886618963651693	**-0.763000348102659**	-0.168463748293433	**-0.594536599809226**
ENSMSEG00005023	green	YB	chr1 (NR)	Il16	**-0.819730571738142**	**-0.863604107237849**	-0.15742779621727	**-0.662302775520872**	0.0438735354997064	**-0.706176311020579**
ENSMSEG00005022	green	YB	chr1 (NR)	Dpy19l3	-0.225310201472817	-0.33339433630356	0.393963382731712	**-0.619273584204529**	0.108084134830743	**-0.727357719035272**
ENSMSEG00005006	green	YB	chr1 (NR)	Kcnj14	**-0.669365410955726**	**-0.77389400880103**	-0.0376546978582063	**-0.63171071309752**	0.104528597845303	**-0.736239310942823**
ENSMSEG00005020	green	YB	chr1 (NR)	Catsperg1	**-0.684757320582118**	**-1.06749425125508**	-0.201114237633649	-0.483643082948469	0.382736930672962	**-0.866380013621431**
ENSMSEG00005023	green	YB	chr1 (NR)	Zfp760	**-0.847456095557802**	**-0.872922089507938**	0.000605162930094946	**-0.848061258487896**	0.0254659939501364	**-0.873527252438033**
ENSMSEG00005016	green	YB	chr1 (NR)	Zfp78	-0.568207094224553	**-0.644034833251005**	0.343601385759449	**-0.911808479984002**	0.0758277390264513	**-0.987636219010453**
ENSMSEG00005000	green	YB	chr1 (NR)	Fam71e1	-0.500626510772446	**-0.749630226569314**	0.269065655749361	**-0.769692166521806**	0.249003715796869	**-1.01869588231867**
ENSMSEG00005010	green	YB	chr1 (NR)	Fxyd3	**-2.21494438857528**	**-2.01151153335096**	**-0.82457063854451**	**-1.39037375003077**	-0.203432855224326	**-1.18694089480645**
ENSMSEG00005012	green	YB	chr1 (NR)	Hddc3	**-3.24617255965038**	**-0.743577883560022**	0.506379133572995	**-3.75255169322337**	**-2.50259467609035**	**-1.24995701713302**
ENSMSEG00005003	green	YB	chr1 (NR)	Zfp51	**-8.2042256825833**	**-0.972766519550022**	**0.658873156198729**	**-8.86309883878203**	**-7.23145916303328**	**-1.63163967574875**
ENSMSEG00005021	green	YB	chr1 (NR)	Rlbp1	**-1.418128838359**	**-2.06085957415659**	-0.357045487313845	**-1.06108335104516**	**0.642730735797587**	**-1.70381408684274**
ENSMSEG00005002	green	YB	chr1 (NR)	2410002F23Ri	**-2.29333683595429**	**-2.35412391025965**	-0.11696832140147	**-2.17636851455282**	0.0607870743053582	**-2.23715558885818**
ENSMSEG00005009	green	YB	chr1 (NR)	Upk1a	**-2.14785916087152**	**-2.5037343646314**	-0.100325505467787	**-2.04753365540373**	0.355875203759883	**-2.40340885916361**
ENSMSEG00005002	green	YB	chr1 (NR)	1700028J19Ri	**-2.49075593153603**	**-2.74601505366328**	-0.257981288176468	**-2.23277464335957**	0.255259122127245	**-2.48803376548681**
ENSMSEG00005012	green	YB	chr1 (NR)		**-3.2857819969356**	**-2.61922244891549**	0.0394536638983601	**-3.32523566083396**	**-0.666559548020113**	**-2.54166971100964**
ENSMSEG00005002	green	YB	chr1 (NR)		**-2.46589173252605**	**-2.88011350952968**	-0.33844379852004	**-2.12744793400601**	0.41422177700363	**-2.65867611281385**
ENSMSEG00005020	green	YB	chr1 (NR)	Zfp59	**-7.09312901021292**	**-5.68549175792752**	0.286116713063857	**-7.37924572327678**	**-1.40763725228541**	**-5.97160847099137**
ENSMSEG00005013	green	YB	chr13 (NR)	Crtam	**-1.0891547249237**	-0.514421566572485	-0.175430724740303	**-0.913724000183399**	-0.574733158351218	-0.338990841832181
ENSMSEG00005008	green	YB	chr1 (R)	Cd70	0.062825495654819	-0.247767858267875	**0.60697339948117**	-0.544147903826351	0.310593353922694	**-0.854741257749045**
ENSMSEG00005005	green	YB	chr13 (R)		**-1.27188717690346**	**0.905160055956945**	**1.07225761646287**	**-2.34414479336633**	**-2.17704723286041**	-0.167097560505924
ENSMSEG00005002	green	YB	chr13 (R)	BC049352	-0.230369186665098	0.0287492177255078	0.52938179537147	**-0.759750982036568**	-0.259118404390606	-0.500632577645962
ENSMSEG00005005	green	YB	chr13 (R)	Myd88	-0.353990574917531	-0.172468475123676	0.381027118297521	**-0.735017693215052**	-0.181522099793855	-0.553495593421197
ENSMSEG00005000	green	YB	chr13 (R)		**-1.98491003994431**	**-1.75804745097366**	0.255185217298334	**-2.24009525724265**	-0.226862588970653	**-2.013232668272**
ENSMSEG00005005	green	YB	unassigned		**-4.1836373250753**	**-5.32449681829181**	0.00697138298077865	**-4.19060870805608**	**1.1408594932165**	**-5.33146820127259**

bold values indicates |logFC|>= log2(1.5) ; threshold to consider differential expression

candidates genes (* influence on phenotype ; ° X* Y females different from other females ; † genes escaping inactiva

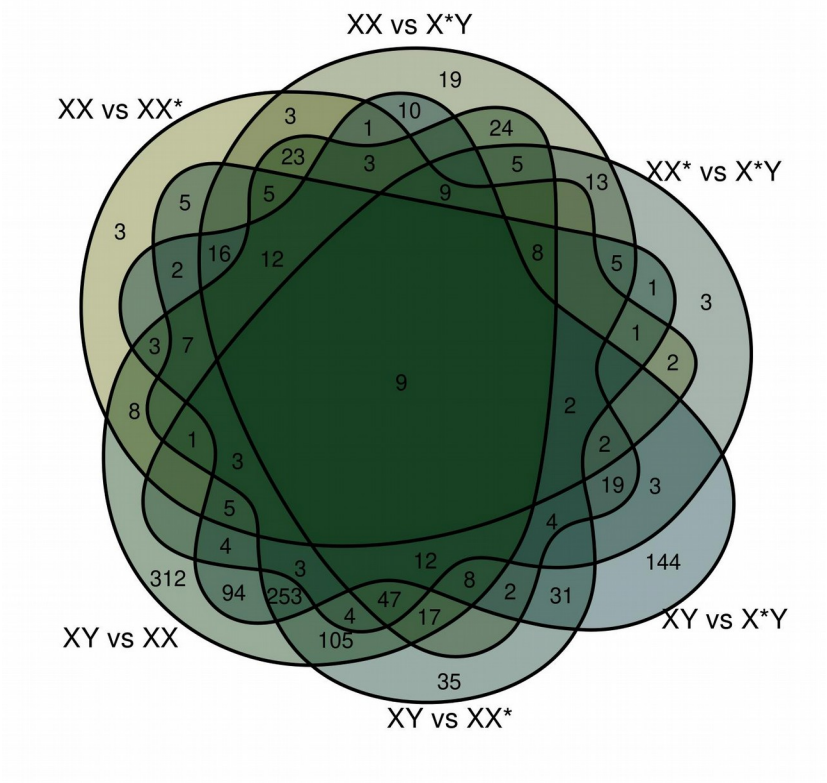

Overlap DEG between contrasts

ID	Description	GeneRatio	BgRatio	pvalue	p.adjust	qvalue	geneID
GO:0006412	translation	77/545	469/11314	4.20E-22	1.37E-18	1.36757274390369E-18	Rpl4/Rbm3/Rps3/Rps28/Rpl32/Rpl24/Rps20/Mrpl41/Mrpl13/Mrps7/Mrps21/ Mrpl19/Rpl7/Rps9/ Rpl36al/Mrpl47/Rpl13/Dph7/Rpl14/Rpl26/Rpl19/Rnf139/Rps14/Chchd1/Rps12/ Rpl39/Rps7/ Rpl22l1/Rps11/Rpl11/Rps13/Rps23/Rpl21/Rpl36/Rpl35/Mrpl20/Eif3m/Mrpl23/ Mrpl49/Fau/Mrps18a/Guf1/Rpl23/Rps5/Mrps18c/Rpl8/Rpl9-ps6/Rpl37a/Eef1g/ Rpl13a/Rpl31/Polr2g/Sars2/Mrpl17/Rpl17/Dcps/Rack1/Eif3e/Mrpl32/Rwdd1/ Rps16/Rps26/Fastkd2/Rplp0/Rps15/Rpl30/Rpl5/Eif3k/Rpl6/Rps21/Rps27a/ Mrps14/Mrpl15/Eif2s2/Mrps28/Magoh/Uqcc2
GO:0043043	peptide biosynthetic process	77/545	486/11314	3.98E-21	6.48E-18	6.48156040140576E-18	Rpl4/Rbm3/Rps3/Rps28/Rpl32/Rpl24/Rps20/Mrpl41/Mrpl13/Mrps7/Mrps21/ Mrpl19/Rpl7/Rps9/Rpl36al/Mrpl47/Rpl13/Dph7/Rpl14/Rpl26/Rpl19/Rnf139/Rps14/ Chchd1/Rps12/Rpl39/Rps7/Rpl22l1/Rps11/Rpl11/Rps13/Rps23/Rpl21/Rpl36/ Rpl35/Mrpl20/Eif3m/Mrpl23/Mrpl49/Fau/Mrps18a/Guf1/Rpl23/Rps5/Mrps18c/ Rpl8/Rpl9-ps6/Rpl37a/Eef1g/Rpl13a/Rpl31/Polr2g/Sars2/Mrpl17/Rpl17/Dcps/ Rack1/Eif3e/Mrpl32/Rwdd1/Rps16/Rps26/Fastkd2/Rplp0/Rps15/Rpl30/Rpl5/ Eif3k/Rpl6/Rps21/Rps27a/Mrps14/Mrpl15/Eif2s2/Mrps28/Magoh/Uqcc2
GO:0033108	mitochondrial respiratory chain complex assembly	26/545	74/11314	2.38E-16	2.59023041312672E-13	2.59023041312671E-13	Ndufb6/Ndufa12/Cox14/Ndufa3/Ndufaf5/Ndufs3/Ndufs4/Cox19/Tmem126a/ Ndufa1/Ndufc1/Ndufaf6/Ndufb2/Ndufs5/Sdhaf2/Oma1/Slc25a33/Ndufb8/Ndufs6/ Ndufaf3/Pet100/Surf1/Uqcc2/Ndufa6/Ndufb4/Ndufb7
GO:0002181	cytoplasmic translation	25/545	72/11314	1.25E-15	1.01901003554227E-12	1.01901003554227E-12	Rps28/Rpl32/Rpl24/Rpl36al/Dph7/Rpl26/Rpl19/Rpl39/Rpl22l1/Rpl11/Rps23/ Rpl36/Eif3m/Rpl8/Rpl9-ps6/Rpl13a/Rpl31/Rpl17/Rwdd1/Rps26/Rplp0/Rpl30/Rpl6/ Rps21/Eif2s2
GO:0006119	oxidative phosphorylation	24/545	81/11314	2.60046245874909E-13	1.6955015231044E-10	1.6955015231044E-10	Ndufb6/Ndufa12/Atp5h/Atpsckmt/Cox7c/Ndufs3/Tefm/Cox7a1/Atp5j/Atp5e/ Uqcrfs1/Cox7a2/Sdhaf2/Slc25a33/Lexm/Cox4i1/Ndufb8/Ndufs6/Antkmt/Atp5o/ Atp5k/Uqcc2/Uqcr10/Nupr1
GO:0010257	NADH dehydrogenase complex assembly	18/545	44/11314	4.73368819656481E-13	2.20454621725732E-10	2.20454621725732E-10	Ndufb6/Ndufa12/Ndufa3/Ndufaf5/Ndufs3/Ndufs4/Tmem126a/Ndufa1/Ndufc1/ Ndufaf6/Ndufb2/Ndufs5/Ndufb8/Ndufs6/Ndufaf3/Ndufa6/Ndufb4/Ndufb7
GO:0032981	mitochondrial respiratory chain complex I assembly	18/545	44/11314	4.73368819656481E-13	2.20454621725732E-10	2.20454621725732E-10	Ndufb6/Ndufa12/Ndufa3/Ndufaf5/Ndufs3/Ndufs4/Tmem126a/Ndufa1/Ndufc1/ Ndufaf6/Ndufb2/Ndufs5/Ndufb8/Ndufs6/Ndufaf3/Ndufa6/Ndufb4/Ndufb7
GO:0009060	aerobic respiration	27/545	118/11314	7.52342203069564E-12	3.06579447750847E-09	3.06579447750847E-09	Ndufb6/Ndufa12/Atp5h/Atpsckmt/Sdhb/Cox7c/Ndufs3/Ndufs4/Tefm/Sirt3/Cox7a1/ Atp5j/Atp5e/Uqcrfs1/Cox7a2/Sdhaf2/Slc25a33/Lexm/Cox4i1/Ndufb8/Ndufs6/ Antkmt/Atp5o/Atp5k/Uqcc2/Uqcr10/Nupr1
GO:0042255	ribosome assembly	15/545	47/11314	2.59050932147263E-09	9.38340043111196E-07	9.38340043111196E-07	Rps28/Rpl24/Mrps7/Brix1/Rps14/Rpl11/Mrpl20/Rps25/Rps5/Rps27/Fastkd2/ Rplp0/Rps15/Rpl5/Rpl6
GO:0022613	ribonucleoprotein complex biogenesis	41/545	312/11314	4.02944155494346E-09	1.24594028773006E-06	1.24594028773006E-06	Rps28/Rpl24/Mrps7/Rpl7/Rps6/Snrpd1/Rpl14/Rpl26/Brix1/Ybey/Rps14/Snrpd3/ Rps7/Pih1d1/Rpl11/Rpl27/Snrpd2/Rpl35/Rbis/Mrpl20/Snrpf/Rps25/Nsa2/Rps5/ Rpl13a/Npm3/Nhp2/Rps27/Rps16/Fastkd2/Rplp0/Rps15/Isg20/Rpl5/Pop5/Rpl6/ Snrpe/Rps21/Rpp38/Eif2s2/Gtf3a
GO:0007005	mitochondrion organization	49/545	414/11314	4.20409299540816E-09	1.24594028773006E-06	1.24594028773006E-06	Ndufb6/Ndufa12/Immp1l/Slirp/Tomm7/Cox14/Ndufa3/Ndufaf5/Timm8a1/Ndufs3/ Ndufs4/Cox19/Tomm5/Tmem126a/Ndufa1/Ndufc1/Micos13/Dnajc19/Atp23/ Cox7a1/Hsd17b10/Ndufaf6/Ndufb2/Ndufs5/Fam162a/Pycard/Cox7a2/Sdhaf2/ Oma1/Slc25a33/Bad/Siva1/Ndufb8/Mrpl17/Ndufs6/Mpv17/Slc25a5/Ndufaf3/Gpx1/ Atpif1/Pet100/Mrpl15/Surf1/Ggnbp1/Uqcc2/Ndufa6/Ndufb4/Pdcd5/Ndufb7
GO:0042254	ribosome biogenesis	34/545	233/11314	6.22712838817594E-09	1.69170321212113E-06	1.69170321212113E-06	Rps28/Rpl24/Mrps7/Rpl7/Rps6/Rpl14/Rpl26/Brix1/Ybey/Rps14/Rps7/Pih1d1/ Rpl11/Rpl27/Rpl35/Rbis/Mrpl20/Rps25/Nsa2/Rps5/Npm3/Nhp2/Rps27/Rps16/ Fastkd2/Rplp0/Rps15/Isg20/Rpl5/Pop5/Rpl6/Rps21/Rpp38/Gtf3a

GO:0022618	ribonucleoprotein complex assembly	23/545	118/11314	7.65934986088049E-09	1.92072927280542E-06	1.92072927280542E-06	Rps28/Rpl24/Mrps7/Snrpd1/Brix1/Rps14/Snrpd3/Pih1d1/Rpl11/Snrpd2/Mrpl20/ Snrpf/Rps25/Rps5/Rpl13a/Rps27/Fastkd2/Rplp0/Rps15/Rpl5/Rpl6/Snrpe/Eif2s2
GO:0045333	cellular respiration	27/545	159/11314	8.91927695574961E-09	2.07691734826741E-06	2.07691734826741E-06	Ndufb6/Ndufa12/Atp5h/Atpsckmt/Sdhb/Cox7c/Ndufs3/Ndufs4/Tefm/Sirt3/Cox7a1/ Atp5j/Atp5e/Uqcrfs1/Cox7a2/Sdhaf2/Slc25a33/Lexm/Cox4i1/Ndufb8/Ndufs6/ Antkmt/Atp5o/Atp5k/Uqcc2/Uqcr10/Nupr1
GO:0042273	ribosomal large subunit biogenesis	15/545	54/11314	2.1800513233172E-08	4.62020914870435E-06	4.62020914870435E-06	Rpl24/Rpl7/Rpl14/Rpl26/Brix1/Rpl11/Rpl35/Mrpl20/Nsa2/Nhp2/Fastkd2/Rplp0/ Rpl5/Rpl6/Gtf3a
GO:0046034	ATP metabolic process	29/545	188/11314	2.36538068269971E-08	4.62020914870435E-06	4.62020914870435E-06	Ndufb6/Ndufa12/Atp5h/Atpsckmt/Gm5426/Cox7c/Ndufs3/Tefm/Cox7a1/Atp5j/ Atp5e/Atp5g2/Uqcrfs1/Cox7a2/Sdhaf2/Slc25a33/Bad/Lexm/Cox4i1/Ndufb8/ Ndufs6/Antkmt/Atp5o/Atp5k/Atpif1/Gck/Uqcc2/Uqcr10/Nupr1
GO:0071826	ribonucleoprotein complex subunit organization	23/545	125/11314	2.40931151926301E-08	4.62020914870435E-06	4.62020914870435E-06	Rps28/Rpl24/Mrps7/Snrpd1/Brix1/Rps14/Snrpd3/Pih1d1/Rpl11/Snrpd2/Mrpl20/ Snrpf/Rps25/Rps5/Rpl13a/Rps27/Fastkd2/Rplp0/Rps15/Rpl5/Rpl6/Snrpe/Eif2s2
GO:0015986	proton motive force-driven ATP synthesis	9/545	18/11314	4.30719971696998E-08	7.80081726517896E-06	7.80081726517896E-06	Atp5h/Atpsckmt/Gm5426/Atp5j/Atp5e/Atp5g2/Antkmt/Atp5o/Atp5k
GO:0006364	rRNA processing	25/545	170/11314	5.61573429599453E-07	9.63541779207483E-05	9.63541779207483E-05	Rps28/Rpl7/Rps6/Rpl14/Rpl26/Brix1/Ybey/Rps14/Rps7/Pih1d1/Rpl11/Rpl27/ Rpl35/Rps25/Nsa2/Npm3/Nhp2/Rps27/Rps16/Rps15/Isg20/Rpl5/Pop5/Rps21/ Rpp38
GO:0000028	ribosomal small subunit assembly	7/545	13/11314	7.7152398728348E-07	0.000121908493168	0.000121908493168	Rps28/Mrps7/Rps14/Rps25/Rps5/Rps27/Rps15

ID	Description	GeneRatio	BgRatio	pvalue	p.adjust	qvalue	geneID
GO:0061564	axon development	36/309	418/11314	8.40811530646821E-10	2.22312270035147E-06	1.8156288253579E-06	Usp9x/Shh/Jun/Nrcam/Notch1/Egr2/Bcl11b/Sema6a/Lrp1/Fstl4/Mef2c/Ptpro/Dlx5/Vash2/Plxna2/Sema3c/Auts2/Sema3e/Lamc2/Nr4a3/Plxna4/Map1b/Tiam1/Slit1/Nfasc/Prkca/Myo5b/Nfib/Lama3/Sema3a/Tnr/Reln/Bmpr2/Pak3/Itga4/Nlgn3
GO:0007409	axonogenesis	34/309	384/11314	1.25352280820495E-09	2.22312270035147E-06	1.8156288253579E-06	Usp9x/Shh/Nrcam/Notch1/Egr2/Bcl11b/Sema6a/Lrp1/Fstl4/Mef2c/Ptpro/Dlx5/Plxna2/Sema3c/Auts2/Sema3e/Lamc2/Nr4a3/Plxna4/Map1b/Tiam1/Slit1/Nfasc/Prkca/Myo5b/Nfib/Lama3/Sema3a/Tnr/Reln/Bmpr2/Pak3/Itga4/Nlgn3
GO:0007411	axon guidance	23/309	192/11314	2.39481478886142E-09	2.35206379673825E-06	1.92093528070383E-06	Shh/Nrcam/Notch1/Egr2/Bcl11b/Sema6a/Lrp1/Mef2c/Ptpro/Dlx5/Plxna2/Sema3c/Sema3e/Lamc2/Nr4a3/Plxna4/Slit1/Nfasc/Nfib/Lama3/Sema3a/Reln/Bmpr2
GO:0097485	neuron projection guidance	23/309	193/11314	2.65245423934396E-09	2.35206379673825E-06	1.92093528070383E-06	Shh/Nrcam/Notch1/Egr2/Bcl11b/Sema6a/Lrp1/Mef2c/Ptpro/Dlx5/Plxna2/Sema3c/Sema3e/Lamc2/Nr4a3/Plxna4/Slit1/Nfasc/Nfib/Lama3/Sema3a/Reln/Bmpr2
GO:0044057	regulation of system process	36/309	445/11314	4.55791732467577E-09	3.23338655012499E-06	2.64071336368584E-06	Glra1/Cacna1e/Chrm2/Tacr1/Notch1/Cacna2d1/Egr2/Scn5a/Akap9/Mef2c/Zdhhc21/Hcn4/Ptpro/Grm1/Hgf/Pclo/Dsp/Nr4a3/Grin2a/Pbx3/Cacna1c/Prkca/Slc8a1/Grin2b/Tenm4/Cckbr/Ryr2/Galr1/Sema3a/Tnr/Reln/Bmpr2/Nos1/Oprm1/Dmd/Nlgn3
GO:0042391	regulation of membrane potential	30/309	343/11314	1.66732965929171E-08	9.85669716917951E-06	8.04998460065052E-06	Glra1/Kcnk13/Jun/Nrcam/Tacr1/Cacna2d1/Slc4a8/Ppid/Scn5a/Kdr/Akap9/Mef2c/Hcn4/Cacna1i/Pclo/Dsp/Grik3/Grin2a/Cacna1c/Scn8a/Slc8a1/Grin2b/Ryr2/Npas4/Reln/Kcnh5/Kcnh7/Oprm1/Dmd/Nlgn3
GO:0001508	action potential	16/309	105/11314	2.26744766571429E-08	1.14894812432694E-05	9.38348267074546E-06	Glra1/Nrcam/Tacr1/Cacna2d1/Scn5a/Akap9/Hcn4/Cacna1i/Dsp/Grin2a/Cacna1c/Scn8a/Grin2b/Ryr2/Kcnh7/Dmd
GO:0050679	positive regulation of epithelial cell proliferation	18/309	142/11314	5.70285504103799E-08	2.52850335382022E-05	2.06503382538639E-05	Shh/Sox9/Jun/Tacr1/Notch1/Scn5a/Notch2/Kdr/Erbb4/Dlx5/Vash2/Nr4a3/Rictor/Prkca/Foxp2/Bmpr2/Osr1/Itga4
GO:0035637	multicellular organismal signaling	15/309	111/11314	3.1928741772863E-07	0.000123280102351	0.000100683110017	Glra1/Cacna1e/Nrcam/Cacna2d1/Scn5a/Akap9/Hcn4/Cacna1i/Dsp/Cacna1c/Nfasc/Scn8a/Slc8a1/Ryr2/Tnr
GO:0060284	regulation of cell development	32/309	437/11314	3.47561607980168E-07	0.000123280102351	0.000100683110017	Shh/Tnik/Rest/Notch1/Egr2/Heyl/Notch2/Fbn1/Sema6a/Kdr/Lrp1/Fstl4/Zdhhc21/Dlx2/Plxna2/Sema3c/Sema3e/Plxna4/Map1b/Tiam1/Slit1/Tenm4/Myo5b/Trib1/Spry4/Sema3a/Tnr/Reln/Bmpr2/Pak3/Nos1/Oprm1
GO:0051960	regulation of nervous system development	31/309	432/11314	8.30423730822959E-07	0.000267773906657	0.000218691493514	Shh/Tnik/Rest/Notch1/Egr2/Heyl/Sema6a/Kdr/Lrp1/Fstl4/Dlx2/Plxna2/Sema3c/Hgf/Sema3e/Plxna4/Map1b/Tiam1/Slit1/Prkca/Tenm4/Myo5b/Sema3a/Tnr/Reln/Bmpr2/Pak3/Nos1/Lingo4/Oprm1/Nlgn3
GO:0050767	regulation of neurogenesis	27/309	353/11314	1.31009812847336E-06	0.000387243171808	0.000316262285049	Shh/Tnik/Rest/Notch1/Egr2/Heyl/Sema6a/Kdr/Lrp1/Fstl4/Dlx2/Plxna2/Sema3c/Sema3e/Plxna4/Map1b/Tiam1/Slit1/Tenm4/Myo5b/Sema3a/Tnr/Reln/Bmpr2/Pak3/Nos1/Oprm1
GO:0007507	heart development	32/309	468/11314	1.56981265514804E-06	0.000408410394722	0.000333549599001	Shh/Tbc1d32/Adam19/Sox9/Jun/Rest/Notch1/Scn5a/Heyl/Notch2/Fbn1/Kdr/Lrp1/Mef2c/Erbb4/Sema3c/Sh3pxd2b/Dsp/Ccn1/Plxna4/Myh11/Cacna1c/Rbm20/Sik1/Slc8a1/Tenm4/Ryr2/Bmpr2/Acan/Osr1/Itga4/Dusp6
GO:0048736	appendage development	16/309	143/11314	1.73481498305334E-06	0.000408410394722	0.000333549599001	Fras1/Shh/Tbc1d32/Sox9/Notch1/Atrx/Notch2/Fmn1/Rc3h2/Dlx5/Plxna2/Sema3c/Slc7a11/Cacna1c/Bmpr2/Osr1
GO:0060173	limb development	16/309	143/11314	1.73481498305334E-06	0.000408410394722	0.000333549599001	Fras1/Shh/Tbc1d32/Sox9/Notch1/Atrx/Notch2/Fmn1/Rc3h2/Dlx5/Plxna2/Sema3c/Slc7a11/Cacna1c/Bmpr2/Osr1
GO:0050678	regulation of epithelial cell proliferation	22/309	255/11314	1.84227976192461E-06	0.000408410394722	0.000333549599001	Shh/Sox9/Jun/Tacr1/Notch1/Scn5a/Bcl11b/Notch2/Kdr/Mef2c/Erbb4/Brca2/Dlx5/Vash2/Nr4a3/Rictor/Prkca/Foxp2/Nfib/Bmpr2/Osr1/Itga4

GO:0034765	regulation of ion transmembrane transport	26/309	342/11314	2.32334691528706E-06	0.000484759500501	0.000395904068785	Cacna1e/Kcnk13/Cacna2d1/Scn5a/Akap9/Mef2c/Hcn4/Cybb/Lrrc55/Kcnb2/Grin2a/Arc/Cacna1c/Scn8a/Prkca/Hecw1/Slc8a1/Ryr2/Reln/Osr1/Kcnh5/Kcnh7/Nos1/Oprm1/Dmd/Nlgn3
GO:0050808	synapse organization	28/309	396/11314	3.86384097355804E-06	0.000695239057806	0.000567803150797	Nrcam/Dgkb/Rest/Ncan/Mef2c/Erbb4/Ptpro/Igfn1/Pclo/Sema3e/Slc7a11/Grin2a/Arc/Nfasc/Tanc2/Pcdhb16/Prkca/Cdh9/Grin2b/Myo5b/Npas4/Tnr/Reln/Pak3/Pcdh17/Bsn/Lingo4/Nlgn3
GO:0048675	axon extension	14/309	118/11314	3.87446609297972E-06	0.000695239057806	0.000567803150797	Usp9x/Sema6a/Lrp1/Sema3c/Auts2/Sema3e/Plxna4/Map1b/Slit1/Myo5b/Sema3a/Tnr/Bmpr2/Nlgn3
GO:0060560	developmental growth involved in morphogenesis	20/309	228/11314	4.25138575353664E-06	0.000695239057806	0.000567803150797	Usp9x/Shh/Sox9/Notch1/Sema6a/Fmn1/Lrp1/Fstl4/Sema3c/Auts2/Sema3e/Plxna4/Map1b/Slit1/Myo5b/Sema3a/Tnr/Bmpr2/Itga4/Nlgn3

gene_id	gene_nam	contrast	estimate	SE	df	z.ratio	p.value	FDR	bias	Allele
ENSMSEG00005000951	Wdr13	ref - alt	0.551064666946172	0.144874833775297	Inf	3.80372941653126	0.000142533866948	0.0003142223885	unbiased	X/X*
ENSMSEG00005001222	Ap2a1	ref - alt	-0.014362904000362	0.118912810370914	Inf	-0.120785169869933	0.903861196826682	0.932707830767959	unbiased	1neo-X/1neo-X*
ENSMSEG00005001389	Atp6ap2	ref - alt	0.499589550499065	0.122627967265308	Inf	4.07402619190607	4.62072814722585E-05	0.000113431136552	unbiased	X/X*
ENSMSEG00005001538	Myh14	ref - alt	0.260883879297056	0.166048785104823	Inf	1.57112790155234	0.116152942806337	0.156483825725204	unbiased	1neo-X/1neo-X*
ENSMSEG00005002231	Med25	ref - alt	-0.067822596338761	0.147857502693269	Inf	-0.45870243378491	0.646447866085303	0.753939104923421	unbiased	1neo-X/1neo-X*
ENSMSEG00005002478	Sh3kbp1	ref - alt	0.650587566141149	0.156970010338451	Inf	4.14466154865114	3.40315970405527E-05	9.5342923161884E-05	unbiased	X/X*
ENSMSEG00005002693		ref - alt	0.651182981460913	0.177174756350345	Inf	3.67537111310183	0.000237503920254	0.000470160821727	unbiased	X/X*
ENSMSEG00005002808	Eif1ax	ref - alt	0.294039372947247	0.139476625988538	Inf	2.10816235955845	0.035016947909168	0.050696178316258	unbiased	X/X*
ENSMSEG00005002968	Xk	ref - alt	0.777230297770487	0.190151999167817	Inf	4.08741586295157	4.36204794105415E-05	0.000111347013232	unbiased	X/X*
ENSMSEG00005002993		ref - alt	0.737997746725297	0.155272933413666	Inf	4.75290657876076	2.00513011096898E-06	8.84080094381779E-06	unbiased	X/X*
ENSMSEG00005003036	Mbtps2	ref - alt	0.19724720701063	0.155695354698805	Inf	1.26687920389281	0.205198485754411	0.265390041575705	unbiased	X/X*
ENSMSEG00005003230	Pdha1	ref - alt	0.534899002947509	0.11503275475632	Inf	4.64997125454062	3.31981295957681E-06	1.23854560414981E-05	unbiased	X/X*
ENSMSEG00005003375	Map7d2	ref - alt	0.497032301633654	0.133766194666061	Inf	3.71567945753756	0.000202658368183	0.000409538785703	unbiased	X/X*
ENSMSEG00005003487	Cnksr2	ref - alt	0.765298077263516	0.126082651137121	Inf	6.06981270112426	1.28059513566405E-09	1.38019697954903E-08	unbiased	X/X*
ENSMSEG00005003814	Mboat7	ref - alt	-0.167537760609719	0.148855178358932	Inf	-1.125508446913	0.260373639838916	0.332318987689143	unbiased	1neo-X/1neo-X*
ENSMSEG00005003867	Cnot3	ref - alt	0.018576385572935	0.151440999525069	Inf	0.1226641770141	0.90237303218453	0.932707830767959	unbiased	1neo-X/1neo-X*
ENSMSEG00005003962		ref - alt	0.382124008225004	0.112058273599008	Inf	3.41004725445269	0.000649516246787	0.001145510471607	unbiased	X/X*
ENSMSEG00005003995	Prkcg	ref - alt	0.096821388218869	0.118641005543959	Inf	0.81608704996178	0.414450350034653	0.508882075359005	unbiased	1neo-X/1neo-X*
ENSMSEG00005004010	Drp2	ref - alt	0.596816071621513	0.145249600524387	Inf	4.10889991756851	3.97548302240072E-05	0.000107117181437	unbiased	X/X*
ENSMSEG00005004061	Gpm6b	ref - alt	0.90825856017689	0.1233970273825	Inf	7.36045737440269	1.83281154494731E-13	4.44456799649723E-12	unbiased	X/X*
ENSMSEG00005004392	Cstf2	ref - alt	0.112117298120706	0.206518945148737	Inf	0.542891103961227	0.587204781380091	0.703195849307022	unbiased	X/X*
ENSMSEG00005004536	Eepd1	ref - alt	0.054067221270276	0.193897371401994	Inf	0.278844529347343	0.780364139736187	0.850509230948428	unbiased	13aut/13neo-X*
ENSMSEG00005004927		ref - alt	0.329827693902544	0.148100737102132	Inf	2.22704964442608	0.025943956080205	0.038129753633029	unbiased	X/X*
ENSMSEG00005004967	Tceal5	ref - alt	0.562961671441611	0.108166914425611	Inf	5.20456439412232	1.94452189492131E-07	1.38861487781079E-06	unbiased	X/X*
ENSMSEG00005004972	Bex1	ref - alt	0.524785241318146	0.125038611473234	Inf	4.19698551619379	2.70491224727074E-05	8.19926524953942E-05	unbiased	X/X*
ENSMSEG00005004988	Eif2s3x	ref - alt	0.811162154058027	0.116467735742647	Inf	6.9646941179522	3.29118046654471E-12	6.38489010509673E-11	X dose	X/X*
ENSMSEG00005005046	Maged1	ref - alt	0.716092737909815	0.115882796708178	Inf	6.17945681543327	6.43225253325445E-10	7.79910619657102E-09	unbiased	X/X*
ENSMSEG00005005643	Pgk1	ref - alt	-0.000944733183161	0.111529698553286	Inf	-0.008470687139085	0.993241450336281	0.993241450336281	unbiased	X/X*
ENSMSEG00005005666	Taf9b	ref - alt	0.556287997842746	0.21711415038798	Inf	2.56219134887647	0.010401399417428	0.016273157153073	unbiased	X/X*
ENSMSEG00005007059	Kcnj11	ref - alt	-0.013423020332141	0.193381110398212	Inf	-0.06941226216201	0.944661468668167	0.958527080730109	unbiased	1neo-X/1neo-X*
ENSMSEG00005007546	Magt1	ref - alt	0.562118918153541	0.140465987205678	Inf	4.00181516775627	6.2858394842809E-05	0.00014179684418	unbiased	X/X*
ENSMSEG00005008781	Slc9a7	ref - alt	0.6216882165778	0.1542715991257	Inf	4.02982934059852	5.58173620194357E-05	0.000132055710144	unbiased	X/X*
ENSMSEG00005008786	Anln	ref - alt	-0.244196960512041	0.171816874076589	Inf	-1.42126296863711	0.155240324798604	0.203490696019791	unbiased	13aut/13neo-X*
ENSMSEG00005009413	Tro	ref - alt	0.559615787935423	0.135101769953216	Inf	4.14217954457008	3.44020856769685E-05	9.5342923161884E-05	unbiased	X/X*
ENSMSEG00005010727	Armcx3	ref - alt	0.54146259322788	0.149221845743149	Inf	3.62857455978586	0.000284990445847	0.000531616793215	unbiased	X/X*
ENSMSEG00005010739	Armcx4	ref - alt	1.25954265548074	0.267734871431715	Inf	4.70444006320626	2.54563635986406E-06	9.87706907627254E-06	unbiased	X/X*
ENSMSEG00005010764	Frmpd4	ref - alt	0.788457360364271	0.19234263178956	Inf	4.09923350340196	4.14520665654528E-05	0.000108671633969	unbiased	X/X*
ENSMSEG00005010794	Tspyl2	ref - alt	0.542261350241252	0.112647099591175	Inf	4.81380658897794	1.48082132510115E-06	7.55998255446378E-06	unbiased	X/X*
ENSMSEG00005010868	Iqsec2	ref - alt	0.512123482481591	0.14468574252207	Inf	3.53955734376158	0.000400798684439	0.000733537214916	unbiased	X/X*
ENSMSEG00005011162	Smc1a	ref - alt	0.49123192986559	0.120660843757509	Inf	4.0711793036423	4.67757264131163E-05	0.000113431136552	unbiased	X/X*
ENSMSEG00005011733	Ube2s	ref - alt	0.008141157583699	0.126399783840908	Inf	0.064408002421478	0.948645358248355	0.958527080730109	unbiased	1neo-X/1neo-X*
ENSMSEG00005014280	Snx19	ref - alt	0.266020575670602	0.165446325461766	Inf	1.60789654849166	0.107857837908602	0.149460146816206	unbiased	13aut/13neo-X*

ENSMSEG00005014686	Ecsit	ref - alt	-0.032335380642936	0.140675858761212 Inf	-0.229857353832284	0.818202615761442	0.872150040976482 unbiased	13aut/13neo-X*
ENSMSEG00005015155	Vrk3	ref - alt	0.037457562534901	0.159799674513839 Inf	0.234403246745391	0.814671938316037	0.872150040976482 unbiased	1neo-X/1neo-X*
ENSMSEG00005015797	**Dlg3**	**ref - alt**	**0.379489621704903**	**0.157937863653342 Inf**	**2.40277798449804**	**0.016271062547422**	**0.025052270906348 unbiased**	**X/X***
ENSMSEG00005015840	Hspbp1	ref - alt	0.088665637085656	0.152422208449637 Inf	0.581710749289875	0.5607615298223	0.679923354909539 unbiased	1neo-X/1neo-X*
ENSMSEG00005016028		**ref - alt**	**0.978708361442589**	**0.184032568601223 Inf**	**5.3181258560996**	**1.04841542008642E-07**	**8.47469131236521E-07 unbiased**	**X/X***
ENSMSEG00005016101		**ref - alt**	**0.952366788347964**	**0.19705731659935 Inf**	**4.83294304816037**	**1.34529282397483E-06**	**7.24963355141993E-06 unbiased**	**X/X***
ENSMSEG00005016117	**Zmym3**	**ref - alt**	**0.480972660616309**	**0.185327273912526 Inf**	**2.59526107767239**	**0.009451909199549**	**0.015030085120595 unbiased**	**X/X***
ENSMSEG00005016379	Zfp426	ref - alt	-0.065240521868401	0.179754493289176 Inf	-0.36294237031086	0.716647934769735	0.808312205496097 unbiased	13aut/13neo-X*
ENSMSEG00005016419	Zfp266	ref - alt	-0.062520356981335	0.204523725815777 Inf	-0.305687551563821	0.759842552312652	0.842464719558135 unbiased	13aut/13neo-X*
ENSMSEG00005016625	Kirrel3	ref - alt	0.096626835689073	0.195448344510843 Inf	0.494385541770155	0.621033922903896	0.734637689288755 unbiased	13aut/13neo-X*
ENSMSEG00005016853	**Dcps**	**ref - alt**	**0.617161273582023**	**0.219311526489786 Inf**	**2.81408498431462**	**0.004891629458441**	**0.007908134291147 MB**	13aut/13neo-X*
ENSMSEG00005016910	Gm49373	ref - alt	-0.06103589058637	0.155310532075023 Inf	-0.392992605014619	0.694324943237064	0.792347288164649 unbiased	13aut/13neo-X*
ENSMSEG00005017294		ref - alt	0.267062785249045	0.169014758659239 Inf	1.58011517673132	0.114080492298186	0.155856447224283 -YB	X/X*
ENSMSEG00005017471	**Chm**	**ref - alt**	**0.479573080261886**	**0.137303369641123 Inf**	**3.49279905886775**	**0.000477986040753**	**0.000858604554686 unbiased**	**X/X***
ENSMSEG00005017514	**Syn1**	**ref - alt**	**0.729961153682661**	**0.140753171206673 Inf**	**5.18610804591275**	**2.14734259455277E-07**	**1.38861487781079E-06 unbiased**	**X/X***
ENSMSEG00005017611		ref - alt	0.200670695462151	0.189213985378231 Inf	1.06054896027383	0.288894928405453	0.359266769940114 -YB	X/X*
ENSMSEG00005017716		**ref - alt**	**0.610032273849439**	**0.141483955523181 Inf**	**4.31167104138173**	**1.62025366847507E-05**	**5.06982599490586E-05 unbiased**	**X/X***
ENSMSEG00005018016	**Huwe1**	**ref - alt**	**0.360259671340118**	**0.123444806390663 Inf**	**2.91838662049509**	**0.003518478027876**	**0.005884351184552 FB2**	**X/X***
ENSMSEG00005018084	**Pcyt1b**	**ref - alt**	**1.43910766373057**	**0.130748298065811 Inf**	**11.0067028406458**	**3.54749771506593E-28**	**3.44107278361395E-26 unbiased**	**X/X***
ENSMSEG00005018446	**Nap1l3**	**ref - alt**	**0.847297860387204**	**0.232033295670294 Inf**	**3.65162188443493**	**0.000260589370671**	**0.000495630763825 unbiased**	**X/X***
ENSMSEG00005018452		**ref - alt**	**1.03691871966277**	**0.212794125951195 Inf**	**4.87287285317541**	**1.0998701330673E-06**	**6.27572958279579E-06 unbiased**	**X/X***
ENSMSEG00005020240	Fcgrt	ref - alt	-0.060624621816435	0.202188746880084 Inf	-0.299841720926191	0.764297889908411	0.842464719558135 unbiased	1neo-X/1neo-X*
ENSMSEG00005020826	Prr12	ref - alt	0.168227793718095	0.156954157961755 Inf	1.07182756992705	0.283797487428133	0.35751112052635 FB3	1neo-X/1neo-X*
ENSMSEG00005021265	Ncapd3	ref - alt	-0.036367644170876	0.216621948074659 Inf	-0.16788531584224	0.866673502420853	0.913775323204595 unbiased	13aut/13neo-X*
ENSMSEG00005021302	**Slc16a2**	**ref - alt**	**0.944966531850823**	**0.152229711316489 Inf**	**6.20750393388199**	**5.38327618407312E-10**	**7.45968271221561E-09 unbiased**	**X/X***
ENSMSEG00005021391	**Pbdc1**	**ref - alt**	**0.588886170235535**	**0.161074214589158 Inf**	**3.65599280888981**	**0.000256188535973**	**0.000495630763825 unbiased**	**X/X***
ENSMSEG00005021470	**Magee1**	**ref - alt**	**0.74217266653303**	**0.113934925266483 Inf**	**6.51400494446422**	**7.31730868368134E-11**	**1.18296490386182E-09 unbiased**	**X/X***
ENSMSEG00005021871	**Hdac6**	**ref - alt**	**0.639801199854653**	**0.143064918969508 Inf**	**4.4721040242648**	**7.74537316947221E-06**	**2.78259702755113E-05 unbiased**	**X/X***
ENSMSEG00005021952	**Ccdc120**	**ref - alt**	**0.722134717433199**	**0.238504167167941 Inf**	**3.02776561939361**	**0.002463690901085**	**0.004192596796584 unbiased**	**X/X***
ENSMSEG00005022450		ref - alt	-0.090971778205727	0.202275002183174 Inf	-0.449743058825165	0.652895719727499	0.753939104923421 unbiased	1neo-X/1neo-X*
ENSMSEG00005022451	**Wdr45**	**ref - alt**	**0.548767341337677**	**0.123756841210224 Inf**	**4.43423843054859**	**9.23983246245188E-06**	**3.09056465123391E-05 unbiased**	**X/X***
ENSMSEG00005022496	**Ftsj1**	**ref - alt**	**1.05977245535185**	**0.221408729900707 Inf**	**4.78649805645475**	**1.69716582038137E-06**	**7.83928974176155E-06 unbiased**	**X/X***
ENSMSEG00005022544	**Pqbp1**	**ref - alt**	**0.625526992884965**	**0.120354691178134 Inf**	**5.19736278463078**	**2.0213564137631E-07**	**1.38861487781079E-06 unbiased**	**X/X***
ENSMSEG00005022559	**Slc35a2**	**ref - alt**	**0.623467259921955**	**0.142814878563452 Inf**	**4.36556237132499**	**1.26796114297497E-05**	**4.0997410289524E-05 unbiased**	**X/X***
ENSMSEG00005022587		**ref - alt**	**0.499747538592835**	**0.131747444889817 Inf**	**3.79322376240983**	**0.000148704041193**	**0.000320539822126 unbiased**	**X/X***
ENSMSEG00005022704	**Taf1**	**ref - alt**	**1.75666814941678**	**0.225797578784559 Inf**	**7.7798360765103**	**7.26185823265206E-15**	**3.52200124283625E-13 X dose**	**X/X***
ENSMSEG00005022714	Tfe3	ref - alt	0.428454626332862	0.221261691476745 Inf	1.93641575942617	0.0528168008631	0.07424970556117 unbiased	X/X*
ENSMSEG00005022736	**Pcsk1n**	**ref - alt**	**0.648411286718554**	**0.108023926248498 Inf**	**6.00247842526062**	**1.94328090163007E-09**	**1.88498247458117E-08 unbiased**	**X/X***
ENSMSEG00005022757	**Pim2**	**ref - alt**	**0.522189382416305**	**0.182509445149832 Inf**	**2.86116360710873**	**0.004220891703398**	**0.006939432122536 unbiased**	**X/X***
ENSMSEG00005022822	**Porcn**	**ref - alt**	**0.658914008917703**	**0.158555718930071 Inf**	**4.15572527666637**	**3.24257265015317E-05**	**9.53119839590477E-05 unbiased**	**X/X***
ENSMSEG00005022896	**Sh3bgrl**	**ref - alt**	**0.64409102357075**	**0.136608389338116 Inf**	**4.71487166118748**	**2.41863147666211E-06**	**9.77530221817601E-06 unbiased**	**X/X***
ENSMSEG00005022903	**Phka1**	**ref - alt**	**0.430782916092454**	**0.189562713624308 Inf**	**2.27250870097913**	**0.023055803069374**	**0.03494395152702 unbiased**	**X/X***
ENSMSEG00005022929	**Tmem47**	**ref - alt**	**0.939398306884303**	**0.122740359261927 Inf**	**7.65354046976216**	**1.95520068307544E-14**	**6.32181554194392E-13 unbiased**	**X/X***

ENSMSEG00005022946	**Itm2a**	**ref - alt**	**0.401236771998644**	**0.177994975016955**	**Inf**	**2.25420280522203**	**0.024183412404353**	**0.036089092357266**	**unbiased**	**X/X***
ENSMSEG00005022991	**Rragb**	**ref - alt**	**0.720981979553389**	**0.150118259277398**	**Inf**	**4.80276005746318**	**1.56493371651964E-06**	**7.58992852512024E-06**	**unbiased**	**X/X***
ENSMSEG00005023023	**Suv39h1**	**ref - alt**	**0.780158557549575**	**0.164685690662446**	**Inf**	**4.73725770837404**	**2.1662961597325E-06**	**9.13611858669791E-06**	**unbiased**	**X/X***
ENSMSEG00005023081	**Nono**	**ref - alt**	**0.742418229566728**	**0.124575176024624**	**Inf**	**5.9596000845303**	**2.52855961905129E-09**	**2.22972984589068E-08**	**unbiased**	**X/X***
ENSMSEG00005023098	**Ogt**	**ref - alt**	**0.660886318341723**	**0.128712242262038**	**Inf**	**5.13460341244202**	**2.82739595877345E-07**	**1.71410880000641E-06**	**unbiased**	**X/X***
ENSMSEG00005023112	**Ophn1**	**ref - alt**	**0.776528789498994**	**0.205641769703485**	**Inf**	**3.7761238420515**	**0.000159287816127**	**0.000333937070788**	**unbiased**	**X/X***
ENSMSEG00005023129	Syap1	ref - alt	0.230905556649699	0.148988431365536	Inf	1.54982205352027	0.121184232252975	0.161025623678611	unbiased	X/X*
ENSMSEG00005023135	**Stard8**	**ref - alt**	**0.52839194748389**	**0.131363535548526**	**Inf**	**4.02236393286402**	**5.76169400859155E-05**	**0.00013306769496**	**unbiased**	**X/X***
ENSMSEG00005023211	**Cdkl5**	**ref - alt**	**0.68433655087779**	**0.154097746893399**	**Inf**	**4.44092509250766**	**8.95729733926502E-06**	**3.09056465123391E-05**	**unbiased**	**X/X***
ENSMSEG00005023225	Nhsl2	ref - alt	0.458307589482544	0.226160242017018	Inf	2.0264728468413	0.042716352525935	0.060933620514937	FB2	X/X*
ENSMSEG00005023228	**Yipf6**	**ref - alt**	**0.596297354570026**	**0.185495548916363**	**Inf**	**3.21461812994169**	**0.001306181581388**	**0.002262493096333**	**unbiased**	**X/X***

Bold indicate genes that passed significance thresholds = true allelic imbalance

gene_id	gene_name	contrast	estimate	SE	df	z.ratio	p.value	FDR	bias	Allele
ENSMSEG00005000542	Atf5	ref - alt	-0.056352936551142	0.247887114800334	Inf	-0.22733306084317	0.820164767173613	0.951585464381571	unbiased	1neo-X*/1neo-Y
ENSMSEG00005000914	Shank1	ref - alt	0.124562722641765	0.186088692674005	Inf	0.669372871891669	0.50325765220212	0.917897034171841	unbiased	1neo-X*/1neo-Y
ENSMSEG00005001150	Slc17a6	ref - alt	-0.111897873914755	0.18673521709428	Inf	-0.599232837040369	0.549017628282594	0.917897034171841	unbiased	1neo-X*/1neo-Y
ENSMSEG00005001222	Ap2a1	ref - alt	-0.161884670426996	0.191334952834196	Inf	-0.846079966200839	0.397508135929963	0.862903886188663	unbiased	1neo-X*/1neo-Y
ENSMSEG00005001253	Iglon5	ref - alt	-0.07132932114797	0.188882587602624	Inf	-0.377638415765642	0.705699222639367	0.925087582009118	unbiased	1neo-X*/1neo-Y
ENSMSEG00005001298	Kcnc3	ref - alt	0.158832774718324	0.188922668316492	Inf	0.840729046089062	0.400499744578005	0.862903886188663	unbiased	1neo-X*/1neo-Y
ENSMSEG00005001413	Tbc1d17	ref - alt	0.004175371410481	0.203978932757615	Inf	0.020469620828162	0.98366874606422	1	unbiased	1neo-X*/1neo-Y
ENSMSEG00005001538	Myh14	ref - alt	0.178075265912503	0.22096020631916	Inf	0.805915548681591	0.420291545248353	0.865124476937435	unbiased	1neo-X*/1neo-Y
ENSMSEG00005001765	Lrrc4b	ref - alt	-0.052446475372539	0.219654764776818	Inf	-0.238767756419159	0.81128567380411	0.951585464381571	unbiased	1neo-X*/1neo-Y
ENSMSEG00005001863	Zfp658	ref - alt	0.031748698314581	0.239682735160161	Inf	0.132461348512923	0.894619393000304	0.975597872539125	unbiased	1neo-X*/1neo-Y
ENSMSEG00005001882	Zfp719	ref - alt	-0.045985113241824	0.237186211366495	Inf	-0.193877683600959	0.846271658046851	0.951585464381571	unbiased	1neo-X*/1neo-Y
ENSMSEG00005001964	Smim17	ref - alt	-0.20430046351273	0.239707189034004	Inf	-0.852291766200424	0.394052174846701	0.862903886188663	unbiased	1neo-X*/1neo-Y
ENSMSEG00005002231	Med25	ref - alt	-0.138150338480816	0.237392091503166	Inf	-0.581950045623041	0.560600329470621	0.917897034171841	unbiased	1neo-X*/1neo-Y
ENSMSEG00005002592	Zfp715	ref - alt	0.034916265106228	0.207929653585419	Inf	0.167923451533496	0.86664350044239	0.960843591825258	unbiased	1neo-X*/1neo-Y
ENSMSEG00005002618	Nup62	ref - alt	0.089079630053687	0.212484437618148	Inf	0.419228961199364	0.675048808239117	0.925087582009118	unbiased	1neo-X*/1neo-Y
ENSMSEG00005003798	Tsen34	ref - alt	0.49594269307428	0.188526243192898	Inf	2.63062947988009	0.008522689742793	0.107812025246329	unbiased	1neo-X*/1neo-Y
ENSMSEG00005003814	Mboat7	ref - alt	0.078312603435754	0.189630782323394	Inf	0.412974109352144	0.67962558283706	0.925087582009118	unbiased	1neo-X*/1neo-Y
ENSMSEG00005003867	Cnot3	ref - alt	-0.101964926656688	0.196551563435868	Inf	-0.518769349244873	0.603921594535864	0.917897034171841	unbiased	1neo-X*/1neo-Y
ENSMSEG00005003892	Prpf31	ref - alt	0.166061035922174	0.198026980011892	Inf	0.838577833748723	0.40170625374413	0.862903886188663	unbiased	1neo-X*/1neo-Y
ENSMSEG00005003928	**Ndufa3**	**ref - alt**	**-0.85301412152227**	**0.188535855710524**	**Inf**	**-4.52441323857239**	**6.05632905711946E-06**	**0.000383062812863**	**MB**	1neo-X*/1neo-Y
ENSMSEG00005003995	Prkcg	ref - alt	0.016474837203505	0.191185131273511	Inf	0.086172167750514	0.931329555307261	0.993772001118516	unbiased	1neo-X*/1neo-Y
ENSMSEG00005004051		ref - alt	0.342944751126829	0.268538531516794	Inf	1.27707837378035	0.201574579066799	0.671031164525002	unbiased	1neo-X*/1neo-Y
ENSMSEG00005004098	Cacng7	ref - alt	-0.042420715883952	0.199461423428456	Inf	-0.212676291760082	0.831579460150518	0.951585464381571	unbiased	1neo-X*/1neo-Y
ENSMSEG00005004535	Gas2	ref - alt	-0.41173472112176	0.270071697763993	Inf	-1.52453857449943	0.127374228424462	0.5653628033577	unbiased	1neo-X*/1neo-Y
ENSMSEG00005004536	Eepd1	ref - alt	0.556571645554194	0.258318322268784	Inf	2.15459608387776	0.031193455761021	0.239149827501164	unbiased	13aut/13neo-X*
ENSMSEG00005004582	**Chrna7**	**ref - alt**	**-0.774977198807577**	**0.211139774745981**	**Inf**	**-3.67044627067515**	**0.000242127363407**	**0.00765727786776**	**unbiased**	1neo-X*/1neo-Y
ENSMSEG00005004590	Otud7a	ref - alt	-0.277477902277539	0.20537510536088	Inf	-1.35107856324632	0.176670267569729	0.638536824216305	unbiased	1neo-X*/1neo-Y
ENSMSEG00005005597	**Ldha**	**ref - alt**	**2.0240117367405**	**0.235489181569437**	**Inf**	**8.59492450248163**	**8.33195588140354E-18**	**1.05399241899755E-15**	**X dose**	1neo-X*/1neo-Y
ENSMSEG00005005631	Spty2d1	ref - alt	0.262942466276025	0.215767888568131	Inf	1.21863576652185	0.222982467590891	0.696476102475253	unbiased	1neo-X*/1neo-Y
ENSMSEG00005005670	Ptpn5	ref - alt	-0.042048236243501	0.185988967289597	Inf	-0.226079196289254	0.82113982468469	0.951585464381571	unbiased	1neo-X*/1neo-Y
ENSMSEG00005005689	Bax	ref - alt	-0.199731110689468	0.19239231014691	Inf	-1.03814497854386	0.299202563890453	0.780394316126645	unbiased	1neo-X*/1neo-Y
ENSMSEG00005005760	Lmtk3	ref - alt	0.030199739863633	0.194688104437193	Inf	0.155118567469415	0.87672784463339	0.960843591825258	FB3	1neo-X*/1neo-Y
ENSMSEG00005005911	Tmem143	ref - alt	0.437213806422745	0.244545163208333	Inf	1.7878652788985	0.073797745869758	0.424337038751106	unbiased	1neo-X*/1neo-Y
ENSMSEG00005005952	Kdelr1	ref - alt	0.098024704167613	0.198974735212395	Inf	0.492648999195687	0.622260619686785	0.917897034171841	unbiased	1neo-X*/1neo-Y
ENSMSEG00005005976	Grin2d	ref - alt	0.01481508578514	0.250774586852672	Inf	0.059077301137552	0.952890538125798	0.993772001118516	unbiased	1neo-X*/1neo-Y
ENSMSEG00005006000	Ruvbl2	ref - alt	-0.196710294246056	0.244241997723179	Inf	-0.805390948648421	0.420594113293694	0.865124476937435	unbiased	1neo-X*/1neo-Y
ENSMSEG00005006073	**Sergef**	**ref - alt**	**0.736319352425155**	**0.23453096554171**	**Inf**	**3.13954002075774**	**0.001692132995351**	**0.035675803985322**	**unbiased**	1neo-X*/1neo-Y
ENSMSEG00005006106	Kcnc1	ref - alt	0.253481276365998	0.192637838973353	Inf	1.31584364586368	0.188226526601176	0.645008361234239	unbiased	1neo-X*/1neo-Y
ENSMSEG00005006175	Car11	ref - alt	-0.119760158175874	0.186700990335508	Inf	-0.64145432737481	0.521227545702402	0.917897034171841	unbiased	1neo-X*/1neo-Y
ENSMSEG00005006189	Mamstr	ref - alt	-0.712195375530639	0.265019865104003	Inf	-2.68732826971725	0.007202612833025	0.09590847614502	unbiased	1neo-X*/1neo-Y
ENSMSEG00005006193	Tmem86a	ref - alt	0.204794412646013	0.246482924535798	Inf	0.830866531755508	0.406049032366729	0.863280715872121	unbiased	1neo-X*/1neo-Y
ENSMSEG00005006298	Tsg101	ref - alt	0.225637600900865	0.187876312517315	Inf	1.2009901507944	0.229755021918218	0.708878299333037	unbiased	1neo-X*/1neo-Y
ENSMSEG00005006318	Abcc8	ref - alt	-0.395685079054524	0.198401802958939	Inf	-1.99436231502601	0.046112473743986	0.315309617762932	unbiased	1neo-X*/1neo-Y
ENSMSEG00005006424	**Kcnj14**	**ref - alt**	**-0.883767540168596**	**0.20080526294482**	**Inf**	**-4.40111741698449**	**1.07694823527725E-05**	**0.00054493580705**	**YB**	1neo-X*/1neo-Y
ENSMSEG00005006485	**Hsd17b14**	**ref - alt**	**0.725408042778164**	**0.239972057713638**	**Inf**	**3.02288545462157**	**0.002503769948846**	**0.045246699789862**	**-YB**	1neo-X*/1neo-Y
ENSMSEG00005006496	Zfp329	ref - alt	-0.281984051337145	0.215746798849721	Inf	-1.30701383677799	0.191208012223589	0.645008361234239	unbiased	1neo-X*/1neo-Y

ENSMSEG00005006563	Gtf2h1	ref - alt	0.085522173438164	0.224459195988727	Inf	0.381014344551331	0.703192604545408	0.925087582009118 unbiased	1neo-X*/1neo-Y
ENSMSEG00005006585	Zfp606	ref - alt	0.125163142954004	0.241567127605445	Inf	0.518129863921035	0.604367665168641	0.917897034171841 unbiased	1neo-X*/1neo-Y
ENSMSEG00005006726	Saal1	ref - alt	0.208029913504162	0.197280787178703	Inf	1.05448643265866	0.291660268979802	0.77673734791463 unbiased	1neo-X*/1neo-Y
ENSMSEG00005006756	Zfp369	ref - alt	20.863631175598	1550.87349815148	Inf	0.013452825907765	0.989266521664848	1 unbiased	1neo-X*/1neo-Y
ENSMSEG00005006759	Ppfia3	ref - alt	-0.081973582959674	0.195151263261973	Inf	-0.420051510758769	0.674447824188732	0.925087582009118 unbiased	1neo-X*/1neo-Y
ENSMSEG00005006801	Ftl1-ps1	ref - alt	0.315773807318795	0.184601549613857	Inf	1.7105696457008	0.087160586445938	0.450925299632904 unbiased	1neo-X*/1neo-Y
ENSMSEG00005006865	Nomo1	ref - alt	-0.093090423066012	0.196050505805517	Inf	-0.474828782937996	0.634909015731511	0.917897034171841 unbiased	1neo-X*/1neo-Y
ENSMSEG00005007020	Gys1	ref - alt	-0.056618893999508	0.228341165177333	Inf	-0.247957454169672	0.804167325597665	0.951585464381571 unbiased	1neo-X*/1neo-Y
ENSMSEG00005007059	Kcnj11	ref - alt	-0.103184236235229	0.196022982377994	Inf	-0.526388462125616	0.598618330558175	0.917897034171841 unbiased	1neo-X*/1neo-Y
ENSMSEG00005007475	**Rps11**	**ref - alt**	**0.648789327929549**	**0.198868540857121**	**Inf**	**3.26240301826159**	**0.001104719651702**	**0.027949407188066 MB**	1neo-X*/1neo-Y
ENSMSEG00005007577	Pih1d1	ref - alt	-0.294799540220644	0.241206654306869	Inf	-1.22218659791032	0.221637070845383	0.696476102475253 MB	1neo-X*/1neo-Y
ENSMSEG00005007624	Aldh16a1	ref - alt	0.093331939792219	0.232437503945168	Inf	0.401535630903332	0.688025810512419	0.925087582009118 unbiased	1neo-X*/1neo-Y
ENSMSEG00005007714	Rras	ref - alt	-0.297959655210023	0.201137649363301	Inf	-1.48137186724222	0.138507507154276	0.587742704379833 MB	1neo-X*/1neo-Y
ENSMSEG00005007755	Luzp2	ref - alt	-0.319575436227733	0.209556155630817	Inf	-1.52501097028494	0.127256361436356	0.5653628033577 unbiased	1neo-X*/1neo-Y
ENSMSEG00005007787		ref - alt	0.017358198609758	0.19265048430977	Inf	0.09010202425366	0.928206140642968	0.993772001118516 unbiased	1neo-X*/1neo-Y
ENSMSEG00005007828		ref - alt	0.094745367589366	0.186952004194109	Inf	0.506789793443422	0.612302318555929	0.917897034171841 unbiased	1neo-X*/1neo-Y
ENSMSEG00005007974	**Lsr**	**ref - alt**	**-0.653581580353755**	**0.215317515571229**	**Inf**	**-3.03543155149188**	**0.002401917362194**	**0.045246699789862 YB**	1neo-X*/1neo-Y
ENSMSEG00005007978		ref - alt	0.124190380231384	0.220953322687777	Inf	0.562066135601292	0.574070959996126	0.917897034171841 unbiased	1neo-X*/1neo-Y
ENSMSEG00005008093	Gemin7	ref - alt	-6.93889390390723E-17	0.245527320172086	Inf	-2.82611886084363E-16	1	1 unbiased	1neo-X*/1neo-Y
ENSMSEG00005008135	Clasrp	ref - alt	0.049392755329575	0.240755183834211	Inf	0.205157598449005	0.837448996303476	0.951585464381571 unbiased	1neo-X*/1neo-Y
ENSMSEG00005008224	Eml2	ref - alt	0.339297097256768	0.191434775260933	Inf	1.7723900832244	0.07632982681136	0.429143248517204 unbiased	1neo-X*/1neo-Y
ENSMSEG00005008322	Mark4	ref - alt	-0.156004248476581	0.256259480805974	Inf	-0.608774543622443	0.542673889136353	0.917897034171841 unbiased	1neo-X*/1neo-Y
ENSMSEG00005008404	Dmpk	ref - alt	-0.020619287202736	0.208727123473493	Inf	-0.098785854275208	0.921308300205145	0.991876595540007 unbiased	1neo-X*/1neo-Y
ENSMSEG00005008427	U2af1l4	ref - alt	-0.272347708451673	0.220396929774585	Inf	-1.23571462057217	0.216564660969177	0.693555180065846 unbiased	1neo-X*/1neo-Y
ENSMSEG00005008540	Dmwd	ref - alt	-0.174002448379992	0.187217247101476	Inf	-0.929414629655774	0.352674248975751	0.841760235762878 unbiased	1neo-X*/1neo-Y
ENSMSEG00005008661		ref - alt	0.143894179660069	0.235522139467049	Inf	0.610958188413538	0.541227260987913	0.917897034171841 unbiased	1neo-X*/1neo-Y
ENSMSEG00005008670	Mag	ref - alt	-0.043422161450278	0.197605867816007	Inf	-0.219741255308819	0.826072672747506	0.951585464381571 unbiased	1neo-X*/1neo-Y
ENSMSEG00005008713	Rtn2	ref - alt	-0.036679882496405	0.18659537509912	Inf	-0.196574446054304	0.844160569507557	0.951585464381571 unbiased	1neo-X*/1neo-Y
ENSMSEG00005008786	Anln	ref - alt	-0.060624621816434	0.231251434934257	Inf	-0.262158900046044	0.793198938494252	0.951585464381571 unbiased	13aut/13neo-X*
ENSMSEG00005008907	Lrfn3	ref - alt	0.259511195485082	0.297038655190416	Inf	0.873661360063468	0.382302699597392	0.862903886188663 unbiased	1neo-X*/1neo-Y
ENSMSEG00005008935	Lin37	ref - alt	0.056123324212286	0.192040096586791	Inf	0.292247948265957	0.770097053551971	0.951585464381571 unbiased	1neo-X*/1neo-Y
ENSMSEG00005008992	Arhgap33	ref - alt	-0.296898727556703	0.188806112263842	Inf	-1.57250591094111	0.115833269410937	0.552939946433343 unbiased	1neo-X*/1neo-Y
ENSMSEG00005009015	Bcam	ref - alt	-0.423614426613841	0.226803645290781	Inf	-1.86775845719205	0.061795746374564	0.372245805542017 unbiased	1neo-X*/1neo-Y
ENSMSEG00005009050	Clptm1	ref - alt	-0.207947889890431	0.184580701330277	Inf	-1.12659605468906	0.259913307968275	0.736214681556673 unbiased	1neo-X*/1neo-Y
ENSMSEG00005009094	Qpctl	ref - alt	0.335355541921137	0.215999375236665	Inf	1.55257644404618	0.120524356866015	0.559551853629746 unbiased	1neo-X*/1neo-Y
ENSMSEG00005009246	Gramd1a	ref - alt	-0.357791638638805	0.1908426541686	Inf	-1.87479911237618	0.06082036535886	0.372245805542017 unbiased	1neo-X*/1neo-Y
ENSMSEG00005009361	Clip3	ref - alt	0.010570922960011	0.185239709315604	Inf	0.057066181970737	0.954492475382606	0.993772001118516 unbiased	1neo-X*/1neo-Y
ENSMSEG00005009708	Kmt2b	ref - alt	-0.193852754393143	0.194825819033357	Inf	-0.995005463623651	0.319733607064005	0.790749922398068 unbiased	1neo-X*/1neo-Y
ENSMSEG00005009990	Fxyd7	ref - alt	0.115879019849045	0.187511461665211	Inf	0.617983662545064	0.536586108051032	0.917897034171841 unbiased	1neo-X*/1neo-Y
ENSMSEG00005010042	Lgi4	ref - alt	-0.250372365093006	0.188174915293427	Inf	-1.33052997368216	0.183343717407318	0.645008361234239 unbiased	1neo-X*/1neo-Y
ENSMSEG00005010106	Zfp84	ref - alt	0.201866152866926	0.239096676749686	Inf	0.844286736273889	0.398509196074285	0.862903886188663 unbiased	1neo-X*/1neo-Y
ENSMSEG00005010136	Zfp30	ref - alt	-0.616186139423818	0.248546085147961	Inf	-2.47916252254385	0.01316912854974	0.138824563461839 unbiased	1neo-X*/1neo-Y
ENSMSEG00005010158	Zfp790	ref - alt	0.218689200964831	0.27080620931438	Inf	0.807548695129636	0.419350431493372	0.865124476937435 unbiased	1neo-X*/1neo-Y
ENSMSEG00005010182	Zfp940	ref - alt	0.726669872598588	0.258791270409461	Inf	2.80793811726666	0.004985980692525	0.070080728622713 FB2	1neo-X*/1neo-Y
ENSMSEG00005010258	Zfp74	ref - alt	0.163325056103299	0.237664950302624	Inf	0.687207162416393	0.491952191506669	0.917897034171841 unbiased	1neo-X*/1neo-Y
ENSMSEG00005010444	Zfp382	ref - alt	-0.046883585898851	0.221111342337109	Inf	-0.212036096399666	0.832078873662989	0.951585464381571 unbiased	1neo-X*/1neo-Y
ENSMSEG00005010486	Cox7a1	ref - alt	-0.171358251996685	0.224669642062326	Inf	-0.76271208884175	0.445635119412265	0.896323905333178 MB	1neo-X*/1neo-Y

ENSMSEG00005010588	Tbcb	ref - alt	-0.181934784404682	0.193677720751503	Inf	-0.939368677505825	0.347541488957299	0.837409492439967 unbiased	1neo-X*/1neo-Y
ENSMSEG00005011055	Zfp260	ref - alt	0.078390633945724	0.203756564030892	Inf	0.384726913307385	0.700439753214569	0.925087582009118 unbiased	1neo-X*/1neo-Y
ENSMSEG00005011262	Fan1	ref - alt	0.006079046076382	0.231795091494707	Inf	0.026225948259654	0.97907711927952	1 unbiased	1neo-X*/1neo-Y
ENSMSEG00005011302	Pcsk6	ref - alt	-0.388613268072672	0.19412384994367	Inf	-2.00188316987036	0.045297298152518	0.315309617762932 unbiased	1neo-X*/1neo-Y
ENSMSEG00005011345	Mtmr10	ref - alt	0.080472353222574	0.209756690662986	Inf	0.383646180573414	0.701240707202309	0.925087582009118 unbiased	1neo-X*/1neo-Y
ENSMSEG00005011399	Igf1r	ref - alt	-0.174487157461345	0.19851979320273	Inf	-0.87894085847227	0.37943334347896	0.862903886188663 unbiased	1neo-X*/1neo-Y
ENSMSEG00005011432	Selenos	ref - alt	-0.270793854423259	0.204183647620397	Inf	-1.32622694118336	0.184764537991046	0.645008361234239 MB	1neo-X*/1neo-Y
ENSMSEG00005011444	Mphosph10	ref - alt	-0.272530267431179	0.194090959435477	Inf	-1.4041368450331	0.160278103727757	0.627929548459552 unbiased	1neo-X*/1neo-Y
ENSMSEG00005011459	Mcee	ref - alt	0.641322112695361	0.220628187140808	Inf	2.90680044561152	0.003651460562916	0.059090218654714 unbiased	1neo-X*/1neo-Y
ENSMSEG00005011468	Lins1	ref - alt	0.258041491165488	0.203812765604536	Inf	1.26607129048125	0.205487560062587	0.675173411634214 unbiased	1neo-X*/1neo-Y
ENSMSEG00005011526		ref - alt	0.319942934670002	0.217728592949376	Inf	1.46945759551384	0.141708715285256	0.587742704379833 unbiased	1neo-X*/1neo-Y
ENSMSEG00005011556	Zswim9	ref - alt	0.660140884091775	0.230119665189321	Inf	2.86868522752575	0.00412181775208	0.061342346545662 FB3	1neo-X*/1neo-Y
ENSMSEG00005011672	Zfp324	ref - alt	-0.463284678996992	0.265826814520557	Inf	-1.74280642015956	0.081367434498597	0.447520889742285 unbiased	1neo-X*/1neo-Y
ENSMSEG00005011679	Rps5	ref - alt	0.096063286404498	0.189453314929465	Inf	0.507055188980268	0.612116095581279	0.917897034171841 MB	1neo-X*/1neo-Y
ENSMSEG00005011690		ref - alt	-0.100604699121299	0.200515842250328	Inf	-0.501729429416866	0.615857860142045	0.917897034171841 unbiased	1neo-X*/1neo-Y
ENSMSEG00005011705	Zfp128	ref - alt	0.174802724379926	0.208786006676751	Inf	0.837233908355562	0.40246110106823	0.862903886188663 unbiased	1neo-X*/1neo-Y
ENSMSEG00005011720	Chsy1	ref - alt	-0.040224801310509	0.201425446749218	Inf	-0.199700693034033	0.841714671729318	0.951585464381571 unbiased	1neo-X*/1neo-Y
ENSMSEG00005011733	Ube2s	ref - alt	0.054317221271578	0.188597841378134	Inf	0.288005530045664	0.773342505578379	0.951585464381571 unbiased	1neo-X*/1neo-Y
ENSMSEG00005011734	Fam189a1	ref - alt	0.161372609876632	0.190488993895068	Inf	0.847149258216592	0.396911932148403	0.862903886188663 unbiased	1neo-X*/1neo-Y
ENSMSEG00005011743	Leng8	ref - alt	0.265522774283071	0.187533369096761	Inf	1.41586948265228	0.156813721414985	0.627929548459552 FB3	1neo-X*/1neo-Y
ENSMSEG00005011775	**U2af2**	**ref - alt**	**2.2225423853205**	**0.248345407331527**	**Inf**	**8.94939998770959**	**3.57419804314928E-19**	**9.04272104916767E-17 unbiased**	1neo-X*/1neo-Y
ENSMSEG00005011812	Ccdc106	ref - alt	0.241835684326362	0.223825842108138	Inf	1.08046364105501	0.279935769261433	0.761545694872501 unbiased	1neo-X*/1neo-Y
ENSMSEG00005011852	Snrpa1	ref - alt	-0.529144204289677	0.21589463707536	Inf	-2.45093723242868	0.014248479711448	0.144194614679851 MB	1neo-X*/1neo-Y
ENSMSEG00005011886	Apba2	ref - alt	0.202065639018776	0.185524047882037	Inf	1.08916143931517	0.276082700155418	0.759227425427399 unbiased	1neo-X*/1neo-Y
ENSMSEG00005011894	Ppp6r1	ref - alt	0.210014259872418	0.207597463559088	Inf	1.01164174297651	0.311709379494231	0.790749922398068 unbiased	1neo-X*/1neo-Y
ENSMSEG00005011987	Kmt5c	ref - alt	-0.293347809987459	0.308389615815358	Inf	-0.951224668223249	0.341490338514304	0.83074091965499 unbiased	1neo-X*/1neo-Y
ENSMSEG00005012029	Ttyh1	ref - alt	-0.440751514288177	0.184019332946708	Inf	-2.39513700669603	0.016614155888102	0.150120765703211 unbiased	1neo-X*/1neo-Y
ENSMSEG00005012199	Zik1	ref - alt	-0.066249385541201	0.244490860527256	Inf	-0.270968760952175	0.786415058851289	0.951585464381571 unbiased	1neo-X*/1neo-Y
ENSMSEG00005012407	Syt5	ref - alt	-0.095031278672964	0.190223764011275	Inf	-0.49957627096124	0.617373469656271	0.917897034171841 unbiased	1neo-X*/1neo-Y
ENSMSEG00005013199	Klf13	ref - alt	-0.025317807984289	0.214282277228228	Inf	-0.118151665698996	0.905947486797172	0.983711219569461 unbiased	1neo-X*/1neo-Y
ENSMSEG00005014067	Smg9	ref - alt	0.044059989794031	0.205113352212745	Inf	0.214808004055883	0.829917012232947	0.951585464381571 unbiased	1neo-X*/1neo-Y
ENSMSEG00005014126	**Xrcc1**	**ref - alt**	**0.854990206010361**	**0.267914011997225**	**Inf**	**3.19128588921738**	**0.001416410498725**	**0.032577441470669 -YB**	1neo-X*/1neo-Y
ENSMSEG00005014233	Kcnn4	ref - alt	-0.232622295268752	0.27556140198091	Inf	-0.844175902708129	0.398571118044984	0.862903886188663 unbiased	1neo-X*/1neo-Y
ENSMSEG00005014268	Zfp428	ref - alt	-3.88578058618805E-16	0.280370887293707	Inf	-1.38594296422704E-15	0.999999999999999	1 unbiased	1neo-X*/1neo-Y
ENSMSEG00005014280	Snx19	ref - alt	0.379489621704905	0.234198805652235	Inf	1.6203738556567	0.105151992487315	0.532069081985816 unbiased	13aut/13neo-X*
ENSMSEG00005014301	Irgq	ref - alt	0.458247807686084	0.199730750415826	Inf	2.29432777242384	0.021771678475346	0.189939126009051 -YB	1neo-X*/1neo-Y
ENSMSEG00005014444	Ethe1	ref - alt	0.360002734031407	0.228297365336235	Inf	1.57690270976714	0.114817912950577	0.552939946433343 unbiased	1neo-X*/1neo-Y
ENSMSEG00005014686	Ecsit	ref - alt	-0.091807549253123	0.206034694029505	Inf	-0.44559266916462	0.65589150693971	0.925087582009118 unbiased	13aut/13neo-X*
ENSMSEG00005015198	Pold1	ref - alt	0.180521376289807	0.199641586922715	Inf	0.904227315923361	0.365874878621837	0.857095780475229 unbiased	1neo-X*/1neo-Y
ENSMSEG00005015262	Pnkp	ref - alt	0.306619273471532	0.208489796378719	Inf	1.4706680077262	0.141380922174386	0.587742704379833 unbiased	1neo-X*/1neo-Y
ENSMSEG00005015286	Syt3	ref - alt	0.096767551934994	0.208467264669505	Inf	0.464185837946332	0.642514606781843	0.918396584835064 unbiased	1neo-X*/1neo-Y
ENSMSEG00005015313	Etfb	ref - alt	0.259998643703365	0.198245267672406	Inf	1.31149987465529	0.189688936051482	0.645008361234239 unbiased	1neo-X*/1neo-Y
ENSMSEG00005015735	Shisa7	ref - alt	-0.07750356115486	0.191789089912846	Inf	-0.404108289945374	0.686133089162443	0.925087582009118 unbiased	1neo-X*/1neo-Y
ENSMSEG00005015770	Nat14	ref - alt	4.64905891561784E-16	0.217130207048093	Inf	2.14113871064845E-15	0.999999999999998	1 unbiased	1neo-X*/1neo-Y
ENSMSEG00005015813		ref - alt	-0.170957798143639	0.253951776429987	Inf	-0.673190006964851	0.500826417858401	0.917897034171841 unbiased	1neo-X*/1neo-Y
ENSMSEG00005015840	Hspbp1	ref - alt	-0.014117881545786	0.190772244190753	Inf	-0.074003855255114	0.941007317624799	0.993772001118516 unbiased	1neo-X*/1neo-Y
ENSMSEG00005015850	Fiz1	ref - alt	0.620928972748146	0.214146318154076	Inf	2.89955474416046	0.003736930824014	0.059090218654714 unbiased	1neo-X*/1neo-Y

ENSMSEG00005015876		ref - alt	0.197139919285479	0.188921230041557	Inf	1.04350325922668	0.296715272112249	0.780394316126645	unbiased	1neo-X*/1neo-Y
ENSMSEG00005015953	Zfp772	ref - alt	0.341749293722056	0.29513411041162	Inf	1.15794576657175	0.246886169100258	0.726304660260061	unbiased	1neo-X*/1neo-Y
ENSMSEG00005016009	Brsk1	ref - alt	-0.014949137558467	0.184508709666817	Inf	-0.081021311056059	0.935425004447592	0.993772001118516	unbiased	1neo-X*/1neo-Y
ENSMSEG00005016047	Isoc2a	ref - alt	0.112572752190978	0.188056503598209	Inf	0.59861132179451	0.549432104356375	0.917897034171841	unbiased	1neo-X*/1neo-Y
ENSMSEG00005016078	Gm3854	ref - alt	0.306166887125884	0.243250944596724	Inf	1.25864624136801	0.208158136873435	0.675179597807425	unbiased	1neo-X*/1neo-Y
ENSMSEG00005016112	Zfp667	ref - alt	0.54875267567805	0.215671899422329	Inf	2.54438652948236	0.010946987245425	0.125890353322385	unbiased	1neo-X*/1neo-Y
ENSMSEG00005016177	Zfp444	ref - alt	-0.042559614418796	0.206681362071873	Inf	-0.205918975916153	0.836854202450451	0.951585464381571	unbiased	1neo-X*/1neo-Y
ENSMSEG00005016222		ref - alt	0.10573723444171	0.183667688481043	Inf	0.575698618064895	0.564818909594807	0.917897034171841	unbiased	1neo-X*/1neo-Y
ENSMSEG00005016244	Epn1	ref - alt	0.190701116570617	0.190344943298111	Inf	1.00187119902601	0.316405804327191	0.790749922398068	unbiased	1neo-X*/1neo-Y
ENSMSEG00005016379	Zfp426	ref - alt	-0.417161147871357	0.229724360464248	Inf	-1.81592037965986	0.069382586615506	0.408227777063328	unbiased	13aut/13neo-X*
ENSMSEG00005016419	Zfp266	ref - alt	-0.275411979859963	0.275980797058086	Inf	-0.997938924721623	0.318308975518193	0.790749922398068	unbiased	13aut/13neo-X*
ENSMSEG00005016477	Nfkbib	ref - alt	-0.136859182717198	0.241283812623094	Inf	-0.567212450886555	0.570569849825087	0.917897034171841	unbiased	1neo-X*/1neo-Y
ENSMSEG00005016530	Sirt2	ref - alt	0.386853260913566	0.201002812127591	Inf	1.92461616242465	0.054277395892964	0.352107209254357	unbiased	1neo-X*/1neo-Y
ENSMSEG00005016625	Kirrel3	ref - alt	0.22314355131421	0.244391542732462	Inf	0.913057583005182	0.361212257364301	0.854081318814657	unbiased	13aut/13neo-X*
ENSMSEG00005016626		ref - alt	-0.046493634239052	0.185448207317224	Inf	-0.250709537243034	0.802038686484527	0.951585464381571	unbiased	1neo-X*/1neo-Y
ENSMSEG00005016853	Dcps	ref - alt	0.495616205102462	0.252227705309555	Inf	1.96495545362156	0.049419393594958	0.329029120513799	MB	13aut/13neo-X*
ENSMSEG00005016910	Gm49373	ref - alt	0.150480950938296	0.221712849531411	Inf	0.678720025728493	0.497315275046649	0.917897034171841	unbiased	13aut/13neo-X*
ENSMSEG00005017056	Tmem145	ref - alt	0.063178901621532	0.233088577098714	Inf	0.271051041659479	0.78635177550993	0.951585464381571	unbiased	1neo-X*/1neo-Y
ENSMSEG00005017189	Sertad1	ref - alt	-0.303307390354861	0.216667042164383	Inf	-1.39987783709506	0.161549903880231	0.627929548459552	unbiased	1neo-X*/1neo-Y
ENSMSEG00005017479	Irf2bp1	ref - alt	0.076961041136129	0.220599286787755	Inf	0.348872574598011	0.727184975426583	0.929180801933967	unbiased	1neo-X*/1neo-Y
ENSMSEG00005017836	Psmc4	ref - alt	0.410066664021061	0.18801389336956	Inf	2.18104447853241	0.02918012681543	0.23070537763449	unbiased	1neo-X*/1neo-Y
ENSMSEG00005017870	Zfp626	ref - alt	-0.105360515657825	0.289470239622393	Inf	-0.363977021593878	0.715875168328031	0.929180801933967	unbiased	1neo-X*/1neo-Y
ENSMSEG00005018006	Fbl	ref - alt	0.239891408615431	0.202971884419509	Inf	1.18189476981755	0.237247457519944	0.720871168595737	unbiased	1neo-X*/1neo-Y
ENSMSEG00005018032	BC024978	ref - alt	0.194156014440957	0.314396400774368	Inf	0.617551644874893	0.536870927850049	0.917897034171841	unbiased	1neo-X*/1neo-Y
ENSMSEG00005018083	Sptbn4	ref - alt	-0.217442577075982	0.19472960568703	Inf	-1.11663851168813	0.264148918168875	0.736214681556673	unbiased	1neo-X*/1neo-Y
ENSMSEG00005018166	Pld3	ref - alt	0.482682087505505	0.189303423698836	Inf	2.54978002021456	0.010779090902979	0.125890353322385	unbiased	1neo-X*/1neo-Y
ENSMSEG00005018210	Nell1	ref - alt	0.087613605252335	0.188587406685465	Inf	0.464578238771058	0.642233518965838	0.918396584835064	unbiased	1neo-X*/1neo-Y
ENSMSEG00005018376	Supt5	ref - alt	0.230069319667169	0.200462281857309	Inf	1.14769380820944	0.251094988177227	0.730195770216532	unbiased	1neo-X*/1neo-Y
ENSMSEG00005018382	Arhgap35	ref - alt	0.038482730495927	0.186995731715653	Inf	0.205794699926327	0.836951281437307	0.951585464381571	unbiased	1neo-X*/1neo-Y
ENSMSEG00005018401	Pnmal2	ref - alt	0.396182642314245	0.191894643790443	Inf	2.06458416185338	0.038962363110383	0.281642224769343	FB3	1neo-X*/1neo-Y
ENSMSEG00005018456	Npas1	ref - alt	-0.438135890397714	0.198311944181837	Inf	-2.20932678667088	0.027151919332554	0.221594696488262	unbiased	1neo-X*/1neo-Y
ENSMSEG00005018499	Sae1	ref - alt	-0.276111695438935	0.186284116358058	Inf	-1.48220739823152	0.138285118652061	0.587742704379833	unbiased	1neo-X*/1neo-Y
ENSMSEG00005018543	Slc8a2	ref - alt	0.066560766518337	0.189390580155936	Inf	0.351447080755198	0.725252966831283	0.929180801933967	unbiased	1neo-X*/1neo-Y
ENSMSEG00005018675	Slc6a5	ref - alt	0.287682072451783	0.20812041992132	Inf	1.38228662310282	0.166883711674861	0.630172821697608	FB3	1neo-X*/1neo-Y
ENSMSEG00005018676	Rps16	ref - alt	-0.007380107297623	0.184194361638704	Inf	-0.040066955535256	0.968039746299159	1	MB	1neo-X*/1neo-Y
ENSMSEG00005018703	2310022A10R	ref - alt	-0.232445943976523	0.204042247644511	Inf	-1.13920497671393	0.254617670319877	0.732025802169646	unbiased	1neo-X*/1neo-Y
ENSMSEG00005018739	Ppp5c	ref - alt	0.317102974783365	0.18539784643076	Inf	1.71039189984223	0.087193427887564	0.450925299632904	unbiased	1neo-X*/1neo-Y
ENSMSEG00005018804	Selenow	ref - alt	-0.376051222901869	0.264426060540503	Inf	-1.42214130533578	0.154985233835186	0.627929548459552	unbiased	1neo-X*/1neo-Y
ENSMSEG00005018863	Nav2	ref - alt	0.161268147596123	0.23747617942901	Inf	0.67909189032718	0.497079640564409	0.917897034171841	FB3	1neo-X*/1neo-Y
ENSMSEG00005018911		ref - alt	0.532373959972191	0.221295236078956	Inf	2.40571812301574	0.016140713218606	0.150120765703211	unbiased	1neo-X*/1neo-Y
ENSMSEG00005018946		ref - alt	0.044486872259356	0.183802294483087	Inf	0.242036544671369	0.808751846363267	0.951585464381571	unbiased	1neo-X*/1neo-Y
ENSMSEG00005018955	Actn4	ref - alt	-0.116506807113353	0.185830080742167	Inf	-0.626953433201172	0.530689760174696	0.917897034171841	unbiased	1neo-X*/1neo-Y
ENSMSEG00005019007	Meis3	ref - alt	0.071021269748343	0.195342712133578	Inf	0.363572661465752	0.716177144604915	0.929180801933967	unbiased	1neo-X*/1neo-Y
ENSMSEG00005019063	Herc2	ref - alt	-0.028658677751803	0.185609571308913	Inf	-0.154403016771724	0.877291975144801	0.960843591825258	unbiased	1neo-X*/1neo-Y
ENSMSEG00005019099	Strn4	ref - alt	-0.020716371753749	0.187456872797411	Inf	-0.110512735247311	0.912002750467043	0.986054255846846	unbiased	1neo-X*/1neo-Y
ENSMSEG00005019146	Ccdc9	ref - alt	0.0761236954728	0.196721370796468	Inf	0.386962001965508	0.698784338777229	0.925087582009118	unbiased	1neo-X*/1neo-Y
ENSMSEG00005019210	Bicra	ref - alt	0.146982190348646	0.238952663392718	Inf	0.615110073525656	0.538482029914551	0.917897034171841	unbiased	1neo-X*/1neo-Y

ENSMSEG00005019281	Zc3h4	ref - alt	-0.127833371509885	0.264680271062412 Inf	-0.482972799584829	0.629115049694641	0.917897034171841 unbiased	1neo-X*/1neo-Y
ENSMSEG00005019288	Paf1	ref - alt	-0.157760792051358	0.212111190778127 Inf	-0.743764586265417	0.457018908252885	0.896323905333178 unbiased	1neo-X*/1neo-Y
ENSMSEG00005019367	Sipa1l3	ref - alt	0.080852096629095	0.208264650746675 Inf	0.388218050155039	0.69785467658026	0.925087582009118 unbiased	1neo-X*/1neo-Y
ENSMSEG00005019405	**Kptn**	**ref - alt**	**-0.794797116821234**	**0.19806716113679 Inf**	**-4.01276573188389**	**6.00114633017059E-05**	**0.002530483369222 YB**	1neo-X*/1neo-Y
ENSMSEG00005019499	Ankrd27	ref - alt	-0.106190047020205	0.192865233679713 Inf	-0.550591959961808	0.581913421625858	0.917897034171841 unbiased	1neo-X*/1neo-Y
ENSMSEG00005019502	**Zfp541**	**ref - alt**	**4.77068462446566**	**0.733139772525986 Inf**	**6.5071965854868**	**7.6566188262308E-11**	**6.45708187678797E-09 -YB**	1neo-X*/1neo-Y
ENSMSEG00005019599	**Fkrp**	**ref - alt**	**0.839750654751821**	**0.228246250445695 Inf**	**3.67914326352369**	**0.000234018786656**	**0.00765727786776 -YB**	1neo-X*/1neo-Y
ENSMSEG00005019608	Garre1	ref - alt	-0.169292056503621	0.226190400104452 Inf	-0.748449343674376	0.454189168989463	0.896323905333178 unbiased	1neo-X*/1neo-Y
ENSMSEG00005019609	Akt2	ref - alt	-0.090572815503446	0.190216555421233 Inf	-0.4761563224761	0.633963013863926	0.917897034171841 unbiased	1neo-X*/1neo-Y
ENSMSEG00005019693	**Ppp1r14a**	**ref - alt**	**0.649879200311427**	**0.195485670027743 Inf**	**3.32443396090976**	**0.000885982137942**	**0.024905942322135 unbiased**	1neo-X*/1neo-Y
ENSMSEG00005019760	Atp10a	ref - alt	-0.046883585898852	0.202665813143185 Inf	-0.231334457310409	0.81705497951842	0.951585464381571 unbiased	1neo-X*/1neo-Y
ENSMSEG00005019785	Cebpg	ref - alt	-0.11583181552512	0.257731444672515 Inf	-0.449428340698984	0.653122690758827	0.925087582009118 unbiased	1neo-X*/1neo-Y
ENSMSEG00005019809	Nipa1	ref - alt	0.549599009691952	0.227147428549338 Inf	2.4195695861579	0.015538887349512	0.150120765703211 unbiased	1neo-X*/1neo-Y
ENSMSEG00005019848	Pak4	ref - alt	0.088292607145679	0.26653314959249 Inf	0.331263136614232	0.740445733529444	0.941370706446982 -YB	1neo-X*/1neo-Y
ENSMSEG00005019864	Yif1b	ref - alt	-0.206961260731102	0.192845803042631 Inf	-1.07319556591725	0.283183379743784	0.762185053991249 unbiased	1neo-X*/1neo-Y
ENSMSEG00005019870	Nipa2	ref - alt	0.137358416047825	0.19747890869123 Inf	0.69555993071945	0.486704467065295	0.917897034171841 unbiased	1neo-X*/1neo-Y
ENSMSEG00005019886	Map3k10	ref - alt	0.083046357217745	0.19652131716597 Inf	0.422581928593574	0.672600313831356	0.925087582009118 unbiased	1neo-X*/1neo-Y
ENSMSEG00005019975	Cyfip1	ref - alt	0.029462032730317	0.188253357083304 Inf	0.156502031022372	0.875637318445787	0.960843591825258 unbiased	1neo-X*/1neo-Y
ENSMSEG00005019978	Mctp2	ref - alt	-22.0210839676334	1550.87349844486 Inf	-0.014199149053559	0.98867109887588	1 unbiased	1neo-X*/1neo-Y
ENSMSEG00005019979	Snrpa	ref - alt	0.498246841559132	0.223612205647581 Inf	2.22817372654685	0.025868932382407	0.2181613297583 unbiased	1neo-X*/1neo-Y
ENSMSEG00005020064	Timm50	ref - alt	-0.138998874806655	0.222850074118632 Inf	-0.623732683762359	0.53280315481974	0.917897034171841 unbiased	1neo-X*/1neo-Y
ENSMSEG00005020205	Eif3k	ref - alt	-0.051008839827252	0.188349078661667 Inf	-0.270820755746192	0.786528895453942	0.951585464381571 MB	1neo-X*/1neo-Y
ENSMSEG00005020211	Numbl	ref - alt	0.151806012868003	0.252457100492466 Inf	0.601314094837801	0.547630803456747	0.917897034171841 unbiased	1neo-X*/1neo-Y
ENSMSEG00005020240	Fcgrt	ref - alt	-0.114113306767422	0.208933252984483 Inf	-0.546171110330135	0.58494832269052	0.917897034171841 unbiased	1neo-X*/1neo-Y
ENSMSEG00005020322	Ccdc97	ref - alt	-0.24362208265775	0.208586358291104 Inf	-1.16796747713362	0.242819883857019	0.722746242539127 unbiased	1neo-X*/1neo-Y
ENSMSEG00005020363	Itpkc	ref - alt	0.05129329438755	0.259284963200078 Inf	0.197825950855351	0.843181241556106	0.951585464381571 unbiased	1neo-X*/1neo-Y
ENSMSEG00005020450	Megf8	ref - alt	0.269840934810512	0.193798502850322 Inf	1.39237884112511	0.163807708293796	0.627929548459552 unbiased	1neo-X*/1neo-Y
ENSMSEG00005020562	Egln2	ref - alt	0.006659292089978	0.194155089545947 Inf	0.034298828351869	0.972638859161146	1 unbiased	1neo-X*/1neo-Y
ENSMSEG00005020566	Gabrb3	ref - alt	0.137823147760767	0.184212872772435 Inf	0.748173271967943	0.454355650520263	0.896323905333178 unbiased	1neo-X*/1neo-Y
ENSMSEG00005020621	Cic	ref - alt	0.103121589406705	0.190512477815805 Inf	0.541285224931077	0.588311002788454	0.917897034171841 unbiased	1neo-X*/1neo-Y
ENSMSEG00005020665	Gabra5	ref - alt	0.294271882130838	0.190108015558099 Inf	1.54791938292	0.121641707310814	0.559551853629746 unbiased	1neo-X*/1neo-Y
ENSMSEG00005020729	Irf3	ref - alt	0.437622219742696	0.255974039522009 Inf	1.70963516675318	0.087333358426926	0.450925299632904 unbiased	1neo-X*/1neo-Y
ENSMSEG00005020731	Fam98c	ref - alt	0.012987195526812	0.199375069233043 Inf	0.06513951607275	0.948062917950333	0.993772001118516 unbiased	1neo-X*/1neo-Y
ENSMSEG00005020738	Axl	ref - alt	0.172371225940786	0.226916198972665 Inf	0.759625036560526	0.447478749259207	0.896323905333178 unbiased	1neo-X*/1neo-Y
ENSMSEG00005020819	Zfp112	ref - alt	-0.013841051411873	0.200442970937343 Inf	-0.069052316213172	0.944947976526671	0.993772001118516 unbiased	1neo-X*/1neo-Y
ENSMSEG00005020887	Rcn3	ref - alt	-0.502728413533372	0.19931864031901 Inf	-2.5222348132054	0.01166118378375	0.128273021621252 unbiased	1neo-X*/1neo-Y
ENSMSEG00005021009	Zfp180	ref - alt	-0.240141127682781	0.242442379269287 Inf	-0.990508047341219	0.321925857735182	0.790749922398068 unbiased	1neo-X*/1neo-Y
ENSMSEG00005021123	Mypop	ref - alt	-0.07924937165414	0.207781572477015 Inf	-0.381407122438187	0.702901176798396	0.925087582009118 unbiased	1neo-X*/1neo-Y
ENSMSEG00005021264	B9d2	ref - alt	0.449267730766558	0.240220358383707 Inf	1.87023170637743	0.061451648546877	0.372245805542017 unbiased	1neo-X*/1neo-Y
ENSMSEG00005021265	Ncapd3	ref - alt	0.163629423781804	0.272666068065652 Inf	0.600109228634953	0.548433442548627	0.917897034171841 unbiased	13aut/13neo-X*
ENSMSEG00005021291	Grik5	ref - alt	-0.136798301769869	0.207505301290742 Inf	-0.659252081363438	0.509733907815129	0.917897034171841 unbiased	1neo-X*/1neo-Y
ENSMSEG00005021349	Atp1a3	ref - alt	-0.099122109442329	0.18322616305566 Inf	-0.54098229089815	0.588519789005051	0.917897034171841 unbiased	1neo-X*/1neo-Y
ENSMSEG00005021570	Hnrnpul1	ref - alt	0.033738139631852	0.195134022052694 Inf	0.172897269665981	0.86273217782513	0.960843591825258 unbiased	1neo-X*/1neo-Y
ENSMSEG00005021617	Dedd2	ref - alt	-0.226527649298448	0.192521352532244 Inf	-1.17663649418061	0.239340625146411	0.720871168595737 unbiased	1neo-X*/1neo-Y
ENSMSEG00005021862	Erf	ref - alt	-0.080364509768027	0.203228300694742 Inf	-0.395439559811789	0.692518518536272	0.925087582009118 unbiased	1neo-X*/1neo-Y
ENSMSEG00005022045	Bckdha	ref - alt	-0.170625517030764	0.209696333293037 Inf	-0.813679067970756	0.415828828617641	0.865124476937435 unbiased	1neo-X*/1neo-Y
ENSMSEG00005022047	Tarsl2	ref - alt	-0.260443034289597	0.191455774687608 Inf	-1.36033000161292	0.17372551845446	0.636993567666354 unbiased	1neo-X*/1neo-Y

ENSMSEG00005022245	Mef2a	ref - alt	-0.098217628145444	0.20010288163013	Inf	-0.490835650867785	0.623542692723243	0.917897034171841	X dose	1neo-X*/1neo-Y
ENSMSEG00005022401	Pop4	ref - alt	-0.115760790275615	0.204574376365333	Inf	-0.565861631023072	0.57148784623489	0.917897034171841	-X*B	1neo-X*/1neo-Y
ENSMSEG00005022416	Tjp1	ref - alt	-0.109750863959121	0.189168481485207	Inf	-0.580175212580026	0.561796467465467	0.917897034171841	unbiased	1neo-X*/1neo-Y
ENSMSEG00005022428	Tshz3	ref - alt	-0.23386432105931	0.209723623773875	Inf	-1.11510719131701	0.264804490204179	0.736214681556673	unbiased	1neo-X*/1neo-Y
ENSMSEG00005022450		ref - alt	0.050189744523855	0.201071161553808	Inf	0.249611849536283	0.802887534008699	0.951585464381571	unbiased	1neo-X*/1neo-Y
ENSMSEG00005022518	Ccne1	ref - alt	0.119346757632566	0.244624497886276	Inf	0.487877373949886	0.62563670180279	0.917897034171841	unbiased	1neo-X*/1neo-Y
ENSMSEG00005022529	Tm2d3	ref - alt	0.138776512577672	0.198266954601623	Inf	0.699947769190862	0.483959923593624	0.917897034171841	unbiased	1neo-X*/1neo-Y
ENSMSEG00005022553	Pepd	ref - alt	-0.003696861881328	0.201619390257811	Inf	-0.018335844963129	0.985370932122502	1	unbiased	1neo-X*/1neo-Y
ENSMSEG00005022644	Vstm2b	ref - alt	-0.177206456127183	0.228052029378211	Inf	-0.777043978123502	0.437132824280641	0.891891972120986	unbiased	1neo-X*/1neo-Y
ENSMSEG00005022662	Pdcd2l	ref - alt	-0.361013345537329	0.264853324521623	Inf	-1.36306895973229	0.172860778306169	0.636993567666354	MB	1neo-X*/1neo-Y
ENSMSEG00005022819	Zfp536	ref - alt	0.121185556802222	0.211722435886487	Inf	0.572379381026932	0.567064981569991	0.917897034171841	unbiased	1neo-X*/1neo-Y
ENSMSEG00005022859	Dpy19l3	ref - alt	-0.556287997842746	0.264283531856755	Inf	-2.10489088720163	0.035300807125275	0.262679535373372	YB	1neo-X*/1neo-Y
ENSMSEG00005022890	Gpi1	ref - alt	-0.300974535958882	0.188489534265058	Inf	-1.59677054289733	0.110316864435075	0.5472581706289	unbiased	1neo-X*/1neo-Y
ENSMSEG00005022920	Slc7a10	ref - alt	0.19723426596357	0.192546732972617	Inf	1.02434491055021	0.305672392397669	0.789133829353166	unbiased	1neo-X*/1neo-Y
ENSMSEG00005022961	Lrp3	ref - alt	0.11880358591428	0.186638419342116	Inf	0.636544106690641	0.524421842407275	0.917897034171841	unbiased	1neo-X*/1neo-Y
ENSMSEG00005023072	Lsm14a	ref - alt	0.146603474191872	0.229943172988983	Inf	0.637563934976648	0.523757578677555	0.917897034171841	unbiased	1neo-X*/1neo-Y
ENSMSEG00005023097	Gpatch1	ref - alt	0.039220713153282	0.215252319385371	Inf	0.182208086144075	0.855419427394712	0.957615553676381	unbiased	1neo-X*/1neo-Y
ENSMSEG00005023113	Uri1	ref - alt	-0.06791120561621	0.209075460969884	Inf	-0.324816720724544	0.745319788849241	0.94282953289429	unbiased	1neo-X*/1neo-Y

Bold indicate genes that passed significance thresholds = true allelic imbalance

S.4 The evolution of gene expression on sex and neo-sex chromosomes: detecting signs of degeneration ?

Supplemental Information

Supplemental methods

a) Animals, sampling and RNA extractions.

Individuals were reared in our breeding colony (CECEMA, University of Montpellier) established from wild caught animals in a South African population. We collected tissues from virgin individuals aged between 6-9 months old. Five individuals of each genotype (XX, XX*, X*Y and XY) were euthanised by cervical dislocation and kidneys were collected afterwards. Genotypes were assessed by PCR of *Sry* (Veyrunes et al., 2010a) or by karyotyping (Veyrunes et al., 2010b). Samples were kept in RNAlater® (ThermoFisher) for 48h at 4°C and then stored at -80°C until processing. Only one kidney, randomly chosen between left and right, was used and the whole tissue was extracted following RNeasy® Plus Mini Kit (Qiagen) protocol. For each individual, we first grounded the tissue in liquid nitrogen using a mortar and a pestle. We then added a lysis buffer (6 µL of β-mercapto added to 6000 µL of RLT Plus per sample) to homogenize shredded materials, and RNA was purified following Qiagen provided protocol. Total RNA was eluted in 50 µL of RNase free water. Samples were then stored at -80°C until further use.

b) Sequencing and mapping

Unstranded libraries' preparation and sequencing (Novogene, Cambridge, UK) using NovaSeq 6000 PE150 generated an average of ~46 millions of 150 pb paired-end reads. We assessed reads quality using FastQC v0.11.5. Reads were trimmed for minimal quality (set at 30), minimal length (set at 75 bp), and adaptors and N bases were removed using Cutadapt v3.5. Trimmed reads were then mapped on the masked *Mus minutoides* XX reference genome using STAR software v2 (https://www.ncbi.nlm.nih.gov/data-hub/genome/GCA_902729485.2/), with a 3 mismatch tolerance threshold. Gene quantification at the exon level was performed using the featureCounts software (Subread v 2.0) with a minimum mapping quality of 10.

c) Differential expression analysis

We filtered out read counts with a minimal read depth below 10 in at least 5 individuals and compared expression between the four genotypes using edgeR (i.e., multiple pairwise comparisons leading to 6 contrasts of genotype in total). We used a Benjamini-Hochberg correction for multiple testing and used a false discovery rate (FDR) threshold of 5% to detect differentially expressed genes (DEG). We normalized expression data of DEG using the TMM method, $\log_2$ transformed the values and further scaled expression to compare genes between genotypes. Gene expression was averaged between individuals within a genotypic group, and DEG were clustered according to their expression patterns

across genotype using a K-means hierarchical clustering method. This allows to detect patterns of expression that could reflect degeneration (i.e., underexpression of genes in individuals with X*, $1^{Neo\text{-}X*}$ and/or $1^{Neo\text{-}Y}$ and $13^{Neo\text{-}X*}$chromosomes) but also other changes in gene expression. These genes were tested for enrichment using permutation tests on each genomic compartment: autosome, X/X*, chr1 (i.e., $1^{Neo\text{-}X/X*/Y}$) with NR, NRY and R regions, and chr13 (i.e., $13^{Neo\text{-}X*}$) with NR and R regions. Because X*-linked autosome 16 is recombining, we included it in the 'autosome' genomic compartment.

d) Orientate changes in expression : comparison with *M. mattheyi*.

Raw read counts data including both species were normalized across species using TMM normalization and a log2 transformation in edgeR. We kept only genes expressed in *M.minutoides* to evaluate the evolution of gene expression (unbiased and DEG). We compared expression for each genotype to that of *M. mattheyi* in each clusters identified in the previous analysis (i.e., whether differential expression is due to an up-regulation or a down-regulation in comparison to the ancestral state). Expression changes were measured as the ratio of *M. minutoides* expression above the expression in *M. mattheyi*, which is averaged between the sexes :

$$Expression\,ratio = \log_2\left(\frac{TMM_{minutoides}+1}{\left(TMM_{mattheyi\,♀+♂}/2\right)+1}\right)$$

Ratios were further standardized by the averaged expression ratio of unbiased genes to correct for inter-species variability.

e) Allele specific expression of sex and neo-sex -linked genes

We tested for the degeneration of alleles in non-recombining regions and dosage compensation by comparing alleles' expression at the gene level. SNPs fixed in non-recombining regions were previously identified using whole genome DNA resequencing data (Saunders et al., in prep). We used the ASEReadCounter command from GATK v4.1 to retrieve reference and alternative allele counts at the SNP level . We filtered mapped reads for mapping quality, base quality and minimum number of bases that pass filters with the following parameters : *--min-mapping-quality 10 --min-base-quality 10 -min-depth 10*. Allele counts at the gene level were then obtained using the ASEReadCounter* pipeline (Mendelevich et al., 2020). We further kept genes with a minimal count of 10 reads in at least 5 allelic counts out of the 10 (2 alleles x 5 sample replicates). We used XX* females to investigate X* and $1^{Neo\text{-}X*}$ alleles' degeneration, XX* and X*Y females for $13^{Neo\text{-}X*}$ alleles' degeneration, and X*Y and XY individuals for $1^{Neo\text{-}Y}$ alleles' degeneration. We kept $1^{Neo\text{-}Y}$-linked genes identified in both X*Y and XY genotypes to eliminate a phenotypic sex effect (gene degeneration on $1^{Neo\text{-}Y}$ is independent of gonadal sex). We filtered genes with misdiagnosed alleles: reference and alternate alleles observed in

XX females, X alleles present in X*Y and $13^{Neo\text{-}X*}$ alleles present in XX and XY individuals. We modelled allele counts at the gene level fitting a negative binomial distribution, using alleles' origin and gene ensembl IDs as fixed effects, with an interaction term. We did not account for inter-genotype variability in models including two genotypes and tested each genomic compartment separately due to convergence issues. We adjusted p-values for multiple testing using a 'Benjamini-Hochberg' correction and genes below a 5% FDR threshold were considered to have a true allelic imbalance. One outlier female driving allelic imbalance results for X/X* alleles was removed from the analysis.

f) DEG enrichment on each genomic compartment.

We first tested for an enrichment using permutation tests: we reassigned genes on X:X* (non-recombining and recombining regions separately), neo-sex chromosomes (non-recombining and recombining regions separately) and autosomes a 1000 times, and compared expected frequencies of DEG in each cluster with a degeneration pattern (i.e., random distribution) to observed frequencies. P.values were defined by the number of times expected frequencies were even or greater observed frequencies, over the 1000 permutations. In a second analysis, we compared DEG frequencies on each genomic compartment to that of autosomes using Pearson χ^2 tests.

Supplemental References

Mendelevich, A., Vinogradova, S., Gupta, S., Mironov, A. A., Sunyaev, S., & Gimelbrant, A. A. (2020). Unexpected variability of allelic imbalance estimates from RNA sequencing. *BioRxiv* https://doi.org/10.1101/2020.02.18.948323

Veyrunes, F., Chevret, P., Catalan, J., Castiglia, R., Watson, J., Dobigny, G., Robinson, T. J., & Britton-Davidian, J. (2010a). A novel sex determination system in a close relative of the house mouse. *Proceedings of the Royal Society B: Biological Sciences*, *277*(1684), 1049-1056. https://doi.org/10.1098/rspb.2009.1925

Veyrunes, F., Catalan, J., Tatard, C., Cellier-Holzem, E., Watson, J., Chevret, P., Robinson, T. J., & Britton-Davidian, J. (2010b). Mitochondrial and chromosomal insights into karyotypic evolution of the pygmy mouse, Mus minutoides, in South Africa. *Chromosome Research*, *18*(5), 563-574. https://doi.org/10.1007/s10577-010-9144-9

Supplemental Tables

Table S1. Differentially expressed genes (DEG) enrichment in non-recombining regions and comparison with autosomes. N values indicate the number of genes in each category with observed frequencies. Asterisks indicate p.value significance from Pearson χ^2 and permutation tests.***p<0.001, **p≤0.01,*p≤0.05.

	Autosome		**chr1**						**chr13**				**X/X***		
	R		NR			NRY			NR				NR		
Clusters	*N (Freq$_{obs}$)*	*p.val (perm.)*	*N (Freq$_{obs}$)*	p.val (χ^2 test)	*p.val (perm.)*	*N (Freq$_{obs}$)*	p.val (χ^2 test)	*p.val (perm.)*	*N (Freq$_{obs}$)*	p.val (χ^2 test)	*p.val (perm.)*	*N (Freq$_{obs}$)*	p.val (χ^2 test)	*p.val (perm.)*
FB	23 (0.002)	0.34	0	0.79	1	1 (0.002)	0.5	0.05*	0	0.5	1	0	0.57	1
MB	68 (0.007)	0.11	2 (0.003)	0.82	0.01**	1 (0.002)	0.92	0.05*	1 (0.008)	0.5	0.56	0	0.85	1
MBxG	46 (0.004)	0.98	1 (0.002)	0.8	0.19	1 (0.002)	0.8	0.05*	1 (0.008)	0.5	0.48	2 (0.007)	0.45	0.4
-YB	5 (0.0005)	1	5 (0.008)	**<0.001*** **	**0.001*** **	8 (0.01)	**<0.001*** **	**<0.001*** **	0	0.5	1	1 (0.003)	0.2	0.34
-X*B	28 (0.003)	0.92	0	0.83	1	2 (0.003)	0.5	0.005**	1 (0.008)	0.42	0.36	2 (0.007)	0.23	0.22
X dose	5 (0.0005)	1	3 (0.005)	**0.002** **	**0.003** **	13 (0.02)	**<0.001*** **	**<0.001*** **	0	0.5	1	3 (0.01)	**<0.001*** **	**0.02***
YB	9 (0.0009)	1	6 (0.009)	**<0.001*** **	**<0.001*** **	7 (0.01)	**<0.001*** **	**<0.001*** **	0	0.5	1	0	0.5	1
X*B	36 (0.004)	0.98	2 (0.003)	0.5	0.04*	0	0.88	1	0	0.5	1	5 (0.02)	**<0.001*** **	**0.01** **
Unbiased	9671 (0.98)	-	237 (0.36)	-	-	363 (0.56)		-	127 (0.98)	-	-	273 (0.95)		-

Table S2. Differentially expressed genes (DEG) enrichment in recombining regions and comparison with autosomes. N values indicate the number of genes in each category with observed frequencies. Asterisks indicate p.values' significance from Pearson χ^2 and permutation tests. .***p<0.001, **p≤0.01,*p≤0.05, †p≤0.1. We considered the recombining region of X/X* chromosome enriched in 'X dose' genes because the enrichment was significant using Pearson χ^2 and at the threshold limit using the permutation test, consistent with graphical data (Fig 2b).

	Autosome		**Chr 1 (R)**			**Chr13 (R)**			**X/X* (R)**		
Clusters	*N (Freq$_{obs}$)*	*p.val (perm.)*	*N (Freq$_{obs}$)*	p.val (χ^2 test)	*p.val (perm.)*	*N (Freq$_{obs}$)*	p.val (χ^2 test)	*p.val (perm.)*	*N (Freq$_{obs}$)*	p.val (χ^2 test)	*p.val (perm.)*
FB	23 (0.002)	0.34	1 (0.0006)	0.86	0.98	1 (0.002)	0.5	0.74	0	0.5	1
MB	68 (0.007)	0.11	0	0.5	1	3 (0.005)	0.66	0.77	2 (0.01)	0.43	0.37
MBxG	46 (0.004)	0.98	0	0.99	1	6 (0.009)	0.08	0.08	3 (0.005)	0.5	0.59
Y down-reg	5 (0.0005)	1	0	0.6	0.93	0	0.5	0.68	0	0.5	0.25
X* down-reg	28 (0.003)	0.92	0	0.97	1	4 (0.006)	0.12	0.15	2 (0.01)	0.1	0.11
X dose	5 (0.0005)	1	0	0.6	0.97	0	0.5	0.73	2 (0.01)	**<0.001*** **	**0.06** †
Y up-reg	9 (0.0009)	1	0	0.77	0.96	1 (0.002)	0.5	0.7	0	0.5	0.29
X* up-reg	36 (0.004)	0.98	0	0.99	1	4 (0.006)	0.24	0.3	3 (0.02)	**0.02***	**0.05***
Unbiased	9671 (0.98)	-	1568 (0.99)		-	621 (0.98)		-	179 (0.95)		-

Annexe

Veyrunes, F., Perez, J., Heitzmann, L., Saunders, P. A., & Givalois, L. (2022). Separating the effects of sex hormones and sex chromosomes on behavior in the African pygmy mouse Mus minutoides , a species with XY female sex reversal [*BioRxiv*]. Evolutionary Biology. https://doi.org/10.1101/2022.07.11.499546

bioRxiv preprint doi: https://doi.org/10.1101/2022.07.11.499546; this version posted July 12, 2022. The copyright holder for this preprint (which was not certified by peer review) is the author/funder, who has granted bioRxiv a license to display the preprint in perpetuity. It is made available under aCC-BY-NC-ND 4.0 International license.

Separating the effects of sex hormones and sex chromosomes on behavior in the African pygmy mouse *Mus minutoides*, a species with XY female sex reversal.

Frederic Veyrunes (1), Julie Perez (1), Louise Heitzmann (1), Paul A Saunders (1), Laurent Givalois (2)

(1) ISEM, Institut des Sciences de l'Evolution de Montpellier UMR 5554, CNRS, Université de Montpellier, IRD, EPHE, Montpellier, France
(2) MMDN, Laboratoire Mécanismes Moléculaires dans les Démences Neurodégénératives, UMR 1198, Université de Montpellier, EPHE, INSERM, Montpellier, France

Corresponding author: Frederic Veyrunes
frederic.veyrunes@umontpellier.fr

bioRxiv preprint doi: https://doi.org/10.1101/2022.07.11.499546; this version posted July 12, 2022. The copyright holder for this preprint (which was not certified by peer review) is the author/funder, who has granted bioRxiv a license to display the preprint in perpetuity. It is made available under aCC-BY-NC-ND 4.0 International license.

ABSTRACT

In mammals, most sex differences in phenotype are controlled by gonadal hormones, but recent work on transgenic mice have shown that sex chromosomes can have a direct influence on sex-specific behaviors. In this study, we take advantage of the naturally occurring sex reversal in a mouse species, *Mus minutoides*, to investigate for the first time the relationship between sex chromosomes, hormones and behaviors in a wild species. In this model, a feminizing variant of the X chromosome, named X*, produces three types of females with different sex chromosome complements (XX, XX*, and X*Y), associated with alternative behavioral phenotypes, while all males are XY. We thus compared the levels of three major circulating steroid hormones (testosterone, corticosterone and estradiol) in the four sex genotypes to disentangle the influence of sex chromosomes and sex hormones on behavior. First, we did not find any difference in testosterone levels in the three female genotypes, although X*Y females are notoriously more aggressive. Second, in agreement with their lower anxiety-related behaviors, X*Y females and XY males display lower baseline corticosterone concentration than XX and XX* females. Instead of a direct hormonal influence, this result rather suggests that sex chromosomes may have an impact on the baseline corticosterone level, which in turn may influence behaviors. Third, estradiol concentrations do not explain the enhanced reproductive performance and maternal care behavior of the X*Y females compared to the XX and XX* females. Overall, this study highlights that most of the behaviors varying along with sex chromosome complement of this species are driven by genetic factors rather than steroid hormone concentrations.

bioRxiv preprint doi: https://doi.org/10.1101/2022.07.11.499546; this version posted July 12, 2022. The copyright holder for this preprint (which was not certified by peer review) is the author/funder, who has granted bioRxiv a license to display the preprint in perpetuity. It is made available under aCC-BY-NC-ND 4.0 International license.

INTRODUCTION

The developmental processes leading from a single genome to two sexually dimorphic phenotypes are remarkably complex and remain poorly understood (Mank, 2017; Naqvi et al., 2019). In mammals, sex development can be divided into two main components: sex determination and sex differentiation. Sex determination is the process by which the bipotential embryonic gonads develop into either testes or ovaries, which depends exclusively on the sex chromosomes; sex differentiation involves the subsequent events that ultimately produce either the male or female phenotype, driven mostly by gonadal steroid hormones (review in Arnold, 2012). However, in the last two decades, several studies on genetically manipulated mice have challenged this view, highlighting the direct influence of the sex chromosomes on sex differences in behavior and brain, such as some aspects of aggressiveness, parental behavior, food consumption, social interactions, anxiety, or brain structures and functions (e.g. de Vries et al., 2002; Gatewood et al., 2006; Arnold, 2012, 2019; Lentini et al., 2013; Corre et al., 2016). Although mammalian XX/XY sex determination is extremely conserved, a few species escape this convention and present unusual sex determination systems (Parma et al., 2016; Saunders & Veyrunes, 2021). The African pygmy mouse, *Mus minutoides* is the latest addition to this short list of odd mammals, owing to the presence of a third sex chromosome named X* (Veyrunes et al., 2010). This is a mutant copy of the X chromosome that differs cytogenetically from the ancestral X and is feminizing. Therefore, three female genotypes are found: XX, XX* and X*Y, while all males are XY. Previous works showed that sex-reversed females (X*Y) may represent up to 75% of the females in some wild populations (Veyrunes et al., 2010). They are fully fertile with typical ovaries without apparent signs of testicular tissue (Rahmoun et al., 2014), they have a higher lifetime reproductive success than the XX and XX* females, including larger litter size despite the cost of losing lethal YY embryos (Saunders et al., 2014),

bioRxiv preprint doi: https://doi.org/10.1101/2022.07.11.499546; this version posted July 12, 2022. The copyright holder for this preprint (which was not certified by peer review) is the author/funder, who has granted bioRxiv a license to display the preprint in perpetuity. It is made available under aCC-BY-NC-ND 4.0 International license.

and they also show enhanced maternal care behaviors compared to other females (Heitzmann et al. 2022). On the other hand, they display some masculinized behaviors, such as enhanced aggressiveness, lower anxiogenic response (Saunders et al., 2016) and higher bite-force performance (Ginot et al., 2017). Therefore, the X* effect goes well beyond sex reversal, and is at the origin of a complex X*Y phenotype with opposite results on the two components of sex development (i.e., sex determination and sex differentiation): gonad feminization and partial masculinization of behaviors. Phenotypic sexes of the X*Y gonads and brain are thus partially dissociated, a unique feature in a wild mammal species. Moreover, gonadal sex and chromosomal sex also are partially uncoupled (XX *vs*. X*Y females, and XY males *vs*. X*Y females), offering a promising model to investigate the influence of sex chromosome complements versus steroid hormones on sexual dimorphism in brain and behavioral traits. To date, the behavioral differences observed in the three *M. minutoides* female genotypes have been mostly attributed to genetic effects (Saunders et al., 2016; Ginot et al., 2017) on basis that X*Y females are characterized by complete sex reversal with typical ovarian anatomy (no ovotestes) and normal anogenital distance. This suggests a low level of circulating androgens (Rahmoun et al., 2014), but the question remains open. In this study, we thus compared the levels of three circulating steroid hormones (testosterone, corticosterone and estradiol) in the four sex genotypes (XY males, and XX, XX* and X*Y females) to disentangle the influence of sex-linked genes and steroid hormones on the masculinized behaviors observed in X*Y females (Saunders et al., 2016; Ginot et al., 2017).

MATERIALS AND METHODS

Animals

Mice were bred in our own breeding colony (CECEMA, University of Montpellier), established from wild-derived animals (for further details see Saunders et al., 2014). Females were housed

bioRxiv preprint doi: https://doi.org/10.1101/2022.07.11.499546; this version posted July 12, 2022. The copyright holder for this preprint (which was not certified by peer review) is the author/funder, who has granted bioRxiv a license to display the preprint in perpetuity. It is made available under aCC-BY-NC-ND 4.0 International license.

in same-sex groups of 3-4 individuals per cage, and males in individual cages (to prevent agonistic behaviors). They were provided with *ad libitum* food and water, and the light regime was set to 15:9h (light:dark). The genotype of females was determined by PCR amplification of the Y-specific *Sry* gene from tail biopsies or culture of fibroblasts from skin biopsies. The animal age varied between 8 and 10 months, and all blood/urine samples were collected at the same time of the day (± 2 h). Experimental procedures were in accordance with the European guidelines and were approved by the French Ethical Committee on animal care and use (No. CEEA-LR- 12170).

Hormone assays

As the African pygmy mouse is one of the smallest mammal species in the world (Boel et al., 2020), the amount of blood that could be collected from each individual was limited. This prevented testing all samples in duplicate and measuring the three steroid hormones in the same animal (one mouse for each hormone). Moreover, for a limited number of animals, reduced volumes of plasma, serum or urine were collected and had to be used diluted with kit's sample diluents or SAMPLEDIL (ref: KLZZ731). Nevertheless, all samples were within the range of robust minimal assay sensitivity. The numbers of animals used for the different measurements are listed in Table 1.

Testosterone: animals were euthanized by decapitation and trunk blood collected in Eppendorf tubes. After 30 min at room temperature, blood samples were centrifuged and serum was collected and stored at -20 °C. Testosterone concentrations were measured using an ELISA kit (IBL International ref: RE52151) following the manufacturer's instructions. To fall within the sensitivity range of the assay, serum from males were tested at two dilutions (1:5 and 1:10), and the hormone concentration was calculated by the mean of values obtained at each dilution. This

bioRxiv preprint doi: https://doi.org/10.1101/2022.07.11.499546; this version posted July 12, 2022. The copyright holder for this preprint (which was not certified by peer review) is the author/funder, who has granted bioRxiv a license to display the preprint in perpetuity. It is made available under aCC-BY-NC-ND 4.0 International license.

also allowed to obtained pseudo-duplicates that confirmed an excellent dilution pattern, and a very good assay precision with a low intra-assay coefficient of variability.

Corticosterone: plasma corticosterone concentrations were measured at baseline (no stress) and after stress induction. For baseline corticosterone, mice were taken from the cage and rapidly decapitated to collect trunk blood. For the post-stress corticosterone measurement, mice were placed in a glass beaker (diameter 12.5 cm), filled with 1.4L of water (22 ± 1 °C) and forced to swim for 10 min, then animals were rapidly decapitated. In both cases, blood samples were collected in EDTA-coated Eppendorf tubes, centrifuged at 4 °C, and plasma was collected and stored at -20°C. Corticosterone concentrations were measured with a conventional ELISA kit (ENZO Life Sciences; ref: ADI-900-097) following the manufacturer's instructions, as previously reported (Canet et al., 2020).

17ß-Estradiol: the inconclusive results obtained with serum (most concentrations below the standard curve) led to its quantification in urine samples that have shown to give interpretable results in mice (e.g. deCantazaro et al., 2004). Urine was collected upon handling mice and pipetted on a clean surface, and stored at -20 °C. As estradiol concentration varies along the estrous cycle (e.g. Wood et al., 2007), this study focused arbitrarily on the diestrus and estrus stages. To determine the estrous cycle phase, just after urine collection, females were held by the tail, and the vagina was flushed twice with 10 µl of sterile water using a pipette tip. The vaginal smear was placed on a glass slide, stained with Giemsa, and viewed under a light microscope (10x magnification). The diestrus phase was defined by the exclusive presence of leukocytes, and the estrus phase by the presence of large and squamous-type epithelial cells without nucleus. Urinary estradiol concentrations were measured with an ELISA kit (IBL International ref: 30121045) following the manufacturer's instructions and protocol in deCantazaro et al. (2004).

bioRxiv preprint doi: https://doi.org/10.1101/2022.07.11.499546; this version posted July 12, 2022. The copyright holder for this preprint (which was not certified by peer review) is the author/funder, who has granted bioRxiv a license to display the preprint in perpetuity. It is made available under aCC-BY-NC-ND 4.0 International license.

Statistical analysis

Final steroid concentrations were calculated from hormone-specific standard curves corrected for an individual's sample volume. All statistical analysis were performed on R v3.6.3. We used a non-parametric test, Kruskall-Wallis, to test differences in testosterone level between the four genotypes. Post-hoc pairwise comparisons were made using *dunn.test* with a Benjamini-Hochberg p-value adjustment to account for multiple testing. Baseline and stress-induced corticosterone concentration were analyzed separately fitting a linear model with individuals' genotype as the only predictor. We used a log-transformation of corticosterone baseline-level to account for heteroscedasticity. Post-hoc pairwise comparisons were made using *emmeans* package with Tukey adjustments of p-values to account for multiple testing. We also fitted a linear model to investigate estradiol level using 'genotype' and 'estrous cycle phase' (estrus *vs.* diestrus) as predictors. We included an interaction between both predictors with the assumption that female estradiol level may vary with the estrous cycle and independently between genotypes (i.e., estradiol variation between estrus and diestrus states may differ between genotypes). Post-hoc comparisons were made using *emmeans* package with Tukey adjustments of p-values to account for multiple testing.

RESULTS AND DISCUSSION

Sex-reversed *M. minutoides* females show a combination of phenotypic traits not seen in concordant individuals of either sex. For some phenotypic traits, X*Y females can be viewed as "super females" as called by Knight (2017), with a greater reproductive output (Saunders et al., 2014) and enhanced maternal care (for example, they retrieve pups faster and with a higher probability; Heitzmann et al. 2022) compared to XX and XX* females. Conversely, for other aspects, they are more similar to males: lower anxiety-related behavior and enhanced aggressiveness (Saunders et al., 2016). That similarity between X*Y females and males extends

bioRxiv preprint doi: https://doi.org/10.1101/2022.07.11.499546; this version posted July 12, 2022. The copyright holder for this preprint (which was not certified by peer review) is the author/funder, who has granted bioRxiv a license to display the preprint in perpetuity. It is made available under aCC-BY-NC-ND 4.0 International license.

to whole-organism performance with higher bite force than other females, and even a tendency (though not statistically significant) to bite harder than males (Ginot et al., 2017). In summary, sex reversal changes not only the gonadal sex, but also some behavioral and life history traits, and is at the origin of a new female sexual phenotype (Heitzmann et al., 2022). Therefore, to untangle the role of genetic *versus* hormonal effects on these behavioral differences observed among females, we compared the levels of three major circulating sex steroid hormones in the different genotypes.

Testosterone is ubiquitous in vertebrates and is the key mediator in the expression of many male morphological and behavioral traits (Trainor and Marler, 2002; Giammanco et al., 2005; Preston et al., 2012; McEvoy et al. 2015; and references therein). More particularly, it is thought to be the major sex steroid regulating male aggressive behavior and dominance, in a wide variety of fish, reptile, bird, and mammal species (including humans). For example, high rates of aggression generally correlate with elevated testosterone levels (Giammanco et al., 2005; Yu and Shi, 2009; Cantarero et al., 2015; St Clair Yewers et al., 2017; Denson et al. 2018), and male aggressiveness can be reduced by castration and restored by administration of androgens (Giammanco et al. 2005). In humans, higher testosterone concentrations are observed in perpetrators of violent crimes, in soldiers with antisocial behaviors, in subjects with impulsive behaviors, and in athletes during competition (review in Giammanco et al., 2005). In vertebrates, testosterone is mostly produced by Leydig cells in testes, while smaller quantities are also produced by ovaries, and adrenal glands in both sexes (Nelson, 2010). Although aggressiveness and testosterone may be lower in females, the more limited literature data shows a similar positive relationship between testosterone and aggression, albeit less so (Giammanco et al., 2005; Denson et al., 2018). In the African pygmy mice, we found a high sexual dimorphism of serum testosterone levels as expected ($p < 0.001$ between males and XX and

bioRxiv preprint doi: https://doi.org/10.1101/2022.07.11.499546; this version posted July 12, 2022. The copyright holder for this preprint (which was not certified by peer review) is the author/funder, who has granted bioRxiv a license to display the preprint in perpetuity. It is made available under aCC-BY-NC-ND 4.0 International license.

XX* females; p = 0.002 between males and X*Y females); however, we did not detect any difference among the three female genotypes (Fig. 1). Therefore, the aggressive behavior and stronger bite force (another indicator of aggressive performance) of X*Y females are unlikely to be directly mediated by the circulating testosterone level. This result adds to the increasing evidence that the relationship between aggression and testosterone is not straightforward (e.g. Huyghe et al., 2009; McEvoy et al., 2015; Cantarero et al., 2015; St Clair Yewers et al., 2017), which might be explained by the fact that aggressiveness is highly context-dependent (e.g. social experience or motivation) and includes complex behavioral patterns with different underlying physiological mechanisms and metabolic pathways. This is especially relevant in females: in females more than males, it would be simplistic to reduce hormone-mediated aggressive behavior to testosterone concentration only (review in Denson et al., 2018). In *M. minutoides*, the clear-cut contrast of aggressiveness in controlled experiments between X*Y females and XX and XX* females (in the resident-intruder test, X*Y females show an attack latency at least twice shorter and a number of aggressions at least twice higher than in the other female genotypes; Saunders et al., 2016) may also suggest a direct effect of the sex chromosome complement on the behavior of X*Y females. Specifically, the Y chromosome includes at least one gene, *Sts*, that has been shown to influence aggressiveness in mice (Mortaud et al., 2010). Two other important candidates are X-linked genes, the Androgen Receptor (*AR*) which mediates the actions of testosterone (Davey & Grossman 2016), and the Monoamine oxidase A (*MaoA*) that is well known to influence aggressiveness (Cases et al., 1995). Following the rise of the X* chromosome, differences of expression could have evolved between the X and X* copies.

Although glucocorticoids (i.e., mainly corticosterone in rodents) may be involved in aggression, they are best known as stress hormones (Romero, 2004; Bonier et al., 2009).

bioRxiv preprint doi: https://doi.org/10.1101/2022.07.11.499546; this version posted July 12, 2022. The copyright holder for this preprint (which was not certified by peer review) is the author/funder, who has granted bioRxiv a license to display the preprint in perpetuity. It is made available under aCC-BY-NC-ND 4.0 International license.

Corticosterone secreted by adrenal glands is increasingly employed as a physiological indices of the relative health conditions and as a stress index of individuals or populations (review in Bonier et al., 2009). The interpretation of corticosterone concentrations is complicated by the fact that its secretion can be classified in two types based on the secretion dynamics, the receptors bound, and the physiological and behavioral effects (Romero, 2004; Rensel and Schoech, 2011). The baseline corticosterone is the amount of hormone secreted on a continuous low-level basis, and is involved in the maintenance of energetic balances and homeostasis. Elevated baseline corticosterone levels are assumed to predict a low relative fitness of individuals, associated with multiple deleterious characteristics, such as chronic stress, poor body conditions, reallocation of resources away from reproductive behaviors, infertility (e.g. Romero and Wikelski, 2001; Strasser and Heath, 2013; review in Bonier et al., 2009). The second type of secretion takes place when a stressful stimulus is perceived, stress responses are thus initiated which trigger activation of the hypothalamo-pituitary-adrenal axis with a rapid and intense release of corticosterone. This abrupt increase of circulating corticosterone modulates specific physiological and behavioral traits to help the organism to cope with the stressor, thus promoting short-term survival, and will remain high for a few hours (Wingfield and Sapolsky, 2003; Romero, 2004). Acute elevation of corticosterone has been associated with escape behavior, suppression of territorial behavior and reproductive activity, reduction of parental care and energy reallocation (Wingfield et al., 1998; Sapolsky et al., 2000; Miller et al. 2009). Therefore, differences in baseline or stress-induced corticosterone concentrations among individuals may have completely different physiological and behavioral consequences, and it is essential to consider both. In *M. minutoides*, X*Y females and XY males display lower baseline corticosterone levels than XX and XX* females; concentrations were significantly lower in sex-reversed females than in XX* ($p = 0.003$) and XX females ($p = 0.01$), tended to be lower though not significant in males than in XX* ($p = 0.054$) and XX females ($p = 0.14$),

bioRxiv preprint doi: https://doi.org/10.1101/2022.07.11.499546; this version posted July 12, 2022. The copyright holder for this preprint (which was not certified by peer review) is the author/funder, who has granted bioRxiv a license to display the preprint in perpetuity. It is made available under aCC-BY-NC-ND 4.0 International license.

and were similar between X*Y females and males ($p = 0.54$), as well as between XX and XX* females ($p = 0.99$); whereas the stress-induced concentrations were comparable in the four groups (Fig. 2A-B). According to the Glucocorticoid-Fitness hypothesis (Bonier et al., 2009), the lower baseline corticosterone concentration in X*Y females suggests lower anxiety and greater relative fitness. This assumption is congruent with the life-history and behavioral traits measured in captivity: X*Y females display (i) a greater probability of breeding and produce significantly more offspring during their lifetime than XX and XX* females (Saunders et al., 2014), and (ii) lower anxiety-related behavior compared with the other females but similar to males (Saunders et al., 2016). This might suggest that anxiety-related behaviors are influenced by sex hormones only; however, the finding that animals harboring a Y chromosome have a lower baseline corticosterone than XX and XX* females, rather suggests a direct effect of the sex chromosome complements. We show that irrespective of the gonadal sex, the chromosomal sex also may have an impact on steroid concentrations, which in turn may influence behaviors.

Finally, we investigated estradiol levels in females since the reproductive performances (Saunders et al., 2014) and the maternal care behavior (Heitzmann et al. 2022) of the three female genotypes differ. Estrogens, particularly estradiol, exert powerful influences on the mammalian female reproductive physiology and behavior. For example, estradiol plays critical roles in regulating estrous cycling, preparing the uterus for embryo implantation, inducing sexual receptivity and facilitating lordosis, and on the onset and maintenance of maternal behaviors (reviews in Kelley & Brenowitz, 2002; deCatanzaro, 2015). In *M. minutoides*, urinary estradiol levels were comparable among female genotypes at diestrus, and marginally lower in XX females during estrus ($p = 0.053$ and $p = 0.11$ in comparison to X*Y and XX*, respectively) (Fig. 3). Our data also show a trend for higher estradiol levels at estrus than diestrus in X*Y ($p = 0.048$) and XX* females ($p = 0.08$), as reported in the house mouse (e.g. Wood et al., 2007),

bioRxiv preprint doi: https://doi.org/10.1101/2022.07.11.499546; this version posted July 12, 2022. The copyright holder for this preprint (which was not certified by peer review) is the author/funder, who has granted bioRxiv a license to display the preprint in perpetuity. It is made available under aCC-BY-NC-ND 4.0 International license.

but not in XX females (p = 0.92) (Fig. 3). In our laboratory colony, XX females show lower breeding performance and lower pup retrieval behavior than X*Y females (Saunders et al., 2014; Heitzmann et al. 2022), which fits with the trend in estradiol level differences observed. However, the finding that XX* have comparable reproductive traits and maternal care behaviors to XX females, but the same estradiol concentration as X*Y females rules out any causal link. Conversely, these results strongly suggest an advantageous feature of the X*Y complement, and it is tempting to attribute it to the X* chromosome that evolved towards a female uniparental transmission and may have accumulated female-beneficial genes. But this hypothesis does not explain why XX* females, which also harbor the X* chromosome and retain random inactivation of the X and X* chromosomes (Veyrunes and Perez, 2018), do not present a more intermediate phenotype. Other hypotheses are discussed by Saunders et al (2014), particularly concerning the X chromosome copy number (one in X*Y *vs*. two in XX and XX*) that has been shown to influence the expression of hundreds of autosomal genes in the house mouse (Wijchers et al., 2010). Finally, the low level of estradiol concentration and the absence of detectable variations between estrus and diestrus in XX females are noteworthy, and might be related to their apparent smaller ovaries and fewer follicles compared to XX* and X*Y females (Rahmoun et al., 2014); this result requires further investigations.

Overall, there is a substantial body of evidence about sex differences in many aspects of brain development and function and also behavior (reviews in Arnold and Chen, 2009; Ngun et al., 2011; Arnold, 2012; de Vries & Forger, 2015). Although such differences are mostly due to steroid hormone levels, recent data indicate that the sex-specific genetic architecture and expression of sex-linked genes also play a direct role on sexual dimorphism (e.g. de Vries et al., 2002; Gatewood et al., 2006; McPhie-Lalmansingh et al., 2008; Lentini et al., 2013; Corre et al., 2016; Arnold, 2019). The direct effect of the sex chromosome complement on behavior

bioRxiv preprint doi: https://doi.org/10.1101/2022.07.11.499546; this version posted July 12, 2022. The copyright holder for this preprint (which was not certified by peer review) is the author/funder, who has granted bioRxiv a license to display the preprint in perpetuity. It is made available under aCC-BY-NC-ND 4.0 International license.

and brain has been mostly assessed using transgenic mouse strains, called the "Four core genotypes" model (see De Vries et al., 2002; Cox et al. 2014 for a description). But these strains show some limitations, including the fact that these mice are genetically manipulated, have poor fertility, and that the *Sry* gene is absent in XY females (Ngun et al., 2011). The sex determination system of *M. minutoides*, shaped by one million years of natural selection (Veyrunes et al., 2013), in which gonadal sex and chromosomal sex are partially dissociated, offers a unique framework to investigate the relationship between sex chromosomes, hormones and behaviors in a wild species. The hormonal profile of each female genotype obtained in this study confirmed that most of the sexually dimorphic behaviors of this species are driven by genetic factors rather than steroid hormone concentrations (Table 2). They also highlight the need to consider naturally occurring sex reversal with alternative phenotypes, as observed in the pygmy mouse or in the bearded dragon (Li et al., 2016), to better understand the large spectrum of behaviors under the direct influence of genetic factors and as such, to challenge the classical view of steroid hormone predominance in the induction of sex differences in non-gonadal organs and behavior.

ACKNOWLEDGMENTS

We are grateful to RAM-CECEMA animal facility and Marie Challe for her help in maintaining the breeding colony. This study was supported by the ANR grant SEXREV (no. 18-CE02-0018-01).

REFERENCES

Arnold, A.P. (2012). The end of gonad-centric sex determination in mammals. Trends Genet. **28**, 55-61.

Arnold, A.P. (2019). Rethinking sex determination of non-gonadal tissues. Curr. Top. Dev. Biol. **134**, 289–315

bioRxiv preprint doi: https://doi.org/10.1101/2022.07.11.499546; this version posted July 12, 2022. The copyright holder for this preprint (which was not certified by peer review) is the author/funder, who has granted bioRxiv a license to display the preprint in perpetuity. It is made available under aCC-BY-NC-ND 4.0 International license.

Arnold, A.P. and Chen, X. (2009). What does the "four core genotypes" mouse model tell us about sex differences in the brain and other tissues? Front. Neuroendocrinol. **30**, 1–9

Boel, M., Romestaing, C., Duchamp, C., Veyrunes, F., Renaud, S., Roussel, D. and Voituron, Y. (2020). Improved mitochondrial coupling as a response to high mass-specific metabolic rate in extremely small mammals. J. Exp. Biol. **223**, jeb215558

Bonier, F., Martin, P.R., Moore, I.T. and Wingfield, J.C. (2009). Do baseline glucocorticoids predict fitness? Trends Ecol. Evol. **24**, 634-642.

Canet, G., Pineau, F., Zussy, C., Hernandez, C., Hunt, H., Chevallier, N., Perrier, V., Torrent, J., Belanoff, J., Meijer, O.C., Desrumaux, C. and Givalois, L. (2020). Glucocorticoid receptors signaling impairment potentiates amyloid-β oligomers-induced pathology in an acute model of Alzheimer's disease. FASEB J. **34**, 1150-1168.

Cantarero, A., Laaksonen, T., Jarvisto, P.E., Gil, D., Lopez-Arrabe, J., Redondo, A.J. and Moreno, J. (2015). Nest defence behaviour and testosterone levels in female pied flycatcher. Ethology **121**, 946-657.

Cases, O., Seif, I., Grimsby, J. and Gaspar, P. (1995). Aggressive behavior and altered amounts of brain serotonin and norepinephrine in mice lacking MAOA. Science **268**, 1763–1766.

Corre, C., Friedel, M., Vousden, D.A., Metcalf, A., Spring, S., Qiu, L.R., Lerch, J.P. and Palmert, M.R. (2016). Separate effects of sex hormones and sex chromosomes on brain structure and function revealed by high-resolution magnetic resonance imaging and spatial navigation assessment of the Four Core Genotype mouse model. Brain Struct. Funct. **221**, 997-1016.

Cox, K.H., Bonthuis, P.J. and Rissman, E.F. (2014). Mouse model systems to study sex chromosome genes and behavior: Relevance to humans. Front. Neuroendocr. **35**, 405-419.

Davey, R.A. and Grossman, M. (2016). Androgen Receptor structure, function and biology: from bench to bedside. Clin. Biochem. Rev. **37**, 3-15.

De Vries, G.J. and Forger, N.G. (2015). Sex differences in the brain: a whole body perspective. Biol. Sex. Differ. **6**, 15.

De Vries, G.J., Rissman, E.F., Simerly, R.B., Yang, L.Y., Scordalakes, E.M., Auger, C.J., Swain, A., Lovell-Badge, R., Burgoyne, P.S. and Arnold, A.P. (2002). A model system for study of sex chromosome effects on sexually dimorphic neural and behavioral traits. J. Neurosci. **22**, 9005–9014.

deCantazaro, D., Muir, C., Beaton, E.A. and Jetha, M. (2004). Non-invasive repeated measurement of urinary progesterone, 17 b-estradiol, and testosterone in developing, cycling, pregnant, and postpartum female mice. Steroids **69**, 687-696.

Denson, T.F., O'Dean, S.M., Blake, K.R. and Beames, J.R. (2018). Aggression in women: behavior, brain and hormones. Front. Behav. Neurosci. **12**, 81.

Gatewood, J.D., Wills, A., Shetty, S., Xu, J., Arnold, A.P., Burgoyne, P.S. and Rissman, E.F. (2006). Sex chromosome complement and gonadal sex influence aggressive and parental behaviors in mice. J. Neurosci. 26, 2335–2342.

Giammanco, M., Tabacchi, G., Giammanco, S., Di Malo, D. and La Guardia, M. (2005). Testosterone and aggressiveness. Med. Sci. Monit. 11, RA136-145.

bioRxiv preprint doi: https://doi.org/10.1101/2022.07.11.499546; this version posted July 12, 2022. The copyright holder for this preprint (which was not certified by peer review) is the author/funder, who has granted bioRxiv a license to display the preprint in perpetuity. It is made available under aCC-BY-NC-ND 4.0 International license.

Ginot, S., Claude, J., Perez, J. and Veyrunes, F. (2017). Sex reversal induces size and performance differences among females of the African pygmy mouse, *Mus minutoides*. J. Exp Biol. **220**, 197-1951.

Heitzmann, L., Challe, M., Perez, J., Castell, L., Galibert, E., Martin, A., Valjent, E. and Veyrunes F. (2022). Genotypic sex shapes maternal care in the African Pygmy mouse, *Mus minutoides*. BioRxiv doi.org/10.1101/2022.04.05.487174

Huyghe, K., Husak, J.F., Herrel, A., Tadic, Z., Moore, I.T., Van Damma, R. and Vanhooydonck, B. (2009). Relationships between hormones, physiological performance and immunocompetence in a color-polymorphic lizard species, *Podarcis melisellensis*. Horm. Behav. **55**, 488-494.

Kelley, D. B. and Brenowitz, E. (2002). Hormonal influences on courtship behaviors, in: Becker, J.B., Breedlove, S.M., Crews, D. (Eds), Behavioral Endocrinology 2. MIT Press, London, pp 289-330.

Knight, K. (2017). X*Y super female pygmy mice have larger heads and superior bites. J. Exp. Biol. **220**, 1931-1932

Lentini, E., Kasahara, M., Arver, S. and Savic, I. (2013). Sex differences in the human brain and the impact of sex chromosomes and sex hormones. Cereb. Cortex **23**, 2322-2336.

Li, H., Holleley, C.E., Elphick, M., Georges, A. and Shine, R. (2016). The behavioural consequences of sex reversal in dragons. Proc. R. Soc. B. **283**, 20160217.

Mank, J.E. (2017). The Transcriptional architecture of phenotypic dimorphism. Nature Ecol. Evol, **1**, 6.

McEvoy, J., While, G.M., Jones, S.M. and Wapstra, E. (2015). Examining the role of testosterone in mediating short-term aggressive responses to social stimuli in a lizard. PLoS ONE **10**, e0125015

McPhie-Lalmansingh, A., Tejada, L., Weaver, J. and Rissman, E. (2008). Sex chromosome complement affects social interactions in mice. Horm. Behav. **54**, 565–70.

Miller, D.A., Vleck, C.M. and Otis, D.L. (2009). Individual variation in baseline and stress-induced corticosterone and prolactin levels predicts parental effort by nesting mourning doves. Horm. Behav. **56**, 457-464.

Mortaud, S. Nicolas, L., Pinoteau, W., Tordjman, S., Carlier, M. and Roubertoux, P.L. (2010). Brain pathways mediating the pro-aggressive effect of the steroid sulfatase (*Sts*) gene. Behav. Genet. **40**, 211–219.

Naqvil, S., Godfrey, A.K., Hughes, J.F., Goodheart, M.L., Mitchell, R.N. and Page, D.C. (2019). Conservation, acquisition, and functional impact of sex-biased gene expression in mammals. Science **365**, eaaw7317.

Nelson, R.J. (2010). Hormones and behavior: basic concepts, in: Breed, M.D., Moore, J. (Eds), Encyclopedia of animal behavior. Academic Press, pp 97-105.

Ngun, T.C., Ghahramani, N., Sanchez, F.J., Bocklandt, S. and Vilain, E. (2011). The genetics of sex differences in brain and behavior. Front. Neuroendocrinol. 32, 227-246.

Parma, P., Veyrunes, F. and Pailhoux, E. (2016). Sex reversal in non-human placental mammals. Sex. Dev. **10**, 326-344.

bioRxiv preprint doi: https://doi.org/10.1101/2022.07.11.499546; this version posted July 12, 2022. The copyright holder for this preprint (which was not certified by peer review) is the author/funder, who has granted bioRxiv a license to display the preprint in perpetuity. It is made available under aCC-BY-NC-ND 4.0 International license.

Preston, B.T., Stevenson, I.R., Lincoln, G.A., Monfort, S.L., Pilkington, J.G. and Wilson, K. (2012). Testes size, testosterone production and reproductive bahaviour in a natural mammalian mating system. J. Anim. Ecol. **81**, 296-305.

Rahmoun, M., Perez, J., Sauders, P.A., Boizet-Bonhoure, B, Wilhelm, D, Poulat, F. and Veyrunes, F. (2014). Anatomical and molecular analyses of XY ovaries from the African pygmy mouse *Mus minutoides*. Sex. Dev. **8**, 356–63.

Rensel, M.A. and Schoech, S.J. (2011). Repeatability of baseline and stress-induced corticosterone levels across early life stages in the Florida scrub-jay (*Aphelocoma coerulescens*). Horm. Behav. **59**, 497-502.

Romero, L.M. (2004). Physiological stress in ecology: lessons from biomedical research. Trends Ecol. evol. **19**, 249-255.

Romero, L.M. and Wikelski, M. (2001). Corticosterone levels predict survival probabilities of Galapagos marine iguanas during El Nino events. Proc. Natl. Acad. Sci. U. S. A. **98**, 7366-7370.

Sapolsky, R.M., Romero, L.M. and Munck, A.U. (2000). How do glucocorticoids influence stress-responses? integrating permissive, suppressive, stimulatory, and adaptative actions. Endocr. Rev. **21**, 55-89.

Saunders, P.A. and Veyrunes, F. (2021) Unusual Mammalian Sex Determination Systems: A Cabinet of Curiosities. Genes. **12**, 1770.

Saunders, P.A., Franco, T., Sottas, C., Maurice, T., Ganem, G. and Veyrunes, F. (2016). Masculinised behaviour of XY females in a mammal with naturally occurring sex reversal. Sci. Rep. **6**, 22881.

Saunders, P.A., Perez, J., Rahmoun, M., Ronce, O., Crochet, P.A. and Veyrunes, F. (2014). XY females do better than the XX in the African pygmy mouse, *Mus minutoides*. Evolution **68**, 2119-2127.

St Clair Yewers, M., Jessop, T.S. and Stuart-Fox, D. (2017). Endocrine differences among colour morphs in a lizard with alternative behavioural strategies. Horm. Behav. **93**, 118-127.

Strasser, E.H. and Heath, J.A. (2013). Reproductive failure of a human-tolerant species, the American kestrel, is associated with stress and human disturbance. J. Appl. Ecol. **50**, 912-919.

Trainor, B.C. and Marler, C.A. (2002). Testosterone promotes paternal behaviour in a monogamous mammal via conversion to estrogen. Proc. R. Soc. B **269**, 823-829.

Veyrunes, F., Chevret, P., Catalan, J., Castiglia, R., Watson, J., Dobigny, G., Robinson, T.J. and Britton-Davidian, J. (2010). A novel sex determination system in a close relative of the house mouse. Proc. R. Soc. B **277**, 1049–1056.

Veyrunes, F. and Perez, J. (2018). X inactivation in a mammal species with three sex chromosomes. Chromosoma **127**, 261-267.

Veyrunes, F., Perez, J., Paintsil, S.N.C., Fichet-Calvet, E. and Britton-Davidian, J. (2013). Insights into the evolutionary history of the X-Linked sex reversal mutation in *Mus minutoides*: clues from sequence analyses of the Y-linked *Sry* gene. Sex. Dev. **7**, 244–52.

Wijchers, P.J., Yandim, C., Panousopoulou, E., Ahmad, M., Harker, N., Saveliev, A., Burgoyne, P.S. and Festenstein. R. (2010). Sexual dimorphism in mammalian autosomal gene regulation is determined not only by *Sry* but by sex chromosome complement as well. Dev. Cell **19**, 477–484.

bioRxiv preprint doi: https://doi.org/10.1101/2022.07.11.499546; this version posted July 12, 2022. The copyright holder for this preprint (which was not certified by peer review) is the author/funder, who has granted bioRxiv a license to display the preprint in perpetuity. It is made available under aCC-BY-NC-ND 4.0 International license.

Wingfield, J.C., Maney, D.L., Breuner, C.W., Jacobs, J.D., Lynn, S., Ramenofskky, M. and Richardson, R.D. (1998). Ecological bases of hormone-behavior interactions: the "emergency life history stage". Am. Zool. **38**, 191-206.

Wingfield, J.C. and Sapolsky, R.M. (2003). Reproduction and resistance to stress: when and how. J. Neuroendocrinol. **15**, 711-724.

Wood, G.A., Fata, J.E., Watson, K.L.M. and Khokha, R. (2007). Circulating hormones and estrous stage predict cellular and stromal remodeling in murine uterus. Reproduction **133**, 1035-1044.

Yu, Y.Z. and Shi, J.X. (2009). Relationship between levels of testosterone and cortisol in saliva and aggressive behaviors of adolescents. Biomed. Environ. Sci. **22**, 44-49.

FIGURES AND TABLES

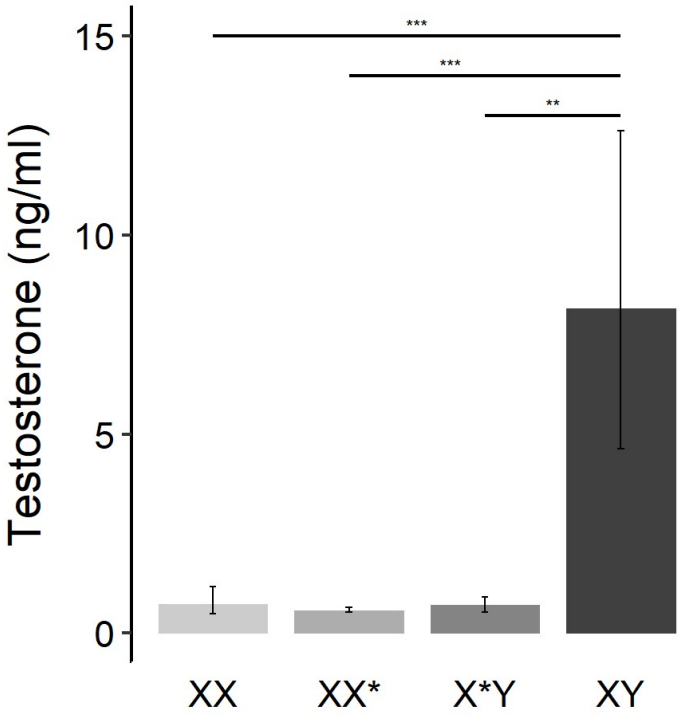

Fig. 1: Serum testosterone concentrations of the four sex genotypes, XX, XX* and X*Y females, and XY males. Values are means ± IC 95 %. *** $p < 0{,}001$, ** $p < 0{,}01$.

bioRxiv preprint doi: https://doi.org/10.1101/2022.07.11.499546; this version posted July 12, 2022. The copyright holder for this preprint (which was not certified by peer review) is the author/funder, who has granted bioRxiv a license to display the preprint in perpetuity. It is made available under aCC-BY-NC-ND 4.0 International license.

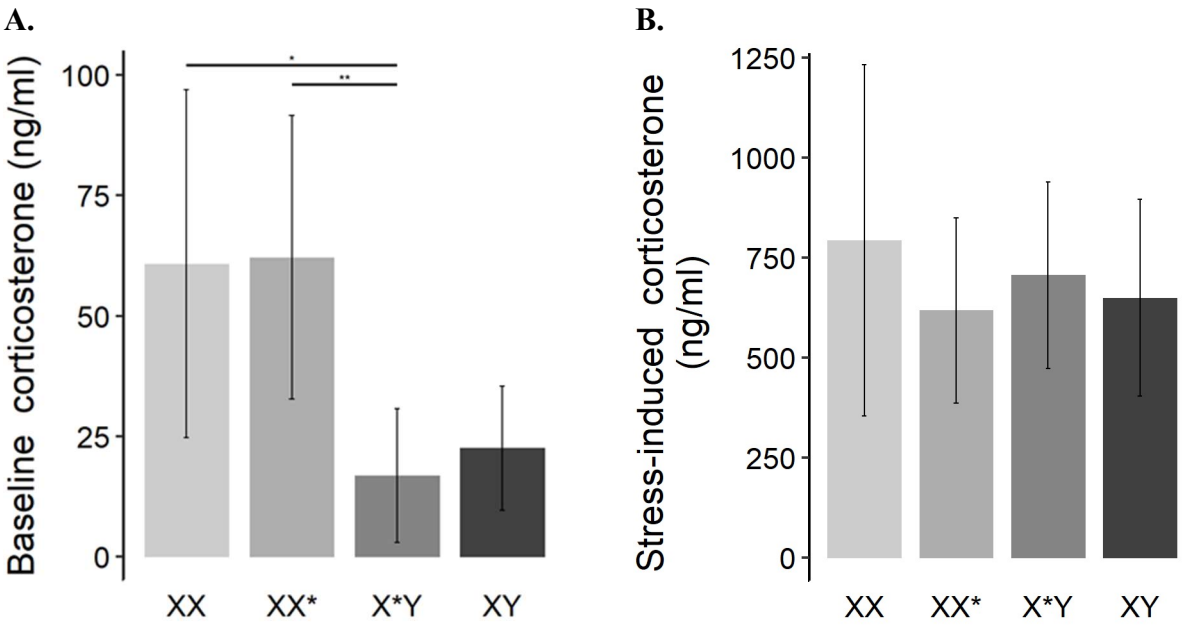

Fig. 2: Plasma corticosterone concentrations of the four sex genotypes, XX, XX* and X*Y females, and XY males. (**A**) Baseline and (**B**) stress-induced concentrations. Values are means ± IC 95 %. **p < 0,01, *p < 0,05.

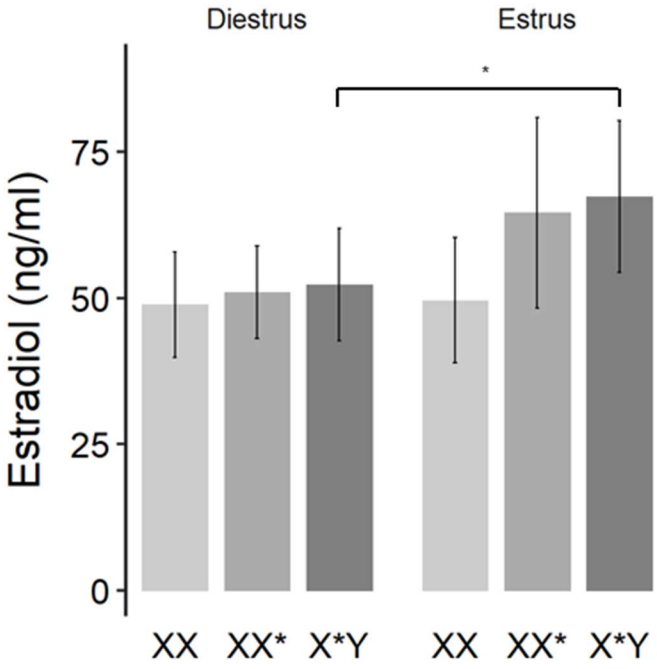

Fig. 3: Urinary estradiol concentrations of the three female genotypes, XX, XX* and X*Y, at diestrus and estrus stages. Values are means ± IC 95 %. *p < 0,05.

bioRxiv preprint doi: https://doi.org/10.1101/2022.07.11.499546; this version posted July 12, 2022. The copyright holder for this preprint (which was not certified by peer review) is the author/funder, who has granted bioRxiv a license to display the preprint in perpetuity. It is made available under aCC-BY-NC-ND 4.0 International license.

Table 1: Number of mice involved in each hormone assay.

Sex	**Female**			**Male**
Genotype	**XX**	**XX***	**X*Y**	**XY**
Testosterone	10	10	10	10
Corticosterone (baseline)	8	10	10	13
Corticosterone (after stress)	8	12	13	11
Estradiol (diestrus)	12	11	13	NA
Estradiol (estrus)	13	13	12	NA

Table 2: Hormonal profiles of the four sex genotypes. Comparison between hormonal profile expected according to behavioral traits they display, and hormonal profile observed.

	Hormonal profile expected			
	Aggressive behavior	Anxiety-related behavior	Reproduction, maternal care	Hormonal profile observed
XX females	T ↘	C ↗	E ↘	T → C ↗ E → or ↘
XX* females	T ↘	C ↗	E ↘	T → C ↗ E →
X*Y females	T ↗	C ↘	E ↗	T → C ↘ E →
XY males	T ↗↗	C ↘	NA	T ↗↗ C ↘

T = testosterone ; C = baseline corticosterone ; E estradiol ; ↗ = high concentration ; → = no difference between females ; ↘ = low concentration; double arrows indicate substantial difference.

bioRxiv preprint doi: https://doi.org/10.1101/2022.07.11.499546; this version posted July 12, 2022. The copyright holder for this preprint (which was not certified by peer review) is the author/funder, who has granted bioRxiv a license to display the preprint in perpetuity. It is made available under aCC-BY-NC-ND 4.0 International license.

Abstract :
The brain, like any other organ, is sexually dimorphic. Gonadal hormones were long thought to be the main, if not the only, biological factor at the basis of brain sexual differentiation and subsequent behaviours. In the last two decades, a few studies have challenged this hormone-centered view and showed that sex chromosomes can also have an influence. However, the role of sex chromosomes is far from being understood, and the majority of these studies are based on transgenic mice, which may limit interpretations especially when we are interested in phenotypes shaped by natural and sexual selection. The African pygmy mouse, *Mus minutoides*, is a wild mouse species with a polygenic sex determination system, which allows to tackle these questions. In this species, there are three sex chromosomes: the classical X and Y, as well as a feminizing chromosome, called X*. Hence, there are three female genotypes in natural populations: XX, XX*, X*Y, and males are XY. Previous studies have shown that X*Y females considerably differ from the other females: they have a greater reproductive success, they are more aggressive and less anxious than XX and XX* females, which have similar phenotypes. There is thus a dichotomy between gonadal sex and phenotypic sex, that questions the direct impact of sex chromosomes on brain sexual differentiation. Here, we show that sex chromosomes influence maternal care strategies of females (X*Y females differ from XX/XX* females), rather than impacting on their quality. We have identified a promising candidate for the neural basis of some of these behaviours: the dopaminergic system. Preliminary results also suggest that the latter, rather than steroid hormones, is likely to drive the enhanced territorial aggression in X*Y females. Furthermore, we show that sex chromosomes have a pervasive and sometimes dominant influence on the differentiation of the whole brain transcriptome. Most importantly, we show that the steady phenotypic similarities between XX and XX* females coincide with a preferential inactivation of the X* chromosome, highlighting potential sexual conflicts between X and X*. Through these analyses, we were also able to further identify candidate genes at the basis of females phenotypic divergences (e.g. reproductive cycle and behavioural traits). In sum, these multidisciplinary approaches allowed us to describe the genotype-phenotype relationship in the African pygmy mouse, and show that the emergence of the X* chromosome has opened avenues for the diversification of sexual phenotypes, underpinned by the new evolutionary trajectories of the sex chromosomes.

Key words : Brain, sexual dimorphism, sex chromosomes, hormones, African pygmy mouse, sex reversal

Résumé :
Le cerveau, comme tout autre organe, est sexuellement dimorphique. On a longtemps considéré que le principal, voire l'unique facteur biologique à la base de la différenciation sexuelle du cerveau, et des comportements sus-jacents, était les hormones secrétées par les gonades. Au cours des deux dernières décennies, quelques études ont défié cette vision hormone-centrée et ont démontré que les chromosomes sexuels peuvent également avoir une influence. Cependant, le rôle de ces derniers est loin d'être compris, et la majorité de ces études se basent sur des souris transgéniques, ce qui peut limiter les interprétations, surtout lorsque l'on s'intéresse à des phénotypes façonnés par la sélection naturelle et sexuelle. La souris naine africaine, *Mus minutoides* est une souris sauvage avec un déterminisme du sexe polygénique, qui permet d'aborder ces questions. On retrouve chez cette souris trois chromosomes sexuels : les classiques X et Y, ainsi qu'un chromosome féminisant, appelé X*, menant donc à trois génotypes femelles dans les populations naturelles : XX, XX*, X*Y, tandis que les mâles sont XY. De précédentes études ont montré que les femelles X*Y diffèrent considérablement des autres femelles : elles ont un plus grand succès reproducteur, sont plus agressives et moins anxieuses que les femelles XX et XX* qui, elles, ont des phénotypes similaires. Il y a donc une dichotomie entre le sexe gonadique et le sexe phénotypique chez cette espèce qui questionne l'impact direct des chromosomes sexuels sur la différenciation sexuelle du cerveau. Nous montrons, ici, que les chromosomes sexuels influencent les stratégies de soins maternels des différentes femelles (les femelles X*Y sont différentes des femelles XX/XX*), plutôt que d'en impacter la qualité. Nous avons identifié un candidat à la base neurale de certains de ces comportements : le système dopaminergique. Des résultats préliminaires suggèrent aussi que ce dernier, plutôt que les hormones stéroïdiennes, semble réguler l'agressivité territoriale accrue des femelles X*Y. En outre, nous montrons que les chromosomes sexuels ont une influence omniprésente et parfois prédominante sur la différenciation du transcriptome du cerveau. Mais surtout, nous montrons que les constantes similitudes phénotypiques entre les femelles XX et XX* coïncident avec une inactivation préférentielle du X*, soulignant de potentiels conflits sexuels entre le X et le X*. Par le biais de ces analyses, nous avons également pu identifier davantage de gènes candidats à la base des divergences phénotypiques (ex : cycle de reproduction et comportements) observées entre les femelles. En somme, ces approches pluridisciplinaires nous ont permis de décrire la relation génotype-phénotype chez la souris naine africaine, et montrent que l'émergence du chromosome X* a ouvert des voies à la diversification des phénotypes sexuels, sous-tendus par les nouvelles trajectoires évolutives des chromosomes sexuels.

Mots clés : cerveau, dimorphisme sexuel, chromosomes sexuels, hormones, souris naine africaine, inversion du sexe